Ant Colony Optimisation Algorithms for Solving Multi-Objective Power-Aware Metrics for Mobile Ad Hoc Networks

by

Demetrakis Constantinou

Department of Computer Science

School of Information Technology

University of Pretoria

Pretoria

South Africa

August 2010

Ant Colony Optimisation Algorithms for Solving Multi-Objective Power-Aware Metrics for Mobile Ad Hoc Networks

by

Demetrakis Constantinou

Abstract

A mobile ad hoc network (MANET) is an infrastructure-less multi-hop network where each node communicates with other nodes directly or indirectly through intermediate nodes. Thus, all nodes in a MANET basically function as mobile routers participating in some routing protocol required for deciding and maintaining the routes. Since MANETs are infrastructure-less, self-organizing, rapidly deployable wireless networks, they are highly suitable for applications such as military tactical operations, search and rescue missions, disaster relief operations, and target tracking.

Building such ad-hoc networks poses a significant technical challenge because of energy constraints and specifically in relation to the application of wireless network protocols.

As a result of its highly dynamic and distributed nature, the routing layer within the wireless network protocol stack, presents one of the key technical challenges in MANETs. In particular, energy efficient routing may be the most important design criterion for MANETs since mobile nodes are powered by batteries with limited capacity and variable recharge frequency, according to application demand. In order to conserve power it is essential that a routing protocol be designed to guarantee data delivery even should most of the nodes be asleep and not forwarding packets to other nodes. Load distribution constitutes another important approach to the optimisation of active communication energy. Load distribution enables the maximisation of the network lifetime by facilitating the avoidance of over-utilised nodes when a route is in the process of being selected.

Routing algorithms for mobile networks that attempt to optimise routes while attempting to retain a small message overhead and maximise the network lifetime has been put forward. However certain of these routing protocols have proved to have a

negative impact on node and network lives by inadvertently over-utilising the energy resources of a small set of nodes in favour of others. The conservation of power and careful sharing of the cost of routing packets would ensure an increase in both node and network lifetimes.

This thesis proposes simultaneously, by using an ant colony optimisation (ACO) approach, to optimise five power-aware metrics that do result in energy-efficient routes and also to maximise the MANET's lifetime while taking into consideration a realistic mobility model. By using ACO algorithms a set of optimal solutions – the Pareto-optimal set – is found.

This thesis proposes five algorithms to solve the multi-objective problem in the routing domain.

The first two algorithms, namely, the energy efficiency for a mobile network using a multi-objective, ant colony optimisation, multi-pheromone (EEMACOMP) algorithm and the energy efficiency for a mobile network using a multi-objective, ant colony optimisation, multi-heuristic (EEMACOMH) algorithm are both adaptations of multi-objective, ant colony optimisation algorithms (MOACO) which are based on the ant colony system (ACS) algorithm. The new algorithms are constructive which means that in every iteration, every ant builds a complete solution. In order to guide the transition from one state to another, the algorithms use pheromone and heuristic information.

The next two algorithms, namely, the energy efficiency for a mobile network using a multi-objective, MAX-MIN ant system optimisation, multi-pheromone (EEMMASMP) algorithm and the energy efficiency for a mobile network using a multi-objective, MAX-MIN ant system optimisation, multi-heuristic (EEMMASMH) algorithm, both solve the above multi-objective problem by using an adaptation of the MAX-MIN ant system optimisation algorithm.

The last algorithm implemented, namely, the energy efficiency for a mobile network using a multi-objective, ant colony optimisation, multi-colony (EEMACOMC) algorithm uses a multiple colony ACO algorithm.

From the experimental results the final conclusions may be summarised as follows:

- Ant colony, multi-objective optimisation algorithms are suitable for mobile ad hoc networks. These algorithms allow for high adaptation to frequent changes in the topology of the network.

- All five algorithms yielded substantially better results than the non-dominated sorting genetic algorithm (NSGA-II) in terms of the quality of the solution.
- All the results prove that the EEMACOMP outperforms the other four ACO algorithms as well as the NSGA-II algorithm in terms of the number of solutions, closeness to the true Pareto front and diversity.

Thesis supervisor: Prof. AP Engelbrecht
Department of Computer Science

Acknowledgments

I would like to thank professor AP Engelbrecht, my thesis supervisor, for his insight, motivation and ongoing support.

The sacrifices demanded by this thesis have impacted most strongly on my family and friends to whom I would like to express my gratitude for their moral support and encouragement over these past years.

Finally, I would like to dedicate this research to my dear sister–in–law who died unexpectedly at a young age recently leaving behind five children.

Contents

List of Algorithms

List of Tables

List of Figures

Chapter 1

Introduction

This thesis proposes to simultaneously optimise five power-aware metrics for energy efficiency in maximising mobile ad-hoc network (MANET) lifetime, taking in consideration a realistic mobility model, using an ant colony optimisation (ACO) approach. The ACO approach addresses a hardware independent routing protocol implementation within MANETs. Using the proposed algorithms, a set of optimal solutions, the Pareto-optimal set, is found based on ACO. Section 1.1 introduces MANETs. Section 1.2 emphasizes the importance of reducing energy consumption for MANETs. Section 1.3 briefly describes how this thesis solves the energy consumption problem for MANETs. Section 1.4 states the primary objectives of this thesis. Section 1.5 explains the contribution of this thesis, and Section 1.6 gives the thesis outline.

1.1 Mobile Ad Hoc Network

Mobile devices coupled with wireless network interfaces will become an essential part of future computing environments consisting of infrastructured and infrastructure-less mobile networks. Wireless local area networks based on IEEE 802.11 technology are the most prevalent infrastructured mobile networks, where a mobile node communicates with a fixed base station, and thus a wireless link is limited to one hop between the node and the base station. A MANET is an infrastructure-less multi-hop network where each node communicates with other nodes directly or indirectly through intermediate nodes [35, 117]. Thus, all nodes in a MANET basically function as mobile routers participating in some routing protocol required for deciding and maintaining the (potentially) dynamically changing routes. Since MANETs are infrastructure-less, self-organizing, rapidly deployable wireless networks, they are highly suitable for applications such as:

- Military tactical operations [86, 100] for fast and possibly short term establishment of military communications for troop deployments in hostile and/or unknown en-

vironments.

- Search and rescue missions [114] for communication in areas with little or no wireless infrastructure support.
- Disaster relief operations [162] for communication in environments where the existing infrastructure is destroyed or left inoperable.
- Law enforcement [201] for secure and fast communication during law enforcement operations.
- Commercial use [26] for creating communications in exhibitions, conferences, and large gatherings.

Building such ad hoc networks poses a significant technical challenge due to multiple constraints imposed by the environment [36, 82]. As a result, the device used in the field must weigh as little as possible. Furthermore, since mobile devices are battery operated, they need to be energy conserving in order to maximise battery lifetime. Several technologies are in the process of being developed with the aim of achieving energy conservation by targeting specific components of the computer and optimising the energy consumption of these components. For example, low-power displays, algorithms to reduce the power consumption of disk drives, low-power I/0 devices, and low-power central processing units (CPUs) all contribute to overall energy savings.

As a result of the highly dynamic and distributed nature of MANETs, routing tends to be one of the key issues in MANETs [48, 174]. In particular, energy efficient routing may constitute the most important design criterion for MANETs since mobile nodes are powered by batteries with limited capacity. Power failure of a mobile node not only affects the node itself, but also the ability of the node to forward packets on behalf of other nodes and, thus, the overall network lifetime.

A mobile node not only consumes its battery energy when it is actively sending or receiving packets, but it also consumes battery energy when idle and listening to the wireless medium for any possible communication requests from other nodes. Thus, energy efficient routing protocols minimise either the active communication energy which is required to transmit and receive data packets or the energy consumed during inactive periods. In terms of protocols that belong to the former category, the active communication energy may be reduced by adjusting the radio power of each node just enough

to reach the receiving node, and no more. This transmission power control approach may be extended to determine the optimal routing path that will minimise the total transmission energy required to deliver data packets to their destinations. In terms of those protocols that minimise the energy consumed for data transfer during inactive periods, each node may save the inactivity energy by switching its mode of operation to sleep/power-down mode or by simply turning the mode of operation off when there is no data to be either transmitted or received. This will result in substantial energy savings, especially in cases where the network environment is characterised by a low duty cycle of communication activities. However, a well-designed routing protocol is required to guarantee data delivery even if most of the nodes sleep and do not forward packets to other nodes.

Another important approach to the optimisation of active communication energy is the load distribution approach [111]. While the primary focus of the above two approaches is to minimise the energy consumption of individual nodes, the main goal of the load distribution method is to balance the energy usage amongst the nodes and to maximise the network lifetime by avoiding over-utilised nodes when selecting a routing path. While it is not clear whether any particular algorithm or class of algorithms is the best for all scenarios, there are definite advantages and disadvantages to each protocol, and each protocol is suited for certain situations. However, it is possible to combine and integrate the existing solutions and metrics for energy efficiency in order to offer a more energy efficient routing mechanism.

1.2 Reducing Energy Consumption for MANETs

The research focus in MANETs, in the past years, has been on developing strategies for reducing the energy consumption of the communication subsystem and increasing the lifetime of the nodes. Recent studies have stressed the need for designing medium access control (MAC) and routing protocols to ensure longer battery life. Much research has been done on designing protocols that increase the lifetime of nodes and the network [33, 109]. The research and developed algorithms were done with reference to the MAC, network and transport layers. Power-aware MAC protocols such as the power-aware multi-access protocol (PAMAS) [185] have been designed for battery energy savings that intelligently turn off radios when they can not transmit or can not receive packets.

The mobile ad-hoc network routing problem is difficult because of node mobility [7, 105, 206, 215]. With mobility, physically available routes may become invalid due to the topology change by node movement or link failure (i.e. may not be found by the routing algorithm), causing packets to be dropped and leading to throughput degradation and increasing control overhead. When two nodes previously within the transmission range move far away, the connection is lost. Vice versa, when two nodes move into the transmission range, a connection is gained. Thus, two conflicting goals are encountered: on the one hand, in order to optimise routes, frequent topology updates are required, while on the other hand, frequent topology updates result in higher message overhead.

Routing algorithms for mobile networks have been presented that attempt to optimise routes while attempting to keep message overhead small [33, 78, 97, 107, 116, 125, 138, 139, 157, 160, 182, 204]. Different routing protocols use one or more of a small set of metrics to determine optimal paths. Some of these metrics, however, have a negative impact on node and network life by inadvertently overusing the energy resources of a small set of nodes in favour of others.

Conserving power and carefully sharing the cost of routing packets will ensure that node and network life are increased. Singh *et al.* [184] presented several power-aware metrics that do result in energy-efficient routes. These metrics are

1. to minimise energy consumed per packet,
2. to maximise time to network partition,
3. to minimise variance in node power levels,
4. to minimise cost per packet, and
5. to minimise maximum node cost.

Many real-world problems require the simultaneous optimisation of a number of objective functions, referred to as *multi-objective optimisation problems* (MOP) [37, 147]. Some of these objectives may be in conflict with one another. A typical MOP simultaneously involves some competing objectives. The solution to a MOP requires a suitable definition of optimality (usually called *Pareto optimality*). MOPs normally have not one, but an infinite set of solutions, which represent possible trade-offs among the objectives (such solutions constitute the so-called *Pareto-optimal set* [155]). For MOPs

the main task is to optimise a vector function, say $\mathbf{f}(\mathbf{x}) = (f_1(\mathbf{x}), f_2(\mathbf{x}), ..., f_n(\mathbf{x}))$. A typical way to approach these problems is to transform the MOPs into single-objective (or scalar) problems (e.g. by using a linear aggregating function). This approach does, indeed, make sense if the functions $f_1, f_2, ..., f_n$ are of the same type and expressed in the same units, but otherwise (for instance, if f_1 denotes distance, f_2 denotes time, and so on) the scalarised problem might be meaningless. Also transforming the MOPs into a single-objective problem might not be feasible when there are trade-offs among the sub-objectives.

1.3 Solving Multi-Objective Power-Aware Metrics with Ant Colony Optimisation Algorithms

This research presents five multi-objective algorithms for simultaneously optimising the five power-aware metrics used for determining routes in wireless ad hoc networks, whilst, at the same time, taking into account the reference point group mobility (RPGM) model [29].

The proposed algorithms constitute new versions of the multi-objective ant colony system [53], the max-min ant system [195], and the multiple colony ant system [76].

1.4 Objectives

The primary objectives of this thesis can be summarised as follows:

- To develop and test multi-objective ant optimisation algorithms, in order to simultaneously optimise the five power-aware routing metrics described in Section 1.2 while taking in consideration a realistic mobility model.
- To obtain empirical results to support the predictions offered by the proposed algorithms.

1.5 Contributions

The main contributions of this work are:

- Development of the first dynamic multi-objective ant optimisation algorithms to simultaneously optimise five power-aware objectives for energy efficiency and the MANET's lifetime, taking in consideration a realistic mobility model.
- The evaluation of the scalability of the five dynamic multi-objective ant optimisation algorithms with different network sizes.
- The experimental evaluation of the response of the five algorithms to varying node mobility.

1.6 Thesis Outline

Chapter 2 contains an introduction to MANETs which is, in turn, followed by a comprehensive review of recent work conducted which addresses energy efficient and low-power design within the network layer. The chapter also examines different mobility models.

Chapter 3 starts with an introduction to combinatorial optimisation. An overview of the foraging behaviour of real ants is then presented, and this is, in turn, followed by a discussion on ant colony optimisation algorithms.

Chapter 4 commences with a theoretical overview of the multi-objective problem (MOP), which is followed by a discussion of the concepts of Pareto-optimal set and Pareto-optimal front. In view of the fact that ACO methods for MOO problems form the basis of the work presented in this thesis the focus then shifts to the application of ACO algorithms to MOO problems. A brief introduction of the evolutionary algorithms for solving multi-objective optimisation problems is then presented, and the NSGA-II algorithm is described in detail. Performance metrics used to compare multi-objective algorithms are discussed.

Chapter 5 discusses the concept of optimisation within dynamic environments since the optimisation problem considered in this thesis is within the context of a dynamic environment. A formal definition of a dynamic optimisation problem (DOP) is presented, followed by an overview of the main characteristics of DOPs. The ant algorithms for DOP are discussed, the performance metrics for DOP are described, and dynamic multi-objective optimisation examined.

Chapter 6 describes in detail the five metrics for power-aware routing, and the multi-objective optimisation problem is reformulated. This is followed by a description of the

new multi-objective ant colony optimisation algorithms for simultaneously optimising the five power-aware routing metrics. These new algorithms are adaptations of multi-objective ant colony optimisation algorithms.

Chapter 7 presents an empirical analysis of the behaviour of the multi-objective ant colony optimisation algorithms which were introduced in Chapter 6. The results are presented and evaluated.

Chapter 8 presents a summary of the findings of this thesis. Topics for future research are also discussed.

Appendix A and appendix B respectively list abbreviations and symbols used in this thesis along with their explanations.

Appendix C displays symbols used in this thesis to formulate the multi-objective optimisation problem for power-aware routing metrics.

Appendix D and appendix E respectively contain tables and graphs to visualise the results of the empirical analysis of the ant-based algorithm control parameters.

Appendix F displays the algorithms results for different scenarios.

Appendix G presents a three dimensional graphs to illustrate the influence of change frequency and change severity on the performance metrics.

Appendix H contains the results of the Mann-Whitney U test for each pair of algorithms to be compared.

Appendix I summarises the optimisation criteria results.

Appendix J presents FluxViz graphs to illustrate the influence of change frequency and change severity on the optimisation criteria for different number of nodes.

Chapter 2

Energy Efficient Network Protocols for Mobile Ad Hoc Networks

This chapter provides a review of mobile ad hoc networks (MANETs) and their main components. A discussion of multi-hop MANETs is also presented. An overview of the different mobility models is given. This is followed by a survey of different energy efficient protocols within the network layer.

2.1 Introduction

A mobile ad hoc network (MANET) refers to a collection of wireless mobile nodes which form a self-configuring network without using any existing, fixed infrastructure [35, 117]. As wireless networks become an integral component of the modern communication infrastructure, energy efficiency becomes an important design consideration in view of the limited battery life of mobile terminals. Power conservation techniques are commonly used in the hardware design of such systems. Since the network interface is a significant consumer of power, there has been much research conducted into low-power design of the entire network protocol stack of wireless networks in an effort to enhance energy efficiency. This chapter presents a comprehensive summary of recent work done on energy efficient and low-power design within the network layer. Table 2.1 illustrates the open systems interconnection (OSI) based protocol stack for a generic wireless network.

The mobility model plays a very important role in determining the protocol performance in MANETs [47, 123, 174]. Thus, it is essential to study and analyse various mobility models and their effect on MANET protocols. This chapter surveys and examines different mobility models which have been proposed in recent research literature.

A great body of knowledge about MANETs has been produced and many researchers in the field are now trying to apply this knowledge to the field of wireless sensor networks

Table 2.1: Protocol stack for a generic wireless network

Application and Services
OS and Middleware
Transport
Network
Data link (LLC, MAC)
Physical

(WSNs) because MANETs and WSNs are very similar. Both are distributed wireless networks and routing between two nodes may involve the use of intermediate relay nodes. Both networks are usually battery-powered and therefore there is a big concern on minimizing power consumption. Both MANETs and WSNs use a wireless channel and finally, self-management is necessary because of the distributed nature of both networks.

The remainder of this chapter is organised as follows. Section 2.2 provides a description of MANETs and their main components. Section 2.3 discusses multi-hop MANETs. Section 2.4 surveys and examines different mobility models. Section 2.5 discusses power-aware protocols within the network layer. Section 2.6 discusses bio-inspired routing for MANETs and, finally, Section 2.7 summarises and concludes the chapter.

2.2 Power Consumption and Communication for MANETs

In ad hoc mobile wireless networks, energy consumption is an important issue as most mobile hosts operate on limited battery resources. Conservation of energy is, therefore, critical in order to prolong the lifetime of the network. Instruction level modelling mobile systems run on the limited energy which is available within a battery. Thus the energy consumed by the system, or by the software running on the system, determines the duration of battery life.

There are two main consumers of energy on a MANET node, namely, the central processing unit and the radio (transmitter/receiver). These energy consumers are described in the following subsections.

2.2.1 Central Processing Unit

The microprocessor draws a current each time a program is executed. The average power consumed by a microprocessor while running a certain program is given by $P_o = I_c * V_s$, where P_o is the average power, I_c is the average current, and V_s the supply voltage [202]. Since power is the rate at which energy is consumed, the energy consumed by a program is given by $E = P_o * T_e$ where T_e is the execution time of the program. T_e, in turn, is given by $T_e = N_c * c_p$ where N_c is the number of clock cycles utilised by the program and c_p is the clock period.

Thus, together with the power cost of the hardware component it is important to also estimate the power cost of the software component. In order to systematically analyse the power cost of the software component it is necessary to estimate the power cost of the individual instructions.

Power Cost Measurement Method

It is obvious that a good instruction-level energy model is essential in order to evaluate software in terms of the power metric and also to help search the design space for low power software implementations. The instruction-level power analysis technique was first developed at Princeton University [128, 202, 203]. The technique is based on measurements of the current drawn by the processor as it executes certain instructions repeatedly. Power models for the Intel 486DX2, the Fujitsu SPARClite 934, and the Fujitsu DSP processor have been developed using this method. In order to model the energy consumption of the microprocessor, individual instructions must be considered. Each instruction involves specific processing demands across various units of the CPU. In terms of this model each instruction in the instruction set is assigned a fixed energy cost which is termed the base energy cost. The variation in the base costs of a given instruction is then quantified as a result of different operands and address values. The base energy cost of a program is based on the sum of the base energy costs of each instruction executed. However, during the execution of a program, certain inter-instruction effects occur of which the energy contribution is not accounted for if only the base costs are taken into account. The circuit state constitutes the first type of inter-instruction effect, while the second type is related to the resource constraints that may lead to stalls and cache misses. The energy cost of these effects is also modelled and used to obtain the

Table 2.2: Subset of the base cost table for the 486DX2

Number	*Instruction*	*Base Cost(mA)*	*Cycles*
1	NOP	275.7	1
2	MOV DX,BX	302.4	1
3	MOV DX,[BX]	428.3	1
4	MOV DX,[BX][DI]	409.0	2
5	MOV [BX],DX	521.7	1
6	MOV [BX][DI],DX	451.7	2
7	ADD DX,BX	313.6	1
8	ADD DX,[BX]	400.1	2
9	ADD [BX],DX	415.7	3
10	SAL BX,1	300.8	3
11	SAL BX,CL	306.5	3
12	LEA DX,[BX]	364.4	1
13	LEA DX,[BX][DI]	345.2	2
14	JMP label	373.0	3
15	JZ label	375.7	3
16	JZ label	355.9	1
17	CMP BX,DX	298.2	1
18	CMP [BX],DX	388.0	2

total energy cost of a program.

Certain instructions involve multiple cycles within a given pipeline stage. The base energy cost of the instruction is merely the observed average current value multiplied by the number of cycles taken by the instruction in that specific stage. Table 2.2 [203] summarises the CPU base costs for certain 486DX2 instructions.

Methodologies for analysing the energy consumption of embedded software help to verify whether an embedded design meets the energy constraints. These methodologies may also be used to guide the design of embedded software in such a way that the design meets these constraints.

Operating Modes

The CPU has four operating modes, namely, power down, power save, active, and idle. Power down shuts down the processor while the external interrupts (switch, button) remain on. Power save shuts down the processor while external interrupts and an asynchronous timer (external oscillator) remain on. The active mode leaves everything on,

while the idle mode shuts down the processor while the peripheral universal asynchronous receiver transmitter (UART), serial peripheral interface (SPI), and analogue to digital converter (ADC) remain on.

2.2.2 Radio

Radios have three operating modes, namely, transmit, receive, and power off. Thus, the total power consumption at a node is dependent on the operating modes of the two subsystems, i.e. the CPU and radio. All two subsystems must be used sparingly in order to prolong the lifetime of the network. As has been proved by several wireless network researchers [12, 50, 164, 187] the radio consumes the most energy of these two subsystems. At the communication distances which are typical in MANETs, the receiving and transmitting data involve similar costs [166]. Therefore, it is essential that protocols that account explicitly for receive power be developed. The primary cost of radio power consumption does not come from the number of packets transmitted but from the time spent by the nodes in a state of idle listening.

Idle listening is the time spent listening while waiting to receive packets. Stemm and Katz [189] observed that idle listening dominates the energy costs of network interfaces in hand-held devices. Overhearing constitutes a secondary cost of radio power consumption. Since radios are broadcast mediums, nodes receive all communications, including those destined for other nodes. Clearly, in order to reduce power consumption in radios, the radio must be switched off during idle times.

An important challenge for the communication block unit is the design of a wakeup radio – a low-power radio that is able to receive very simple communication and, in particular, is able to detect whether communication with its own node is desired. In such a case the wakeup radio may power up the main radio that receives the actual communication. Unfortunately, switching the radio off means that a neighbouring node that detects an interesting event is not able to wake up the radio's node. This may lead to missed events and packets, thus both increasing latency and wasting energy. Accordingly, a challenge to radio technology is to develop an ultra low power communication channel which is able to wake up neighbouring nodes on demand. Currently, such wakeup radios still constitute an area of active research in chip design and communications research [131, 209].

Researchers are investigating protocols across software layers for controlling radio

on/off times. Current approaches, which have been designed and implemented for real-world TinyOS applications, have focused on MAC-layer and application-layer techniques. Great Duck Island (GDI) for habitat monitoring [137] uses MAC-layer low-power-listening [197], while TinyDB [136] uses application-layer duty cycling [28] when deployed.

2.3 Multi-Hop MANETs

Multi-hop topologies play a significant role in MANETs. There are two main reasons for the importance of multi-hops. Firstly, the MANET itself has no wired or power-rich infrastructure. Therefore, in order to connect to the outside world, data must travel hop by hop to the nearest access point. Secondly, in terms of wireless communication, it is more energy efficient to transmit over several short distances than over a few long distances. Short distances also have better signal-to-noise ratios (because the environment is more homogenous), and this results in fewer retransmissions per hop due to packet loss [164].

However, there are inherent problems in multi-hop MANETs. Asynchronous events may trigger sudden bursts of traffic that could lead to collisions, congestion, and channel capture [214]. The problems that arise for wireless multi-hop networks are as a result of hidden nodes and exposed nodes. A hidden node refers to a node within the interfering range of the intended destination but out of the sensing range of the sender. Hidden nodes cause collisions at the destination when they transmit during the destination's reception. An exposed node refers to a node which is within the sensing range of the sender but out of the interfering range of the destination. Exposed nodes cease transmitting despite the fact that no collisions will take place at the destination.

In view of the fact that the MAC is a shared and scarce resource in a wireless multi-hop ad hoc network, efficient control of access to this shared media tends to become complicated. There has been considerable effort expended in designing MAC layer protocols, and several possible MAC layer protocols have been proposed [3, 217, 221]. The widely adopted IEEE 802.11 distributed coordination function (DCF) MAC protocol does not work well in wireless multi-hop networks primarily because DCF was designed for single communication cell networks [217]. The basic DCF access mechanism is carrier sense multiple access/collision avoidance (CSMA/CA) which uses physical carrier sense

and the request-to-send/clear-to-send (RTS/CTS) handshake for collision avoidance [99]. The latter is extremely effective in avoiding hidden nodes in single communication cells. However, the hidden node problem still exists in multi-hop networks. There is no scheme which addresses the exposed node problem which is far more harmful in multi-hop networks. In order to understand the reason why this is the case, it must be stated that in a carrier sense wireless network,

- the communication (transmitting) range and sensing (receiving) range are not symmetric,
- the interfering range and sensing range are much larger than the communication range, and
- collisions occur at the receiver and not the transmitter.

The larger interfering and sensing ranges are the cause of severe unfairness while end-to-end packets yield problems in multi-hop networks. While larger interfering ranges exacerbate the hidden node problem, larger sensing ranges exacerbate the exposed node problem.

2.4 Mobility Models

Performance evaluation of a protocol for a MANET should test the protocol under realistic conditions including, but not limited to, a sensible transmission range, limited buffer space for the storage of messages, representative data traffic models, and realistic movements of the mobile users (i.e. a mobility model).

A mobility model should attempt to mimic the movements of real mobile nodes (MNs). Changes in the speed and direction of MNs must occur and within reasonable time slots; for example, it is not desirable for MNs to travel in straight lines at constant speeds throughout the course of the entire simulation because real MNs generally do not travel in such a restricted manner. Different entity and group mobility models for ad hoc networks have been developed [13, 29, 124]. This research uses the reference point group mobility model (RPGM) [29].

In the remainder of this section the reference point group mobility model is described. Reference point group mobility model (RPGM) is a group mobility model, where group movements are based upon the path traveled by a logical centre.

At the beginning of a simulation, the RPGM model divides mobile nodes into groups. Each group has a logical centre whose movement defines the entire group's motion behavior including location, speed, direction and acceleration.

Each individual node has one reference point which movement is determined by that of the group. The motion of each node is determined by two vectors, a group motion vector and an individual motion vector with respect to the node's reference point. The net motion vector of each node is the sum of the two vectors. The group motion is defined by specifying a sequence of check points along the path corresponding to given time intervals. As time goes by, a group moves from one check point to the next on a continuing basis. By proper selection of check points, many realistic situations can easily be modeled, where a group must reach predefined destinations within given time intervals to accomplish the group's task. There are different ways to create various moving scenarios by changing the pattern of check points [101].

This thesis generates group motion patterns using the random waypoint model. Every time the group reaches its destination, all nodes inside the group pause for a certain time and then restart the moving process.

The group motion vector maps out the location of the reference centre, while the node-dependent random motion vectors, added to the group motion vector, give the positions of the node. The RPGM model describes the group membership of a mobile node by its physical displacement from the group reference center. For example, at time t the location of the i-th node in the j-th group is given by

$$\mathbf{x}_{j,i}(t) = \mathbf{y}_{j,i}(t) + \mathbf{z}_{j,i}(t) \tag{2.1}$$

where $\mathbf{y}_{j,i}(t)$ is the reference location and $\mathbf{z}_{j,i}(t)$ is the local displacement.

The node-dependent local displacement or random motion vector, $\mathbf{z}_{j,i}(t)$, denotes the effect of the mobile nodes having their own localised movements while following the general group motion defined by the reference centre. RPGM is illustrated in Figure 2.1.

In Figure 2.1, five MNs are initially placed in the lower left-hand corner of the simulation area. A black square represents the group centre while the circles near the group centre represent the MNs in the group. One circle in Figure 2.1 is grey in order to distinguish it from the other MNs in the group. The movement of the grey circle will be examined. RPGM first calculates the reference point of each MN using the group motion

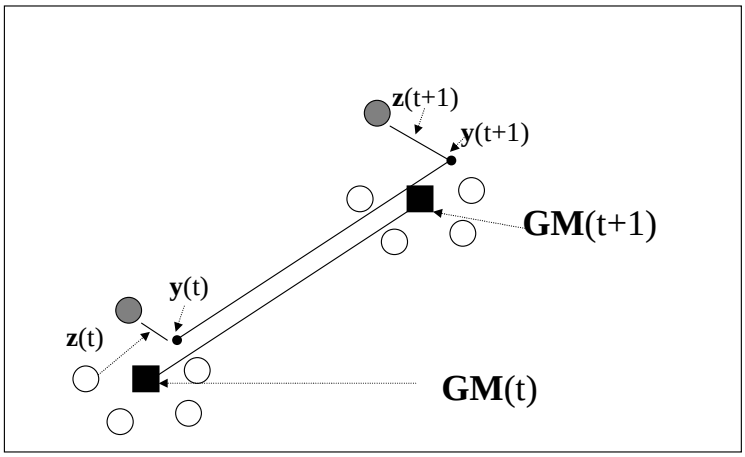

Figure 2.1: Movements of MNs using RPGM

vector, $\mathbf{GM}(t)$. $\mathbf{GM}(t)$ may be randomly chosen or predefined. The current reference point of the grey MN, $\mathbf{y}(t)$, moves towards the right-hand corner of the simulation area alongside the group centre. This location becomes the new reference point, $\mathbf{y}(t+1)$, for the grey MN. Finally, the new position of the grey MN is calculated by summing a random motion vector, $\mathbf{z}(t+1)$, with the new reference point, $\mathbf{y}(t+1)$. The length of $\mathbf{z}(t+1)$ is uniformly distributed within a specified radius centred at $\mathbf{y}(t+1)$ while its direction is uniformly distributed between 0 and 2π. This process is repeated for each MN in the group.

The RPGM model is a very good approach for realizing group mobility in tactical scenarios, because relative positions of nodes inside the groups can be modeled explicitly using an appropriate choice of parameters.

2.5 Network and Power Saving Routing Protocols

Routing of packets and congestion control are the main functions of the network layer [133]. In wireless mobile networks the network layer has the added functionality of routing under mobility constraints and mobility management including user location update. This section discusses energy efficient routing algorithms which were developed for wireless networks.

A switch is a device with several inputs and outputs that acts like a traffic junction to forward messages. Switches consist of a fabric and a set of ports which allow packets to flow from one link to another. Switches act as intersections as they forward messages arriving from one input link to a different output link. The advantage of a packet switched data network is its ability to scale beyond single hop communication. By connecting switches the network may be expanded to allow messages to be sent over multiple hops to non-adjacent nodes. Packet switched networks contain many pathways and this creates the problem of how to find a route from one node to another. A route connects nodes via one or more intermediate switches. Routes are discovered by exchanging information about links in order to construct route tables which contain directions to each node in the network. A packet switched network may be represented as a graph of nodes which are connected by links or edges. Each edge is assigned a cost which is derived from the characteristics of the link. The aim of a routing algorithm is to find the least cost path between two non-adjacent nodes in the network and to create a table which maps each destination to one of the output ports of the switches.

Ad hoc routing algorithms may be categorised into two types: table driven and on-demand [168]. Table driven algorithms send periodical broadcasts in order to maintain a route table. Algorithms classified as on-demand construct routes only when the routes are needed. Both types of algorithms use controlled flooding to find routes. The difference between these two approaches is the frequency with which flooding takes place. In terms of an on-demand protocol, flooding takes place only when a node desires a route to a new destination. On the other hand, because routing information is constantly propagated and maintained in table driven routing protocols, a route to every other node in the ad hoc network is always available, regardless of whether or not it is needed. This feature, although useful for datagram traffic, incurs substantial flooding traffic and power consumption.

Ad hoc routing algorithms may also be classified as active or reactive routing algorithms [216]. Routing algorithms that attempt to determine routes in advance are classified as active routing algorithms. Routing algorithms which take action only when a link is broken are classified as reactive.

Subsections 2.5.1 to 2.5.7 respectively discuss power efficient data gathering and aggregation protocols, dynamic source routing, distance vector routing, routing for maximum system lifetime, temporally ordered routing algorithms, volcano routing schemes,

and destination sequenced distance vector, power-aware protocols. Subsection 2.5.8 presents a routing algorithm for network capacity maximisation (CMAX) in a wireless network. Subsection 2.5.9 presents the online maximum lifetime (OML) routing algorithm to maximise lifetime in a wireless network. Subsection 2.5.10 discusses other power-aware routing algorithms with respect to different metrics while Subsection 2.5.11 discusses power-aware routing algorithms for networks with frequent topological changes. These routing protocols employ power efficient methods for data gathering, aggregation and sending in order to achieve long network lifetimes.

2.5.1 Power Efficient Data Gathering and Aggregation Protocol

Tan and Korpeoglu [200] proposed two algorithms for enhancing network lifetime, namely, the power efficient data gathering and aggregation protocol (PEDAP) and the power efficient data gathering and aggregation protocol power-aware (PEDAP-PA). Both are routing protocols based on optimal minimum spanning trees (MST) [34]:

Definition 2.5.1. Minimum spanning tree:

Given a connected, undirected, graph $G = (V, L)$ a spanning tree, T_s, denotes an acyclic subset of edges, $T_s \subseteq L$, that connects all the vertices together.

Assuming G is weighted, the cost of a spanning tree, T_s, is the sum of edge weights, C_s, in the spanning tree, given as

$$C_s(T_s) = \sum_{(u,w)\,\in\, T_s} c_{s,uw} \tag{2.2}$$

where $(u, w) \in T_s$ is an edge and $c_{s,uw}$ is the weight of edge (u, w). A MST is a spanning tree of minimum weight.

PEDAP minimises the total energy expended in the system in a round of communication in which each round corresponds to an aggregation of data which is transmitted from different MANET nodes to the sink by computing a minimum spanning tree over the MANET. The data packets are then routed to the base station over the edges of the computed minimum spanning tree. PEDAP prolongs a satisfactory lifetime for the first node while providing a satisfactory lifetime for the last node. PEDAP constructs minimum energy consuming routing tables for each round of communication.

PEDAP-PA extends PEDAP by balancing the energy consumption among the nodes. PEDAP-PA provides a near optimal lifetime for the first node although the lifetime of the last node is slightly decreased.

Both algorithms consider that locations of wireless nodes are fixed and that the base station knows all the locations of the nodes a priori. The nodes are in direct communication range of each other and are able to transmit to and receive from the base station. The nodes aggregate or fuse the data received (via the minimum spanning tree) from the other nodes with their own data, and produce one packet only regardless of the number of packets received. In each round a special node is randomly selected to assume the responsibility for sending the fused data to the base station. Both algorithms assume that the quality of the system dramatically decreases after the first node dies. However, this is not always the case if the redundancy of a wireless network is considered.

2.5.2 Dynamic Source Routing

Dynamic source routing (DSR) [107] uses one or more of a small set of metrics to determine optimal paths. The most common metric used is shortest-hop routing [173]. DSR is a routing protocol for ad hoc networks that uses dynamic source routing of packets between hosts that wish to communicate. Source routing is a routing technique in which the sender of a packet determines the complete sequence of nodes through which to forward the packet. The sender lists this route explicitly in the header of the packet and identifies each forwarding hop by the address of the next node to which it must transmit the packet on its way to the destination host. The sender uses a route discovery algorithm to discover a route to the destination host dynamically. A route maintenance procedure is used to inform the sender of any routing errors. DSR uses no periodic routing advertisement messages, thereby reducing network bandwidth overhead, particularly during periods when little or no significant host movement is taking place. Battery power is also conserved on the mobile hosts – both by not sending the advertisements and by having no need to receive the advertisements. DSR adapts quickly to routing changes when host movement is frequent, yet requires little or no overhead during periods in which hosts move less frequently.

2.5.3 Distance Vector Routing

Distance vector routing (DVR) [97] refers to a decentralised algorithm which applies a distance vector to each route. A distance vector has two components – magnitude and direction. The magnitude represents the cost or distance of the route while the direction identifies the output port which leads to the destination. Switches which use the distance vector algorithm maintain local route tables containing a cost and next hop address for each destination in the network. Messages are forwarded by consulting the route table for the correct destination. Routes are selected by competing for the lowest cost path until a stable state is reached. Occasionally, routes do not stabilise and this causes loops to be formed.

2.5.4 Routing for Maximum System Lifetime

Chang and Tassiulas [33] presented several proposals on ways in which to model the system lifetime of ad hoc networks when the total energy in the network limits lifetime. They proposed routing algorithms with which to select routes and the corresponding power levels so as to maximise the elapsed time until the batteries of the nodes are depleted. Instead of minimising the energy consumed, the focus of the routing algorithms is on maximising the lifetime of the system. In order to achieve this, instead of minimising the absolute power consumed, traffic is routed in such a way that the energy consumption is balanced among the nodes in proportion to the available energy of the nodes. The proposals of Chang and Tassiulas are applicable to networks which are either static or else to networks with slowly changing topology to the extent that there is enough time to balance the traffic optimally during the periods between successive topology changes.

2.5.5 Temporally Ordered Routing Algorithm

Park and Corson [156, 157] presented a new distributed routing protocol for mobile multi-hop wireless networks known as temporally ordered routing algorithm (TORA). TORA is extremely quick in creating and maintaining loop-free multi-path routing to destinations for which routing is required while simultaneously minimising communication overhead. TORA adapts speedily to topological changes and has the ability to detect network partitions and to erase all invalid routes within a finite time. TORA is a link reversal algorithm which routes messages by assigning a height value to each node. Heights

impose a temporary order on the set of nodes from highest to lowest. Messages may flow only via nodes in descending height order. Heights are negotiated between immediate neighbours on demand by sending a query message, and, thus, triggering further queries which elevate the height of the originator. Intermediate nodes are assigned heights in descending order toward the destination. A query packet consists of a quintuplet which contains the time of a link request, the identifier address of the originator, the reference height of the originator, and the forwarding node height. A sequence number orders the queries, thus reducing the chances of a loop being created by older requests. At any given time the same quintuplet with node identifier i is associated with each node i. This quintuplet represents the height of the node. Route maintenance is performed when a broken link is detected. The height of a node at the point of failure is lowered, thus causing a link reversal. If it is not possible to reach a destination, then routes toward the destination are flushed from the network.

This protocol is best-suited for use in large, dense mobile networks in which the reaction of the protocol to link failures typically involves a localised single pass of the distributed algorithm only. This capability is unique among protocols which are stable in the face of network partitions, and results in the high degree of adaptability of the protocol. In order to verify convergence in a MANET protocol it is necessary to consider states which are reachable not only in terms of the events of the protocol itself but also in terms of changes of topology [219, 220].

The TORA protocol guarantees that no loops will occur, provides multiple routes and minimal communication overhead even in highly dynamic environments. TORA aims to minimise routing discovery overhead, and, in doing so, prefers instant routes to optimal routes. The protocol supports source-initiated, on-demand routing for networks with a high rate of mobility as well as destination oriented, proactive routing for networks with lesser mobility.

2.5.6 Volcano Routing Scheme

Ganjali and McKeown [78] proposed the volcano routing scheme (VRS) algorithm which routes packets successfully even if the topology changes extremely rapidly. VRS does not need to discover routes, or exchange routing information. It merely balances the load locally between adjacent pairs of nodes. Ganjali and McKeown demonstrated that VRS keeps the system stable for various models of mobility, different communication

patterns, and different volumes of flow in the network. The VRS is a potential-based routing scheme. The key principle in potential-based routing is to define K scalar fields on the network one for each destination node. More formally, a single-valued potential, denoted by P_u^f, is associated with any flow f at a given node u. At each node u of the network, packets destined to D_f, the destination of the f-th flow, are routed in the direction (i.e. the next hop) that the potential field decreases the most for flow f.

Normally, the potential function depends on the topology of the network and it is chosen in such a way that each packet is directed toward its destination. In VRS, the potential function is totally different, and is simply based on the number of packets buffered at each node of the network and not on the connectivity of the network. At a given node, u, and for a given flow, f, the potential function, P_u^f, is equal to the number of packets of flow that reside at node u. VRS forwards packets from nodes which have more buffered packets to those nodes which have fewer buffered packets.

The performance of VRS is based on several metrics, namely, packet loss, distribution of queue size, and the length of the path taken by packets. Simulations suggest that, when the network is not highly loaded, the average and maximum queue sizes do not change with the communication range, the number of nodes, and the mobility process [78]. However, when the network becomes highly loaded as a result of reducing the communication range or decreasing the number of nodes, the queue sizes increase. For a fixed number of nodes in the network expansion of the communication range of each node increases the average degree of each node, and this, in turn, enhances the connectivity of the network and reduces the packet loss ratio. If the communication range of each node is fixed then increasing the number of nodes in the network will reduce the packet loss.

2.5.7 Destination Sequenced Distance Vector

Destination sequenced distance vector (DSDV) [160] is a proactive protocol which models mobile computers as routers. The mobile computers cooperate to forward packets as needed to each other. Packets are transmitted between the stations (mobile computers) of the network by using routing tables which are stored at each station of the network. Each routing table, at each of the stations, lists all the available destinations as well as the number of hops to each destination. Each route table entry is tagged with a sequence number. This sequence number is generated by the destination station. In order to maintain the consistency of the routing tables in a dynamically varying topology, each

station periodically transmits routing table updates and transmits updates immediately when significant new information becomes available. Older routes will be discarded in favour of newer or cheaper routes (with fewer hop counts). The routing table updates may be sent in two ways:

1. a full dump which sends the full routing table to the neighbours and is able to span several packets, or

2. an incremental update which sends only those entries with a metric (hop count) change since the last update.

Route updates must be sent sufficiently frequently in order to locate all the nodes in the network, thus creating a high communication overhead when the topology is dynamic. Temporary routing loops may be caused by a delay in the propagation of accurate route information. The aim of DSDV is to prevent the propagation of false or out of date information by appending a sequence number to distance vector routing. DSDV has a moderate memory requirement of $O(n)$, where n is the number of nodes. No simulation studies have yet been performed in order to examine the convergence of the algorithm.

2.5.8 Routing for Network Capacity Maximisation in Energy-Constrained Ad Hoc Networks

Kar *et al.* [115] developed a capacity-competitive algorithm known as CMAX. CMAX carries out admission control, i.e. the algorithm may occasionally reject messages that are deemed to be too detrimental to the residual capacity of the network. Network capacity is defined as the total volume of message data that is successfully carried by the network.

Before describing the CMAX algorithm, the following terminology will be defined: The wireless network is modelled as a directed graph, $G = (V, L)$. V is the set of nodes in the network with $n = |V|$ the number of nodes. L is the edge set. There is a directed edge, $(u, w) \in L$, from node u to node w if and only if a single-hop transmission from u to w is possible. Let $E_u > 0$ be the initial energy of node u and let $e_u^c \geq 0$ denote the current energy of node u. For each $(u, w) \in L$ let $E_{uw} > 0$ denote the energy required to do a single-hop transmission from node u to node w. Following a single-hop message

transmission from u to w the current energy in node u becomes $e_u^c - E_{uw}$. Note that this single-hop transmission is possible only if $e_u^c \geq E_{uw}$.

To calculate E_{uw}, the most common model for power attenuation is used. In this model signal power attenuates at the rate $\frac{c_a}{d^{h_d}}$, where c_a is a media dependent constant, d is the distance from the signal source, and h_d is another constant between 2 and 4 [170]. Therefore, $E_{uw} = E_{wu} = c * d_{uw}^{h_d}$, where d_{uw} is the Euclidean distance between nodes u and w, and c is a constant.

Let $\kappa(u) = 1 - e_u^c/E_u$ be the fraction of initial energy of node u that has been used so far, where E_u is the initial energy of node u. Let ζ and σ represent two constants. CMAX changes the weight of every edge (u, w) from E_{uw} to $E_{uw} * (\zeta^{\kappa(u)} - 1)$. The shortest source-to-destination path, P, in the resulting graph is determined using the new weight. If the length of this path is more than σ, then the routing request is rejected (admission control); otherwise, path P is accepted as the route. Algorithm 1 summarises the CMAX algorithm.

Algorithm 1 CMAX Algorithm

Step 1: {Initialize}
Eliminate from G every edge (u, w) for which $e_u^c < E_{uw}$;
Change the weight of every remaining edge (u, w) to $E_{uw} * (\zeta^{\kappa(u)} - 1)$;
Step 2: {Shortest Path}
Let P be the shortest source-to-destination path in the modified graph.
Step 3: {Wrap Up}
If no path is found in Step 2, the route is not possible;
If the length of P is more than σ, reject the route;
Otherwise, use P for the route;

2.5.9 The Online Maximum Lifetime Heuristic

In order to maximise lifetime, it is necessary to delay the depletion of the energy of a node to a level below that needed to transmit to its closest neighbour for as long as possible [94]. This objective may be attained by using a two-step algorithm, namely, the online maximum lifetime (OML) heuristic algorithm. The OML is used to find a path for each routing request, $r_i = (s_i, d_i)$, where s_i is the source node and d_i is the destination node. In the first step, OML removes from G all edges (u, w) such that $e_u^c < E_{uw}$ as these edges require more energy than is available for a transmit. Let the resulting graph

be $G^{'} = (V, L^{'})$. In the next step OML determines the minimum energy path, $P_i^{'}$, from s_i to d_i in the pruned graph $G^{'}$. This may be done by using Dijkstra's shortest path algorithm [175]. In cases in which there is no s_i to d_i path in the pruned graph $G^{'}$ then the routing request r_i will fail. Assume that such a $P_i{'}$ exists. Using $P_i{'}$, OML computes the residual energy, e_u^r as $e_u^r = e_u^c - E_{uw}$, for all edges $(u, w) \in P_i^{'}$. The minimum residual energy, e_{min}^r, is then calculated as

$$e_{min}^r = min\{e_u^r | u \in P_i{'} \text{ AND } u \neq d_i\} \tag{2.3}$$

Let $G^{''} = (V, L^{''})$ be obtained from $G^{'}$ by removing all edges $(u, w) \in L^{'}$ with $e_u^c - E_{uw} < e_{min}^r$. That is, all edges whose use would result in a residual energy below e_{min}^r are pruned from $L^{'}$. This pruning is an attempt to prevent the depletion of energy from nodes that are low on energy.

The second step finds the path to be used to route request r_i. In order to find the path, OML begins with $G^{''}$ as above and assigns weights to each $(u, w) \in L^{''}$. The weight assignment is done to balance the desire to minimise total energy consumption as well as the desire to prevent the depletion of node energy. Let $e_u^m = min\{E_{uw} | (u, w) \in L^{''}\}$ be the energy needed by node u to transmit a message to its nearest neighbour in $G^{''}$. Let $\phi(u, w)$ a function whose use prevent the depletion of the energy of node u, below that needed to transmit to the closest neighbour of u; $\phi(u, w)$ is defined as

$$\phi(u, w) = \begin{cases} 0 & \text{if } e_u^c - E_{uw} > e_u^m \\ c & \text{otherwise} \end{cases} \tag{2.4}$$

where c is a non-negative constant. For each $u \in V$, define

$$\kappa(u) = \frac{e_{min}^r}{e_u^c} \tag{2.5}$$

where $\kappa(u)$ is the fraction of u's initial energy that has been used so far.
The weight, $E_{uw}^{''}$, assigned to edge $(u, w) \in L^{''}$ is

$$E_{uw}^{''} = (E_{uw} + \phi(u, w))(\zeta^{\kappa(u)} - 1) \tag{2.6}$$

where ζ is another non-negative constant.

From equation (2.6), the weighting function, through ϕ, assigns a high weight to edges whose use on a routing path causes a node's residual energy to become low. Also, all edges emanating from a node whose current energy is small relative to e^r_{min} are assigned a high weight because of the $\zeta^{\kappa(u)}$ term. Thus the weighting function discourages the use of edges whose use on a routing path is likely to result in the failure of a future route.

Algorithm 2 gives the OML algorithm to select a path for request r_i.

Algorithm 2 General Procedure of OML

Step 1: **Compute** G'';
$G' = (V, L')$ where $L' = L - \{(u, w)|e^c_u < E_{uw}\}$;
Let P'_i be a shortest path from s_i to d_i in G' using Dijkstra's algorithm;
If there is no such P'_i, the route request fails and the algorithm terminates;
Compute the minimum residual energy e^r_{min} for all nodes other than d_i on P'_i using equation (2.3);
Let $G'' = (V, L'')$ where $L'' = L' - \{(u, w)|e^c_u - E_{uw} < e^r_{min}\}$;
Step 2: **Find route path**
Compute the weight E''_{uw} for each edge of L'' using equation (2.6);
Let P''_i be a shortest path from s_i to d_i in G'';
Use P''_i to route from s_i to d_i;

2.5.10 Other Power-Aware Routing Algorithms and Metrics

Energy conservation is a critical issue in wireless networks for node and network lifetime, as the nodes are powered by batteries [211]. This subsection surveys recent routing protocols for wireless networks in which energy awareness is an essential consideration. The most interesting research issue in respect of these power-aware routing protocols consists of ways in which to optimise different metrics.

Singh *et al.* [186] addressed routing of unicast traffic (unicast refers to the sending of information packets to a single destination) with respect to battery power consumption. Their research focused on the design of protocols to reduce energy consumption and to increase the lifetime of each mobile node, thus also increasing network lifetime. This goal may be attained by minimising the energy of mobile nodes, not only during active communication, but also when the mobile nodes are inactive.

Transmission power control and load distribution are two approaches to minimising the active communication energy. Sleep/power-down mode is used to minimise energy

during inactivity. In order to minimise the active communication energy, five different metrics are defined from which to study the performance of power-aware routing protocols. These energy-related metrics have been used to determine an energy efficient routing path instead of finding the shortest paths. The metrics are [186]:

- **Energy consumed per packet:**

  This metric is useful in order to provide the minimum power path through which the overall energy consumption for delivering a packet is minimised. Each wireless link is annotated with the link cost in terms of transmission energy over the link. The minimum power path is that path which minimises the sum of the link costs along the path. However, a routing algorithm using this metric may result in unbalanced energy spending among mobile nodes. Nodes that are unfairly burdened in order to support several packet-relaying functions consume more battery energy and run out of energy earlier than other nodes, thus disrupting the overall functionality of the ad hoc network.

- **Time to network partition:**

  This metric maximises the network lifetime. Given a network topology, a minimal set of MNs exists so that the removal of these MNs would cause the network to partition. The traffic in these MNs should be divided in such a way that their power is depleted at equal rates. Given alternative routing paths, this metric favours the selection of that path which will result in the longest network operation time.

- **Variance in node power levels:**

  This metric is based on the premise that all MNs in the network operate at the same priority level, thus ensuring that all mobile nodes are equal and that no single mobile node is penalised or advantaged over any other. All mobile nodes in the network remain powered on for as long as possible.

- **Cost per packet:**

  Metrics other than energy consumed per packet need to be adopted in order to maximise the lifetime of all the mobile nodes in the network. The cost per packet metric creates routes in such a way that mobile nodes with depleted energy reserves do not form part of many routes.

- **Maximum node cost:**

  This metric attempts to minimise the cost experienced by a mobile when routing a packet. By minimising the cost per mobile node significant reductions in the maximum mobile cost are obtained. Also, the maximum node cost metric delays mobile failure, and reduces variance in mobile power level.

In order to conserve energy all metrics need to be minimised, except the time to network partition metric which needs to be maximised. As a result, a minimal cost routing protocol with respect to the five energy efficient metrics is more appropriate instead of a shortest hop routing protocol. Thus, although packets may be routed through longer paths, the paths contain mobile nodes that have greater energy reserves. Also, routing traffic through lightly loaded mobile nodes conserves energy because contention and retransmission are minimised.

The above approach to routing in wireless ad hoc networks requires that every mobile node has knowledge of the locations of every other mobile node and the links between them. This creates significant communication overhead and increases delays. Stojmenovic and Lin [191] addressed this issue by proposing a power, cost, and power-cost global positioning system (GPS) which is based on a localised routing algorithm, where nodes make routing decisions based solely on the location of their neighbours and on the location of the destination.

The power-aware localised routing algorithm attempts to minimise the total power needed to route a message between a source and a destination. The loop-free localised power efficient routing algorithm may be described as follows: The source (or an intermediate node), S, should select one of its neighbours, A, to forward packets toward destination, D, with the goal of reducing the total power needed for the packet transmission. Only those neighbours that are closer to the destination than S are considered. Node A becomes the source and the algorithm proceeds recursively until the destination is reached – if possible.

The cost-aware localised routing algorithm is aimed at extending the worst case lifetime of batteries. The loop-free localised cost aware routing algorithm may be described as follows: The cost, $c(A)$, of a route from S to D via neighbouring node A is the sum of the cost, $f(A)$, of node A and the estimated cost of the route from A to D. If the destination is one of the neighbours of node S, which currently holds the packet, then the packet will be delivered to D. Otherwise, S will select that neighbour, A, which

minimises $c(A)$. The algorithm proceeds until the destination is reached, if possible, or until a node has no neighbouring node to the destination other than itself.

Combined power-cost algorithms both minimise the total power needed and maximise remaining battery lifetime.

Stojmenovic and Lin [191] proved empirically that these localised power, cost, and power-cost efficient routing algorithms are loop-free. These routing algorithms achieve very high delivery rates for dense networks, but low delivery rates for sparse networks. Control messages are used to update the positions of all nodes in order to maintain the efficiency of the routing algorithms. These control messages also consume power which means that the most advantageous trade-off for moving nodes must be established.

These routing algorithms were tested on static networks with high connectivity [191]. Power efficient methods tend to select well positioned neighbouring nodes in forwarding messages while cost efficient methods favour nodes with more power remaining.

Shah and Rabaey [181] presented an energy aware routing algorithm for low energy wireless networks. Network survivability was considered as the primary metric. They demonstrated that network lifetimes may be increased up to 40% as against comparable schemes such as directed diffusion routing. Energy aware routing builds per-sink cost fields to direct data delivery. A sender probabilistically picks a receiver to which each packet has to be forwarded. The basic principle is that, in order to occasionally increase the survival of networks, it may be necessary to use sub-optimal paths. This will ensure that the power of the optimal path is not depleted, and that the network degrades as a whole rather than being partitioned. To prevent energy depletion of the optimal path, multiple paths are found between the source and the destination, and each path is assigned a certain probability of being selected, depending on the energy metric. In order for each packet to be sent from the source to the destination one of the paths is randomly chosen, depending on the probabilities. This means that none of the paths is used all the time, thus preventing energy depletion. Also, different paths are tried continuously, hence improving tolerance to nodes moving around in the network.

Energy aware routing is also a reactive routing protocol. It is also a destination-initiated protocol in terms of which the data consumer initiates the route request and subsequently maintains the route.

2.5.11 Power-Aware Routing Algorithms for Networks with Frequent Topological Changes

Routing in mobile ad hoc networks is difficult because the topology may change rapidly [105, 215]. By the time new paths have been discovered the network could change again. In extreme cases packets may circulate endlessly, thus causing the system to become unstable. It is difficult to describe and to constrain mobility for frequently changing networks. There will not be enough time to balance traffic optimally between successive topology changes. For this reason existing routing algorithms are of little use. However, existing algorithms such as the distance vector routing [160] have proved to be effective in situations in which topology changes slowly.

Gafni and Bertsekas [71] considered the problem of maintaining communication between the nodes of a data network and a central station in the presence of frequent topological changes as, for example, in mobile packet radio (PR) networks. They proposed distributed algorithms for generating loop-free routes, and thus forming the basis for the development of contingency routing algorithms.

These distributed algorithms have the following properties:

1. They work on unknown communication topologies.

2. They implement a directed acyclic graph (DAG) over the network topology, where all directed paths lead to the destination.

3. In the event of changes to the topology of the network, a new DAG is created using an iterative method.

In such distributed algorithms each PR is assigned a generalised number (i.e. an element of a suitable totally ordered set). Link directions will always be oriented from higher to lower numbers. This prevents loops from forming and provides reliable secondary routes that may be used for transmitting connectivity information and data to the station when the primary routes fail. When a PR loses all its routes to the station, a reversal process is executed whereby, on the basis of the numbers of its neighbours, the PR selects a number according to the rules of one of the algorithms proposed. This number is broadcast to all the PR's neighbours informing them of any reversals in the direction of communications that affect them.

There is a possibility that some numbers may become too large, for example, if the network becomes disconnected. Accordingly, an error detection scheme is required to ensure that each PR operates on the basis of correct numbers for all its neighbours.

These distributed algorithms – referred to as Gafni-Bertsekas (GB) algorithms – are designed for operation in connected networks. GB algorithms do exhibit instability in parts of the network which have become partitioned from the destination.

Stergaard [190] presented a distributed algorithm for a network with dynamic changing topology. This distributed algorithm is termed the efficient distributed hormone graph gradient (EDHGG). EDHGG provides information on topological distance in communication networks with dynamic changing topologies. From a functional point of view this algorithm is an improved version of the algorithm which was presented by Gafni and Bertsekas [71], with two additional features:

1. From a given node, the length of any directed path to the destination is equal to the shortest undirected path to the destination.

2. Each node knows its topological distance from the destination.

EDHGG is based on topological distance (i.e. the number of hops between two nodes) and is capable of dealing with changing topologies in the connectivity graph using only local information, without global synchronisation. The algorithm generates messages only when the topology of the graph changes.

2.6 Bio-inspired Routing for MANETs

In addition to the classical MANET routing algorithms, the focus of the MANET research community has also been on the application of nature inspired engineering approaches to solve the MANET routing problem [31]. The term bio-inspired has been introduced to demonstrate the strong relation between a particular system or algorithm, which has been proposed to solve a specific problem, and a biological system, which follows a similar procedure or has similar capabilities.

A number of MANET routing protocols have been designed [2], which deal with the extremely dynamic nature of MANET networks [69]. These protocols are mainly

inspired by ant colony behaviours, resulting in distributed, self-organizing, and adaptive algorithms. The first ACO routing algorithms developed were the ant based control (ABC) algorithm [178] for circuit-switched telephone networks and AntNet [31] for connectionless IP data networks. ACO implementations for different routing protocols developed since then have based their design on either AntNet [14, 44, 113, 180, 210] or ABC [196].

ABC is a proactive algorithm designed for load balancing in a circuit switched system. ABC is used for call controlling (distributes the calls over multiple switches) and maintains only one routing table whose rows show the destination. Calls between nodes are routed as a function of the pheromone distributions at each intermediate node.

AntNet is an adaptive, distributed, mobile agents-based algorithm which was based on the stigmergic communication found in natural ant colonies. The operation of AntNet is based on two types of agents:

- forward ants who gather information about the state of the network, and
- backward ants who use the collected information to adapt the routing tables of nodes on their path.

The routing tables of each visited node are updated based on trip times. AntNet has been used to simultaneously optimize the *throughput* (delivered bits/sec), *average delay* for data packets (sec), and *network's capacity usage*. However, AntNet has a scalability problem with larger scale networks, because each node has to generate many ants for updating routing tables. In large networks, both overhead and loss of protocol packets grow for distant destinations. Furthermore, ants may carry outdated information for long travel times. Another problem which may arise when implementing AntNet on a real network is the synchronization of the internal clocks of the nodes in the network.

The popularity of MANETs has lead to an increasing need to address MANETs security issues. There are a number of proposals for secure MANETs that are based on artificial immune systems (AISs) [39]. Artificial immune systems (AIS) are algorithms and systems that use the human immune system as inspiration. Sarafijanovic and Boudec [176] presented an AIS security solution that can detect misbehavior in the dynamic source routing (DSR) protocol [107]. Mazhar and Farooq [145] addressed anomaly detection in MANETs using AIS, while Mazhar [144] proposed two security frameworks for securing MANET protocols based on the AIS approach, i.e BeeAIS based on self

non-self discrimination from adaptive immune system and BeeAIS-DC based upon the danger theory [39]

.

2.7 Summary

As a result of the power constraint characteristics of MANETs, it is vital to enhance the longevity of the nodes in the network in order to prolong network lifetime. Low power design as applied to the implementation of all protocols, and in particular (in reference to this thesis), the routing protocols, remains one of the most important research areas in terms of MANETs. This chapter provided a survey of existing algorithms at the network layer that address the energy efficiency of MANETs. The next chapter discusses the ant colony optimisation meta-heuristic approach for solving combinatorial optimisation problems. In late chapters, energy aware optimisation algorithms are developed to based on the ant colony optimisation meta-heuristic.

Chapter 3

Combinatorial Optimisation and Ant Colony Optimisation Meta-Heuristic

This chapter reviews basic definitions of concepts related to optimisation. The ant colony meta-heuristic, viewed in the general context of combinatorial optimisation, is then discussed. This is followed by a detailed description as well as a guide to three major ant colony optimisation algorithms, namely, the ant system, the ant colony system, and the MAX-MIN ant system.

3.1 Introduction

Ant colony optimisation (ACO) [54, 56] refers to a recent meta-heuristic approach for solving difficult combinatorial optimisation problems. ACO was inspired by the pheromone trail laying and following behaviour of real ants which use pheromones as a communication medium. With reference to this biological example, ACO is based on the indirect communication of a colony of simple agents, termed artificial ants, which is mediated by (artificial) pheromone trails. The pheromone trails in ACO algorithms serve as distributed, numerical information which the ants use to construct probabilistic solutions to the problem under investigation and which the ants adapt during the algorithm's execution to reflect their search experience.

The ant system (AS) was the first ACO algorithm [56] developed to solve the travelling salesman problem (TSP) [127]. Despite initial encouraging results, AS was not able to compete with state-of-the-art algorithms for the TSP [57]. Nevertheless, AS did play an important role in stimulating further research on algorithmic variants which did obtain far more improved computational performance [53, 56, 73, 195]. Motivated by

this success, the ACO meta-heuristic was proposed [54, 56] as a common framework for the existing applications and algorithmic variants. Algorithms which follow the ACO meta-heuristic are generically referred to as ACO algorithms for the remainder of this thesis.

The rest of chapter 3 is organised as follows: Section 3.2 provides an overview of computational complexity, Section 3.3 discusses meta-heuristics in general, Section 3.4 gives an overview of the ant colony optimisation meta-heuristic, while Section 3.5 provides a detailed description of three major ant colony optimisation algorithms.

3.2 Computational Complexity

An important criterion for the classification of problems is the time required by algorithms to find a solution to the given problem. This issue is addressed by the theory of computational complexity [154] and, in particular, by the theory of NP-completeness [80]. The subject of computational complexity theory is dedicated to classifying problems in terms of their degree of complexity.

The time-complexity of an algorithm is measured by a time-complexity function that offers, depending on the size of the problem instance, the maximal run-time needed by the algorithm to solve an instance of that problem. The size of a problem instance reflects the volume of data required to encode an instance in a compact form. An intuitive understanding of the size of an instance of the problem often suffices; for example, the size of TSP [127] instance may be measured by the number of cities to be visited. Typically the time-complexity is detailed in terms of the number of elementary operations required to solve the problem, for example, the number of value assignments or comparisons. Time complexity is formalised by the $O(.)$ notation: Let $f : N \rightarrow N$ and $g : N \rightarrow N$ be two functions. Then, $f(n) = O(g(n))$ if there are positive integers c and n_0 such that for all $n > n_0$, $f(n) \leq c.g(n)$.

An algorithm runs in polynomial time if the runtime is bounded by a polynomial. If it is not possible for the runtime to be bounded by a polynomial then the algorithm is said to be an exponential time algorithm. In complexity theory a distinction is made between efficiently solvable problems (easy problems) and inherently intractable problems (difficult problems). Usually, a problem is considered to be efficiently solvable if it is possible to find a solution in a number of steps bounded by a polynomial of the input

size. If the number of steps needed to solve an instance grows super-polynomially then that problem is considered to be inherently intractable.

The theory of NP-completeness distinguishes between two basic classes of problems: the class NP of tractable problems and the NP-complete class of problems. The class NP consists of those problems that may be solved by a nondeterministic polynomial-time algorithm (composed of a guessing stage and a checking stage). The NP-complete class is the class comprising the most difficult problems. If it is possible to solve an NP-complete problem by a polynomial time algorithm, then all problems in NP may be solved in polynomial time.

Many problems of practical and theoretical importance within the fields of artificial intelligence and operations research are of a combinatorial nature [9, 32, 127, 135, 205]. Combinatorial optimisation problems involve finding values for discrete variables such that certain conditions are satisfied. Problems of combinatorial nature may be classified either as optimisation or constraint satisfaction problems. The goal of combinatorial optimisation problems is to find an optimal arrangement, grouping, ordering, or selection of discrete objects.

The TSP [127] is probably the most widely known combinatorial optimisation problem, where the goal is to find a closed tour through a set of cities. Other examples of combinatorial optimisation problems are assignment [32], scheduling [9], and vehicle routing problems [205]. Constraint satisfaction problems (CSP) [135] require a solution to be found that satisfies a given set of constraints. An important special case of the CSP is the well-known satisfiability problem in propositional logic [122]. Other CSP problems are graph coloring [25], temporal and spatial reasoning [5], as well as resource allocation [151].

Combinatorial optimisation problems are often extremely difficult to solve. For example, no algorithm exists for finding the optimal solution to a TSP within polynomial time [153]. Similarly, no algorithm is guaranteed to decide in polynomial time whether a given CSP instance is satisfiable or not. These problems are classified as NP-complete. The class of NP-complete problems has the important distinction that no polynomial time algorithm for any of its members exists to date and, consequently, these problems are considered as inherently intractable from a computational point of view. Thus, in the worst case, any algorithm that endeavours to solve an NP-complete problem will require exponential execution time. In particular, the TSP and the CSP belong to this

class and are thus among the most difficult combinatorial problems.

Algorithmic approaches to combinatorial optimisation problems may be classified as either exact or approximate [96]. Exact algorithms are guaranteed to find an optimal solution in finite time by systematically searching the solution space. However, due to the NP-completeness of many combinatorial optimisation problems, the time needed to solve these problems may grow exponentially in the worst case. As a result of the fact that there are several problems for which exact algorithms display poor performance, several types of approximate algorithms have been developed that provide high quality solutions to combinatorial problems in short computation time [62, 108].

Approximate algorithms may be classified into two main types: construction algorithms and local search algorithms [193]. Construction algorithms generate solutions from scratch by adding solution components step by step. The best known examples are greedy construction heuristics [24]. The main advantage of the greedy heuristics is speed: the algorithms are very quick and return reasonably good solutions. However, these solutions are not guaranteed to be optimal with respect to small local changes and solutions may be further improved by a local search.

Local search algorithms start from some given solution and try to find a better solution within an appropriately defined neighbourhood of the current solution. Should a better solution be found, this solution then replaces the current solution and the local search is continued from this point. The most basic local search algorithm, termed iterative improvement [59], applies these steps repeatedly until it is no longer possible to find a better solution in the neighbourhood of the current solution and stops in a local optimum. A disadvantage of this algorithm is that it may stop at poor quality local minima. In order to avoid these disadvantages, many generally applicable extensions of local search algorithms have been proposed [81, 118, 192, 193]. Local search algorithms may be improved by either accepting worse solutions and, thus, allowing the local search to escape from local optima, or by generating good starting solutions for local search algorithms which guide towards better solutions. In the latter case, the experience gained during the run of the algorithm is often used to guide the search in subsequent iterations.

General-purpose techniques have been designed to allow for a further improvement in solution quality. These methods are termed meta-heuristics [152]. A meta-heuristic is defined as a general heuristic method which is used to guide an underlying construction or local search algorithm towards promising regions of the search space containing high

quality solutions. In other words, a meta-heuristic may be seen as a general algorithmic framework which may be applied to different combinatorial optimisation problems with relatively few modifications if given some underlying, problem specific method. The problem considered in this thesis is a combinatorial optimisation problem.

The next section describes meta-heuristics in more detail.

3.3 Meta-Heuristics

Meta-heuristics are high-level strategies which guide an underlying, more problem specific heuristic, in enhancing the performance of this heuristic. Meta-heuristics are applicable to a wide range of different combinatorial optimisation problems [20]. The main goal is to avoid the disadvantages of iterative improvement and, in particular, multiple descent by allowing the local search to escape from local optima. Many of the meta-heuristic methods may be interpreted as introducing a bias so that high quality solutions are produced quickly. This bias may take various forms and it may be cast as descent bias (based on the objective function), memory bias (based on previous decisions), or experience bias (based on prior performance) [193]. Many of the meta-heuristic approaches rely on probabilistic decisions which were made during the search [193]. However, the main difference in terms of pure random search is that meta-heuristics do not use randomness blindly, but in an intelligent, biased form.

When applied to combinatorial optimisation problems, the main aim of meta-heuristic algorithms is to provide efficient solution techniques in order to yield high quality solutions within a reasonable amount of time.

The next section discusses one of the most popular and efficient meta-heuristics, namely, the ant colony optimisation (ACO) meta-heuristic. The algorithms proposed in this thesis are using an ACO approach.

3.4 Ant Colony Optimisation Meta-Heuristic

Ant colony optimisation (ACO) is a meta-heuristic proposed by Dorigo [51].

The inspiring source of ACO is the foraging behaviour of real ants. The foraging behaviour [45] enables the ants to find shortest paths between food sources and their nests. While walking from food sources to the nest and vice versa, ants deposit a

substance called pheromone on the ground. In this way a pheromone trail is formed. When they decide about a direction to go they choose, in probability, paths marked by strong pheromone concentrations. This basic behaviour is the basis for a cooperation interaction which leads to the emergence of shortest paths.

One of the basic principles of ACO is the use of an algorithmic counterpart of the pheromone trail as a medium for cooperation and communication among a colony of artificial ants. This medium of communication is guided by positive feedback.

Artificial ants posses characteristics of the real ants foraging behaviour. Artificial ants are also enriched with additional capabilities to make them more effective and efficient.

The rest of the section is organised as follows. Subsection 3.4.1 discusses ant algorithms and the foraging behaviour of real ants. Subsection 3.4.2 describes the relation between natural and artificial ants. Subsection 3.4.3 discusses a general framework for the ant colony optimisation meta-heuristic.

3.4.1 Ant Algorithms and Foraging Behaviour of Real Ants

Ant algorithms were first proposed by Dorigo *et al.* [51, 55] as a multi-agent approach to difficult combinatorial optimisation problems, e.g. the travelling salesman problem and the quadratic assignment problem (QAP). There is currently much ongoing research in the scientific community with the aim of extending and applying ant-based algorithms to the many different discrete optimisation problems [21, 38]. Recent applications of ant-based algorithms cover problems such as vehicle routing [27, 205], sequential ordering [66, 75], graph colouring [4], routing in communications networks [98], amongst others.

Ant algorithms were inspired by observations of real ant colonies [45, 141]. Ants are social insects, that is, insects that live in colonies and whose behaviour is directed more to the survival of the colony as a whole than to that of a single individual component of the colony. Social insects have captured the attention of many scientists [54, 58] because of the high structuration level such colonies are capable of, especially when compared to the relative simplicity of the individuals within the colony.

An important and interesting form of behaviour on the parts of ants is their foraging behaviour [56], and, in particular, the way in which ants find the shortest paths between food sources and their nest. Ants are able to detect pheromone and probabilistically choose the next path to follow based on pheromone concentrations. Pheromone trails enable ants to find their way back to the food source (or to the nest). Also, pheromone

trails may be used by other ants to find the location of food sources which have been discovered by other ants. It has been demonstrated experimentally [45] that this pheromone trail following behaviour may give rise to the emergence of shortest paths. In other words, when more paths are available from the nest to a food source, a colony of ants may be able to exploit the pheromone trails left by the individual ants in order to discover the shortest path from the nest to the food source and back again.

In order to study the foraging behaviour of ants under controlled conditions, Deneubourg *et al.* [45] set up the binary bridge experiment. In this laboratory experiment, as illustrated in Figure 3.1, the nest was separated from the food source by a bridge with two equally long branches. Initially, both branches were free of any pheromones. After a finite time period, one of the branches was selected, with most of the ants following the path, despite the fact that both branches were of the same length. This selection of one of the branches is as a result of random fluctuations in path selection which cause higher concentrations on the one path.

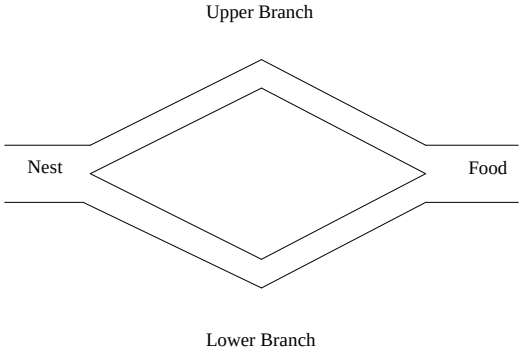

Figure 3.1: Binary bridge experiment

From this experiment, referred to as the binary bridge experiment, a simple, formal model was developed to characterise the path selection process [45, 159]. This probabilistic model makes the assumption that ants deposit the same amount of pheromone. This assumption implies that pheromone evaporation is not taken into account. It is also assumed that the amount of pheromone on a branch is proportional to the number of ants that used the branch in the past. The probability of choosing a branch at a certain time depends on the total amount of pheromone on the branch, which is, in turn, proportional to the number of ants that have used the branch until that time. More precisely, if U_m and L_m respectively denote the numbers of ants that have used the upper

and lower branches after m ants have crossed the bridge, then $U_m + L_m = m$. Pasteels *et al.* [159] found empirically that the probability, $P_U(m)$, with which the $(m+1)$-th ant chooses the upper branch is given as

$$P_U(m) = \frac{(U_m + z)^h}{(U_m + z)^h + (L_m + z)^h} \tag{3.1}$$

where z quantifies the degree of attraction of an unexplored branch, and h is the bias to using pheromone deposits in the decision process. The probability, $P_L(m)$, that an ant chooses the lower branch is $P_L(m) = 1 - P_U(m)$.

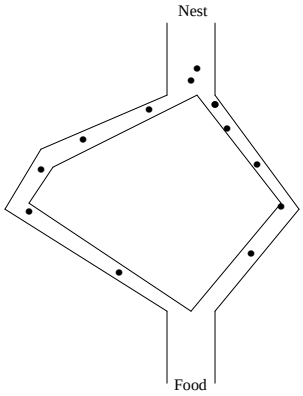

Figure 3.2: Ants start exploring the double bridge

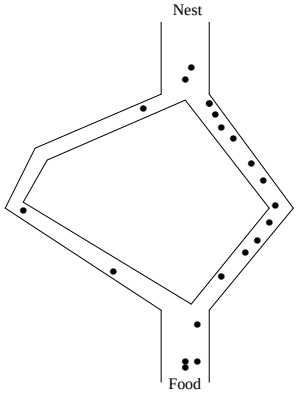

Figure 3.3: Shortest path selection by forager ants

Goss *et al.* [83] extended the binary bridge experiment such that one of the branches of the bridge is longer than the other, as illustrated in Figures 3.2 and 3.3. Dots in these figures indicate ants. Initially, paths are chosen randomly with approximately the same number of ants following both paths. However, over time, more and more ants follow the shorter path, since ants that follow the shortest path return to the nest earlier than those ants on the longer path. The pheromone on the shorter path is, therefore, reinforced sooner than that on the longer path.

The above process represents a form of distributed optimisation mechanism to which each single ant makes a very small contribution. It is interesting to note that, although a single ant is, in principle, capable of constructing a solution (i.e. of finding a path

between the nest and food reservoir), it is only the ensemble of ants, that is the ant colony, which presents the shortest path finding behaviour. In a sense, this behaviour may be viewed as an emergent property of the ant colony. It is also interesting to note that ants are able to perform this specific behaviour using a simple form of indirect communication mediated by pheromone laying which is known as stigmergy [84].

Stigmergetic communication is at work via the pheromone that ants deposit on the ground while walking. Correspondingly, artificial ants simulate pheromone laying by modifying appropriate pheromone variables associated to problem states visited, while building solutions to the optimisation problem under consideration. Also, according to the stigmergetic communication model, artificial ants have local access only to these pheromone variables.

Another important aspect of the foraging behaviour of real ants, that is exploited by artificial ants, is the coupling between the autocatalytic (positive feedback) mechanism [55] and the implicit evaluation of solutions. Implicit solution evaluation is the fact that shorter paths (which correspond to lower cost solutions) will be completed earlier than longer paths and therefore, shorter paths will receive pheromone reinforcement more quickly. Implicit solution evaluation coupled with autocatalysis may be very effective: the shorter the path, the sooner the pheromone is deposited by the ants and the greater the number of ants that use the shorter path. As a result of the stronger attraction of ants via the high pheromone concentrations, autocatalysis causes the shortest paths to be favoured. This may cause premature convergence (stagnation) [51, 56], where ants converge too quickly on the same path. Consequently, ants barely explore, and exploit too much. The result of stagnation is that a suboptimal solution may be found. Pheromone trail evaporation and stochastic (based on random choice) state transitions are used to address these autocatalysis drawbacks. Evaporation causes pheromone concentrations on paths to decrease, thereby increasing the probability of selecting longer paths.

3.4.2 Relation Between Natural and Artificial Ants

The artificial ant is a simple, computational agent that builds feasible solutions to the problem being optimised by exploiting the available pheromone trails and heuristic information [52, 54]. Real and artificial ant colonies share a number of characteristics. The most important of these characteristics are summarised as follows [54]:

- Natural and artificial ants both use a colony of individuals that interact and collaborate in order to solve a given task.
- Natural and artificial ants both modify their "environment" through stigmergic communication based on pheromones. In the case of artificial ants the *(artificial) pheromone trail* consists of numeric information which is only locally available.
- Natural and artificial ants both share a common task, i.e. the search for the shortest path from an origin (the ant nest) to a certain goal state (the food).
- As do real ants, artificial ants build solutions iteratively by applying a local stochastic transition policy in order to move between adjacent states.

However, these characteristics alone do not allow for the development of efficient algorithms for difficult combinatorial problems. Artificial ants live in a discrete world and possess additional capabilities:

- Artificial ants make use of heuristic information in the stochastic transition policy used to select next links in the path being constructed.
- Artificial ants possess a memory that stores the path followed.
- The amount of pheromone deposited by artificial ants is a function of the quality of the solution discovered.
- Pheromone evaporation in ACO algorithms is different to the pheromone evaporation in nature, since the inclusion of an evaporation mechanism is a key question to avoid the algorithm becoming stuck in local optima.

3.4.3 General Framework for Ant Colony Optimisation Meta-Heuristic

Several ACO algorithms exist, which are collectively referred to as ant colony optimisation meta-heuristics. These algorithms model and exploit the behaviour of ants to be applied to solve graph-based, NP-hard, combinatorial optimisation problems.

The main characteristics of ACO are:

1. **Autocatalytic**: The system uses positive feedback as a way of auto-reinforcement. This process is iterative, and soon almost all ants will be choosing the best path.

2. **Distributed computation**: A number of agents are searching for the best solution.

3. **Constructive heuristics**: A "greedy force" which balances the decisions of ants in terms of shorter paths or paths with more pheromone.

The problem to solve with an ACO algorithm is represented by a graph, $G = (V, L)$, where V denotes the set of nodes and L is a matrix which represents the connections between nodes. The graph has $N_G = |V|$ nodes.

ACO algorithms are essentially construction algorithms: For each algorithm iteration, every artificial ant constructs a solution to the problem by travelling on a construction graph. Each link, $(i, j) \in L$, of the graph, which represents a possible step that an ant may make, possesses two kinds of information in order to guide ant movements:

- **Heuristic information** which measures the heuristic preference of moving from node i to node j. This heuristic information is denoted by η_{ij}.

- **Artificial pheromone trail information** which measures the "learned desirability" of the movement and mimics the real pheromone that natural ants deposit. This pheromone information is denoted by τ_{ij}.

The ACO meta-heuristic framework consists of three parts, namely, Ants_generation_and_activity(), EvaporatePheromone(), and DaemonActions() (refer to Algorithm 3).

Ants_generation_and_activity() After initialising each link of the problem graph with a very small amount of pheromone and defining the starting node of each ant, each ant iteratively constructs a solution during each iteration.

The transition rule assigns a probability to each possible link leading from the current node. This probability expresses the desirability of each link and is calculated as a function of pheromone concentrations on the link and heuristic information. While moving, an ant keeps in memory the partial solution it has built in terms of the path the ant was walking on the construction path. As ants construct paths (i.e. solutions to the

optimisation problem), a pheromone update rule is executed to update pheromone concentrations on links. The exact way in which the pheromone update rule is implemented differs based on the specific ACO algorithm used. Depending on the algorithm used, all ants can update pheromone on all links along the traversed path (referred to as the online step-by-step pheromone trail update). Once every ant has generated a solution, the ant can deposit an amount of pheromone which is a function of the quality of the ant's solution (referred to as the global or online delayed pheromone trail update).

EvaporatePheromone() Pheromone evaporation is used to increase exploration of alternative paths, thereby reducing the chance of premature stagnation. For each link, (i, j), pheromone evaporation is implemented using

$$\tau_{ij}(t) = (1 - \rho)\tau_{ij}(t), \quad \forall (i, j) \in L \tag{3.2}$$

where $\rho \in [0, 1]$ specifies the rate at which pheromones evaporate.

DaemonActions() Since not all ACO algorithms make use of daemon actions, the daemon actions are indicated as optional. Daemon actions can be used to implement centralised actions which cannot be performed by single ants. An example daemon action is the use of a local optimisation procedure applied to the solutions built by the ants. Pheromone updates performed by the daemon are called *o*ffline pheromone updates.

A generic ACO meta-heuristic algorithm is summarised in Algorithm 3. The high-level description in Algorithm 3 consists of the above three main components of ACO algorithms, namely, ant generation and activation, pheromone evaporation, and daemon actions gathered in the schedule_activities construct. The schedule_activities construct does not specify how these three activities are scheduled and synchronised. This is up to the algorithm design.

Action *ants_generation_and_activity* creates a new ant and activates that ant. The procedure *new_active_ant* is called for each ant to construct a path from source to destination node. The procedure refers to an ant routing table which is maintained for each ant. Each entry in an ant routing table is a value obtained by a functional composition of the pheromone and heuristic values of the link of the corresponding nodes. The abstract specification of *new_active_ant()* allows for the implementation of any ACO instances.

Algorithm 3 Generic ACO Meta-Heuristic

```
procedure ACO_Meta_Heuristic()
while termination_criterion_not_satisfied do
    begin schedule_activities
      ants_generation_and_activity();
      pheromone_evaporation();
      daemon_actions(); {optional}
    end schedule_activities
end while
end procedure

procedure ants_generation_and_activity()
while available_resources do
    schedule_the_creation_of_a_new_ant();
    new_active_ant();
end while
end procedure

procedure new_active_ant() {ant lifecycle}
initialise_ant();
M= update_private_ant_memory();
i = starting_node;
D = target_node;
T = ∅; {ant solution}
while i ≠ D do
   Build set of neighbours for i; {using M}
   A = read_local_ant_routing_table(); {problem specific heuristic information and pheromone information}
   Assign probability p_ij to each neighbour node j based on A, M, and problem_constraints;
   Select next node j according to transition policy based on p_ij and problem_constraints;
   T = T ∪ j;
   i = j;
   if online_step_by_step_pheromone_update then
      deposit_pheromone_on_the_visited_arc();
      update_ant_routing_table();
   end if
   M= update_private_ant_memory();
end while
if online_delayed_pheromone_update then
   evaluate_solution();
   deposit_pheromone_on_all_visited_arcs();
   update_ant_routing_table();
end if
die(); {when ant finish building a solution and depositing pheromone the ant is deleted from the system}
end procedure
```

3.5 Ant Colony Optimisation Algorithms

The term ACO meta-heuristic (ACO-MH) is used to represent all instances of ACO variants [52, 54]. ACO refers to an algorithm which is a specific instance of the generic algorithm presented in Algorithm 3.

The ACO-MH comprises a wide class of algorithms that may manifest very different implementations. However, the ACO-MH is not sufficiently general to cover the full family of ant algorithms. The fast ant system [198, 199] is an example of an ant algorithm which is not covered by the ACO-MH. The fast ant system is a construction algorithm based on the operation of a single ant without using explicit pheromone evaporation.

The next subsections discuss three different instances of the ACO-MH, namely, the ant system [56], the ant colony system [53], and the MAX-MIN ant system [194]. The algorithms presented in this thesis are adaptations of these three ACO algorithms. The complete algorithm for each of these ACO instances is given. The three algorithms vary in their transition rules and their pheromone trail update rules.

3.5.1 Ant System

The ant system (AS), developed by Dorigo *et al.* [56], was the first algorithm inspired by the behaviour of real ants. Even though AS was developed to solve the travelling salesman problem (TSP) [74], it can be applied to a more general class of combinatorial optimisation problems [27, 67, 75, 140]. The AS deviates from the natural metaphor in that artificial ants possess a degree of memory. Memory is achieved by maintaining a tabu list of already visited cities. This is used to prevent revisiting cities. The tabu list is selected using the ant's private memory, M (refer to the generic ACO meta-heuristic in Algorithm 3).

In AS, at each construction step an ant k chooses to go to the next node with a probability that is computed as:

$$p_{ij}^k(t) = \begin{cases} \frac{(\tau_{ij}(t))^\alpha (\eta_{ij}(t))^\beta}{\sum_{u \in N_i^k(t)} (\tau_{iu}(t))^\alpha (\eta_{iu}(t))^\beta} & \text{if} \quad j \in N_i^k(t) \\ 0 & \text{otherwise} \end{cases} \tag{3.3}$$

where $N_i^k(t)$ is the set of feasible nodes for ant k which is currently located at node i; $N_i^k(t) = V(i) \backslash TL^k(t)$, where $TL^k(t)$ is the tabu list for ant k, storing the ant's partial

tour and $V(i)$ is the set of neighbouring nodes for ant k which is currently located at node i; τ_{ij} represents the *a posteriori effectiveness* of the move from node i to node j, as expressed in the pheromone intensity of the corresponding link, (i, j); η_{ij} represents the *a priori effectiveness* of the move from i to j (i.e. the attractiveness, or desirability of the move) computed using a specific heuristic; α is a positive constant used to amplify the influence of pheromone concentrations; β is an adjustable parameter that controls the relative influence of the attractiveness, $\eta_{ij}(t)$, of node j. The heuristic information, η_{ij}, adds an explicit bias towards the most attractive solutions and is, therefore, a problem dependent function.

The transition probability as given in equation (3.3) balances pheromone intensity, τ_{ij}, and heuristic information, η_{ij}. The best balance between exploration and exploitation is achieved through proper selection of the parameters α and β. Therefore, the transition probability is a trade-off between heuristic (which indicates that close nodes should be chosen with high probability, thus implementing a greedy constructive heuristic) and pheromone trail intensity at time t (which indicates that links with a high traffic load are more desirable than links with a low traffic load, thus implementing the autocatalytic process). The ant's decision table, A_i, for node i (refer to Algorithm 3), is obtained by the composition of the local pheromone trail values with the local heuristic values as in equation (3.3).

Pheromone evaporation is implemented as given in equation (3.2). Once all ants have constructed a solution, pheromones are laid on the links, and the amount of pheromone on the trails is calculated using

$$\tau_{ij}(t+1) \leftarrow \tau_{ij}(t) + \Delta\tau_{ij}(t) \tag{3.4}$$

where $\tau_{ij}(t)$ represents the pheromone concentration associated with link (i, j), and $\Delta_{ij}(t)$ is the total amount of pheromone deposited by all ants on link (i, j), defined as

$$\Delta\tau_{ij}(t) = \sum_{k=1}^{n_k} \Delta\tau_{ij}^{k}(t) \tag{3.5}$$

with

$$\Delta\tau_{ij}^{k}(t) = \begin{cases} \frac{Q}{L^{k}(t)} & \text{if} \quad \text{link } (i,j) \text{ occurs in path described by } TL^{k}(t) \\ 0 & \text{otherwise} \end{cases} \tag{3.6}$$

where Q is a parameter that specifies the amount of pheromones ant k has to distribute throughout its trail, $L^{k}(t)$ is the tour length of ant k or the quality of the complete path constructed by the ant k, and n_k is the number of ants. Ants with a minimum tour length deposit a greater amount of pheromone on the links that form part of their trails, while longer tours receive smaller pheromone deposits.

The AS algorithm is summarised in Algorithm 4.

3.5.2 Ant Colony System Optimisation

This section describes the ant colony system (ACS) – an ACO meta-heuristic introduced by Dorigo and Gambardella [53] in order to improve the performance of AS. ACS differs from AS in four aspects:

1. a different transition rule is used,
2. a different pheromone update rule is defined,
3. local pheromone updates are introduced, and
4. candidate lists are used to provide additional local heuristic information.

Each of these differences is discussed next.

ACS transition rule

The ACS transition rule, also referred to as a *pseudo-random-proportional* action rule [74], was developed explicitly to balance the exploration and the exploitation abilities of the algorithm. Ant k, currently located at node i, selects the next node, j, to move to using the rule,

$$j = \begin{cases} Arg\ Max_{u \in N_i^k(t)}\{\tau_{iu}(t)\eta_{iu}^{\beta}(t)\} & \text{if } r \leq r_0, \\ J & \text{otherwise} \end{cases} \tag{3.7}$$

Algorithm 4 General Procedure of Ant System Algorithm

$t = 0$;
$TL^{best}(t) = \emptyset$; {shortest path}
$L^{best}(t) = 0$; {tour length of the shortest path}
Initialise all parameters, i.e. α, β, ρ, Q, n_k, τ_0;
Place all ants, $k = 1, ..., n_k$;
for each link (i, j) **do**
  $\tau_{ij}(t) = \tau_0$; {Initialise pheromones to the small value τ_0}
  $\eta_{ij}(t) = \frac{1}{d_{ij}}$; { d_{ij} represents the distance between the nodes i and j }
end for
repeat
  for all ant $k = 1, ..., n_k$ **do**
    $TL^k(t) =$ starting_node of ant k;
    $i =$ starting_node of ant k;
    repeat
      From current node i, select next node j with probability as defined in equation (3.3);
      Add j to the ordered list $TL^k(t)$;
      $i = j$;
    until full path has been constructed
    $L^k(t)$=length of the tour described by $TL^k(t)$;
    if $L^k(t) < L^{best}(t)$ **then**
      $TL^{best}(t) = TL^k(t)$;
    end if
  end for
  for each link (i, j) **do**
    Apply evaporation using equation (3.2);
    Calculate $\Delta\tau_{ij}(t)$ using equation (3.5);
    Update pheromone using equation (3.4);
  end for
  for each link (i, j) **do**
    $\tau_{ij}(t + 1) = \tau_{ij}(t)$;
  end for
  $t = t + 1$;
until Stopping condition is true
Return $TL^{best}(t)$;

where r is a real random variable uniformly distributed in the interval $[0, 1]$, r_0 is a tuneable parameter ($0 \leq r_0 \leq 1$), and $J \in N_i^k(t)$ is a node that is randomly selected according to probability,

$$p_{iJ}^k(t) = \frac{\tau_{iJ}(t)\eta_{iJ}^\beta(t)}{\sum_{u \in N_i^k(t)} \tau_{iu}(t)\eta_{iu}^\beta(t)} \tag{3.8}$$

where $N_i^k(t)$ is a set of valid nodes to visit and β is an adjustable parameter that controls the relative influence of the attractiveness, $\eta_{ij}(t)$, of node j. The ACS transition rule uses $\alpha = 1$ and may be omitted. If $\beta = 0$, only pheromone amplification is at work, and this will, in turn, lead to the rapid selection of tours which may prove to be far from optimal. When $r \leq r_0$ exploitation is facilitated. The selection of the next node is then heavily influenced by the distances between nodes and existing pheromone concentrations by choosing the best local compromise between distance and pheromone concentration. When $r > r_0$ exploration is favoured. Greater emphasis may be placed on exploitation instead of exploration by increasing the value of r_0.

Pheromone global update

The ant that performed the best tour is allowed to update the concentrations of pheromone on the corresponding links globally. Gambardella and Dorigo [53] implemented two methods of selecting the best tour (best path), $TL^{bt}(t)$, namely

- **iteration-best** in terms of which $TL^{bt}(t)$ represents the best path found during the current iteration, t, denoted as $TL^{ib}(t)$, and
- **global-best** in terms of which $TL^{bt}(t)$ represents the best path globally which has been found from the beginning of the trial, denoted as $TL^{gb}(t)$.

The pheromone concentration, $\tau_{ij}(t)$, is then modified by an amount, $\Delta\tau_{ij}(t)$, as follows:

$$\Delta\tau_{ij}(t) = \begin{cases} \frac{1}{L^{bt}(t)} & \text{if } (i,j) \in TL^{bt}(t) \\ 0 & \text{otherwise} \end{cases} \tag{3.9}$$

where $L^{bt}(t)$ represents the length of the tour described by $TL^{bt}(t)$.

Only the best tour is reinforced through the global update as follows (including pheromone evaporation),

$$\tau_{ij}(t+1) \leftarrow (1-\rho_g)\tau_{ij}(t) + \rho_g \Delta\tau_{ij}(t) \tag{3.10}$$

where $\rho_g (0 \leq \rho_g \leq 1)$ is a parameter governing global pheromone decay.

The ACS global update rule results in the search being more directed by encouraging ants to search in the vicinity of the best solution found thus far. This strategy favours exploitation and is applied after all ants have constructed a solution.

Local update

When, while performing a tour, ant k is on node i and selects node $j \in N_i^k(t)$ as the next node to hop to, the pheromone concentration of (i, j) is immediately reinforced by a fixed amount τ_0. The pheromone decays simultaneously using

$$\tau_{ij}(t) \leftarrow (1-\rho_l)\tau_{ij}(t) + \rho_l \tau_0 \tag{3.11}$$

where $\rho_l (0 \leq \rho_l \leq 1)$ is a parameter which governs local pheromone decay, and τ_0 is a small positive constant. Experimental results demonstrated that $\tau_0 = 1/(n_G L_{nn})$ provided good results [53]; n_G is the number of nodes in graph G, and L_{nn} is the tour length produced by the nearest neighbour heuristic [172].

Candidate list

A candidate list is a list of preferred nodes to be visited from a given node. When an ant is in node i, instead of examining all the unvisited neighbours of i, the ant chooses the node to move to among those in the candidate list. Only if no candidate list node has unvisited status then other nodes are examined. The candidate list contains $n_c < N_i^k(t)$ nodes ordered by increasing cost, and the list is scanned sequentially and according to the ant tabu list to avoid already visited cities.

ACS is summarised in Algorithm 5.

Algorithm 5 General Procedure of Ant Colony System Algorithm

$t = 0$; Initialise parameters β, ρ_g, ρ_l, r_0, n_k, τ_0;
Place all ants, $k = 1, ..., n_k$;
for each link (i, j) **do**
  $\tau_{ij}(t) = \tau_0$;
  $\eta_{ij}(t) = \frac{1}{d_{ij}}$; { d_{ij} represents the distance between the nodes i and j }
end for
$TL^{gb}(t) = \emptyset$;
$L^{gb}(t) = 0$;
repeat
  for all ants $k = 1, ..., n_k$ **do**
    $TL^k(t) =$ starting_node of ant k;
    $i =$ starting_node of ant k;
    repeat
      From current node i, select next node $j \in N_i^k(t)$ using equations (3.7) and (3.8);
      Add j to the ordered list $TL^k(t)$;
      $i = j$;
      Apply local update using equation (3.11);
    until full path has been constructed;
    $L^k(t)$=length of the tour described by $TL^k(t)$;
  end for
  for $k = 1, ..., n_k$ **do**
    if $L^k(t) < L^{gb}(t)$ **then**
      $TL^{gb}(t) = TL^k(t)$;
      $L^{gb}(t) = L^k(t)$;
    end if
  end for
  for each link $(i, j) \in TL^{gb}(t)$ **do**
    Apply global update using equation (3.10);
  end for
  for each link (i, j) **do**
    $\tau_{ij}(t + 1) = \tau_{ij}(t)$;
  end for
  $TL^{gb}(t + 1) = TL^{gb}(t)$;
  $L^{gb}(t + 1) = L^{gb}(t)$;
  $t = t + 1$;
until Stopping condition is true;
Return $TL^{gb}(t)$ as the solution;

3.5.3 MAX-MIN Ant System

Stützle and Hoos [194] introduced the max-min ant system (MMAS) in order to address the premature stagnation problem of AS. The main difference between MMAS and AS is that pheromone intensities are restricted within given intervals, $\tau_{min} \leq \tau_{ij} \leq \tau_{max}$ for all τ_{ij}, where τ_{min} and τ_{max} are two tunable parameters. By choosing appropriate values for τ_{min} and τ_{max} stagnation is reduced. Additional differences with AS as stated in [194] are:

- After each iteration only the best ant is allowed to deposit pheromones following the ACS model.
- Trails are initialised with the highest possible volume of pheromone τ_{max} to incite high exploration of trails at the commencement of the search process.

In order to limit the stagnation of the search a direct influence on the pheromone limits is exerted by restricting the allowed range of the possible pheromone strength. Pheromone strength is bounded by an upper and lower limit (thus MAX-MIN). A range $[\tau_{min}, \tau_{max}]$ is imposed to all τ_{ij} components. A bound on the upper level is given as [195]

$$\tau_{max}(t) = \left(\frac{1}{1-\rho}\right)\frac{1}{L^{ib}(t)} \tag{3.12}$$

where ρ is the evaporation factor and $L^{ib}(t)$ is the cost of the iteration-best path at iteration t (alternatively the global-best path). The upper level is, therefore, time-dependent. Before the first iteration the pheromone strength on all links is set to a certain high value to ensure that, after the first iteration, the pheromones correspond to τ_{max}. The lower bound may be calculated as [195]

$$\tau_{min}(t) = \frac{\tau_{max}(t)(1 - p_{best}^{1/(n_G-1)})}{(\frac{n_G}{2} - 1)p_{best}^{1/(n_G-1)}} \tag{3.13}$$

where n_G denotes the number of nodes in graph, G, and p_{best} is the probability at which the best solution is constructed. The term, $\frac{n_G}{2} - 1$, represents the average number of nodes from which an ant has to choose.

The transition rule is the same as that of AS while the global update is the same as that of ACS. As a result of the evaporation coefficient, all pheromones are decreased

at the end of each iteration while the pheromones on the links pertaining to the best solution are increased. The pheromone upper bound helps to avoid search stagnation by preventing only one trail from accumulating high values of pheromone. By limiting the amount of pheromone in a given trail, the probability of an ant choosing that particular trail is also limited.

The max-min algorithm is summarised in Algorithm 6. The iteration-best solution is used to update pheromone concentrations.

3.6 Summary

Ant colony optimisation (ACO) has been used for the last decade to design effective algorithms to solve combinatorial optimisation problems.

This chapter provided an overview of the basic principles of combinatorial problems. ACO meta-heuristics for solving combinatorial optimisation problems were discussed, including the most popular ACO algorithms. The ACO algorithms discussed in this chapter are stochastic, population-based search algorithms. Optimal solutions are incrementally constructed by a number of agents working cooperatively by exchanging information obtained about the search space.

The ACO algorithms discussed in this chapter were developed to solve

- static and well defined combinatorial optimisation problems; that is, problems for which all the necessary information is both available and does not change during the optimisation process, and
- single-objective optimisation problems.

In order to apply ACO algorithms to dynamic problems, the algorithms have to be adapted to ensure good exploration abilities during the entire optimisation process. Similarly, ACO algorithms have to be adapted to solve multi-objective optimisation problems (MOPs).

Chapter 4 shows how ACO algorithms can be adapted to solve MOPs, while Chapter 5 explains how ACO algorithms can be adapted to solve dynamic optimisation problems.

Algorithm 6 General Procedure of Max-Min Ant System Algorithm

Initialise parameters α, β, ρ, n_k, p_{best}, τ_{min}, τ_{max};
$t = 0$, $\tau_{max}(0) = \tau_{max}$, $\tau_{min}(0) = \tau_{min}$;
Place all ants, $k = 1, ..., n_k$;
for each link (i, j) **do**
  $\tau_{ij}(t) = \tau_{max}(0)$;
  $\eta_{ij}(t) = \frac{1}{d_{ij}}$; { d_{ij} represents the distance between the nodes i and j }
end for
repeat
  $TL^{ib}(t) = \emptyset$; {$TL^{ib}(t)$ is the iteration-best solution}
  $L^{ib}(t) = 0$;
  for all ant $k = 1, ..., n_k$ **do**
    $TL^k(t) =$ starting_node of ant k;
    $i =$ starting_node of ant k;
    repeat
      From current node i, select next node j with probability as defined in equation (3.3);
      Add j to the ordered list $TL^k(t)$;
      $i = j$;
    until full path has been constructed;
    $L^k(t)$=length of the tour described by $TL^k(t)$;
    if k=1 OR $L^k(t) < L^{ib}(t)$ **then**
      $TL^{ib}(t) = TL^k(t)$;
      $L^{ib}(t)$=length of the tour described by $TL^{ib}(t)$;
    end if
  end for
  for each link $(i, j) \in TL^{ib}(t)$ **do**
    Apply global update using equation (3.10);
  end for
  for each link (i, j) **do**
    Constrict $\tau_{ij}(t)$ to be in $[t_{min}(t), \tau_{max}(t)]$;
  end for
  $TL^{ib}(t + 1) = TL^{ib}(t)$;
  $L^{ib}(t + 1) = L^{ib}(t)$;
  $t = t + 1$;
  Update $\tau_{max}(t)$ using equation (3.12);
  Update $\tau_{min}(t)$ using equation (3.13);
until Stopping condition is true;
Return $TL^{ib}(t)$ as the solution;

Chapter 4

Multi-Objective Optimisation

Ant colony optimisation (ACO) algorithms were originally proposed for single-objective optimisation problems [51, 52, 53, 54, 56, 195]. For many real-world problems it is necessary to optimise more than one conflicting objective (multi-objective optimisation) simultaneously. In this respect, an ACO has to be modified in order for it to be applicable to multi-objective optimisation problems [11, 79, 134].

This chapter provides an overview of the different aspects of multi-objective optimisation. A definition of Pareto-optimality is provided and various multi-objective optimisation algorithm classes are discussed. The adaptation of ACO algorithms for multi-objective optimisation problems is discussed. In addition to the ACO algorithms for multi-objective optimisation, the elitist non-dominated sorting genetic algorithm (NSGA-II) is also described in detail. The NSGA-II is included in this chapter, as it is used to compare the results with those of the ACO algorithms proposed in this thesis. Performance metrics that can be used to compare the performance of multi-objective algorithms are also discussed.

4.1 Introduction

Many real-world problems require the simultaneous optimisation of a number of objective functions. This is referred to as multi-objective optimisation (MOO) [208] and presents a situation in which certain of the required objectives may be in conflict with one another. An example of a multi-objective problem (MOP) is compressor design where the major objectives are the maximisation of overall isentropic efficiency, the maximisation of mass flow rate, the maximisation of total pressure ratio, the minimisation of weight, and the maximisation of durability. Another example of a MOP is routing in data communication networks, where the objectives may include minimisation of routing cost, minimisation of route length, minimisation of congestion, and maximisation of the

utilisation of physical infrastructure. There is an important trade-off between the last two objectives, as minimisation of congestion is achieved by reducing the utilisation of links. A reduction in utilisation, on the other hand, means that infrastructure, for which high installation and maintenance costs are incurred, is under-utilised. Solutions to such problems require a balance between conflicting objectives.

The remainder of this chapter is organised as follows: Section 4.2 provides a theoretical overview of the multi-objective problem (MOP). Section 4.3 discusses the concepts of Pareto-optimal set and Pareto-optimal front. Section 4.4 presents a summary of MOO algorithm classes. Section 4.5 demonstrates the way in which ACO can be adapted to solve multi-objective problems. Section 4.6 discusses evolutionary multi-objective optimisation (EMO) and the NSGA-II algorithm. Section 4.7 discusses performance metrics for comparing the performance of multi-objective algorithms.

4.2 Multi-Objective Optimisation Problem

Let $S \subseteq \mathbb{R}^{n_x}$ denote the n_x-dimensional search space defined by a finite set of decision variables. Let $\mathbf{x} = (x_1, x_2, ..., x_{n_x}) \in S$ refer to a *decision vector*. A single objective function, $f_k(\mathbf{x})$, is defined as $f_k : \mathbb{R}^{n_x} \rightarrow \mathbb{R}$. Let $\mathbf{f}(\mathbf{x}) = (f_1(\mathbf{x}), f_2(\mathbf{x}), ..., f_{n_o}(\mathbf{x})) \in \mathcal{O} \subseteq \mathbb{R}^{n_o}$ be an objective vector containing n_o objective function evaluations; $\mathcal{O}$ is referred to as the *objective space*. The search space, S, is also referred to as the *decision space*. Let $\mathcal{F} \subseteq S$ denote the feasible space which is constrained by n_g-inequality and n_h-equality constraints, i.e.

$$\mathcal{F} = \{\mathbf{x} : g_m(\mathbf{x}) \leq 0,\ h_l(\mathbf{x}) = 0,\ m = 1, ..., n_g;\ l = 1, ..., n_h\} \tag{4.1}$$

where g_m and h_l are the inequality and equality constraints respectively. With no constraints the feasible space is the same as the search space, S.

Using the notation above, a multi-objective optimisation problem is defined as:

$$\begin{aligned} &\text{minimise} && \mathbf{f}(\mathbf{x}) \\ &\text{subject to} && \mathbf{x} \in \mathcal{F} \\ & && \mathbf{x} \in [x_{min},\ x_{max}]^{n_x} \end{aligned} \tag{4.2}$$

Solutions, $\mathbf{x}^*$, to the MOP are in the feasible space, $\mathcal{F} \subseteq S$. In order for $\mathbf{x}^*$ to be in the feasible space, $\mathcal{F}$, both the inequality and equality constraints have to be satisfied. The main issue in MOO is the presence of conflicting objectives, where improvement in one objective may result in deterioration in another objective. Trade-offs do exist between such conflicting objectives, however, and the task is to find solutions which balance these trade-offs. Such a balance may be achieved when a solution is unable to effect an improvement in any of the objectives without degrading one or more of the other objectives. These solutions are referred to as non-dominated solutions of which many may exist.

Therefore, the objective when solving a MOP is to produce a set of acceptable compromises rather than a single solution. This set of solutions is referred to as the non-dominated set or the Pareto-optimal set. The plot of the objective functions whose non-dominated solutions are in the Pareto-optimal set is called the Pareto front.

4.3 Pareto-Optimality

This section presents a number of definitions which pertain to MOO.

Definition 4.3.1. Domination: For two decision vectors, $\mathbf{x}$ and $\mathbf{z}$, $\mathbf{x}$ dominates $\mathbf{z}$, noted $\mathbf{x} \prec \mathbf{z}$, if and only if $\mathbf{x}$ is equally good or better than $\mathbf{z}$ for each of the objectives to optimise, i.e.

$$f_k(\mathbf{x}) \leq f_k(\mathbf{z}),\ \forall k \in \{1, 2, .., n_o\} \wedge \exists k \in \{1, 2, .., n_o\} | f_k(\mathbf{x}) < f_k(\mathbf{z}) \tag{4.3}$$

The concept of dominance is illustrated in Figure 4.1 for a two-objective function, $\mathbf{f}(\mathbf{x}) = (f_1(\mathbf{x}), f_2(\mathbf{x}))$. The shaded area denotes the area of the objective vectors which are dominated by $\mathbf{f}$.

Definition 4.3.2. Weak domination: A decision vector, $\mathbf{x}$, weakly dominates a decision vector, $\mathbf{z}$, noted $\mathbf{x} \preceq \mathbf{z}$, if and only if $\mathbf{x}$ is not worse than $\mathbf{z}$ for each of the objectives to optimise, i.e.

$$f_k(\mathbf{x}) \leq f_k(\mathbf{z}),\ \forall k \in \{1, 2, .., n_o\} \tag{4.4}$$

Definition 4.3.3. Pareto-optimal: A decision vector $\mathbf{x}^* \in \mathcal{F}$ is termed a Pareto-optimal solution for the MOP (refer to equation (4.2)) if there does not exist a decision

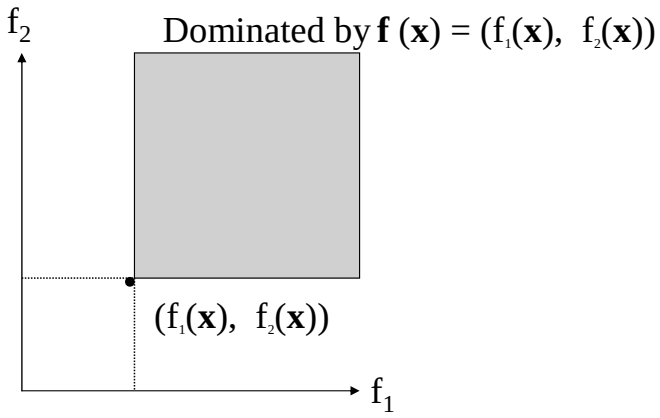

Figure 4.1: The concept of dominance

vector, $\mathbf{x} \neq \mathbf{x}^* \in \mathcal{F}$ that dominates $\mathbf{x}^*$, i.e. $\nexists \mathbf{x} : f_k(\mathbf{x}) < f_k(\mathbf{x}^*)\ \forall k \in \{1, 2, .., n_o\}$. An objective vector $\mathbf{f}^*(\mathbf{x})$ is Pareto-optimal if $\mathbf{x}$ is Pareto-optimal.

In words, a decision vector, $\mathbf{x}^*$, is Pareto optimal if there exists no feasible vector of decision variables $\mathbf{x} \in \mathcal{F}$ which would decrease some criterion without causing a simultaneous increase in at least one other criterion. The presence of multiple objective functions, usually conflicting among them, give rise to a set of optimal solutions called the *Pareto-optimal set*.

Definition 4.3.4. Pareto-optimal set: The set of all Pareto-optimal decision vectors form the Pareto-optimal set, $\mathcal{P}^*$. That is,

$$\mathcal{P}^* = \{\mathbf{x}^* \in \mathcal{F} | \ \nexists \mathbf{x} \in \mathcal{F} : \mathbf{x} \prec \mathbf{x}^*\} \tag{4.5}$$

Therefore, the Pareto-optimal set contains the set of solutions, or balanced trade-offs, for the MOP. The corresponding objective vectors are referred to as the Pareto-optimal front $\mathcal{PF}^*$.

Definition 4.3.5. Pareto-optimal front: Given the objective vector, $\mathbf{f}(\mathbf{x})$, and the Pareto-optimal solution set, $\mathcal{P}^*$, then the Pareto-optimal front, $\mathcal{PF}^*$ is defined as

$$\mathcal{PF}^* = \{\mathbf{f}(\mathbf{x}^*) = (f_1(\mathbf{x}^*), f_2(\mathbf{x}^*), ..., f_{n_o}(\mathbf{x}^*)) | \mathbf{x}^* \in \mathcal{P}^*\} \tag{4.6}$$

An example of a Pareto front is illustrated in Figure 4.2. Figure 4.3 illustrates the assignment of an *objective vector,* $\mathbf{f}$, to the *decision vector,* $\mathbf{x}$.

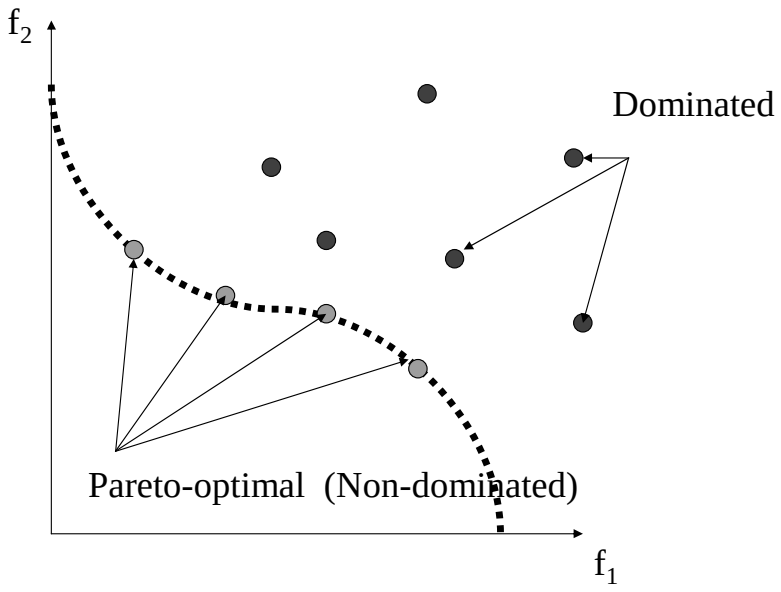

Figure 4.2: Pareto-optimal front for objectives f_1 and f_2

4.4 Multi-Objective Optimisation Algorithm Classes

It may be computationally expensive to generate the Pareto front [224]. Owing to the computational complexity, exact methods to find all non-dominated solutions are not feasible.

For this reason, a number of stochastic search strategies such as particle swarm optimisation (PSO) [60, 63], evolutionary algorithms (EAs) [15], tabu search [81], simulated annealing [118], and ant colony optimisation (ACO) [54, 56] have been developed. These strategies endeavour to find a set of solutions for which the objective vectors are not too far removed from the optimal objective vectors.

MOO involves guiding the search towards the true Pareto front while maintaining a diverse set of non-dominated solutions. The task of MOO is thus reduced to finding an

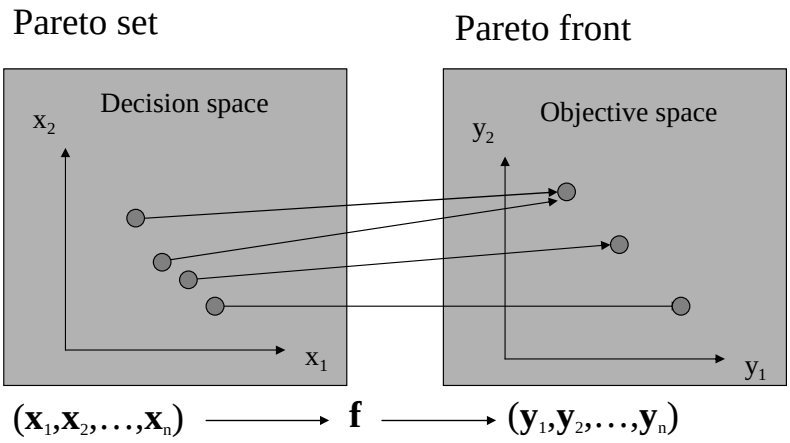

Figure 4.3: Mapping between decision space and objective space

approximation to the true Pareto front such that

- the distance to the true Pareto front is minimised,
- the set of non-dominated solutions, i.e. the Pareto-optimal set, is as diverse as possible, and
- non-dominated solutions which have already been found are maintained.

The first objective is addressed by assigning an appropriate fitness function in order to quantify the quality of a solution in the presence of multiple optimisation criteria. In terms of the second objective, methods are used which preserve the diversity of non-dominated solutions [42, 226]. The third objective which, in essence, addresses both the first two objectives is achieved by using archives of previously found non-dominated solutions [120]. The use of archives is a type of elitist strategy, where the best solutions are maintained in a repository.

Depending on the fitness assignment strategy, classes of MOO algorithms are grouped into:

- **Aggregation-based methods**. The objectives are aggregated into a single parameterised objective function. The parameters of this function are systematically

varied during the optimisation run in order to find a set of non-dominated solutions instead of a single trade-off solution. The aggregation-based method is referred to as the weighted sum method [143]. Another aggregation-based method is the epsilon-constraint method [46, 213], which involves optimising a primary objective and expressing the other objectives in the form of inequality constraints.

Although aggregation methods have been successfully applied to solve MOPs, the following disadvantages of these methods should be noted:

- Aggregation methods can find only one solution with a single application of the algorithm. To find more than one solution repetitive applications of the algorithm are required. However, repetitive applications do not guarantee that distinct Pareto-optimal solutions will be found.
- Optimal values for the weights are problem dependent. Care must be taken when choosing the values of the weights in order to ensure that an acceptable solution is found.

- **Criterion-based methods**. Criterion-based methods [76, 142] switch between the objectives during the optimisation process, i.e. different stages of the optimisation process use different objectives.

- **Dominance-based methods**. One of the most important issues in MOO is that of determining when one solution is better than another with respect to all objectives. To address this issue the notion of dominance is used (refer to Section 4.3).

  Dominance-based MOO algorithms [104, 177], using an archive, provide an efficient way in which to find multiple Pareto-optimal solutions simultaneously in a single simulation run.

The following paragraphs briefly describe MOO algorithms that make use of Pareto dominance to find a set of non-dominated solutions.

Evolutionary algorithms (EA) refers to a class of stochastic optimisation methods that simulate the process of natural evolution [224]. As a result of the population-based nature of EAs, EAs have been widely used in multi-objective optimisation as the population-based nature of EAs allows the generation of several elements of the Pareto-optimal set with a single run [16, 40, 167].

Particle swarm optimisation (PSO) [60, 61] refers to a population based stochastic optimisation technique which was inspired by the social behaviour of bird flocking. PSO algorithms have been adapted to maintain a set of non-dominated solutions using the Pareto dominance [102, 158, 171].

Ant colony optimisation (ACO) algorithms have been adapted to solve MOPs [30, 49, 76, 85, 104, 177]. Most of the ACO algorithms adapt the way that pheromone and heuristic information is used to increase diversity. Diversity is improved by ensuring better exploration by artificial ants.

The rest of the chapter focuses on describing these MOO ACO algorithms, as MOO ACO algorithms are used in this thesis to solve the multi-objective power-aware routing problem.

4.5 Ant Colony Optimisation for Multi-Objective Optimisation

Ant colonies are increasingly used to solve various optimisation problems [51, 52, 53, 54, 56, 195]. Most of these applications of ACO algorithms are for single-objective optimisation. For many real-world problems it is necessary to optimise more than one conflicting objective simultaneously. In this respect, ACO algorithms have been adapted to find a set of acceptable non-dominated solutions that cover, in the best way possible, the various regions of the true Pareto front.

This section describes the different ways in which ACO has been adapted to solve MOPs in general and is organised as follows: Subsection 4.5.1 discusses the different issues with MOACO algorithms, while Subsections 4.5.2 to 4.5.6 respectively discuss the single colony, single-pheromone, single-heuristic matrix methods, the single colony, single-pheromone, multi-heuristic matrix methods, the single colony, multi-pheromone, single-heuristic matrix methods, the single colony, multi-pheromone, multi-heuristic matrix methods, and the multi-colony MOO algorithms.

4.5.1 Introduction

Very few studies have dealt with MOO using multi-objective ACO algorithms (MOACOs). The design of a MOACO algorithm should address the following issues [79, 134]:

- **The management of the pheromone information in MOO.** ACO algorithms for single objective problems represent the pheromone information in terms of a single pheromone matrix (or vector) in which each entry in the matrix corresponds to the desirability of the move from node i to node j. One pheromone matrix represents one objective, because pheromone updates are proportional to some objective function expressing the quality of a solution (trail) or partial solution.

  So, the issue is to change the way in which the pheromone matrix is used to account for multiple objectives. This can be achieved either by keeping a single pheromone matrix [142], where pheromone updates are proportional to a weighted sum of updates, where each update corresponds to an objective, or using multiple pheromone matrices, one for each objective [104].

  The essential difference between single and multi-pheromone matrix methods is that those algorithms that use multiple pheromone matrices are able to keep objective specific history information completely partitioned, whereas those that use a single pheromone matrix must combine this information.

  When a MOACO algorithm uses multiple pheromone information and a one-to-one pheromone to objective mapping is used then ideally the pheromone information contained in a single matrix will reflect which solution components advantage a particular objective.

  The choice of the pheromone model depends on design issues such as how the solution construction process uses pheromone information and how pheromone matrices are updated and decayed.

  The reduction in memory associated with using a single pheromone matrix versus multiple pheromone matrices is also a motivating factor when choosing a pheromone model [10]. To make positive use of the extra memory required by multiple pheromone matrices, pheromone matrices must contain different information by being updated or decayed non-uniformly or by being mapped differently during the pheromone update and solution construction processes.

- **The management of heuristic information in MOO.** Single-objective ACO algorithms use one heuristic information matrix to represent the attractiveness of each edge with reference to a single objective. In a multi-objective optimisation

problem with n_o objectives, n_o different cost factors (heuristic information functions) are defined between each pair of nodes, one for each objective. The heuristic information must then be changed to account for multiple objectives. This can be achieved by using two different strategies. The first strategy is to consider an aggregation of the different objectives into a single heuristic information, where each entry is an aggregated value of the attractiveness of each edge [27, 49, 72]. A second strategy is to consider each different objective separately. In this case separate heuristic information matrices are maintained, one for each objective function [56, 76, 177].

- **Pareto archival.** Single-objective ACO algorithms have all ants converging to a single solution. MOACO has to have the ability to find multiple solutions, which can be achieved using a Pareto archive. Pareto archival is the method by which multiple Pareto optimal solutions are stored for post algorithm run-time analysis or use [30, 104, 148, 161]. A storage repository (called an archive) is used to store the non-dominated solutions that are found.

- **Balancing exploration against exploitation.** The balance between exploration and exploitation is guided by the ants' memory, the pheromone matrices with pheromone information accumulated by all the ants from the beginning of the search process, the problem-specific heuristic information, the pheromone evaporation, and the pheromone update.

  Balancing exploration against exploitation is necessary in order to meet the two MOACO goals:

  - to find a number of solutions that are close to the Pareto front (quality enhancing behaviour), and
  - to maintain a coverage of solutions along the entire Pareto front (diversity preserving behaviour).

  The use of several colonies can serve to achieve a balance between exploration and exploitation. Communication between colonies emphasises exploitation by recruiting colonies to work in the same region of the search space. Less communication has an explorative effect, since each colony is more likely to be searching in a different part of the search space.

- **Pheromone update.** In single objective optimisation problems, the best performing ACO algorithms often use only the best solutions of each iteration (iteration-best strategy) or, since the start of the algorithm (best-so-far strategy), for updating the pheromones. However, in the multi-objective case it is more difficult to determine which are the best solutions to be chosen for the pheromone update.

  Two different ways of implementing the pheromone update are possible: the *selection by dominance* strategy [104, 177] and the *selection by objective* strategy [76]. The selection by dominance strategy allows only the non-dominated solutions to update pheromone concentrations. An iteration-best strategy would consider the non-dominated solutions among those generated in the current iteration; a best-so-far strategy would be obtained by choosing only solutions of an archive of the non-dominated solutions found since the start of the algorithm.

  The selection by objective strategy allows solutions that find the best values for each objective within the current cycle or since the start of the algorithm to update pheromone concentrations.

  If the selection by objective strategy is used and multiple pheromone information is considered, each pheromone matrix associated with each objective will be updated by the solution with the best objective value for the respective objective. Selection by objective has two benefits:

  – As in MMAS and ACS, one solution per pheromone matrix only will be allowed to deposit pheromones, which leads to improved performance compared to the original AS (see Sections 3.5.2 and 3.5.3). As a result the advanced techniques used in the MMAS and ACS algorithms may easily be adapted to multi-objective problems.

  – Each pheromone matrix focuses on one objective only, and thus the aggregation of all the pheromone matrices by means of a weight vector truly regulates the relative importance of each objective.

Recently, different ACO algorithms for multi-objective problems have been developed which address the issues mentioned above. Gravel *et al.* [85] proposed a MOACO based on the AS algorithm using a single heuristic information matrix and a single pheromone matrix. Schaerer and Barán [177] adapted the ACS to use two heuristic matrices and

a single pheromone matrix, while Pinto *et al.* [161] adapted the MMAS to use multiple heuristic matrices and a single pheromone matrix. Cardoso *et al.* [30] and Doerner *et al.* [49] modified the AS and ACS respectively to employ a pheromone matrix for each of the objectives using a single heuristic matrix information. Iredi *et al.* [104] adapted the AS for two objectives by including two pheromone matrices and two heuristic matrices – one for each objective. Mora *et al.* [148] adapted the ACS to use two heuristic matrices and two pheromone matrices.

With respect to the number of colonies used, either one colony can be used [177], or one colony for each objective function [142]. The above algorithms all use only one colony. Gambardella *et al.* [76] and Iredi *et al.* [104] have proposed the use of multiple colonies, where each colony focus on the optimisation of one of the objectives. Using several colonies can serve different goals. The usual aim is to have colonies that specialise to find good solutions in different regions of the Pareto front, but it could also be used to let each colony specialise on a given objective.

MOACO algorithms can be classified according to different criteria. One of them could be whether the algorithm returns a set of non-dominated solutions, i.e. if it looks for a set of Pareto solutions during its run, or it just gives a single solution as output. Another interesting criterion is the way the pheromone information is updated.

For the purpose of this thesis, MOACO algorithms are examined and classified into:

- single colony, single-pheromone matrix, single-heuristic matrix algorithms,
- single colony, single-pheromone matrix, multi-heuristic matrix algorithms,
- single colony, multi-pheromone matrix, single-heuristic matrix algorithms,
- single colony, multi-pheromone matrix, multi-heuristic matrix algorithms, and
- multi-colony algorithms.

The following subsections provide a short overview of these classes of algorithms.

4.5.2 Single Colony, Single-Pheromone, Single-Heuristic Matrix Methods

Gravel *et al.* [85] proposed a MOACO called a multiple objective ACO metaheuristic (MOACOM). MOACOM is based on the AS algorithm and uses a single heuristic

information matrix and a single pheromone matrix. Each value of the heuristic information matrix and each value of the pheromone matrix is the result of the aggregation of information associated with every objective. Considering these two matrices, the AS transition rule is applied to build the ants' solutions.

MOACOM deals with the multiple objectives in a lexicographic order, a priori established by the decision maker. At the end of each iteration, only the first solution according to the lexicographic order considered is taken into account and the pheromone matrix is updated on the basis of the evaluation of the primary objective. Each ant k deposits $\Delta\tau_{ij}^k$ pheromone on each link (i, j) used by the ant as follows:

$$\Delta\tau_{ij}^k = \frac{Q}{f^0(\mathbf{T}_k)} \tag{4.7}$$

where Q is a constant related to the amount of pheromone laid by the ants, f^0 is the primary objective function, and $\mathbf{T}_k$ is the solution built by the ant k.

MOACOM uses elite solution storage, and hence does not maintain populations of non-dominated solutions. As such, MOACOM saves on the computation costs associated with maintaining a non-dominated solution set.

4.5.3 Single Colony, Single-Pheromone, Multi-Heuristic Matrix Methods

Single colony, single-pheromone, multi-heuristic matrix methods use one pheromone matrix and multiple heuristic matrices, one for each of the sub-objectives.

Schaerer and Barán [177] adapted the ACS to use two heuristic matrices. The algorithm, referred to as multi-objective ant colony system (MOACS), changes the ACS transition rule to

$$j = \begin{cases} Arg\ Max_{u \in N_i^k(t)}\{\tau_{iu}(t)(\eta_{iu}^1)^{\beta\lambda_k}(t)(\eta_{iu}^2)^{\beta(1-\lambda_k)}(t)\} & \text{if } r \leq r_0, \\ J & \text{otherwise} \end{cases} \tag{4.8}$$

where β weights the relative importance of the heuristic matrices of the different objectives with respect to the pheromone matrix, λ_k is computed for each ant k as $\lambda_k = \frac{k}{n_k}$, where n_k is the number of ants, and $J \in N_i^k(t)$ is a node that is randomly selected according to probability,

$$p_{iJ}^{k}(t) = \frac{\tau_{iJ}(t)(\eta_{iJ}^{1})^{\beta\lambda_k}(t)(\eta_{iJ}^{2})^{\beta(1-\lambda_k)}(t)}{\sum_{u\in N_i^k(t)} \tau_{iu}(t)(\eta_{iu}^{1})^{\beta\lambda_k}(t)(\eta_{iu}^{2})^{\beta(1-\lambda_k)}(t)} \tag{4.9}$$

The local pheromone update is the same as for the original ACS, with τ_0 initially calculated as follows:

$$\tau_0 = \frac{1}{\bar{f}^1 \bar{f}^2} \tag{4.10}$$

where $\bar{f}^1$ and $\bar{f}^2$ are the average objective values over a set of heuristically obtained solutions (prior the execution of the ant algorithm) for the objective functions, f^1 and f^2, respectively. The value of τ_0 is not fixed during the algorithm run, but undergoes adaptation taking a new value $\tau_0^{'}$. Every time an ant k builds a complete solution, $\mathbf{T}_k$, this solution is compared to the current set of non-dominated solutions, $\mathcal{P}$, to check whether $\mathbf{T}_k$ is a non-dominated solution. If $\mathbf{T}_k$ is a non-dominated solution it is included in $\mathcal{P}$ while the solutions dominated by $\mathbf{T}_k$ are deleted from $\mathcal{P}$. At the end of each iteration, $\tau_0^{'}$ is calculated by applying equation (4.10) with the average values of each objective function taken from the solutions currently included in $\mathcal{P}$. If $\tau_0^{'} > \tau_0$, then $\tau_0 = \tau_0^{'}$, and the pheromone matrices are reinitialised to the new value of τ_0; otherwise, the global update is performed for each solution, $\mathbf{T}_p$, in $\mathcal{P}$ by applying the following rule:

$$\tau_{ij} = (1-\rho)\tau_{ij} + \frac{\rho}{f^1(\mathbf{T}_p)f^2(\mathbf{T}_p)},\ \forall (i,j) \in \mathbf{T}_p \tag{4.11}$$

Instead of relying on multiple pheromone matrices to guide objective specific solution construction, MOACS uses multiple heuristic matrices (one per objective) which are weighted in a specific way for each ant to bias solution construction toward different objective trade-offs. In other words, MOACS achieves diversity across the Pareto front through the use of heuristics rather than pheromones.

Pinto *et al.* [161] presented a multi-objective algorithm based on MMAS referred to as M-MMAS. M-MMAS simultaneously optimises four objectives (f^1, f^2, f^3, f^4), using a single pheromone matrix, τ, and three heuristic matrices (M-MMAS uses the same heuristic matrix for two of the objectives since both objectives are functions of the same heuristic information). The MMAS transition rule is changed to

$$p_{ij}^k(t) = \begin{cases} \frac{\tau_{ij}^\alpha(t)\prod_{l=1}^3(\eta_{ij}^l)^{\beta_l}(t)}{\sum_{h\in N_i^k(t)}\tau_{ih}^\alpha(t)\prod_{l=1}^3(\eta_{ih}^l)^{\beta_l}(t)} & \text{if} \quad j \in N_i^k(t) \\ 0 & \text{otherwise} \end{cases} \tag{4.12}$$

where β_1, β_2, and β_3 determine the relative influence among heuristic information.

The global update is performed for each solution, $\mathbf{T}_p$, of the current set of non-dominated solutions by applying the following rule:

$$\tau_{ij} = (1-\rho)\tau_{ij} + \Delta\tau^p, \quad \forall(i,j) \in \mathbf{T}_p \tag{4.13}$$

where

$$\Delta\tau^p = \frac{1}{f^1(\mathbf{T}_p) + f^2(\mathbf{T}_p) + f^3(\mathbf{T}_p) + f^4(\mathbf{T}_p)} \tag{4.14}$$

The upper limit, τ_{max}, for the pheromone matrix is

$$\tau_{max} = \frac{\Delta\tau^p}{(1-\rho)} \tag{4.15}$$

The lower limit, τ_{min}, for the pheromone matrix is

$$\tau_{min} = \frac{\Delta\tau^p}{2n_k(1-\rho)} \tag{4.16}$$

Other MOACO approaches that use single pheromone and multiple heuristic matrices can be found in [72, 177].

4.5.4 Single Colony, Multi-Pheromone, Single-Heuristic Matrix Methods

This class of MOACO addresses the management of the pheromone information (refer to Section 4.5.1) using one pheromone matrix for each sub-objective. Assuming that n_o sub-objectives need to be optimised, n_o pheromone matrices are used.

Cardoso *et al.* [30] extended the AS to maintain multiple pheromone matrices. The AS transition rule (refer to equation (3.3)) is changed to

$$p_{ij}^k(t) = \frac{\eta_{ij}^\beta(t) \prod_{l=1}^{n_o} (\tau_{ij}^l)^{\alpha_l}(t)}{\sum_{h \in N_i^k(t)} \eta_{ih}^\beta(t) \prod_{l=1}^{n_o} (\tau_{ih}^l)^{\alpha_l}(t)} \tag{4.17}$$

where τ_{ij}^l represents the pheromone information for the l-th objective, η_{ij} is the heuristic information, $N_i^k(t)$ is the feasible neighbourhood of ant k at node i, β determines the relative importance of the heuristic information, and each α_l controls the influence of the corresponding objective.

After each iteration, evaporation is applied separately for the pheromone of each objective as follows:

$$\tau_{ij}^l = (1 - \rho_l)\tau_{ij}^l \tag{4.18}$$

where ρ_l is the pheromone evaporation rate for the l-th objective (a different evaporation rate is considered for each pheromone matrix).

At every iteration and for each objective, each ant k deposits $\Delta\tau_{ij}^l$ pheromone on each link (i, j) used by the ant, where

$$\Delta\tau_{ij}^l = \frac{Q}{f^l(\mathbf{T}_k)} \tag{4.19}$$

and Q is a constant related to the amount of pheromone laid by the ants, and f^l is the l-th objective function. Non-dominated solutions generated in each iteration are stored in an archive.

Similar to Cardoso *et al.*, Doerner *et al.* [49] modified the ACS to employ a pheromone matrix for each of the objectives. The ACS transition rule (refer to equation (3.7)) is changed to

$$j = \begin{cases} Arg\ Max_{u \in N_i^k(t)} \{(\sum_{l=1}^{n_o} w_l \tau_{iu}^l(t))\eta_{iu}^\beta(t)\} & \text{if } r \leq r_0, \\ J & \text{otherwise} \end{cases} \tag{4.20}$$

where w_l is the weight assigned to the pheromone matrix of each objective function, and $J \in N_i^k(t)$ is a node that is randomly selected according to probability,

$$p_{iJ}^k(t) = \frac{(\sum_{l=1}^{n_o} w_l \tau_{iJ}^l(t))\eta_{iJ}^\beta(t)}{\sum_{u \in N_i^k(t)} (\sum_{l=1}^{n_o} w_l \tau_{iu}^l(t))\eta_{iu}^\beta(t)} \tag{4.21}$$

Pheromone update was carried out by using two different ants which had discovered the best and the second-best solution generated in the current iteration for each l-th objective. The global pheromone information is updated for each l-th objective according to equation (3.10), as follows:

$$\tau_{ij}^{l}(t+1) = (1-\rho)\tau_{ij}^{l}(t) + \rho\Delta\tau_{ij}^{l}(t) \tag{4.22}$$

where $\Delta\tau_{ij}^{l}(t)$ has the following values:

$$\Delta\tau_{ij}^{l}(t) = \begin{cases} 15 & \text{if edge } (i,j) \in \text{ best and second-best solutions,} \\ 10 & \text{if edge } (i,j) \in \text{ best solution,} \\ 5 & \text{if edge } (i,j) \in \text{ second-best solution,} \\ 0 & \text{otherwise} \end{cases} \tag{4.23}$$

4.5.5 Single Colony, Multi-Pheromone, Multi-Heuristic Matrix Methods

Iredi *et al.* [104] adapted the AS for two objectives by including two pheromone matrices (τ and $\tau^{'}$) and two heuristic matrices (η and $\eta^{'}$) – one for each objective. The AS transition rule (refer to equation (3.3)) is changed to

$$p_{ij}^{k}(t) = \begin{cases} \dfrac{\tau_{ij}^{\alpha\lambda_k}(t)\tau_{ij}^{'\alpha(1-\lambda_k)}(t)\eta_{ij}^{\beta\lambda_k}(t)\eta_{ij}^{'\beta(1-\lambda_k)}(t)}{\sum_{h\in N_i^k(t)}\tau_{ih}^{\alpha\lambda_k}(t)\tau_{ih}^{'\alpha(1-\lambda_k)}(t)\eta_{ih}^{\beta\lambda_k}(t)\eta_{ih}^{'\beta(1-\lambda_k)}(t)} & \text{if} \quad j \in N_i^k(t) \\ 0 & \text{otherwise} \end{cases} \tag{4.24}$$

where λ_k is different for each ant k, in order to force the ants to search in different regions of the Pareto front; λ_k is calculated as the ratio of the ant index to the total number of ants.

Every ant that generates a solution in the non-dominated front for the current iteration is allowed to update both pheromone matrices, τ and $\tau^{'}$, by depositing an amount equal to $\frac{1}{n_p}$, where n_p is the number of ants that constructed a non-dominated solution. Then, all non-dominated solutions for the current iteration are added to an external archive and this archive is sorted to remove any dominated solutions. At the end of the algorithm execution, the external archive is returned as the final set of solutions.

Mora *et al.* [148] adapted the ACS to use two heuristic matrices and two pheromone matrices. The algorithm referred to as hCHAC changes the ACS transition rule to

$$j = \begin{cases} Arg\ Max_{u \in N_i^k(t)}\{\tau_{iu}^{\alpha\lambda_k}(t)\tau_{iu}^{'\alpha(1-\lambda_k)}(t)\eta_{iu}^{\beta\lambda_k}(t)\eta_{iu}^{'\beta(1-\lambda_k)}(t)\} & \text{if } r \leq r_0, \\ J & \text{otherwise} \end{cases} \tag{4.25}$$

where $J \in N_i^k(t)$ is a node that is randomly selected according to probability,

$$p_{ij}^k(t) = \begin{cases} \frac{\tau_{ij}^{\alpha\lambda_k}(t)\tau_{ij}^{'\alpha(1-\lambda_k)}(t)\eta_{ij}^{\beta\lambda_k}(t)\eta_{ij}^{'\beta(1-\lambda_k)}(t)}{\sum_{h \in N_i^k(t)} \tau_{ih}^{\alpha\lambda_k}(t)\tau_{ih}^{'\alpha(1-\lambda_k)}(t)\eta_{ih}^{\beta\lambda_k}(t)\eta_{ih}^{'\beta(1-\lambda_k)}(t)} & \text{if} \quad j \in N_i^k(t) \\ 0 & \text{otherwise} \end{cases} \tag{4.26}$$

where λ_k is calculated as the ratio of the ant index to the total number of ants.

The local pheromone update is the same as for the original ACS, with different initial values τ_0 and $\tau_0^{'}$ for each objective, initially calculated as follows:

$$\tau_0 = \frac{1}{N_G f^1(\mathbf{T}^{worst})} \tag{4.27}$$

$$\tau_0^{'} = \frac{1}{N_G f^2(\mathbf{T}^{worst})} \tag{4.28}$$

where $\mathbf{T}^{worst}$ is the worst solution heuristically obtained prior to the execution of the ant algorithm and f^1 and f^2 are the objective functions.

Every ant k that generates a solution, T_k, in the non-dominated front for the current iteration is allowed to update both pheromone matrices, τ and $\tau^{'}$, by depositing an amount equal to $\frac{1}{f^1(\mathbf{T}_k)}$ and $\frac{1}{f^2(\mathbf{T}_k)}$ respectively. Then, all non-dominated solutions for the current iteration are added to an external archive and this archive is sorted to remove

any dominated solutions. At the end of the algorithm execution, the external archive is returned as the final solutions.

4.5.6 Multi-Colony MOACO Algorithms

The first implementations of ACO algorithms made use of only one colony of ants to construct solutions. These algorithms have been adapted to use multiple colonies [76, 104, 142, 146]. One of the first applications of multiple colony ACO algorithms was to solve MOP. This section discusses such algorithms.

MOPs are solved by assigning to each colony the responsibility for optimising one of the objectives. Each colony is independent of the other colonies in the sense that it has its own ants and its own pheromone information to the extent that, when an ant from a certain colony constructs the ant's solution, the ant is guided by the pheromone information from the ant's own colony only. After every iteration of the ant algorithm for each colony, the colony computes the new pheromone information.

Three aspects define the behaviour of the multiple colonies:

- The set of weight vectors which are used to aggregate multiple pheromone information.

  The image of the optimal Pareto set in the objective space is a trade-off surface between the different objectives. Over this surface, two solutions can be said to belong to different regions with respect to the differences in the objective vectors of the two solutions, for example, if the distance between their respective objective vectors is more than a given value.

  The use of single pheromone information does not in itself force each colony to focus on a certain region. However, when multiple pheromone information is used, the set of weight vectors that each colony uses in order to aggregate its multiple pheromone information defines in some way a region in the objective space on which the colony focuses the search. Choosing the set of weights forces each colony to approximate a different region of the optimal Pareto set.

  The infinite set of weights defines all the possible directions that can be taken to approximate the optimal Pareto set. Any finite subset Γ of maximally dispersed weight vectors defines a region for the entire optimal Pareto set. A partition of

Γ defines regions in the optimal Pareto set that can be either disjoint or overlapping regions depending on whether disjoint partitions of Γ are considered or not. Then, the multiple colonies can use i) the same partition of Γ, ii) disjoint, or iii) overlapping partitions of Γ.

As for the single colony algorithm, in multi-colony algorithm the ants in a colony use different λ-values. That is, when making decisions ants weight the relative importance of each optimisation objective differently. Given the number of colonies n_c and the number of ants per colony, n_k/n_c, Iredi *et al.* [104] proposed the following possibilities to define each weight value λ_k for each ant k, where $k \in [1, n_k/n_c]$:

- Single region: for all colonies the values of λ_k are in the interval $[0, 1]$, computed as

$$\lambda_k = \frac{k-1}{n_k/n_c - 1} \tag{4.29}$$

  An alternative could be to use different λ_k-values in the colonies so that λ_k-values of the ants in the colonies are in different subintervals of $[0, 1]$. Thus, the colonies weight the optimisation sub-objectives differently.

- Disjoint regions: each colony, c, have distinct λ_k-values, computed as

$$\lambda_k = (c-1)n_k/n_c + k \tag{4.30}$$

- 50% overlapping regions: the interval of values of λ_k for colony c overlaps by 50% with the interval for colony $c-1$ and colony $c+1$. Colony c has ants with

$$\lambda_k \in \left[\frac{c-1}{n_c+1}, \frac{c+1}{n_c+1}\right] \tag{4.31}$$

- The pheromone update strategy.

  In order to enforce specialisation of the colonies, each ant deposits pheromone on one colony only. The pheromone update strategies described for the single colony approach may also be applied to multiple colonies. The selection by dominance method is adapted straightforwardly to the multi-colony approach. That is, the ants belonging to the Pareto set of the candidate set are distributed between colonies and are allowed to deposit pheromone. In selection by objective,

the Pareto set of the candidate set is, somehow, distributed among the colonies. Then, for each colony, the best solution in respect of each objective is allowed to deposit pheromone.

The pheromone update strategy must select the colony from which each solution updates the pheromone information.

Iredi *et al.* [104] presented two different methods to determine in which colony an ant should update the pheromone matrix:

1. Method 1 – Update by origin: an ant only updates the pheromone matrices in its own colony. Using this method other colonies help to detect which of the solutions in the local non-dominated front of a colony might be dominated. The update by origin method enforces both colonies to search in different regions of the non-dominated front.
2. Method 2 – Update by region: the sequence of solutions along the non-dominated front is split into n_c parts of equal size. Ants that have found solutions in the c-th part update in the colony c, $c \in [1, n_c]$. This method may be used with bi-objective problems only, because for more than two objectives, a set of non-dominated objective vectors may just be partially sorted.

- Cooperation between colonies.

  Cooperation is achieved by colonies exchanging solutions so that the pheromone updates of one colony are influenced by solutions from other colonies. Another alternative is to form the candidate set – from which the best solutions have been selected in order to update the pheromone information – with solutions from all colonies.

  If no cooperation takes place between colonies, then a reasonable way for pheromone update in the multi colony algorithm is that only those ants that found a solution which is in the local non-dominated front of the colony, update the colony's pheromone information. Therefore the results are the same as with a multi-start approach where a single colony ant algorithm is run several times and the global non-dominated front at the end is determined from the non-dominated fronts of all runs. This approach significantly increases the processing speed and decreases the number of evaluations for each iteration.

Middendorf *et al.* [146] demonstrated that if a high solution quality is required or the overall performance of the algorithm needs to be increased, information exchange between the colonies is important. Information exchange allows the colonies to profit from the good solutions found by other colonies. Information exchange also allows colonies to search in different regions of the search space by using different pheromone matrices, thus, improving diversity.

To balance exploration against exploitation, the colonies cooperate with a given communication policy specifying the details of what kind of information to exchange, when to exchange it, and among which colonies.

In the remainder of this section multi-colony methods for multi-objective optimisation are described.

Mariano and Morales [142] proposed a multi-colony ACO approach where one colony of ants exists for each objective. Mariano and Morales studied a problem in which every objective was influenced by parts of a solution only, so that an ant from colony c received a (partial) solution from an ant from colony $c-1$ and then tried either to improve or to extend this solution with respect to the c-th sub-objective. A final solution that had passed through all the colonies was allowed to update the pheromone information when it formed part of the non-dominated front.

Gambardella *et al.* [76] adapted the ACS for two objectives by defining two ant colonies each dedicated to the optimisation of a different objective function. Each colony maintains its own pheromone matrix, initialised to have a bias towards an initial solution. A local heuristic is first used to obtain the initial solution TL^{gb}, which is then improved by the two colonies, each with respect to a different objective: TL^{gb} is updated each time one of the colonies computes an improved feasible solution and represents the best path globally that has been found from the beginning of the trial. The colonies cooperate by exchanging TL^{gb} which is used for global pheromone updating. The pheromone global update is performed with TL^{gb} using equation (3.10).

Both previous approaches used a lexicographical order to decide the order of importance of each objective. That is, no two objectives could be assigned the same importance.

Iredi *et al.* [104] proposed an approach for bi-criteria optimisation based on multiple ant colonies without considering a lexicographical order. The ant algorithm for each colony adapted the AS for two objectives by including two pheromone matrices (τ and

$\tau^{'}$) and two heuristic matrices (η and $\eta^{'}$) – one for each objective (refer to Section 4.5.5). Each colony specialised in finding satisfactory non-dominated solutions in different parts of the Pareto front.

In order to achieve collaboration between the colonies, the ants within an iteration place their solutions into a global solution pool that is shared by the other colonies. The pool is used to determine the non-dominated front of all the solutions pertaining to that iteration. Subsequently, only those ants that had found a solution which was in the global, non-dominated front are allowed to update the pheromone information. Cooperation was activated after each iteration at which point all colonies had found a solution.

Iredi *et al.* [104] showed that cooperation between the colonies permits the finding of good solutions along the whole Pareto front. Heterogeneous colonies were used in which the ants have different preferences as regards the sub-objectives when constructing a solution. This choice of heterogeneous colonies has a considerable impact on the performance of the algorithms.

Alaya *et al.* [6] proposed a multi-colony ant algorithm to solve a multi-objective optimisation problem with any number n_o of objectives. The proposed algorithm uses $n_o + 1$ ant colonies and n_o pheromone matrices. Each of the l-th colonies ($l \in [1, ..., n_o]$) aims at optimising the l-th objective function and uses one pheromone matrix, τ^l, and one heuristic information function, η^l, defined with respect to the l-th objective. The $(n_o + 1)$-th colony considers, at each construction step, a randomly chosen objective to optimise. The pheromone matrix, τ^{n_o+1}, considered by the (n_o+1)-th colony is the same as the pheromone matrix of the l-th objective function, where $l \in [1, ..., n_o]$ is randomly chosen. The heuristic information η^{n_o+1} considered by the $(n_o + 1)$-th colony is the sum of heuristic informations associated with all objectives, i.e. $\eta^{n_o+1} = \sum_{l=1}^{n_o} \eta^l$.

The ant algorithm for each colony is based on the MAX-MIN ant algorithm. The pheromone update is as follows: For each of the first n_o colonies, pheromone is laid on the components of the best solution, $\mathbf{T}_l^{ib}$, found by the l-th colony during the current iteration, where the quality of solutions is evaluated with respect to the l-th objective, f^l, only.

The quantity, $\Delta\tau_{ij}^l$, of pheromone deposited on each link (i, j) used by the $\mathbf{T}_l^{ib}$ solution, for the l-th pheromone matrix is defined as follows

$$\Delta\tau_{ij}^{l} = \frac{1}{(1 + f^{l}(\mathbf{T}_{l}^{ib}) - f^{l}(\mathbf{T}_{l}^{gb}))} \tag{4.32}$$

where $\mathbf{T}_{l}^{gb}$ is the global best solution since the beginning of the run considering the l-th objective function.

The (n_o+1)-th colony maintains a set of solutions: a best solution for each objective. The $(n_o + 1)$-th colony lays pheromone on each pheromone structure relative to the correspondent objective using equation (4.32).

4.5.7 Summary

This section examined several approaches in which ACO algorithms have been adapted to solve MOPs. Five different approaches have been discussed, namely, the single colony, single-pheromone, single-heuristic matrix, the single colony, single-pheromone, multi-heuristic matrix, the single colony, multi-pheromone, single-heuristic matrix, the single colony, multi-pheromone, multi-heuristic matrix, and the multi-colony approach.

4.6 Evolutionary Multi-Objective Optimisation

Over the past decade, a number of multi-objective evolutionary algorithms (MOEAs) have been suggested [16, 40, 167, 224]. This section briefly describes evolutionary algorithms (EAs) in Subsection 4.6.1 and the elitist non-dominated sorting genetic algorithm (NSGA-II) in Subsection 4.6.2.

4.6.1 Evolutionary Algorithms

EAs are a class of stochastic optimisation methods that simulate the process of natural evolution [224]. Several classes of EAs have been developed, including genetic algorithms, evolutionary programming, and evolution strategies [16]. All of these approaches maintain a population of candidate solutions. During the optimisation process, these candidate solutions are changed through application of selection and variation operators. While selection mimics competition for reproduction and resources among living beings, variation imitates the natural capability of creating "new" living beings by means of recombination and mutation. Although the underlying mechanisms are simple, EAs

have proved to be a general, robust and powerful search mechanism [16]. In particular, EAs have been successful in solving optimisation problems with multiple conflicting objectives [41] and intractable, large and complex search spaces [223].

In EA terminology, candidate solutions are referred to as individuals or chromosomes. The set of candidate solutions is referred to as a population.

Algorithm 7 General Scheme of an Evolutionary Algorithm

```
Initialise population P with random candidate solutions;
while not terminating condition do
  Evaluate each candidate from P;
  Select parents;
  Recombine pair of parents;
  Mutate the resulting offspring;
  Select individuals for the next generation and insert them into P';
  P ← P';
end while
Return P;
```

A generic EA is summarised in Algorithm 7. An EA consists of the following steps: Firstly, an initial population is created at random, and this constitutes the starting point of the evolution process. A loop consisting of the following steps – evaluation (fitness assignment), selection, recombination, and/or mutation – is then executed a certain number of times. Each loop iteration is termed a generation, and a predefined maximum number of generations often serves as the termination criterion of the loop. However, other conditions, for example stagnation in the population or the existence of an individual with sufficient quality, may also be used to terminate the simulation. In the end the best individuals in the final population represent the outcome of the EA. The different steps of the loop are discussed next:

- Evaluation function (fitness function). The evaluation function is a function or procedure that assigns a quality measure to individuals.
- Parent selection mechanism. The role of parent selection or mating selection is to distinguish between individuals based on their quality, in particular, to allow the better individuals to become parents of the next generation. An individual is a parent if it has been selected to undergo variation in order to create offspring.

- Recombination. A binary variation operator is called recombination or crossover. A recombination operator merges information from two parent individuals into one or two offspring individuals.

- Mutation. A unary variation operator is commonly called mutation. A mutation operator is applied to one individual and delivers a (slightly) modified mutant, its child or offspring. A mutation operator is always stochastic: its output - the child - depends on the outcomes of a series of random choices.

- Survivor selection mechanism. The role of survivor selection or environmental selection is to distinguish among individuals from the offspring based on their quality. The fittest will be allowed in the next generation.

4.6.2 Elitist Non-Dominated Sorting Genetic Algorithm

Since this thesis will compare the performance of MOACO algorithms to the performance of the elitist non-dominated sorting genetic algorithm (NSGA-II) on the multi-objective power aware routing problem, this section provides an overview of NSGA-II.

The NSGA-II [42] is one of the most efficient multi-objective evolutionary algorithms using an elitist approach. The fitness assignment of NSGA-II consists of sorting the population on different fronts using the non-domination order relation. Initially, a random parent population P of size N_p is created. The population is sorted on the basis of non-domination. Each solution is assigned a fitness equal to its non-domination level (1 is the best level). Thus, minimisation of fitness is assumed. Binary tournament selection, recombination, and mutation operators are used to create a child population of size N_p. From the first generation onward, the procedure differs, consisting of the main loop:

The parent and child population are combined into the population R_t. R_t is sorted into non-dominated fronts. A new population P' is generated starting from the first non-dominated front until N_p individuals are found. The **crowded comparison operator** is used for the selection process: Between two solutions with differing non-domination fronts, the solution from the lower non-dominated front (with lower rank) is selected. Otherwise, if both the solutions belong to the same non-dominated front then the solution which is located in a region with the lesser number of solutions is included. From P', the child (offspring) population is generated with the standard bimodal crossover and polynomial operators.

At the end of the execution of the algorithm, the best individuals in terms of non-dominance and diversity are chosen.

The NSGA-II consists of the following different modules:

1. **Finding the non-dominated front.** This module does a quick sorting on the solution space obtained after combining the parent and child population, and extracts the set of non-dominated solutions (non-dominated front).

   Algorithm 8 summarises the steps to find the set of non-dominated solutions from a set of solutions.

Algorithm 8 Procedure to Find the Set of Non-Dominated Solutions (Find-Non-Dominated-Front)

```
Input parameter P; {Population from which to extract the non-dominated front}
P' = ∅;
for all p ∈ P ∧ p ∉ P' do
  P' = P' ∪ {p}; {include p in P' temporarily }
  {compare p with other members of P'}
  for all q ∈ P' ∧ q ≠ p do
    if p ≺ q then
      P' = P' \ {q}; {if p dominates a member q of P', delete q }
    else
      if q ≺ p then
        P' = P' \ {p}; {if p is dominated by other members of P', do not include p
        in P'}
      end if
    end if
  end for
end for
Return P';
```

2. **A fast non-dominated sorting approach.** This module strips out the non-dominated fronts one by one from the solution space and then ranks these non-dominated fronts. The solutions belonging to the first non-dominated front are given a rank of 1, and those belonging to the next non-dominated front a rank of 2, and so on. This way the set of non-dominated fronts is extracted from the population to be sorted.

   Algorithm 9 summarises the steps for finding the set of non-dominated fronts.

Algorithm 9 Procedure to Find the Set of Non-Dominated Fronts (Non-Dominated-Sort)

Input parameter P; {Population for which to find the set of non-dominated fronts}
$\mathcal{Z} = \emptyset$; {$\mathcal{Z}$ is the set of non-dominated fronts}
$c = 1$; {c is the non-dominated front counter and is initialized to one}
while $P \neq \emptyset$ **do**
  $\mathcal{Z}_c$ =Find-non-dominated-front(P); {Find the c-th non-dominated front}
  $P = P \setminus \mathcal{Z}_c$; {remove non-dominated solutions from P};
  $\mathcal{Z} = \mathcal{Z} \cup \mathcal{Z}_c$;
  $c = c + 1$;
end while
Return $\mathcal{Z}$;

3. **Density estimation.** It is very important to keep the solution points well spread out. Therefore, efficient measures are required for controlling the crowding (density) in one region. In order to obtain an estimate of the density of the solutions surrounding a particular solution in the population, the average distance of two points on either side of this point along each of the objectives is calculated. This distance is termed the crowding distance.

   The crowding distance computation requires that the population be sorted according to each objective function value in ascending order of magnitude. Thereafter, for each objective function, the boundary solutions (solutions with the smallest and the largest function values) are assigned an infinite distance value. All other intermediate solutions are assigned a distance value equal to the absolute difference in the function values of two adjacent solutions. This calculation is continued in terms of other objective functions. The overall crowding distance value is calculated as the sum of the individual distance values corresponding to each objective. The following crowding-distance-assignment procedure (Algorithm 10) outlines the crowding distance computation procedure for all solutions in a non-dominated set $\mathcal{I}$.

   After all population members in set $\mathcal{I}$ have been assigned a distance metric then any two solutions are compared for the extent of their proximity to other solutions. A solution with a smaller value of this distance measure is, in some sense, more crowded than other solutions. This is exactly what is compared in the crowded comparison operator which is described below.

Algorithm 10 General Procedure of Crowding-distance-assignment

Input parameter $\mathcal{I}$; {A non-dominated set}
$n_{si} = |\mathcal{I}|$; {number of solutions in $\mathcal{I}$}
for all $i \in 1, ..., n_{si}$ **do**
  $\mathcal{I}[i].distance = 0$; {initialise distance}
end for
{n_o number of objectives}
for all $j \in 1, ..., n_o$ **do**
  $\mathcal{I} = sort(\mathcal{I}, j)$; {sort using each j-th objective value}
  $\mathcal{I}[1].distance = \infty$;
  $\mathcal{I}[n_{si}].distance = \infty$;
  for $i = 2\ To\ n_{si} - 1$ **do**
    $\mathcal{I}[i].distance = \mathcal{I}[i].distance + (\mathcal{I}[i+1].j - \mathcal{I}[i-1].j)$; {$\mathcal{I}[i].j$ refers to the j-th objective value of the i-individual in the set $\mathcal{I}$}
  end for
end for
Return $\mathcal{I}$;

4. **Crowded comparison operator.** The crowded comparison operator $\prec_n$ guides the selection process at the various stages of the algorithm towards a uniformly spread-out Pareto-optimal front. The assumption is made that every individual, $\mathcal{I}_i$, in the population possesses two attributes: 1) non-domination rank $\mathcal{I}_{i_{rank}}$ which is based on the non-domination front, and 2) crowding distance $\mathcal{I}_{i_{distance}}$.

   The crowded comparison operator $\prec_n$ is defined as:

   $$\mathcal{I}_i \prec_n \mathcal{I}_j \text{ if } (\mathcal{I}_{i_{rank}} < \mathcal{I}_{j_{rank}}) \text{ or } ((\mathcal{I}_{i_{rank}} = \mathcal{I}_{j_{rank}}) \text{ and } (\mathcal{I}_{i_{distance}} > \mathcal{I}_{j_{distance}}) \quad (4.33)$$

   In other words, in terms of two solutions with differing non-domination ranks the solution with the lower (better) rank is preferred. Otherwise, if both solutions belong to the same front then the solution which is located in a lesser crowded region is preferred.

Using the above procedures – a fast, non-dominated sorting procedure, a fast, crowded distance estimation procedure and a simple crowded comparison operator – the NSGA-II algorithm is summarised in Algorithm 11.

The NSGA-II is a genetic algorithm with $O(n_o N_p^2)$ computational complexity (where n_o denotes the number of objectives and N_p the population size). As a result of the

low computational requirements of NSGA-II, its elitist approach and its parameterless sharing scheme, the NSGA-II was selected as the algorithm to which the five algorithms presented in this thesis will be compared.

Algorithm 11 General Procedure of NSGA-II

Create a random population P_0;
$\mathcal{Z}$ = non-dominated-sort(P_0);
Use binary tournament selection, recombination, and mutation operators to create a child population Q_0 of size N_p.
$t = 0$;
while $t < N_{maxgen}$ **do**
  $R_t = P_t \cup Q_t$; {combine parent and children population}
  $\mathcal{Z}$ = non-dominated-sort(R_t); {$\mathcal{Z} = (\mathcal{Z}_1, \mathcal{Z}_2, ...)$, all non-dominated fronts of R_t}
  $P_{t+1} = \emptyset$;
  $c = 1$;
  {till the parent population is filled}
  while $|P_{t+1}| + |\mathcal{Z}_c| <= N_p$ **do**
    crowding-distance-assignment($\mathcal{Z}_c$); {calculate crowding distance in $\mathcal{Z}_c$};
    $P_{t+1} = P_{t+1} \cup \mathcal{Z}_c$; {include c-th non-dominated front in the parent population}
    $c = c + 1$; {check the next front for inclusion}
  end while
  Sort($\mathcal{Z}_c, \prec_n$); {sort in descending order using $\prec_n$}
  $P_{t+1} = P_{t+1} \cup \mathcal{Z}_c[1 : (N_p - |P_{t+1}|)]$; {Choose the first $(N_p - |P_{t+1}|)$ elements of $\mathcal{Z}_c$ }
  Q_{t+1} = make-new-pop(P_{t+1}); {Use selection, recombination, and mutation operators to create a child population Q_{t+1}}
  $t = t + 1$; {increment the generation counter}
end while
Return P_t;

4.7 Performance Metrics for Multi-Objective Optimisation

It is not an easy task to compare the performance of multi-objective algorithms [22]. In multi-objective optimisation the performance metric must assess a number of solutions, each having a vector of objective values. Performance metrics are hard to define and more than one metric is necessary to evaluate the performance of multi-objective algorithms.

There are several criteria for quantifying the quality of the approximation to the

Pareto front. This section examines a number of performance criteria for MOO. The rest of the section is organised as follows: Section 4.7.1 provides an overview of the goals of multi-objective optimisation, while Section 4.7.2 discusses the perfomance metrics used in this thesis.

4.7.1 Multi-Objective Optimisation Goals

It is relatively simple to define performance metrics for single objective optimisation. However, MOPs do not have a single global optimum solution, but rather a number of optimum solutions that represent a trade-off between the various sub-objectives. The overall aim in MOO is to produce a set of solutions that represent a good approximation to the trade-off surface. A good approximation set should be as close as possible to the true Pareto front and should also provide a good coverage of the true Pareto front. The goal of achieving a good coverage of the trade-off surface, i.e. to maintain diversity and spread of solutions, is of particular interest in multi-objective optimisation.

It is difficult to define a single measure that can be used to quantify the quality of solutions obtained by a multi-objective algorithm (MOA). Instead, MOA performance is characterised using a number of different aspects [37, 208, 227]. This thesis focuses on two aspects of MOA performance:

- Closeness to the true Pareto front, as the distance between the non-dominated set obtained and the true Pareto front.
- Diversity of solutions in the Pareto front.

4.7.2 Performance Metrics

Several criteria have been developed to assess the quality of a MOO algorithm and to compare such algorithms [95, 120, 188]. Some of the criteria require knowledge of the true Pareto-optimal solutions, which are unknown in the optimisation problem presented in this thesis. Taking this limitation into account, the following three criteria are selected: 1) size of the dominated space, 2) spread metric, and 3) the size of the approximated Pareto front (number of non-dominated solutions). The first metric measures the closeness of the obtained non-dominated set to the true Pareto front. The second metric measures the spread of solutions along the non-dominated set obtained, while the last

metric measures the size of the non-dominated set. These three metrics, do not require knowledge of the true Pareto front.

The above three metrics are described below:

1. **Size of the dominated space or hypervolume measure (S_d)**:

   The size of the dominated space is a measure of how much of the objective space is weakly dominated by a given non-dominated set [17, 126, 218]. Consider the non-dominated set $P = \{\mathbf{p_1}, \mathbf{p_2}, ..., \mathbf{p_l}\}$. The size of the space dominated by the set P, denoted by $S_d(P)$, is defined as the volume of the union of hypercubes $\{C_1, ..., C_l\}$, where C_i is a hybercube whose two opposite vertices are $\mathbf{p_i}$ and the origin of the objective space. Since the optimisation problem in this thesis involves the minimisation of five objectives, a reasonable maximum value for each objective is selected for the origin of the objective space. The values of 100.0, 0.1, 500.0, 0.5, and 30.0, corresponding to a maximum value for each of the objectives EP, TNP, VF, CP, and MNC have been selected as the origin of the objective space. These values lead to a maximum hypervolume of 75000. The hypervolume metric measures how well the algorithms performed in identifying solutions along the full extent of the Pareto front. Higher values of $S_d(P)$ indicate more closeness to the true Pareto front and better performance.

2. **Spacing** (SP) or spread metric [179, 208]: The SP metric is used to measure the spread (distribution) of vectors in the current non-dominated set. Schott [179] proposed an SP metric to measure the range (distance) variance of neighbouring vectors in the non-dominated set. The SP is defined as

$$SP = \sqrt{\frac{1}{n_{\mathcal{PF}}} \sum_{i=1}^{n_{\mathcal{PF}}} (\bar{r} - r_i)^2} \tag{4.34}$$

   where $r_i = \min_{j=1,...,n_{\mathcal{PF}}} \sum_{m=1}^{n_o} |f_m^i - f_m^j|$; f_m is the m-th objective function, $\bar{r}$ is the mean of all r_i, $n_{\mathcal{PF}}$ is the number of non-dominated solutions, and n_o is the number of objectives. The smaller the value of SP, the better the distribution in the current non-dominated set. A value of zero indicates that all members of the current Pareto front are equidistantly spaced.

If an MOP has a $\mathcal{PF}$ which is composed of two or more Pareto curves then the distance between the end-points of two successive curves may skew this metric. Therefore, for this kind of Pareto sets, the distance corresponding to the breaks should be removed from the spacing computation.

It should be noted that the objective values should be normalised before calculating the distance. Various normalisation schemes have been proposed in the literature [103, 121].

3. **Number of non-dominated solutions found (ND)** [119, 208]:

   This performance measure quantifies the size of the approximated Pareto front, that is, the number of non-dominated solutions. The ND metric is defined as

$$ND(\mathcal{PF}) = |\mathcal{PF}| \tag{4.35}$$

   The size of the approximated Pareto front may also be calculated with respect to the solution vectors in the decision space.

   The $\bar{n}_{alg}$ metric measures how well the algorithms performed in identifying solutions along the Pareto front. Larger values for $\bar{n}_{alg}$ are preferred as it indicates that many efficient solutions were found which is preferred by the decision maker. The maximum value for $\bar{n}_{alg}$ is 100 which is the size of the archive.

   Although counting the number of non-dominated solutions does provide an indication of the effectiveness of the MOO algorithm in generating desired solutions, ND does not reflect on the distance of $\mathcal{PF}^*$ from these non-dominated solutions. Also, it is not possible to draw any conclusions about any dominance relation between two approximation sets [228].

The three performance metrics are chosen because they address the main functional goals of MOO algorithms (closeness to the true Pareto front and diversity of solution in the $\mathcal{PF}$). This set of three metrics will enable two or more non-dominated solution sets to be compared among each other in terms of their functional achievements. Also, these three metrics are unary and do not require knowledge of the true Pareto front which is uknown in the power aware optimization problem presented in this thesis.

Moreover, the hypervolume indicator is the only unary quality measure that is known to be strictly monotonic with regard to Pareto dominance: whenever a Pareto set approximation entirely dominates another one, then the indicator value of the former will also be better. This property is of high interest and relevance for the problem examined in this thesis which involves a large number of objective functions. The spacing metric has a low computational overhead, and can be used with more than two objectives. A high number of non-dominated solutions, i.e. the cardinality of a non-dominated set, and therefore more route choices is also desired for power aware dynamic optimization problems where it is difficult to obtain many different non-dominated solutions.

4.8 Summary

The main objective of this chapter was to review multi-objective optimisation theory and algorithms used in this thesis, with specific reference to ACO algorithms and the NSGA-II. Different adaptations of ACO algorithms to solve MOPs have been discussed in detail, and a compact description of the NSGA-II was given. Performance metrics for MOO used in this thesis were discussed.

The next chapter discusses ACO optimisation methods for dynamic environments.

Chapter 5

ACO in Dynamic Optimisation Problems

Ant colony optimisation has proved suitable to solve static optimisation problems, that is problems where the objective does not change with time [52, 54]. However, many real-world problems are defined for dynamic environments, where a previously optimum solution may become sub-optimal and new optima may appear.

Dynamic optimisation problems form a class of difficult optimisation problems. Optimisation algorithms applied to dynamic environments must be able to find and track solutions as the environment changes. In this regard, it should be possible to track both the position and value of optima as changes occur, and it should be possible to detect any new optima that appear and those that disappear. Changes in environments may take various forms, such as changes in the objective functions and/or problem constraints. An acceptable solution at a particular point in time may not be acceptable after a change in the environment has occurred.

The power-aware routing problem considered in this thesis is a dynamic optimisation problem: A realistic mobility model is used within MANET, the position of the nodes changes, and both the optimal decision variables (Pareto set) and the optimal objective values (Pareto front) change repeatedly during the optimisation process.

This chapter is organised as follows: Section 5.1 provides a mathematical definition of dynamic optimisation problems. Section 5.2 discusses how ACO algorithms can be adapted for dynamic optimisation problems. Section 5.3 discusses performance metrics for DOP. Section 5.4 describes dynamic multi-objective optimisation (DMOO), while Section 5.5 discusses performance metrics for dynamic multi-objective optimisation problems (DMOP).

5.1 Definition of Dynamic Optimisation Problems

A single-objective dynamic optimisation problem is formally defined as

Definition 5.1.1. Dynamic optimisation problem:

$$\begin{aligned} \text{minimise} \quad & f(\mathbf{x}, \delta(t)), \quad \mathbf{x} = (x_1, ..., x_{n_x}), \delta(t) = (\delta_1(t), ..., \delta_{n_\delta}(t)) \\ \text{subject to} \quad & g_m(\mathbf{x}, \delta(t)) \leq 0, \quad m = 1, ..., n_g \\ & h_m(\mathbf{x}, \delta(t)) = 0, \quad m = 1, ..., n_h \\ & \mathbf{x} \in \mathbb{R}^{n_x} \end{aligned} \tag{5.1}$$

where $\delta(t)$ is a vector of time-dependent objective function control parameters, n_δ is the number of objective function control parameters, and g_m and h_m denote the inequality and equality constraints respectively. The objective is to find and track

$$\mathbf{x}^*(t) = \min_{\mathbf{x}} f(\mathbf{x}, \delta(t)) \tag{5.2}$$

where the solution $\mathbf{x}^*(t)$ is the optimum found at time step t.

Therefore, the task of a dynamic optimisation algorithm is to locate the optimum and track its trajectory as closely as possible and also to search for new optima that may appear. Algorithms should have the ability to track changes in both the position of $\mathbf{x}^*(t)$ and the value of the optimum, $f(\mathbf{x}^*(t))$.

Dynamic environments can be classified into the following classes of problems [61, 64, 68]:

- the location of the optimum changes,
- the location of the optimum remains the same, but its value changes, and
- both the location and value of the optimum change simultaneously.

The difficulty of a dynamic optimisation problem is determined by the frequency, the severity and the predictability of environment change [23]:

- **The frequency of change** determines how often the environment changes, usually in terms of the number of the iterations between each change. As frequency

of change increases, the time available for adaptation becomes shorter and the optimisation task becomes more difficult.

- **The severity of change** determines the amount of displacement of the current location of the optimum. Large displacements make the problem more difficult.
- **The predictability of change** defines the pattern of the change, which can be linear, random or cyclic.

5.2 ACO Algorithms and Dynamic Environments

ACO was developed for static environments in which ants, as a result of the autocatalytic feedback process, converge on a single solution. This characteristic of ACO metaheuristics limits their application to static environments. In order for ACO algorithms to be applied to DOPs, mechanisms should be employed that maintain diversity. These mechanisms should find a trade-off between the opposing goals of preserving pheromone information and sufficient resetting of pheromone information to allow the ants to continuously explore the search space.

ACO algorithms for dynamic environments can be classified into the following approaches:

- **Re-initialisation methods.** The simplest way to enforce exploration is to restart the ant algorithm after each environment change has occurred. However, a simple restart of the ant algorithm will discard all old information about best paths. As a result, it will take longer to find a solution which may prevent re-convergence to a new optimum under frequent changes.
- **New pheromone update methods.** Changes in the search space render pheromone information inaccurate and inconsistent. Therefore, an alternative approach to restarting the ACO algorithm is to develop new approaches to pheromone updates.

  Under the assumption that the change in the environment is relatively small, it is likely that the new optimum will, in some sense, be related to the old one, and it would probably be beneficial to transfer knowledge in the form of pheromone information from the old optimisation run to the new run. On the other hand, if too much information is transferred and the severity of change is high, the next

iteration of the algorithm after the change has occurred may start near a local optimum, and the algorithm may become detained at this local optimum. Thus, a reasonable compromise between these two opposing approaches has to be found.

The rest of this section focuses on such methods.

5.2.1 Re-initialisation Methods

Gambardella *et al.* [77] proposed a complete re-initialisation of all pheromone concentrations when no improvement in the quality of solutions is observed. All pheromone concentrations, τ_{ij}, are re-initialised to $\tau_0 = \frac{1}{QTL^{best}(t)}$, where Q is a parameter and $TL^{best}(t)$ is the tour length of the best solution found so far. While all pheromones are re-initialised, information about the best solution found so far is retained and used to initialise new pheromones on each link. This technique can be applied in dynamic environments when a change in the environment occurs. This diversification mechanism increases exploration while retaining some knowledge from previous environments. Limiting the amount of stored history to the adapted to change elitist solution assists the algorithm to track the optimal solution.

5.2.2 New Pheromone Updates Methods

Stützle [194] proposed that, when stagnation occurs, pheromone values be increased proportionally to the difference between the pheromone value and the largest pheromone value. The increase of pheromone intensity for all links will increase the selection probability for all links. The same increase in pheromone intensity can be applied in dynamic environments when a change in the environment occurs. The relative difference of the pheromone trails will not be very large and, as a consequence, exploration of new paths is increased.

Guntsch and Middendorf [90] proposed three pheromone update rules (strategies) for dynamic environments, namely, the restart strategy, the η-strategy, and the τ-strategy. The strategies distribute a reset-value, $\gamma_i \in [0, 1]$, to each node i. These reset values are used to reinitialise the pheromone values on all links incident to i, as follows:

$$\tau_{ij}(t+1) = (1-\gamma_i)\tau_{ij} + \gamma_i \frac{1}{n_G - 1} \tag{5.3}$$

where n_G is the number of nodes in the representation graph.

The reset-values for each strategy are calculated as follows:

- **Restart strategy:** This strategy is a global pheromone modification strategy which reinitialises all the pheromone values by the same degree. For each node, i,

$$\gamma_i = \lambda_R \tag{5.4}$$

  where $\lambda_R \in [0, 1]$ is a strategy-specific parameter.

  This strategy acts globally without considering the position of the environment change. Consequently the ant algorithm may need more time to find the optimum. The most extensive resetting of pheromone values should generally be performed in the close vicinity of the changed node. With lower values of λ_R, a trade-off between exploration and exploitation would be achieved. With higher values of λ_R virtually all pheromone information is reset and the ant algorithm needs more time to rediscover a good solution.

- **η-strategy:** The η-strategy uses heuristic-based information to decide to what degree pheromone values are to be equalised on all links incident to a node i. The equalization of the pheromone values to some degree resets the pheromone values and effectively reduces the influence of experience on the decisions an ant makes to build a solution, thus improving diversity. Each node, i, is given a value, γ_i, proportionate to the nearest changed node j (a node which is inserted or deleted), and equalisation is effected on all links incident to node i. The node, i, receives the reset value

$$\gamma_i = \max\{0, d_{ij}^{\eta}\} \tag{5.5}$$

  where

$$d_{ij}^{\eta} = 1 - \frac{\bar{\eta}}{\lambda_E . \eta_{ij}} \tag{5.6}$$

with

$$\bar{\eta} = \frac{1}{n_G * (n_G - 1)} \sum_{i=1}^{n_G} \sum_{\substack{k=1 \\ k \neq i}}^{n_G} \eta_{ik} \tag{5.7}$$

and $\lambda_E \in [0, \infty)$ is a strategy-specific parameter.

- **τ-strategy:** This strategy uses a distance measure based on pheromone information to equalise those links which are closer to the changed node to a greater extent than links that are further from the changed node. The reset value is

$$\gamma_i = \min\{1, \lambda_\tau d_{ij}^\tau\}, \lambda_\tau \in [0, \infty) \tag{5.8}$$

where

$$d_{ij}^\tau = \max_{T(i,j)} \left\{ \prod_{(x,y) \in T(i,j)} \frac{\tau_{xy}}{\tau_{max}} \right\} \tag{5.9}$$

where $T(i, j)$ is the set of all paths from i to j, and τ_{xy} is the pheromone associated with link (x, y).

All three strategies adapt the pheromone information such that exploration is increased, assisting the algorithm in the detection of new optima. Also, there is adequate transfer of knowledge from previous iterations.

Guntsch *et al.* [93] developed a novel ACO algorithm for dynamic environments, where extensive resetting of pheromone values is performed in the vicinity of change (i.e. local pheromone resetting) and an elitist strategy is proposed for use in dynamic environments. This ACO algorithm combines the three strategies discussed above in order to make ant algorithms more suitable for optimisation in dynamic environments.

In a situation where strong local resetting of pheromones in the area of change is necessary, a combination of the global restart strategy with one of the two more locally acting strategies, i.e. with the $\eta-$strategy or $\tau-$strategy, is applied. In the areas where no change occurs, a lower global resetting of the pheromone values is needed to be able

to change the best solution found. This combination can be realised by having each of the two combined strategies distribute reset-values, and then choosing the maximum of the two reset-values for each node.

A standard elitist strategy for ant algorithms is that an elitist ant, which represents the best solution found so far, updates the pheromone values in every generation. However, this best solution may no longer represent a feasible solution after an environment change. Instead of forgetting the old best solution, Guntsch *et al.* [93] adapted the old best solution so that it becomes a reasonably good solution after the environment changes. Two steps are followed in order to adapt the old best solution: i) all nodes that were deleted after the environment change are also deleted from the old best solution, effectively connecting the predecessors and successors of the deleted nodes, and ii) the nodes that were added after the environment change are inserted individually into the old best solution at the place where they cause the minimum increase in cost. The solution derived from this process is the new solution of the elitist ant.

Using a combination of the three strategies and the heuristic for keeping a modified elitist ant, better solutions are found for different strategy parameters than is the case with the pure strategies alone. The authors proved empirically that using the above strategies and resetting the information only in the area of change performed best when problem changes occur frequently. The novel ACO algorithm was applied successfully to a combinatorial dynamic TSP.

Eyckelhof and Snoek [67] modified the AS to apply it to DOPs by introducing global shaking: All pheromone values are squashed into a pre-defined range, while preserving the relative pheromone rankings. That is, if $\tau_{ij}(t) > \tau_{i'j'}(t)$ holds before shaking, it also holds after shaking.

Shaking is implemented as follows

$$\tau_{ij} = \tau_0 \left(1 + \log(\frac{\tau_{ij}}{\tau_0})\right) \tag{5.10}$$

Shaking is done when an environment change has been detected. The shaking procedure changes the ratio between exploitation and exploration and diversifies search when change occurs.

There is a high probability that paths only have to change in the vicinity of the environment change. Therefore, in addition to global shaking, a local shaking operator was developed which operates in the same way as global shaking, but only within a

defined radius around the area of change. Local shaking showed good performance under increased change frequencies. The higher the change frequency, the more important it is to preserve some of the pheromone information in order to exploit the solutions in the vicinity of the environment change. The local shake algorithm, by smoothing the part of the pheromone matrix which is close to the environment change, combines exploitation of the current pheromone matrix and biased exploration within the area of change.

Guntsch and Middendorf [91] proposed P-ACO, an ACS-based algorithm which uses a population of previously best solutions to update the pheromone matrix. In the usual implementations of the ACO, pheromone values are the incremental result of all the updates since the start of algorithm execution. In P-ACO, on the other hand, the pheromone patterns at time t are those precisely induced by the current ant population $P(t)$ and not the result of all past updates. That is, after one ant has completed its solution, the solution is either added or included by replacement into the population set according to both deterministic and stochastic criteria (population update strategies) based on quality, population size, or age.

If a solution T_k enters the population, then the values of the pheromone variables associated with T_k are correspondingly increased according to an AS-like rule using equations (3.4)-(3.6). On the other hand, if a solution T_k leaves the population, then the corresponding pheromone is decreased by the same amount it was increased when T_k entered the population. In this way, the pheromone values precisely reflect the solutions belonging to the current population $P(t)$ at iteration t. In addition to this specific mechanism, P-ACO makes use of the ACS's transition rule using equations (3.7) and (3.8) for component selection; however, it does not make any use of online step-by-step pheromone updates, since pheromone updates are subject to the fact that solutions are either entering or leaving the population.

Guntsch and Middendorf [92] applied the P-ACO algorithm for DOPs. When a change occurs, heuristic repair of the solutions of the population is applied: the solutions maintained in the population are modified after a change, such that they can also become good solutions after the environment change. Since pheromone values depend only on the solutions in the current population, using the solutions in the current population to update pheromone information automatically adapts the pheromone information to reflect the environment change. To maximise search efficacy the P-ACO algorithm only inserts the best solution from each iteration into the population, thereby maintaining a

small population of elite solutions. The purpose of maintaining a population of solutions is to provide the P-ACO algorithm with a quick way to adjust the pheromone mapping if a change occurs. The P-ACO algorithm has been shown to be more efficient than most ACO algorithms for dynamic combinatorial optimisation [92].

Ramos *et al.* [169] developed distributed pheromone laying over the dynamic environment itself in order to track different optima. The authors show that the self-organised algorithm is able to cope with, and to adapt quickly to unforeseen situations.

5.3 Performance Metrics for Dynamic Optimisation Algorithms

It is far more difficult to quantify the performance of an algorithm on dynamic optimisation problems than on static optimisation problems [19]. The difficulty in quantifying performance in dynamic environments stems from the fact that the global optimum changes over time, resulting in multiple solutions. The ability of the algorithm to respond to these changes over time has to be quantified.

Even though techniques exist to detect environment changes, these techniques are infeasible owing to the additional computational complexity. Morrison [149] provides a summary of performance measures for dynamic environments with respect to evolutionary algorithms:

- Accuracy (Acc): At each environment change, the absolute difference between the value of the best solution of the iteration found just before a change has taken place and the value of the true global optimum before the change is calculated. The average of these differences for all environment changes is then calculated as a measure of performance [207], denoted by Acc, and defined as

$$Acc = \frac{1}{n_c} \sum_{i=1}^{n_c} |f(L^{opt}(t^c)) - f(L^{best}(t^c))| \tag{5.11}$$

  where t^c is the iteration just before a change has taken place, n_c is the number of changes of the fitness landscape (environment) during the run, $L^{opt}(t^c)$ is the

optimum solution, $L^{best}(t^c)$ is the best solution found in the environment after iteration t^c (just before the environment change), and f is the fitness function. If n_I is the number of iterations between changes then $t^c = n_I - 1$.

The smaller the measured value for Acc the better the result. In particular, a value of 0 for Acc means that the algorithm found the optimum every time before the landscape was changed (i.e. n_I iterations were sufficient to track the optimum).

This measure requires knowledge of the iteration when the environment changed and the true optimum for each change. In real problems, the position of the true global optimum is not always available, and when the environment changes is also not usually known.

- Adaptability (Ada): At each environment change, the average of the absolute difference between the value of the best solution found for each iteration and the value of the optimum before the change is calculated. The average of these differences for all environment changes (over the entire run) is then calculated as a measure of performance [207], denoted by Ada, and defined as

$$Ada = \frac{1}{n_c} \sum_{i=1}^{n_c} \frac{1}{n_I} \sum_{t=0}^{n_I - 1} |f(L^{opt}(t^c)) - f(L_i^{best}(t))| \tag{5.12}$$

where $L_i^{best}(t)$ is the best solution found in the environment for iteration t for the fitness landscape after the i-th environment change ($i \in [0, n_c - 1]$).

The smaller the measured value for Ada the better the result. A value of 0 for Ada means that the best solution in the population is the same as the optimum for all iterations, i.e. the optimum is never lost by the algorithm.

Similar to the first measure, Ada requires knowledge of the iteration when the environment changed and the true optimum for each change.

Combining the Acc and the Ada measures, the quality of the search process performed by the algorithm can be evaluated. For example, results with low values for Acc and larger values for Ada indicate that the algorithm loses the optimum after a change is made, but the time interval between changes is long enough to recover.

- At each iteration, the average of the Euclidean distance between each solution of the iteration and the global optimum before the change is calculated. The average over these distances for all iterations before a change and for all environment changes is then calculated as a measure of performance [212], denoted by AED, and defined as

$$AED = \frac{1}{n_c} \sum_{i=1}^{n_c} \frac{1}{n_I} \sum_{t=0}^{n_I - 1} \frac{1}{n_{PF}} \sum_{k=1}^{n_{PF}} ||L^{opt}(t) - L_k^i(t)|| \tag{5.13}$$

  where n_{PF} is the number of solutions at iteration t, $L_k^i(t)$ is the k-th solution at iteration t for the fitness landscape after the i-th environment change, and $||L^{opt}(t) - L_k^i(t)||$ denotes the Euclidean distance between the solutions $L^{opt}(t)$ and $L_k^i(t)$.

  The smaller the measured value for AED the better the result. A value of 0 for AED means that the algorithm has found the optimum at each iteration.

  Again, the problem with the AED measure is the fact that the position of the global optimum in the search space is usually not available, except in test problems. Another problem is that the Euclidian distance does not apply to all problem spaces.

- Best-of-generation average (BOGA): This is the average of the best solution for each iteration over several executions of the algorithm on the same problem [88]. $BOGA$ for algorithm A is defined as

$$BOGA_A(t) = \frac{1}{n_r} \sum_{r=1}^{n_r} L_r^{best}(t) \tag{5.14}$$

  where n_r is the number of runs and $L_r^{best}(t)$ is the best solution for iteration t and run r.

  To compare the performance of one algorithm against another, the BOGA metric is calculated for each iteration before a change in the environment occurs (refers to Equation (5.14)).

  Figure 5.1 illustrates the BOGA metric for algorithms A and B. The run of each algorithm consists of 20 iterations and the frequency of change is 5. Therefore,

during each run the function changes every 5 iterations, resulting in 4 changes per run.

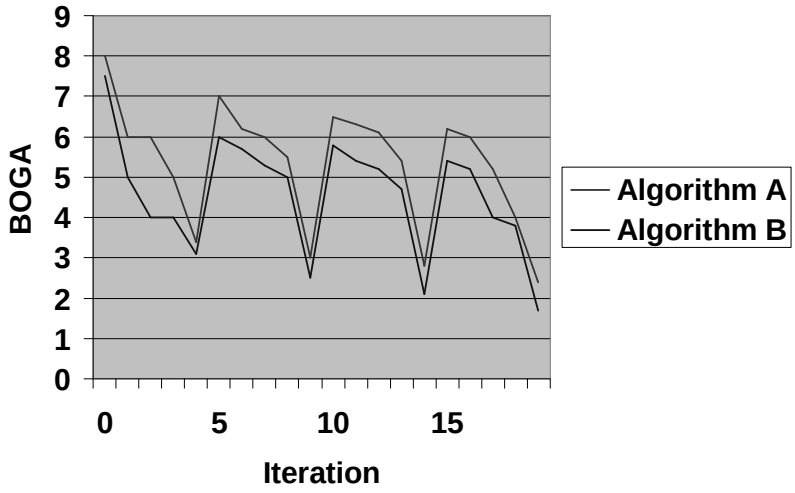

Figure 5.1: Best of generation averages

This method is the most commonly used method to compare the performance of one algorithm against another. However, it does not provide a convenient method for comparing performance across the full range of changes in the environment: Many experiments are required for an accurate measure over all possible changes and using this metric requires the determination of the number of iterations to be used for a representative sample of all the environment changes. In addition, this metric does not provide a convenient method for measuring the statistical significance of the results: it is difficult to determine whether any differences in performance are statistically significant.

- At each iteration, the difference between the value of the best solution of the iteration minus the value of the worst solution within a small window, W, of recent iterations, compared to the value of the best solution within the window minus the value of the worst solution within the window, is calculated as a measure of performance [112], denoted by WA. WA is defined as

$$WA_A(t) = \frac{f(L^{best}(t)) - f(L_W^{worst}(t))}{f(L_W^{best}(t)) - f(L_W^{worst}(t))} \tag{5.15}$$

where $L_W^{best}(t)$ is the best solution within the window $[t-W,...,t]$, and $L_W^{worst}(t)$ is the worst solution within the window $[t-W,...,t]$.

This measure is based on the assumption that the best fitness value will not change much over a small number of iterations, which may not be true. This measure also does not provide a convenient method for comparing performance across the full range of changes in the environment.

Since the position of the global optimum in the search space is not available for the DMOP proposed in this thesis, the $BOGA_A(t)$ measure is used to compare the performance of the developed algorithms.

5.4 Dynamic Multi-objective Optimisation

A dynamic multi-objective optimisation problem (DMOP) is a dynamic optimisation problem (DOP) where at least one of the sub-objectives changes over time.

Solving a DMOP consists of tracking changes in the Pareto-optimal front. New dominated solutions may be found and should be added. It may happen that current solutions in the Pareto-front become dominated after a change and these should be removed.

Very little research has been done on DMOO. Most research in DMOO has been done on EAs [43, 68, 89, 106, 132] and PSO [87].

This section will only discuss a dynamic multi-objective optimisation evolutionary algorithm (DMOEA) proposed by Liu and Wang [132], since this thesis will borrow some of the aspects of this method. Liu and Wang proposed a new DMOEA denoted by DMEA. The DMEA algorithm divides the simulation time of the DMOP into several equal time sub-periods. In each sub-period, the DMOP is approximated by a static multi-objective optimisation problem. As a result, the original DMOP is approximately transformed into several static multi-objective optimisation problems. The comparative study in [132] showed that DMEA is more effective than the compared algorithms with respect to convergence, diversity, and the distribution of the obtained Pareto optimal solutions.

To the author's knowledge no studies exist of the application of ACO algorithms to DMOPs.

5.5 Performance Metrics for Dynamic Multi-Objective Optimisation Problems

Performance measures for DMOPs need to quantify the ability of the algorithm to adapt the Pareto-front under changes in the environment. As indicated in Section 5.3, performance measures for single-objective optimisation problems can be divided into measures that make use of the global optimum and measures independent of the global optimum. In addition, performance measures for MOPs can be divided into measures where the true Pareto front is known and performance metrics where the true Pareto front is unknown (refer to Section 4.7.2).

Since the true Pareto-front is not known for the DMOP proposed in this thesis, the focus of this thesis is on measures that do not require knowledge of the true Pareto-front.

The following performance metrics are used to compare the algorithms of this thesis:

- Number of non-dominated solutions found (ND) [119, 208]

  The number of non-dominated solutions found (refer to Section 4.7.2) is calculated for each iteration before a change to the environment occurs. The average over n_r runs is then calculated for each of these iterations as follows:

$$\overline{ND}^i = \frac{1}{n_r} \sum_{r=1}^{n_r} ND_r^i \tag{5.16}$$

  where ND^i is the number of non-dominated solutions found for iteration i and ND_r^i is the number of non-dominated solutions found for run r at iteration i, which is an iteration before a change occurs in the environment.

  The performance of the algorithm over time is expressed as the average $\overline{ND}^i$ over all iterations, that is,

$$\overline{ND} = \frac{1}{n_c} \sum_{i=1}^{n_c} \overline{ND}^i \tag{5.17}$$

  where n_c is the total number of recorded iterations (or change periods). When comparing the performance of two algorithms, A and B, the total number of times that $\overline{ND}_A^i$ is better than $\overline{ND}_B^i$ is calculated as the performance measure.

The $\overline{ND}$ metric measures how well the algorithms performed in identifying solutions along the Pareto front. Larger values for $\overline{ND}$ are preferred as it indicates that many efficient solutions were found which is preferred by the decision maker. The maximum value for $\overline{ND}$ is 100 which is the size of the archive.

- Size of the dominated space or hypervolume measure (S_d) [17, 218]

  To compare the performance of one algorithm against another, the hypervolume, S_d (refer to Section 4.7.2), is calculated for each iteration before a change to the environment occurs. The average over n_r runs is then calculated for each of these iterations as follows:

$$\overline{S_d}^i = \frac{1}{n_r} \sum_{r=1}^{n_r} S_{d_r}^i \tag{5.18}$$

  where S_d^i is the hypervolume calculated for iteration i and $S_{d_r}^i$ is the hypervolume calculated for run r at iteration i, which is an iteration before a change occurs in the environment.

  The performance of the algorithm over time is expressed as the average $\overline{S_d}^i$ over all iterations, that is,

$$\overline{S_d} = \frac{1}{n_c} \sum_{i=1}^{n_c} \overline{S_d}^i \tag{5.19}$$

  Since the optimisation problem in this thesis involves the minimisation of five objectives, a reasonable maximum value for each objective is selected for the origin of the objective space (refer to Section 4.7.2). The hypervolume metric measures how well the algorithms performed in identifying solutions along the full extent of the Pareto front. Higher values of $\overline{S_d}$ indicate more closeness to the true Pareto front and better performance.

  When comparing the performance of two algorithms, A and B, the total number of times that $\overline{S_{dA}}^i$ is better than $\overline{S_{dB}}^i$ is calculated as the performance measure.

- Spacing (SP) or spread metric [179, 208]

To compare the performance of one algorithm against another, the spacing metric, SP^i (refer to Section 4.7.2), is calculated for each iteration before a change to the environment occurs (refer to Equation (4.34)). The average over n_r runs is then calculated for each of these iterations as follows:

$$\overline{SP}^i = \frac{1}{n_r} \sum_{r=1}^{n_r} SP_r^i \tag{5.20}$$

where SP_r^i is the spacing metric value of run r at iteration i, which is an iteration before a change occurs in the environment.

The performance of the algorithm over time is expressed as the average $\overline{SP}^i$ over all iterations, i.e.

$$\overline{SP} = \frac{1}{n_c} \sum_{i=1}^{n_c} \overline{SP}^i \tag{5.21}$$

The smaller the value of $\overline{SP}$, the better the distribution in the current non-dominated set. A value of zero indicates that all members of the current Pareto front are equidistantly spaced.

When comparing the performance of two algorithms, A and B, the total number of times that $\overline{SP}^i_A$ is better than $\overline{SP}^i_B$ is calculated as the performance measure.

5.6 Summary

This section provided an overview of the main characteristics of dynamic problems and the main goals of an optimisation algorithm for dynamic environments. The use of ant algorithms to handle changes in dynamic environments has been described, and DMOO and performance metrics for DMOO have been discussed.

The following chapter presents the multi-objective optimisation algorithms for power-aware routing metrics.

Chapter 6

Multi-Objective Optimisation Algorithms for Power-Aware Routing Metrics

This chapter formally introduces the multi-objective power-aware routing problem. Five multi-objective ant colony optimisation algorithms are then developed to solve the multi-objective power-aware routing problem.

6.1 Introduction

The mobile ad hoc network routing problem is rendered difficult due to node mobility, time-varying capacity of wireless links, and limited resources. Physically available routes become invalid as a result of topology changes brought about by node movement or link failure (i.e. routes may not be found by the routing algorithm) thus causing packets to be dropped and leading both to throughput degradation and increased control overhead. Control packet overhead (e.g. resource reservation, routing and scheduling) is an expensive operation in mobile ad hoc wireless networks in terms of energy consumption and should be kept to a minimum.

Routing algorithms for mobile networks that attempt to optimise routes while attempting to keep message overhead small have been discussed in Chapter 2. Different routing protocols use one or more of a small set of metrics to determine optimal paths. However, some of these metrics have a negative impact on node and network life by inadvertently overusing the energy resources of a small set of nodes in favour of others (refer to Section 2.5.10).

Conservation of power and careful sharing of the cost of routing packets will ensure that node and network life be increased. The simultaneous optimisation of several power-

aware metrics will result in energy efficient routes and power saving.

This chapter presents new adaptations of the ant colony system (ACS), the max-min ant system (MMAS), and the multiple colony ACO algorithm for solving the MOP power-aware routing problem. This MOP consists of the following five objectives: 1) minimise energy consumed per packet, 2) maximise time to network partition, 3) minimise variance in node power levels, 4) minimise cost per packet, and 5) minimise maximum node cost while taking into consideration a realistic mobility model. This thesis proposes five algorithms for solving this MOP. The first two algorithms, namely, the energy efficiency for mobile networks using multi-objective ant colony optimisation, multi-pheromone (EEMACOMP) algorithm and the energy efficiency for mobile networks using multi-objective ant colony optimisation, multi-heuristic (EEMACOMH) algorithm are adaptations of multi-objective ant colony optimisation algorithms (MOACO) based on the ant colony system (ACS) algorithm. The next two algorithms, namely, the energy efficiency for mobile networks using multi-objective MAX-MIN ant system optimisation, multi-pheromone (EEMMASMP) algorithm and the energy efficiency for mobile network using multi-objective MAX-MIN ant system optimisation, multi-heuristic (EEMMASMH) algorithm solve the above multi-objective problem using an adaptation of the MAX-MIN ant system optimisation algorithm. The last algorithm, namely, the energy efficiency for mobile networks using multi-objective ant colony optimisation, multi-colony (EEMACOMC) algorithm uses a multiple colony ACO algorithm.

One of the objectives of this thesis is to explore different ways of adapting ACO algorithms for the power aware routing problem and to identify which algorithms have a better performance in terms of the optimisation criteria. The management of the pheromone information in MOO is an important factor for the design of a MOACO algorithm. So, the issue is to change the way in which the pheromone matrix is used to account for multiple objectives. This can be achieved either by keeping a single pheromone matrix (EEMACOMH and EEMMASMH), where pheromone updates are proportional to a weighted sum of updates, each update corresponding to an objective, or using multiple pheromone matrices, one for each objective (EEMACOMP and EEMMASMP). EEMACOMC uses multiple colonies, where each colony focuses on the optimisation of one of the objectives. Using several colonies can serve different goals. The usual aim is to have colonies that specialise to find good solutions in different regions of the Pareto front, but it could also be used to let each colony specialise on a given

objective. Finally, EEMACOMP, EEMACOMH and EEMMASMP, EEMMASMH are chosen because they transfer knowledge of the best performing ACO algorithms for single objective optimization, respectively ACS and MMAS, into the multi-objective context for the power aware routing problem.

This chapter is organised as follows. Section 6.2 discusses the suitability of ACO algorithms for the power-aware routing problem. Section 6.3 describes in detail the five metrics for power-aware routing and formulates them mathematically. Section 6.4 formulates the multi-objective optimisation problem. Section 6.5 discusses the mobility model used, namely, the reference point group mobility model. All the changes to the power-aware routing problem formulation resulting from this mobility model are discussed. Section 6.6 presents the five multi-objective ant colony optimisation algorithms proposed in this thesis for simultaneously optimising the five power-aware routing metrics. Section 6.7 describes in detail the elitist non-dominated sorting genetic algorithm for multi-objective power-aware routing (NSGA-II-MPA). The five algorithms proposed will be compared with the NSGA-II-MPA algorithm.

6.2 Suitability of Ant Algorithms for the Power-Aware Routing Problem

The ant algorithms discussed in the previous chapters illustrate the various reasons why it is possible that these types of algorithm could perform well in mobile multi-hop ad hoc networks. Some of these reasons will now be discussed in terms of their relevance to important properties of the power-aware routing problem.

- **Dynamic topology:** The power-aware routing problem is a dynamic optimisation problem because, after applying the mobility model to the MANET, the position of the nodes changes and as a consequence the objective functions change repeatedly. The changes in the environment are responsible for the poor performance of many "classical" routing algorithms in mobile multi-hop ad hoc networks. The ability of ACO algorithms to adapt from the optimum solution for one set of circumstances to the optimal solution to another set of circumstances makes ACO suitable for DOP.

- **Local information:** The power-aware routing problem has certain characteristics, including distributed information, non-stationary stochastic dynamics, and asynchronous evolution of the network status. These characteristics match some of the properties of ACO algorithms, such as the use of local information to generate solutions, indirect communication via the pheromone trails and stochastic state transitions. In contrast to other routing approaches, the ant algorithms use only local information to make stochastic decisions, that is, there is no need to transmit routing tables or other information blocks to other nodes of the network. In addition, ACO algorithms are characterised by the fact that they are multi-agent systems interacting with each other via a form of indirect communication (stigmergy).

- **Link quality:** It is possible to integrate the connection/link quality into the computation of the pheromone concentration, especially into the evaporation process. Link quality is inversely proportional to the cost between nodes and that may easily reflect at the pheromone matrices. Evaporation helps to remove old or poor links from the collective memory of the system. The association of link quality with pheromone information will improve the decision process with respect to the link quality. It is important to note that the link quality approach may be modified so that nodes may also manipulate the pheromone concentration independent of the ants, for example, if a node detects a change in the link quality.

- **Support for multi-path:** Each node has a routing table with entries for all its neighbours. This routing table also contains the pheromone concentration. The decision rule for selecting the next node is based on the pheromone concentration at the current node which is provided for each possible link. Since this decision is stochastic, a set of alternative valid paths can be discovered (multi-path) in order to disperse the data. A multi-path data transfer provides reliable network operations, while considering the energy levels of the nodes.

6.3 Metrics for Power-Aware Routing

This thesis hypothesises that conserving power and carefully sharing the cost of routing packets will ensure that node and network life are increased. This section, therefore,

describes five power-aware metrics that result in energy-efficient routes [186]:

1. **Minimise energy consumed per packet (EP):** This is one of the most obvious metrics that reflects the hypothesis of this thesis in respect of conserving energy. Assume that a certain packet, p, traverses the route $T(s, D)$ which consists of nodes $n_1, ..., n_{n_T}$ where n_1 is the source, s, and n_{n_T} the destination, D. Let E_{ij} denote the energy consumed in transmitting (and receiving) one packet over one hop from node n_i to node n_j and T_p the route which the packet, p, traverses. The energy, $EP(T_p)$, consumed for one packet, p, is denoted by

$$EP(T_p) = \sum_{i=1}^{n_T-1} E_{i(i+1)} \tag{6.1}$$

where n_T is the number of nodes in the route, T_p. The energy, $EP(T)$, consumed for all packets is denoted by

$$EP(T) = \sum_{p=1}^{n_p^T} EP(T_p) \tag{6.2}$$

where n_p^T is the total number of packets from s to D and T is the set of routes T_p, one for each packet p.

Thus, the goal of this metric is to minimise $EP(T)$.

Discussion:

EP facilitates finding the *min-power* path which minimises the overall energy consumption for delivering a packet. Each wireless link is annotated with its transmission energy. The min-power path is that path that minimises the sum of the link costs along the path. In fact, it is interesting to observe that, under light loads, the routes selected when using this metric are identical to the routes selected by shortest-hop routing. This is not a surprising observation because, if the assumption is made that $E_{ij} = E_c, \forall (i, j) \in L$, where E_c is a constant and L is the set of all links, then the power consumed is $(n_T - 1)E_c$. In order to minimise this value n_T needs to be minimised and this is equivalent to finding the shortest-hop path.

In situations where one or more nodes on the shortest-hop path are heavily loaded, the selected route may differ from the route selected by shortest-hop routing. This is as a result of the fact that the amount of energy expended in transmitting one packet over one hop will not be a constant since variable amounts of energy (per hop) may be expended on network contention. Thus, the EP metric will tend to route packets around congested areas (possibly increasing hop-count).

Shortest hop algorithms, while resulting in minimum delay, often result in the early death of some mobile nodes. When mobile nodes are unfairly burdened to support several packet-relaying functions these nodes consume more battery energy and run out of energy earlier than other nodes, thereby creating partitions and disrupting the overall functionality of the ad hoc network. Consider the network illustrated in Figure 6.1 [186]. Here, node 6 will be selected as the route for packets going from 0 to 3, 1 to 4 and 2 to 5, thus providing the shortest hop. As a result, node 6 will expend its battery resources at a faster rate than the other nodes in the network and will be the first node to die. Thus, the EP metric alone does not really meet the goal of increasing node and network life.

2. **Maximise time to network partition (TNP):** The objective of the TNP metric is to divide the load among mobile nodes so that the network will partition in such a way that nodes drain their energy at equal rates. The TNP metric is very important in mission-critical applications such as battle site networks. Optimisation of TNP is very difficult if it has to simultaneously maintain low delay and high throughput. The goal of the TNP metric is to obtain a balanced ad hoc network in order to achieve better performance in terms of execution time and throughput.

   A common approach to balancing network load is to minimise the utilisation of the link with the least capacity:

$$TNP(T_p) = Max_{i,j \in T_p} \left\{ \frac{1}{c^a(i,j)} \right\} \tag{6.3}$$

   with the capacity of link (i, j) defined as

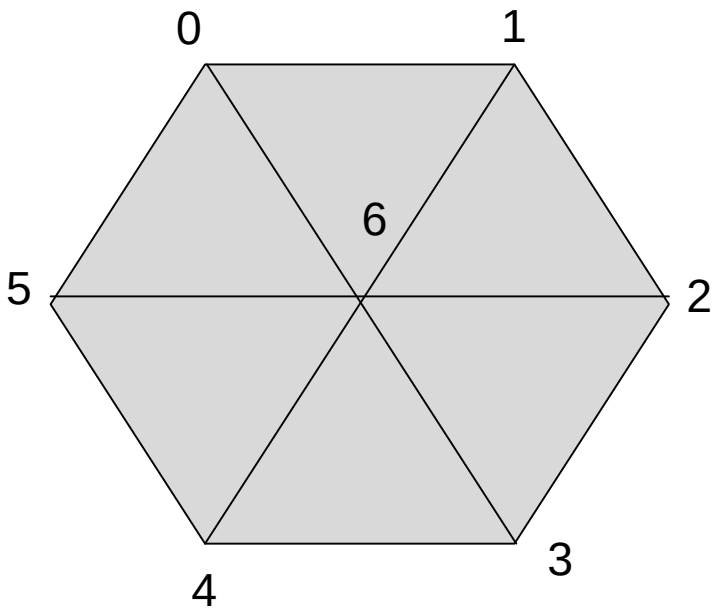

Figure 6.1: A network illustrating the problem with energy per packet as a metric.

$$c^a(i,j) = \frac{e_i^c}{E_{ij}} \tag{6.4}$$

where e_i^c is the current energy of node i, and E_{ij} is the energy expenditure for unit flow transmission over the link (i,j); $c^a(i,j)$ is the capacity of the link (i,j) defined as the number of unit-length messages that may be transmitted along (i,j) before node i runs out of energy.

Discussion: Given a network topology, the maxflow-min-cut theorem [130] may be used to find a minimal set of nodes (i.e. the cut-set nodes) whose removal will cause the network to partition. The routes between these two partitions must pass through one of these cut-set nodes, which are called critical nodes. Therefore, a routing procedure must divide the work among the critical nodes in order to maximise the lifetime of the network. Dividing the work among the critical nodes is similar to the "load balancing" problem, where tasks need to be sent to one of the many servers available so that response time is minimised – this is an NP-complete

problem. If care is not taken that the critical nodes drain their power at an equal rate, there will be delay increases as soon as one of these nodes die as a result of network partition. Achieving equal power drain rate among these nodes requires careful routing, and is similar to the load balancing problem described above. Since nodes in different partitions determine routes independently, it is not possible to achieve the global balance required to maximise the network partition time whilst minimising the average delay. Maximising the network lifetime using the TNP metric is a more fundamental goal of an energy efficient routing algorithm: Given alternative routing paths, TNP selects that path which will result in the longest network operation time.

3. **Minimise variance in node power levels (VNP):** In order to measure quantitatively how well the nodes share the load, the variation factor, VF, is introduced. The VF is defined as the variance of the capacity of the nodes:

$$VF(T_p) = \frac{\sum_{i,j \in T_p} |c^a(i,j) - \mu_T|}{n_T - 1} \tag{6.5}$$

where μ_T is the average capacity for solution T_p, which is computed as

$$\mu_T = \frac{1}{(n_T - 1)} \sum_{i,j \in T_p} c^a(i,j) \tag{6.6}$$

A lower value of VF indicates both a better load distribution and minimum variance in node power and tends to zero for a perfectly balanced load sharing system.

The VNP metric is based on the assumption that all nodes in the network are equally important and that no single node must be penalised more than any other node. The VNP metric ensures that all the nodes in the network remain up and running for as long as possible.

Discussion: A problem with minimising variance in node power levels is similar to "load sharing" in distributed systems, where the objective is to minimise response time while keeping the amount of unfinished work in all nodes the same. This goal may be achieved by using a routing procedure, where each node sends traffic

through the neighbour with the least amount of data waiting to be transmitted, thus avoiding overloading a node.

4. **Minimise cost per packet (CP):** Let $f_i(e_i^e(t))$ denote the node cost or weight of node n_i where $e_i^e(t)$ represents the total energy expended by node n_i thus far.

   The total cost of sending a packet along path $T(s, D) = (s = n_1, n_2, ...D = n_{n_T})$ is defined as the sum of the node costs of all the nodes that lie along that path. The cost CP of sending a packet p from n_1 to n_{n_T} via intermediate nodes $n_2, ..., n_{n_T-1}$ is,

$$CP(T_p) = \sum_{i=1}^{n_T-1} f_i(e_i^e(t)) \tag{6.7}$$

   The goal of the CP metric is to minimise the total cost over all the packets. The paths selected when using the CP metric should be such that those nodes with depleted energy reserves do not lie on many paths. In this way the network partition is extended.

   Discussion: Since f_i represents the reluctance of a node to forward packets, f_i is chosen as [186]

$$f_i(e_i^e(t)) = \frac{1}{E_i - (e_i^e(t))} \tag{6.8}$$

   where E_i is the initial energy of node n_i when the network is deployed.

   Function f_i is the reciprocal of the residual energy of node n_i. Therefore, as the energy of a node decreases, the cost of using that node increases.

   Using equation (6.8), equation (6.7) becomes

$$CP(T_p) = \sum_{i \in T_p} \frac{1}{E_i - (e_i^e(t))} \tag{6.9}$$

   To summarise, the benefits of the CP metric are the following:

- It is possible to incorporate the residual energy characteristics directly into the routing protocol.
- As a side-effect, the CP metric increases the time to network partition and reduces variation in node costs.
- The effects of network congestion are incorporated (as an increase in node cost due to contention).

5. **Minimise maximum node cost (MNC):** The node cost, $C_{n_i}(t)$, is defined as the ratio of the total energy consumed up to time, t, to the initial energy, E_i [65]:

$$C_{n_i}(t) = \frac{E_i - e_i^c(t)}{E_i} \tag{6.10}$$

The MNC metric is then defined as

$$MNC(T_p) = \max_{i \in T_p} C_{n_i}(t), \forall t > 0 \tag{6.11}$$

The objective of this metric is to minimise MNC. Minimising the cost per node significantly reduces the maximum node cost. MNC delays node failure and reduces variance in remaining battery lives because links with high energy cost are avoided.

Since future network lifetime is difficult to estimate, the last three metrics have been included in order to increase network lifetime indirectly. Variance of residual battery energy of mobile nodes is a simple indication of energy balance and may be used to extend network lifetime. The cost-per-packet metric is similar to the energy-per-packet metric but cost-per-packet includes the residual energy life of each node in addition to the transmission energy. The corresponding energy-aware routing protocol prefers wireless links which require low transmission energy, but, at the same time, avoids nodes with low residual energy with high node cost. The outcome of the MNC metric is that each candidate path is annotated with the maximum node cost among the intermediate nodes (equivalently, the minimal residual battery life), and the path with the minimum path cost, is selected. Maximum node cost is also referred to as the max-min path in online max-min (OMM) protocol [165] because this protocol uses the residual battery life of nodes rather than their node cost. It is clear from the above that, in order to maximise network lifetime, it is necessary to achieve a measure of balance between the

energy consumed by a route and the minimum residual energy at the nodes along the chosen route.

The five metrics discussed in this section express, in different ways, the hypothesis of this thesis about conserving energy in the network by selecting routes carefully.

The next section formulates the power-aware routing problem.

6.4 Multi-Objective Optimisation Problem for Power-Aware Routing Metrics Using a Mobility Model

Based on the five metrics defined in Section 6.3, this section defines the dynamic MOP for power-aware routing. The problem is formulated in Section 6.4.1, while Section 6.4.2 discusses the heuristic information used to solve the dynamic MOP.

6.4.1 Problem Formulation

For this thesis, a network is modelled as a directed graph, $G = (V, L)$, where V represents the set of nodes and L is the set of links. The definitions in appendix C are used for the formulation of the power-aware routing problem.

The power-aware routing problem is defined as a dynamic MOP, with the objective to find a path, $T(s, D) = \{s = n_1, n_2, ..., D = n_{n_T}\}$, such that the energy consumed per packet, $EP(T_p)$, utilisation of the most heavily used link, $TNP(T_p)$, variance in node power levels, $VF(T_p)$, cost per packet, $CP(T_p)$, and maximum node cost, $MNC(T_p)$, are minimised (refer to equations (6.1), (6.3), (6.5), (6.9) and (6.11)). More formally, the problem is defined as

$$\text{minimise } \mathbf{f}(T_p) = (EP(T_p),\ TNP(T_p),\ VF(T_p),\ CP(T_p),\ MNC(T_p)) \tag{6.12}$$

An example of a networking routing problem is discussed in the remainder of this section in order to illustrate the multi-objective power-aware problem stated above: Given the network topology of a directed graph G as illustrated in Figure 6.2, the number associated with each link (i, j) denotes the energy, E_{ij}, consumed in transmitting one

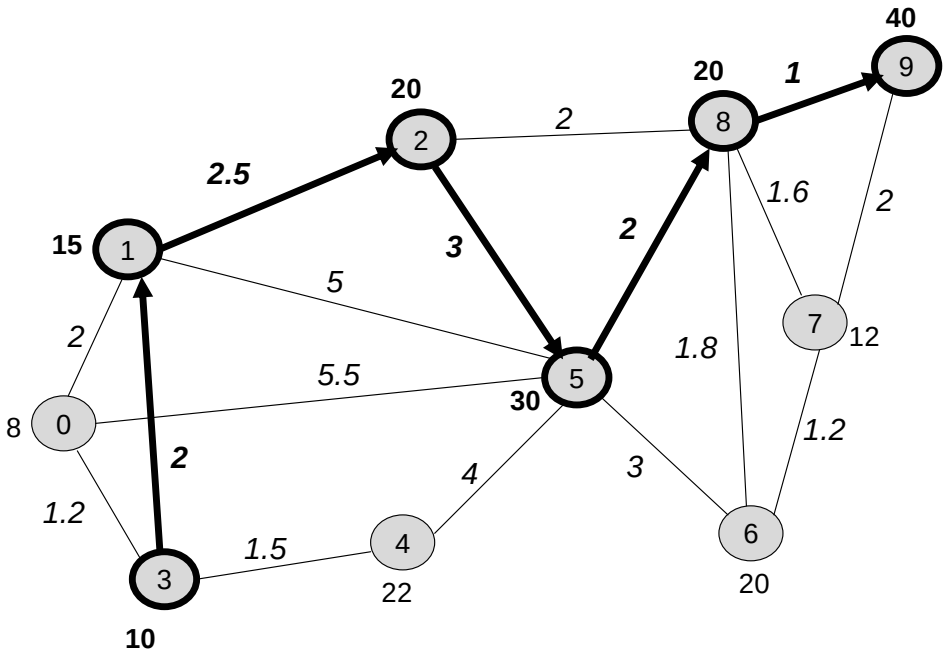

Figure 6.2: A network illustrating the multi-objective optimisation problem

packet over one hop from node i to node j. With each node is associated a number, e_i^c, where e_i^c is the residual power of node i. The initial energy for each node is 50Joule, $n_{pT} = 10$, $s = 3$, and $D = 9$. Table 6.1 presents the values of the objective functions for the random solution, $T_p(3, 9) = (3, 1, 2, 5, 8, 9)$. After finding the set of candidate paths (solutions) from source to destination, and using the concept of non-dominance, the Pareto set is calculated. The objective of the algorithms of this thesis is to calculate the Pareto set in one run and evaluate it just before a change in the environment occurs, using the performance metrics discussed in Section 5.5.

The following subsection presents the heuristic information associated with each sub-objective.

Table 6.1: Objective functions calculated for the route of Figure 6.2

Solution $T_p = (3, 1, 2, 5, 8, 9)$						
(i, j)		$(3, 1)$	$(1, 2)$	$(2, 5)$	$(5, 8)$	$(8, 9)$
E_{ij}		2	2.5	3.0	2	1
i	3	1	2	5	8	9
e_i^c	10	15	20	30	20	40
$\frac{e_i^c}{E_{ij}}$		5.00	6.00	6.66	15.00	20.00
$\frac{1}{e_i^c}$	0.10	0.066	0.050	0.033	0.050	0.025
$EP(T_p)$	10(2+2.5+3+2+1)=105					
$TNP(T_p)$	0.2					
μ_{T_p}	10.53					
$VF(T_p)$	5.57					
$CP(T_p)$	0.1+0.066+0.05+0.033+0.05+0.025=0.324					
$MNC(T_p)$	max(0.8, 0.7, 0.6, 0.4, 0.6, 0.2) =0.8					

6.4.2 Heuristic Information

For each of the five sub-objectives, the heuristic information needed to guide the search to an optimal solution is defined as follows:

- Energy consumed per packet heuristic: Let $\eta_{\nu_{ij}}$ denote the heuristic desirability or the attractiveness of the move from node i to node j which is associated with the objective EP. Then,

$$\eta_{\nu_{ij}} = \frac{1}{E_{ij}} \tag{6.13}$$

  The heuristic information, $\eta_{\nu_{ij}}$, guides the ants to construct good solutions with low energy consumed per packet. For this purpose, the function η_ν creates a matrix that associates a row to each node and a column for each feasible neighbour node. Each entry is calculated according to the energy, E_{ij}, consumed in transmitting one packet over one hop from i to j (refer to equations (6.1) and (6.2)). The motivation for using the energy consumed per packet heuristic information is that, intuitively, good solutions will choose a link with low transmission energy.

- Time to network partition heuristic: Let $\eta_{\xi_{ij}}$ denote the heuristic information associated with the objective TNP. Then,

$$\eta_{\xi_{ij}} = \frac{e_i^c}{E_{ij}} \tag{6.14}$$

The heuristic information, $\eta_{\xi_{ij}}$, guides the ants to construct good solutions with minimal utilisation of the most heavily used link in the network. The assignment of each entry in the matrix created by η_ξ is made according to the current energy, e_i^c, of node i and the energy, E_{ij}, which is consumed in transmitting one packet over one hop from i to j (refer to equation (6.3)). The motivation for using the time to network partition heuristic information is that the use of the least heavily used link in the network delays first node failure (due to node energy depletion), and thus delays network partition.

- Variance in node power levels heuristic: Let $\eta_{\pi_{ij}}$ denote the heuristic information associated with the objective VNP. Then,

$$\eta_{\pi_{ij}} = \frac{1}{|c^a(i,j) - \mu_T|} \tag{6.15}$$

where $c^a(i,j)$ denotes the capacity of link (i,j) and μ_T is the average capacity for all links of T which is computed as in equation (6.6).

The heuristic information, $\eta_{\pi_{ij}}$, guides the ants to construct good solutions with minimum variance in node power level and to send traffic through the nodes with less capacity variation. The assignment of each entry in the matrix created by η_π is made according to the current capacity variation of link (i,j) (refer to equation (6.5)). The motivation for using the variance in node power levels heuristic information is that the performance potential from an energy environment depends on the variation in the energy available across the network. While the amount of energy available is definitely relevant, it is the distribution of this energy in space and time which significantly affects network performance. For instance, if large amounts of energy are available, but concentrated in a small region of the network, then the nodes in those regions without energy supply will limit the total useful lifetime of the network. Energy available in other regions of the network may not be able to meet the performance requirements of the system as a whole.

- Cost per packet heuristic: Let $\eta_{\varrho_{ij}}$ denote the heuristic information associated with the objective CP. Then,

$$\eta_{\varrho_{ij}} = \frac{e_j^c}{E_j} \tag{6.16}$$

where e_j^c is the residual energy of node j and E_j is the initial energy of node j.

The heuristic information, $\eta_{\varrho_{ij}}$, guides the ants to construct good solutions with low cost per packet and to send traffic through nodes with more residual energy (refer to equation (6.9)). The motivation for using the cost per packet heuristic information is that, if routes that pass through nodes with high residual energy are used, network lifetime will be maximised [8].

- Maximum node cost heuristic: Let $\eta_{\varsigma_{ij}}$ denote the heuristic information associated with the objective MNC. Then,

$$\eta_{\varsigma_{ij}} = \frac{E_j}{E_j - e_j^c(t)} \tag{6.17}$$

The heuristic information, $\eta_{\varsigma_{ij}}$, guides the ants to construct good solutions with minimum node cost and to send traffic through links with high residual energy (refer to equation (6.11)). The motivation for using the maximum node cost heuristic information is that network lifetime will be maximised if routes that pass through links with high node cost are avoided [18].

The next section deals with the mobility model used for the multi-objective power-aware routing problem.

6.5 Reference Point Group Mobility Model

This thesis makes use of the reference point group mobility (RPGM) model [29] (refer to Section 2.4). Nodes move in a random fashion using the random way point mobility (RWP) model [29] around a global centre from which the nodes are not able to move farther than a radius of $R_g/2$. This global centre is also mobile, and its motion may follow an arbitrary motion pattern. The RWP model is used to create the motion pattern of the global centre. The effect is that each node will follow the mobility pattern.

RPGM was selected because group motion occurs frequently in ad hoc networks, and RPGM may be readily applied to many existing applications [101]. Moreover, with a proper choice of parameters, RPGM may be used to model several mobility models which have previously been proposed (refer to Section 2.4). RPGM has the advantage of providing a general and flexible framework for describing mobility patterns which are task oriented and time restricted, in addition to being easy to implement and verify. RWP

is one of the widely used models for ad hoc and infrastructure wireless simulations [163] and it has been implemented in several network simulations [110, 183].

The dynamic nature of the power-aware routing problem is determined by the mobility model. The mobility model, in part, makes the problem a dynamic optimisation problem. The R_g determines the severity of change and the pause time, T_{sm}, before applying the mobility model, determines the frequency of change (refer to Section 5.1).

The remainder of this section presents the actions to be taken just before applying the RPGM mobility model and all the updates after the change occurs.

Every T_{sm} seconds, a packet is sent from a source node to a destination node using a random route, T_s, from the Pareto set. The choice of a random route is motivated by the fact that none of the Pareto set solutions is absolutely better than the other non-dominated solutions and all of them are equally acceptable with regards to the satisfaction of all the objectives.

The energy required to do a single-hop transmission from node i to node j is E_{ij}. Therefore, the current energy, e_i^c, for each node $i \in T_s$ is updated according to

$$e_i^c = e_i^c - E_{ij} \tag{6.18}$$

where link $(i, j) \in T_s$.

The RPGM mobility model is applied (refer to Section 6.5) and the distances, d_{ij}, between all nodes i and j belonging to L are recalculated. Since the energy required for transmitting a message along a link (i, j) is proportionate to the distance, d_{ij}, the energy, E_{ij}, for all links $(i, j) \in L$ is recalculated using

$$E_{ij} = max \left\{ \frac{1}{(T_r)^2}, \frac{1}{(T_r)^2} * d_{ij}^2 \right\} \tag{6.19}$$

where T_r is the transmission range of the node and d_{ij} is the Euclidean distance between nodes i and j (refer to Section 2.5.8). The Pareto set is updated by deleting the invalid routes (routes with broken links), i.e. routes for which $E_{ij} > e_i^c$ or $d_{ij} > T_r$. Since the objective functions have been changed, the sub-objectives for all solutions of the current Pareto set are evaluated using equations (6.2), (6.3), (6.5), (6.9), (6.11) and all the dominated solutions are discarded from the Pareto set.

Finally, the heuristic matrices are recalculated (refer to equations (6.13)-(6.17)).

The above steps are summarised in Algorithm 12.

Algorithm 12 General Procedure of ApplyMobilityChanges

Choose a random route, T_s, from P_f;
Send one packet from source to destination using T_s;
for all nodes $i \in T_s$ **do**
  Update e_i^c according to equation (6.18);
end for
Apply the RPGM mobility model (refer to Section 6.5);
for all links $(i, j) \in L$ **do**
  Recalculate d_{ij};
  Recalculate E_{ij} according to equation (6.19);
end for
Delete invalid solutions from P_f;
for all $T \in P_f$ **do**
  Re-evaluate the sub-objectives using equations (6.2), (6.3), (6.5), (6.9), (6.11);
end for
Remove dominated solutions from P_f;
for all links $(i, j) \in L$ **do**
  Recalculate all the heuristic matrices according to equations (6.13)-(6.17);
end for

6.6 Multi-Objective Ant Colony Optimisation

This section presents the five multi-objective ant colony optimisation algorithms proposed in this thesis for simultaneously optimising the five power-aware routing metrics given in Section 6.3.

Subsection 6.6.1 discusses the general framework of the ACO algorithms developed for the power-aware routing problem. Subsections 6.6.2 to 6.6.6 respectively present the EEMACOMP, EEMACOMH, EEMMASMP, EEMMASMH and EEMACOMC multi-objective ACO algorithms.

6.6.1 General Framework of ACO Algorithms for the Power-Aware Routing Problem

An overview of the ACO algorithms for the power-aware routing problem is given below in Figure 6.3.

The remainder of this subsection discusses the solution construction process for each algorithm, the management of the archive, P_f (Pareto set), and the global pheromone update.

Solution construction process. At every iteration of the developed algorithms each ant constructs a complete solution as follows: Starting from the source node, s,

1. Initialise control parameters, and pheromone matrices.
2. Calculate the heuristic matrices.
3. Place all ants at source node s.
4. Repeat for the duration of the simulation time
   (a) Repeat for the duration of pause time {Optimise static problem for power-aware routing }
      i. For each ant
         A. Construct a solution.
         B. Evaluate the solution.
         C. If solution is non-dominated insert it into the archive.
         D. Keep the size of the archive to a predefined limit.
      ii. Apply global pheromone update using all non-dominated solutions of the archive.
   (b) Dynamic aspect for power-aware routing
      i. Send a packet using a solution from the archive.
      ii. Apply RPGM mobility model.
      iii. ApplyMobilityChanges {apply updates due to the mobility of the nodes}
         A. Update energy levels.
         B. Update node distances.
         C. Eliminate invalid solutions from the archive.
         D. Re-evaluate the sub-objectives.
         E. Eliminate dominated solutions from the archive.
         F. Recalculate heuristic information.
      iv. Apply pheromone conservation.
5. Return solutions of the archive.

Figure 6.3: Overview of ACO algorithms for the power-aware routing problem

a non-visited node is selected at each step using an adaptation of the ACS transition rule for the EEMACOMP, EEMACOMH, and EEMACOMC algorithms (refer to Section 3.5.2) and an adaptation of the MAX-MIN transition rule for the EEMMASMP and EEMMASMH algorithms (refer to Section 3.5.3). This process continues until the destination node, D, is reached. When a new node has been added to a candidate solution, a local pheromone update is performed for the EEMACOMP, EEMACOMH, and EEMACOMC algorithms (refer to Section 3.5.2).

Archive management. At the conclusion of each iteration, the Pareto set, P_f, is updated including the non-dominated solutions that have been found thus far. Dominated solutions are removed from P_f. If the number of non-dominated solutions exceeds the predefined archive size, P_{as}, then a truncation operator is used to remove solutions with a lower value of the crowding distance from the archive (refer to Section 4.6.2). The use of the crowding distance guides the selection process at the various stages of the algorithm towards a uniformly spread-out Pareto-optimal front.

Global pheromone update. In the case of multiple pheromone algorithms (EEMACOMP and EEMMASMP) each pheromone matrix associated with each objective is updated using all the solutions of the archive, P_f. That is, every ant that generated a solution in the non-dominated front, P_f, from the beginning of the run is allowed to update all pheromone matrices (refer to Section 4.5.4). In the case of a single pheromone algorithm (EEMACOMH, EEMMASMH) every ant that generated a solution in the non-dominated front from the beginning of the run is allowed to update the pheromone matrix (refer to Section 4.5.3).

The next sections elaborate in detail on the different steps for each of the algorithms.

6.6.2 Energy Efficiency Using Multi-Objective Ant Colony Optimisation, Multi-Pheromone Algorithm

In accordance with the ant colony system (ACS) (refer to Section 3.5.2) the energy efficiency for a mobile network using a multi-objective ant colony optimisation, multi-pheromone (EEMACOMP) algorithm makes use of a colony of ants and several pheromone matrices. This concept has been borrowed from Iredi *et al.* [104] (refer to Section 4.5.4). EEMACOMP calculates five pheromone matrices – one for each optimisation criterion, which, together with a heuristic matrix for each optimisation criterion, are used to calculate transition probabilities. The association of different pheromone matrices for each objective may be useful if the weight of each objective is different and the solution components for each objective must be defined differently (refer to Section 4.5.4).

From equation (3.7), the transition rule for EEMACOMP becomes

$$j = \begin{cases} arg\ \max_{u \in N_i^k(t)} \left\{ \tau_{\nu_{iu}}^{\lambda_\nu}(t)\eta_{\nu_{iu}}^{\beta_\nu}(t) + \tau_{\xi_{iu}}^{\lambda_\xi}(t)\eta_{\xi_{iu}}^{\beta_\xi}(t) + \tau_{\pi_{iu}}^{\lambda_\pi}(t)\eta_{\pi_{iu}}^{\beta_\pi}(t) + \tau_{\varrho_{iu}}^{\lambda_\varrho}(t)\eta_{\varrho_{iu}}^{\beta_\varrho}(t) + \right. \\ \qquad \left. \tau_{\varsigma_{iu}}^{\lambda_\varsigma}(t)\eta_{\varsigma_{iu}}^{\beta_\varsigma}(t) \right\} \quad \text{if } r \leq r_0 \\ J \qquad \text{if } r > r_0 \end{cases} \tag{6.20}$$

where $\lambda_\nu, \lambda_\xi, \lambda_\pi, \lambda_\varrho, \lambda_\varsigma \in (0, 1)$ are user-defined parameters which establish the importance of the objectives; $\tau_{\nu_{ij}}(t)$, $\tau_{\xi_{ij}}(t)$, $\tau_{\pi_{ij}}(t)$, $\tau_{\varrho_{ij}}(t)$ and $\tau_{\varsigma_{ij}}(t)$ are the pheromone matrices, one per objective; $\eta_{\nu_{ij}}(t)$, $\eta_{\xi_{ij}}(t)$, $\eta_{\pi_{ij}}(t)$, $\eta_{\varrho_{ij}}(t)$ and $\eta_{\varsigma_{ij}}(t)$ represent the heuristic information. The parameters β_ν, β_ξ, β_π, β_ϱ, β_ς define the relative influence among heuristic information. The other symbols are as defined in Section 3.5.2. $J \in N_i^k(t)$ is a node

randomly selected based on the probability given by equation (3.8) [104]. According to this equation the probability for EEMACOMP becomes

$$p_{iJ}^{k}(t) = \begin{cases} \dfrac{\left(\tau_{\nu_{iJ}}^{\lambda_\nu}(t)\eta_{\nu_{iJ}}^{\beta_\nu}(t)+\tau_{\xi_{iJ}}^{\lambda_\xi}(t)\eta_{\xi_{iJ}}^{\beta_\xi}(t)+\tau_{\pi_{iJ}}^{\lambda_\pi}(t)\eta_{\pi_{iJ}}^{\beta_\pi}(t)+\tau_{\varrho_{iJ}}^{\lambda_\varrho}(t)\eta_{\varrho_{iJ}}^{\beta_\varrho}(t)+\tau_{\varsigma_{iJ}}^{\lambda_\varsigma}(t)\eta_{\varsigma_{iJ}}^{\beta_\varsigma}(t)\right)}{\sum_{\forall u \in N_i^k(t)}\left(\tau_{\nu_{iu}}^{\lambda_\nu}(t)\eta_{\nu_{iu}}^{\beta_\nu}(t)+\tau_{\xi_{iu}}^{\lambda_\xi}(t)\eta_{\xi_{iu}}^{\beta_\xi}(t)+\tau_{\pi_{iu}}^{\lambda_\pi}(t)\eta_{\pi_{iu}}^{\beta_\pi}(t)+\tau_{\varrho_{iu}}^{\lambda_\varrho}(t)\eta_{\varrho_{iu}}^{\beta_\varrho}(t)+\tau_{\varsigma_{iu}}^{\lambda_\varsigma}(t)\eta_{\varsigma_{iu}}^{\beta_\varsigma}(t)\right)} \\ \qquad \text{if } J \in N_i^k(t) \\ 0 \quad \text{otherwise} \end{cases} \tag{6.21}$$

where $N_i^k(t)$ is a list containing a set of valid nodes to visit from node i.

All objective functions are normalized and bounded by an upper limit value that gives approximately the same magnitude to each objective function [103]. To further reduce any problems which may arise due to difference in magnitude of the objective functions, the above rule uses the sum of the products of the different pheromone and heuristic information matrices instead of the product as used by Iredi *et al.* [104].

The transition rule in equation (6.21) creates a bias towards those nodes which are connected by links with a large amount of pheromone. The same transition rule will bias the search toward minimising energy consumed per packet, utilisation of the link with the least capacity, variance in node power levels, cost per packet, and maximum node cost. Such nodes have a higher probability of being selected.

Heuristic information matrices are calculated at the beginning of the simulation and every time there is a change in the environment using equations (6.13)-(6.17). Pheromone matrix initialisation, and global and local updates are discussed next.

Pheromone matrix initialisation

The five pheromone matrices are initialised as follows:

$$\tau_{\psi_{ij}}(t) = \tau_{0\psi} \tag{6.22}$$

for all $\psi \in \{\nu, \xi, \pi, \varrho, \varsigma\}$, and for all $(i,j) \in L$, where $\tau_{0\psi s}$ are small positive values calculated for each objective, as follows

$$\tau_{0\psi} = \frac{1}{N_G B_\psi} \tag{6.23}$$

where N_G is the number of nodes; $B_\nu = EP(T_\nu)$, where T_ν is the route from source s to destination D with minimal energy consumed per packet; B_ξ is the maximum capacity of all links belonging to T for all paths T from s to D; B_π is the minimal variance of the capacity of all nodes for all paths T from s to D; $B_\varrho = CP(T_\varrho)$, where T_ϱ is the route with minimal cost consumed per packet; B_ς denotes the maximum energy consumed in transmitting one packet over one hop for all links belonging to T and for all paths T from s to D. Routes T, T_ν, and T_ϱ are calculated using greedy heuristics as follows: Starting from the source node, s, a non-visited node is selected at each step according to the heuristic information associated with the corresponding objective. This process continues until the destination node, D, is reached and the greedy algorithm is completed.

Global pheromone update

Once all n_k ants have constructed solutions (refer to Section 6.6.1), the archive (Pareto set), P_f, is updated including the non-dominated solutions that have been found thus far. All the solutions from P_f are then selected to modify the pheromone trails globally. Each pheromone trail associated with each objective is updated using the following global update rules (refer to Section 3.5.2):

$$\tau_{\psi_{ij}}(t+1) = (1-\rho_g)\tau_{\psi_{ij}}(t) + \rho_g \Delta^{\psi}\tau_{ij}(t) \tag{6.24}$$

where $\rho_g \in [0,1]$ is the global evaporation factor, ψ_{ij} represents either ν_{ij}, ξ_{ij}, π_{ij}, ϱ_{ij}, or ς_{ij} depending on the sub-objective, and

$$\Delta^{\psi}\tau_{ij}(t) = \begin{cases} \frac{1}{C(T_k)} \text{ if } i,j \in T_k \\ 0 \quad \text{otherwise} \end{cases} \tag{6.25}$$

for all $T_k \in P_f$, where $C(T_k)$ represents the corresponding objective function.

If ρ_g is small, this strategy favours exploitation by encouraging ants to search in the vicinity of the solutions of the current Pareto front.

Local pheromone update

When a new node is added to a solution being constructed by an ant, a local pheromone update is performed using

$$\tau_{\psi_{ij}}(t+1) = (1-\rho_l)\tau_{\psi_{ij}}(t) + \rho_l \tau_{0\psi} \tag{6.26}$$

where $\tau_{0\psi}$ is the initial amount of pheromone on every link, ψ represents either ν, ξ, π, ϱ, or ς depending on the sub-objective, and $\rho_l \in [0,1]$ is the local evaporation factor.

The EEMACOMP discussed above has been developed for static objective functions. The following subsection discusses an adaptation of EEMACOMP for dynamic objective functions.

Dynamic EEMACOMP

The problem considered in this thesis is a dynamic optimisation problem. Therefore, the static EEMACOMP above has to be adapted to dynamic environments. This section presents an adaptation of EEMACOMP to dynamic environments.

The dynamic ACO algorithm is based on the principle of dividing the simulation time, $S_{T_{tot}}$, into n_{ts} time slices with equal length, $S_{T_{tot}}/T_{sm}$, where T_{sm} is the length of the pause time for the mobility model. T_{sm} is an indication of frequency of change (refer to Section 5.1). During each time slice a problem very similar to a static EEMACOMP is created, and optimisation is carried out. For each of these static problems the aim is to simultaneously minimise the five objectives and to create a Pareto set, P_f, with the best non-dominated solutions that have been found within the time slice. Every T_{sm} seconds the mobility model is applied, the position of the nodes is changed with severity of change, R_g (refer to Section 5.1), and a new static EEMACOMP is created. The concept of a time slice has been introduced to bound the time dedicated to each static problem. A different strategy could be to stop and restart the algorithm each time a new event occurs (i.e. the mobility model is applied). The disadvantage of such an approach is that the time to be dedicated to each static problem would not be known in advance, and, consequently, optimisation may be interrupted before a good local minimum is reached, thus producing unsatisfactory results.

If T_{sm} is small enough, the change in the problem is frequent but a lesser number of iterations are allowed to track new optimal solutions. There is a lower limit to T_{sm} below

which, albeit a small change in the problem, the number of iterations are not enough for an algorithm to track the new optimal solutions adequately. Such a limiting T_{sm} will depend on the chosen algorithm, but importantly allows the best scenario which the chosen algorithm can achieve. The next chapter investigates this aspect and finds such a limiting T_{sm} for the different developed algorithms.

Once a time slice is completed and the respective static problem has been solved by the ACS based EEMACOMP algorithm, each pheromone matrix will contain information on the characteristics of good solutions for this specific problem. In particular, good paths will manifest high values in the corresponding entries of the pheromone matrix for each objective. Pheromone information, together with the current Pareto set, may be passed on to the static problem corresponding to the following time slice since the two problems would potentially be very similar. This operation would prevent optimisation having to restart each time from scratch and would contribute greatly to the good performance of the EEMACOMP algorithm. In case there is no similarity between the two static problems above, the performance of EEMACOMP will be the same as with restarting the optimisation from scratch.

As part of the dynamic EEMACOMP, the ApplyMobilityChanges procedure is called (refer to Algorithm 12) and pheromone conservation rules are applied.

The **ApplyMobilityChanges** procedure sends a message from source to destination, applies the RPGM mobility model and executes all the necessary updates after the change has occured. The P_f archive is re-evaluated and dominated solutions are removed from the archive.

Pheromone conservation rules are applied in order to promote the efficient passing on of information regarding the properties of good solutions from a static problem in one time slice to the static problem in the following time slice. At the end of each time slice the mobility procedure is applied and the environment changes. The distances between nodes are modified, the energy required for transmitting a message along a link (i, j) may be changed and nodes may move out of transmission range or run out of energy. Pheromone trails must be adapted in order to reflect these changes. In order to correct the amount of pheromones, this thesis uses the pheromone update rules for dynamic environments which were proposed by Guntsch and Middendorf [90] (refer to Section 5.2). The choice of these update rules is motivated by the fact that pheromone values are not completely reinitialised but a trace of old values containing characteristics

of good solutions remain. These rules distribute reset-values $\gamma_{\nu_i}, \gamma_{\xi_i}, \gamma_{\pi_i}, \gamma_{\varrho_i}, \gamma_{\varsigma_i} \in [0, 1]$ to each node i. These values determine the amount of re-initialisation of the pheromone values on links j incident to i according to

$$\tau_{\psi_{ij}}(t+1) = (1 - \gamma_{\psi_i})\tau_{\psi_{ij}}(t) + \gamma_{\psi_i}\frac{1}{n_G - 1} \tag{6.27}$$

where ψ_i represents either ν_i, ξ_i, π_i, ϱ_i, or ς_i depending on the sub-objective.

In order to calculate the reset-values, the η-strategy (refer to Section 5.2.2) is used, where heuristic information is applied to decide to what degree pheromone values are equalised. According to the η-strategy, the closer a link is to a modified node, the greater the amount of pheromone which will be removed from this link. The motivation behind the choice of η-strategy is that this specific strategy helps the ants to find new paths by increasing the influence of new links. The measurement of closeness is based on the link costs in terms of the different objectives.

Each node i is assigned the values $\gamma_{\nu_i}, \gamma_{\xi_i}, \gamma_{\pi_i}, \gamma_{\varrho_i}, \gamma_{\varsigma_i}$ proportionate to the distances $d^{\eta}_{\nu_{ij}}$, $d^{\eta}_{\xi_{ij}}$, $d^{\eta}_{\pi_{ij}}$, $d^{\eta}_{\varrho_{ij}}$, and $d^{\eta}_{\varsigma_{ij}}$ from the changed component, j, and equalisation is carried out on all links incident to the changed component. These distances are derived from the heuristics $\eta_{\nu_{ij}}$, $\eta_{\xi_{ij}}$, $\eta_{\pi_{ij}}$, $\eta_{\varrho_{ij}}$, and $\eta_{\varsigma_{ij}}$ such that a high heuristic implies a large distance.

For each pheromone matrix, the $\gamma_{\nu_i}, \gamma_{\xi_i}, \gamma_{\pi_i}, \gamma_{\varrho_i}, \gamma_{\varsigma_i}$ values are calculated using

$$\gamma_{\psi_i} = \max\{0, d^{\eta}_{\psi_{ij}}\} \tag{6.28}$$

with

$$d^{\eta}_{\psi_{ij}} = 1 - \frac{\bar{\eta}_{\psi}}{\lambda_E . \eta_{\psi_{ij}}} \tag{6.29}$$

where ψ represents either ν, ξ, π, ϱ, or ς depending on the sub-objective, and

$$\bar{\eta}_{\psi} = \frac{1}{n_G * (n_G - 1)} \sum_{i=1}^{n_G} \sum_{\substack{j=1 \\ j \neq i}}^{n_G} \eta_{\psi_{ij}} \tag{6.30}$$

where $\lambda_E \in [0, \infty)$ is a strategy-specific parameter.

Algorithm 13 summarises EEMACOMP. In summary, if the environment has changed, then pheromone conservation is applied to allow the ants to explore new, relevant areas of the search space in later iterations.

Algorithm 13 General Procedure of EEMACOMP

$t = 0$; $P_f = \emptyset$; Set timer T_{sm};
Initialise s, D, r_0, β_ν, β_ξ, β_π, β_ϱ, β_ς, λ_ν, λ_ξ, λ_π, λ_ϱ, λ_ς;
Initialize n_k; {number of ants}
Initialize P_{as}; {Maximum archive size}
Initialize $\tau_{0\nu}$, $\tau_{0\xi}$, $\tau_{0\pi}$, $\tau_{0\varrho}$, $\tau_{0\varsigma}$;
for each link (i, j) **do**
  Initialize pheromone matrices $\tau_{\nu_{ij}}(t), \tau_{\xi_{ij}}(t), \tau_{\pi_{ij}}(t), \tau_{\varrho_{ij}}(t), \tau_{\varsigma_{ij}}(t)$ using equation (6.22);
end for
for each link (i, j) **do**
  Calculate $\eta_{\nu_{ij}}, \eta_{\xi_{ij}}, \eta_{\pi_{ij}}, \eta_{\varrho_{ij}}, \eta_{\varsigma_{ij}}$;
end for
Place all ants, $k = 1, ..., n_k$ at source node s;
while $t <= S_{T_{tot}}$ **do**
  {begin resolve static EEMACOMP}
  while T_{sm} seconds not elapsed **do**
    for $k = 1$ to n_k **do**
      $T = \emptyset$;
      $i = s$; {where s the source node and i the current node}
      while $(i \neq D)$ **do**
        Build set $N_i^k(t)$ for node i;
        Assign probability p_{ij}^k to each node of N_i^k according to equation (6.21);
        Select node j of N_i^k using equations (6.20) and (6.21);
        $T = T \cup j$;
        Apply local update pheromone using equation (6.26);
        $i = j$;
      end while
      Evaluate the sub-objectives for solution T using equations (6.2), (6.3), (6.5), (6.9), (6.11) ;
      if T is non-dominated by any $T_x \in P_f$ **then**
        $P_f = P_f \cup T - \{T_y \mid T \prec T_y\}, \forall T_y \in P_f$;
        if size of $P_f > P_{as}$ **then**
          Truncate P_f
        end if
      end if
    end for
    for all $T_k \in P_f$ **do**
      Update_global_pheromone $\forall (i, j) \in T_k$ using equations (6.24)-(6.25);
    end for
  end while
  {end resolve static EEMACOMP}
  Call Procedure ApplyMobilityChanges() (refer to Algorithm 12);
  Apply pheromone conservation $\forall (i, j) \in L$ using equations (6.27)-(6.30);
  $t = t + T_{sm}$;
  Reset timer T_{sm};
end while
Return P_f

6.6.3 Energy Efficiency Using Multi-Objective Ant Colony Optimisation, Multi-Heuristic Algorithm

In accordance with the ant colony system (ACS) (refer to Section 3.5.2), the energy efficiency for mobile networks using a multi-objective ant colony optimisation, multi-heuristic (EEMACOMH) algorithm makes use of a colony of ants, one pheromone matrix and a different heuristic matrix for each objective.

This concept has been borrowed from Iredi *et al.* [104] (refer to Section 4.5.3). The EEMACOMH algorithm is similar to EEMACOMP with the only difference being that EEMACOMH uses a single pheromone matrix instead of five pheromone matrices. This single pheromone matrix represents the desirability of the solution components with regard to all the objectives.

From equation (3.7), the transition rule for EEMACOMH becomes

$$j = \begin{cases} arg\ \max_{u\ \in\ N_i^k(t)} \left\{ \tau_{iu}(t) \times (\eta_{\nu_{iu}}^{\beta_\nu}(t) + \eta_{\xi_{iu}}^{\beta_\xi}(t) + \eta_{\pi_{iu}}^{\beta_\pi}(t) + \eta_{\varrho_{iu}}^{\beta_\varrho}(t) + \eta_{\varsigma_{iu}}^{\beta_\varsigma}(t)) \right\} \\ \qquad\qquad \text{if } \ r \leq r_0 \\ J \qquad\qquad \text{if } r > r_0 \end{cases} \tag{6.31}$$

where $\tau_{ij}(t)$ is the pheromone matrix – the same for all objectives – and $\eta_{\nu_{ij}}(t)$, $\eta_{\xi_{ij}}(t)$, $\eta_{\pi_{ij}}(t)$, $\eta_{\varrho_{ij}}(t)$ and $\eta_{\varsigma_{ij}}(t)$ represent the heuristics. The parameters β_ν, β_ξ, β_π, β_ϱ, and β_ς define the relative influence among heuristic information. The rest of the symbols are as defined in Section 3.5.2. $J \in N_i^k(t)$ is a node randomly selected based on the probability given by equation (3.8). According to this equation the probability for EEMACOMH becomes

$$p_{iJ}^k(t) = \begin{cases} \dfrac{\left(\tau_{iJ}(t) \times (\eta_{\nu_{iJ}}^{\beta_\nu}(t) + \eta_{\xi_{iJ}}^{\beta_\xi}(t) + \eta_{\pi_{iJ}}^{\beta_\pi}(t) + \eta_{\varrho_{iJ}}^{\beta_\varrho}(t) + \eta_{\varsigma_{iJ}}^{\beta_\varsigma}(t))\right)}{\sum_{\forall u \in N_i^k(t)} \left(\tau_{iu}(t) \times (\eta_{\nu_{iu}}^{\beta_\nu}(t) + \eta_{\xi_{iu}}^{\beta_\xi}(t) + \eta_{\pi_{iu}}^{\beta_\pi}(t) + \eta_{\varrho_{iu}}^{\beta_\varrho}(t) + \eta_{\varsigma_{iu}}^{\beta_\varsigma}(t))\right)} \\ \qquad\qquad \text{if } J \ \in \ N_i^k(t) \\ 0 \quad \text{otherwise} \end{cases} \tag{6.32}$$

The solution construction process is as given in Section 6.6.1. Heuristic information matrices are calculated at the beginning of the simulation and every time there is a change

in the environment using equations (6.13)-(6.17). Pheromone matrix initialisation, and global and local updates are discussed next.

Pheromone matrix initialisation

The pheromone matrix is initialised as follows:

$$\tau_{ij}(t) = \tau_0 \tag{6.33}$$

for all $(i, j) \in L$, where τ_0 is a small positive value calculated as

$$\tau_0 = \frac{1}{N_G \times B_a} \tag{6.34}$$

where N_G is the number of nodes, and B_a is the length of the initial solution produced by the nearest neighbour heuristic [70].

Global pheromone update

Once each of the n_k ants has completed its solution, if the ant's solution, T_k, is non-dominated by the solutions of P_f, the solution is stored in the archive, P_f, and solutions of P_f newly dominated by T_k are removed from the archive. All the solutions from P_f are then selected to modify the pheromone trail globally. The pheromone trail is updated using the following global update rule (refer to Section 3.5.2) [161]:

$$\tau_{ij}(t+1) = (1-\rho_g)\tau_{ij}(t) + \rho_g \Delta\tau^k(t),\ \forall\ (i,j) \in T_k \tag{6.35}$$

where

$$\Delta\tau^k = \frac{1}{EP(T_k) + TNP(T_k) + VF(T_k) + CP(T_k) + MNC(T_k)} \tag{6.36}$$

for all $T_k \in P_f$, where each objective value is normalised to ensure that all objectives have approximately the same magnitude [103].

Local pheromone update

When a new node is added to a solution being constructed by an ant, a local pheromone update is performed using

$$\tau_{ij}(t+1) = (1-\rho_l)\tau_{ij}(t) + \rho_l\tau_0 \tag{6.37}$$

where τ_0 is the initial amount of pheromone on every link of L.

The EEMACOMH discussed above has been developed for static objective functions. The following section discusses an adaptation of EEMACOMH for dynamic objective functions.

Dynamic EEMACOMH

As with EEMACOMP (refer to Section 6.6.2) the dynamic EEMACOMH is addressed as a series of static problems with a new problem being defined each time the mobility model is applied. The ApplyMobilityChanges procedure (refer to Algorithm 12) is applied at the end of each time slice.

The pheromone conservation rules are applied as for EEMACOMP, but only one pheromone matrix is updated as follows:

$$\tau_{ij}(t+1) = (1-\gamma_i)\tau_{ij}(t) + \gamma_i\frac{1}{n_G-1} \tag{6.38}$$

where

$$\gamma_i = \max\{0, d_{ij}^{\eta}\} \tag{6.39}$$

with

$$d_{ij}^{\eta} = 1 - \frac{\bar{\eta}}{\lambda_E.(\eta_{\nu_{ij}} + \eta_{\xi_{ij}} + \eta_{\pi_{ij}} + \eta_{\varrho_{ij}} + \eta_{\varsigma_{ij}})} \tag{6.40}$$

where

$$\bar{\eta} = \frac{1}{n_G * (n_G-1)}\sum_{i=1}^{n_G}\sum_{\substack{j=1\\ j\neq i}}^{n_G}(\eta_{\nu_{ij}} + \eta_{\xi_{ij}} + \eta_{\pi_{ij}} + \eta_{\varrho_{ij}} + \eta_{\varsigma_{ij}}) \tag{6.41}$$

where $\lambda_E \in [0, \infty)$ is a strategy-specific parameter.

The EEMACOMH algorithm is very similar to the EEMACOMP algorithm (refer to Algorithm 13) with the following differences in respect of EEMACOMH: a) there is only one pheromone matrix for the EEMACOMH algorithm, b) if the environment is modified, equations (6.38)-(6.41) are used for pheromone conservation, c) equations (6.35) and (6.36) are used for the global pheromone updating, d) the local pheromone update is performed using equation (6.37), and e) the transition rule is applied according to equations (6.31) and (6.32).

In the interests of completeness, Algorithm 14 presents the general procedure of the proposed EEMACOMH algorithm.

6.6.4 Energy Efficiency Using Multi-Objective MAX-MIN Ant System Optimisation, Multi-Pheromone Algorithm

Energy efficiency for mobile networks using the multi-objective MAX-MIN ant system optimisation, multi-pheromone (EEMMASMP) algorithm is based on the MAX-MIN ant system (MMAS) (refer to Section 3.5.3). The EEMMASMP algorithm modifies MMAS with the following changes in order to solve the dynamic multi-objective problem:

- Similar to the previous two algorithms, EEMMASMP finds a set of Pareto optimal solutions termed P_f, instead of finding a single optimal solution as is done by MMAS.
- EEMMASMP solves the dynamic aspect of the multi-objective power-aware routing problem.

In accordance with MMAS, the EEMMASMP algorithm uses a colony of ants and several pheromone matrices. EEMMASMP calculates five pheromone matrices – one for each optimisation criterion – which, together with a heuristic matrix for each optimisation criterion, are used to calculate transition probabilities. This concept has been borrowed from Iredi *et al.* [104] (refer to Section 4.5.4).

The EEMACOMP and EEMMASMP algorithms are very similar. The only difference between EEMACOMP and EEMMASMP is that the ACS (adapted to develop EEMA-

Algorithm 14 General Procedure of EEMACOMH

$t = 0$; $P_f = \emptyset$; Set timer T_{sm};
Initialize s, D, r_0, ρ, $\beta_\nu, \beta_\xi, \beta_\pi, \beta_\varrho, \beta_\varsigma$, n_k;
Initialize P_{as}; {Maximum archive size}
Calculate τ_0 using equation (6.34);
for each link (i, j) **do**
  Initialize pheromone matrix $\tau_{ij}(t) = \tau_0$;
  Calculate $\eta_{\nu_{ij}}, \eta_{\xi_{ij}}, \eta_{\pi_{ij}}, \eta_{\varrho_{ij}}, \eta_{\varsigma_{ij}}$;
end for
Place all ants, $k = 1, ..., n_k$ at source node s;
while $t <= S_{T_{tot}}$ **do**
  {begin resolve static EEMACOMH}
  while T_{sm} seconds not elapsed **do**
    for $k = 1$ to n_k **do**
      $T = \emptyset$;
      $i = s$; {where s the source node and i the current node}
      while $(i \neq D)$ **do**
        Build set $N_i^k(t)$ for i;
        Assign probability p_{ij}^k to each node of N_i^k according to equation (6.32);
        Select node j of N_i^k using equations (6.31) and (6.32);
        $T = T \cup j$;
        Apply local update pheromone using equation (6.37);
        $i = j$;
      end while
      Evaluate the sub-objectives for solution T using equations (6.2), (6.3), (6.5), (6.9), (6.11);
      if T is not dominated by any $T_x \in P_f$ **then**
        $P_f = P_f \cup T - \{T_y \mid T \prec T_y\}, \forall T_y \in P_f$;
        if size of $P_f > P_{as}$ **then**
          Truncate P_f
        end if
      end if
    end for
    for all $T_k \in P_f$ **do**
      Update_global_pheromone $\forall (i, j) \in T_k$ using equations (6.35) and (6.36);
    end for
  end while
  {end resolve static EEMACOMH}
  Call Procedure ApplyMobilityChanges() (refer to Algorithm 12);
  Apply pheromone conservation $\forall (i, j) \in L$ using equations (6.38)-(6.41);
  $t = t + T_{sm}$
  Reset timer T_{sm};
end while
Return P_f

COMP) is replaced with MMAS. The differences between EEMMASMP and EEMA-COMP with reference to MMAS are presented next.

From equation (3.3), the transition rule for EEMMASMP becomes

$$p_{ij}^{k}(t) = \begin{cases} \dfrac{\left(\tau_{\nu_{ij}}^{\alpha\lambda_\nu}(t)\eta_{\nu_{ij}}^{\beta_\nu}(t)+\tau_{\xi_{ij}}^{\alpha\lambda_\xi}(t)\eta_{\xi_{ij}}^{\beta_\xi}(t)+\tau_{\pi_{ij}}^{\alpha\lambda_\pi}(t)\eta_{\pi_{ij}}^{\beta_\pi}(t)+\tau_{\varrho_{ij}}^{\alpha\lambda_\varrho}(t)\eta_{\varrho_{ij}}^{\beta_\varrho}(t)+\tau_{\varsigma_{ij}}^{\alpha\lambda_\varsigma}(t)\eta_{\varsigma_{ij}}^{\beta_\varsigma}(t)\right)}{\sum_{\forall u\in N_i^k(t)}\left(\tau_{\nu_{iu}}^{\alpha\lambda_\nu}(t)\eta_{\nu_{iu}}^{\beta_\nu}(t)+\tau_{\xi_{iu}}^{\alpha\lambda_\xi}(t)\eta_{\xi_{iu}}^{\beta_\xi}(t)+\tau_{\pi_{iu}}^{\alpha\lambda_\pi}(t)\eta_{\pi_{iu}}^{\beta_\pi}(t)+\tau_{\varrho_{iu}}^{\alpha\lambda_\varrho}(t)\eta_{\varrho_{iu}}^{\beta_\varrho}(t)+\tau_{\varsigma_{iu}}^{\alpha\lambda_\varsigma}(t)\eta_{\varsigma_{iu}}^{\beta_\varsigma}(t)\right)} \\ \qquad\qquad \text{if } j \in N_i^k(t) \\ 0 \quad \text{otherwise} \end{cases} \tag{6.42}$$

where α defines the relative influence between the heuristic information and the pheromone levels. The other symbols are as defined in Section 6.6.2.

The solution construction process is as given in Section 6.6.1. Heuristic information matrices are calculated at the beginning of the simulation, and every time there is a change in the environment, using equations (6.13)-(6.17). Pheromone matrix initialisation and global updates are discussed next.

Pheromone matrix initialisation

The five pheromone matrices are initialised using

$$\tau_{\psi_{ij}}(t) = \tau_0 \tag{6.43}$$

for all $(i,j) \in L$, where ψ_{ij} represents either ν_{ij}, ξ_{ij}, π_{ij}, ϱ_{ij}, or ς_{ij} depending on the sub-objective; τ_0 is the upper bound set to some arbitrarily high value in order to achieve a high degree of exploration at the start of the algorithm.

Global pheromone update

Once all n_k ants have constructed solutions (refer to Section 6.6.1), the archive, P_f, is updated including the non-dominated solutions that have been found thus far. All the solutions from P_f are then selected to modify the pheromone trails. Each pheromone trail associated with each objective is updated using equations (6.24)-(6.25) (refer to Section 6.6.2).

If, after application of the global update rule, the pheromone value of a link becomes greater than the maximum value allowed, then the pheromone value of a link is explicitly set as equal to the maximum allowed value (refer to Section 3.5.3) for all pheromone matrices according to the following rules:

$$\text{if } \tau_{\psi_{ij}}(t+1) > \tau_{max_\psi} \text{ then } \tau_{\psi_{ij}}(t+1) = \tau_{max_\psi} \tag{6.44}$$

for all $(i,j) \in T_k$ and for all $T_k \in P_f$, and τ_{max_ψ} is calculated as proposed in Pinto and Barán [161]:

$$\tau_{max_\psi} = \sum_{T_k \in P_f} \frac{1}{(1-\rho_g)C(T_k)} \tag{6.45}$$

where $C(T_k)$ represents the corresponding objective function.

On the other hand, if the pheromone value of a link becomes less than the lower limit, then the pheromone value of a link is explicitly set equal to the lower limit (refer to Section 3.5.3) for all pheromone matrices according to the following rules:

$$\text{if } \tau_{\psi_{ij}}(t+1) < \tau_{min_\psi} \text{ then } \tau_{\psi_{ij}}(t+1) = \tau_{min_\psi} \tag{6.46}$$

for all $(i,j) \in T_k$ and for all $T_k \in P_f$, and τ_{min_ψ} is calculated as proposed in Pinto and Barán [161]:

$$\tau_{min_\psi} = \frac{\tau_{max_\psi}}{2n_k} \tag{6.47}$$

The EEMMASMP discussed above has been developed for static objective functions. EEMMASMP is adapted for dynamic objective functions in the same way as with EEMACOMP (refer to Section 6.6.2).

Algorithm 15 summarises the EEMMASMP algorithm.

Algorithm 15 General Procedure of EEMMASMP

$t = 0$; $P_f = \emptyset$; Set timer T_{sm};
Initialize s, D, τ_0, α, β_ν, β_ξ, β_π, β_ϱ, β_ς, λ_ν, λ_ξ, λ_π, λ_ϱ, λ_ς;
Initialise n_k; {number of ants}
Initialise P_{as}; {Maximum archive size}
for each link (i, j) **do**
  Initialise pheromone matrices $\tau_{\nu_{ij}}(t)$, $\tau_{\xi_{ij}}(t)$, $\tau_{\pi_{ij}}(t)$, $\tau_{\varrho_{ij}}(t)$, $\tau_{\varsigma_{ij}}(t)$ using equation (6.43);
  Calculate $\eta_{\nu_{ij}}$, $\eta_{\xi_{ij}}$, $\eta_{\pi_{ij}}$, $\eta_{\varrho_{ij}}$, $\eta_{\varsigma_{ij}}$;
end for
Place all ants, $k = 1, ..., n_k$ at source node s;
while $t <= S_{T_{tot}}$ **do**
  {begin resolve static EEMMASMP}
  while T_{sm} seconds not elapsed **do**
    for $k = 1$ to n_k **do**
      $T = \emptyset$; $i = s$; {where s the source node and i the current node}
      while $(i \neq D)$ **do**
        Build set $N_i^k(t)$ for i;
        Assign probability p_{ij}^k to each node of $N_i^k(t)$ according to equation (6.42);
        Select node j of $N_i^k(t)$ using equation (6.42);
        $T = T \cup j$;
        $i = j$;
      end while
      Evaluate the sub-objectives for solution T using equations (6.2), (6.3), (6.5), (6.9), (6.11);
      if T is not dominated by any $T_x \in P_f$ **then**
        $P_f = P_f \cup T - \{T_y \mid T \prec T_y\}, \forall T_y \in P_f$;
        if size of $P_f > P_{as}$ **then**
          Truncate P_f
        end if
      end if
    end for
    for all $T_k \in P_f$ **do**
      update_global_pheromone $\forall (i, j) \in T_k$ using equations (6.24)-(6.25);
      Restrict the pheromone intensities within the lower and upper limits, $\forall (i, j) \in T_k$, using equations (6.44)-(6.47);
    end for
  end while
  {end resolve static EEMMASMP}
  Call Procedure ApplyMobilityChanges() (refer to Algorithm 12);
  Apply pheromone conservation $\forall (i, j) \in L$ using equations (6.27)-(6.30);
  Restrict the pheromone intensities within the lower and upper limits, $\forall (i, j), \in L$ using equations (6.44)-(6.47);
  $t = t + T_{sm}$;
  Reset timer T_{sm};
end while
Return P_f

6.6.5 Energy Efficiency Using Multi-objective MAX-MIN Ant System Optimisation, Multi-heuristic Algorithm

In accordance with the max-min ant system (MMAS) (refer to Section 3.5.3) the energy efficiency for mobile networks using a multi-objective MAX-MIN ant system optimisation, multi-heuristic (EEMMASMH) algorithm uses a colony of ants, a single pheromone matrix and a different heuristic matrix for each objective. EEMMASMH is very similar to the EEMMASMP algorithm, the sole difference being that EEMMASMH uses only one pheromone matrix, $\tau_{ij}(t)$. This single pheromone matrix represents the desirability of the solution components with regard to all objectives.

From equation (3.3), the transition rule for EEMMASMH becomes

$$p_{ij}^{k}(t) = \begin{cases} \dfrac{\tau_{ij}^{\alpha}(t)\left(\eta_{\nu_{ij}}^{\beta_{\nu}}(t)+\eta_{\xi_{ij}}^{\beta_{\xi}}(t)+\eta_{\pi_{ij}}^{\beta_{\pi}}(t)+\eta_{\varrho_{ij}}^{\beta_{\varrho}}(t)+\eta_{\varsigma_{ij}}^{\beta_{\varsigma}}(t)\right)}{\sum_{\forall u \in N_i^k(t)} \tau_{iu}^{\alpha}(t)\left(\eta_{\nu_{iu}}^{\beta_{\nu}}(t)+\eta_{\xi_{iu}}^{\beta_{\xi}}(t)+\eta_{\pi_{iu}}^{\beta_{\pi}}(t)+\eta_{\varrho_{iu}}^{\beta_{\varrho}}(t)+\eta_{\varsigma_{iu}}^{\beta_{\varsigma}}(t)\right)} \\ \qquad \text{if } j \in N_i^k(t) \\ 0 \quad \text{otherwise} \end{cases} \tag{6.48}$$

where the symbols are as defined in Section 6.6.2.

The pheromone matrix is initialised as

$$\tau_{ij}(t) = \tau_0 \tag{6.49}$$

for all $(i, j) \in L$, where τ_0 is the upper bound set to some arbitrarily high value in order to achieve a high degree of exploration at the start of the algorithm.

The equations for global pheromone updating are the same as those of EEMACOMH (refer to equations (6.35) and (6.36)).

If, after applying the global update rule, $\tau_{ij}(t+1)$ becomes greater than τ_{max}, then $\tau_{ij}(t+1)$ is explicitly set equal to τ_{max} according to the following rule:

$$\text{if } \tau_{ij}(t+1) > \tau_{max} \text{ then } \tau_{ij}(t+1) = \tau_{max} \tag{6.50}$$

for all $(i,j) \in T_k$ and for all $T_k \in P_f$, where

$$\tau_{max} = \sum_{T_k \in P_f} \frac{1}{(1-\rho_g)(EP(T_k) + TNP(T_k) + VF(T_k) + CP(T_k) + MNC(T_k))} \tag{6.51}$$

On the other hand, if $\tau_{ij}(t+1) < \tau_{min}$ then $\tau_{ij}(t+1)$ is explicitly set equal to τ_{min} according to the following rule:

$$\text{if } \tau_{ij}(t+1) < \tau_{min} \text{ then } \tau_{ij}(t+1) = \tau_{min} \tag{6.52}$$

for all $(i,j) \in T_k$ and for all $T_k \in P_f$, where

$$\tau_{min} = \frac{\tau_{max}}{2n_k} \tag{6.53}$$

The EEMMASMH discussed above has been developed for static objective functions. EEMMASMH is adapted for dynamic objective functions in the same way as with EEMACOMH (refer to Section 6.6.3).

Algorithm 16 summarises the EEMMASMH algorithm.

6.6.6 Energy Efficiency Using Multi-Objective Ant Colony Optimisation, Multi-Colony Algorithm

The multiple colony ACO developed by Gambardella *et al.* [76] and described in Section 4.5.6 was used to solve MOPs by assigning a colony to each objective. This section proposes the energy efficiency for mobile networks using a multi-objective ant colony optimisation, multi-colony (EEMACOMC) algorithm which applies the multi-colony concept to the power-aware routing problem.

Since five objectives are defined for the power-aware routing problem, five colonies are created – one for each of the objectives. These colonies each have the same number of ants, $n_{k_c} = n_k/5$, with $c = 1, ..., 5$.

Each colony implements an ACS, where the transition rule for each sub-objective is

$$j = \begin{cases} arg\ \max_{u \in N_i^k(t)} \{\tau_{\psi_{iu}}(t) \eta_{\psi_{iu}}^{\beta_\psi}(t)\} & \text{if } r \leq r_0, \\ J & \text{otherwise} \end{cases} \tag{6.54}$$

where β_ψ represents either β_ν, β_ξ, β_π, β_ϱ, or β_ς depending on the sub-objective, and

Algorithm 16 General Procedure of EEMMASMH

$t = 0$; $P_f = \emptyset$; Set timer T_{sm};
Initialise s, D, τ_0, α, β_ν, β_ξ, β_π, β_ϱ, β_ς;
Initialize n_k; {number of ants}
Initialize P_{as}; {Maximum archive size}
for each link (i, j) **do**
  Initialise pheromone matrix $\tau_{ij}(t)$, using equation (6.49);
  Calculate $\eta_{\nu_{ij}}$, $\eta_{\xi_{ij}}$, $\eta_{\pi_{ij}}$, $\eta_{\varrho_{ij}}$, $\eta_{\varsigma_{ij}}$;
end for
Place all ants, $k = 1, ..., n_k$ at source node s;
while $t <= S_{T_{tot}}$ **do**
  {begin resolve static EEMMASMH}
  while T_{sm} seconds not elapsed **do**
    for $k = 1$ to n_k **do**
      $T = \emptyset$; $i = s$; {where s the source node and i the current node}
      while $(i \neq D)$ **do**
        Build set $N_i^k(t)$ for i;
        Assign probability p_{ij}^k to each node of $N_i^k(t)$ according to equation (6.48);
        Select node j of $N_i^k(t)$ using equation (6.48);
        $T = T \cup j$;
        $i = j$;
      end while
      Evaluate the sub-objectives for solution T using equations (6.2), (6.3), (6.5), (6.9), (6.11);
      if T is not dominated by any $T_x \in P_f$ **then**
        $P_f = P_f \cup T - \{T_y \mid T \prec T_y\}, \forall T_y \in P_f$;
        if size of $P_f > P_{as}$ **then**
          Truncate P_f
        end if
      end if
    end for
    for all $T_k \in P_f$ **do**
      update_global_pheromone $\forall (i, j) \in T_k$ using equations (6.35) and (6.36);
      Restrict the pheromone intensities within the lower and upper limits, $\forall (i, j) \in T_k$, using equations (6.50)-(6.53);
    end for
  end while
  {end resolve static EEMMASMH}
  Call Procedure ApplyMobilityChanges() (refer to Algorithm 12);
  Apply pheromone conservation $\forall (i, j) \in L$ using equations (6.38)-(6.41);
  Restrict the pheromone intensities within the lower and upper limits, $\forall (i, j) \in L$ using equations (6.50)-(6.53);
  $t = t + T_{sm}$;
  Reset timer T_{sm};
end while
Return P_f

defines the importance of $\eta_{\psi_{iu}}(t)$. The rest of the symbols are as defined in Section 3.5.2. $J \in N_i^k(t)$ is a node that is randomly selected according to probability,

$$p_{iJ}^k(t) = \frac{\tau_{\psi_{iJ}}(t)\eta_{\psi_{iJ}}^{\beta_\psi}(t)}{\sum_{u \in N_i^k(t)} \tau_{\psi_{iu}}(t)\eta_{\psi_{iu}}^{\beta_\psi}(t)} \tag{6.55}$$

At every iteration of the ACS algorithm each ant of a colony constructs a complete solution (optimising the objective of the colony) as follows (refer to Algorithm 17): Starting from the source node, s, a non-visited node is pseudo-randomly selected at each step as in equation (6.54), while equation (6.55) provides the probability of selecting a link. This process continues until the destination node, D, is reached. When a new node has been added to a candidate solution, a local pheromone update is performed using equation (6.26) (refer to Section 3.5.2). The solution created by the ant is inserted into the global archive P_G without being evaluated. The archive, P_G, contains all the candidate solutions.

Algorithm 18 summarises the general procedure for constructing $n_k/5$ solutions for all the ants of a colony.

Algorithm 17 General Procedure of BuildPathMultiColony

input parameters s, D, r_0, β_ψ, τ_ψ, η_ψ;
$T = \emptyset$;
$i = s$; {where s the source node and i the current node}
while $(i \neq D)$ **do**
  Build set $N_i^k(t)$ for i;
  Assign probability p_{ij}^k to each node of $N_i^k(t)$ according to equation (6.54);
  Select node j of $N_i^k(t)$ using equations (6.54) and (6.55);
  $T = T \cup j$;
  Apply local pheromone update using equation (6.26);
  $i = j$;
end while
Return T;

The five pheromone matrices are initialised using equations (6.22)-(6.23) (refer to Section 6.6.2). The cooperation between colonies and the global pheromone updates are discussed next.

Algorithm 18 General Procedure of BuildAllPathsMultiColony

input parameters s, D, r_0, β_ψ, τ_ψ, η_ψ, n_k;
for $k = 1$ to $n_k/5$ **do**
  T = BuildPathMultiColony(s, D, r_0, β_ψ, τ_ψ, η_ψ);
  Insert T in to global archive, P_G;
end for
Return P_G

Cooperation between colonies

The five colonies of ants cooperate and specialise in order to find good solutions in different regions of the Pareto front. In every iteration, the ants in each colony deposit their solutions into a global solution pool (called P_G) that is shared by all colonies. This pool of solutions, P_G, is used to determine the non-dominated front of all solutions from all the colonies in that iteration. Once all the ants from all colonies have constructed their solutions and deposited them in P_G, all the solutions of P_G are evaluated against the sub-objectives using equations (6.2), (6.3), (6.5), (6.9), (6.11). Every solution, T, of P_G is compared with the solutions of P_f and, if T is non-dominated by any solution of P_f, then T is inserted into P_f. All the solutions of P_f which are dominated by T are removed from P_f. If the number of non-dominated solutions exceeds the predefined archive size, P_{as}, a truncation operator is used to remove solutions with a lower value of the crowding distance from the archive (refer to Section 4.6.2). The use of the crowding distance guides the selection process during the various stages of the algorithm towards a uniformly spread-out Pareto-optimal front.

Global pheromone update

Only those ants that found a solution which is in the global non-dominated front are allowed to update pheromones. Each ant uses the update by origin method (refer to Section 4.5.6) to determine in which colony the ant should update the pheromone matrix, that is, the ant updates only in its own colony [104]. The update by origin method imposes a stronger selection pressure on those ants that are allowed to update. The update by origin method might also force the colonies to search in different regions of the non-dominated front.

When only a few solutions from other colonies are in the same region, it is more likely

that a solution from the local non-dominated front of a colony might also appear in the global non-dominated front. Hence, it is more likely that an ant with solutions in less dense areas of the non-dominated front will be allowed to update and, thereby, influence the ensuing search process [104].

The ants of each colony that found a solution which is in the global non-dominated front, P_f, update only the pheromone matrix which is associated with the objective of the colony (refer to Section 4.5.6).

The pheromone trail of each colony is updated using the solutions of P_f as follows:

$$\tau_{\psi_{ij}}(t+1) = (1-\rho_g)\tau_{\psi_{ij}}(t) + \rho_g \Delta^{\psi}\tau_{ij}(t) \tag{6.56}$$

where ψ_{ij} represents either ν_{ij}, ξ_{ij}, π_{ij}, ϱ_{ij}, or ς_{ij} depending on the sub-objective, and

$$\Delta^{\psi}\tau_{ij}(t) = \begin{cases} \frac{1}{C(T_k)} \text{ if } i,j \in T_k \text{ and } T_k \in \text{colony } n_c \\ 0 \qquad\qquad \text{otherwise} \end{cases} \tag{6.57}$$

for all $T_k \in P_f$, where $C(T_k)$ represents the corresponding objective function, and $n_c \in \{1, ..., 5\}$ represents the index of the colony associated with each objective.

The EEMACOMC algorithm discussed above has been developed for static objective functions. EEMACOMC is adapted for dynamic objective functions in the same way as for EEMACOMP (refer to Section 6.6.2).

Algorithm 19 summarises the dynamic EEMACOMC.

Algorithm 19 General Procedure of EEMACOMC

$t = 0$; $P_f = \emptyset$; Set timer T_{sm};
Initialise s, D, r_0, β_ν, β_ξ, β_π, β_ϱ, β_ς;
Initialise n_k; {number of ants}
Initialise $\tau_{0\nu}$, $\tau_{0\xi}$, $\tau_{0\pi}$, $\tau_{0\varrho}$, $\tau_{0\varsigma}$;
Initialise P_{as}; {Maximum archive size}
for each link (i, j) **do**
  Initialise pheromone matrices $\tau_{\nu_{ij}}(t), \tau_{\xi_{ij}}(t), \tau_{\pi_{ij}}(t), \tau_{\varrho_{ij}}(t), \tau_{\varsigma_{ij}}(t)$ using equations (6.22)-(6.23);
end for
for each link (i, j) **do**
  calculate $\eta_{\nu_{ij}}, \eta_{\xi_{ij}}, \eta_{\pi_{ij}}, \eta_{\varrho_{ij}}, \eta_{\varsigma_{ij}}$;
end for
Place all ants, $k = 1, ..., n_k$ at source node s;
while $t <= S_{T_{tot}}$ **do**
  {begin resolve static EEMACOMC}
  while T_{sm} seconds not elapsed **do**
    $P_G = \emptyset$;
    $P_G = P_G \cup BuildAllPathsMultiColony(s, D, r_0, \beta_\nu, \tau_\nu, \eta_\nu, n_k)$;
    $P_G = P_G \cup BuildAllPathsMultiColony(s, D, r_0, \beta_\xi, \tau_\xi, \eta_\xi, n_k)$;
    $P_G = P_G \cup BuildAllPathsMultiColony(s, D, r_0, \beta_\pi, \tau_\pi, \eta_\pi, n_k)$;
    $P_G = P_G \cup BuildAllPathsMultiColony(s, D, r_0, \beta_\varrho, \tau_\varrho, \eta_\varrho, n_k)$;
    $P_G = P_G \cup BuildAllPathsMultiColony(s, D, r_0, \beta_\varsigma, \tau_\varsigma, \eta_\varsigma, n_k)$;
    for all $T \in P_G$ **do**
      Evaluate the sub-objectives for solution T using equations (6.2), (6.3), (6.5), (6.9), (6.11);
      if T is not dominated by any $T_x \in P_f$ **then**
        $P_f = P_f \cup T - \{T_y \mid T \prec T_y\}, \forall T_y \in P_f$;
        if size of $P_f > P_{as}$ **then**
          Truncate P_f;
        end if
      end if
    end for
    for all $T_k \in P_f$ **do**
      Update_global_pheromone $\forall (i, j) \in T_k$ using equations (6.56) and (6.57);
    end for
  end while
  {end resolve static EEMACOMC}
  Call Procedure ApplyMobilityChanges() (refer to Algorithm 12);
  Apply pheromone conservation $\forall (i, j) \in L$ using equations (6.27)-(6.30);
  $t = t + T_{sm}$; Reset timer T_{sm};
end while
Return P_f

6.7 Elitist Non-Dominated Sorting Genetic Algorithm for Multi-Objective Power-Aware Routing

NSGA-II has not yet been applied to the multi-objective power-aware routing problem. This section proposes for the first time to solve the multi-objective power-aware routing problem using an adaptation of the NSGA-II algorithm called NSGA-II multi-objective power-aware algorithm (NSGA-II-MPA).

NSGA-II-MPA modifies the NSGA-II procedure in tracking a new Pareto-optimal front as soon as there is a change in the multi-objective power-aware routing problem. The change in the problem is introduced with the application of the mobility model. Hence, the position of the nodes changes and, as a result, there is a change in objective functions.

As with the five ant algorithms proposed in this thesis, the dynamic multi-objective power-aware routing problem is based on the principle of dividing the simulation time, $S_{T_{tot}}$, into n_{ts} time slices of equal length, $S_{T_{tot}}/T_{sm}$. T_{sm} is the length of the pause time for the mobility model. T_{sm} is an indication of frequency of change (refer to Section 5.1). During each time slice a static problem is created, and optimisation is carried out using the standard NSGA-II. For each of these static problems the aim is to simultaneously minimise the five objectives and to create a population, P_t, with several non-domination fronts that have been found within the time slice. The population, P_t, may be passed on to the static problem corresponding to the following time slice since the two problems would potentially be very similar. This operation would prevent optimisation from having to restart each time from scratch and would contribute greatly to the good performance of the NSGA-II-MPA algorithm. To introduce diversity into the non-dominated solutions obtained by the NSGA-II-MPA algorithm, a number of random solutions are added whenever there is a change in the problem. The number of random solutions is equal to a percentage of the population, P_t. When this percentage of random solutions increases, the performance of NSGA-II-MPA deteriorates. More generations are needed to track the new optimal front. At each change, the P_t archive is re-evaluated and non-dominated sorting is applied.

Considering the power-aware routing problem formulation as given in Section 6.4.1, the NSGA-II-PMA is described in more detail below.

The first iteration consists of the following three steps:

1. **Initialise all parameters**.

2. **Build routing tables**. A procedure for building the routing tables is executed to build possible paths from the source, s, to the destination, D, of the network. This procedure selects the R paths with minimum energy consumed per packet and with minimum cost per packet where R is a parameter of the algorithm. The k shortest path algorithm is used to select the R paths [222].

3. **Calculate initial population, P_0**.

   From the routing tables, $|P_0|$ different random chromosomes are generated. This set of chromosomes is termed the chromosome pool, P_0 (or population), and it forms the first generation. Duplicated solutions in the population are replaced with new randomly generated solutions. A chromosome is represented by a binary string of size $\log_2(R)$, in order to represent R different paths. Each chromosome represents a possible route (path) between the source node, s, and the destination node, D.

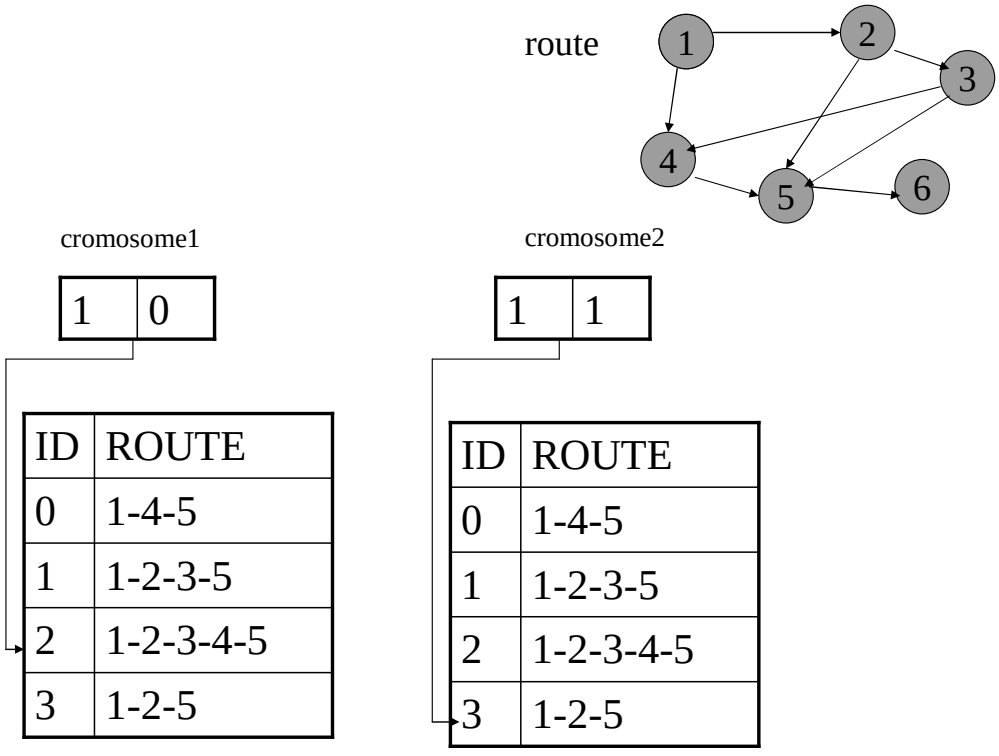

Figure 6.4: Routing tables and chromosomes

In the example of Figure 6.4 the routing table contains 4 paths ($R = 4$) with minimum energy consumed per packet and minimum cost per packet from $s = 1$ to $D = 5$. Each chromosome consists of a binary string of size 2 ($\log_2(4)$) and points to a specific path of the routing table. For example, the chromosome with a binary value of 10 has a decimal value of 2 and points to the path with $id = 2$ (path $1 - 2 - 3 - 4 - 5$).

Parents are selected from the population by using binary tournament selection based on the rank and crowding distance. Out of two individuals the individual with the lowest rank is selected, or, if both individuals have the same rank, the individual with the greater crowding distance is selected (refer to Section 4.6.2). The population selected generates offspring using crossover and mutation operators. Using the genetic operators, a child population Q_0 of size N_p is created.

The simulation (main loop) is run for $S_{T_{tot}}$ seconds with the following instructions: Within the time slice, T_{sm}, the maximum number of allowed generations are used to find the optimal population.

At each iteration, t, the following steps, as for the standard NSGA-II (refer to Section 4.6.2) are applied: The population, P_t, is evaluated against the five sub-objectives. Using binary tournament selection on parent population, P_t, of size N_p, based on the rank and crowding distance and applying crossover and mutation operators, Q_t offspring, of size N_p, are created. The combined population, $R_t = P_t \cup Q_t$, of size $2N_p$, is sorted into different non-domination levels. Individuals are then selected from this combined population to be inserted into the new population on the basis of their non-domination level. If there are more individuals in the last front than there are slots remaining in the new population of size N_p, a diversity preserving mechanism based on rank and the crowding distance on the last front is employed. Individuals from this last front are placed in the new population, P_{t+1}, on the basis of their contribution to diversity in the population.

At the end of time slice, T_{sm}, the ApplyMobilityChangesNSGA procedure, as given in Algorithm 20, and RebuildRoutesUpdatePopulation as given in Algorithm 21, handle the dynamic aspect of the power-aware routing problem.

The ApplyMobilityChangesNSGA procedure sends one packet from the source to the destination. In order to send the packet, a route T_{best} from P_{t+1} is used. T_{best} is the individual with rank 1 and the largest crowding distance. The RPGM mobility model

(refer to Section 6.5) is applied. Energy levels and distances are recalculated (refer to Section 6.5).

The RebuildRoutesUpdatePopulation procedure applies the following modifications to the original NSGA-II procedure, whenever a change in the multi-objective power-aware routing problem occurs:

- All parent solutions are re-evaluated before merging the parent and child populations into a bigger pool. This process allows both offspring and parent solutions to be evaluated using the changed sub-objectives.

- New random solutions are introduced. If N_e represents the first N_e solutions of the population, P_t, a percentage, $\varpi = \frac{N_p - N_e}{N_p}\%$, of the new population is replaced with randomly created solutions which helps to improve exploration. The first N_e solutions of P_t are kept in the archive to maintain elitism. The population, P_t, is completed up to the maximum size N_p, using $N_p - N_e$ new chromosomes generated based on routing tables which are created using the k shortest path algorithm. The final P_t is passed onto the next static problem.

Algorithm 20 General Procedure of ApplyMobilityChangesNSGA

```
Choose the best route, T_best, from P_t;
Send one packet from source to destination using T_best;
for all nodes i ∈ T_best do
  Update e_i^c according to equation (6.18);
end for
Apply the RPGM mobility model (refer to Section 6.5);
for all links (i, j) ∈ L do
  Recalculate d_ij;
  Recalculate E_ij according to equation (6.19);
end for
```

The algorithm moves to the next time slice optimising the new static problem until the end of the simulation.

The NSGA-II algorithm for multi-objective power-aware routing problem is summarised in Algorithm 22.

Algorithm 21 General Procedure for RebuildRoutesUpdatePopulation

Delete invalid routes associated with P_t, i.e. routes for which $E_{ij} > e_i^c$ or $d_{ij} > T_r$;
for all $T \in P_t$ **do**
  Re-evaluate the sub-objectives using equations (6.2), (6.3), (6.5), (6.9), (6.11);
end for
Apply non-dominated-sort on P_t; {refer to Section 4.6.2, Algorithm 9}
Find the first N_e individuals from P_t based on the rank and crowding distance; {An individual is selected if the rank is lesser than the other, or if the rank is the same and the crowding distance is greater than that of the other individuals}
The population P_e with $|P_e| = N_e$ is created;
The corresponding paths, T_{N_e}, are selected; {P_e represent the elitist solutions}
Build routing table T_{N_l} with $N_l = N_p - N_e$ paths from s to D; {Using the k shortest path algorithm}
Complete the routing table, $T_{N_p} = T_{N_l} \cup T_{N_e}$;
From T_{N_p} generate N_p different chromosomes, which form the new generation P_t;
Using the genetic operators on P_t, a child population Q_t of size N_p is created;

6.8 Summary

This chapter presented five new ant-based algorithms to solve the power-aware routing problem. Versions of each algorithm have been developed assuming that the optimisation problem is static. Each algorithm is then adapted to also solve the power-aware routing problem in changing environments under the RPGM mobility model. The chapter also presented an adaptation to the NSGA-II to solve the power-aware routing problem.

The next chapter empirically analyses the five algorithms, and compares their performance to that of the NSGA-II.

Algorithm 22 General Procedure of NSGA-II for the Multi-objective Power-Aware Routing Problem

Initialise E_i, e_i^c, $\forall i \in V$;
Calculate E_{ij}, d_{ij}, $\forall (i,j) \in L$;
Create initial routing tables; {Using the k shortest path algorithm}
Create a random population, P_0, from the routing tables;
Evaluate the sub-objectives for all $T \in P_0$ using equations (6.2), (6.3), (6.5), (6.9), (6.11);
$\mathcal{Z}$ = non-dominated-sort(P_0); {refer to Section 4.6.2, Algorithm 9}
Use binary tournament selection, recombination, and mutation operators to create a child population Q_0 of size N_p;
$simulation\_time = 0$; Set timer T_{sm};
while $simulation\_time <= S_{T_{tot}}$ **do**
  $t = 0$;
  {begin resolving static NSGA-II}
  while T_{sm} seconds not elapsed **do**
    for all $T \in P_t$ **do**
      Re-evaluate the sub-objectives using equations (6.2), (6.3), (6.5), (6.9), (6.11);
    end for
    $R_t = P_t \cup Q_t$; {combine parent and children population}
    $\mathcal{Z}$ = non-dominated-sort(R_t); {$\mathcal{Z} = (\mathcal{Z}_1, \mathcal{Z}_2, ...)$, all non-dominated fronts of R_t}
    $P_{t+1} = \emptyset$;
    $i = 1$;
    {untill the parent population is filled}
    while $|P_{t+1}| + |\mathcal{Z}_i| <= N_p$ **do**
      crowding-distance-assignment($\mathcal{Z}_i$); {calculate crowding distance in $\mathcal{Z}_i$ using Algorithm 10};
      $P_{t+1} = P_{t+1} \cup \mathcal{Z}_i$; {include i-th non-dominated front in the parent population}
      $i = i + 1$; {check the next front for inclusion}
    end while
    Sort($\mathcal{Z}_i, \prec_n$); {sort in descending order using the crowded comparison operator, $\prec_n$}
    $P_{t+1} = P_{t+1} \cup \mathcal{Z}_i[1 : (N_p - |P_{t+1}|)]$; {Choose the first $(N_p - |P_{t+1}|)$ elements of $\mathcal{Z}_i$}
    Q_{t+1} = make-new-pop(P_{t+1}); {Use selection, recombination, and mutation operators to create a child population Q_{t+1}}
    $t = t + 1$; {increment the generation counter}
  end while
  {end resolving static NSGA-II}
  Call Procedure ApplyMobilityChangesNSGA() (refer to Algorithm 20);
  Call procedure RebuildRoutesUpdatePopulation() (refer to Algorithm 21);
  $simulation\_time = simulation\_time + T_{sm}$;
  $P_0 = P_t$;
  $Q_0 = Q_t$;
  Reset T_{sm};
end while
Return P_t;

Chapter 7

Simulation and Empirical Analysis

This chapter contains an empirical study of the performance of the five multi-objective ant colony optimisation algorithms presented in this thesis, and an analysis of the influence of various algorithmic features on performance. The five algorithms are compared to each other and also to a state-of-the-art, multi-objective evolutionary algorithm, the NSGA-II, which was adapted in this thesis (refer to Section 6.7) for the multi-objective, power-aware routing problem. This chapter refers to the adapted NSGA-II as the NSGA-II-MPA. Several numeric simulations are presented and discussed with the goal of validating the algorithms which have been implemented.

The remainder of this chapter is organised as follows: Section 7.1 describes the experimental procedure which was followed in order to test the five algorithms. Section 7.2 presents the empirical analysis of control parameters. Section 7.3 discusses parameter settings for NSGA-II-MPA. Section 7.4 compares the implemented algorithms, while Section 7.5 concludes the chapter.

7.1 Experimental Procedure

Different network configurations (scenarios) are tested for each algorithm and the Pareto fronts are obtained for each of the algorithms. The following subsections describe the different network scenarios, the simulation environment, and the performance measures used to compare the different Pareto fronts.

7.1.1 Network Scenarios

A number of different network scenarios were considered, where the characteristics of each scenario differ in the number of nodes, N_G, pause time, T_{sm}, and the global range of the mobility model, R_g. Table 7.1 illustrates the different values for N_G, T_{sm} and R_g, from which a total of 54 scenarios have been generated as listed in Table 7.2.

Table 7.1: Different simulation parameters used to generate network scenarios

	N_G	T_{sm}	R_g
value 1	30	1 sec	300 m
value 2	100	2 sec	500 m
value 3	300	3 sec	800 m
value 4		4 sec	
value 5		5 sec	
value 6		6 sec	

Table 7.2: List of scenarios for comparing the algorithms

Scenario Name	Configuration	Scenario Name	Configuration
scenario 1a	$N_G = 30$, $R_g = 300$ m, $T_{sm} = 1$ sec	scenario 6a	$N_G = 100$, $R_g = 800$, $T_{sm} = 1$ sec
scenario 1b	$N_G = 30$, $R_g = 300$ m, $T_{sm} = 2$ sec	scenario 6b	$N_G = 100$, $R_g = 800$, $T_{sm} = 2$ sec
scenario 1c	$N_G = 30$, $R_g = 300$ m, $T_{sm} = 3$ sec	scenario 6c	$N_G = 100$, $R_g = 800$, $T_{sm} = 3$ sec
scenario 1d	$N_G = 30$, $R_g = 300$ m, $T_{sm} = 4$ sec	scenario 6d	$N_G = 100$, $R_g = 800$, $T_{sm} = 4$ sec
scenario 1e	$N_G = 30$, $R_g = 300$ m, $T_{sm} = 5$ sec	scenario 6e	$N_G = 100$, $R_g = 800$, $T_{sm} = 5$ sec
scenario 1f	$N_G = 30$, $R_g = 300$ m, $T_{sm} = 6$ sec	scenario 6f	$N_G = 100$, $R_g = 800$, $T_{sm} = 6$ sec
scenario 2a	$N_G = 30$, $R_g = 500$ m, $T_{sm} = 1$ sec	scenario 7a	$N_G = 300$, $R_g = 300$, $T_{sm} = 1$ sec
scenario 2b	$N_G = 30$, $R_g = 500$ m, $T_{sm} = 2$ sec	scenario 7b	$N_G = 300$, $R_g = 300$, $T_{sm} = 2$ sec
scenario 2c	$N_G = 30$, $R_g = 500$ m, $T_{sm} = 3$ sec	scenario 7c	$N_G = 300$, $R_g = 300$, $T_{sm} = 3$ sec
scenario 2d	$N_G = 30$, $R_g = 500$ m, $T_{sm} = 4$ sec	scenario 7d	$N_G = 300$, $R_g = 300$, $T_{sm} = 4$ sec
scenario 2e	$N_G = 30$, $R_g = 500$ m, $T_{sm} = 5$ sec	scenario 7e	$N_G = 300$, $R_g = 300$, $T_{sm} = 5$ sec
scenario 2f	$N_G = 30$, $R_g = 500$ m, $T_{sm} = 6$ sec	scenario 7f	$N_G = 300$, $R_g = 300$, $T_{sm} = 6$ sec
scenario 3a	$N_G = 30$, $R_g = 800$ m, $T_{sm} = 1$ sec	scenario 8a	$N_G = 300$, $R_g = 500$, $T_{sm} = 1$ sec
scenario 3b	$N_G = 30$, $R_g = 800$ m, $T_{sm} = 2$ sec	scenario 8b	$N_G = 300$, $R_g = 500$, $T_{sm} = 2$ sec
scenario 3c	$N_G = 30$, $R_g = 800$ m, $T_{sm} = 3$ sec	scenario 8c	$N_G = 300$, $R_g = 500$, $T_{sm} = 3$ sec
scenario 3d	$N_G = 30$, $R_g = 800$ m, $T_{sm} = 4$ sec	scenario 8d	$N_G = 300$, $R_g = 500$, $T_{sm} = 4$ sec
scenario 3e	$N_G = 30$, $R_g = 800$ m, $T_{sm} = 5$ sec	scenario 8e	$N_G = 300$, $R_g = 500$, $T_{sm} = 5$ sec
scenario 3f	$N_G = 30$, $R_g = 800$ m, $T_{sm} = 6$ sec	scenario 8f	$N_G = 300$, $R_g = 500$, $T_{sm} = 6$ sec
scenario 4a	$N_G = 100$, $R_g = 300$ m, $T_{sm} = 1$ sec	scenario 9a	$N_G = 300$, $R_g = 800$, $T_{sm} = 1$ sec
scenario 4b	$N_G = 100$, $R_g = 300$ m, $T_{sm} = 2$ sec	scenario 9b	$N_G = 300$, $R_g = 800$, $T_{sm} = 2$ sec
scenario 4c	$N_G = 100$, $R_g = 300$ m, $T_{sm} = 3$ sec	scenario 9c	$N_G = 300$, $R_g = 800$, $T_{sm} = 3$ sec
scenario 4d	$N_G = 100$, $R_g = 300$ m, $T_{sm} = 4$ sec	scenario 9d	$N_G = 300$, $R_g = 800$, $T_{sm} = 4$ sec
scenario 4e	$N_G = 100$, $R_g = 300$ m, $T_{sm} = 5$ sec	scenario 9e	$N_G = 300$, $R_g = 800$, $T_{sm} = 5$ sec
scenario 4f	$N_G = 100$, $R_g = 300$ m, $T_{sm} = 6$ sec	scenario 9f	$N_G = 300$, $R_g = 800$, $T_{sm} = 6$ sec
scenario 5a	$N_G = 100$, $R_g = 500$ m, $T_{sm} = 1$ sec	scenario 5d	$N_G = 100$, $R_g = 500$, $T_{sm} = 4$ sec
scenario 5b	$N_G = 100$, $R_g = 500$ m, $T_{sm} = 2$ sec	scenario 5e	$N_G = 100$, $R_g = 500$, $T_{sm} = 5$ sec
scenario 5c	$N_G = 100$, $R_g = 500$ m, $T_{sm} = 3$ sec	scenario 5f	$N_G = 100$, $R_g = 500$, $T_{sm} = 6$ sec

Values of N_G from 30 to 300 represent a small to large network which enables a scalability analysis of the algorithms. Values of T_{sm} from 1 sec to 6 sec determine how often the environment changes and represent high to low change frequencies. Values of R_g from 300 meters to 800 meters determine the amount of displacement of the current location of the optimum and represent low to high change severities.

The performance of each algorithm was tested under all 54 scenarios. For each of the scenarios 30 independent simulations have been executed and results are reported as averages over these simulations. Both the comparative results and the empirical results of the impact of the parameters in terms of the performance of each algorithm are reported in Section 7.4.

In order to test the quality of the solutions, a high initial energy of 400 energy units was used for each node.

7.1.2 Simulation Environment

The simulation environment generates a network topology consisting of a number of nodes. Initial placement of nodes was made randomly within the simulation environment, which is a circular area with a diameter of 300m, 500m, or 800m. Nodes move within this area according to the RPGM model (refer to Section 6.5). The centre of the circular area is also mobile, and its motion follows the RWP model (refer to Section 2.4).

All the nodes have a resting period of T_{sm} seconds. T_{sm} determines the change frequency. The performance of each algorithm was checked for $T_{sm} = 1$, $T_{sm} = 2$, $T_{sm} = 3$, $T_{sm} = 4$, $T_{sm} = 5$, and $T_{sm} = 6$ seconds. After the resting period all the nodes moved in accordance with the RWP mobility model. This process repeated itself throughout the simulation, thus bringing about continuous changes in the topology of the underlying network. The number of changes for each simulation is $S_{T_{tot}} \ / \ T_{sm}$, where $S_{T_{tot}}$ is the total simulation time.

Before the topology changes, a number of iterations of the multi-objective optimisation algorithm had taken place and, at each iteration, each ant had calculated a solution, T, evaluated the solution and, if non-dominated, inserted the solution into the Pareto set, P_s. Thereafter, the solutions in P_s which were dominated by T were deleted from P_s. Before the mobility model was applied again, a packet was sent from the source node to the destination node using a random route, T_s, from the Pareto set list and the ApplyMobilityChanges procedure was executed (refer to Algorithm 12).

7.1.3 Performance Measures

The five proposed algorithms and the NSGA-II-MPA algorithm each produced an estimated Pareto front, $\mathcal{PF}$ ($P_{EEMACOMP}$, $P_{EEMACOMH}$, $P_{EEMMASMP}$, $P_{EEMMASMH}$, $P_{EEMACOMC}$, and $P_{NSGA-II-MPA}$). Each $\mathcal{PF}$ was evaluated using three quantitative metrics, discussed in Section 4.7.2:

- **The ND metric**: The number of non-dominated solutions is computed, noted as $\bar{n}_{alg}$ in the result tables.
- **The spread metric**: The diversity of solutions in each Pareto front is computed using the spread metric, noted $\bar{\varrho}$ in the result tables.
- **The hypervolume measure**: The size of the dominated space is computed using the hypervolume measure, noted $\bar{\xi}$ in the result tables.

Simulation of the five algorithms presented the following practical problems. Firstly, due to mobility, different independent runs of the algorithms produced results that differed significantly. To overcome this high variability, performance measures were calculated as averages over 30 independent runs for each of the algorithms. For each scenario, each algorithm is therefore executed thirty times, with each execution starting from different initial conditions. For each run of an algorithm a Pareto-optimal set of solutions, $\mathcal{PF}$, was computed, one for each network topology. The number of times that one algorithm has a better n_{alg}, ϱ, and ξ average than all the other algorithms before each change, is counted and referred to as n^w_{alg}, ϱ^w, and ξ^w respectively. The total average for all iterations before a change to the environment occurs, further averaged over 30 simulations is calculated for each metric and referred to as $\bar{n}_{alg}$, $\bar{\varrho}$, and $\bar{\xi}$. The standard deviation, and a 95% confidence interval, CI, is provided next to each value.

Secondly, when simulating the algorithms the network topology changes after the mobility model is applied. For fair comparison among the different algorithms, it is important that the algorithms are tested on the same sequence of topology changes. Therefore, based on the mobility model used, a sequence of node changes is determined for each of the 30 runs. All algorithms are then evaluated on these change sequences.

The objective of the experiments is to analyse and compare the performance of the six algorithms according to the metrics listed above.

7.1.4 Sending a Packet

A network initialised with random or uniform pheromone tables will not contain any useful information about good routes. After a short time has elapsed, the largest probabilities in the pheromone tables of each node will define relatively optimal routes. For example, after 500 time steps or 5 seconds, the algorithm will converge on typically good routes in relation to the five objectives, and a packet may be sent from the source to the destination. Therefore, each algorithm runs for the allowed pause time, T_{sm}, before sending a packet.

7.2 Empirical Analysis of the Ant-Based Algorithms Control Parameters

The space of possible control parameter settings for the five ant algorithms is large, including parameters r_0, ρ_l, ρ_g, α, β_ν, β_ξ, β_π, β_ϱ, β_ς, λ_E, λ_ν, λ_ξ, λ_π, λ_ϱ, λ_ς, and P_{as}.

The objective of this section is to perform a sensitivity analysis of these parameters in order to derive suggestions of how the parameters should be initialized for best performance. For each parameter, a number of values were tested while all the other parameters were held constant. The default value of the parameters is: $\beta_\nu = 3.0$, $\beta_\xi = 3.0$, $\beta_\pi = 3.0$, $\beta_\varrho = 3.0$, $\beta_\varsigma = 3.0$, $S_{T_{tot}}$=120sec, $r_0 = 0.5$, $\rho_l = 0.5$, $\rho_g = 0.5$, $\alpha = 1.0$, $\lambda_E = 6$, $\lambda_\nu = 0.2$, $\lambda_\xi = 0.2$, $\lambda_\pi = 0.2$, $\lambda_\varrho = 0.2$, $\lambda_\varsigma = 0.2$, $P_{as} = 100$. These values were obtained using a trial-and-error process for finding preliminary best parameter settings. For each parameter value the Pareto front, $\mathcal{PF}$, was obtained using the process described in Section 7.1.3. The performance metrics listed in Section 7.1.3 were computed for each of these Pareto fronts and used to determine the best values for each control parameter. Due to space limitations, the influence of parameter values is only presented for a 30 nodes network.

The results of the empirical analysis of the ant-based algorithms control parameters are illustrated in Tables D.1-D.18 in Appendix D. Graphs of the performance metrics as a function of the different control parameters, T_{sm} and R_g, based on Tables D.1-D.18, are presented in Appendix E using the FluxViz software [1]. Relations between the different performance metrics and the parameter values with reference to different change frequencies are illustrated in two dimension figures. Each value is the average of

the three change severities. Relations between the different performance metrics and the parameter values with reference to different change severities are also illustrated in two dimension figures, where each value is the average of the six change frequencies.

The following subsections perform an empirical analysis of the sensitivity of the algorithms to the above parameters.

7.2.1 Heuristics vs Pheromone Parameters

Parameters β_ν, β_ξ, β_π, β_ϱ, and β_ς set the relative importance of heuristic versus pheromone information. In the transition rules for the developed algorithms (refer to equations (6.20), (6.31), (6.42), (6.48), and (6.54)), parameters β_ψ, where ψ represents either ν, ξ, π, ϱ, or ς depending on the sub-objective, are the exponents of heuristics, $\eta_{\psi_{ij}}$, which are defined as in equations (6.13)-(6.17). Heuristic values ranged between 0 (high link cost) and 1 (small link cost).

The larger the value of β_ψ, the smaller the emphasis on heuristic information, and learned desirability discovered by pheromone trails is favored. In this case, ants may choose non-optimal paths too quickly. On the other hand, a small value for β_ψ gives higher priority to heuristic information over pheromone and the algorithm becomes more greedy and leads to increased exploration.

In order to find the best value for all β_ψ parameters, values for these parameters were randomly selected from the range $[1, 7]$. The values $(\beta_\nu, \beta_\xi, \beta_\pi, \beta_\varrho, \beta_\varsigma) \in \{(1,1,1,1,1), (3,3,3,3,3), (3.5,4,4.5,4,5), (4.5,5,3.5,4,4), (5,5,5,5,5), (7,7,7,7,7)\}$ were selected and tested. For this study the rest of the parameter values were fixed as in Section 7.2.

Tables D.1-D.3 in appendix D summarise the empirical results for β_ψ using the $\bar{n}_{alg}$, $\bar{\varrho}$ and $\bar{\xi}$ metrics. These results are visualised using the FluxViz software in Figures E.1-E.15 in appendix E. These figures highlights the best results with blue indicating the best values for the $\bar{n}_{alg}$, $\bar{\varrho}$ and $\bar{\xi}$ metrics. Relations between the different performance metrics and the β_ψ values with reference to different change frequencies are illustrated in Figures 7.1-7.3. Relations between the different performance metrics and the β_ψ values with reference to different change severities are illustrated in Figures 7.4-7.6. The β_ψ axis represents the combination of the parameters $(\beta_\nu, \beta_\xi, \beta_\pi, \beta_\varrho, \beta_\varsigma)$ used in the experiments. Axis values of β_ψ=1, 2, 3, 4, 5, 6 respectively refer to parameter combinations $(1,1,1,1,1)$, $(3,3,3,3,3)$, $(3.5,4,4.5,4,5)$, $(4.5,5,3.5,4,4)$, $(5,5,5,5,5)$, and $(7,7,7,7,7)$.

The larger the number of non-dominated solutions, $\bar{n}_{alg}$, the better the effectiveness

of the MOO algorithm in generating desired solutions. A value of zero for $\bar{\varrho}$ indicates that all members of the Pareto front are equidistantly spaced. A higher value of $\bar{\xi}$ indicates that the obtained Pareto front is closer to the true Pareto front.

For each β_ψ parameter combination, referred to as an experiment, six different change frequencies (with $T_{sm} \in \{1, 2, 3, 4, 5, 6\}$) and three different change severities (with $R_g \in \{300, 500, 800\}$) were used. The same applies with the rest of the sections for the empirical analysis of the ant-based algorithms control parameters.

The rest of this section discusses the results obtained from the experiments with regards to the influence of β_ψ on the performance metrics.

1. **Influence of β_ψ on the number of non-dominated solutions, $\bar{n}_{alg}$.**

   Irrespective of the change frequency and change severity, for $(\beta_\nu, \beta_\xi, \beta_\pi, \beta_\varrho, \beta_\varsigma) \in \{(1, 1, 1, 1, 1), (3, 3, 3, 3, 3)\}$ all the algorithms produced a very low number of non-dominated solutions (refer to Figures E.1, E.4, E.7, E.10, E.13, 7.1, 7.4). For values of $(\beta_\nu, \beta_\xi, \beta_\pi, \beta_\varrho, \beta_\varsigma) = (3.5, 4, 4.5, 4, 5)$, $(\beta_\nu, \beta_\xi, \beta_\pi, \beta_\varrho, \beta_\varsigma) = (4.5, 5, 3.5, 4, 4)$, and $(\beta_\nu, \beta_\xi, \beta_\pi, \beta_\varrho, \beta_\varsigma) = (5, 5, 5, 5, 5)$ the best values of $\bar{n}_{alg}$ were obtained. Therefore, β_ψ should be large enough in order to have a strong focus on pheromone information.

   For all the experiments, $\bar{n}_{alg}$ decreased with increase in change frequency, T_{sm} (refer to Figure 7.1), which is expected. As frequency of change increases, the time available for adaptation becomes shorter and it becomes more difficult to find optimum solutions.

   Also, $\bar{n}_{alg}$ decreased with increase in change severity, R_g (refer to Figure 7.4), which is also expected. With high change severity there is a large displacement of the current location of the optimum and it is more difficult to adapt and to find optimal solutions.

2. **Influence of β_ψ on the spread metric, $\bar{\varrho}$.**

   Irrespective of the change frequency and change severity, for $(\beta_\nu, \beta_\xi, \beta_\pi, \beta_\varrho, \beta_\varsigma) \in \{(1, 1, 1, 1, 1), (3, 3, 3, 3, 3)\}$ all the algorithms displayed a higher value for $\bar{\varrho}$ which means less uniformly distributed solutions (refer to Figures E.2, E.5, E.8, E.11, E.14). For all values of $(\beta_\nu, \beta_\xi, \beta_\pi, \beta_\varrho, \beta_\varsigma) \in \{(3.5, 4, 4.5, 4, 5), (4.5, 5, 3.5, 4, 4), (5, 5, 5, 5, 5), (7, 7, 7, 7, 7)\}$ lower values of $\bar{\varrho}$ (more uniformly dis-

tributed solutions) were obtained. Higher values of β_ψ, and therefore a strong focus on pheromone information, produced a better solution spread.

A decrease in change frequency, T_{sm}, leads to more uniformly distributed solutions (refer to Figure 7.2), which is expected. As the change frequency decreases, the time left for adaptation gets larger and there are more iterations available to track the optima. The archive is more likely to become full several times, and each time the crowding distance is used in selecting which solution in the archive will be replaced with a new solution. This promotes diversity among the stored solutions in the archive since those solutions which are in the most crowded areas are most likely to be replaced by a new solution. At the end the archive will contain more non-dominated solutions which are in the least crowded area in the objective space, therefore, maintaining a good spread of non-dominated solutions.

The value of $\bar{\varrho}$ increased with increase in change severity, R_g (refer to Figure 7.5), which is also expected. When R_g increases, more iterations are needed to track the optima after the change occurred and therefore the distribution of solutions decreases correspondingly.

3. **Influence of β_ψ on the hypervolume metric, $\bar{\xi}$.**

   For $(\beta_\nu,\ \beta_\xi,\ \beta_\pi,\ \beta_\varrho,\ \beta_\varsigma) \in \{(1,1,1,1,1),(3,3,3,3,3)\}$ all the algorithms displayed a lower value of the $\bar{\xi}$ metric (refer to Figures E.3, E.6, E.9, E.12, E.15). For all values of $(\beta_\nu,\ \beta_\xi,\ \beta_\pi,\ \beta_\varrho,\ \beta_\varsigma) \in \{(3.5,4,4.5,4,5),(4.5,5,3.5,4,4),(5,5,5,5,5)\}$ the best values of $\bar{\xi}$ were obtained. For $(\beta_\nu,\ \beta_\xi,\ \beta_\pi,\ \beta_\varrho,\ \beta_\varsigma) = (7,7,7,7,7)$ all the algorithms presented a decline in value of the $\bar{\xi}$ metric (refer to Figures 7.3, 7.6) which shows that too much exploitation is not good. These observations are true for all change frequencies (refer to Figure 7.3) and all change severities (refer to Figure 7.6).

   The graphs indicate an increase in $\bar{\xi}$ with decrease in change frequency (refer to Figure 7.3). This result is expected since low change frequency gives more iterations, and theoretically is supposed to produce a uniform distribution of the solutions and closeness of the solutions to the optimal Pareto set, thus increasing the size of the dominated space (hypervolume measure). Also, the graphs indicate an increase of hypervolume, $\bar{\xi}$, with decrease in change severity (refer to Figure 7.6). It is intuitive to assume that smaller change severities are easier to adapt to, primar-

ily by transferring solutions from the past optimisation problem which may help to accelerate the rate of convergence to the optima, after a change has occurred. Therefore the closeness of the solutions to the optimal Pareto set should be getting worse as the change severity increases.

For the values of $(\beta_\nu, \beta_\xi, \beta_\pi, \beta_\varrho, \beta_\varsigma) \in \{(3.5, 4, 4.5, 4, 5), (4.5, 5, 3.5, 4, 4), (5, 5, 5, 5, 5)\}$, all algorithms displayed the best value, with reference to all three metrics. Accordingly, the value of $(\beta_\nu, \beta_\xi, \beta_\pi, \beta_\varrho, \beta_\varsigma) = (3, 4, 4.5, 4, 5)$ was adopted for the remainder of the simulations.

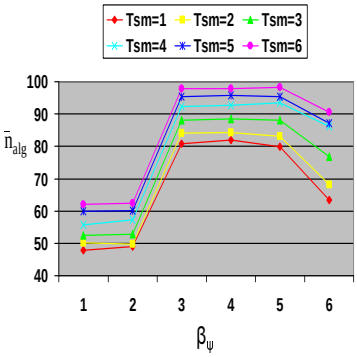

(a) EEMACOMP

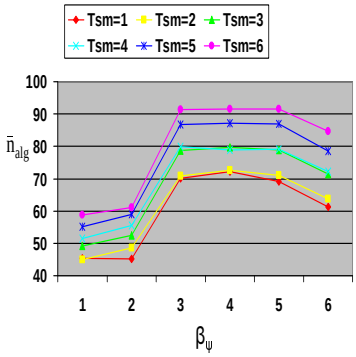

(b) EEMACOMH

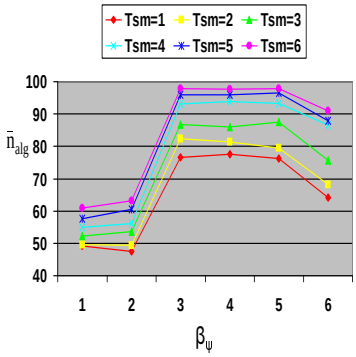

(c) EEMMASMP

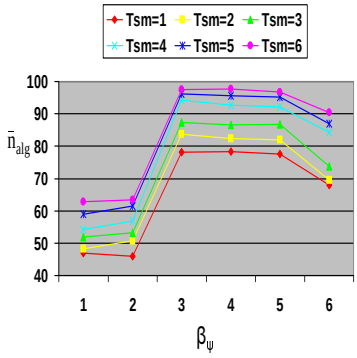

(d) EEMMASMH

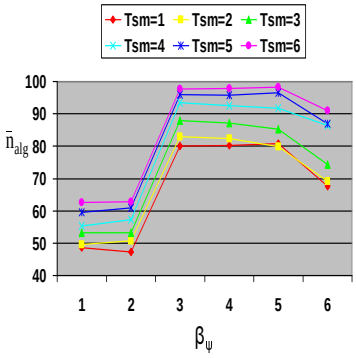

(e) EEMACOMC

Figure 7.1: Influence of β_ψ on $\bar{n}_{alg}$ metric, for different change frequencies, T_{sm}

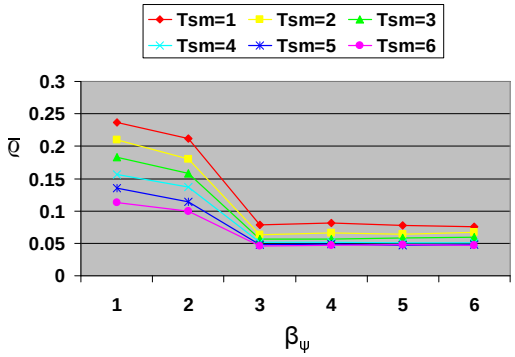

(a) EEMACOMP

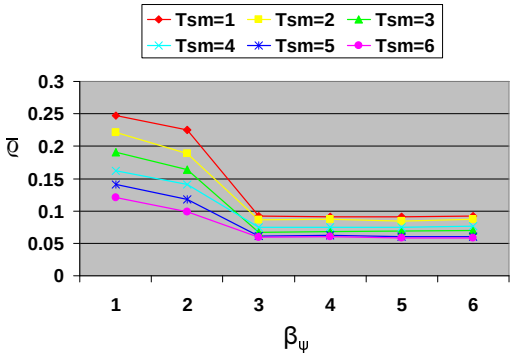

(b) EEMACOMH

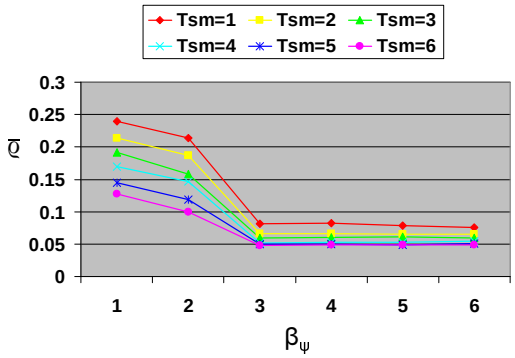

(c) EEMMASMP

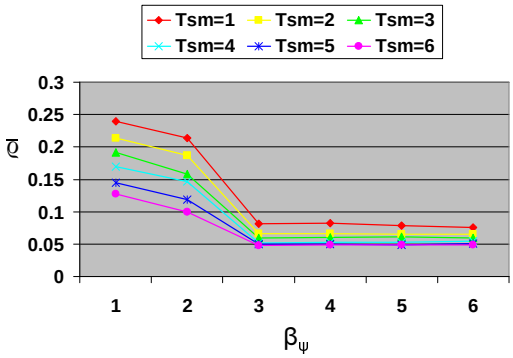

(d) EEMMASMH

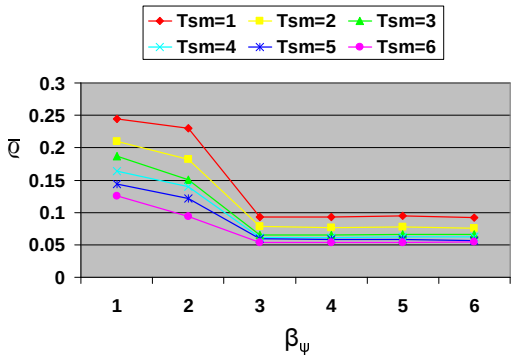

(e) EEMACOMC

Figure 7.2: Influence of β_ψ on $\bar{\varrho}$ metric, for different change frequencies, T_{sm}

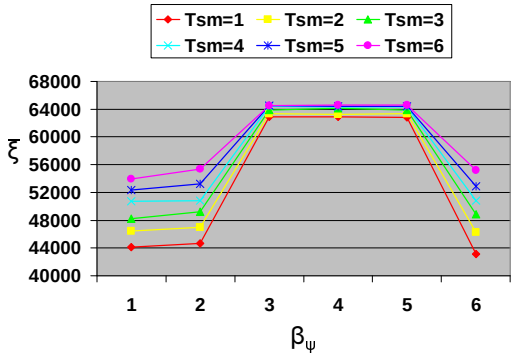

(a) EEMACOMP

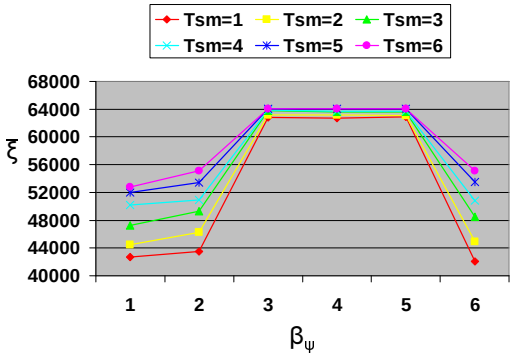

(b) EEMACOMH

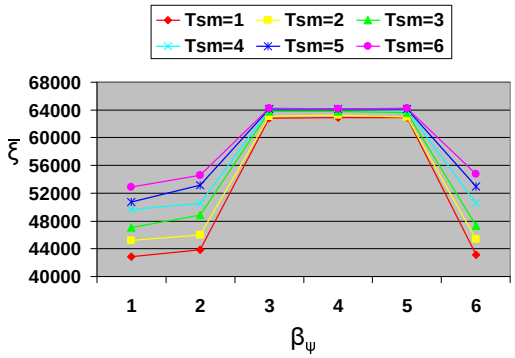

(c) EEMMASMP

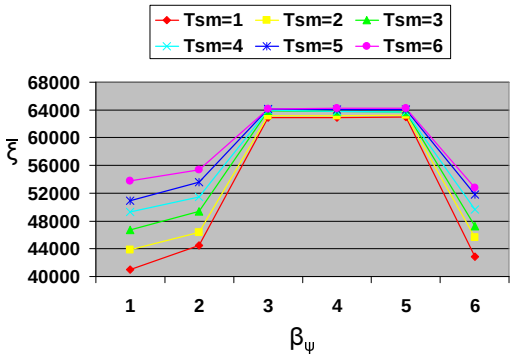

(d) EEMMASMH

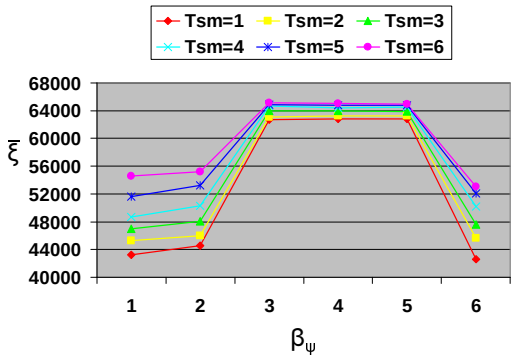

(e) EEMACOMC

Figure 7.3: Influence of β_ψ on $\bar{\xi}$ metric, for different change frequencies, T_{sm}

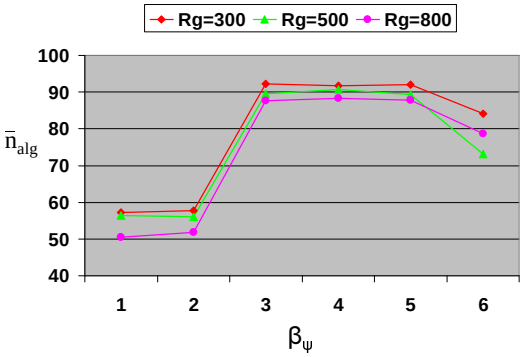

(a) EEMACOMP

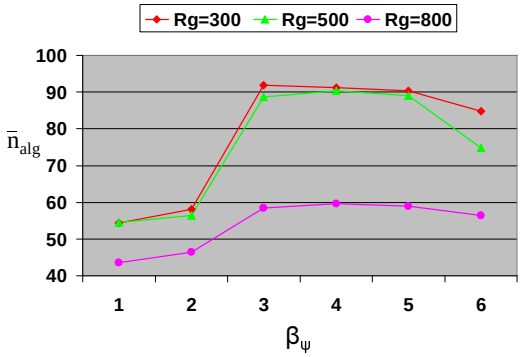

(b) EEMACOMH

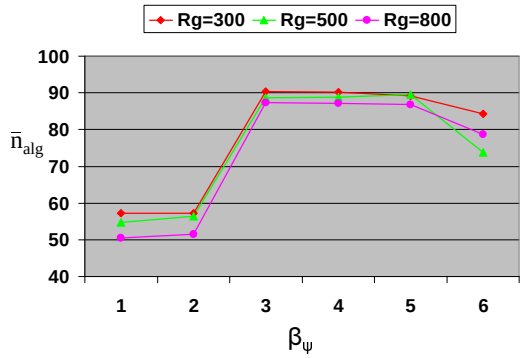

(c) EEMMASMP

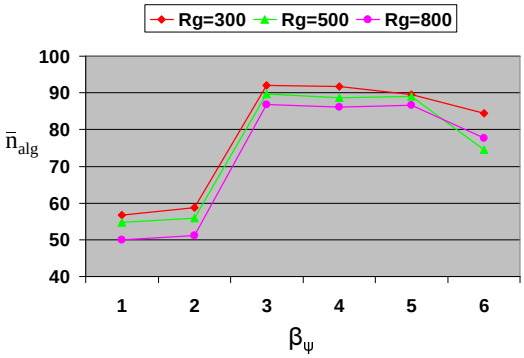

(d) EEMMASMH

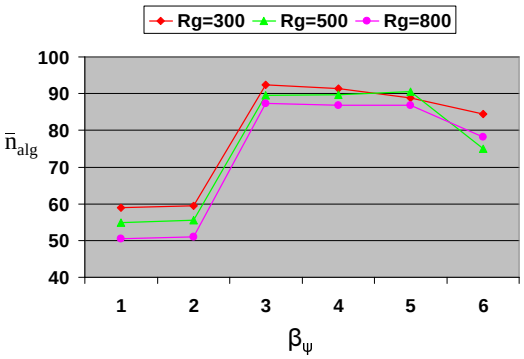

(e) EEMACOMC

Figure 7.4: Influence of β_ψ on $\bar{n}_{alg}$ metric, for different change severities, R_g

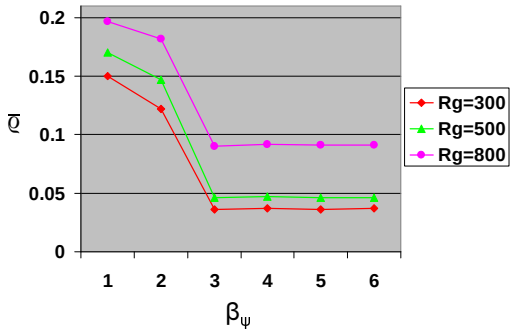

(a) EEMACOMP

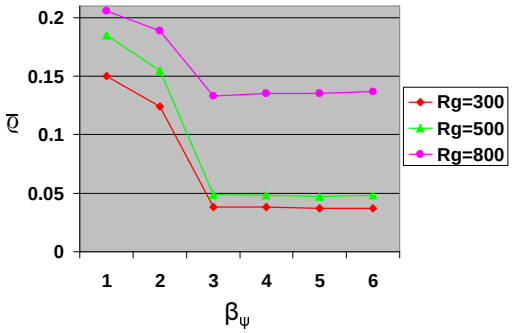

(b) EEMACOMH

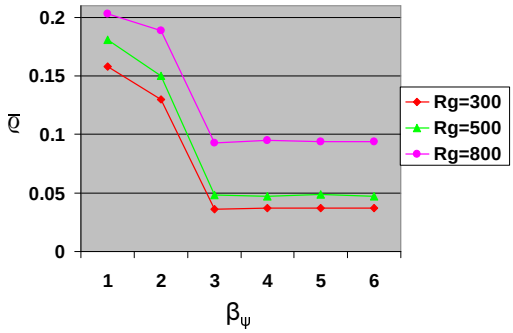

(c) EEMMASMP

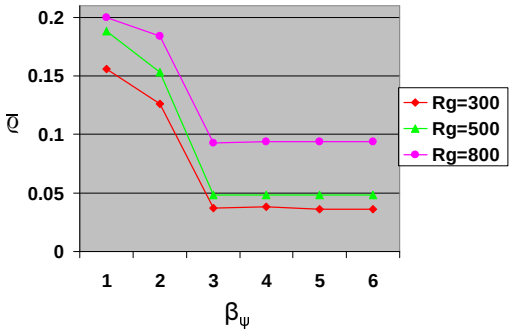

(d) EEMMASMH

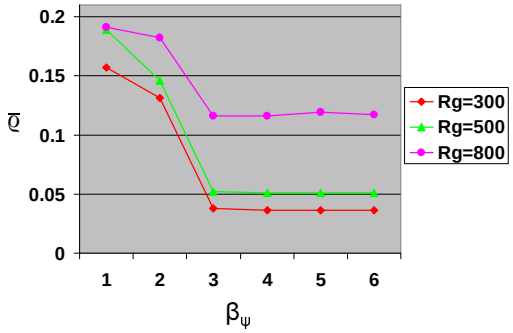

(e) EEMACOMC

Figure 7.5: Influence of β_ψ on $\bar{\varrho}$ metric, for different change severities, R_g

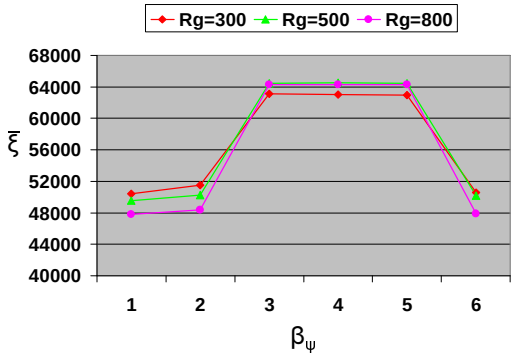

(a) EEMACOMP

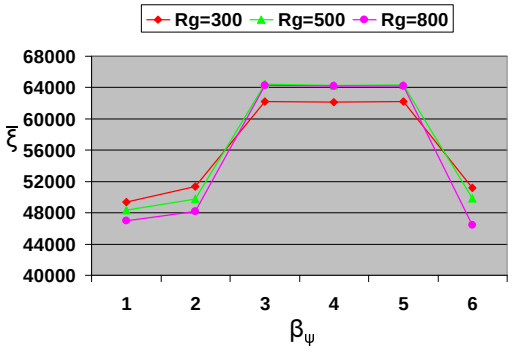

(b) EEMACOMH

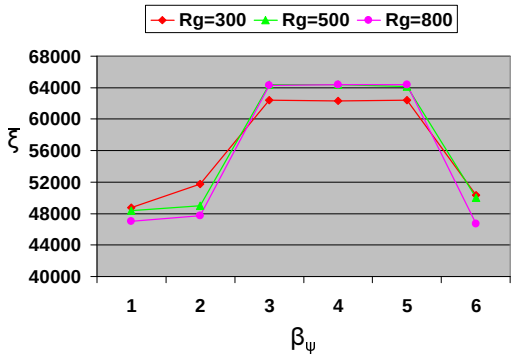

(c) EEMMASMP

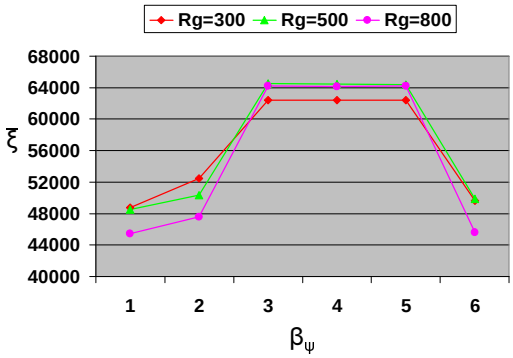

(d) EEMMASMH

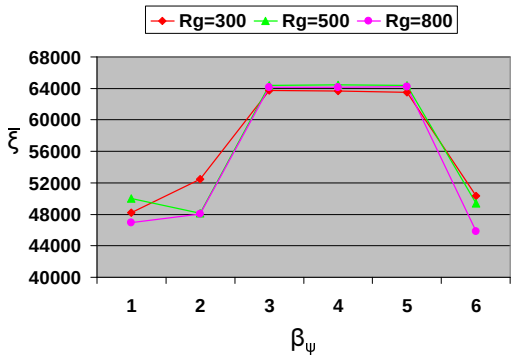

(e) EEMACOMC

Figure 7.6: Influence of β_ψ on $\bar{\xi}$ metric, for different change severities, R_g

7.2.2 Exploration Vs Exploitation Parameter, r_0

The parameter, r_0, is used in the ACS transition rule (refer to equations (6.20), (6.31), (6.54)) to control the balance between exploration and exploitation of the search space. Parameter r_0 takes values within the interval $[0, 1]$. When r_0 approaches zero, exploration is favoured. More focus can be given on exploitation instead of exploration by increasing the value of r_0.

In order to find the best value for r_0, five values were considered, namely $r_0 \in \{0.1,\ 0.3,\ 0.5,\ 0.7,\ 0.9\}$.

Since r_0 is an ACS specific parameter, the influence of r_0 is investigated only for the EEMACOMP, EEMACOMH and EEMACOMC algorithms, as these make use of the ACS equation to compute the transition probability (see equations (6.20), (6.31), (6.54)).

Tables D.4-D.6 summarise the empirical results for r_0 using the $\bar{n}_{alg}$, $\bar{\varrho}$ and $\bar{\xi}$ metrics. Results are visualised in Figures E.16-E.24. Relations between the different performance metrics and the r_0 values with reference to different change frequencies are illustrated in Figures 7.7-7.9. Relations between the different performance metrics and the r_0 values with reference to different change severities are illustrated in Figures 7.10-7.12.

The following parameter values were used based on the result of the previous section: $\beta_\nu = 3.5$, $\beta_\xi = 4.0$, $\beta_\pi = 4.5$, $\beta_\varrho = 4.5$, and $\beta_\varsigma = 5.0$. The rest of the parameter values were fixed as in Section 7.2.

The rest of this section discusses the results obtained from the experiments with regards to the influence of r_0 on the performance metrics.

1. **Influence of r_0 on the number of non-dominated solutions, $\bar{n}_{alg}$.**

   For the values of $r_0 \in \{0.5,\ 0.7,\ 0.9\}$ all the algorithms produced the largest $\bar{n}_{alg}$ irrespective of change frequencies and change severities. For $r_0 = 0.1$ and $r_0 = 0.3$ results are similar to the values of $r_0 \in \{0.5,\ 0.7,\ 0.9\}$ for lower change frequencies ($T_{sm} \in \{3, 4, 5, 6\}$). For $r_0 = 0.1$ and $r_0 = 0.3$ and higher change frequencies ($T_{sm} = 1$ and $T_{sm} = 2$) all the algorithms produced a very low number of non-dominated solutions compared to larger values of T_{sm} (refer to Figure 7.7). This result is expected because for $r_0 = 0.1$ and $r_0 = 0.3$ there is a high exploration of the search space and if the change frequency is too high environment changes may occur before convergence. That is, high exploration negatively affected the

number of non-dominated solutions for high change frequencies. For the values of $r_0 \in \{0.5,\ 0.7,\ 0.9\}$ all the algorithms produced the largest $\bar{n}_{alg}$ for high change frequencies which indicates that exploitation should be preferred under high change frequencies.

For all the experiments, $\bar{n}_{alg}$ increased with decrease in change frequency, T_{sm} (refer to Figure 7.7). This result is expected as low change frequencies provides more time to explore the search space, thereby finding more solutions.

The EEMACOMH algorithm produced the lowest number of non-dominated solutions for $R_g = 800$, for all values of r_0 (refer to Figure 7.10(b)).

Independent of change frequency and change severity, the best values for r_0 are $r_0 \in \{0.5,\ 0.7,\ 0.9\}$ (refer to Tables D.4-D.6 and Figures E.16, E.19, E.22).

2. **Influence of r_0 on the spread metric, $\bar{\varrho}$.**

   For values of $r_0 \in \{0.5,\ 0.7,\ 0.9\}$ all the algorithms produced a lower spread metric value producing more uniformly distributed solutions.

   Values of $r_0 = 0.1$ and $r_0 = 0.3$ produced the largest spread metric value with high change frequencies ($T_{sm} = 1$ and $T_{sm} = 2$). That is, high exploration negatively affected the solution spread for high change frequencies. The values of $r_0 = 0.1$ and $r_0 = 0.3$ produced a low spread metric value with low change frequencies ($T_{sm} \in \{3, 4, 5, 6\}$), for all ACO algorithms.

   The graphs indicate an increase in $\bar{\varrho}$ (i.e. deterioration in the solution spread) with increase in change severity (refer to Figure 7.11). When R_g increases, more iterations are needed to track the optima after the change occurred and therefore less time is available to reach a good distribution of solutions.

   The best values for the solution spread are produced with $r_0 = 0.5$, irrespective of change frequencies and change severities (refer to Tables D.4-D.6 and Figures E.17, E.20, E.23).

3. **Influence of r_0 on the hypervolume metric, $\bar{\xi}$.**

   For all change frequencies and all change severities the values of $r_0 = 0.1$ and $r_0 = 0.3$ produced the worst results for the hypervolume metric (refer to Figures E.18, E.21, E.24). That is, high exploration negatively affected the $\bar{\xi}$ metric. This is

related to the fact that the computational load of the hypervolume calculation sharply increases, the more criteria are considered (when the number of objectives increases). Combined with a high exploration of the search space, environment changes may occur before convergence thus affecting the hypervolume.

The graphs indicate an increase in $\bar{\xi}$ with decrease in change frequency (refer to Figure 7.9). Also, the graphs indicate an increase in $\bar{\xi}$, with decrease in change severity (refer to Figure 7.12).

The best values for the hypervolume were produced with $r_0 = 0.5$, for all change frequencies and all change severities.

A value of $r_0 = 0.5$ offers the best trade-off between metrics $\bar{n}_{alg}$, $\bar{\varrho}$ and $\bar{\xi}$ for all change frequencies and all change severities. Therefore, a value of 0.5 for r_0 was adopted for the remainder of the simulations.

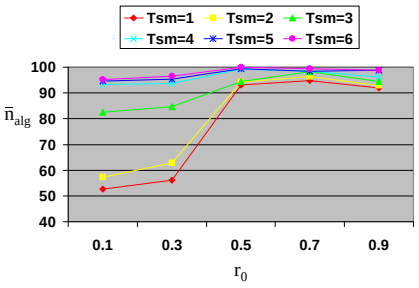

(a) EEMACOMP

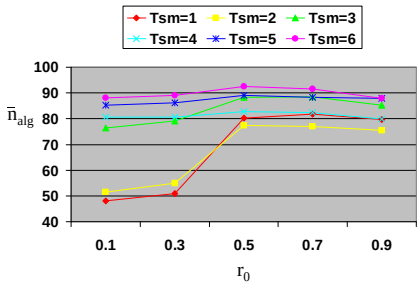

(b) EEMACOMH

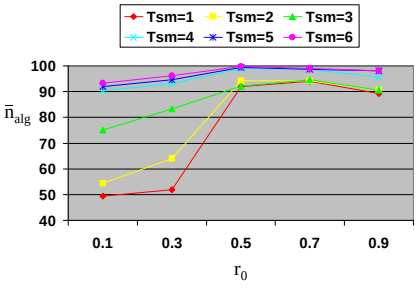

(c) EEMACOMC

Figure 7.7: Influence of r_0 on $\bar{n}_{alg}$ metric, for different change frequencies, T_{sm}

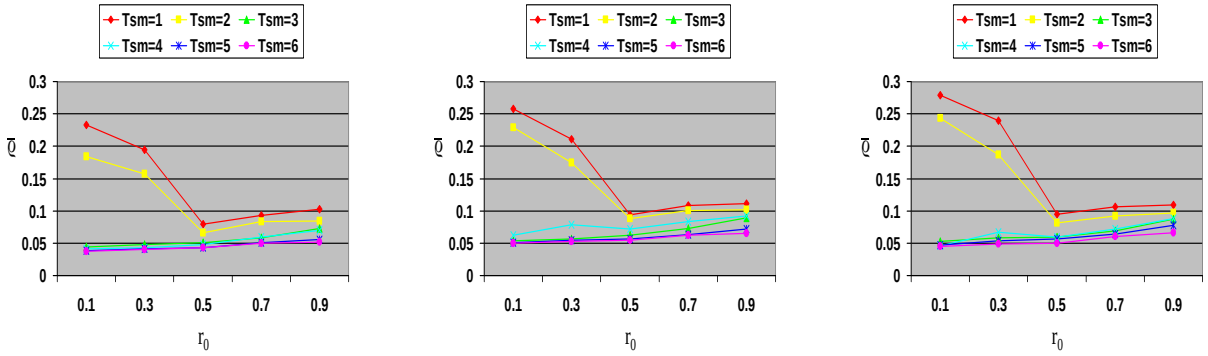

(a) EEMACOMP (b) EEMACOMH (c) EEMACOMC

Figure 7.8: Influence of r_0 on $\bar{\varrho}$ metric, for different change frequencies, T_{sm}

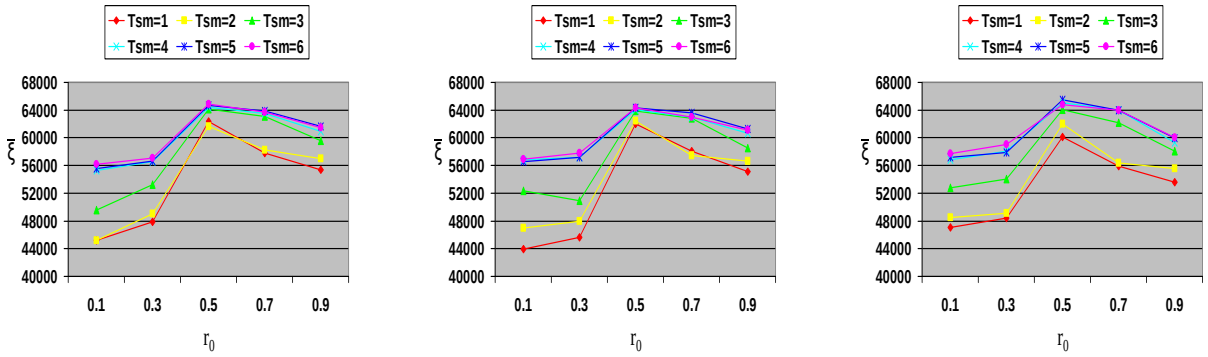

(a) EEMACOMP (b) EEMACOMH (c) EEMACOMC

Figure 7.9: Influence of r_0 on $\bar{\xi}$ metric, for different change frequencies, T_{sm}

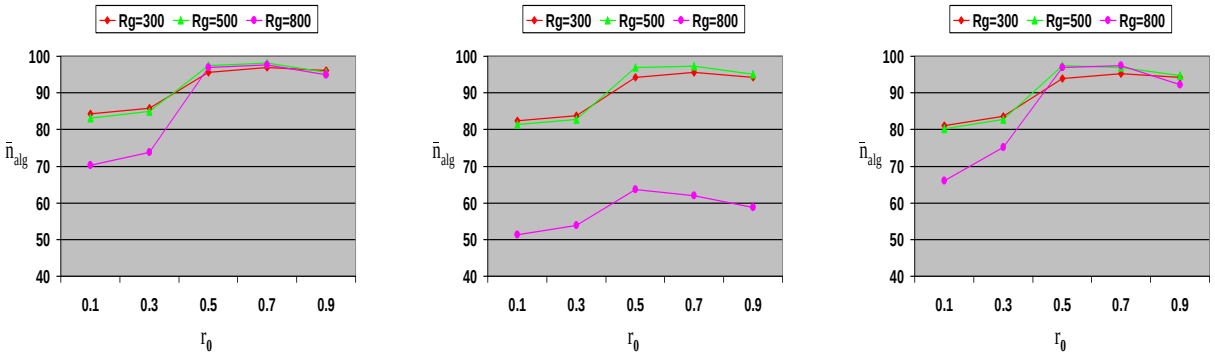

(a) EEMACOMP (b) EEMACOMH (c) EEMACOMC

Figure 7.10: Influence of r_0 on $\bar{n}_{alg}$ metric, for different change severities, R_g

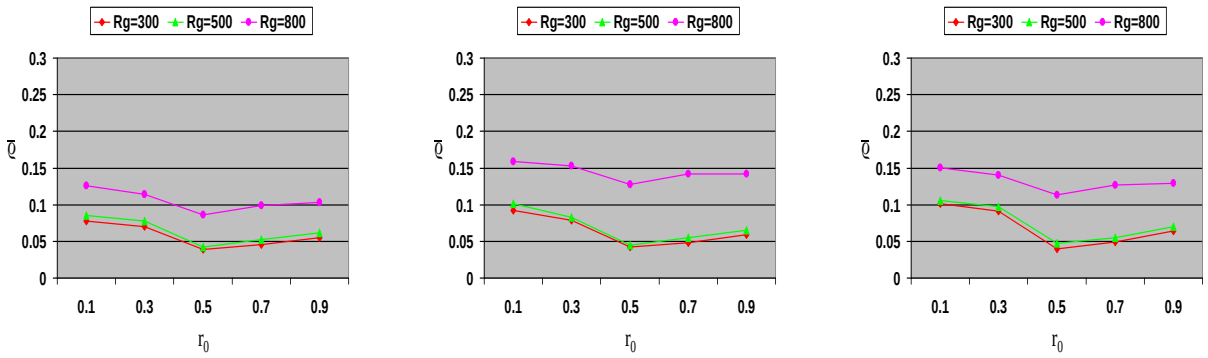

(a) EEMACOMP (b) EEMACOMH (c) EEMACOMC

Figure 7.11: Influence of r_0 on $\bar{\varrho}$ metric, for different change severities, R_g

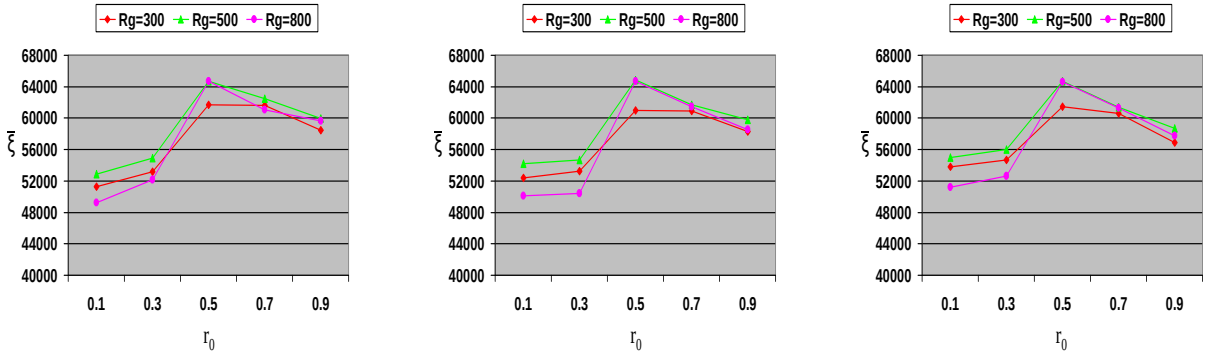

(a) EEMACOMP (b) EEMACOMH (c) EEMACOMC

Figure 7.12: Influence of r_0 on $\bar{\xi}$ metric, for different change severities, R_g

7.2.3 Local Decay Parameter, ρ_l

After each solution construction step, the local updating rule is applied for all the ACS based algorithms (refer to equations (6.26) and (6.37)). The local decay parameter, ρ_l, determines the rate at which pheromone on all the paths are evaporated after each step. Parameter ρ_l has values within the interval $[0, 1]$. A high value of ρ_l leaves less pheromone at each step. Consequently, the ants have less information on other ants' paths, and the

search is less focused, favouring exploration. More focus can be given on exploitation instead of exploration by decreasing the value of ρ_l.

In order to find the best value for ρ_l, five values for ρ_l were considered, namely $\rho_l \in \{0.1,\ 0.3,\ 0.5,\ 0.7,\ 0.9\}$. Since ρ_l is an ACS parameter, the influence of ρ_l is investigated only for the EEMACOMP, EEMACOMH and EEMACOMC algorithms, as these make use of the ACS local update rule. The following parameter values were used based on the result of sections 7.2.1-7.2.2: $\beta_\nu = 3.5$, $\beta_\xi = 4.0$, $\beta_\pi = 4.5$, $\beta_\varrho = 4.5$, $\beta_\varsigma = 5.0$, and $r_0 = 0.5$. The rest of the parameter values were fixed as in Section 7.2.

Tables D.7-D.9 summarise the empirical results for control parameter ρ_l using the $\bar{n}_{alg}$, $\bar{\varrho}$ and $\bar{\xi}$ performance metrics. Results are visualised in Figures E.25-E.33 and 7.13-7.18.

The rest of this subsection discusses the results obtained from the experiments with regards to the influence of ρ_l on the performance metrics.

1. **Influence of ρ_l on the number of non-dominated solutions, $\bar{n}_{alg}$.**

   All the algorithms produced high values for $\bar{n}_{alg}$ for all values of ρ_l and low change frequencies ($T_{sm} \in \{5, 6\}$). For values of $\rho_l = 0.1$ and $\rho_l = 0.3$ and high change frequencies ($T_{sm} \in \{1, 2, 3, 4\}$) (refer to Figure 7.13) all the algorithms struggled to find many non-dominated solutions. It is clear that too much exploitation (small ρ_l) is not good under high change frequency with regard to $\bar{n}_{alg}$. In fact, this observation is true for change frequencies $T_{sm} \in \{1, 2, 3, 4\}$ and all change severities (refer to Figures E.25, E.28, E.31, 7.13, 7.16).

   For all the experiments, $\bar{n}_{alg}$ decreased with increase in change frequency (refer to Figure 7.13). This result is expected since, as frequency of change increases, the time available for adaptation becomes shorter and it becomes more difficult to find optimum solutions.

   Results for $R_g = 800$ show that the EEMACOMH algorithm produced the lowest number of non-dominated solutions (refer to Figure 7.16(b)).

   The best results for the $\bar{n}_{alg}$ metric were obtained with $\rho_l \in \{0.5, 0.7\}$, irrespective of change frequencies and change severities (refer to Tables D.7-D.9 and Figures E.25, E.28, E.31, 7.13, 7.16).

2. **Influence of ρ_l on the spread metric, $\bar{\varrho}$.**

Results for $\rho_l = 0.1$ and $\rho_l = 0.3$ show that all the algorithms failed in obtaining a good spread in the found non-dominated solutions (refer to Figures E.26, E.29, E.32), irrespective of change severities and for change frequencies $T_{sm} \in \{1, 2, 3, 4\}$. The spacing metric for $\rho_l = 0.9$ is also higher (obtaining less uniformly distributed solutions) than the spacing metric obtained with $\rho_l \in \{0.5, 0.7\}$. It is also clear that too much exploration (very large ρ_l) and too much exploitation (small ρ_l) is not good (refer to Figures 7.14 and 7.17). In fact this observation is true for all change frequencies and all change severities. A balance of exploration and exploitation is needed, which is achieved with a $\rho_l \in \{0.5, 0.7\}$ (refer to Tables D.7-D.9 and Figures 7.14 and 7.17).

The graphs indicate a deterioration in the solution spread with increase in change frequency (refer to Figure 7.14). A decrease in change frequency leads to more uniformly distributed solutions, which is expected (refer to Section 7.2.1 on page 160).

The graphs indicate a deterioration in the solution spread with increase in change severity (refer to Figure 7.17). That is, high change severity negatively affected the solution spread.

3. **Influence of ρ_l on the hypervolume metric, $\bar{\xi}$.**

   Irrespective of the change frequency and change severity, all algorithms succeeded in obtaining good performance with respect to the hypervolume metric (refer to Figures E.27, E.30, E.33). A general trend that is observed over all values of T_{sm} and R_g is that performance peaks at $\rho_l = 0.5$ and $\rho_l = 0.7$. Again this indicates that a balance between exploration and exploitation is best for this dynamic environment, since a high value of ρ_l which favours exploration and a low value of ρ_l which favours exploitation produced the lowest values for the hypervolume (refer to Figures 7.15 and 7.18).

   The graphs indicate in most cases an increase in $\bar{\xi}$ with decrease in change frequency (refer to Figure 7.15). This result is expected, since low change frequency gives more time for adaptation and is supposed to produce a uniform distribution of the solutions and closeness of the solutions to the optimal Pareto set.

A value of $\rho_l = 0.5$ and $\rho_l = 0.7$ offers the best trade-off between metrics $\bar{n}_{alg}$, $\bar{\varrho}$ and $\bar{\xi}$ for all change frequencies and all change severities. Accordingly, the value of 0.5 for ρ_l

was adopted for the remainder of the simulations.

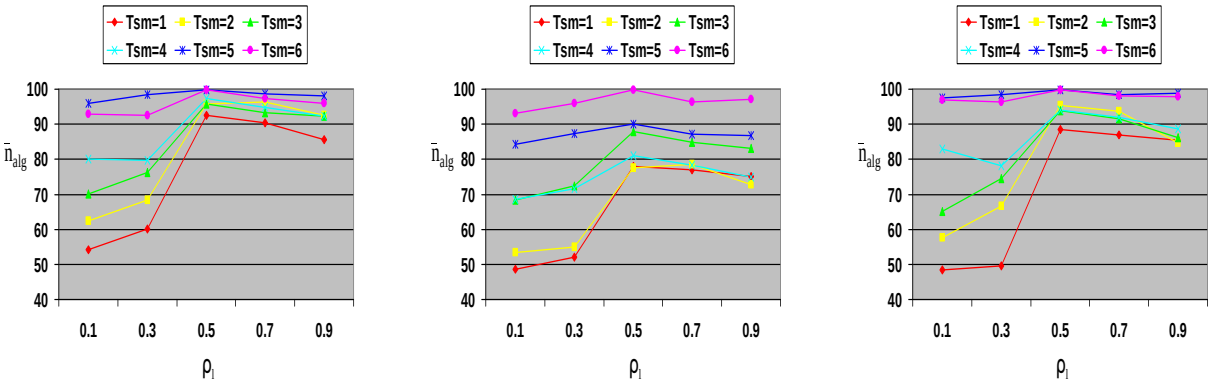

(a) EEMACOMP (b) EEMACOMH (c) EEMACOMC

Figure 7.13: Influence of r_l on $\bar{n}_{alg}$ metric, for different change frequencies, T_{sm}

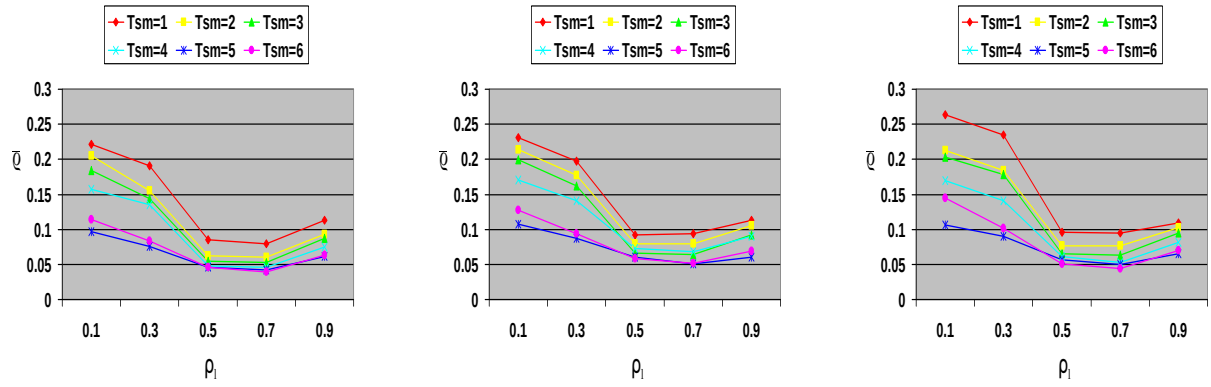

(a) EEMACOMP (b) EEMACOMH (c) EEMACOMC

Figure 7.14: Influence of r_l on $\bar{\varrho}$ metric, for different change frequencies, T_{sm}

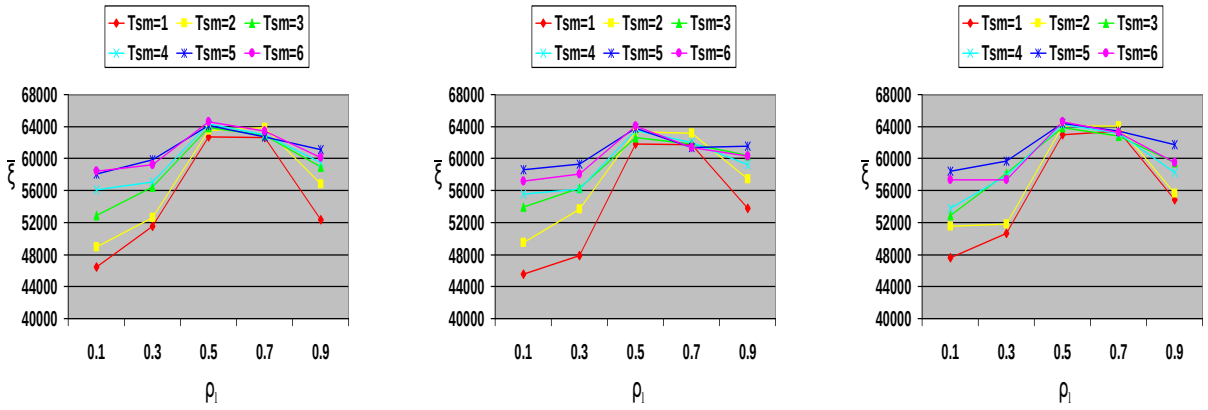

(a) EEMACOMP (b) EEMACOMH (c) EEMACOMC

Figure 7.15: Influence of r_l on $\bar{\xi}$ metric, for different change frequencies, T_{sm}

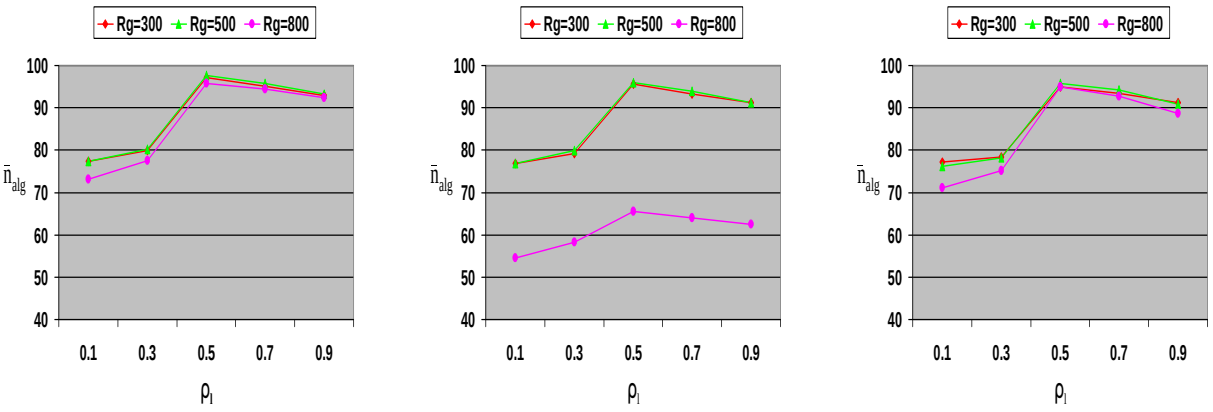

(a) EEMACOMP (b) EEMACOMH (c) EEMACOMC

Figure 7.16: Influence of r_l on $\bar{n}_{alg}$ metric, for different change severities, R_g

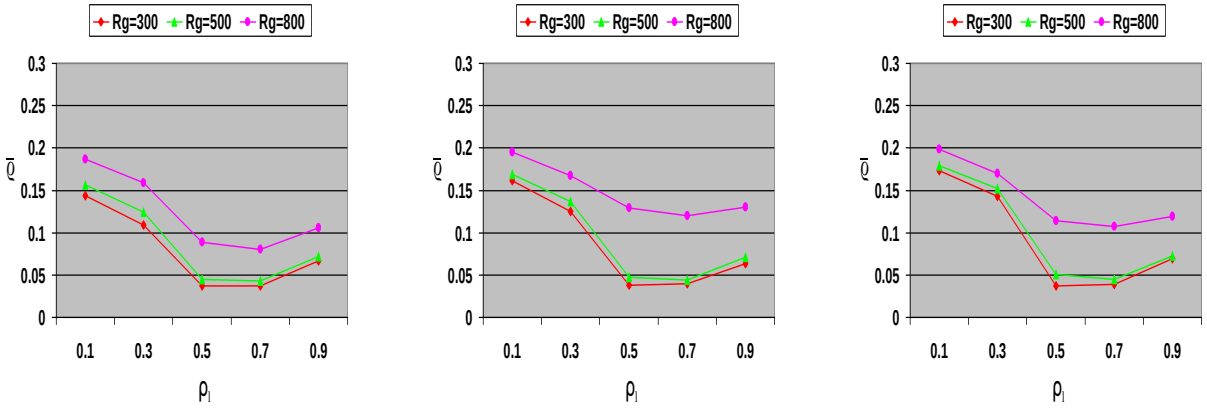

(a) EEMACOMP (b) EEMACOMH (c) EEMACOMC

Figure 7.17: Influence of r_l on $\bar{\varrho}$ metric, for different change severities, R_g

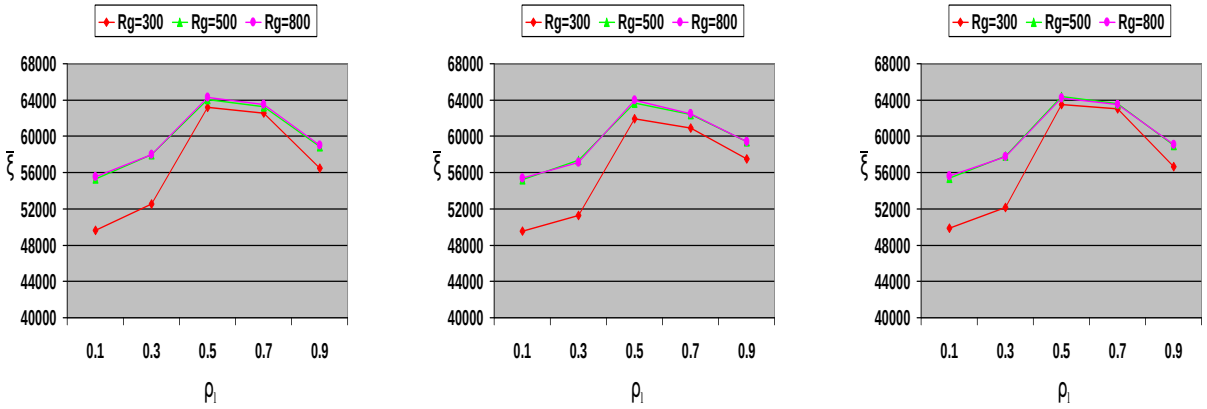

(a) EEMACOMP (b) EEMACOMH (c) EEMACOMC

Figure 7.18: Influence of r_l on $\bar{\xi}$ metric, for different change severities, R_g

7.2.4 Global Decay Parameter, ρ_g

After each iteration, all ants found a solution and the global updating rule is applied (refer to equations (6.24), (6.35), and (6.56). The global decay or global evaporation parameter, ρ_g, sets the amount of pheromone that evaporate on the paths after each loop, as for ρ_l. A high value of ρ_g will help finding more solutions instead of focusing on a specific solution.

In order to find the best value for ρ_g, five values were considered, namely $\rho_g \in \{0.1, 0.3, 0.5, 0.7, 0.9\}$. The influence of ρ_g was investigated for all five algorithms.

The following parameter values were used based on the result of sections 7.2.1-7.2.3: $\beta_\nu = 3.5$, $\beta_\xi = 4.0$, $\beta_\pi = 4.5$, $\beta_\varrho = 4.5$, $\beta_\varsigma = 5.0$, $r_0 = 0.5$, and $\rho_l = 0.5$. The rest of the parameter values were fixed as in Section 7.2.

Tables D.10-D.12 summarise the empirical results for control parameter ρ_g using the $\bar{n}_{alg}$, $\bar{\varrho}$ and $\bar{\xi}$ metrics. Results are visualised in Figures E.34-E.48 and 7.19-7.24.

The rest of this subsection discusses the results obtained from the experiments.

1. **Influence of ρ_g on the number of non-dominated solutions, $\bar{n}_{alg}$.**

   Parameter ρ_g follows similar trends as for ρ_l with reference to $\bar{n}_{alg}$, except that there is no real trend between $\bar{n}_{alg}$ and the change frequency (refer to Figures E.25, E.28, E.31, E.34, E.37, E.40, E.43, E.46). Values of $\rho_g \in \{0.5, 0.7\}$ performed the best for all change frequencies (refer to Figure 7.19) and for all change severities (refer to Figure 7.22).

2. **Influence of ρ_g on the spread metric, $\bar{\varrho}$.**

   Results for $\rho_g = 0.1$ and $\rho_g = 0.3$ show that all the algorithms failed in obtaining a good spread in the found non-dominated solutions (refer to Figures E.35, E.38, E.41, E.44, E.47), irrespective of change severities and change frequencies. For $\rho_g = 0.9$, the spread metric is higher than the spread metric obtained with $\rho_g \in \{0.5, 0.7\}$. It seems to be a general trend for all results thus far that too much exploration (very large ρ_g) and too much exploitation (small ρ_g) is not good. For $\rho_g = 0.9$ there is high pheromone evaporation and the search is very random. Consequently, it takes more time for the algorithms to converge to a solution. That explains the high value of $\bar{\varrho}$. For $\rho_g = 0.1$ and $\rho_g = 0.3$ there is high pheromone concentration and ants tend to converge to the same solution. There is a too early convergence to sub-optimal solutions, which again explains the high value of $\bar{\varrho}$.

Again, parameter ρ_g follows the same trends as for ρ_l with reference to $\bar{\varrho}$. Values of $\rho_g \in \{0.5, 0.7\}$ performed the best (refer to Tables D.10-D.12 and Figures 7.20 and 7.23).

3. **Influence of ρ_g on the hypervolume metric, $\bar{\xi}$.**

   Parameter ρ_g follows the same trends as for ρ_l with reference to $\bar{\xi}$ (refer to Figures E.27, E.30, E.33, E.36, E.39, E.42, E.45, E.48).

   A general trend that was observed over all values of T_{sm} and R_g is that performance peaks at $\rho_g = 0.5$ and $\rho_g = 0.7$ (refer to Figures 7.21 and 7.24). Again this indicates that a balance between exploration and exploitation is best for this dynamic environment.

A value of $\rho_g = 0.5$ and $\rho_g = 0.7$ offered the best trade-off between metrics $\bar{n}_{alg}$, $\bar{\varrho}$ and $\bar{\xi}$ for all change frequencies and all change severities. Accordingly, the value of $\rho_g = 0.7$ was adopted for the remainder of the simulations.

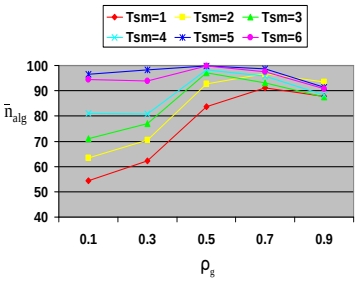

(a) EEMACOMP

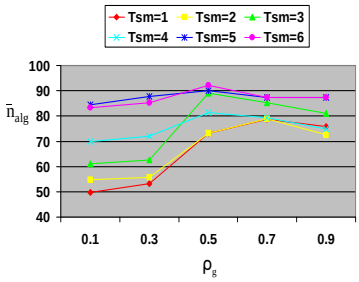

(b) EEMACOMH

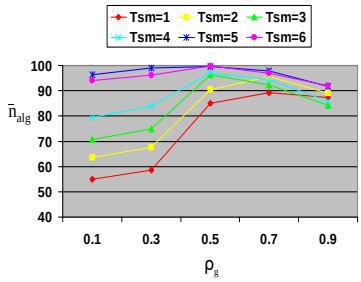

(c) EEMMASMP

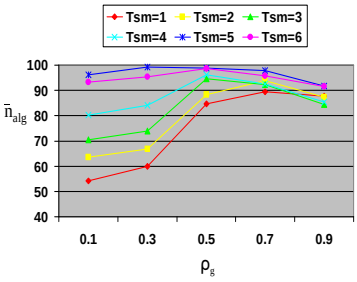

(d) EEMMASMH

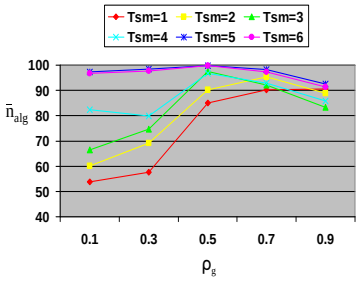

(e) EEMACOMC

Figure 7.19: Influence of ρ_g on $\bar{n}_{alg}$ metric, for different change frequencies, T_{sm}

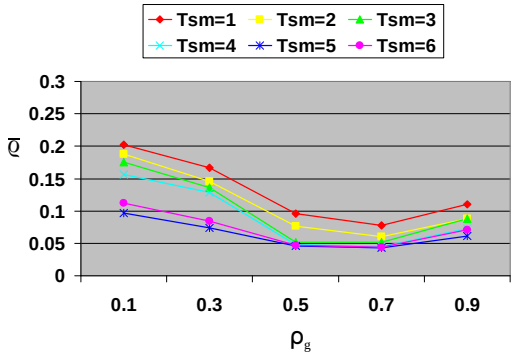

(a) EEMACOMP

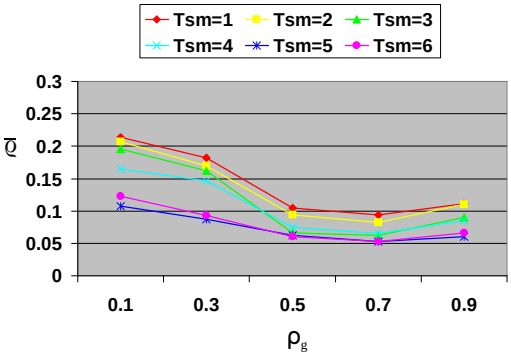

(b) EEMACOMH

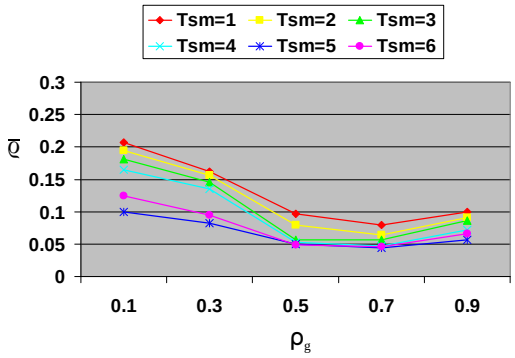

(c) EEMMASMP

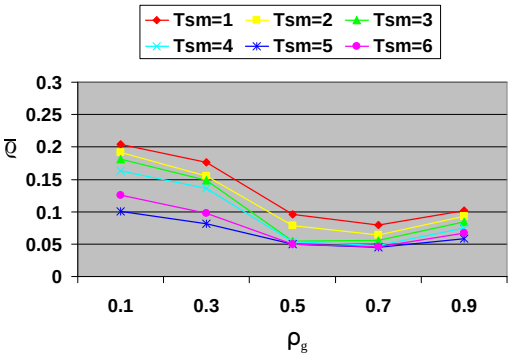

(d) EEMMASMH

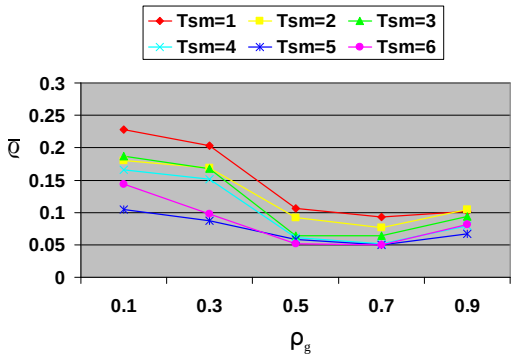

(e) EEMACOMC

Figure 7.20: Influence of ρ_g on $\bar{\varrho}$ metric, for different change frequencies, T_{sm}

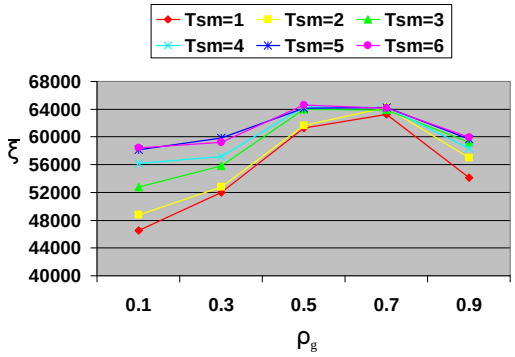

(a) EEMACOMP

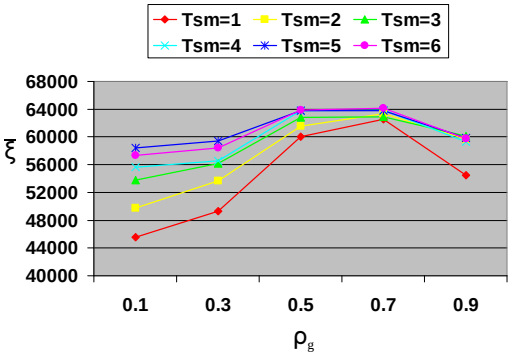

(b) EEMACOMH

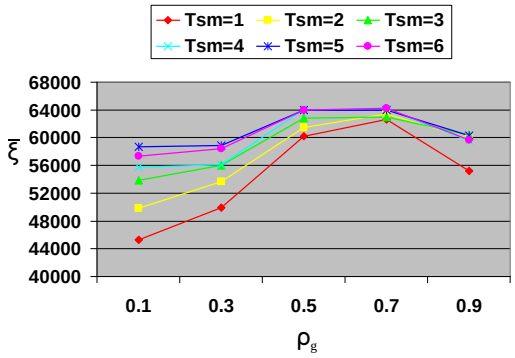

(c) EEMMASMP

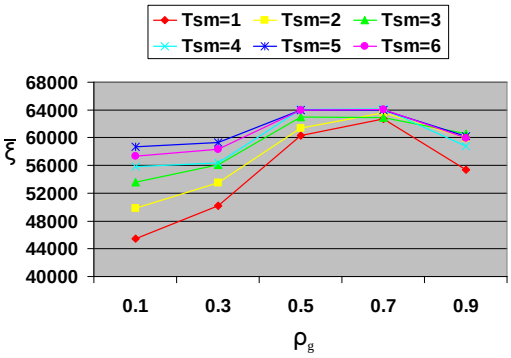

(d) EEMMASMH

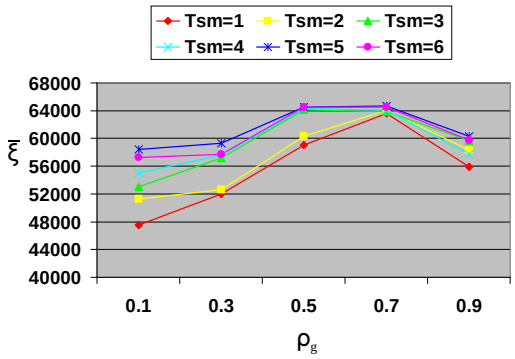

(e) EEMACOMC

Figure 7.21: Influence of ρ_g on $\bar{\xi}$ metric, for different change frequencies, T_{sm}

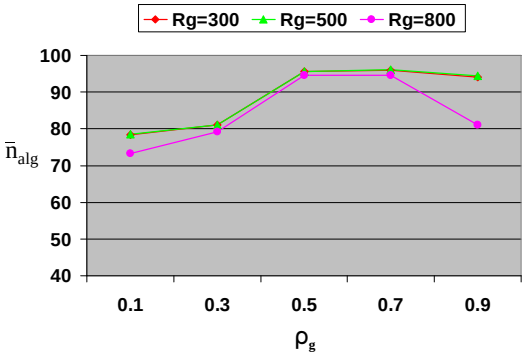

(a) EEMACOMP

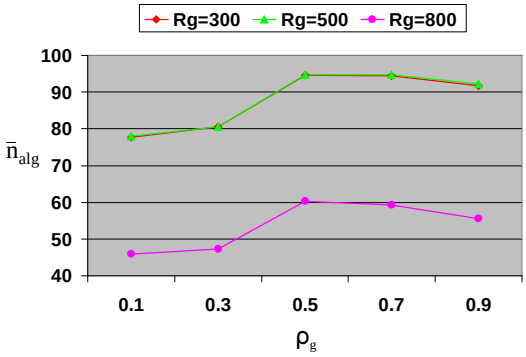

(b) EEMACOMH

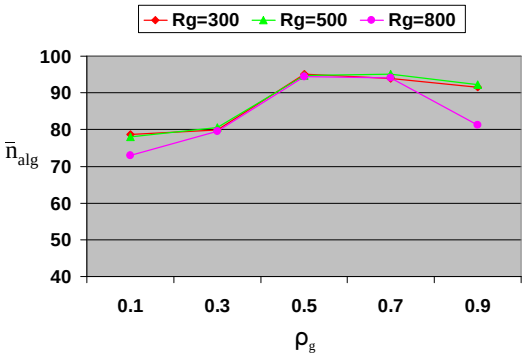

(c) EEMMASMP

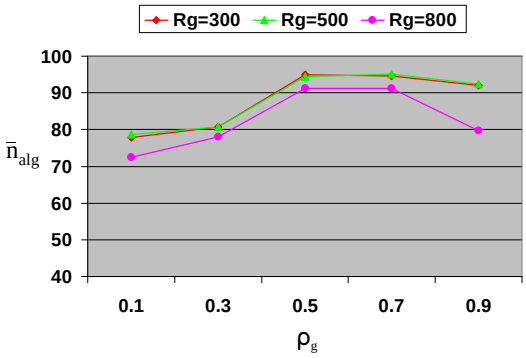

(d) EEMMASMH

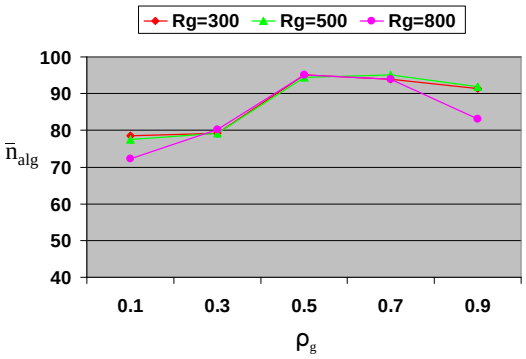

(e) EEMACOMC

Figure 7.22: Influence of ρ_g on $\bar{n}_{alg}$ metric, for different change severities, R_g

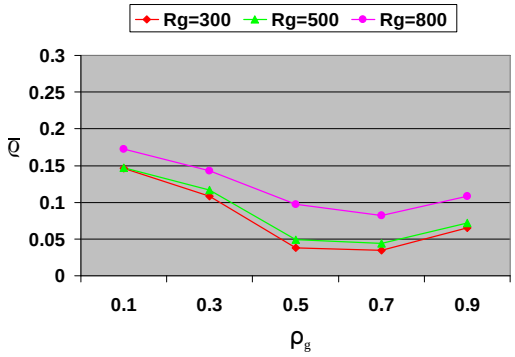

(a) EEMACOMP

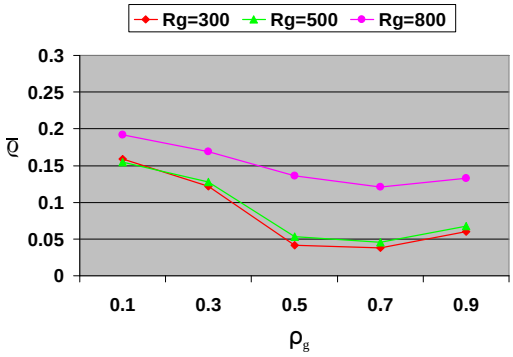

(b) EEMACOMH

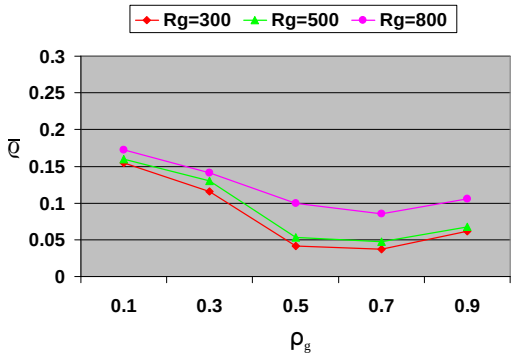

(c) EEMMASMP

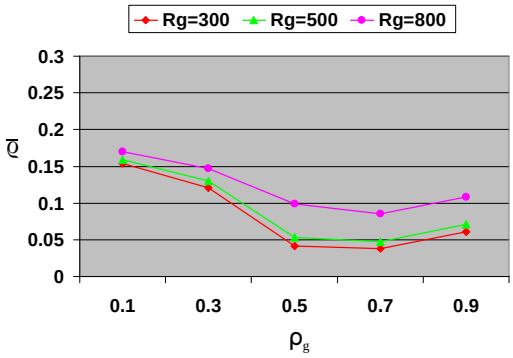

(d) EEMMASMH

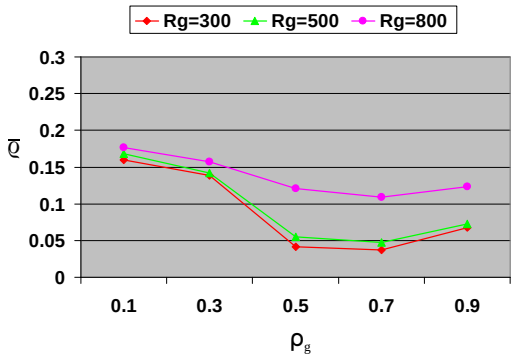

(e) EEMACOMC

Figure 7.23: Influence of ρ_g on $\bar{\varrho}$ metric, for different change severities, R_g

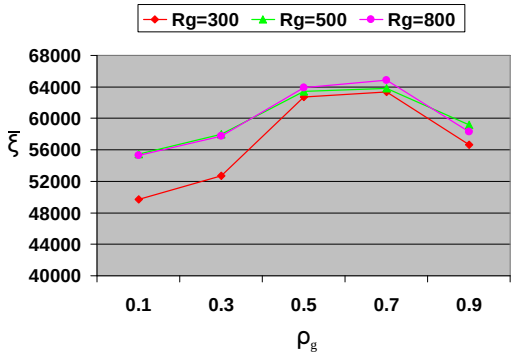

(a) EEMACOMP

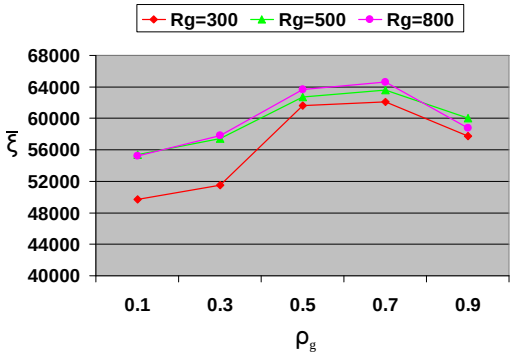

(b) EEMACOMH

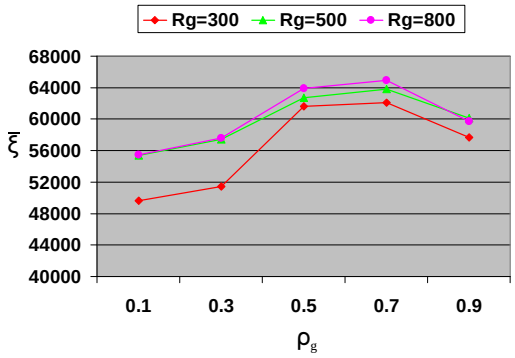

(c) EEMMASMP

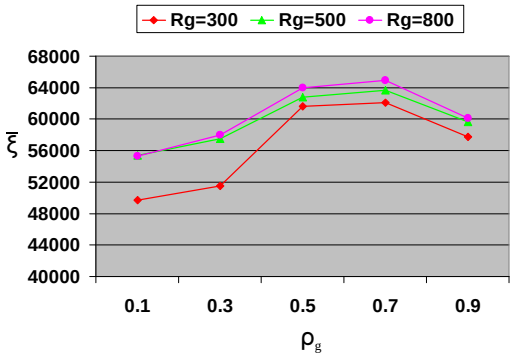

(d) EEMMASMH

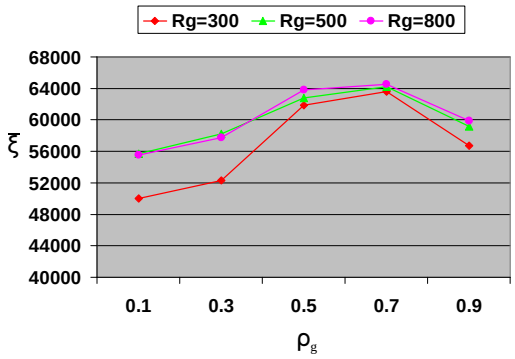

(e) EEMACOMC

Figure 7.24: Influence of ρ_g on $\bar{\xi}$ metric, for different change severities, R_g

7.2.5 Importance of the Pheromone Trail Concentrations Parameter, α

As illustrated in equations (6.42) and (6.48), α controls the balance between exploration and exploitation. Diversification of the solution searching process in the solution space can be emphasized by decreasing the value of α and exploitation can be increased by increasing the value of α. If $\alpha = 0$, no pheromone information is used, i.e. previous search experience is neglected. The search then degrades to a stochastic greedy search.

Because α is used only in equations (6.42) and (6.48), the influence of α was investigated only for EEMMASMP and EEMMASMH. For the other three algorithms, α was set to one.

In order to find the best value for α, six values were considered, namely $\alpha \in \{1,\ 1.5,\ 2,\ 2.5,\ 3,\ 3.5\}$.

The following parameter values were used based on the results of sections 7.2.1-7.2.4: $\beta_\nu = 3.5$, $\beta_\xi = 4.0$, $\beta_\pi = 4.5$, $\beta_\varrho = 4.5$, $\beta_\varsigma = 5.0$, $r_0 = 0.5$, $\rho_l = 0.5$, and $\rho_g = 0.7$. The rest of the parameter values were fixed as in Section 7.2.

Tables D.13-D.15 summarise the empirical results for α using the $\bar{n}_{alg}$, $\bar{\varrho}$ and $\bar{\xi}$ metrics. Results are visualised in Figures E.49-E.54 and 7.25-7.30. The rest of this section discusses the results obtained from the experiments with regards to the influence of α on the performance metrics.

1. **Influence of α on the number of non-dominated solutions, $\bar{n}_{alg}$.**

   For $\alpha = 3$ and $\alpha = 3.5$ all the algorithms produced a very low number of non-dominated solutions compared to lower values of α. The best values for α are for $\alpha \in \{1,\ 1.5,\ 2,\ 2.5\}$, for all change frequencies and all change severities (refer to Tables D.13-D.15 and Figures E.49, E.52, 7.25 and 7.28). For these values all algorithms produced a very large number of non-dominated solutions.

   The graphs indicate a small decrease in the number of non-dominated solutions with increase in change frequency which is expected (refer to Figures E.49, E.52 and 7.25). As pointed out in section 7.2.1 on page 159, as change frequency increases, the time available for adaptation becomes shorter and it becomes harder to find optimum solutions.

   Also, there is a small decrease in the number of non-dominated solutions with increase in change severity (refer to Figures E.49, E.52 and 7.28).

2. **Influence of α on the spread metric, $\bar{\varrho}$.**

   The graphs indicate a small deterioration of the solution spread with higher values of α (refer to Figures E.50 and E.53). The best values for the solution spread were produced with $\alpha \in \{1,\ 1.5,\ 2\}$, for all change frequencies and all change severities.

   Figure 7.26 indicates a deterioration of the solution spread (i.e. higher $\bar{\varrho}$) with increase in change frequency which is expected (refer to Section 7.2.1 on page 160). Also, there is a deterioration of the solution spread with increase in change severity (refer to Figure 7.29). This result is expected since, when R_g increases, more iterations are needed to track the optima after the change occurred and therefore less time is available to reach a good distribution of solutions.

3. **Influence of α on the hypervolume metric, $\bar{\xi}$.**

   Values of $\alpha \in \{1,\ 3,\ 3.5\}$ produced the worst results for the hypervolume metric (refer to Figures E.51 and E.54). This observation is true for all change frequencies (refer to Figure 7.27) and all change severities (refer to Figure 7.30). That is, high exploration and high exploitation negatively affected the $\bar{\xi}$ metric.

   The graphs indicate a small increase in $\bar{\xi}$, with decrease in change frequency (refer to Figure 7.27).

   There is no pattern between $\bar{\xi}$ and R_g, which indicates insensitivity of $\bar{\xi}$ to R_g (refer to Figure 7.30).

   The best values for the hypervolume were produced with $\alpha \in \{1.5,\ 2,\ 2.5\}$, for all change frequencies and all change severities (refer to Tables D.13-D.15 and Figures E.51, E.54, 7.27 and 7.30).

A value of $\alpha = 1.5$ offered the best trade-off between metrics $\bar{n}_{alg}$, $\bar{\varrho}$ and $\bar{\xi}$ for all change frequencies and all change severities. Accordingly, the value of $\alpha = 1.5$ was adopted for the remainder of the simulations.

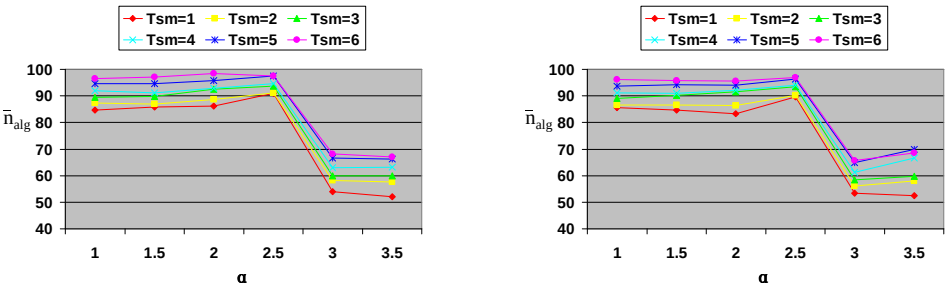

(a) EEMMASMP (b) EEMMASMH

Figure 7.25: Influence of α on $\bar{n}_{alg}$ metric, for different change frequencies, T_{sm}

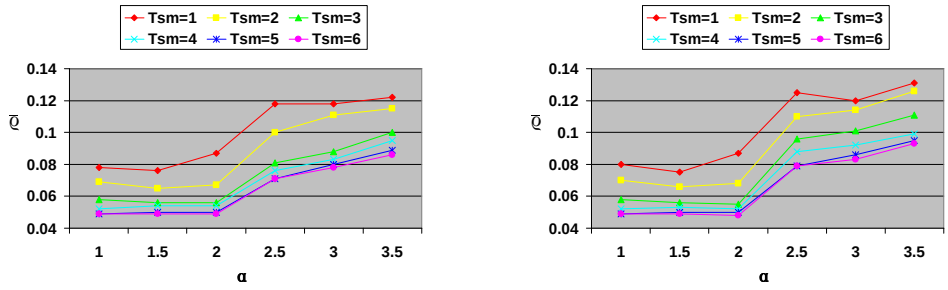

(a) EEMMASMP (b) EEMMASMH

Figure 7.26: Influence of α on $\bar{\varrho}$ metric, for different change frequencies, T_{sm}

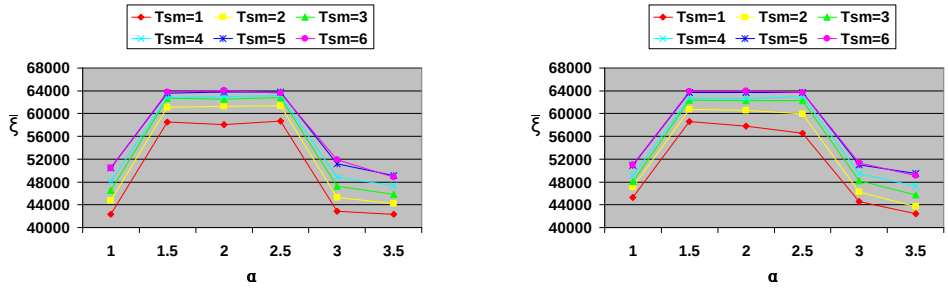

(a) EEMMASMP (b) EEMMASMH

Figure 7.27: Influence of α on $\bar{\xi}$ metric, for different change frequencies, T_{sm}

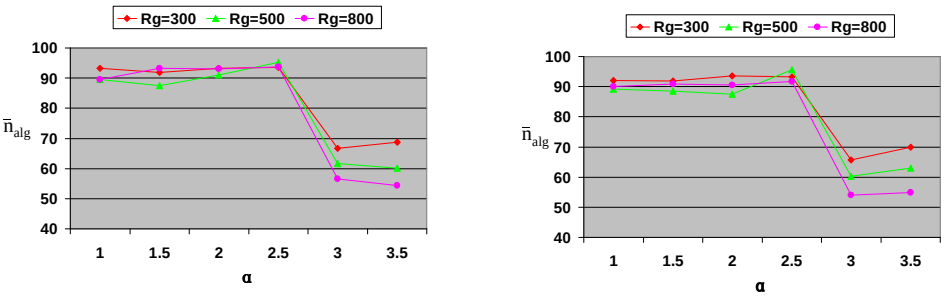

(a) EEMMASMP (b) EEMMASMH

Figure 7.28: Influence of α on $\bar{n}_{alg}$ metric, for different change severities, R_g

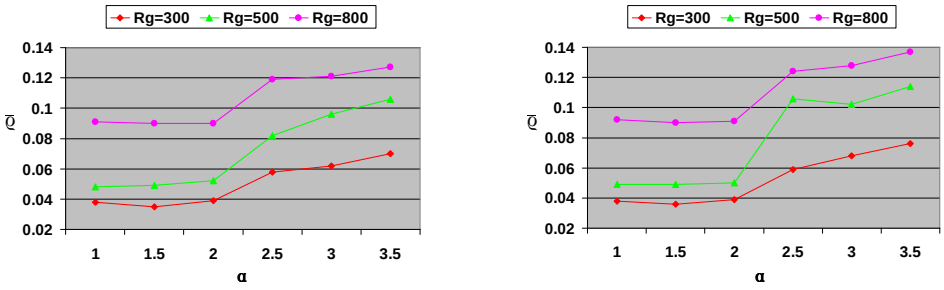

(a) EEMMASMP (b) EEMMASMH

Figure 7.29: Influence of α on $\bar{\varrho}$ metric, for different change severities, R_g

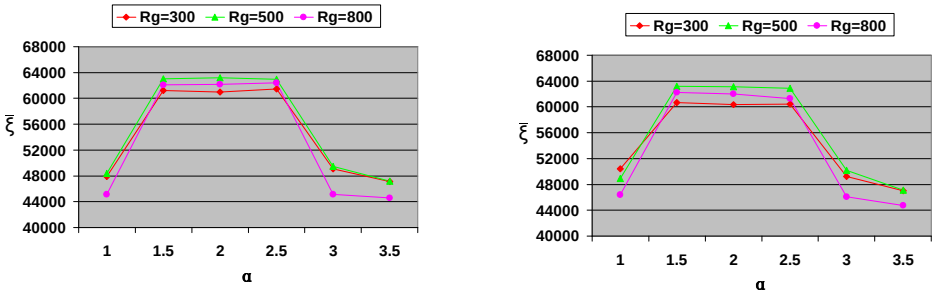

(a) EEMMASMP (b) EEMMASMH

Figure 7.30: Influence of α on $\bar{\xi}$ metric, for different change severities, R_g

7.2.6 η-Strategy Parameter

The η-strategy parameter, noted λ_E, is used to determine the reset value to reinitialise pheromone values on links. The η-strategy is applied after a change in the environment occurs in order to promote diversity. If $\lambda_E \rightarrow \infty$ there is no pheromone conservation and exploration is emphasized. For lower values of λ_E there is a higher pheromone conservation and exploitation is promoted.

All algorithms were run using the η-strategy. The influence of λ_E on the performance metrics $\bar{n}_{alg}$, $\bar{\varrho}$, and $\bar{\xi}$ was therefore evaluated. In order to find the best value for λ_E, four values for λ_E were considered, namely $\lambda_E \in \{2,\ 4,\ 6,\ 8\}$.

The following parameter values were used based on the result of sections 7.2.1-7.2.5: $\beta_\nu = 3.5$, $\beta_\xi = 4.0$, $\beta_\pi = 4.5$, $\beta_\varrho = 4.5$, $\beta_\varsigma = 5.0$, $r_0 = 0.5$, $\rho_l = 0.5$, $\rho_g = 0.7$, and $\alpha = 1.5$. The rest of the parameter values were fixed as in Section 7.2.

Tables D.16-D.18 summarise the empirical results for the control parameter λ_E using the $\bar{n}_{alg}$, $\bar{\varrho}$ and $\bar{\xi}$ metrics. Results are visualised in Figures E.55-E.69 and 7.31-7.36.

The rest of this subsection discusses the results obtained from the experiments with regards to the influence of λ_E on the performance metrics $\bar{n}_{alg}$, $\bar{\varrho}$, and $\bar{\xi}$.

1. **Influence of λ_E on the number of non-dominated solutions, $\bar{n}_{alg}$.**

   Results for $\lambda_E = 2$ and $\lambda_E = 8$ show that all the algorithms struggled to find many non-dominated solutions irrespective of change frequency (refer to Figure 7.31) and irrespective of change severity (refer to Figure 7.34). All the algorithms produced the largest number of non-dominated solutions for $\lambda_E = 4$ and $\lambda_E = 6$ (refer to Figures E.55, E.58, E.61, E.64, E.67).

   The graphs indicate a decrease in the number of non-dominated solutions with increase in change frequency (refer to Figure 7.31).

   Results for $R_g = 800$ show that the EEMACOMH algorithm produced the lowest number of non-dominated solutions irrespective of the λ_E value (refer to Figure 7.34(b)).

2. **Influence of λ_E on the spread metric, $\bar{\varrho}$.**

Irrespective of the change frequency and change severity, for $\lambda_E = 2$ and $\lambda_E = 8$ all the algorithms displayed a higher value for $\bar{\varrho}$ which means less uniformly distributed solutions (refer to Figures E.56, E.59, E.62, E.65, and E.68). For $\lambda_E = 4$ and $\lambda_E = 6$ lower values of $\bar{\varrho}$ (more uniformly distributed solutions) were obtained.

A decrease in change frequency lead to more uniformly distributed solutions (refer to Figure 7.32). As pointed out in section 7.2.1 on page 160, as frequency of change decreases, the time available for adaptation becomes larger and the crowding distance operator is applied more times on the archive. At the end the archive will contain more non-dominated solutions which are in the least crowded area in the objective space, therefore, maintaining a good spread of non-dominated solutions.

The graphs indicate a deterioration of the solution spread with increase in change severity (refer to Figure 7.35). That is, high change severity negatively affected the solution spread. When the change severity increases there is not much information gained from the past to reuse, and it takes more time to optimise the problem and less time to explore, which explains the poor distribution of solutions as R_g increases.

The best solution distribution is produced with $\lambda_E = 4$ and $\lambda_E = 6$, for all change frequencies and all change severities (refer to Tables D.16-D.18 and Figures E.56, E.59, E.62, E.65, E.68, 7.32, 7.35).

3. **Influence of λ_E on the hypervolume metric, $\bar{\xi}$.**

   A general trend that is observed over all values of T_{sm} and R_g is that performance with reference to the hypervolume metric peaks at $\lambda_E = 4$ and $\lambda_E = 6$ (refer to Figures E.57, E.60, E.63, E.66, E.69, 7.33, and 7.36). Again, this indicates that a balance between exploration and exploitation is best for this dynamic environment. With $\lambda_E = 4$ and $\lambda_E = 6$, the relative difference of the pheromone trails is small enough to increase exploration of new paths and large enough to increase exploitation of existing paths.

   The graphs indicate an increase in $\bar{\xi}$ with decrease in change frequency (refer to Figure 7.33).

   There is no pattern between $\bar{\xi}$ and R_g, which indicates insensitivity of $\bar{\xi}$ to R_g (refer to Figure 7.36), excluding the EEMACOMH which showed a decrease in $\bar{\xi}$

with $R_g = 800$ (refer to Figure 7.36(b)).

A value of $\lambda_E = 4$ and $\lambda_E = 6$ offered the best trade-off between metrics $\bar{n}_{alg}$, $\bar{\varrho}$ and $\bar{\xi}$ for all change frequencies and all change severities. Accordingly, the value off $\lambda_E = 6$ was adopted for the remainder of the simulations.

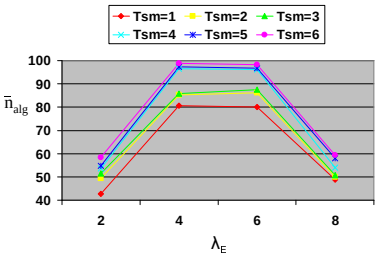

(a) EEMACOMP

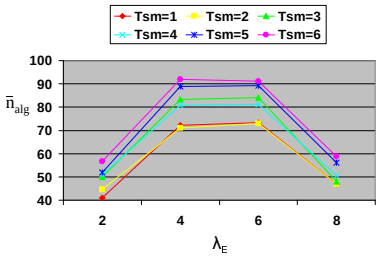

(b) EEMACOMH

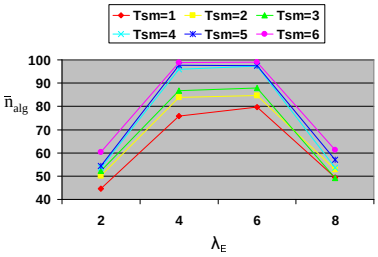

(c) EEMMASMP

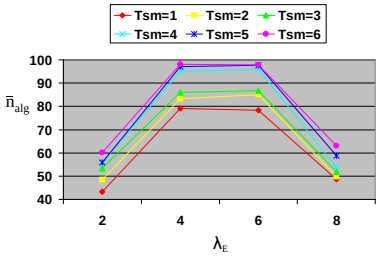

(d) EEMMASMH

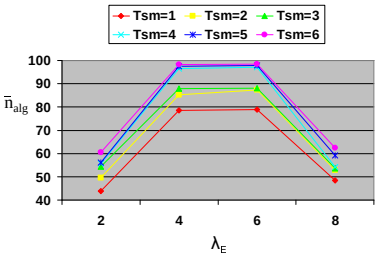

(e) EEMACOMC

Figure 7.31: Influence of λ_E on $\bar{n}_{alg}$ metric, for different change frequencies, T_{sm}

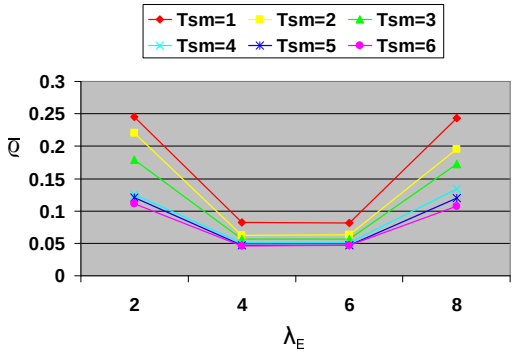

(a) EEMACOMP

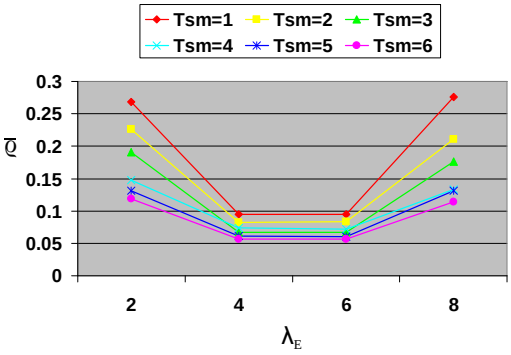

(b) EEMACOMH

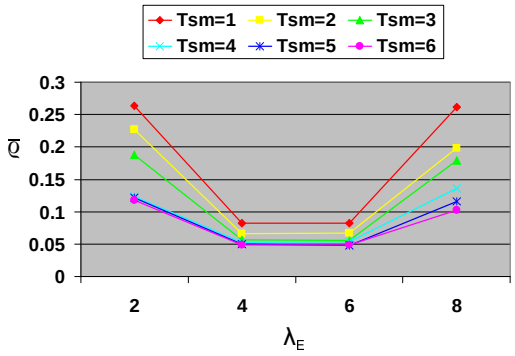

(c) EEMMASMP

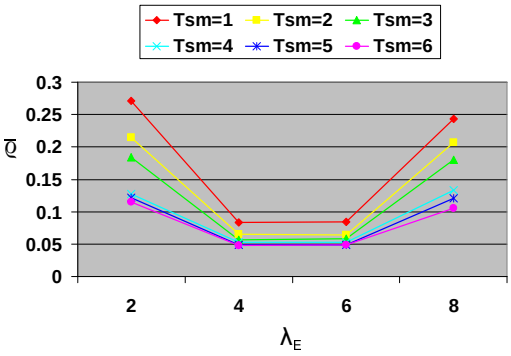

(d) EEMMASMH

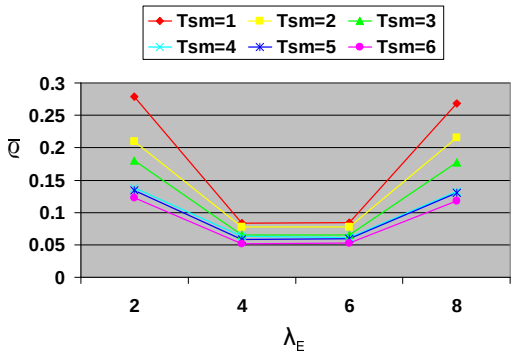

(e) EEMACOMC

Figure 7.32: Influence of λ_E on $\bar{\varrho}$ metric, for different change frequencies, T_{sm}

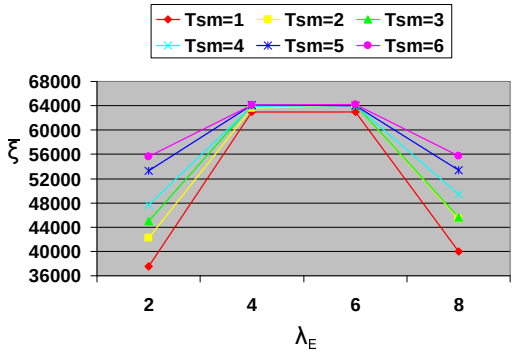

(a) EEMACOMP

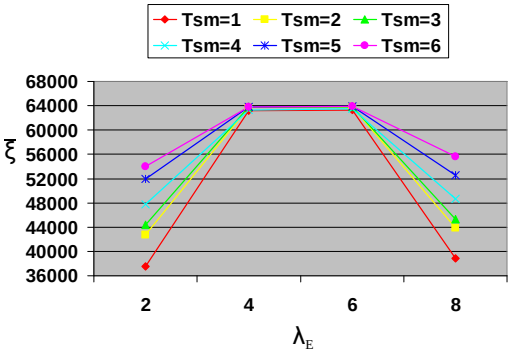

(b) EEMACOMH

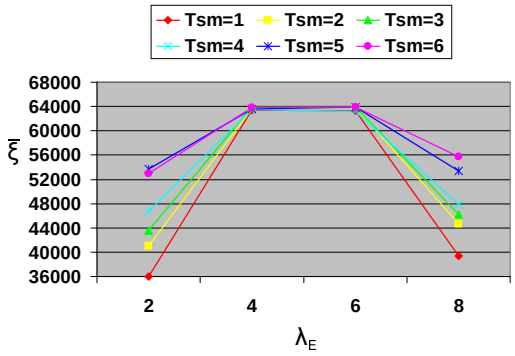

(c) EEMMASMP

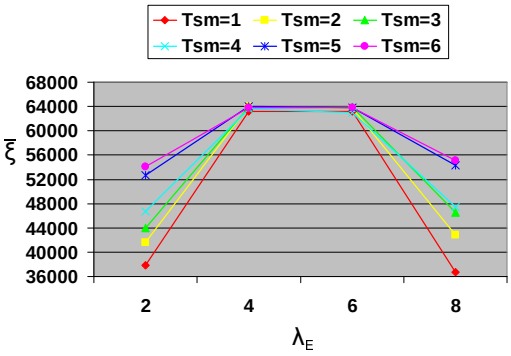

(d) EEMMASMH

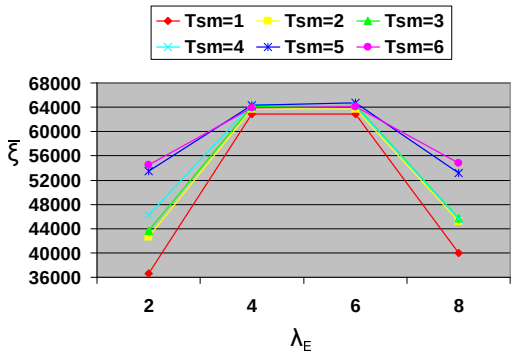

(e) EEMACOMC

Figure 7.33: Influence of λ_E on $\bar{\xi}$ metric, for different change frequencies, T_{sm}

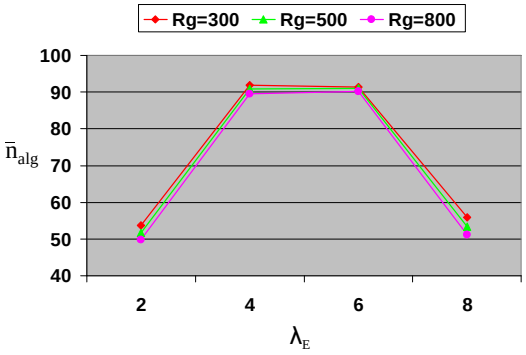

(a) EEMACOMP

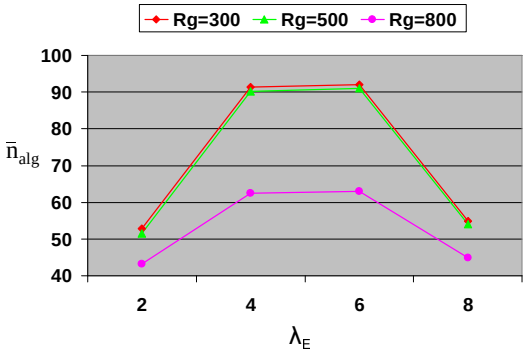

(b) EEMACOMH

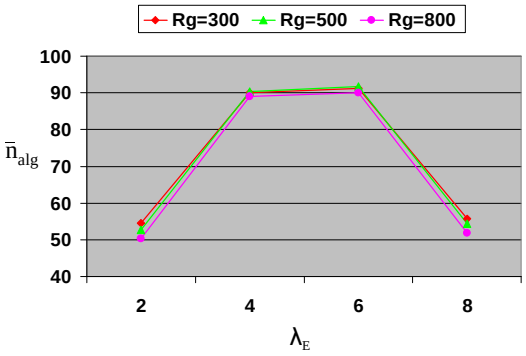

(c) EEMMASMP

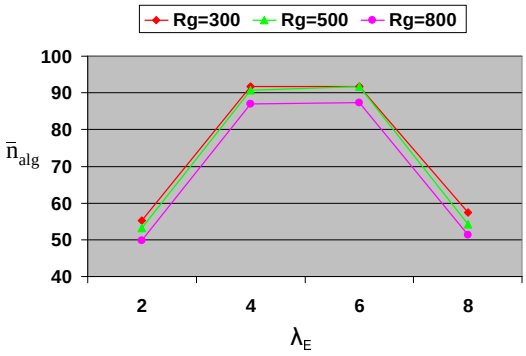

(d) EEMMASMH

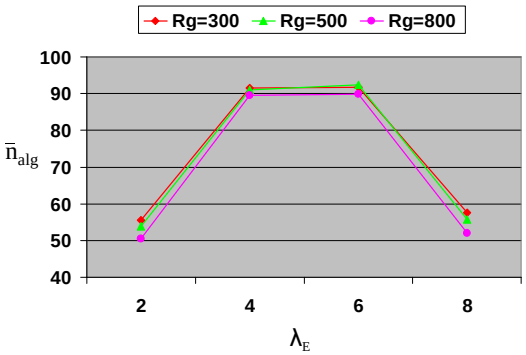

(e) EEMACOMC

Figure 7.34: Influence of λ_E on $\bar{n}_{alg}$ metric, for different change severities, R_g

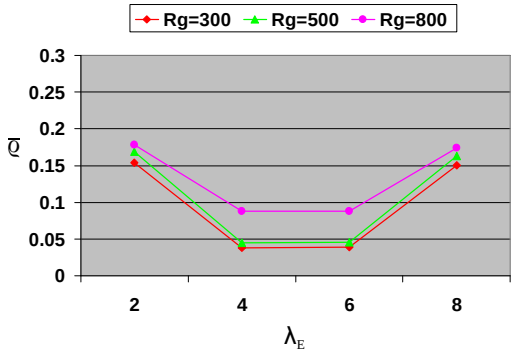

(a) EEMACOMP

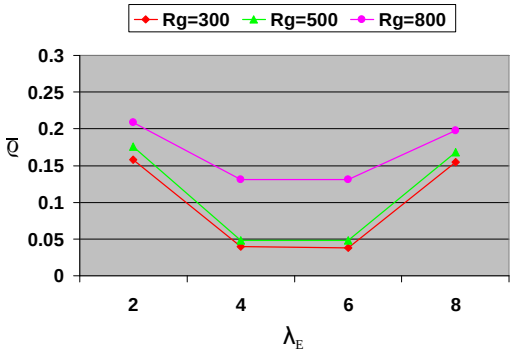

(b) EEMACOMH

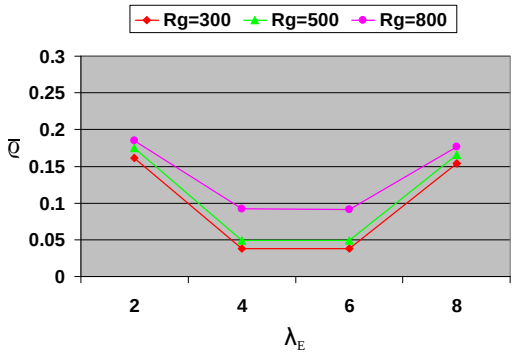

(c) EEMMASMP

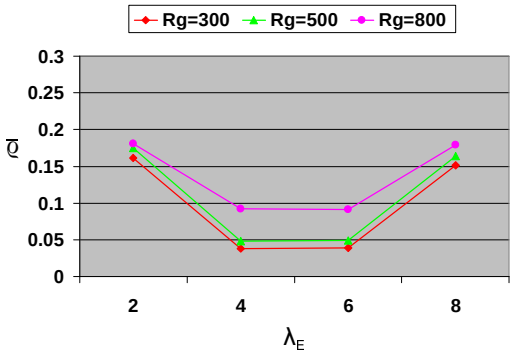

(d) EEMMASMH

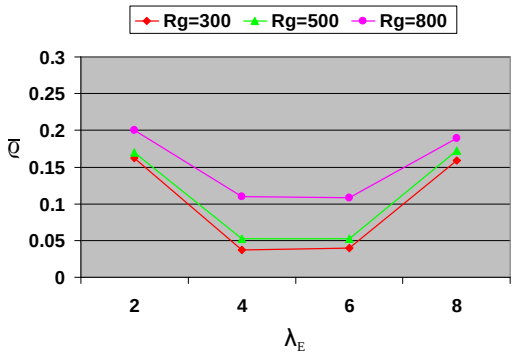

(e) EEMACOMC

Figure 7.35: Influence of λ_E on $\bar{\varrho}$ metric, for different change severities, R_g

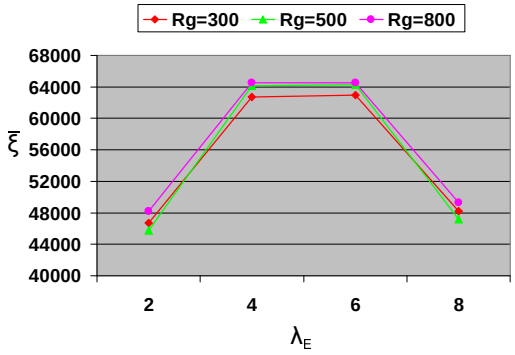

(a) EEMACOMP

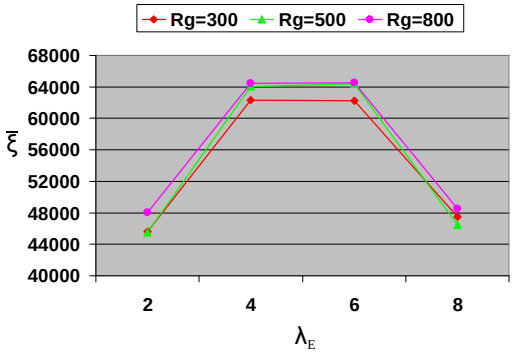

(b) EEMACOMH

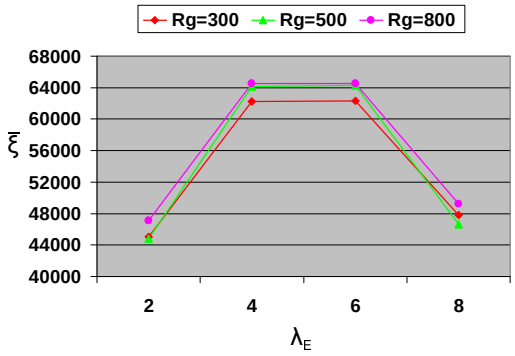

(c) EEMMASMP

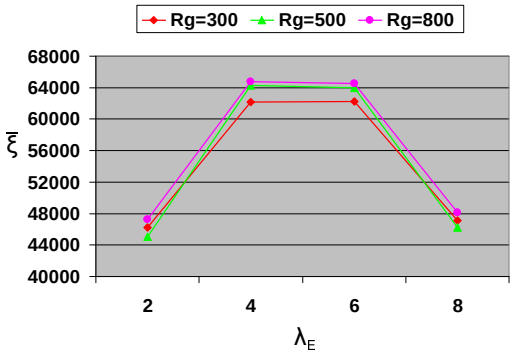

(d) EEMMASMH

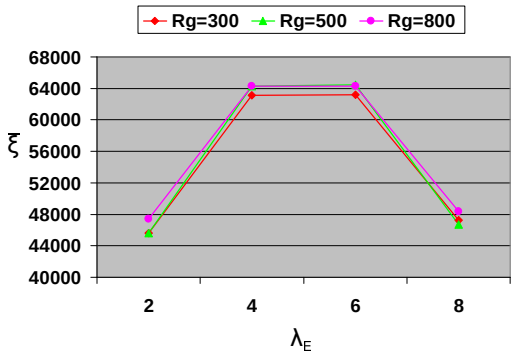

(e) EEMACOMC

Figure 7.36: Influence of λ_E on $\bar{\xi}$ metric, for different change severities, R_g

7.2.7 Importance of the Objectives Parameters

The parameters λ_ν, λ_ξ, λ_π, λ_ϱ, $\lambda_\varsigma \in [0, 1]$ are user-defined parameters which set the importance of the objectives in the search. For this thesis the assumption was made that the objectives have the same importance in the search. Therefore, the value for all λ_ψ was set to 0.2. It is suggested that future research investigates the influence of different values for these parameters on performance.

7.2.8 Pareto Archive Size

The size of the archive is fixed. If the number of solutions is more than the archive size, solutions which have high density in the objective space, i.e. solutions with a lower value of the crowding distance (refer to Section 4.6.2), are removed. On the other hand if the archive is not full, the current non-dominated solutions are added until the archive becomes full. Keeping a bound on the archive size may be important because the Pareto-optimal set may be infinitely large, but also because updating and searching through the archive will become very time-consuming if the archive is allowed to grow without bound.

The size of the Pareto archive was limited to 100 since this value has been used by different researchers [120, 225].

7.2.9 Summary of Ant Based Control Parameters which Affect Exploration and Exploitation

In order for ACO algorithms to be applied to DOPs, mechanisms should be employed that maintain diversity. This section summarises the control parameters for ACO algorithms which influence the exploration and exploitation.

- **Heuristics vs Pheromone Parameters, β_ψ**

  Parameters β_ψ=β_ν, β_ξ, β_π, β_ϱ, and β_ς set the relative importance of heuristic versus pheromone information. The larger the value of β_ψ, the smaller the emphasis on heuristic information, and learned desirability discovered by pheromone trails is favored. On the other hand, a small value for β_ψ gives higher priority to heuristic information over pheromone and the algorithm becomes more greedy and leads to increased exploration.

Higher values of β_ψ, and therefore a strong focus on pheromone information, produce a better solution spread. The highest number of non-dominated solutions and the best value for the hypervolume metric are obtained with a balance between exploration and exploitation which is achieved for the values of $(\beta_\nu,\ \beta_\xi,\ \beta_\pi,\ \beta_\varrho,\ \beta_\varsigma) \in \{(3.5, 4, 4.5, 4, 5),\ (4.5, 5, 3.5, 4, 4), (5, 5, 5, 5, 5)\}$.

- **Exploration Vs Exploitation Parameter,** r_0

  The parameter, r_0, is used in the ACS transition rule (refer to equations (6.20), (6.31), (6.54)) to control the balance between exploration and exploitation of the search space. Parameter r_0 takes values within the interval $[0, 1]$. When r_0 approaches zero, exploration is favoured. More focus can be given on exploitation instead of exploration by increasing the value of r_0.

  Irrespective of change frequencies and change severities, high exploration negatively affected the number of non-dominated solutions while for high exploitation all the algorithms produced the largest number of non-dominated solutions.

  The best values for the hypervolume and the solution spread were produced with a balance between exploration and exploitation which is achieved for the value of $r_0 = 0.5$, for all change frequencies and all change severities.

- **Local Decay Parameter,** ρ_l

  The local decay parameter, ρ_l, determines the rate at which pheromone on all the paths are evaporated after each step. Parameter ρ_l has values within the interval $[0, 1]$. A high value of ρ_l leaves less pheromone at each step. Consequently, the ants have less information on other ants' paths, and the search is less focused, favouring exploration. More focus can be given on exploitation instead of exploration by decreasing the value of ρ_l.

  A balance of exploration and exploitation is needed, which is achieved with a $\rho_l \in \{0.5, 0.7\}$. These values offer the best trade-off between metrics $\bar{n}_{alg}$, $\bar{\varrho}$ and $\bar{\xi}$ for all change frequencies and all change severities.

- **Global Decay Parameter,** ρ_g

  The global decay or global evaporation parameter, ρ_g, sets the amount of pheromone that evaporate on the paths after each iteration, as for ρ_l. A high value of ρ_g will help to find more solutions instead of focusing on a specific solution.

Irrespective of change frequencies and change severities, a balance of exploration and exploitation is needed, which is achieved with a $\rho_g \in \{0.5, 0.7\}$. These values offer the best trade-off between metrics $\bar{n}_{alg}$, $\bar{\varrho}$ and $\bar{\xi}$.

- **Pheromone Trail Concentrations Parameter,** α

  Diversification of the solution searching process in the solution space (exploration) can be emphasized by decreasing the value of α and exploitation can be increased by increasing the value of α. If $\alpha = 0$, no pheromone information is used, i.e. previous search experience is neglected. The search then degrades to a stochastic greedy search.

  For high values of α (high exploitation) all the algorithms produced a very low number of non-dominated solutions compared to lower values of α. The best values for α for the $\bar{n}_{alg}$ metric are for $\alpha \in \{1,\ 1.5,\ 2,\ 2.5\}$, for all change frequencies and all change severities

  There is a small deterioration of the solution spread with higher values of α. The best values for the solution spread were produced with $\alpha \in \{1,\ 1.5,\ 2\}$, for all change frequencies and all change severities.

  High exploration and high exploitation negatively affected the $\bar{\xi}$ metric. The best values for the hypervolume were produced with $\alpha \in \{1.5,\ 2,\ 2.5\}$, for all change frequencies and all change severities.

- **η-Strategy Parameter**

  The η-strategy parameter, noted λ_E, is used to determine the reset value to reinitialise pheromone values on links. The η-strategy is applied after a change in the environment occurs in order to promote diversity. If $\lambda_E \rightarrow \infty$ there is no pheromone conservation and exploration is emphasized. For lower values of λ_E there is a higher pheromone conservation and exploitation is promoted.

  A general trend that is observed over all values of change frequency and change severity is that performance with reference to all the three metrics peaks at $\lambda_E = 4$ and $\lambda_E = 6$. Again, this indicates that a balance between exploration and exploitation is best for this dynamic environment. With $\lambda_E = 4$ and $\lambda_E = 6$, the relative difference of the pheromone trails is small enough to increase exploration of new paths and large enough to increase exploitation of existing paths.

7.2.10 Summary of Ant Based Control Parameters

The performed empirical analysis of the ant based algorithms control parameters (refer to Sections 7.2.1-7.2.8) showed that the performance and quality of the ACO algorithms is sensitive to control parameters. The empirical analysis showed that a balance between exploration and exploitation is good for the dynamic power aware optimization problem. Also, high exploration negatively affected the number of non-dominated solutions and the solution spread for high change frequencies.

Table 7.3 summarises the simulation control parameters and their values as resulted from this empirical study for the proposed multi-objective power-aware routing ACO algorithms.

7.3 NSGA-II-MPA Parameters

The control parameters of NSGA-II-MPA have been optimised using the same process as described and conducted in section 7.2 for the ant-based algorithms. Table 7.4 lists the values for the NSGA-II-MPA parameters that produced the best results for these experiments.

7.4 Algorithm Comparison

This section has as its main objective to compare the EEMACOMP, EEMACOMH, EEMMASMP, EEMMASMH, and EEMACOMC algorithms to each other and also to the NSGA-II-MPA.

The remainder of this section is organised as follows: Subsection 7.4.1 describes the followed experimental procedure. Section 7.4.2 discusses performance with reference to the number of non-dominated solutions. Performance with reference to the spacing metric is covered in Section 7.4.3. Section 7.4.4 discusses the results with reference to the hypervolume metric. Section 7.4.5 analyses the performance of the algorithms over time with reference to the performance metrics. Section 7.4.6 discusses the performance of the optimisation criteria (power-aware routing objectives). Section 7.4.7 gives an overview of the ranking of the algorithms. Section 7.4.8 discusses the computational complexity of the algorithms, while Section 7.4.9 gives a summary of the overall performance of the algorithms.

Table 7.3: Simulation parameters for the MOO ACO algorithms

Parameter	Value	Applicable Algorithms
Number of Nodes, N_G	30, 100, 300	ALL
Transmission Range, T_r	400m	ALL
R_g	300m, 500m, 800m	ALL
Simulation Time	120	ALL
Mobility Model	RPGM	ALL
Number of Ants	25	ALL
Source Node, S	4	ALL
Destination Node, D	28 if $N_G = 30$ 98 if $N_G = 100$ or $N_G = 300$	ALL
Network Timer, T_{sm}	1, 2, 3, 4, 5, 6 sec	ALL
Exploration Vs Exploitation Parameter, r_0	0.5	EEMACOMP, EEMACOMH, EEMACOMC
Local Evaporation Parameter, ρ_l	0.5	EEMACOMP, EEMACOMH, EEMACOMC
Global Evaporation Parameter, ρ_g	0.7	ALL
α	1.50	EEMMASMP, EEMMASMH
Initial Energy for Node i, E_i	400	ALL
η-Strategy Parameter, λ_E	6	ALL
λ_ν	0.2	EEMACOMP, EEMMASMP
λ_ξ	0.2	EEMACOMP, EEMMASMP
λ_π	0.2	EEMACOMP, EEMMASMP
λ_ϱ	0.2	EEMACOMP, EEMMASMP
λ_ς	0.2	EEMACOMP, EEMMASMP
β_ν	3.5	ALL
β_ξ	4.0	ALL
β_π	4.5	ALL
β_ϱ	4.5	ALL
β_ς	5.0	ALL
Pareto Archive Size	100	ALL

Table 7.4: Simulation parameters for the NSGA-II algorithm

Parameter	value
Population size	100
Crossover probability	0.9
Mutation probability	0.125
R	256
N_e	30

7.4.1 Experimental Procedure

Each estimated pareto front, $\mathcal{PF}$, produced by the EEMACOMP, EEMACOMH, EEMMASMP, EEMMASMH, EEMACOMC, and NSGA-II-MPA algorithms is evaluated using three performance metrics, namely the $\bar{n}_{alg}$, $\bar{\varrho}$, and $\bar{\xi}$ (refer to Section 7.1.3). The performance of each algorithm was tested under different scenarios for different change frequencies, change severities and number of nodes as outlined in section 7.1.1. The influence of the change frequency, the change severity and the number of nodes on the performance of each algorithm was evaluated. For each of the scenarios 30 simulations were executed and results are reported as averages over these simulations together with the standard deviations.

Results obtained from the EEMACOMP, EEMACOMH, EEMMASMP, EEMMASMH, EEMACOMC, and NSGA-II-MPA algorithms are summarised in Tables F.1 to F.54 in the appendix F. Each table represents the results of the execution for each algorithm, for a specific scenario. A total of 54 scenarios, generated as listed in Table 7.2 for different values combinations of $N_G \in \{30, 100, 300\}$, $T_{sm} \in \{1, 2, 3, 4, 5, 6\}$, and $R_g \in \{300, 500, 800\}$, were tested.

In each table, the following information is provided for each algorithm:

- $\bar{n}_{alg}$: average number of non-dominated solutions found by each algorithm.
- $\bar{\varrho}$: average value of the spacing metric.
- $\bar{\xi}$: average value of the hypervolume metric.
- n^w_{alg} : number of times that the algorithm has a better $\bar{n}_{alg}$ than the others, for each environment change.

- ϱ^w : number of times that the algorithm has a better $\bar{\varrho}$ than the others, for each environment change.
- ξ^w : number of times that the algorithm has a better $\bar{\xi}$ than the others, for each environment change.
- *Rank* : overall rank of the algorithm. For each of the performance metrics the algorithm is ranked according to the number of times that the algorithm has a better performance than all the other algorithms with reference to this performance metric, for each environment change. The algorithm's average rank is calculated and then the algorithm is ranked accordingly.
- CI : the 95% confidence intervals using the t-test for each algorithm and each performance metric.

For all of the experiments, the algorithms used the best found values for the control parameters as listed in tables 7.3 and 7.4.

Appendix G presents three dimensional graphs to illustrate the influence of change frequency, T_{sm}, and change severity, R_g, on the performance metrics, $\bar{n}_{alg}$, $\bar{\varrho}$, and $\bar{\xi}$ for different number of nodes, based on Tables F.1 to F.54.

For each algorithm the following hypotheses or questions were investigated :

1. Is there a statistical significant difference in the performance of the algorithms?
2. Does performance deteriorate with increase in change frequency?
3. Does performance deteriorate with increase in change severity?
4. Are the algorithms scalable?
5. Is there an algorithm that is less affected by change frequency / change severity?

To test whether there is a statistical significant difference in the performance of any two algorithms, algorithm1 and algorithm2, with reference to the performance metric, p_{metric}, the following two hypotheses were considered:

$$H_0 : \quad \mu^{p_{metric}}_{algorithm1} = \mu^{p_{metric}}_{algorithm2}$$
$$H_1 : \quad \mu^{p_{metric}}_{algorithm1} > \mu^{p_{metric}}_{algorithm2}$$

where H_0 is the null hypothesis and H_1 is the alternative hypothesis.

In order to test these hypotheses the Mann-Whitney U test [129] was applied over the 30 p_{metric} values (one for each simulation) for each algorithm and for each T_{sm}, R_g and N_G combination. A 95% confidence level was used together with a 1-tail test. The critical value for U is 317, where U is the test statistic for the Mann-Whitney test. Results are illustrated in appendix H using Fluxviz [1] graphs. Each graph contains 4 axes. The first axis represents the change frequency, T_{sm}, the second axis represents the change severity, R_g, and the third axis represents the number of nodes, N_G. The last axis represents the results of the Mann-Whitney U test one for each of the T_{sm}, R_g and N_G combinations. Each combination corresponds to a specific scenario. If the null hypothesis, H_0, is accepted for a specific scenario, the value of 0 and the symbol "$\approx$" are displayed next to the scenario (last axis), showing that there is no statistical significant difference between the performance of the two compared algorithms. If H_0 is rejected the value of one and the symbol ">" are displayed next to the scenario, showing that the first algorithm is better than the second one for the respective scenario.

7.4.2 Number of Non-Dominated Solutions Metric

This subsection analyses the empirical results of each algorithm in terms of the average number of non-dominated solutions metric, $\bar{n}_{alg}$. The $\bar{n}_{alg}$ metric measures how well the algorithms performed in identifying solutions along the Pareto front. Larger values for $\bar{n}_{alg}$ are preferred as it indicates that many efficient solutions were found which is preferred by the decision maker.

Figures G.1-G.3 in Appendix G illustrate the influence of T_{sm} and R_g on the $\bar{n}_{alg}$ metric under different N_G values, using the values of Tables F.1 to F.54. The following observations can be made from the figures and tables:

1. **Influence of T_{sm} on the $\bar{n}_{alg}$ metric.**

   Figures G.1-G.3 indicate that $\bar{n}_{alg}$ increased for all ACO algorithms as T_{sm} increases (change frequency decreases). Figures G.1(f), G.2(f) and G.3(f) indicate that $\bar{n}_{alg}$ increased for the NSGA-II-MPA algorithm as T_{sm} increases, for all scenarios, excluding those with $N_G \in \{100, 300\}$ and $R_g = 800$.

Table 7.5 displays the average values for $\bar{n}_{alg}$ over all the N_G and R_g values while Figure 7.37 illustrates the results of Table 7.5. Table 7.5 and Figure 7.37 indicate that $\bar{n}_{alg}$ increased for each algorithm as change frequency decreases. This result is expected as low change frequencies (high pause time, T_{sm}) provides more time to explore the search space, thereby finding more solutions.

Table 7.5: Average value for $\bar{n}_{alg}$ over all the N_G and R_g values

	T_{sm}					
$\mathcal{PF}$	1	2	3	4	5	6
$P_{EEMACOMP}$	78.56	82.48	85.68	86.87	88.26	91.26
$P_{EEMACOMH}$	52.70	54.57	57.99	57.29	61.50	63.85
$P_{EEMMASMP}$	75.60	77.79	80.01	80.72	83.18	85.78
$P_{EEMMASMH}$	72.52	75.47	77.88	79.15	81.41	83.82
$P_{EEMACOMC}$	72.69	76.18	76.70	78.56	81.02	83.23
$P_{NSGA-II-MPA}$	34.99	39.40	41.67	41.58	41.33	41.72

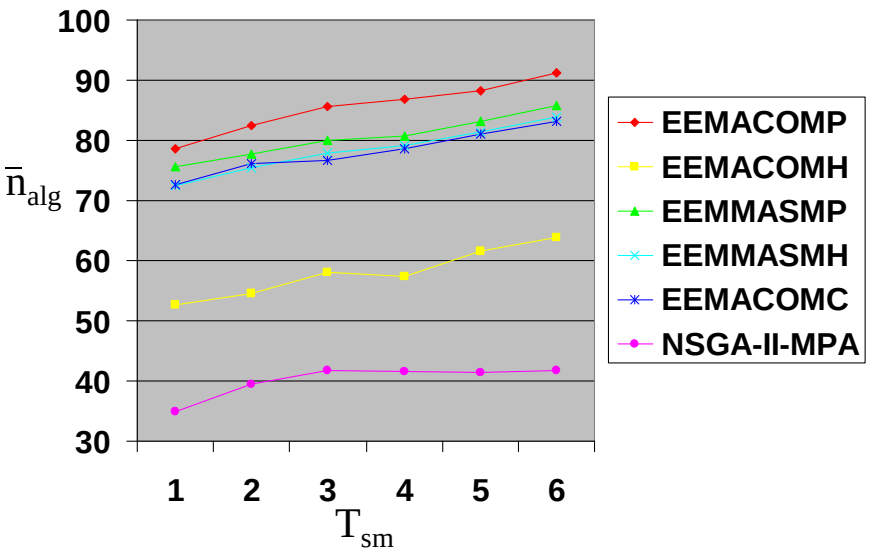

Figure 7.37: Average value for $\bar{n}_{alg}$ over all the N_G and R_g values

It is also to be noted from Table 7.5 and Figure 7.37 that EEMACOMH and NSGA-II-MPA are significantly worse than the other algorithms. In other words, EEMACOMH and NSGA-II-MPA do not scale well with reference to T_{sm}.

2. **Influence of R_g on the $\bar{n}_{alg}$ metric.**

Figures G.1-G.3 show that in most cases the number of non-dominated solutions decreased with increase in change severity, R_g. For the rest of the scenarios, $\bar{n}_{alg}$ increased when R_g increased to 500, and decreased again with $R_g = 800$. In order to better visualise the relation between R_g and $\bar{n}_{alg}$, Table 7.6 displays the average values for $\bar{n}_{alg}$ over all the N_G and T_{sm} values while Figure 7.38 illustrates the results of Table 7.6.

Table 7.6: Average value for $\bar{n}_{alg}$ over all the N_G and T_{sm} values

	R_g		
$\mathcal{PF}$	300	500	800
$P_{EEMACOMP}$	99.25	88.87	68.48
$P_{EEMACOMH}$	75.93	69.46	34.05
$P_{EEMMASMP}$	97.33	83.68	60.66
$P_{EEMMASMH}$	94.92	81.82	58.90
$P_{EEMACOMC}$	95.75	82.02	57.57
$P_{NSGA-II-MPA}$	53.15	41.62	25.92

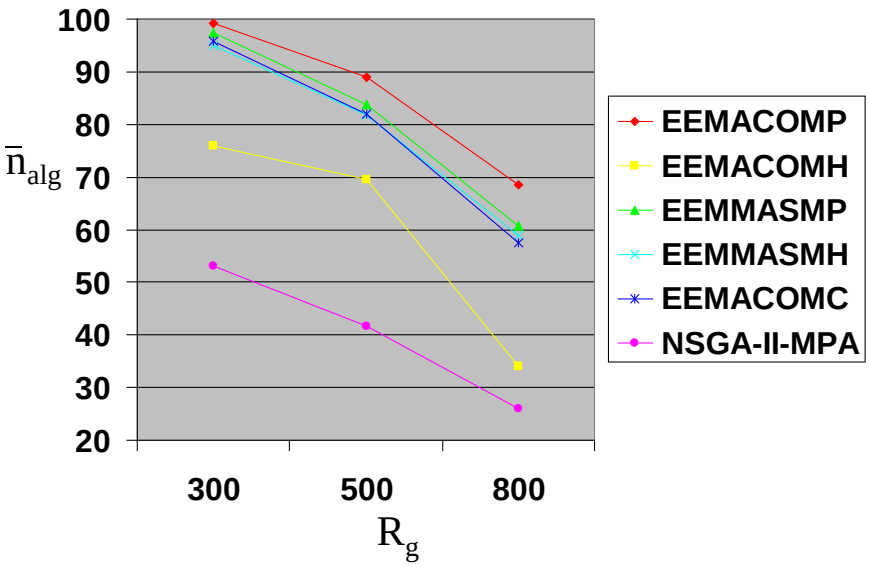

Figure 7.38: Average value for $\bar{n}_{alg}$ over all the N_G and T_{sm} values

Table 7.6 and Figure 7.38 show that when $\bar{n}_{alg}$ is taken as the average value over all the N_G and T_{sm} values, the number of non-dominated solutions decreased with increase in R_g. This trend is expected, because an increase in change severity, R_g, causes only some of the nodes to be within transmission range. The number of alternative paths by which to send a packet from source to destination and the number of non-dominated solutions therefore decreases.

It is also to be noted from Table 7.6 and Figure 7.38 that EEMACOMH and NSGA-II-MPA are affected the most by the change severity.

3. **Performance of multi-pheromone approaches vs single-pheromone approaches with reference to the $\bar{n}_{alg}$ metric.**

   Multi-pheromone approaches are EEMACOMP and EEMMASMP where a pheromone matrix is associated with each objective. Single-pheromone approaches are EEMACOMH and EEMMASMH where one pheromone matrix is associated with all the objectives.

   Figures G.1(a), G.2(a), G.3(a), G.1(c), G.2(c), and G.3(c) illustrate the influence of R_g and T_{sm} on the $\bar{n}_{alg}$ metric for the multi-pheromone approaches, while figures G.1(b), G.2(b), G.3(b), G.1(d), G.2(d), and G.3(d) illustrate the influence of R_g and T_{sm} on the $\bar{n}_{alg}$ metric for the single-pheromone approaches. The figures show that the multi-pheromone approaches produced a larger $\bar{n}_{alg}$ in most scenarios compared to single pheromone approaches.

   To test whether there is a statistical significant difference in the performance of the multi-pheromone approach, EEMACOMP, and the single pheromone approach, EEMACOMH, the following two hypotheses were considered:

$$H_0: \quad \mu^{\bar{n}_{alg}}_{EEMACOMP} = \mu^{\bar{n}_{alg}}_{EEMACOMH}$$
$$H_1: \quad \mu^{\bar{n}_{alg}}_{EEMACOMP} > \mu^{\bar{n}_{alg}}_{EEMACOMH}$$

   In order to test these hypotheses the Mann-Whitney U test was applied over all scenarios for the EEMACOMP and EEMACOMH.

Figure H.1 illustrates the results of the Mann-Whitney U test. Results show that the multi-pheromone approach, EEMACOMP, produced significantly more non-dominated solutions than the single pheromone approach, EEMACOMH, for 95% of the scenarios (all scenarios except scenarios with $\{N_G = 30,\ R_G = 300,\ T_{sm} \in \{3, 4, 5, 6\}\}$ and $\{N_G = 30,\ R_G = 500,\ T_{sm} \in \{3, 5, 6\}\}$). EEMACOMP increases the coverage of the solution space, therefore finding more non-dominated solutions than the EEMACOMH algorithm.

Following the same procedure as with EEMACOMP and EEMACOMH, to test whether there is a statistical significant difference in the performance of the multi-pheromone approach, EEMMASMP, and the single pheromone approach, EEMMASMH, the following two hypotheses were considered:

$$H_0: \ \mu^{\bar{n}_{alg}}_{EEMMASMP} = \mu^{\bar{n}_{alg}}_{EEMMASMH}$$
$$H_1: \ \mu^{\bar{n}_{alg}}_{EEMMASMP} > \mu^{\bar{n}_{alg}}_{EEMMASMH}$$

Results of the Mann-Whitney U test are illustrated in Figure H.2. The Mann-Whitney U test shows that EEMMASMP produced significantly more non-dominated solutions than EEMMASMH for all scenarios, excluding those with $\{N_G = 30,\ R_G \in \{300, 500\},\ \forall T_{sm}\}$ and $\{N_G = 300,\ R_G = 500,\ T_{sm} \in \{1, 2, 3\}\}$ (72% of the scenarios).

For the scenarios where the null hypothesis is rejected, EEMMASMP increases the coverage of the solution space, therefore finding more non-dominated solutions than the EEMMASMH algorithm.

4. **Performance of the multi-colony approach vs single-colony approaches with reference to the $\bar{n}_{alg}$ metric.**

   EEMACOMC is a multi-colony approach assigning a colony to each objective, while EEMACOMP, EEMACOMH, EEMMASMP, and EEMMASMH are single-colony approaches assigning the same colony for all objectives.

   Figures G.1(a), G.2(a), G.3(a), G.1(b), G.2(b), G.3(b), G.1(c), G.2(c), G.3(c), G.1(d), G.2(d), and G.3(d) illustrate the influence of R_g and T_{sm} on the $\bar{n}_{alg}$ metric

for the single-colony approaches, while figures G.1(e), G.2(e), and G.3(e) illustrate the influence of R_g and T_{sm} on the $\bar{n}_{alg}$ metric for the multi-colony approach.

Figures G.1(a), G.1(e), G.2(a), G.2(e), G.3(a), and G.3(e) show that the single-colony approach, EEMACOMP, produced in most scenarios more non-dominated solutions than the multi-colony approach, EEMACOMC.

To test whether there is a statistical significant difference in the performance of EEMACOMP and EEMACOMC the following two hypotheses were considered:

$$\begin{aligned} H_0: &\quad \mu^{\bar{n}_{alg}}_{EEMACOMP} = \mu^{\bar{n}_{alg}}_{EEMACOMC} \\ H_1: &\quad \mu^{\bar{n}_{alg}}_{EEMACOMP} > \mu^{\bar{n}_{alg}}_{EEMACOMC} \end{aligned}$$

Results of the Mann-Whitney U test are illustrated in Figure H.3. The Mann-Whitney U test shows that EEMACOMP is significantly better than EEMACOMC with reference to the $\bar{n}_{alg}$ metric for all scenarios with $N_G > 30$, excluding scenarios with $\{T_{sm} = 6,\ R_G = 300,\ N_G = 100\}$ and $\{T_{sm} = 1,\ R_G = 800,\ N_G = 100\}$ (better for 63% of the scenarios).

Figures G.1(b), G.1(e), G.2(b), G.2(e), G.3(b), and G.3(e) show that the multi-colony approach, EEMACOMC, produced in most scenarios more non-dominated solutions than the single-colony approach, EEMACOMH.

To test whether there is a statistical significant difference in the performance of EEMACOMC and EEMACOMH the following two hypotheses were considered:

$$\begin{aligned} H_0: &\quad \mu^{\bar{n}_{alg}}_{EEMACOMC} = \mu^{\bar{n}_{alg}}_{EEMACOMH} \\ H_1: &\quad \mu^{\bar{n}_{alg}}_{EEMACOMC} > \mu^{\bar{n}_{alg}}_{EEMACOMH} \end{aligned}$$

Results of the Mann-Whitney U test are illustrated in Figure H.4. The Mann-Whitney U test shows that EEMACOMC is significantly better than EEMACOMH with reference to the $\bar{n}_{alg}$ metric for all scenarios, excluding those with $\{N_G = 30,\ R_g = 300,\ T_{sm} \in \{3, 4, 5, 6\}\}$ and $\{N_G = 30,\ R_g = 500,\ T_{sm} \in \{5, 6\}\}$ (better for 88% of the scenarios).

5. **Performance of ACO approaches vs the NSGA-II-MPA approach with reference to the $\bar{n}_{alg}$ metric.**

   Figures G.1-G.3 show that all the ACO approaches displayed a higher value for $\bar{n}_{alg}$ when compared to the NSGA-II-MPA approach.

   To test whether there is a statistical significant difference in the performance of the ACO approaches and the NSGA-II-MPA approach the following two hypotheses were considered:

$$H_0: \quad \mu_{ACO}^{\bar{n}_{alg}} = \mu_{NSGA-II-MPA}^{\bar{n}_{alg}}$$
$$H_1: \quad \mu_{ACO}^{\bar{n}_{alg}} > \mu_{NSGA-II-MPA}^{\bar{n}_{alg}}$$

   where ACO takes the values EEMACOMP, EEMACOMH, EEMMASMP, EEMMASMH, and EEMACOMC.

   Results of the Mann-Whitney U tests are illustrated in Figures H.5-H.9. The Mann-Whitney U tests show that all the ACO approaches excluding EEMACOMH found significantly more non-dominated solutions than the NSGA-II-MPA approach, for all scenarios. EEMACOMH produced significantly more non-dominated solutions than NSGA-II-MPA for all scenarios, excluding those with $\{N_G \in \{100, 300\}$, $R_g = 800\ \}$ (better for 77% of the scenarios).

6. **Performance of ACS approaches vs MAX-MIN approaches with reference to the $\bar{n}_{alg}$ metric**.

   EEMACOMP and EEMACOMH are ACS approaches, while EEMMASMP and EEMMASMH are MAX-MIN approaches. Figures G.1(a), G.2(a), G.3(a), G.1(b), G.2(b), and G.3(b) illustrate the influence of R_g and T_{sm} on the $\bar{n}_{alg}$ metric for the ACS approaches, while Figures G.1(c), G.2(c), G.3(c), G.1(d), G.2(d), and G.3(d) illustrate the influence of R_g and T_{sm} on the $\bar{n}_{alg}$ metric for the MAX-MIN approaches.

   Figures G.1(a), G.1(c), G.1(d), G.2(a), G.2(c), G.2(d), G.3(a), G.3(c), and G.3(d) show that the ACS approach, EEMACOMP, produced a higher $\bar{n}_{alg}$ for higher number of nodes compared to the MAX-MIN approaches, EEMMASMP, and EEMMASMH.

To test whether there is a statistical significant difference in the performance of the EEMACOMP, and the EEMMASMP and EEMMASMH, approaches, the following two hypotheses were considered:

$$H_0: \ \mu^{\bar{n}_{alg}}_{EEMACOMP} = \mu^{\bar{n}_{alg}}_{EEMAXMIN}$$
$$H_1: \ \mu^{\bar{n}_{alg}}_{EEMACOMP} > \mu^{\bar{n}_{alg}}_{EEMAXMIN}$$

where EEMAXMIN takes the values EEMMASMP and EEMMASMH.

In order to test these hypotheses the Mann-Whitney U test was applied and the results are illustrated in Figures H.10 and H.11. Figure H.10 shows that EEMACOMP produced significantly more non-dominated solutions than EEMMASMP for all scenarios with $N_G = 100$ and $R_g = 800$, scenarios with $N_G = 300$, irrespective of T_{sm} and R_g, and scenarios with $\{R_g = 800,\ N_G = 30,\ T_{sm} \in \{1, 2, 3, 4\}\}$ (better for 63% of the scenarios). Figure H.11 shows that EEMACOMP produced significantly more non-dominated solutions than EEMMASMH for all scenarios, excluding those with $\{R_g = 300,\ N_G = 30,\ \forall T_{sm}\}$, $\{R_g = 500,\ N_G = 30,\ T_{sm} \in \{1, 3, 4, 5, 6\}\}$, $\{R_g = 800,\ N_G = 30,\ T_{sm} = 1\}$, and $\{R_g = 500,\ N_G = 100,\ T_{sm} = 6\}$ (better for 75% of the scenarios).

Figures G.1(b), G.1(c), G.1(d), G.2(b), G.2(c), G.2(d), G.3(b), G.3(c), and G.3(d) show that the MAX-MIN approaches, EEMMASMP and EEMMASMH, produced on average a higher $\bar{n}_{alg}$ compared to the ACS approach EEMACOMH.

To test whether there is a statistical significant difference in the performance of the EEMMASMP and EEMMASMH approaches, and the EEMACOMH approach, the following two hypotheses were considered:

$$H_0: \ \mu^{\bar{n}_{alg}}_{EEMAXMIN} = \mu^{\bar{n}_{alg}}_{EEMACOMH}$$
$$H_1: \ \mu^{\bar{n}_{alg}}_{EEMAXMIN} > \mu^{\bar{n}_{alg}}_{EEMACOMH}$$

In order to test these hypotheses the Mann-Whitney U test was applied and the results are illustrated in Figures H.12 and H.13. Figure H.12 shows that EEMMASMP produced significantly more non-dominated solutions than EEMACOMH

for all scenarios, except those with $\{R_g = 300,\ N_G = 30,\ T_{sm} \in \{3,4,5,6\}\}$ and $\{R_g = 500,\ N_G = 30,\ T_{sm} \in \{3,5,6\}\}$ (better for 87% of the scenarios). Figure H.13 shows the same results when comparing EEMMASMH and EEMACOMH.

7. **Influence of N_G on the $\bar{n}_{alg}$ metric.**

   Figures G.1-G.3 show that $\bar{n}_{alg}$ decreased for each algorithm as the number of nodes, N_G, increased. With increase in number of nodes the computational complexity is much higher and there is not enough time for the algorithms to explore the search space and to track the optima after the change occurred, thereby finding less solutions.

7.4.3 Spacing Metric

This subsection analyses the empirical results of each algorithm in terms of the average spacing metric, $\bar{\varrho}$. The spacing metric serves as an indicator of the distribution of solutions in the obtained Pareto front for each algorithm. The higher the value of $\bar{\varrho}$, the less uniformity in the distribution of solutions. The ideal value for the spacing metric is zero, in which case all solutions would be equidistantly spaced. Smaller values for $\bar{\varrho}$ are therefore preferred.

Figures G.4-G.6 in Appendix G illustrate the influence of T_{sm} and R_g on the $\bar{\varrho}$ metric under different N_G values, using the values of Tables F.1 to F.54. The following observations can be made from the figures and tables:

1. **Influence of T_{sm} on the $\bar{\varrho}$ metric.**

   Figures G.4-G.6 show that the solution spread improved ($\bar{\varrho}$ decreased) with decrease in change frequency. In order to derive different trends, Table 7.7 displays the average values for $\bar{\varrho}$ over all the N_G and R_g values while Figure 7.39 illustrates the results of Table 7.7.

   Table 7.7 and Figure 7.39 indicate that the solution spread improved with decrease in change frequency. Lower change frequencies provide more time to explore the search space. This helps to identify solutions along the full extent of the Pareto front and keeps the solutions more uniformly distributed in the whole Pareto-

Table 7.7: Average value for $\bar{\varrho}$ over all the N_G and R_g values

	T_{sm}					
$\mathcal{PF}$	1	2	3	4	5	6
$P_{EEMACOMP}$	0.084	0.070	0.062	0.057	0.056	0.050
$P_{EEMACOMH}$	0.129	0.114	0.101	0.102	0.097	0.087
$P_{EEMMASMP}$	0.093	0.082	0.072	0.068	0.065	0.059
$P_{EEMMASMH}$	0.098	0.085	0.077	0.073	0.070	0.066
$P_{EEMACOMC}$	0.110	0.095	0.084	0.080	0.077	0.070
$P_{NSGA-II-MPA}$	0.188	0.139	0.133	0.134	0.139	0.136

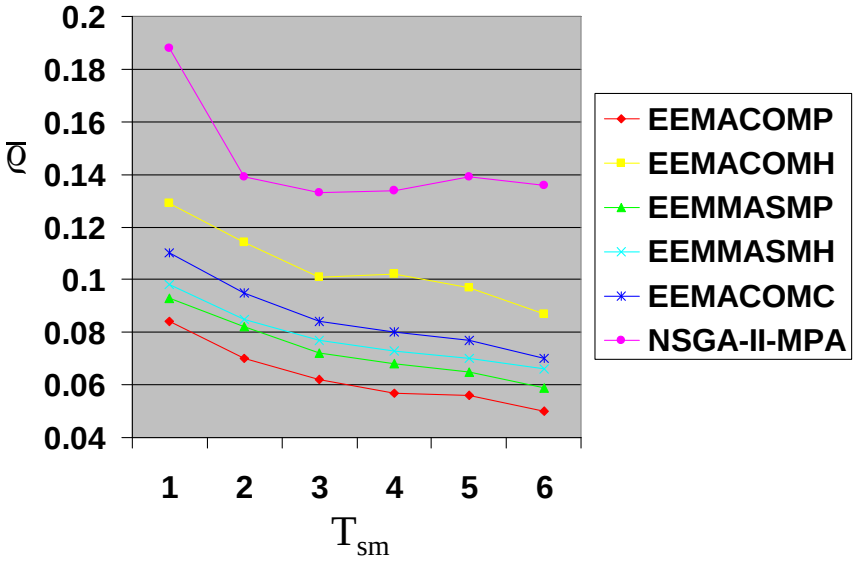

Figure 7.39: Average value for $\bar{\varrho}$ over all the N_G and R_g values

optimal set, instead of gathering in a small region. A decrease in change frequency leads to more uniformly distributed solutions, which justifies the obtained results.

It is also to be noted from Table 7.7 and Figure 7.39 that EEMACOMP is better than the other algorithms while NSGA-II-MPA is significantly worse than all the ACO algorithms.

2. **Influence of R_g on the $\bar{\varrho}$ metric.**

Figures G.4-G.6 show that, for all the ACO algorithms, the solution spread deteriorated with increase in change severity, R_g. The same applied to the NSGA-II-MPA algorithm for scenarios with $N_G = 30$. For scenarios with $N_G > 30$, NSGA-II-MPA had a strange behaviour: For scenarios with $N_G = 100$ (refer to Figure G.5(f)), NSGA-II-MPA had the worst solution spread for $R_g = 300$. With $R_g = 300$, the network has a small diameter and combined with a medium number of nodes ($N_G = 100$) may produce many redundant solutions. Redundancy may slow down the optimisation process and have a negative impact on the exploration ability of the algorithm. For scenarios with $N_G = 300$ (refer to Figure G.6(f)), NSGA-II-MPA had a parabolic behaviour with worst $\bar{\varrho}$ at $R_g = 500$ and best $\bar{\varrho}$ at $R_g = 300$. With $N_G = 300$ and $R_g = 300$, the redundancy of solutions is probably not uniform and may be beneficial for the optimisation process. From these solutions many new solution candidates may be reached, thus improving diversity.

In order to derive different trends, Table 7.8 displays the average values for $\bar{\varrho}$ over all the N_G and T_{sm} values while Figure 7.40 illustrates the results of Table 7.8. Table 7.8 and Figure 7.40 indicate that when $\bar{\varrho}$ is taken as the average value over all the N_G and T_{sm} values, $\bar{\varrho}$ increased (the solution spread deteriorated) with increase in R_G for all algorithms.

Table 7.8: Average value for $\bar{\varrho}$ over all the N_G and T_{sm} values

	R_g		
$\mathcal{PF}$	300	500	800
$P_{EEMACOMP}$	0.034	0.057	0.100
$P_{EEMACOMH}$	0.057	0.098	0.163
$P_{EEMMASMP}$	0.040	0.068	0.112
$P_{EEMMASMH}$	0.043	0.073	0.120
$P_{EEMACOMC}$	0.043	0.071	0.145
$P_{NSGA-II-MPA}$	0.106	0.125	0.200

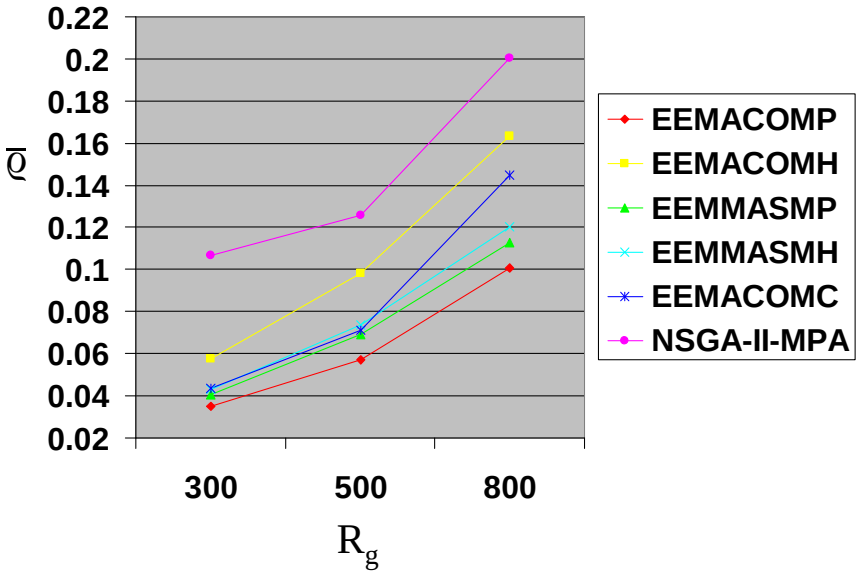

Figure 7.40: Average value for $\bar{\varrho}$ over all the N_G and T_{sm} values

The global range, R_g, relates to the connectivity of the network. When R_g is small the network is highly connected which means that it is easy to move from any one vertex to any other vertex in a few steps. Thus, the network has a small diameter and many alternate disjoint paths between vertices. With a high value of R_g, only part of the nodes are within transmission range from one another, and the number of alternative paths available to send a packet from source to destination decreases. Thus, it is logical that the diversity will deteriorate when the network range increases. On the other side, when the change severity, R_g, increases, it becomes more difficult for the optimiser to adapt current solutions to a changing environment. There is not much information gained from the past to reuse and it takes more time to optimise the problem and less time to explore, which explains the poor distribution of solutions as R_g increases.

It is also to be noted from Table 7.8 and Figure 7.40 that NSGA-II-MPA is significantly worse than all the ACO algorithms.

3. **Performance of multi-pheromone approaches vs single-pheromone ap-**

proaches with reference to $\bar{\varrho}$ metric.

Figures G.4(a), G.5(a), G.6(a), G.4(c), G.5(c), and G.6(c) illustrate the influence of R_g and T_{sm} on the $\bar{\varrho}$ metric for the multi-pheromone approaches, while Figures G.4(b), G.5(b), G.6(b), G.4(d), G.5(d), and G.6(d) illustrate the influence of R_g and T_{sm} on the $\bar{\varrho}$ metric for the single-pheromone approaches.

Figures G.4(a), G.4(b), G.5(a), G.5(b), G.6(a), and G.6(b) show that the multi-pheromone approach, EEMACOMP, outperformed the corresponding single pheromone approach, EEMACOMH, in terms of the solution spread. To test whether there is a statistical significant difference in the performance of the two approaches, the following two hypotheses were considered:

$$\begin{aligned} H_0: &\quad \mu^{\bar{\varrho}}_{EEMACOMP} = \mu^{\bar{\varrho}}_{EEMACOMH} \\ H_1: &\quad \mu^{\bar{\varrho}}_{EEMACOMP} > \mu^{\bar{\varrho}}_{EEMACOMH} \end{aligned}$$

In order to test these hypotheses the Mann-Whitney U test was applied over all scenarios for EEMACOMP and EEMACOMH.

Figure H.14 illustrates the results of the Mann-Whitney U test. Results show that the multi-pheromone approach, EEMACOMP, had a significantly better solution spread than the single pheromone approach, EEMACOMH, except for the scenario with $T_{sm} = 1$, $N_G = 30$, and $R_G = 500$ (better for 98% of the scenarios). EEMACOMP improves the coverage of the solution space, therefore, leading to more uniformly distributed solutions.

Figures G.4(c), G.4(d), G.5(c), G.5(d), G.6(c), and G.6(d) show that the multi-pheromone approach, EEMMASMP, produced results similar to the corresponding single pheromone approach, EEMMASMH, in terms of the solution spread. Following the same procedure as with EEMACOMP and EEMACOMH, the Mann-Whitney U test has been applied for EEMMASMP and EEMMASMH. The Mann-Whitney U test shows that there is no statistical significant difference in the average performance between EEMMASMP and EEMMASMH with reference to the $\bar{\varrho}$ metric except for 33% of the scenarios, i.e scenarios with ($R_g = 300$, $N_G = 100$, $T_{sm} \in \{3, 5, 6\}$), ($R_g = 800$, $N_G = 100$, $T_{sm} = 1$), ($R_g = 300$, $N_G = 300$,

$T_{sm} \in \{1, 3, 4, 5, 6\}$), ($R_g = 500$, $N_G = 300$, $T_{sm} \in \{2, 3, 4\}$), ($R_g = 500$, $N_G = 300$, $T_{sm} = 6$), and ($R_g = 800$, $N_G = 300$, $T_{sm} \in \{1, 3, 4, 5, 6\}$) (refer to Figure H.15).

4. **Performance of the multi-colony approach vs single-colony approaches with reference to $\bar{\varrho}$ metric**.

   Figures G.4(a), G.5(a), G.6(a), G.4(b), G.5(b), G.6(b), G.4(c), G.5(c), G.6(c), G.4(d), G.5(d), and G.6(d) illustrate the influence of R_g and T_{sm} on the $\bar{\varrho}$ metric for the single-colony approaches, while figures G.4(e), G.5(e), and G.6(e) illustrate the influence of R_g and T_{sm} on the $\bar{\varrho}$ metric for the multi-colony approach.

   Figures G.4(a), G.4(e), G.5(a), G.5(e), G.6(a), and G.6(e) show that the single-colony approach, EEMACOMP, produced in most scenarios a better solution spread than the multi-colony approach, EEMACOMC. To test whether there is a statistical significant difference in the performance of EEMACOMP and EEMACOMC the following two hypotheses were considered:

$$H_0: \quad \mu^{\bar{\varrho}}_{EEMACOMP} = \mu^{\bar{\varrho}}_{EEMACOMC}$$
$$H_1: \quad \mu^{\bar{\varrho}}_{EEMACOMP} > \mu^{\bar{\varrho}}_{EEMACOMC}$$

   Results of the Mann-Whitney U test are illustrated in Figure H.16. The Mann-Whitney U test shows that EEMACOMP is significantly better than EEMACOMC with reference to the $\bar{\varrho}$ metric for all scenarios, excluding scenarios with $\{N_G = 30, R_g = 300, T_{sm} \in \{3, 4, 6\}\}$, $\{N_G = 30, R_g = 500, T_{sm} = 5\}$, and $\{N_G = 100, R_g = 500, T_{sm} = 6\}$ (better for 90% of the scenarios).

   Figures G.4(b), G.4(e), G.5(b), G.5(e), G.6(b), and G.6(e) show that the multi-colony approach, EEMACOMC produced in most scenarios a better solution spread than the single-colony approach, EEMACOMH.

   To test whether there is a statistical significant difference in the performance of EEMACOMC and EEMACOMH the following two hypotheses were considered:

$$H_0: \quad \mu^{\bar{\varrho}}_{EEMACOMC} = \mu^{\bar{\varrho}}_{EEMACOMH}$$
$$H_1: \quad \mu^{\bar{\varrho}}_{EEMACOMC} > \mu^{\bar{\varrho}}_{EEMACOMH}$$

Results of the Mann-Whitney U test are illustrated in Figure H.17. The Mann-Whitney U test shows that EEMACOMC is significantly better than EEMACOMH with reference to the $\bar{\varrho}$ metric for all scenarios, excluding scenarios with $\{N_G = 30,\ R_g = 300,\ T_{sm} \in \{2,3\}\}$, $\{N_G = 30,\ R_g = 500,\ T_{sm} = 6\}$, $\{N_G = 30,\ R_g = 800,\ T_{sm} \in \{3,5\}\}$, and $\{N_G = 100,\ R_g = 800,\ T_{sm} = 1\}$ (better for 89% of the scenarios).

5. **Performance of ACO approaches vs NSGA-II-MPA approach with reference to $\bar{\varrho}$ metric**.

   Figures G.4-G.6 show that all the ACO approaches produced in most scenarios a better solution spread compared to the NSGA-II-MPA approach.

   To test whether there is a statistical significant difference in the performance of the ACO approaches and the NSGA-II-MPA approach the following two hypotheses were considered:

$$H_0: \ \mu^{\bar{\varrho}}_{ACO} = \mu^{\bar{\varrho}}_{NSGA-II-MPA}$$
$$H_1: \ \mu^{\bar{\varrho}}_{ACO} > \mu^{\bar{\varrho}}_{NSGA-II-MPA}$$

   Results of the Mann-Whitney U tests are illustrated in Figures H.18-H.22. The Mann-Whitney U tests show that all the ACO approaches produced significantly better solution spread than the NSGA-II-MPA approach for all scenarios, excluding the following scenarios: $\{N_G = 30,\ R_g = 500,\ T_{sm} \in \{1,2\}\}$, $\{N_G = 100,\ R_g = 500,\ T_{sm} \in \{3,4,5,6\}\}$, $\{N_G = 100,\ R_g = 800,\ T_{sm} \in \{4,5,6\}\}$, and $\{N_G = 300,\ R_g = 800,\ T_{sm} \in \{3,4\}\}$ for EEMACOMP (better for 80% of the scenarios), $\{N_G = 30,\ R_g = 500,\ T_{sm} \in \{1,2,3\}\}$, $\{N_G = 100,\ R_g = 500,\ T_{sm} \in \{1,2\}\}$, and $\{N_G = 300,\ R_g = 300,\ T_{sm} \in \{1,2,4,5,6\}\}$ for EEMACOMH (better for 83% of the scenarios), $\{N_G = 30,\ R_g = 500,\ T_{sm} \in \{1,2,3\}\}$, $\{N_G = 100,\ R_g = 500,\ T_{sm} \in \{1,2,6\}\}$, and $\{N_G = 300,\ R_g = 800,\ T_{sm} \in \{2,5\}\}$ for EEMMASMP (better for 85% of the scenarios), $\{N_G = 30,\ R_g = 500,\ T_{sm} \in \{1,2,3\}\}$, $\{N_G = 100,\ R_g = 500,\ T_{sm} \in \{2,6\}\}$, and $\{N_G = 300,\ R_g = 800,\ T_{sm} \in \{5,6\}\}$ for EEMMASMH (better for 87% of the scenarios), and $\{N_G = 30,\ R_g = 500,\ T_{sm} \in \{2,3\}\}$, $\{N_G = 100,$

$R_g = 500, \forall\ T_{sm}\ \}$, and $\{N_G = 300,\ R_g = 800,\ T_{sm} \in \{6\}\}$ for EEMACOMC (better for 83% of the scenarios).

6. **Performance of ACS approaches vs MAX-MIN approaches with reference to $\bar{\varrho}$ metric**.

   Figures G.4(a), G.5(a), G.6(a), G.4(b), G.5(b), and G.6(b) illustrate the influence of R_g and T_{sm} on the $\bar{\varrho}$ metric for the ACS approaches, while Figures G.4(c), G.5(c), G.6(c), G.4(d), G.5(d), and G.6(d) illustrate the influence of R_g and T_{sm} on the $\bar{\varrho}$ metric for the MAX-MIN approaches.

   Figures G.4(a), G.4(c), G.4(d), G.5(a), G.5(c), G.5(d), G.6(a), G.6(c), and G.6(d) show that the ACS approach, EEMACOMP, produced in most scenarios a better solution spread for $N_G > 30$ compared to the MAX-MIN approaches, EEMMASMP and EEMMASMH.

   To test whether there is a statistical significant difference in the performance of EEMACOMP and the EEMMASMP and EEMMASMH approaches, the following two hypotheses were considered:

$$H_0: \quad \mu^{\bar{\varrho}}_{EEMACOMP} = \mu^{\bar{\varrho}}_{EEMAXMIN}$$
$$H_1: \quad \mu^{\bar{\varrho}}_{EEMACOMP} > \mu^{\bar{\varrho}}_{EEMAXMIN}$$

   In order to test these hypotheses the Mann-Whitney U test was applied and the results are illustrated in Figures H.23 and H.24. Figure H.23 shows that EEMACOMP, produced a significantly better solution spread than EEMMASMP for $N_G > 30$ excluding scenario with $\{N_G = 100,\ R_g = 800,\ T_{sm} = 1\}$ (better for 65% of the scenarios), while Figure H.24 indicates that EEMACOMP, produced a significantly better solution spread than EEMMASMH for $N_G > 30$ (better for 66% of the scenarios).

   Figures G.4(b), G.4(c), G.4(d), G.5(b), G.5(c), G.5(d), G.6(b), G.6(c), and G.6(d) show that the MAX-MIN approaches, EEMMASMP and EEMMASMH, produced

in most scenarios a better solution spread compared to the ACS approach EEMACOMH.

To test whether there is a statistical significant difference in the performance of the EEMMASMP and EEMMASMH approaches, and the EEMACOMH approach, the following two hypotheses were considered:

$$H_0: \ \mu^{\bar{\varrho}}_{EEMAXMIN} = \mu^{\bar{\varrho}}_{EEMACOMH}$$
$$H_1: \ \mu^{\bar{\varrho}}_{EEMAXMIN} > \mu^{\bar{\varrho}}_{EEMACOMH}$$

In order to test these hypotheses the Mann-Whitney U test was applied and the results are illustrated in Figures H.25 and H.26. Figure H.25 shows that EEMMASMP had a significantly better solution spread than EEMACOMH, except for scenarios with $\{N_G = 30,\ R_g = 300,\ T_{sm} \in \{1, 2\}\}$, and $\{N_G = 30,\ R_g = 500,\ T_{sm} \in \{1, 2, 3, 4, 6\}\}$ (better for 87% of the scenarios). Figure H.26 indicates that EEMMASMH had a significantly better solution spread than EEMACOMH for all scenarios, except those with $\{N_G = 30,\ R_g = 300,\ T_{sm} = 1\}$, and $\{N_G = 30,\ R_g = 500,\ T_{sm} \in \{1, 2, 3, 4, 5, 6\}\}$ (better for 87% of the scenarios).

7. **Influence of N_G on the $\bar{\varrho}$ metric.**

   Figures G.4-G.6 show that when the number of nodes increased from 100 to 300 the distribution of solutions for all algorithms deteriorated. This is both an interesting and an unexpected result, which is possibly related to the computational complexity of the algorithms and scalability. The problem with scalability is that, as the number of nodes increases, it becomes necessary for the routing protocol to search more nodes in order to reach the destination, thus affecting diversity. When the number of nodes increased from 30 to 100 the distribution of solutions for all algorithms improved.

7.4.4 Hypervolume Metric

This subsection analyses the empirical results of each algorithm in terms of the hypervolume metric, $\bar{\xi}$. The hypervolume metric measures how well the algorithms performed

in identifying solutions along the full extent of the Pareto front. High values of the hypervolume metric indicate the closeness of the solutions to the optimal Pareto set.

Figures G.7-G.9 in Appendix G illustrate the influence of T_{sm} and R_g on the $\bar{\xi}$ metric under different N_G values, using the values of Tables F.1 to F.54. The following observations can be made from the figures and tables:

1. **Influence of T_{sm} on the hypervolume metric, $\bar{\xi}$.**

   Figures G.7-G.9 show a small increase of $\bar{\xi}$ as change frequency decreases, for all the ACO algorithms. This observation is confirmed when looking at Table 7.9 and Figure 7.41. Table 7.9 displays the average values for $\bar{\xi}$ over all the N_G and R_g values while Figure 7.41 illustrates the results of Table 7.9. This observation is expected as change frequency determines how often the problem changes and it seems intuitive to assume that a high change frequency makes a problem more difficult for an algorithm to solve as less time is available at each T_{sm} to reach the new global optima and optimise the multi-objective problem. Low change frequency gives more iterations, and theoretically is supposed to produce a uniform distribution of the solutions and closeness of the solutions to the optimal Pareto set.

Table 7.9: Average value for $\bar{\xi}$ over all the N_G and R_g values

	T_{sm}					
$\mathcal{PF}$	1	2	3	4	5	6
$P_{EEMACOMP}$	60831.05	61552.60	61894.07	62010.58	62179.96	62485.17
$P_{EEMACOMH}$	59205.85	59677.70	59843.11	59936.95	60076.63	60365.10
$P_{EEMMASMP}$	60410.77	60999.21	61421.41	61440.03	61678.51	61995.58
$P_{EEMMASMH}$	60264.39	60804.01	61252.15	61290.71	61489.01	61811.21
$P_{EEMACOMC}$	61033.57	61753.97	62181.59	62308.67	62439.49	62701.89
$P_{NSGA-II-MPA}$	61514.60	60201.54	60078.20	60028.05	60041.14	60048.25

2. **Influence of R_g on the hypervolume metric, $\bar{\xi}$.**

   For the ACO algorithms there are different observations according to the number of nodes. Figure G.7 shows an increase in $\bar{\xi}$ when R_g increases to 500 and a decrease in $\bar{\xi}$ when R_g increases to 800, for scenarios with $N_G = 30$. For most scenarios with $N_G = 100$, there is an increase in $\bar{\xi}$ with increase in change severity (refer to Figure G.8). For scenarios with $N_G = 300$, Figure G.9 shows an increase in $\bar{\xi}$ with decrease in change severity.

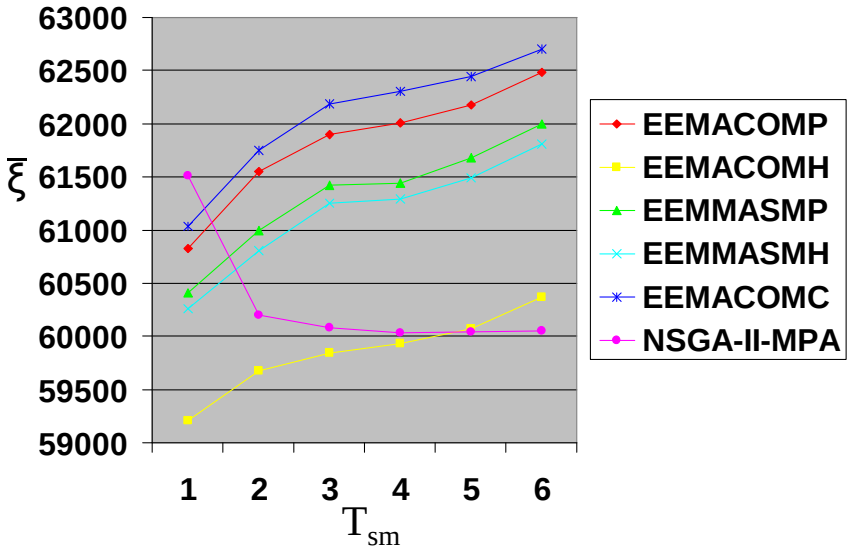

Figure 7.41: Average value for $\bar{\xi}$ over all the N_G and R_g values

For the NSGA-II-MPA algorithm, Figure G.7(f) shows an increase in $\bar{\xi}$ with increase in change severity, for scenarios with $N_G = 30$. For scenarios with $N_G = 100$, there is a decrease in $\bar{\xi}$ when R_g increases to 500 and an increase in $\bar{\xi}$ when R_g increases to 800 (refer to Figure G.8(f)). For scenarios with $N_G = 300$, Figure G.9(f) shows an increase in $\bar{\xi}$ when R_g increases to 500, and a decrease in $\bar{\xi}$ when R_g increases to 800.

Table 7.10: Average value for $\bar{\xi}$ over all the N_G and T_{sm} values

	R_g		
$\mathcal{PF}$	300	500	800
$P_{EEMACOMP}$	62046.719	62895.465	60677.192
$P_{EEMACOMH}$	60746.295	61105.342	57976.182
$P_{EEMMASMP}$	61491.817	62542.096	60083.312
$P_{EEMMASMH}$	61459.620	62419.858	59746.060
$P_{EEMACOMC}$	62708.710	62870.936	60783.509
$P_{NSGA-II-MPA}$	57908.890	59735.745	63251.480

Table 7.10 displays the average values for $\bar{\xi}$ over all the N_G and T_{sm} values while Figure 7.42 illustrates the results of Table 7.10. Table 7.10 and Figure 7.42 show

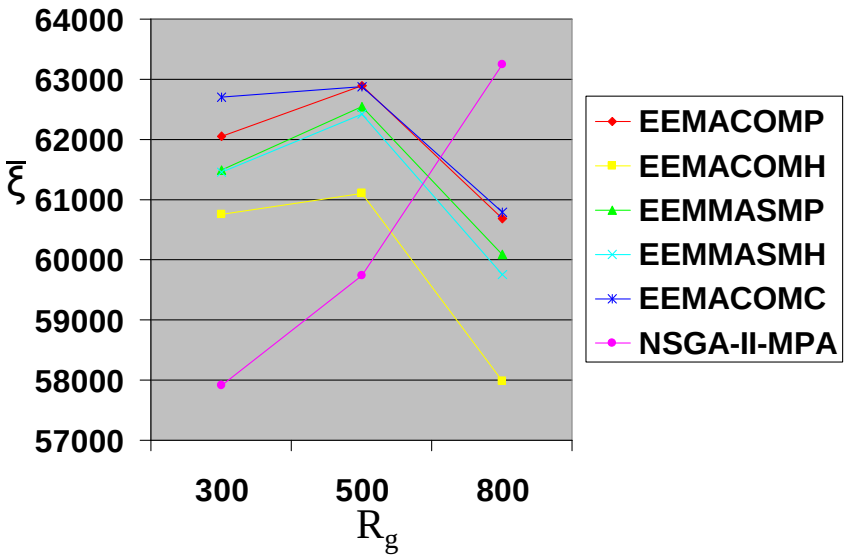

Figure 7.42: Average value for $\bar{\xi}$ over all the N_G and T_{sm} values

that when $\bar{\xi}$ is taken as the average value over all the N_G and T_{sm} values, $\bar{\xi}$ sharply decreases for $R_g = 800$ for the ACO algorithms and $\bar{\xi}$ sharply increases for $R_g = 800$ for the NSGA-II-MPA, outperforming the ACO algorithms. The expected result is a decrease in $\bar{\xi}$ with increase in change severity: It is a common assumption that smaller change severities are easier to adapt to, primarily by transferring solutions from the past optimisation problem which may help to accelerate the rate of convergence to the optima, after a change has occurred. Since R_g determines the change severity, the convergence to the optima, and therefore the closeness of the solutions to the optimal Pareto set, should be getting worse as the change severity increases.

3. **Performance of multi-pheromone approaches vs single-pheromone approaches with reference to the hypervolume metric.**

   Figures G.7(a), G.8(a), G.9(a), G.7(c), G.8(c), and G.9(c) illustrate the influence of R_g and T_{sm} on the $\bar{\xi}$ metric for the multi-pheromone approaches, while figures G.7(b), G.8(b), G.9(b), G.7(d), G.8(d), and G.9(d) illustrate the influence of

R_g and T_{sm} on the $\bar{\xi}$ metric for the single-pheromone approaches.

Figures G.7(a), G.7(b), G.8(a), G.8(b), G.9(a), and G.9(b) show that the multi-pheromone approach, EEMACOMP, displayed a higher value for the $\bar{\xi}$ metric compared to the single pheromone approach, EEMACOMH.

To test whether there is a statistical significant difference in the performance of EEMACOMP and EEMACOMH the following two hypotheses were considered:

$$H_0: \ \mu^{\bar{\xi}}_{EEMACOMP} = \mu^{\bar{\xi}}_{EEMACOMH}$$
$$H_1: \ \mu^{\bar{\xi}}_{EEMACOMP} > \mu^{\bar{\xi}}_{EEMACOMH}$$

In order to test these hypotheses the Mann-Whitney U test was applied over all scenarios for the EEMACOMP and EEMACOMH.

Figure H.27 illustrates the results of the Mann-Whitney U test. Results show that EEMACOMP produced a significantly higher value for the $\bar{\xi}$ metric than EEMACOMH for all scenarios, excluding those with $\{N_G = 30,\ R_g = 500,\ T_{sm} = 1\}$ and $\{N_G = 30,\ R_g = 800,\ T_{sm} = 1\}$ (better for 96% of the scenarios).

4. **Performance of the multi-colony approach vs single-colony approaches with reference to the hypervolume metric.**

   Figures G.7(a), G.8(a), G.9(a), G.7(b), G.8(b), G.9(b), G.7(c), G.8(c), G.9(c), G.7(d), G.8(d), and G.9(d) illustrate the influence of R_g and T_{sm} on the $\bar{\xi}$ metric for the single-colony approaches, while figures G.7(e), G.8(e), and G.9(e) illustrate the influence of R_g and T_{sm} on the $\bar{\xi}$ metric for the multi-colony approach.

   Figures G.7(b), G.7(e), G.8(b), G.8(e), G.9(b), and G.9(e) show that the multi-colony approach, EEMACOMC, produced in most scenarios a higher value for the hypervolume metric than the single-colony approach, EEMACOMH.

   To test whether there is a statistical significant difference in the performance of EEMACOMC and EEMACOMH the following two hypotheses were considered:

$$H_0: \ \mu^{\bar{\xi}}_{EEMACOMC} = \mu^{\bar{\xi}}_{EEMACOMH}$$
$$H_1: \ \mu^{\bar{\xi}}_{EEMACOMC} > \mu^{\bar{\xi}}_{EEMACOMH}$$

Results of the Mann-Whitney U test are illustrated in Figure H.28. The Mann-Whitney U test shows that EEMACOMC is significantly better than EEMACOMH with reference to the $\bar{\xi}$ metric for all scenarios, excluding scenarios with $\{N_G = 30,\ R_g = 500,\ T_{sm} = 1\}$ and $\{N_G = 30,\ R_g = 800,\ T_{sm} \in \{2, 6\}\}$ (better for 94% of the scenarios).

5. **Performance of ACO approaches vs the NSGA-II-MPA approach with reference to the hypervolume metric.**

   Figures G.7-G.9 and Tables F.1 to F.54 show that all the ACO approaches displayed a higher value for the hypervolume metric when compared to the NSGA-II-MPA approach, except for scenarios with $N_G = 300$ and $R_g \in \{500, 800\}$ and for scenarios with $N_G = 30$ and $R_g = 800$.

   To test whether there is a statistical significant difference in the performance of the ACO approaches and the NSGA-II-MPA approach the following two hypotheses were considered:

$$H_0: \ \mu^{\bar{\xi}}_{ACO} = \mu^{\bar{\xi}}_{NSGA-II-MPA}$$
$$H_1: \ \mu^{\bar{\xi}}_{ACO} > \mu^{\bar{\xi}}_{NSGA-II-MPA}$$

   Results of the Mann-Whitney U tests are illustrated in Figures H.29-H.33. The Mann-Whitney U tests show that all the ACO approaches displayed a significantly higher value for the hypervolume than the NSGA-II-MPA approach for all scenarios, excluding the following scenarios: $\{N_G = 30,\ R_g = 800,\ T_{sm} = 1\}$, $\{N_G = 100,\ R_g = 300,\ T_{sm} = 2\}$, $\{N_G = 100,\ R_g = 500,\ T_{sm} = 1\}$, and $\{N_G = 100,\ R_g = 800,\ T_{sm} = 1\}$ for EEMACOMP, EEMMASMP and EEMMASMH (better for 92% of the scenarios), $\{N_G = 30,\ R_g = 800,\ T_{sm} = 1\}$, $\{N_G = 100,\ R_g = 300,\ T_{sm} = 4\}$,

and $\{N_G = 100,\ R_g = 800,\ T_{sm} \in \{2, 3, 4\}$ for EEMACOMH (better for 90% of the scenarios), $\{N_G = 30,\ R_g = 800,\ T_{sm} \in \{1, 2\}\}$, $\{N_G = 100,\ R_g = 300,\ T_{sm} = 2\}$, and $\{N_G = 100,\ R_g = 500,\ T_{sm} = 1\}$ for EEMACOMC (better for 92% of the scenarios).

6. **Performance of ACS approaches vs MAX-MIN approaches with reference to the hypervolume metric**.

   Tables F.1 to F.54 and Figures G.7-G.9 show no trend between the performance of the ACS approaches and the MAX-MIN approaches with reference to the hypervolume metric.

7. **Influence of N_G on the hypervolume metric.**

   Figures G.7-G.9 show that, for scenarios with $N_G = 300$ and $R_g = 800$, all algorithms displayed a lower value for the hypervolume metric.

   There are two possible explanations for this result:

   (a) Computational complexity of the algorithms: As the number of nodes increases it becomes necessary for the routing protocol to search more nodes in order to reach the destination, which, in turn, increases the convergence time and affects closeness towards the true Pareto front.

   (b) Premature convergence towards local optima: With a high number of nodes the population tends to contain similar individuals and the diversity decreases rapidly. The suboptimal solutions which may have helped in finding the global optima are deleted too rapidly and the closeness towards the true Pareto front gets worst.

7.4.5 Performance of the Algorithms Over the Environmental Changes

This subsection compares the performance of the algorithms for each environment change. For each environmental change the average values for all the solutions of the iteration before a change to the environment occurs were calculated for each metric. These values were then averaged over all R_g and N_G and further averaged over the 30 simulations. The obtained values are referred to as $\bar{n}_{alg}$, $\bar{\varrho}$, and $\bar{\xi}$.

Figure 7.43 visualises the performance of the algorithms over time with reference to $\bar{n}_{alg}$. The graphs show that, for all change frequencies, there is little variance in $\bar{n}_{alg}$ over time. This shows the ability of all the algorithms, excluding the EEMACOMH and the NSGA-II-MPA, to react to change and find an adequate number of non-dominated solutions. Also, results show that transferring of solutions from the environment before the change occurs helps to accelerate search after the environment has changed and find a satisfactory number of non-dominated solutions. Therefore, in each environment, good solutions were likely to be found where good solutions have been in the previous environment. The EEMACOMP algorithm found more non-dominated solutions than all the other algorithms and the NSGA-II-MPA found the least number of non-dominated solutions. For low change frequencies all algorithms displayed the largest values for $\bar{n}_{alg}$.

Figure 7.43(a) shows a linear decrease over time for the NSGA-II-MPA algorithm for $T_{sm} = 1$ (high change frequency). NSGA-II-MPA had less time to react to changes and the time to find solutions was increased at each environment change.

Figure 7.43(f) shows an increase of $\bar{n}_{alg}$ over time for the EEMACOMH algorithm for $T_{sm} = 6$ (low change frequency). The optimiser had enough time to exploit the solutions transferred from the previous environment and improve the tracking performance of the optima and reduce the time to find solutions.

Figure 7.44 visualises the performance of the algorithms over time with reference to $\bar{\varrho}$. The graphs show that, for all change frequencies, $\bar{\varrho}$ had a very small value, showing a very good distribution of the solutions. For NSGA-II-MPA, $\bar{\varrho}$, remained constant over time for $T_{sm} \in \{3, 4, 5, 6\}$ and displayed an increase over time for $T_{sm} = 1$. For all ACO algorithms, $\bar{\varrho}$ remained at relatively the same level, for all environment changes, which again shows the robustness of the ACO algorithms. The assumption can be made here that a diverse spread of non-dominated solutions can adapt more easily to changes when the environment change is not too severe. For severe environment changes, the performance of the algorithms are similar to restarting the optimisation from scratch, and the optimum tracking becomes difficult. That is the case for NSGA-II-MPA, for $T_{sm} = 1$.

The EEMACOMP algorithm had the best solution spread and the NSGA-II-MPA had the worst solution spread compared to the rest of the algorithms.

Figure 7.45 visualises the performance of the algorithms over time with reference to the $\bar{\xi}$ metric. The graphs show high values of $\bar{\xi}$ for all change frequencies. The value

of $\bar{\xi}$ is similar for all environment changes, showing that there is a good adaptability to environment changes by all the algorithms. The size of the objective space which is dominated by the non-dominated solutions is over 80% of the total hypervolume of 75000, where 75000 is the maximum hypervolume calculated using the values of 100.0, 0.1, 500.0, 0.5, and 30.0, corresponding to a maximum value for each of the objectives. This indicates the closeness of the solutions to the optimal set and the good spread of solutions across the objective space. All algorithms displayed a similar value of $\bar{\xi}$.

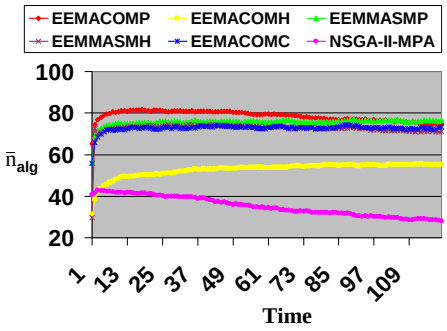

(a) $T_{sm} = 1$

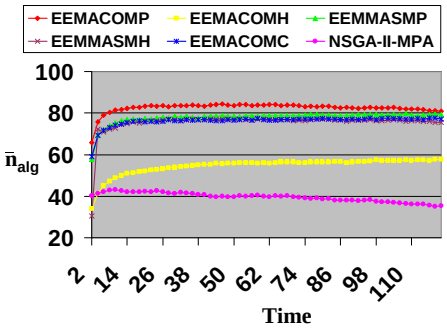

(b) $T_{sm} = 2$

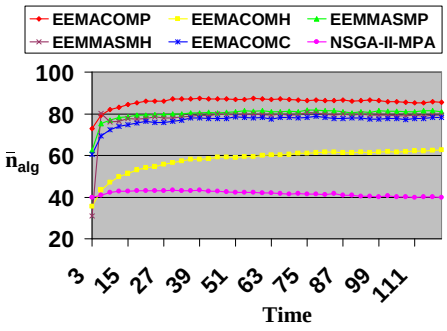

(c) $T_{sm} = 3$

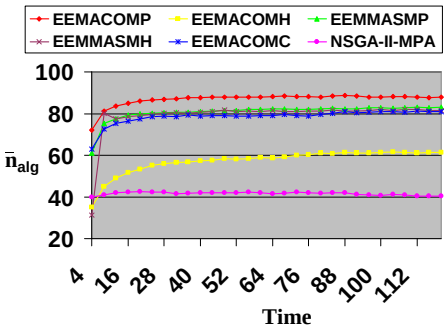

(d) $T_{sm} = 4$

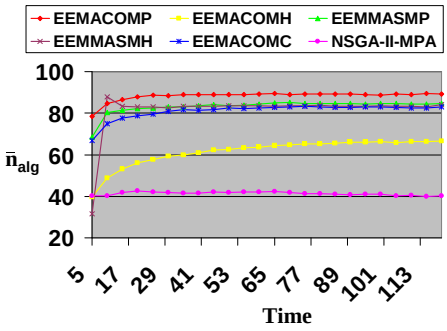

(e) $T_{sm} = 5$

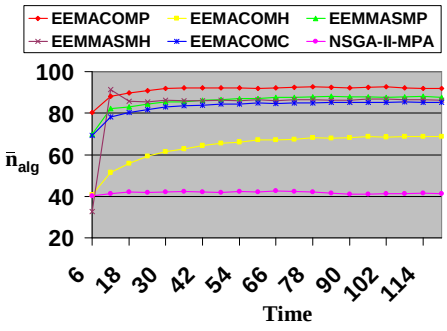

(f) $T_{sm} = 6$

Figure 7.43: Performance of the algorithms over time with regard to the number of non-dominated solutions metric, $\bar{n}_{alg}$

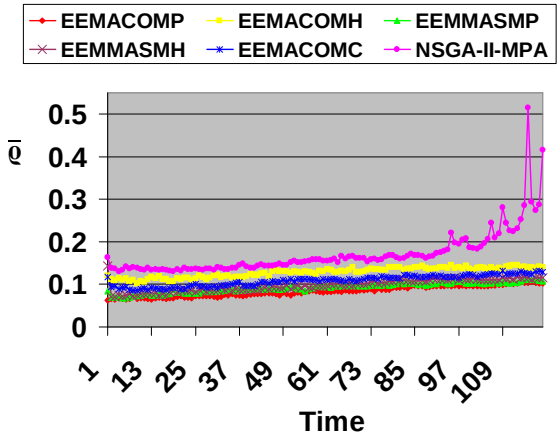

(a) $T_{sm} = 1$

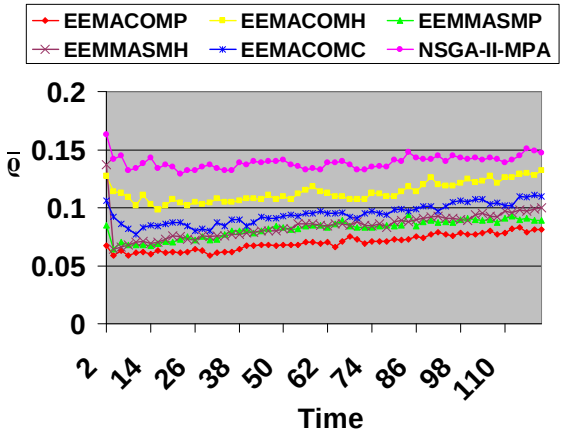

(b) $T_{sm} = 2$

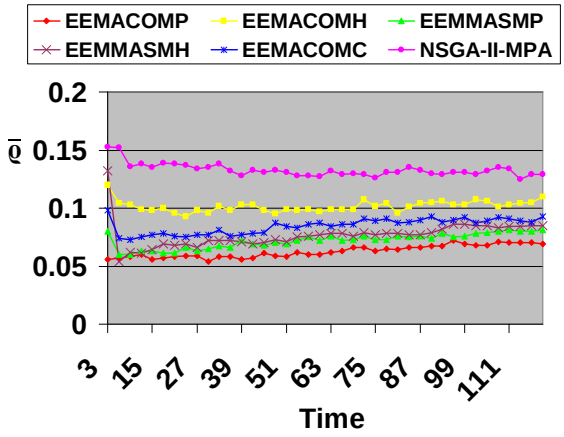

(c) $T_{sm} = 3$

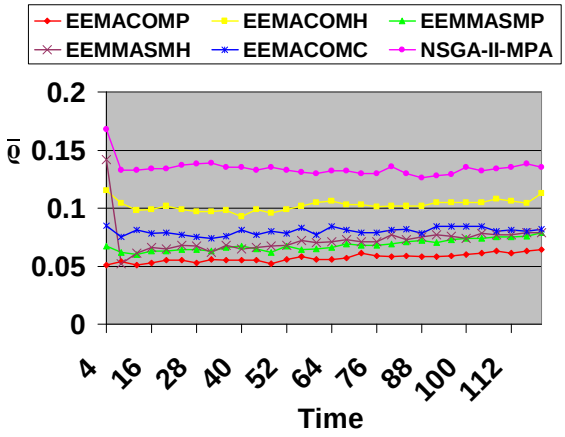

(d) $T_{sm} = 4$

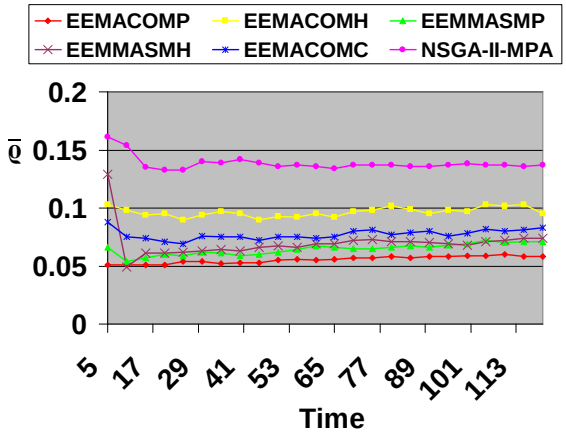

(e) $T_{sm} = 5$

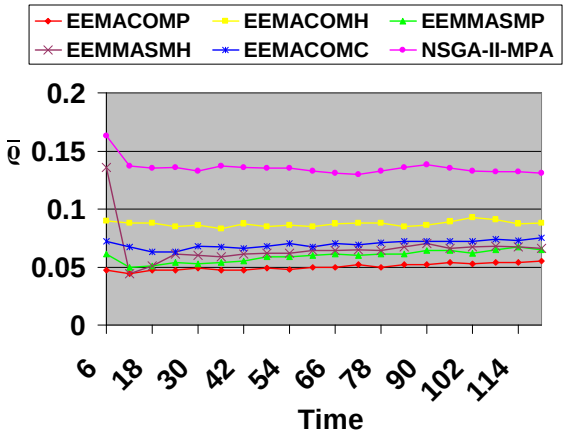

(f) $T_{sm} = 6$

Figure 7.44: Performance of the algorithms over time with regard to the spacing metric, $\bar{\varrho}$

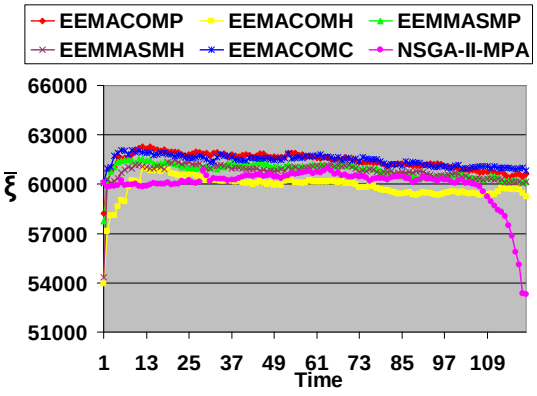

(a) $T_{sm} = 1$

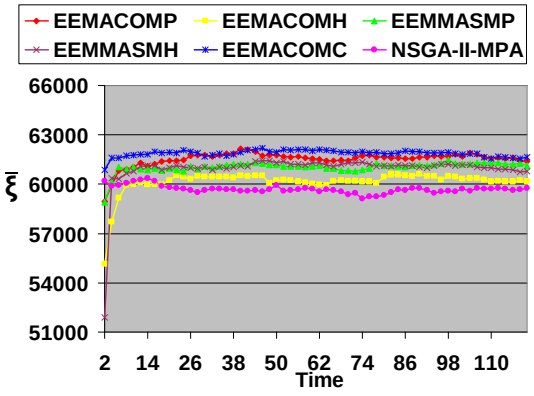

(b) $T_{sm} = 2$

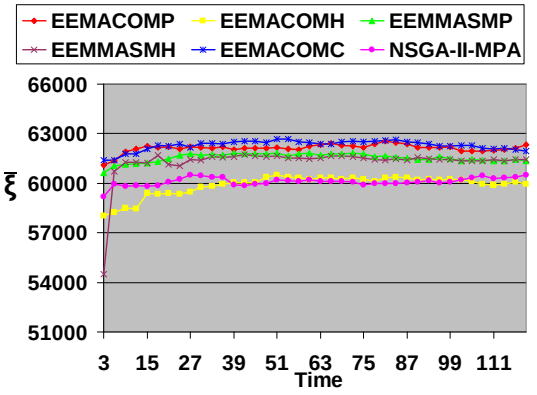

(c) $T_{sm} = 3$

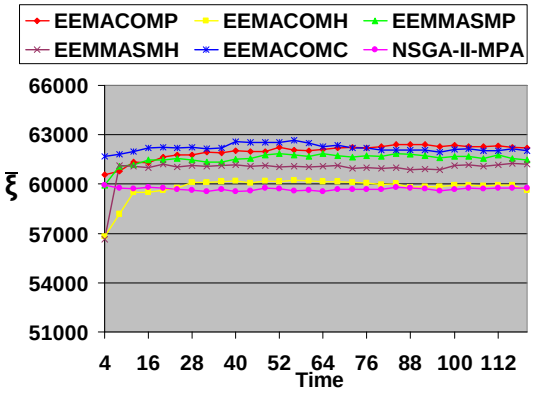

(d) $T_{sm} = 4$

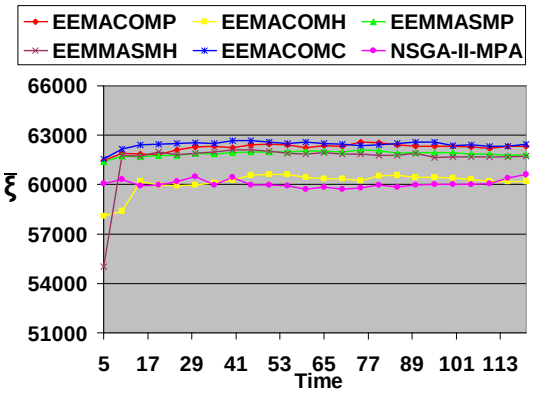

(e) $T_{sm} = 5$

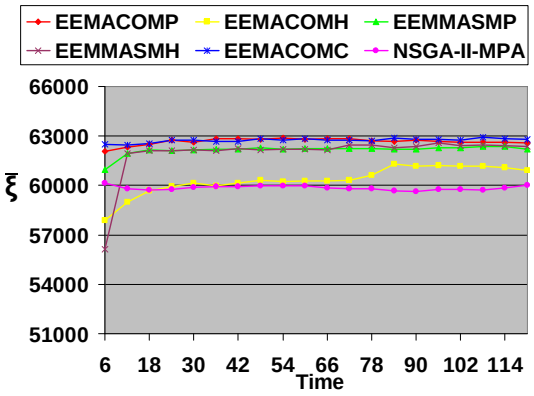

(f) $T_{sm} = 6$

Figure 7.45: Performance of the algorithms over time with regard to the hypervolume metric, $\bar{\xi}$

7.4.6 Optimization Criteria

This section analyses the performance of each algorithm in terms of the optimisation criteria (objective functions). The performance of each algorithm was tested under different scenarios for different change frequencies, change severities, and number of nodes as outlined in section 7.1.1. For each scenario the Pareto front, $\mathcal{PF}$, produced by the EEMACOMP, EEMACOMH, EEMMASMP, EEMMASMH, EEMACOMC, and NSGA-II-MPA algorithms is estimated. The influence of the change frequency, the change severity, and the number of nodes on the value of each objective function is evaluated.

For each of the scenarios 30 simulations have been executed and results were reported as averages over these simulations over all environment changes together with the standard deviations.

Results obtained from the EEMACOMP, EEMACOMH, EEMMASMP, EEMMASMH, EEMACOMC, and NSGA-II-MPA algorithms are summarised in Tables I.1 to I.45 in appendix I for the different scenarios. Based on these tables, appendix J illustrates the influence of change frequency, T_{sm}, and change severity, R_g, on the EP, TNP, VNP, CP, and MNC optimisation criteria (refer to Section 6.3 for a discussion of these criteria) for different number of nodes, N_G, using Fluxviz graphs.

Figures J.1-J.3 visualise the influence of T_{sm} and R_g on the EP criterion based on the results of Tables I.1-I.9. Figures J.4-J.6 visualise the influence of T_{sm} and R_g on the TNP criterion based on the results of Tables I.10-I.18. Figures J.7-J.9 visualise the influence of T_{sm} and R_g on the VNP criterion based on the results of Tables I.19-I.27. Figures J.10-J.12 graphically illustrate the influence of T_{sm} and R_g on the CP criterion based on the results of Tables I.28-I.36, while Figures J.13-J.15 visualise the influence of T_{sm} and R_g on the MNC criterion based on the results of Tables I.37-I.45.

The algorithms were compared in terms of the value of the objective functions. To test whether there is a statistical significant difference in the performance of any two algorithms with reference to the optimisation criteria, the Mann-Whitney U test as outlined in section 7.4.1 was applied.

- **Energy consumed per packet, EP, objective**

  Tables I.1-I.9 and Figures J.1-J.3 show no variation in EP with increase in change frequency for $N_G = 30$ and no pattern between EP and change frequency for

$N_G \in \{100, 300\}$.

Table 7.11 displays the average values of EP over all the N_G and R_g values using the results of Tables I.1-I.9. Figure 7.46 illustrates the results of Table 7.11. Table 7.11 and Figure 7.46 indicate no significant difference in EP value as change frequency increases. It is also to be noted from Table 7.11 and Figure 7.46 that when EP is taken as the average value over all the N_G and R_g values, NSGA-II-MPA is significantly better than the other algorithms, showing a very low EP.

Table 7.11: Average value of the EP objective over all the N_G and R_g values

	T_{sm}					
$\mathcal{PF}$	1	2	3	4	5	6
$P_{EEMACOMP}$	8.60	8.77	8.58	8.43	8.54	8.28
$P_{EEMACOMH}$	9.90	10.47	10.39	10.32	10.62	10.22
$P_{EEMMASMP}$	8.86	9.07	8.86	8.82	8.89	8.52
$P_{EEMMASMH}$	9.10	9.29	9.08	9.05	9.09	8.75
$P_{EEMULTCOL}$	8.72	8.90	8.66	8.60	8.68	8.34
$P_{NSGA-II-MPA}$	2.58	2.55	2.53	2.51	2.52	2.52

Tables I.1-I.9 and Figures J.1-J.3 indicate an increase in EP with increase in R_g for $N_G = 30$. For $N_G = 100$, EEMACOMC and NSGA-II-MPA produced the highest EP for $R_g = 800$, while the rest of the algorithms produced the highest EP for $R_g = 300$. For $N_G = 300$, EEMACOMH, EEMACOMC and NSGA-II-MPA produced the highest EP for $R_g = 800$ and no real trend between EP and change severity for $R_g \in \{300, 500\}$, while the rest of the algorithms presented no pattern between EP and change severity.

In order to better visualise the relation between R_g and EP, Table 7.12 displays the average values of EP over all the N_G and T_{sm} values while Figure 7.47 illustrates the results of Table 7.12. Table 7.12 and Figure 7.47 indicate that EP increased for each algorithm as R_g increased to the value of 800. This trend is expected, because an increase in change severity, R_g, causes only some of the nodes to be within transmission range and paths with minimum energy consumed per packet may not be possible. It is also to be noted from Table 7.12 and Figure 7.47 that when EP is taken as the average value over all the N_G and T_{sm} values, NSGA-II-MPA is significantly better than the other algorithms, showing a very low EP.

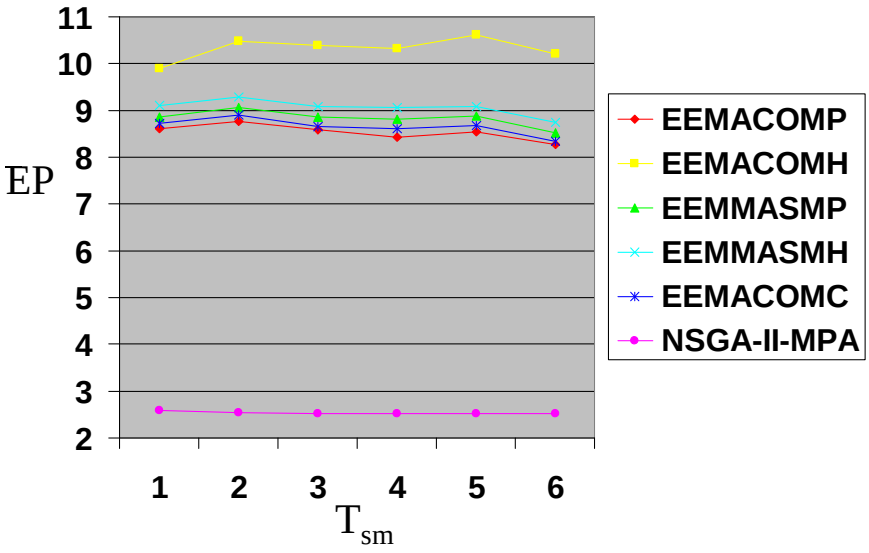

Figure 7.46: Average value of the EP objective over all the N_G and R_g values

Table 7.12: Average value of the EP objective over all the N_G and T_{sm} values

	R_g		
$\mathcal{PF}$	300	500	800
$P_{EEMACOMP}$	8.87	7.56	9.17
$P_{EEMACOMH}$	9.67	9.51	11.78
$P_{EEMMASMP}$	8.88	7.96	9.67
$P_{EEMMASMH}$	8.89	8.15	10.14
$P_{EEMULTCOL}$	7.75	7.59	10.61
$P_{NSGA-II-MPA}$	2.26	2.21	3.14

Tables I.1-I.9 and Figures J.1-J.3 show that the EP value increased significantly when the number of nodes increased to $N_G = 300$. This is an unexpected result which is possibly related to the computational complexity of the algorithms. As the number of nodes increases, it becomes necessary for the routing protocol to search more nodes in order to reach the destination, thus affecting diversity and the finding of the paths with the least energy consumed per packet.

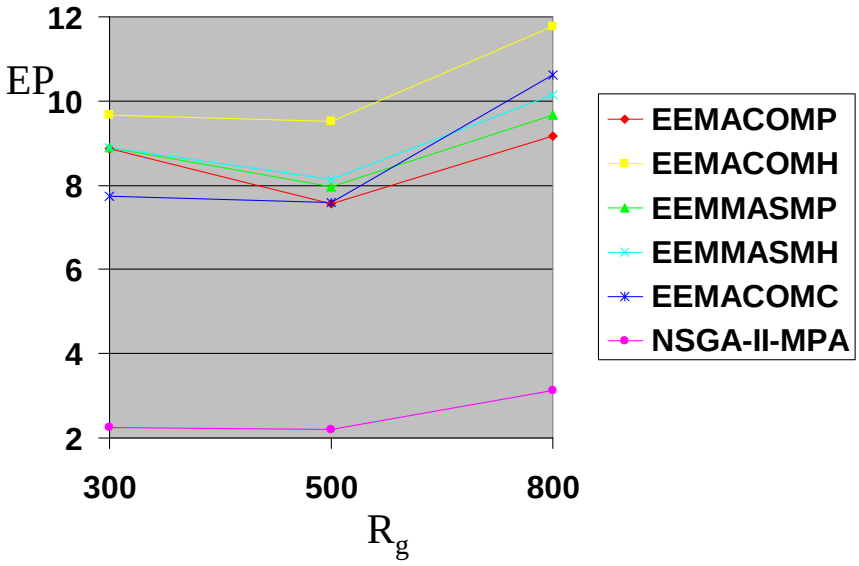

Figure 7.47: Average value of the EP objective over all the N_G and T_{sm} values

Tables I.1-I.9 show that all the ACO approaches displayed a higher value for EP and therefore worst performance when compared to the NSGA-II-MPA approach. To test whether there is a statistical significant difference in the performance of the NSGA-II-MPA approach and the ACO approaches, the following two hypotheses were considered:

$$H_0: \quad \mu^{EP}_{NSGA-II-MPA} = \mu^{EP}_{ACO}$$
$$H_1: \quad \mu^{EP}_{NSGA-II-MPA} > \mu^{EP}_{ACO}$$

where ACO takes the values EEMACOMP, EEMACOMH, EEMMASMP, EEMMASMH, and EEMACOMC.

Results of the Mann-Whitney U tests were the same for all the compared algorithms, as illustrated in Figure 7.48. The Mann-Whitney U tests show that the NSGA-II-MPA had a significantly lower energy consumed per packet than all the ACO algorithms for all the scenarios. This is possibly related to the effects of the

k shortest path algorithm used for NSGA-II-MPA, which selects the first R paths with minimum energy consumed per packet and with minimum cost per packet (refer to Section 6.7).

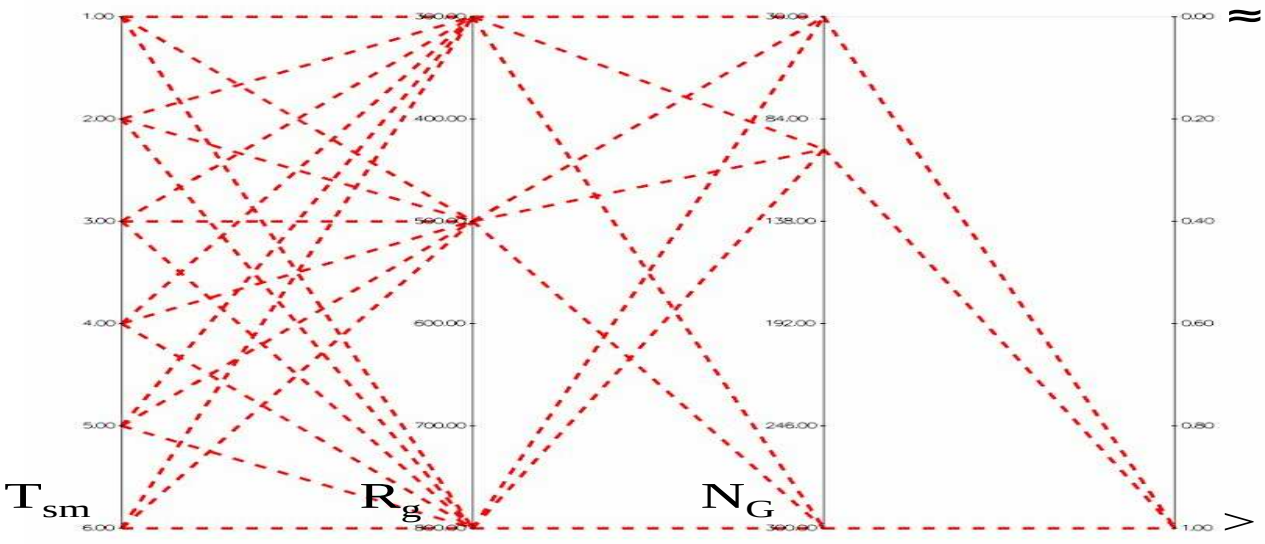

Figure 7.48: Comparing the NSGA-II-MPA algorithm against the ACO algorithms with regard to EP using the Mann-Whitney U test

- **Utilisation of the most heavily used link, TNP, objective**

  Tables I.10-I.18 and Figures J.4-J.6 indicate a small decrease in TNP with decrease in change frequency for all algorithms. In addition, the NSGA-II-MPA displayed a high value of TNP for $T_{sm} = 1$, showing a bad performance for high change frequency.

  Table 7.13 displays the average values of TNP over all the N_G and R_g values using the results of Tables I.10-I.18. Figure 7.49 illustrates the results of Table 7.13. Table 7.13 and Figure 7.49 indicate a very small decrease or no difference for TNP as T_{sm} increased (change frequency decreased), except for the NSGA-II-MPA algorithm which displayed a high value of TNP for $T_{sm} = 1$. Low change frequencies provide more time to better optimise the TNP objective.

Table 7.13: Average value of the TNP objective over all the N_G and R_g values

	T_{sm}					
$\mathcal{PF}$	1	2	3	4	5	6
$P_{EEMACOMP}$	0.0024	0.0022	0.0021	0.0021	0.0020	0.0020
$P_{EEMACOMH}$	0.0026	0.0024	0.0023	0.0022	0.0022	0.0022
$P_{EEMMASMP}$	0.0024	0.0022	0.0021	0.0021	0.0020	0.0020
$P_{EEMMASMH}$	0.0024	0.0022	0.0021	0.0021	0.0021	0.0021
$P_{EEMULTCOL}$	0.0023	0.0022	0.0022	0.0022	0.0021	0.0021
$P_{NSGA-II-MPA}$	0.0130	0.0026	0.0024	0.0023	0.0023	0.0022

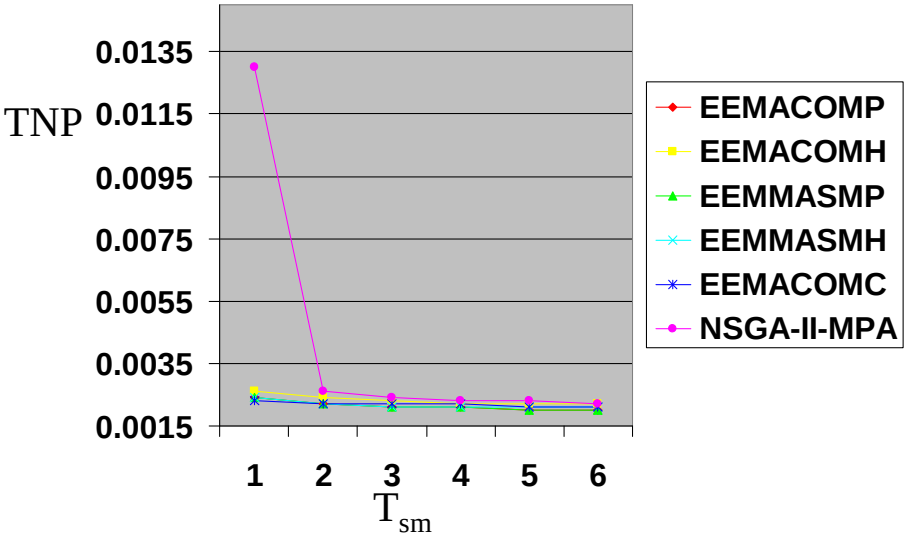

Figure 7.49: Average value of the TNP objective over all the N_G and R_g values

Tables I.10-I.18 and Figures J.4-J.6 indicate an increase in TNP with increase in change severity for all algorithms. In addition, the NSGA-II-MPA displayed a high value of TNP for $N_G = 100$, $R_g = 300$ and $T_{sm} = 1$.

In order to better visualise the relation between R_g and TNP, Table 7.14 displays the average values for TNP over all the N_G and T_{sm} values, while Figure 7.50 illustrates the results of Table 7.14. Table 7.14 and Figure 7.50 indicate that TNP increased for each algorithm as R_g increased. This trend is expected, because an increase in change severity, R_g, causes only some of the links to be valid, and it may not be possible to minimise or avoid the utilisation of the link with the least capacity.

Table 7.14: Average value of the TNP objective over all the N_G and T_{sm} values

	R_g		
$\mathcal{PF}$	300	500	800
$P_{EEMACOMP}$	0.0014	0.0018	0.0033
$P_{EEMACOMH}$	0.0014	0.0019	0.0036
$P_{EEMMASMP}$	0.0014	0.0018	0.0033
$P_{EEMMASMH}$	0.0014	0.0018	0.0033
$P_{EEMULTCOL}$	0.0014	0.0019	0.0033
$P_{NSGA-II-MPA}$	0.0021	0.0020	0.0083

Tables I.10-I.18 and Figures J.4-J.6 show that the TNP value decreased when the number of nodes increased. This is an expected result because as the number of nodes increases, more links are available and therefore it becomes more easy to minimise the utilisation of the link with the least capacity.

Tables I.10-I.18 show that all the ACO approaches displayed a lower value for the TNP for scenarios with $N_G = 300$ when compared to the NSGA-II-MPA approach. To test whether there is a statistical significant difference in the performance of the ACO approaches and the NSGA-II-MPA approach for $N_G = 300$, the following two hypotheses were considered:

$$H_0 : \quad \mu_{ACO}^{TNP} = \mu_{NSGA-II-MPA}^{TNP}$$
$$H_1 : \quad \mu_{ACO}^{TNP} > \mu_{NSGA-II-MPA}^{TNP}$$

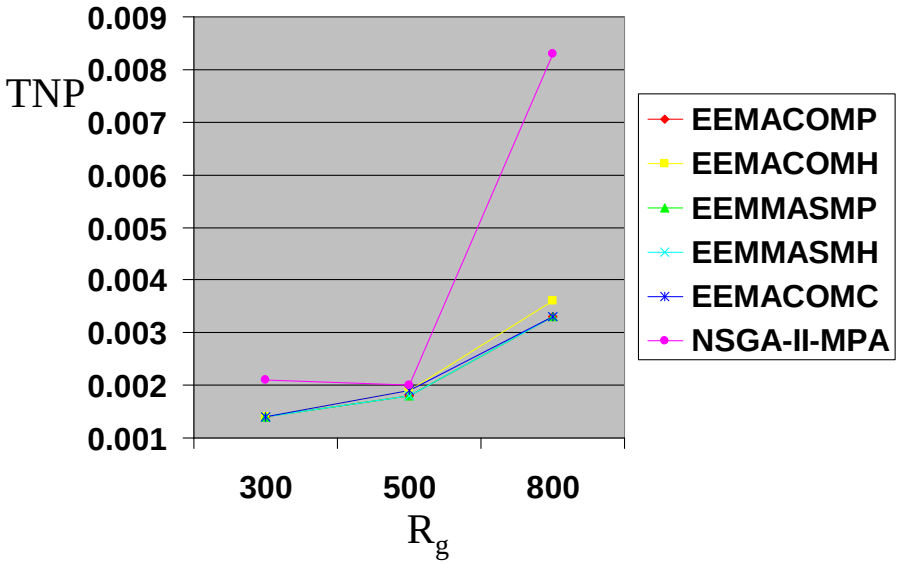

Figure 7.50: Average value of the TNP objective over all the N_G and T_{sm} values

Results of the Mann-Whitney U tests were the same for all the compared algorithms as illustrated in Figure 7.51. The Mann-Whitney U tests show that all ACO approaches are significantly better than the NSGA-II-MPA approach with reference to the TNP objective for $N_G = 300$. There is no significant difference between ACO approaches and the NSGA-II-MPA approach with reference to the TNP objective for $N_G \in \{30, 100\}$.

- **Variance in node power levels, VNP, objective**

  Tables I.19-I.27 and Figures J.7-J.9 show no pattern between VNP and change frequency.

  Table 7.15 displays the average values of VNP over all the N_G and R_g values using the results of Tables I.19-I.27. Figure 7.52 illustrates the results of Table 7.15. Table 7.15 and Figure 7.52 indicate a small decrease in VNP with a decrease in change frequency for the ACO algorithms and a small increase in VNP with

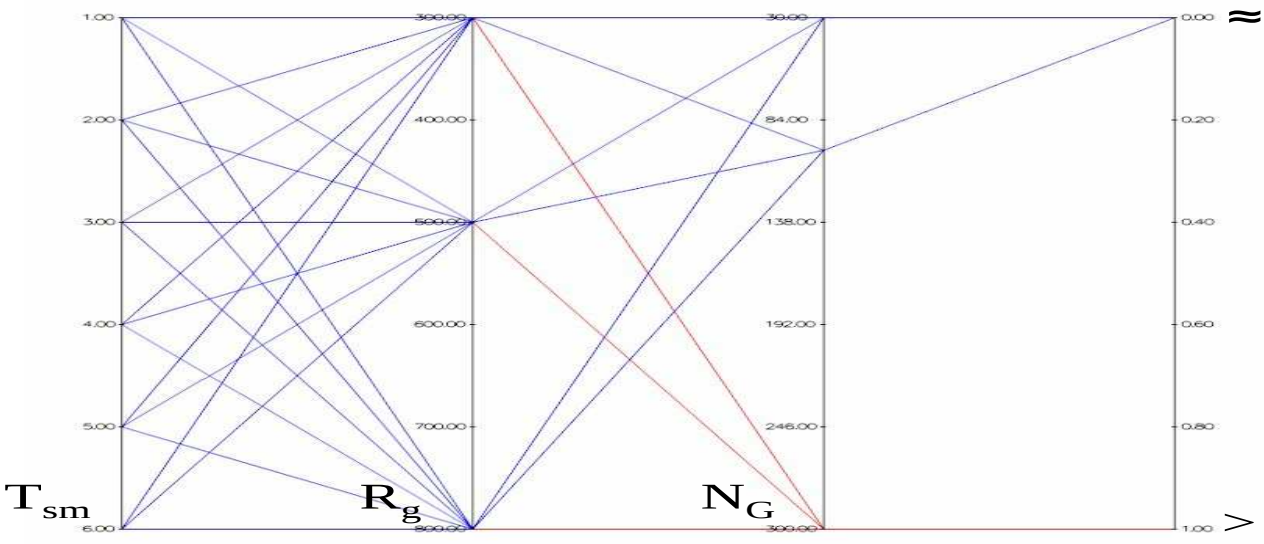

Figure 7.51: Comparing the ACO algorithms against the NSGA-II-MPA algorithm with regard to the TNP objective using the Mann-Whitney U test

a decrease in change frequency for the NSGA-II-MPA. Low change frequencies deteriorate the optimisation of the VNP for the NSGA-II-MPA.

Table 7.15: Average value of the VNP objective over all the N_G and R_g values

	T_{sm}					
$\mathcal{PF}$	1	2	3	4	5	6
$P_{EEMACOMP}$	81.53	80.63	80.55	80.07	79.29	78.78
$P_{EEMACOMH}$	90.00	89.60	87.98	88.16	86.32	85.55
$P_{EEMMASMP}$	82.95	82.46	82.75	82.18	81.17	80.82
$P_{EEMMASMH}$	83.33	82.70	83.08	82.54	81.95	81.03
$P_{EEMULTCOL}$	76.27	76.17	76.94	76.27	76.48	76.07
$P_{NSGA-II-MPA}$	114.67	117.40	119.43	121.03	120.62	121.65

Tables I.19-I.27 and Figures J.7-J.9 indicate a decrease in VNP with increase in R_g for $N_G = 30$. For $N_G = 100$ all the single-colony ACO algorithms produced the highest VNP for $R_g = 500$ and the lowest VNP for $R_g = 300$, while the EEMACOMC and the NSGA-II-MPA algorithms produced the lowest VNP for

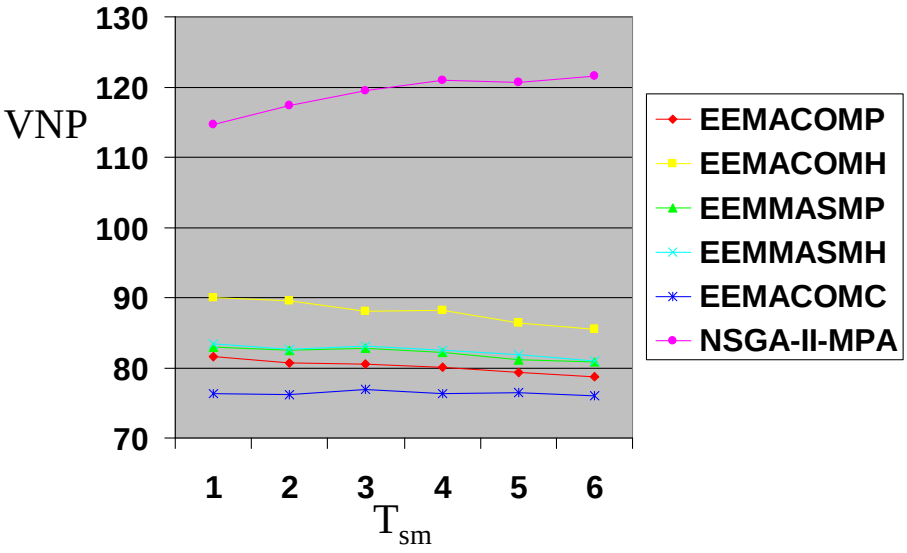

Figure 7.52: Average value of the VNP objective over all the N_G and R_g values

$R_g = 800$.

Table 7.16 displays the average values of VNP over all the N_G and T_{sm} values while Figure 7.53 illustrates the results of Table 7.16. Table 7.16 and Figure 7.53 indicate an increase in VNP with increase in change severity from 300 to 500 and then a decrease in VNP with increase in change severity from 500 to 800 for the ACO algorithms. The NSGA-II-MPA produced a decrease in VNP with increase in change severity. High change severities improve the optimisation of the VNP.

Table 7.16: Average value of the VNP objective over all the N_G and T_{sm} values

	R_g		
$\mathcal{PF}$	300	500	800
$P_{EEMACOMP}$	76.67	82.16	81.59
$P_{EEMACOMH}$	80.11	90.63	93.06
$P_{EEMMASMP}$	78.13	84.41	83.63
$P_{EEMMASMH}$	78.41	84.78	84.13
$P_{EEMULTCOL}$	75.57	81.00	72.53
$P_{NSGA-II-MPA}$	128.68	123.23	105.48

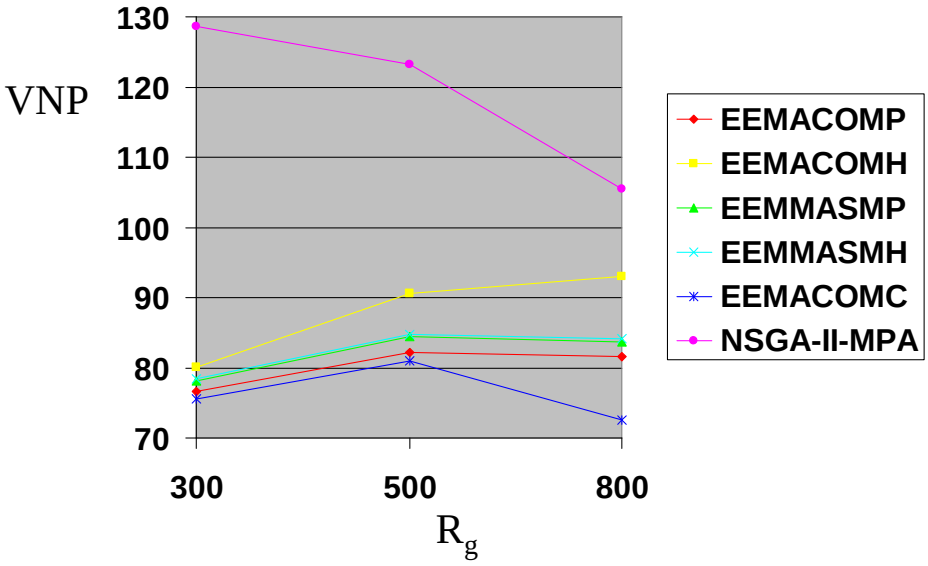

Figure 7.53: Average value of the VNP objective over all the N_G and T_{sm} values

Tables I.19-I.27 and Figures J.7-J.9 show no trend between the VNP value and the number of nodes.

Tables I.19-I.27 show that all the ACO approaches except the EEMACOMH approach, displayed a lower value for the VNP for all scenarios when compared to the NSGA-II-MPA approach. The EEMACOMH approach displayed a lower value for VNP for all scenarios except for scenarios with $R_g = 800$ and $N_G \in \{100, 300\}$ when compared to the NSGA-II-MPA approach. To test whether there is a statistical significant difference in the performance of EEMACOMP, EEMMASMP, EEMMASMH, and EEMACOMC and the NSGA-II-MPA approach, the following two hypotheses were considered:

$$H_0: \quad \mu_{ACO}^{VNP} = \mu_{NSGA-II-MPA}^{VNP}$$
$$H_1: \quad \mu_{ACO}^{VNP} > \mu_{NSGA-II-MPA}^{VNP}$$

where ACO takes the values EEMACOMP, EEMMASMP, EEMMASMH, and EEMACOMC.

Results of the Mann-Whitney U tests were the same for all the compared algorithms as illustrated in Figure 7.54. The Mann-Whitney U tests show that the EEMACOMP, EEMMASMP, EEMMASMH, and EEMACOMC approaches are significantly better than the NSGA-II-MPA approach with reference to the VNP objective for all scenarios.

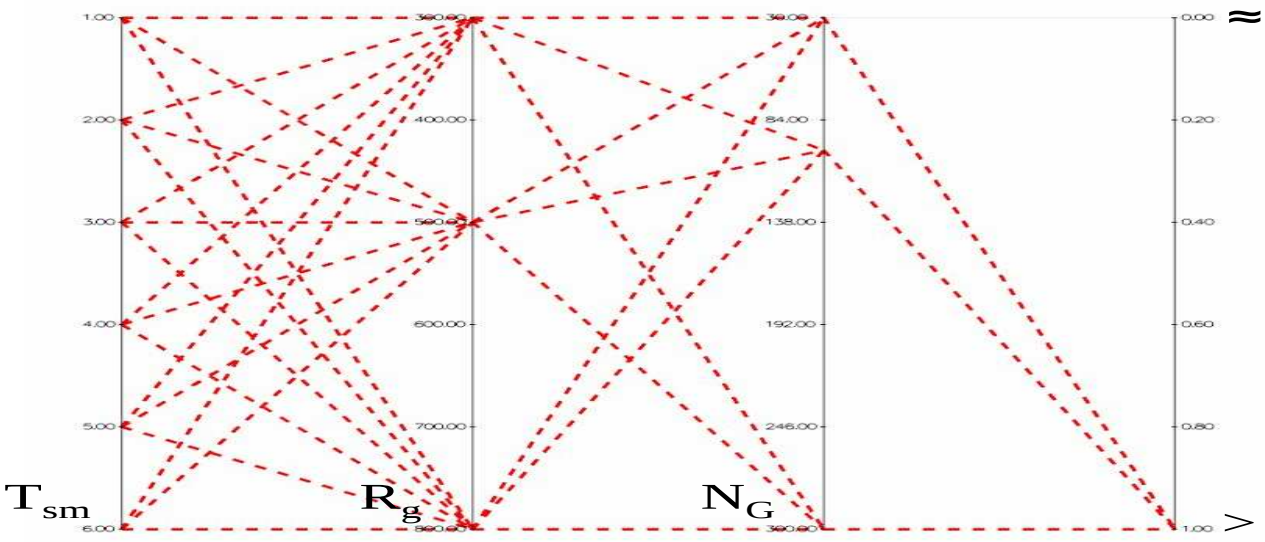

Figure 7.54: Comparing EEMACOMP, EEMMASMP, EEMMASMH, and EEMACOMC against the NSGA-II-MPA algorithm with regard to the VNP objective using the Mann-Whitney U test

To test whether there is a statistical significant difference in the performance of EEMACOMH and the NSGA-II-MPA approach for all scenarios except for scenarios with $R_g = 800$ and $N_G \in \{100, 300\}$, the following two hypotheses were considered:

$$H_0 : \ \mu^{VNP}_{EEMACOMH} = \mu^{VNP}_{NSGA-II-MPA}$$
$$H_1 : \ \mu^{VNP}_{EEMACOMH} > \mu^{VNP}_{NSGA-II-MPA}$$

Results of the Mann-Whitney U tests are illustrated in Figure 7.55. The Mann-Whitney U tests show that the EEMACOMH approach is significantly better than the NSGA-II-MPA approach with reference to the VNP objective for all scenarios except for scenarios with $R_g = 800$ and $N_G \in \{100, 300\}$.

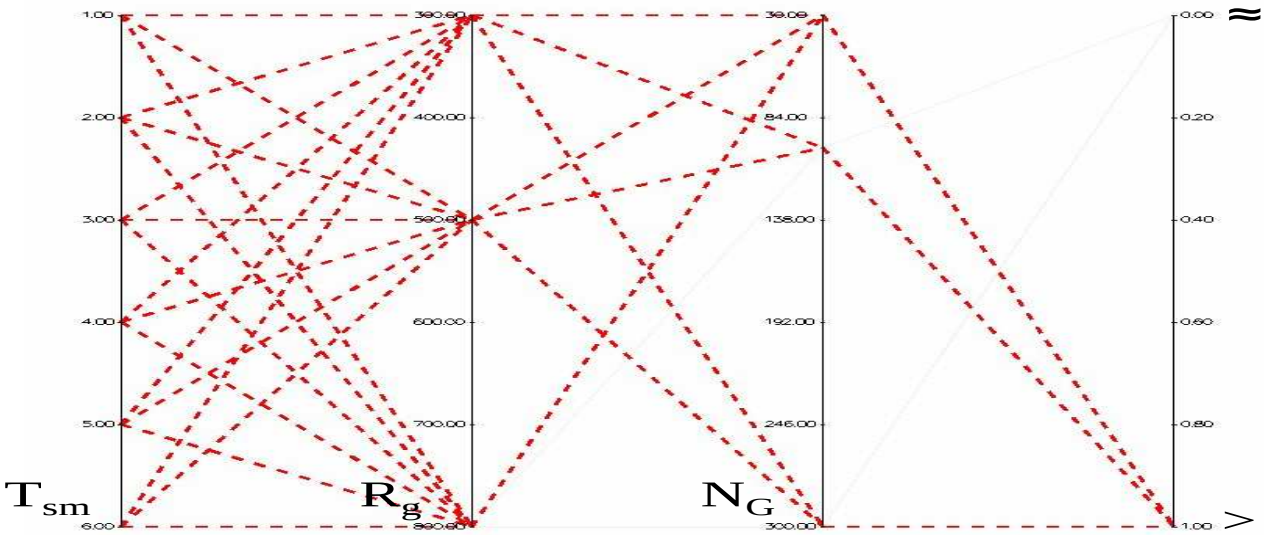

Figure 7.55: Comparing the EEMACOMH against the NSGA-II-MPA algorithm with regard to the VNP objective using the Mann-Whitney U test

- **Cost per packet, CP, objective**

  Tables I.28-I.36 and Figures J.10-J.12 show no trend between the CP value and the change frequency for $N_G = 300$, while for $N_G \in \{30, 100\}$ there is no difference in CP value as change frequency increases.

  Table 7.17 displays the average values of CP over all the N_G and R_g values using the results of Tables I.28-I.36. Figure 7.56 illustrates the results of Table 7.17. Table 7.17 and Figure 7.56 indicate no difference in CP value with change frequency variation except for NSGA-II-MPA which produced a higher value of CP for $T_{sm} = 1$. It is also to be noted from Table 7.17 and Figure 7.56 that when CP is taken

as the average value over all the N_G and R_g values, NSGA-II-MPA is significantly better than the other algorithms, showing a very low CP.

Tables I.28-I.36 and Figures J.10-J.12 show no trend between the CP value and the change severity for $N_G \in \{30, 300\}$. For $N_G = 100$, the CP value increased with increase in R_g for all ACO algorithms, while the NSGA-II-MPA algorithm produced the lowest CP for $R_g = 800$.

Table 7.17: Average value of the CP objective over all the N_G and R_g values

	T_{sm}					
$\mathcal{PF}$	1	2	3	4	5	6
$P_{EEMACOMP}$	0.043	0.044	0.043	0.043	0.043	0.042
$P_{EEMACOMH}$	0.050	0.054	0.053	0.054	0.055	0.053
$P_{EEMMASMP}$	0.045	0.047	0.045	0.045	0.046	0.044
$P_{EEMMASMH}$	0.047	0.048	0.047	0.047	0.047	0.045
$P_{EEMULTCOL}$	0.040	0.041	0.039	0.039	0.040	0.038
$P_{NSGA-II-MPA}$	0.017	0.010	0.010	0.010	0.010	0.010

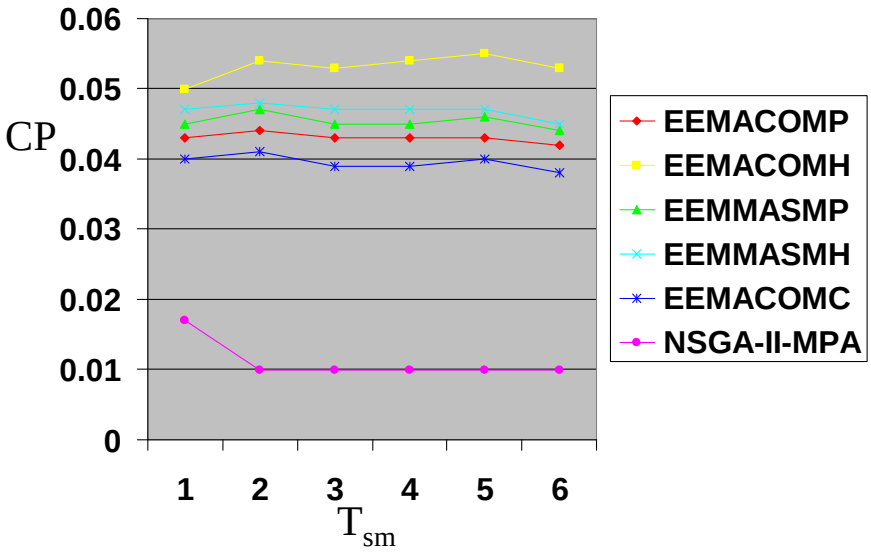

Figure 7.56: Average value of the CP objective over all the N_G and R_g values

Table 7.18 displays the average values of CP over all the N_G and T_{sm} values, while Figure 7.57 illustrates the results of Table 7.18. Table 7.18 and Figure 7.57 indicate that CP was higher for $R_g = 300$ which is not expected, because low change severity is supposed to delay the energy depletion of a node and therefore to maintain a low cost of using that node and lower value of CP.

Table 7.18: Average value of the CP objective over all the N_G and T_{sm} values

	R_g		
$\mathcal{PF}$	300	500	800
$P_{EEMACOMP}$	0.051	0.039	0.038
$P_{EEMACOMH}$	0.056	0.050	0.053
$P_{EEMMASMP}$	0.052	0.042	0.042
$P_{EEMMASMH}$	0.052	0.043	0.044
$P_{EEMULTCOL}$	0.043	0.037	0.038
$P_{NSGA-II-MPA}$	0.012	0.010	0.012

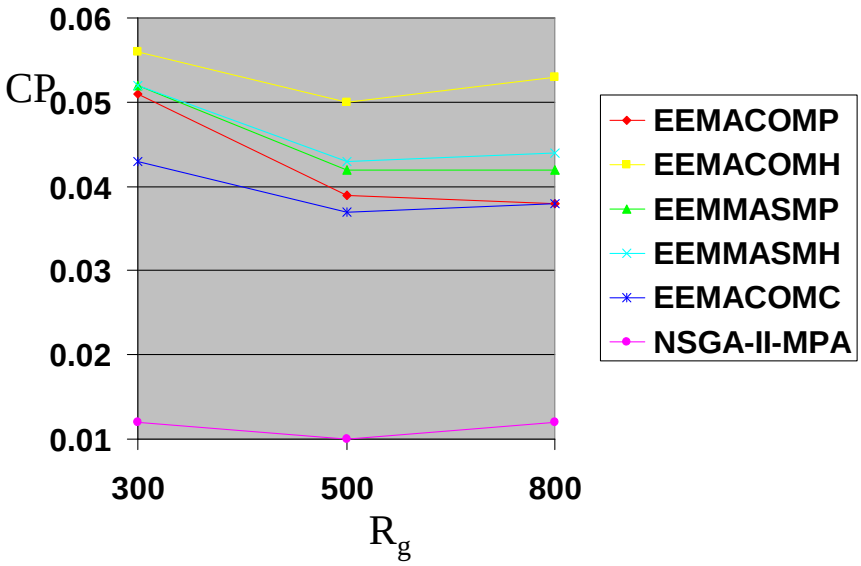

Figure 7.57: Average value of the CP objective over all the N_G and T_{sm} values

Tables I.28-I.36 show that the CP value increased when the number of nodes increased. This is an expected result because as the number of nodes increases, paths

consist on average of more nodes, and therefore the value of the CP objective which is a function of the residual energy of each node of the path increases.

Tables I.28-I.36 show that all the ACO approaches displayed a higher value for CP and therefore worst performance for all scenarios when compared to the NSGA-II-MPA approach. To test whether there is a statistical significant difference in the performance of the NSGA-II-MPA approach and the ACO approaches, the following two hypotheses were considered:

$$H_0: \quad \mu^{CP}_{NSGA-II-MPA} = \mu^{CP}_{ACO}$$
$$H_1: \quad \mu^{CP}_{NSGA-II-MPA} > \mu^{CP}_{ACO}$$

Results of the Mann-Whitney U tests were the same for all the compared algorithms as illustrated in Figure 7.58. The Mann-Whitney U tests show that the NSGA-II-MPA approach is significantly better than all the ACO approaches with reference to the CP objective for all scenarios. Again, this is possibly related to the effects of the k shortest path algorithm used in NSGA-II-MPA, which selects the first R paths with minimum energy consumed per packet and with minimum cost per packet (refer to Section 6.7).

- **Maximum node cost, MNC, objective**

  Tables I.37-I.45 and Figures J.13-J.15 indicate a decrease in MNC with decrease in change frequency for all algorithms.

  Table 7.19 displays the average values of MNC over all the N_G and R_g values using the results of Tables I.37-I.45. Figure 7.59 illustrates the results of Table 7.19. Table 7.19 and Figure 7.59 indicate an exponential decrease for MNC as change frequency decreased for all ACO algorithms and a small decrease for MNC as change frequency decreased for NSGA-II-MPA. That is an expected result, because low change frequencies give more time for the algorithms to find paths with low energy cost links.

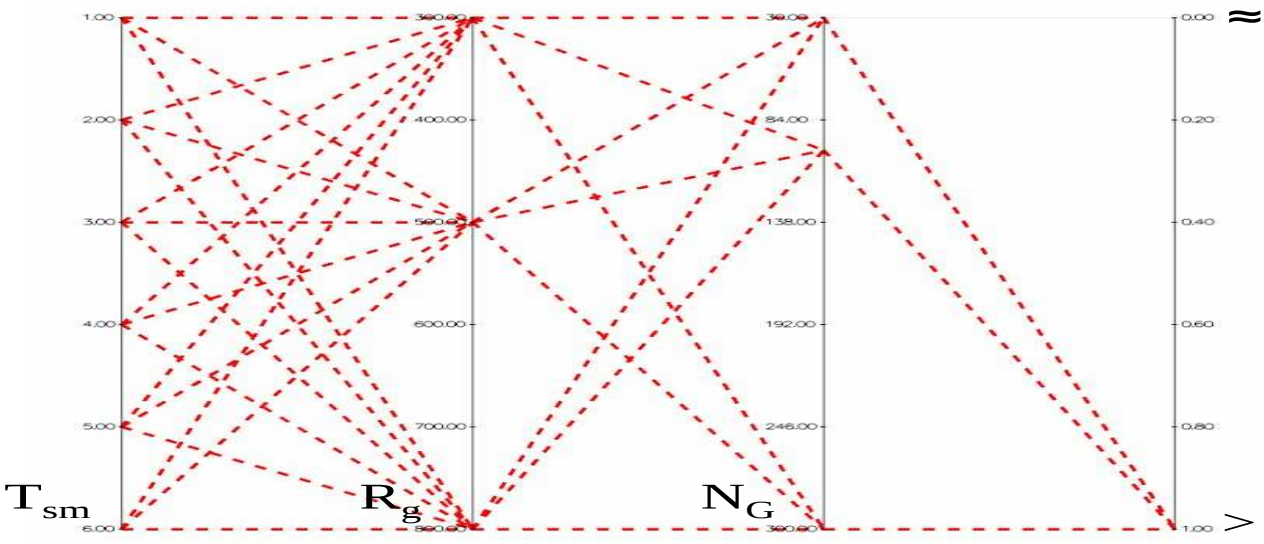

Figure 7.58: Comparing the NSGA-II-MPA algorithm against the ACO algorithms with regard to the CP objective using the Mann-Whitney U test

Tables I.37-I.45 and Figures J.13-J.15 indicate an increase in MNC with increase in change severity for most scenarios and for all algorithms.

Table 7.20 displays the average values for MNC over all the N_G and T_{sm} values while Figure 7.60 illustrates the results of Table 7.20. Table 7.20 and Figure 7.60 indicate that MNC increased for each ACO algorithm as R_g increased. This trend is expected, because an increase in change severity, R_g, causes only some of the links to be valid and it may not be possible to always find paths with low energy cost links. The value of MNC for NSGA-II-MPA increased when R_g increased from 500 to 800.

Tables I.37-I.45 and Figures J.13-J.15 show that the MNC value had a small increase when the number of nodes increased.

Tables I.37-I.45 and Figures J.13-J.15 show that all the ACO approaches displayed a higher value for MNC for all scenarios except for scenarios with $N_G = 300$ and $R_g = 800$ when compared to the NSGA-II-MPA approach. To test whether there is a statistical significant difference in the performance of the NSGA-II-MPA

Table 7.19: Average value of the MNC objective over all the N_G and R_g values

	T_{sm}					
$\mathcal{PF}$	1	2	3	4	5	6
$P_{EEMACOMP}$	2.830	2.023	1.727	1.569	1.485	1.410
$P_{EEMACOMH}$	2.794	1.999	1.778	1.602	1.518	1.456
$P_{EEMMASMP}$	3.091	2.219	1.830	1.678	1.580	1.475
$P_{EEMMASMH}$	3.067	2.220	1.828	1.665	1.579	1.516
$P_{EEMULTCOL}$	3.736	2.577	2.057	1.751	1.610	1.556

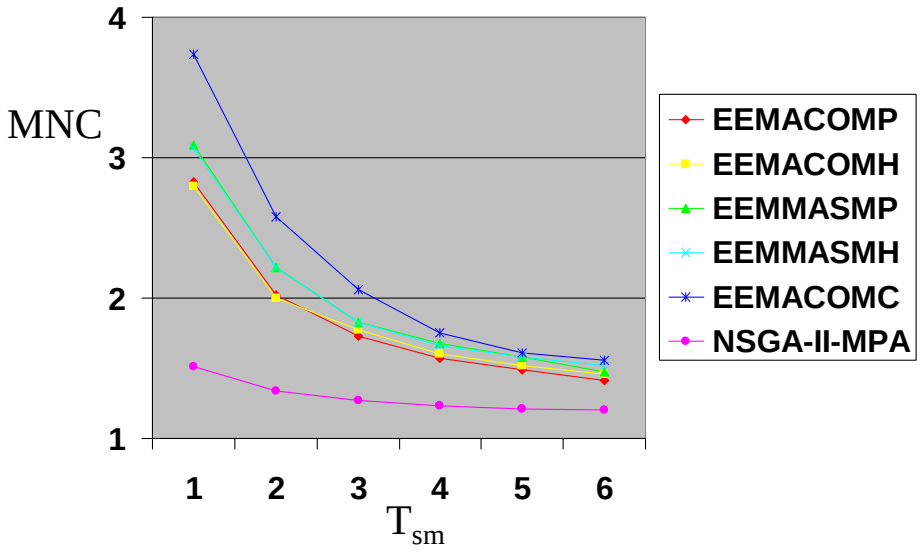

Figure 7.59: Average value of the MNC objective over all the N_G and R_g values

Table 7.20: Average value of the MNC objective over all the N_G and T_{sm} values

	R_g		
$\mathcal{PF}$	300	500	800
$P_{EEMACOMP}$	1.612	1.749	2.160
$P_{EEMACOMH}$	1.666	1.760	2.148
$P_{EEMMASMP}$	1.772	1.870	2.294
$P_{EEMMASMH}$	1.766	1.870	2.302
$P_{EEMULTCOL}$	1.802	2.011	2.830
$P_{NSGA-II-MPA}$	1.240	1.143	1.500

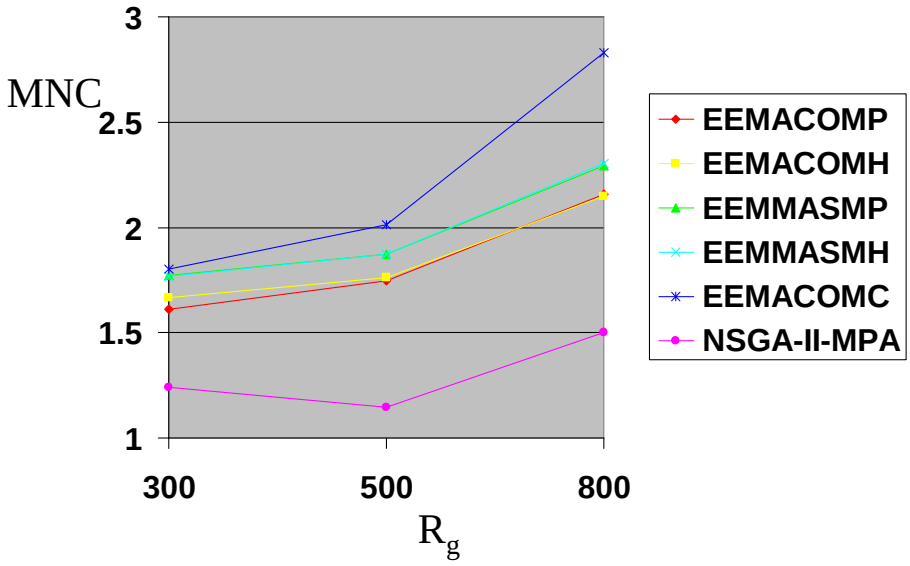

Figure 7.60: Average value of the MNC objective over all the N_G and T_{sm} values

approach and the ACO approaches the following two hypotheses were considered:

$$H_0: \quad \mu^{MNC}_{NSGA-II-MPA} = \mu^{MNC}_{ACO}$$
$$H_1: \quad \mu^{MNC}_{NSGA-II-MPA} > \mu^{MNC}_{ACO}$$

Results of the Mann-Whitney U tests were the same for all the compared algorithms as illustrated in Figure 7.61. The Mann-Whitney U tests show that the NSGA-II-MPA approach is significantly better than all the ACO approaches with reference to the MNC objective for all scenarios except for scenarios with $N_G = 300$ and $R_g = 800$ where the NSGA-II-MPA approach is equal to the ACO approaches.

The remainder of this section analyses the value of each optimisation criterion for each environment change.

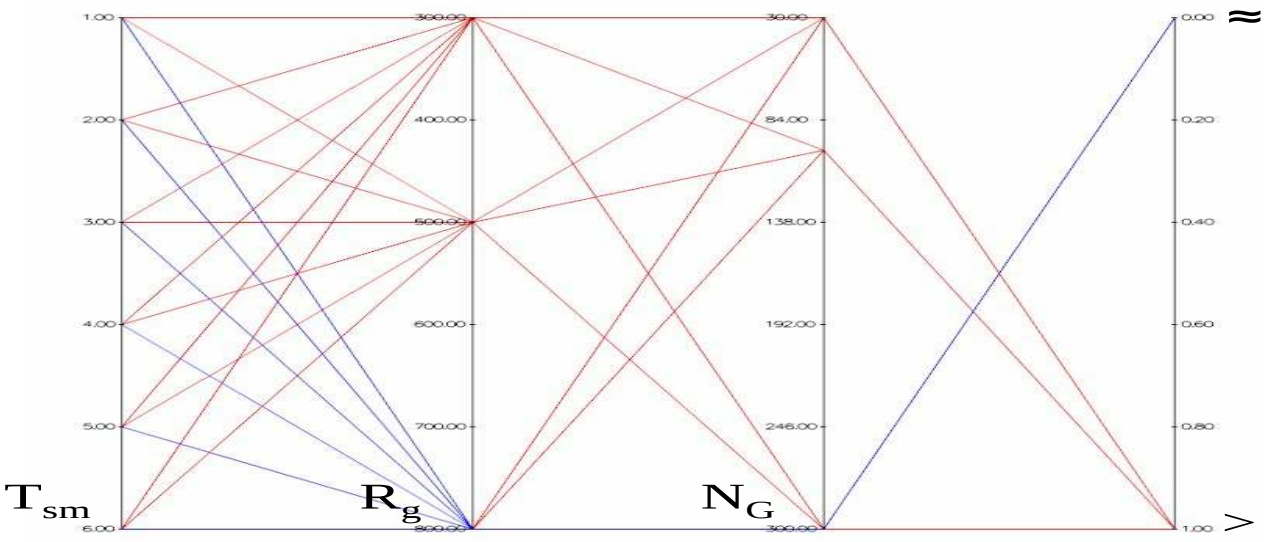

Figure 7.61: Comparing the NSGA-II-MPA algorithm against the ACO algorithms with regard to the MNC objective using the Mann-Whitney U test

Optimization criteria over time

For each optimisation criterion and for each iteration before a change to the environment occurs, the average value of that criterion is computed over all the number of solutions for this iteration, further averaged over all 30 simulations for all R_g and N_G values per T_{sm} value.

Figure 7.62 visualises the energy consumed per packet, EP, over time. For all change frequencies, a slight decrease in EP is observed over time. This decrease over time in EP shows that transferring solutions from the environment before the change occurs helps to accelerate the rate of convergence to the optima after the change occurred. Therefore more time is available to find solutions with equal or lower energy consumed per packet after the environment has changed. For all environment changes the NSGA-II-MPA produced a very low EP compared to the ACO algorithms.

Figure 7.63 visualises the utilisation of the most heavily used link, TNP, over time. All algorithms minimise the TNP criterion to a very low value. Because of this low value of TNP, the load among mobile nodes is divided so that the network will partition in such a way that nodes drain their energy at equal rates. This will help to maximise the

time to network partition. In addition, for NSGA-II-MPA, Figures 7.63(a) and 7.63(b) indicate an exponential increase for TNP over time for $T_{sm} = 1$ and $T_{sm} = 2$.

Figure 7.64 visualises the variance in node power levels, VNP, over time. NSGA-II-MPA displayed the highest value for VNP over all change frequencies, indicating a bad load distribution. It is also to be noted from Figures 7.64(b)-7.64(d) that for the NSGA-II-MPA, VNP decreased over time for $T_{sm} \in \{2, 3, 4\}$ which is good. Otherwise, for all algorithms, the value of VNP had a very small variation for all environment changes. This small variation of VNP, together with the relatively low value for VNP, will ensure that all the nodes in the network remain up and running for as long as possible.

Figure 7.65 visualises the cost per packet, CP, criterion over time. NSGA-II-MPA produced the best CP value, having a small value for all environment changes. Even-though NSGA-II-MPA produced the best cost results, all the ant algorithms achieved very low cost solutions. Minimising CP achieves the objective of avoiding those nodes with depleted energy reserves since these nodes have high node cost. In this way, network partition is delayed.

Figure 7.66 visualises the maximum node cost, MNC, over time. EEMACOMC produced the worst MNC values (highest MNC values), while NSGA-II-MPA produced the best MNC values. All algorithms produced low MNC values for all change frequencies, and environment changes. This will help delay node failure and reduce variance in remaining battery lives.

For all algorithms, there is a very small variation at each environment change in the values of the EP, TNP, CP, and VNP objectives. This shows the robustness and adaptability of all the algorithms to the environment changes.

7.4.7 Ranking Of The Algorithms Based On Performance Criteria

Tables 7.21-7.29 give the average rank of the algorithms for each scenario based on the results of Tables F.1-F.54. Symbols n_{alg}^{w}, ϱ^{w}, and ξ^{w} are defined in Section 7.4.1. For each of the performance metrics, each algorithm is ranked according to the number of times that the algorithm had a better performance than all the other algorithms with reference to this performance metric, for each environment change. The algorithm's average rank over all the performance criteria is calculated and then the algorithm is

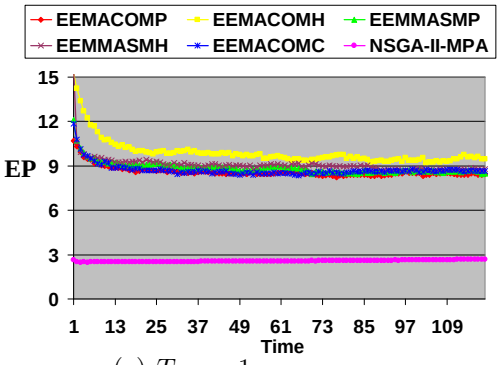

(a) $T_{sm} = 1$

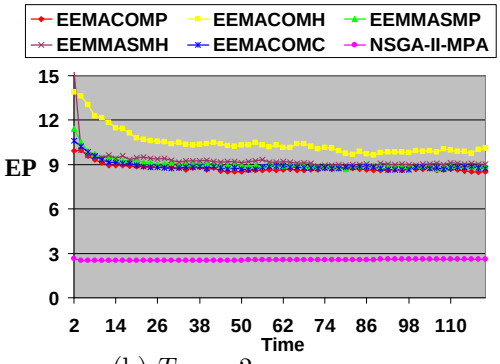

(b) $T_{sm} = 2$

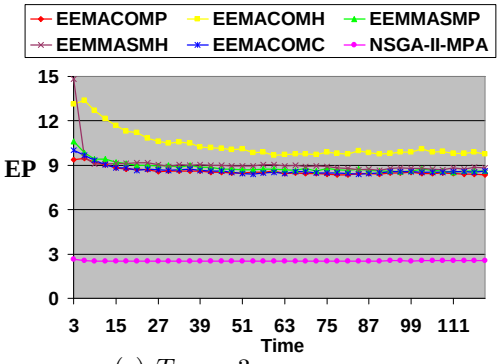

(c) $T_{sm} = 3$

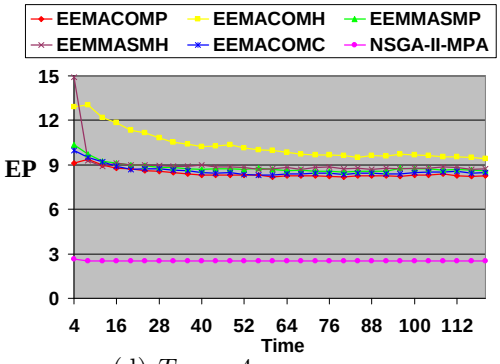

(d) $T_{sm} = 4$

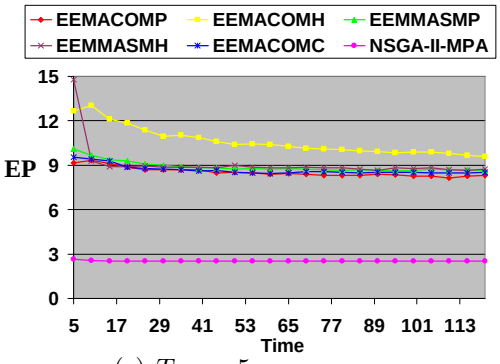

(e) $T_{sm} = 5$

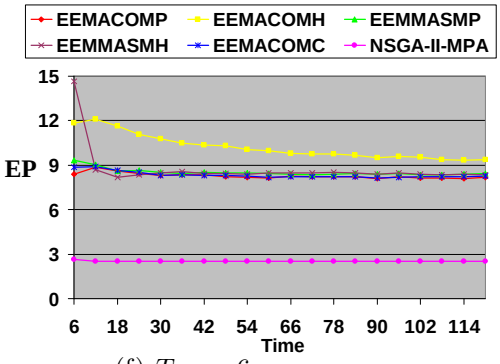

(f) $T_{sm} = 6$

Figure 7.62: Energy consumed per packet, EP, criterion over time

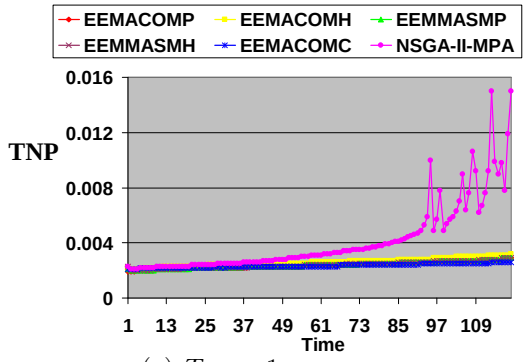

(a) $T_{sm} = 1$

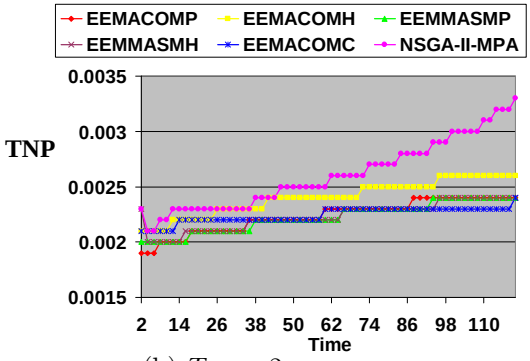

(b) $T_{sm} = 2$

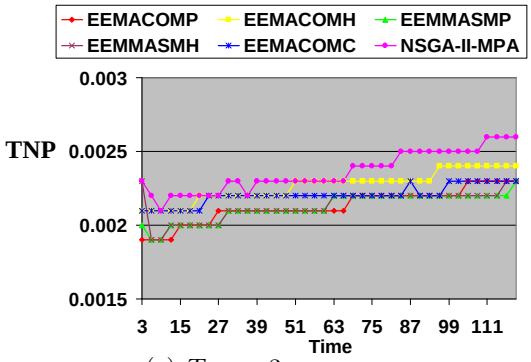

(c) $T_{sm} = 3$

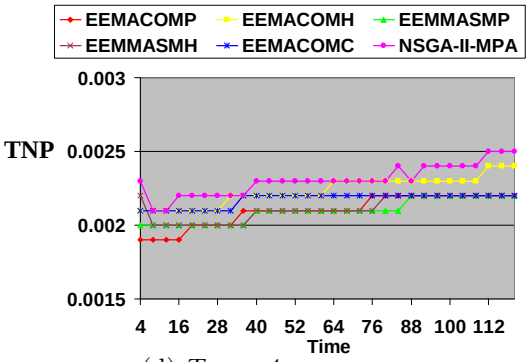

(d) $T_{sm} = 4$

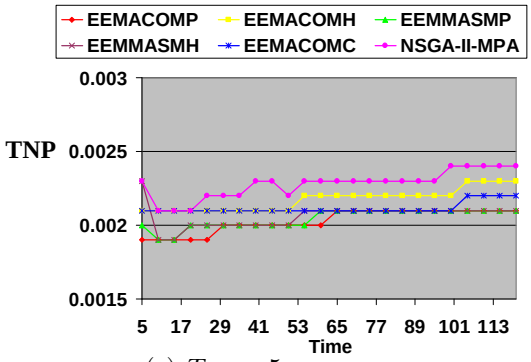

(e) $T_{sm} = 5$

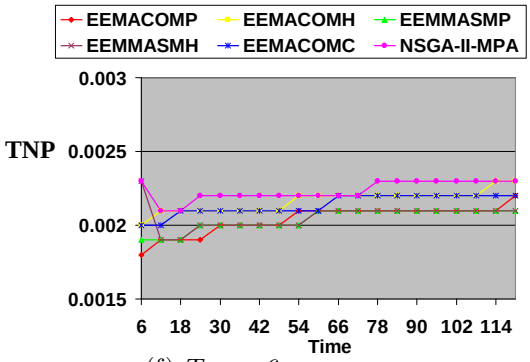

(f) $T_{sm} = 6$

Figure 7.63: Utilisation of the most heavily used link, TNP, criterion over time

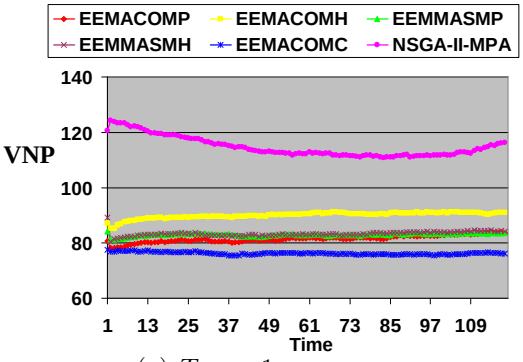

(a) $T_{sm} = 1$

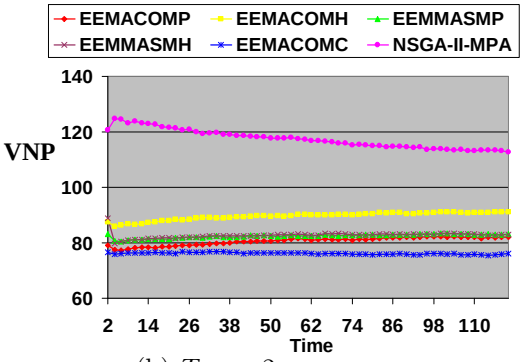

(b) $T_{sm} = 2$

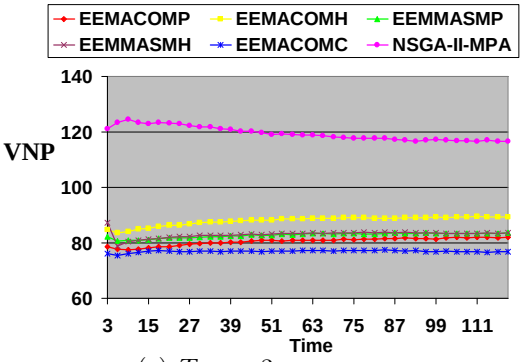

(c) $T_{sm} = 3$

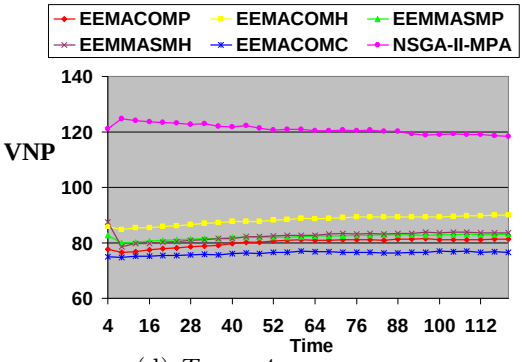

(d) $T_{sm} = 4$

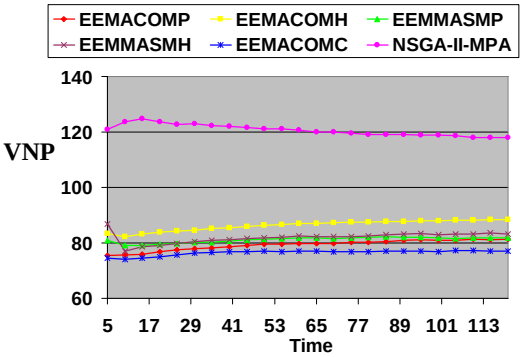

(e) $T_{sm} = 5$

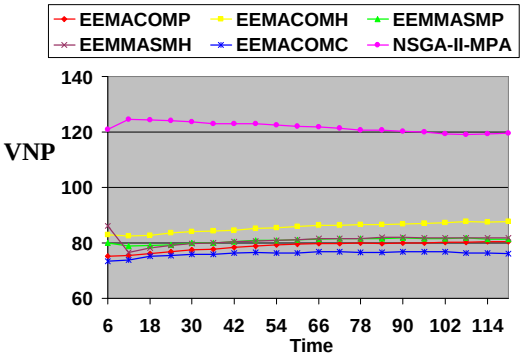

(f) $T_{sm} = 6$

Figure 7.64: Variance in node power levels, VNP, criterion over time

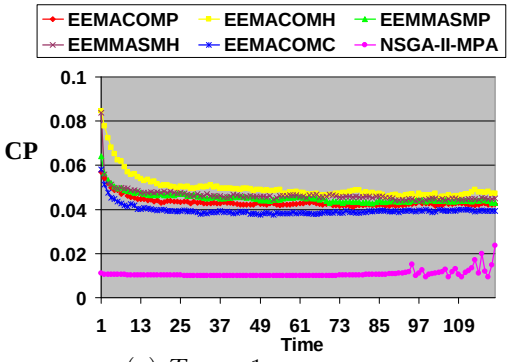

(a) $T_{sm} = 1$

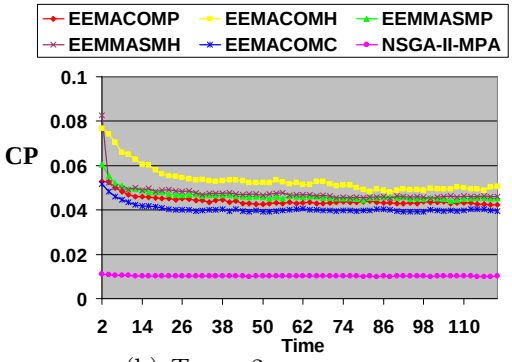

(b) $T_{sm} = 2$

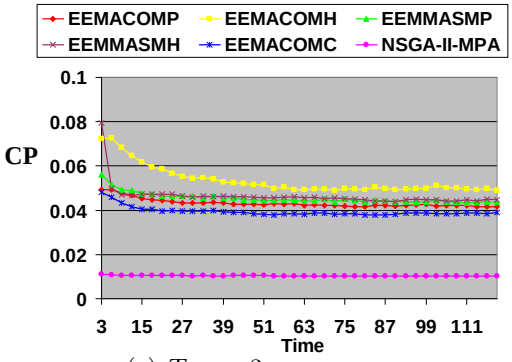

(c) $T_{sm} = 3$

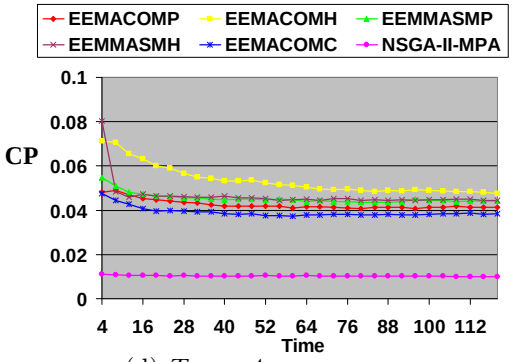

(d) $T_{sm} = 4$

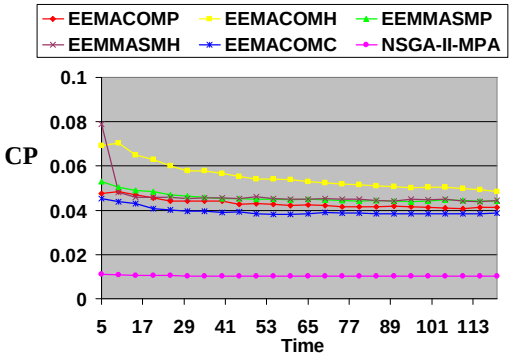

(e) $T_{sm} = 5$

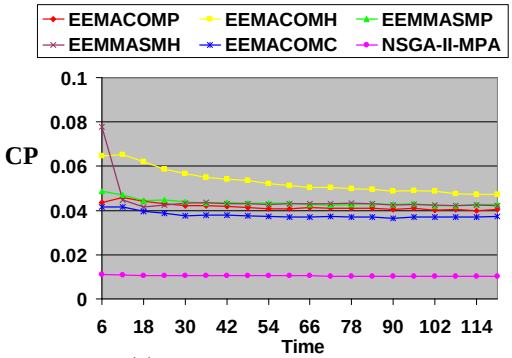

(f) $T_{sm} = 6$

Figure 7.65: Cost per packet, CP, criterion over time

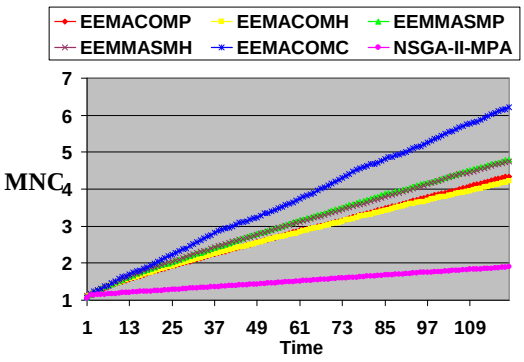

(a) $T_{sm} = 1$

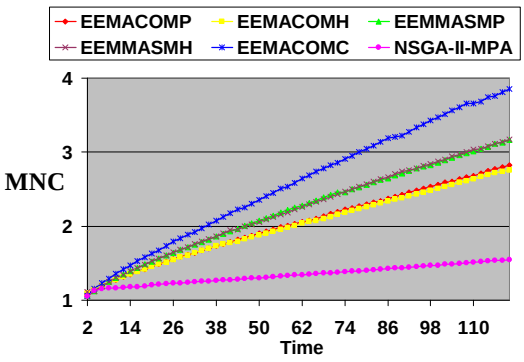

(b) $T_{sm} = 2$

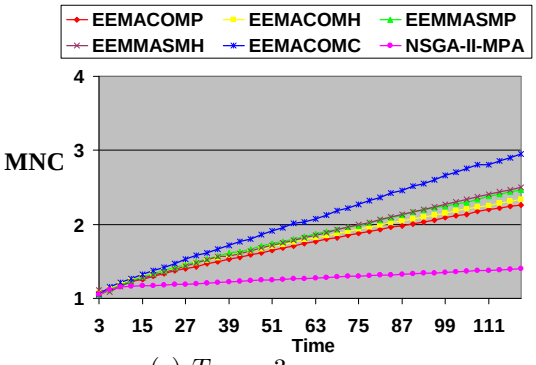

(c) $T_{sm} = 3$

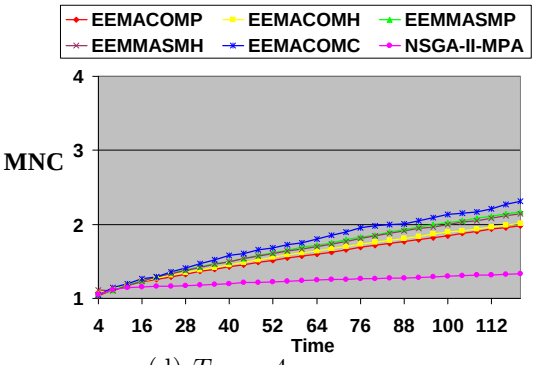

(d) $T_{sm} = 4$

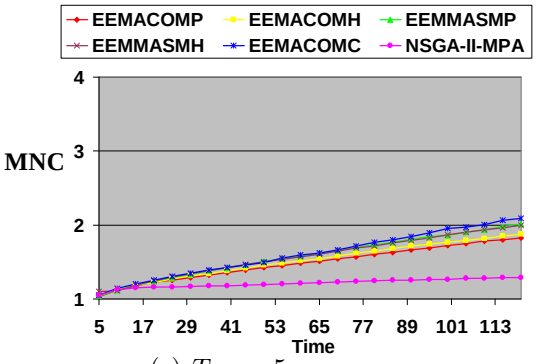

(e) $T_{sm} = 5$

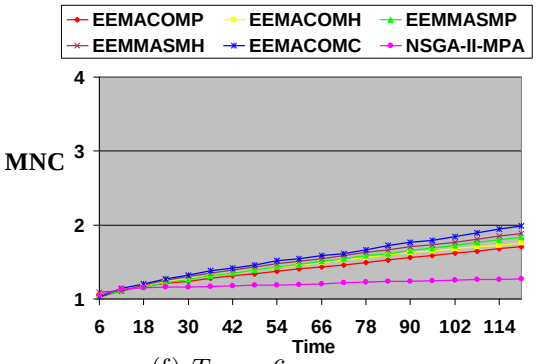

(f) $T_{sm} = 6$

Figure 7.66: Maximum node cost, MNC, criterion over time

ranked accordingly. Table 7.30 gives the average rank of the algorithms over all the scenarios, together with the standard deviation.

Tables 7.24-7.29 indicate that EEMACOMP ranked overall in first place for 88% of the scenarios with $N_G > 30$. For scenarios with $N_G = 30$, EEMACOMP ranked overall in first place for 44% of the scenarios (refer to Tables 7.21-7.23). EEMACOMH is ranked overall last for 87% of the scenarios. The NSGA-II-MPA algorithm had a better $\bar{\xi}$ than the other algorithms for almost all environment changes for scenarios with $N_G = 300$ and $R_g \in \{500, 800\}$ (refer to Tables 7.28-7.29).

Table 7.30 indicates that the EEMACOMP algorithm had on average the best rank over all the scenarios, while the EEMACOMH algorithm had on average the worst rank over all the scenarios.

Table 7.21: Ranks for scenarios with $N_G = 30$, $R_g = 300$

	T_{sm}																							
	1				2				3				4				5				6			
$\mathcal{PF}$	n^w_{alg}	ϱ^w	ξ^w	rank	n^w_{alg}	ϱ^w	ξ^w	rank	n^w_{alg}	ϱ^w	ξ^w	rank	n^w_{alg}	ϱ^w	ξ^w	rank	n^w_{alg}	ϱ^w	ξ^w	rank	n^w_{alg}	ϱ^w	ξ^w	rank
$\mathcal{P}_{EEMACOMP}$	0	3	0	4	0	0	0	5	0	0	0	4	0	0	0	4	0	0	0	4	0	0	0	4
$\mathcal{P}_{EEMACOMH}$	0	0	0	5	0	0	0	5	0	0	0	4	0	0	0	4	0	0	0	4	0	0	0	4
$\mathcal{P}_{EEMMASMP}$	5	0	0	3	1	0	0	3	0	0	0	4	0	1	0	3	0	0	0	4	0	0	0	4
$\mathcal{P}_{EEMMASMH}$	0	0	0	5	0	1	0	3	0	1	0	3	0	0	0	4	0	1	0	3	0	1	0	3
$\mathcal{P}_{EEMACOMC}$	10	0	120	1	0	0	60	1	0	0	40	1	0	0	30	1	0	0	24	1	0	1	20	1
$\mathcal{P}_{NSGA-II-MPA}$	0	117	0	2	0	59	0	2	0	39	0	2	0	29	0	2	0	23	0	2	0	18	0	2

Table 7.22: Ranks for scenarios with $N_G = 30$, $R_g = 500$

	T_{sm}																							
	1				2				3				4				5				6			
$\mathcal{PF}$	n^w_{alg}	ϱ^w	ξ^w	rank	n^w_{alg}	ϱ^w	ξ^w	rank	n^w_{alg}	ϱ^w	ξ^w	rank	n^w_{alg}	ϱ^w	ξ^w	rank	n^w_{alg}	ϱ^w	ξ^w	rank	n^w_{alg}	ϱ^w	ξ^w	rank
$\mathcal{P}_{EEMACOMP}$	5	54	9	1	0	31	13	1	0	29	6	1	0	28	0	2	0	18	0	2	0	14	0	2
$\mathcal{P}_{EEMACOMH}$	0	6	4	5	1	7	0	5	0	1	0	5	0	1	0	3	0	0	0	5	0	0	0	3
$\mathcal{P}_{EEMMASMP}$	4	43	20	2	0	9	4	4	0	6	0	3	0	3	0	3	0	3	0	3	0	0	0	3
$\mathcal{P}_{EEMMASMH}$	2	16	35	4	1	13	10	3	0	4	0	4	0	0	0	5	0	1	0	4	0	0	0	3
$\mathcal{P}_{EEMACOMC}$	1	1	52	3	0	0	33	2	0	0	34	2	0	0	30	1	0	2	24	1	0	6	20	1
$\mathcal{P}_{NSGA-II-MPA}$	0	0	0	6	0	0	0	6	0	0	0	6	0	0	0	5	0	0	0	5	0	0	0	3

Table 7.23: Ranks for scenarios with $N_G = 30$, $R_g = 800$

	T_{sm}																							
	1				2				3				4				5				6			
$\mathcal{PF}$	n^w_{alg}	ϱ^w	ξ^w	rank	n^w_{alg}	ϱ^w	ξ^w	rank	n^w_{alg}	ϱ^w	ξ^w	rank	n^w_{alg}	ϱ^w	ξ^w	rank	n^w_{alg}	ϱ^w	ξ^w	rank	n^w_{alg}	ϱ^w	ξ^w	rank
$\mathcal{P}_{EEMACOMP}$	6	28	23	4	11	43	31	1	4	13	39	1	6	20	29	1	4	14	17	1	3	11	20	1
$\mathcal{P}_{EEMACOMH}$	0	0	0	6	0	0	0	6	0	0	0	5	0	0	0	5	0	0	0	5	0	0	0	5
$\mathcal{P}_{EEMMASMP}$	21	50	19	2	0	9	1	4	5	8	1	3	4	6	1	3	3	2	2	4	2	3	0	3
$\mathcal{P}_{EEMMASMH}$	9	42	56	1	0	8	24	3	5	19	0	2	4	4	0	4	1	8	3	2	5	6	0	2
$\mathcal{P}_{EEMACOMC}$	73	0	0	3	49	0	0	2	14	0	0	3	13	0	0	2	8	0	2	3	5	0	0	3
$\mathcal{P}_{NSGA-II-MPA}$	0	0	22	5	0	0	4	5	0	0	0	5	0	0	0	5	0	0	0	5	0	0	0	5

Table 7.24: Ranks for scenarios with $N_G = 100$, $R_g = 300$

	T_{sm}																							
	1				2				3				4				5				6			
$\mathcal{PF}$	n^w_{alg}	ϱ^w	ξ^w	rank	n^w_{alg}	ϱ^w	ξ^w	rank	n^w_{alg}	ϱ^w	ξ^w	rank	n^w_{alg}	ϱ^w	ξ^w	rank	n^w_{alg}	ϱ^w	ξ^w	rank	n^w_{alg}	ϱ^w	ξ^w	rank
$\mathcal{P}_{\mathcal{EEMACOMP}}$	118	114	32	1	47	59	39	1	8	39	40	1	12	27	29	1	2	24	23	1	3	20	20	1
$\mathcal{P}_{\mathcal{EEMACOMH}}$	0	0	0	6	0	0	0	6	0	0	0	5	0	0	0	5	0	0	0	4	0	0	0	3
$\mathcal{P}_{\mathcal{EEMMASMP}}$	0	1	0	5	2	0	0	3	2	0	0	4	3	0	0	3	0	0	0	4	0	0	0	3
$\mathcal{P}_{\mathcal{EEMMASMH}}$	2	1	1	4	1	0	1	3	5	0	0	2	2	0	1	2	1	0	0	3	0	0	0	3
$\mathcal{P}_{\mathcal{EEMACOMC}}$	0	4	1	3	0	1	0	5	2	1	0	3	0	3	0	3	0	0	1	2	0	0	0	3
$\mathcal{P}_{\mathcal{NSGA-II-MPA}}$	0	0	86	2	0	0	20	2	0	0	0	5	0	0	0	5	0	0	0	4	0	0	0	2

Table 7.25: Ranks for scenarios with $N_G = 100$, $R_g = 500$

	T_{sm}																							
	1				2				3				4				5				6			
$\mathcal{PF}$	n^w_{alg}	ϱ^w	ξ^w	rank	n^w_{alg}	ϱ^w	ξ^w	rank	n^w_{alg}	ϱ^w	ξ^w	rank	n^w_{alg}	ϱ^w	ξ^w	rank	n^w_{alg}	ϱ^w	ξ^w	rank	n^w_{alg}	ϱ^w	ξ^w	rank
$\mathcal{P}_{\mathcal{EEMACOMP}}$	56	119	70	1	34	59	52	1	36	38	39	1	9	30	29	1	4	24	23	1	6	20	20	1
$\mathcal{P}_{\mathcal{EEMACOMH}}$	0	0	0	5	0	0	0	5	0	0	0	5	0	0	0	4	0	0	0	4	0	0	0	4
$\mathcal{P}_{\mathcal{EEMMASMP}}$	61	0	2	2	13	0	2	2	3	0	0	3	6	0	0	2	5	0	0	3	1	0	0	3
$\mathcal{P}_{\mathcal{EEMMASMH}}$	2	1	1	4	6	1	1	3	1	1	1	2	3	0	1	3	6	0	1	2	4	0	0	2
$\mathcal{P}_{\mathcal{EEMACOMC}}$	0	0	0	5	0	0	5	4	0	0	0	5	0	0	0	4	0	0	0	4	0	0	0	4
$\mathcal{P}_{\mathcal{NSGA-II-MPA}}$	0	0	47	3	0	0	0	5	0	1	0	4	0	0	0	4	0	0	0	4	0	0	0	4

Table 7.26: Ranks for scenarios with $N_G = 100$, $R_g = 800$

	T_{sm}																							
	1				2				3				4				5				6			
$\mathcal{PF}$	n^w_{alg}	ϱ^w	ξ^w	rank	n^w_{alg}	ϱ^w	ξ^w	rank	n^w_{alg}	ϱ^w	ξ^w	rank	n^w_{alg}	ϱ^w	ξ^w	rank	n^w_{alg}	ϱ^w	ξ^w	rank	n^w_{alg}	ϱ^w	ξ^w	rank
$\mathcal{P}_{\mathcal{EEMACOMP}}$	63	0	4	3	57	9	0	1	40	8	0	1	30	12	0	1	23	16	0	1	19	13	0	1
$\mathcal{P}_{\mathcal{EEMACOMH}}$	0	0	0	4	0	0	0	4	0	0	0	4	0	0	0	4	0	0	0	5	0	0	0	5
$\mathcal{P}_{\mathcal{EEMMASMP}}$	0	0	0	4	0	0	0	4	0	0	0	4	0	0	0	4	0	0	0	5	0	0	0	5
$\mathcal{P}_{\mathcal{EEMMASMH}}$	0	0	0	4	0	0	0	4	0	0	0	4	0	0	0	4	1	1	0	4	1	2	0	4
$\mathcal{P}_{\mathcal{EEMACOMC}}$	55	0	67	2	1	0	60	2	0	0	40	2	0	0	30	2	0	0	24	2	0	0	20	2
$\mathcal{P}_{\mathcal{NSGA-II-MPA}}$	2	120	49	1	2	51	0	3	0	32	0	3	0	18	0	3	0	7	0	3	0	5	0	3

Table 7.27: Ranks for scenarios with $N_G = 300$, $R_g = 300$

	T_{sm}																							
	1				2				3				4				5				6			
$\mathcal{PF}$	n^w_{alg}	ϱ^w	ξ^w	rank	n^w_{alg}	ϱ^w	ξ^w	rank	n^w_{alg}	ϱ^w	ξ^w	rank	n^w_{alg}	ϱ^w	ξ^w	rank	n^w_{alg}	ϱ^w	ξ^w	rank	n^w_{alg}	ϱ^w	ξ^w	rank
$\mathcal{P}_{\mathcal{EEMACOMP}}$	118	114	0	1	60	57	0	1	39	39	0	1	29	27	0	1	24	23	0	1	15	18	0	1
$\mathcal{P}_{\mathcal{EEMACOMH}}$	0	0	0	6	0	0	0	5	0	0	0	5	0	0	0	5	0	0	0	4	0	0	0	6
$\mathcal{P}_{\mathcal{EEMMASMP}}$	0	3	0	3	0	0	0	5	0	0	0	5	0	2	0	3	0	0	0	4	2	0	0	4
$\mathcal{P}_{\mathcal{EEMMASMH}}$	1	0	0	5	0	2	0	3	1	0	0	3	0	2	0	3	0	0	0	4	2	1	0	3
$\mathcal{P}_{\mathcal{EEMACOMC}}$	0	1	120	2	0	0	60	2	0	0	40	2	0	0	30	2	0	0	24	2	0	0	20	2
$\mathcal{P}_{\mathcal{NSGA-II-MPA}}$	1	2	0	3	0	1	0	4	0	1	0	3	0	0	0	5	0	1	0	3	0	1	0	5

Table 7.28: Ranks for scenarios with $N_G = 300$, $R_g = 500$

	T_{sm}																							
	1				2				3				4				5				6			
$\mathcal{PF}$	n^w_{alg}	ϱ^w	ξ^w	rank	n^w_{alg}	ϱ^w	ξ^w	rank	n^w_{alg}	ϱ^w	ξ^w	rank	n^w_{alg}	ϱ^w	ξ^w	rank	n^w_{alg}	ϱ^w	ξ^w	rank	n^w_{alg}	ϱ^w	ξ^w	rank
$\mathcal{P}_{\mathcal{EEMACOMP}}$	119	118	0	1	59	58	0	1	39	39	0	1	29	29	0	1	23	23	0	1	19	19	0	1
$\mathcal{P}_{\mathcal{EEMACOMH}}$	0	0	0	5	0	0	0	5	0	0	0	4	0	0	0	4	0	0	0	4	0	0	0	4
$\mathcal{P}_{\mathcal{EEMMASMP}}$	0	1	0	4	0	1	0	4	0	0	0	4	0	0	0	4	0	0	0	4	0	0	0	4
$\mathcal{P}_{\mathcal{EEMMASMH}}$	1	1	0	3	1	1	0	3	1	1	0	3	1	1	0	3	1	1	0	3	1	1	0	3
$\mathcal{P}_{\mathcal{EEMACOMC}}$	0	0	0	5	0	0	0	5	0	0	0	4	0	0	0	4	0	0	0	4	0	0	0	4
$\mathcal{P}_{\mathcal{NSGA-II-MPA}}$	0	0	120	2	0	0	60	2	0	0	40	2	0	0	30	2	0	0	24	2	0	0	20	2

Table 7.29: Ranks for scenarios with $N_G = 300$, $R_g = 800$

	T_{sm}																							
	1				2				3				4				5				6			
$\mathcal{PF}$	n^w_{alg}	ϱ^w	ξ^w	rank	n^w_{alg}	ϱ^w	ξ^w	rank	n^w_{alg}	ϱ^w	ξ^w	rank	n^w_{alg}	ϱ^w	ξ^w	rank	n^w_{alg}	ϱ^w	ξ^w	rank	n^w_{alg}	ϱ^w	ξ^w	rank
$\mathcal{P}_{\mathcal{EEMACOMP}}$	0	5	0	2	2	3	0	2	35	18	0	2	28	18	0	1	21	17	0	1	18	17	0	1
$\mathcal{P}_{\mathcal{EEMACOMH}}$	0	0	0	4	0	0	0	4	0	0	0	5	0	0	0	4	0	0	0	4	0	0	0	6
$\mathcal{P}_{\mathcal{EEMMASMP}}$	0	0	0	4	0	1	0	3	1	7	0	3	1	1	0	3	2	4	0	3	0	2	0	3
$\mathcal{P}_{\mathcal{EEMMASMH}}$	0	2	0	3	0	0	0	4	1	0	0	4	0	0	0	4	0	0	0	4	1	1	0	3
$\mathcal{P}_{\mathcal{EEMACOMC}}$	0	0	0	4	0	0	0	4	0	0	0	5	0	0	0	4	0	0	0	4	1	0	0	5
$\mathcal{P}_{\mathcal{NSGA-II-MPA}}$	120	113	120	1	58	56	60	1	30	15	40	1	1	11	30	2	1	3	24	2	0	0	20	2

Table 7.30: Average rank of all algorithms with respect to all performances measures

$\mathcal{PF}$	rank
$\mathcal{P}_{\mathcal{EEMACOMP}}$	1.555 ± 1.040
$\mathcal{P}_{\mathcal{EEMACOMC}}$	2.833 ± 1.313
$\mathcal{P}_{\mathcal{EEMMASMH}}$	3.259 ± 0.850
$\mathcal{P}_{\mathcal{EEMMASMP}}$	3.481 ± 0.794
$\mathcal{P}_{\mathcal{NSGA-II-MPA}}$	3.259 ± 1.494
$\mathcal{P}_{\mathcal{EEMACOMH}}$	4.666 ± 0.824

7.4.8 Computational Complexity of the Algorithms

The runtime complexity of each algorithm can be analysed by investigating the runtime behavior of the sub-routines of the corresponding algorithm. The approximated worst case asymptotic complexity of each algorithm is estimated as follows:

- EEMACOMP algorithm

  The initialisation process has a worst case complexity of $O(c_1 n_o N_G^2)$, while the solution construction process has a worst case complexity of $O(c_2 n_o N_G^2)$. When checking whether to insert a new solution into the $\mathcal{PF}$, EEMACOMP performs a non-dominance check of worst case complexity $O(c_3 n_o P_{as})$. The worst case complexity for the crowding distance used in order to keep a bound on the archive size is $O(c_4 n_o P_{as}^2)$. The EEMACOMP global pheromone update has a worst case complexity of $O(c_5 n_o N_G P_{as})$ and the ApplyMobilityChanges procedure has a worst case complexity of $O(c_6 n_o P_{as} + c_7 n_o N_G^2)$. The pheromone conservation rule has a worst case complexity of $O(c_8 n_o N_G^2)$. The worst case complexity of EEMACOMP is $O(c_9 n_o P_{as} + c_{10} n_o P_{as}^2 + c_{11} n_o N_G P_{as} + c_{12} n_o N_G^2) = O(n_o N_G^2)$ where n_o is the number of objectives, P_{as} is the archive size, N_G is the number of nodes, and $c_1, c_2, ..., c_{12}$ are constants.

- EEMACOMH algorithm

  The EEMACOMH algorithm has a similar worst case complexity as EEMACOMP except for the global pheromone update, which has a worst case complexity of $O(c_5 N_G P_{as})$ and the pheromone conservation rule which has a worst case complexity of $O(c_8 N_G^2)$. The worst case complexity of EEMACOMH is $O(n_o N_G^2)$.

  Comparing EEMACOMP with EEMACOMH, the use of multiple pheromone ma-

trices requires an additional cost of $O(5c_5(n_o-1)N_G P_{as})$ due to the global pheromone update. EEMACOMP also requires an additional cost of $O(c_8(n_o-1)N_G^2)$ due to the pheromone conservation.

- EEMMASMP algorithm

  The EEMMASMP algorithm has a similar worst case complexity as EEMACOMP except for an additional processing for restricting the pheromones by an upper and lower limit in the order of $O(5c_{12}n_oN_G^2)$, where c_{12} is a constant. The worst case complexity of EEMMASMP is $O(n_oN_G^2)$.

- EEMMASMH algorithm

  The EEMMASMH algorithm has a similar worst case complexity as EEMACOMH except for additional processing in the order of $O(13c_{12}N_G^2)$ due to the restriction of the pheromones by an upper and lower limit, where c_{12} is a constant. The worst case complexity of EEMMASMH is $O(n_oN_G^2)$.

- EEMACOMC algorithm

  The EEMACOMC algorithm has a similar worst case complexity as EEMACOMP.

- NSGA-II-MPA has a worst case complexity $O(n_oN_G^2 + N_G\log(N_G) + k\log(k)) = O(n_oN_G^2)$ where $O(N_G\log(N_G) + k\log(k))$ is the worst case complexity of the k-shortest path algorithm.

The NSGA-II-MPA algorithm has the lowest worst case complexity because it does not require pheromone updates, and the complexity of the $k-$shortest path algorithm is less than the pheromone updates used in the ACO algorithms.

EEMMASMP has the highest worst case complexity because of the multi-pheromone processing and the restriction of pheromones by the highest and lowest limits. Also, EEMACOMP has a higher worst case complexity than EEMMASMH because of the multi-pheromone processing which occurs more frequently than the restriction of pheromones by the highest and lowest limits.

A fair ranking of the algorithms in terms of their worst case computational complexity is: NSGA-II-MPA $<$ EEMACOMH $<$ EEMMASMH $<$ EEMACOMC $\leq$ EEMACOMP $<$ EEMMASMP.

7.4.9 Overall Performance of Algorithms

Based on the analysis of the empirical results presented in Subsections 7.4.2-7.4.7, this subsection summarises the performance of the developed algorithms in terms of the $\bar{n}_{alg}$, $\bar{\varrho}$ and $\bar{\xi}$ metrics and the optimisation criteria.

A comparison of each algorithm for each scenario reveals the following conclusions:

- When change frequency, T_{sm}, decreased, all algorithms displayed lower values, and therefore good results for the spacing metric for most scenarios. The solutions are more uniformly distributed in the whole Pareto-optimal set, instead of gathering in a small region.
- When change severity, R_g, increased, the number of non-dominated solutions decreased as well and the value of the $\bar{\varrho}$ metric increased for all algorithms.
- All algorithms displayed a high value for $\bar{\xi}$ irrespective of T_{sm}, R_g, and N_G. High values of $\bar{\xi}$ show closeness of the solutions to the optimal Pareto set, and to some extent, the spread of the solutions across objective space.
- All algorithms displayed a very low value for the $\bar{\varrho}$ metric (below 0.3), showing that they produced uniformly distributed solutions.
- The EEMACOMH algorithm is affected the most when change severity increased to 800, producing a much smaller number of non-dominated solutions and a worst solution spread compared to the rest of the ACO algorithms.
- All ACO algorithms compared to the NSGA-II-MPA algorithm displayed a higher value for $\bar{n}_{alg}$ for 90% of the scenarios.
- A larger number of nodes combined with higher change severity negatively affected the performance of the ACO algorithms in terms of the number of non-dominated solutions and solution spread, even though the value of $\bar{\varrho}$ is still low and under 0.3.
- The EEMACOMP algorithm found the largest number of non-dominated solutions from EEMACOMH for all scenarios with $N_G > 30$ (66.6% of the scenarios). Also, EEMACOMP found the largest number of non-dominated solutions from EEMMASMP, EEMMASMH, and EEMACOMC for all scenarios with $N_G = 100$ and

$R_g = 800$ and scenarios with $N_G = 800$ (44.4% of the scenarios). The EEMACOMP algorithm produced a better solution spread than EEMACOMH for 82% of the scenarios, a better solution spread than EEMMASMP and EEMACOMC for 66% of the scenarios, a better solution spread than EEMMASMH for 77% of the scenarios, and better solution spread than NSGA-II-MPA for 88% of the scenarios.

- For all environment changes, the EEMACOMP algorithm found more non-dominated solutions than all the other algorithms and the NSGA-II-MPA found the least number of non-dominated solutions (refer to Figure 7.43).
- For all environment changes, the EEMACOMP algorithm had the best solution spread and the NSGA-II-MPA had the worst solution spread (refer to Figure 7.44).
- For all algorithms, there is a very small variation at each environment change in the values of the $\bar{n}_{alg}$, $\bar{\varrho}$, and $\bar{\xi}$ metrics, and the values of the EP, TNP, CP, and VNP objectives. This shows the robustness and adaptability of all the algorithms to the environment changes.
- The NSGA-II-MPA approach had a lower energy consumed per packet than all the ACO approaches and for all the scenarios.
- All ACO approaches are better than the NSGA-II-MPA approach with reference to the utilisation of the most heavily used link, TNP, objective for $N_G = 300$.
- The EEMACOMP, EEMMASMP, EEMMASMH, and EEMACOMC approaches are better than the NSGA-II-MPA approach with reference to the variance in node power levels, VNP, objective for all scenarios. The EEMACOMH approach is better than the NSGA-II-MPA approach with reference to the VNP objective for all scenarios except for scenarios with $R_g = 800$ and $N_G \in \{100, 300\}$.
- The NSGA-II-MPA approach had a lower cost per packet, CP, than all ACO approaches for all scenarios.
- The NSGA-II-MPA approach had a lower maximum node cost, MNC, than all ACO approaches for all scenarios except for scenarios with $N_G = 300$ and $R_g = 800$.

- EEMACOMP had the highest rank with reference to the performance criteria for most scenarios, and the highest average rank over all scenarios and performance criteria.
- EEMACOMH had the lowest average rank over all scenarios and performance criteria.
- If all objectives have the same importance it is recommended to use the EEMACOMP, EEMMASMP, EEMMASMH, or EEMACOMC ACO algorithms (especially the EEMACOMP), which provide more closeness to the true Pareto front and maintain better distribution of solutions in the Pareto front. If any of the EP, CP, or MNC objectives have a higher priority than the other objectives, it is recommended to use the NSGA-II-MPA algorithm.

7.5 Summary

This chapter presented an empirical study of the performance of the five ant multi-objective optimisation algorithms presented in this thesis and the role played by the various algorithmic features.

The experimental procedures and results of parameter tuning were given.

The five algorithms were compared with one another and with the NSGA-II, which was adapted in this thesis for the multi-objective, power-aware routing problem. Different scenarios were tested for each algorithm according to the values of different ACO and NSGA-II parameters and the Pareto fronts for each algorithm were obtained.

The experimental results showed that the five ACO algorithms, excluding the EEMACOMH algorithm, outperformed, on most scenarios, the NSGA-II-MPA algorithm in terms of the number of solutions and spacing metric. All algorithms produced similar results for the hypervolume metric for most of the scenarios. The NSGA-II-MPA approach had a lower energy consumed per packet, and lower cost per packet than all the ACO approaches and for all the scenarios. Also, the NSGA-II-MPA approach had a lower maximum node cost than all the ACO approaches for most scenarios. All ACO approaches had a lower utilisation of the most heavily used link than the NSGA-II-MPA for $N_G = 300$ and less variance in node power levels for most of the scenarios.

By minimising the five optimisation criteria for the power-aware routing problem,

the proposed ACO algorithms minimised the energy consumed per packet and spread the traffic over the network to make all nodes have similar amounts of consumed energy. Maximum energy consumption has been reduced which means that the lifetime of the first node to die is extended using the ACO approaches. Consequently, MANETS network lifetime was maximised and network partitioning was delayed.

In addition, the results demonstrated that EEMACOMP outperformed the other four ACO algorithms and the NSGA-II-MPA algorithm in terms of the number of solutions and spacing metric in most scenarios and produced the best rank. Therefore, in light of the results presented, the EEMACOMP approach is recommended by this study for the multi-objective, power-aware routing problem.

Chapter 8

Conclusion

8.1 Summary

As a special type of network, mobile ad hoc networks (MANETs) have increasingly been the focus of research in recent years. The network topology in MANETs usually changes with time. Therefore, as a result of the highly dynamic and distributed nature of MANETs, routing protocols are being presented with new challenges since traditional routing protocols may not be suitable for MANETs. In particular, energy efficient routing may be the most important design criterion for MANETs since mobile nodes are powered by batteries with limited capacity.

The main purpose of this thesis was to study ant algorithms as applied to the dynamic environment of mobile ad hoc networks and, specifically, to resolve the five power-aware metrics which were presented by Singh *et al.* [184]. These metrics aim to minimise the energy consumed per packet, maximise the time needed to network partition, minimise the variance in node power levels, minimise cost per packet, and minimise maximum node cost. Taking into consideration a realistic mobility model using an ant colony optimisation (ACO) approach, this thesis proposed to simultaneously optimise the five power-aware metrics for energy efficiency and maximising the lifetime of MANETs. A set of optimal solutions, the Pareto-optimal set, is found using ACO algorithms.

This thesis proposed five algorithms with which to solve the above multi-objective optimisation problem. The first two algorithms are the energy efficiency for mobile networks using multi-objective ant colony optimisation, multi-pheromone (EEMACOMP) algorithm and the energy efficiency for mobile networks using multi-objective ant colony optimisation, multi-heuristic (EEMACOMH) algorithm. These two algorithms are adaptations of multi-objective ant colony optimisation algorithms (MOACO) based on the ant colony system (ACS) algorithm.

The next two algorithms, namely, the energy efficiency for mobile networks using

multi-objective MAX-MIN ant system optimisation, multi-pheromone (EEMMASMP) algorithm and the energy efficiency for mobile networks using multi-objective MAX-MIN ant system optimisation, multi-heuristic (EEMMASMH) algorithm succeeded in solving the above multi-objective optimisation problem by using an adaptation of the MAX-MIN ant system optimisation algorithm.

The last algorithm implemented, namely, the energy efficiency for mobile networks using multi-objective ant colony optimisation, multi-colony (EEMACOMC) uses a multiple colony ACO algorithm.

In addition, this thesis used an adaptation of the NSGA-II algorithm called NSGA-II multi-objective power-aware algorithm (NSGA-II-MPA) to solve the multi-objective power-aware routing problem.

For each algorithm the following hypotheses or questions were investigated:

1. Is there a statistical significant difference in the performance of the algorithms?
2. Does performance deteriorate with increase in change frequency?
3. Does performance deteriorate with increase in change severity?
4. Are the algorithms scalable?
5. Is there an algorithm that is less affected by change frequency / change severity?
6. How is the performance of the algorithms over time?

The performance of each algorithm was tested under different scenarios for different change frequencies, change severities and number of nodes as outlined in Section 7.1.1. For each of the scenarios 30 simulations were executed and results were reported as averages over these simulations. Each estimated pareto front, $\mathcal{PF}$, produced by the EEMACOMP, EEMACOMH, EEMMASMP, EEMMASMH, EEMACOMC, and NSGA-II-MPA algorithms was evaluated using three performance metrics, namely the number of non-dominated solutions, $\bar{n}_{alg}$, the spread metric, $\bar{\varrho}$, and the hypervolume metric, $\bar{\xi}$ (refer to Section 7.1.3).

8.2 Conclusions

On the basis of the experimental results the final conclusions are summarised as follows:

- The EEMACOMP algorithm found a largest number of non-dominated solutions and produced a better solution spread compared to the rest of the algorithms, for high percentage of scenarios.
- All ACO algorithms compared to the NSGA-II-MPA algorithm displayed a higher value for $\bar{n}_{alg}$ for 90% of the scenarios and they produced a better solution spread for high percentage of scenarios.
- Performance for $\bar{n}_{alg}$ and $\bar{\varrho}$ metrics deteriorate with increase in change frequency, for all algorithms.
- Performance for $\bar{n}_{alg}$ and $\bar{\varrho}$ metrics deteriorate with increase in change severity, for all algorithms.
- The EEMACOMH algorithm is affected the most when change severity increased to 800, producing a much smaller number of non-dominated solutions and a worst solution spread compared to the rest of the ACO algorithms.
- A larger number of nodes combined with higher change severity negatively affected the performance of the ACO algorithms in terms of the number of non-dominated solutions and solution spread, even though the value of $\bar{\varrho}$ is still low and under 0.3.
- All the algorithms had a good performance over time. This shows the robustness and adaptability of all the algorithms to the environment changes.
- All algorithms displayed a high value for $\bar{\xi}$ irrespective of T_{sm}, R_g, and N_G. High values of $\bar{\xi}$ show closeness of the solutions to the optimal Pareto set, and to some extent, the spread of the solutions across objective space.
- EEMACOMP had the highest rank with reference to the performance criteria for most scenarios, and the highest average rank over all scenarios and performance criteria.

In summary, based on the simulations it can be concluded that using ant multi-objective optimisation to simultaneously optimise the five power-aware metrics is extremely beneficial because the traffic is spread over the network, thus forcing all nodes to have similar amounts of consumed energy. Maximum energy consumption has been reduced which means that the lifetime of the first node to die is extended using the ACO

approaches. Consequently, MANETS network lifetime was maximised and network partitioning was delayed.

This is the first time the power-aware routing multi-objective optimisation problem has been solved using an ant colony optimisation algorithm. All five algorithms presented in this thesis were shown to outperform the NSGA-II-MPA algorithm in terms of the performance metrics in most scenarios. Also, all the ACO approaches had a lower variance in node power levels and a lower utilisation of the most heavily used link than the NSGA-II-MPA approach. In addition, all ACO algorithms produced a very good solution distribution, high number of non-dominated solutions and dominated a high percentage of the objective space, showing closeness to the true Pareto front.

8.3 Future Work

Specific recommendations to develop and extend this work further and areas of future research include:

- Other mobility models such as the random waypoint mobility model can be studied in order to model different realistic situations of the movements of mobile nodes and study the behaviour of the proposed algorithms. Finally, these different mobility models may be compared in order to demonstrate their effects on the performance of the proposed ant routing algorithms.
- A detailed comparison of the performance of the ant-based algorithms with other meta-heuristics can be conducted.
- The influence of the control parameters on the ant-based algorithms under different number of nodes can be analysed.
- The influence of different weights for the objective parameters, λ_ψ, on the ant-based algorithms can be examined.
- The impact of the Pareto archive size on the performance of the ant-based algorithms can be analysed.
- Other performance metrics such as diversity in the objective space (DOM) proposed by Morrison and De Jong [150], and their application to the evaluation and

comparison of the developed multi-objective optimisation algorithms for the power aware routing problem can be investigated.

Bibliography

[1] Fluxviz software: http://fluxviz.sourceforge.net.

[2] Next Generation Intelligent Networks Research Center (NeXGIN RC), http://nexginrc.org, 10 June 2010.

[3] LAN MAN Standards Committee of the IEEE Computer Society, Wireless LAN Medium Access Control (MAC) and Physical Layer (PHY) Specification, IEEE, New York, NY, USA. *IEEE Std 802.11-1999 edition*, 1999.

[4] S-H. Ahn, S-G. Lee, and T-C. Chung. Modified Ant Colony System for Coloring Graphs. In *Proceedings of the Joint Conference of the Fourth International Conference on Information, Communications and Signal Processing, and the Fourth Pacific Rim Conference on Multimedia*, pages 1849–1853, 2003.

[5] M. Aiello. *Spatial Reasoning: Theory and Practice*. PhD thesis, Institute for Logic, Language and Computation Universiteit van Amsterdam, 2002.

[6] I. Alaya, C. Solnon, and K. Ghdira. Ant Colony Optimisation for Multi-objective Optimisation Problems. In *Proceedings of the 19th IEEE International Conference on Tools with Artificial Intelligence*, pages 450–457. IEEE Computer Society, 2007.

[7] F. Alnajjar and Y. Chen. SNR/RP Aware Routing Algorithm: Cross-Layer Design For MANETs. *International Journal of Wireless and Mobile Networks*, 1(2):127–136, 2009.

[8] A.Misra and S. Banerjee. MRPC: Maximizing Network Lifetime for Reliable Routing in Wireless Environments. In *Proceedings of IEEE Wireless Communications and Networking Conference*, pages 800–806, 2002.

[9] E.J. Anderson, C. Glass, and C.N. Potts. Machine scheduling. In E. Aarts and J. K. Lenstra, editors, *Local Search in Combinatorial Optimisation*, pages 361–414. John Wiley and Sons, 1997.

[10] D. Angus. Crowding Population-Based Ant Colony Optimization for the Multi-Objective TSP. In *2007 IEEE Symposium on Computational Intelligence in Multi-Criteria Decision-Making*, pages 333–340. IEEE Press, 2007.

[11] D. Angus and C. Woodward. Multiple Objective Ant Colony Optimisation. *Swarm Intelligence*, 3(1):69–85, 2009.

[12] G. Asada, M. Dong, T.S. Lin, F. Newberg, G. Pottie, W.J. Kaiser, and H.O. Marcy. Wireless Integrated Network Sensors: Low Power Systems on a Chip. In *Proceedings of the 24th European Solid-State Circuits Conference*, pages 1–8, 1998.

[13] N. Aschenbruck, E. Gerhands-Padilla, and P. Martini. A Survey on Mobility Models for Performance Analysis in Tactical Mobile Networks. *Journal of Telecommunication and Information Technology*, 2:54–61, 2008.

[14] E. K. Asl, M. Damanafshan, M. Abbaspour, M. Noorhosseini, and K. Shekoufandeh. EMP-DSR: An Enhanced Multi-path Dynamic Source Routing Algorithm for MANETs Based on Ant Colony Optimization. In *Proceedings of the Third Asia International Conference on Modelling and Simulation*, pages 692–697. IEEE Press, 2009.

[15] T. Bäck. *Evolutionary Algorithms Theory and Practice: Evolution Strategies, Evolutionary Programming, Genetic Algorithms*. Oxford University Press, New York, USA, 1996.

[16] T. Bäck, U. Hammel, and H.P. Schwefel. Evolutionary Computation: Comments on the History and Current State. *IEEE Transactions on Evolutionary Computation*, 1(1):3–17, 1997.

[17] J. Bader and E. Zitzler. HypE: An Algorithm for Fast Hypervolume-Based Many-Objective Optimization. TIK Report 286, Computer Engineering and Networks Laboratory (TIK), ETH Zurich, 2008.

[18] S. Banerjee and A. Misra. Minimum Energy Paths for Reliable Communication in Multi-Hop Wireless Networks. In *Proceedings of Mobihoc*, pages 146–156, 2002.

[19] S. Bird and X. Li. Informative Performance Metrics for Dynamic Optimisation Problems. In *Proceedings of the 9th Annual Conference on Genetic and Evolutionary Computation*, pages 18–25, 2007.

[20] C. Blum and A. Roli. Metaheuristics in Combinatorial Optimisation: Overview and Conceptual Comparison. *ACM Computing Surveys*, 35(3):268–308, 2003.

[21] E. Bonabeau, M. Dorigo, and G. Theraulaz. *Swarm Intelligence: From Natural to Artificial Swarm Intelligence*. Oxford University Press, 1999.

[22] P.A.N. Bosman and D. Thierens. The Balance Between Proximity and Diversity in Multi-objective Evolutionary Algorithms. *IEEE Transactions on Evolutionary Computation*, 7:174–188, 2003.

[23] J. Branke. *Evolutionary Optimisation in Dynamic Environments*. Kluwer Academic Publishers, Massachusetts USA, 2002.

[24] G. Brassard and P. Bratley. *Fundamentals of Algorithmics*. Prentice Hall, Englewood Cliffs, NJ, 1996.

[25] R.L. Brooks. On Colouring the Nodes of a Network. In *Proceedings Cambridge Philos*, volume 37, pages 194–197, 1941.

[26] A. Budgor and O. Diaz. Final Report on Utility of Commercial Wireless Study: A Technology Roadmap for Disaster Response. *NORTHCOM Disaster Relief Comms Report*, 2006.

[27] B. Bullnheimer, R.F. Hartl, and C. Strauss. An Improved Ant System Algorithm for the Vehicle Routing Problem. *Annals of Operation Research*, 89:319–328, 1999.

[28] P. Buonadonna, J. Hellerstein, W. Hong, D. Gay, and S. Madden. TASK: Sensor Network in a Box. In *Proceedings of the Second European Workshop on Wireless Sensor Neworks*, pages 133–144, 2005.

[29] T. Camp, J. Boleng, and V. Davies. A Survey of Mobility Models for Ad Hoc Networks Research. *Wireless Communications and Mobile Computing: Special Issue on Mobile Ad Hoc Networking Research, Trends and Applications*, 2(5):483–502, 2002.

[30] P. Cardoso, M. Jesús, and A. Márquez. MONACO – Multi-Objective Network Optimization Based on an ACO. In *Proceedings of Enguentros de Geometría Computacional*, 2003.

[31] G. Di Caro and M. Dorigo. AntNet: Distributed Stigmergetic Control for Communications Networks. *Journal of Artificial Intelligence Research*, 9:317–365, 1998.

[32] E. Çela. *The Quadratic Assignment Problem: Theory and Algorithms*. Kluwer Academic Publishers, 1998.

[33] C. Chang and L. Tassiulas. Maximum Lifetime Routing in Wireless Sensor Networks. *IEEE/ACM Transactions on Networking*, 12(4):609–619, 2004.

[34] D. Cheriton and R.E. Tarjan. Finding Minimum Spanning Trees. *SIAM Journal on Computing*, 5:724–742, 1976.

[35] K.W. Chin, J. Judge, A. Williams, and R. Kermode. Implementation Experiences with MANET Routing Protocols. *ACM/SIGCOMM Computer Communications Review*, 2002.

[36] I. Chlamtac, M. Conti, and J.-N. Liu. Mobile Ad Hoc Networking: Imperatives and Challenges. *Ad Hoc Networks*, 1(1):13–64, 2003.

[37] C.A. Coello Coello, D.A. Van Veldhuizen, and G.B. Lamont. *Evolutionary Algorithms for Solving Multi-Objective Problems*. Kluwer Academic Publishers, 2002.

[38] D. Corne, M. Dorigo, and F. Glover. New Methods in Optimisation. *McGraw-Hill*, 1999.

[39] L. de Castro and J. Timmis. *Artificial Immune Systems: A New Computational Intelligence Approach*. Springer-Verlag, 2002.

[40] K. Deb. *Multi-objective Optimisation using Evolutionary Algorithms*. John Wiley & Sons, Chichester, UK, 2001.

[41] K. Deb. Unveiling Innovative Design Principles By Means of Multiple Conflicting Objectives. *Engineering Optimization*, 35:445–470, 2003.

[42] K. Deb, A. Pratap, S. Agrawal, and T. Meyarivan. Fast and Elitist Multi-Objective Genetic Algorithm: NSGA-II. *IEEE Transactions on Evolutionary Computation*, 6(2):182–197, 2002.

[43] K. Deb, U.B. Rao, and S. Karthik. Dynamic Multi-Objective Optimisation and Decision-Making Using Modified NSGA-II: A Case Study on Hydro-Thermal Power Scheduling Bi-Objective Optimisation Problems. Technical Report KanGAL Report No. 2006008, Kanpur Genetic Algorithms Laboratory, 2006.

[44] P. Deepalakshmi and S. Radhakrishnan. Ant Colony Based QoS Routing Algorithm For Mobile Ad Hoc Networks. *International Journal of Recent Trends in Engineering*, 1(1):459–462, 2009.

[45] J.L. Deneubourg, S. Aron, S. Goss, and J.M. Pasteels. The Self-organizing Exploratory Pattern of the Argentine Ant. *Journal of Insect Behavior*, 13:159–168, 1990.

[46] S. Deng. On Approximate Solutions in Convex Vector Optimisation. *SIAM Journal on Control and Optimisation*, 35(6):2128–2136, 1997.

[47] B. Divecha, A. Abraham, C. Grosan, and S. Sanyal. Impact of Node Mobility on MANET Routing Protocols Models. *Journal of Digital Information Management*, 5(1):19–23, 2007.

[48] D.L. Djenouri, A. Derhab, and N. Badache. Ad Hoc Networks Routing Protocols and Mobility. *International Arab Journal of Information Technology*, 3(2):126–133, 2006.

[49] K. Doerner, J. Gutjahr, R. Hartl, C. Strauss, and C. Stummer. Pareto Ant Colony Optimisation: A Metaheuristic Approach to Multiobjective Portfolio Selection. *Annals of Operations Research*, 131:79–99, 2004.

[50] L. Doherty, B.A. Warneke, B.E. Boser, and K.S.J. Pister. Energy and Performance Considerations for Smart Dust. *International Journal of Parallel Distributed Systems and Networks*, 4(3):121–133, 2001.

[51] M. Dorigo. *Optimisation, Learning and Natural Algorithms*. PhD thesis, Dipartimento di Elettronica, Politecnico di Milano, IT, 1992.

[52] M. Dorigo and G. Di Caro. The Ant Colony Optimisation Meta-Heuristic. In D. Corne, M. Dorigo, and F. Glover, editors, *New Ideas in Optimisation*, pages 11–32. McGraw-Hill, 1999.

[53] M. Dorigo and L.M. Gambardella. Ant Colony System: A Cooperative Learning Approach to the Traveling Salesman Problem. *IEEE Transactions on Evolutionary Computation*, 1(1):53–66, 1997.

[54] M. Dorigo, L.M Gambardella, and G. Di Caro. Ant Algorithms for Discrete Optimisation. *Artificial Life*, 5(2):137–172, 1999.

[55] M. Dorigo, V. Maniezzo, and A. Colorni. Positive Feedback as a Search Strategy. Technical Report 91-016, Dipartimento di Elettronica, Politecnico di Milano, IT, 1991.

[56] M. Dorigo, V. Maniezzo, and A. Colorni. Ant System: Optimisation by a Colony of Cooperating Agents. *IEEE Transactions on Systems, Man, and Cybernetics-Part B*, 26(1):29–41, 1996.

[57] M. Dorigo and T. Stützle. The Ant Colony Optimisation Metaheuristic: Algorithms, Applications, and Advances. Technical Report IRIDIA-2000-32, IRIDIA, Universite Libre de Brussels, Belgium, 2000.

[58] M. Dorigo and T. Stützle. *Ant Colony Optimisation*. MIT Press, 2004.

[59] J. Dorn. Iterative Improvement Methods for Knowledge-Based Scheduling. *AICOM*, 8:20–34, 1995.

[60] R.C. Eberhart and J. Kennedy. A New Optimiser Using Particle Swarm Theory. In *Proceedings of Sixth International Symposium on Micro Machine and Human Science*, pages 39–43, 1995.

[61] R.C. Eberhart and Y. Shi. Tracking and Optimising Dynamic Systems with Particle Swarms. In *Proceedings of the IEEE Congress on Evolutionary Computation*, volume 1, pages 94–100, 2001.

[62] M. Ehrgott. Approximation Algorithms for Combinatorial Multicriteria Optimization Problems. *International Transactions in Operational Research*, 7(1):5–31, 2000.

[63] A.P. Engelbrecht. *Fundamentals of Computational Swarm Intelligence*. John Wiley & Sons, 2005.

[64] A.P. Engelbrecht. *Fundamentals of Computational Swarm Intelligence*. John Wiley & Sons, 2006.

[65] S.C. Ergen and P. Varaiya. Energy Efficient Routing with Delay Guarantee for Sensor Networks. *ACM Wireless Networks*, 13:679–690, 2006.

[66] L.F. Escudero. An Inexact Algorithm for the Sequential Ordering Problem. *European Journal of Operational Research*, 37:232–253, 1988.

[67] C.J. Eyckelhof and M. Snoek. Ant Systems for a Dynamic TSP. In *Ant Algorithms: Third International Workshop, ANTS 2002*, pages 88–99. Springer Verlag, 2002.

[68] M. Farina, K. Deb, and P. Amato. Dynamic Multiobjective Optimisation Problems. In *IEEE Transactions on Evolutionary Computation. Test Cases, Approximations, and Applications*, volume 8, pages 425–442, 2004.

[69] M. Farooq and G. Di Caro. Routing Protocols for Next Generation Intelligent Networks Inspired by Collective Behaviors of Insect Societies. In C. Blum and D. Merkle, editors, *Swarm Intelligence: Introduction and Applications. Natural Computing Series*, pages 101–160. Springer-Verlag, 2008.

[70] M.M. Flood. The Traveling Salesman Problem. *Operations Research 4*, pages 61–75, 1956.

[71] E. Gafni and D. Bertsekas. Distributed Algorithms for Generating Loop-free Routes in Networks with Frequently Changing Topology. *IEEE Transactions on Communications*, 29(1):11–18, 1981.

[72] C. Gagné, M. Gravel, and W. Price. Scheduling a Single Machine Where Setup Times are Sequence Dependent Using an Ant-Colony Heuristic. In *Abstract Proceedings of ANTS*, pages 157–160, 2000.

[73] L.M. Gambardella and M. Dorigo. Ant-Q: A Reinforcement Learning Approach to the TSP. In *Proceedings of ML-95, Twelfth International Conference on Machine Learning*, pages 252–260. Morgan Kaufmann, 1995.

[74] L.M. Gambardella and M. Dorigo. Solving Symmetric and Asymmetric TSPs by Ant Colonies. In *Proceedings of IEEE International Conference on Evolutionary Computation*, pages 622–627, 1996.

[75] L.M. Gambardella and M. Dorigo. AHAS-SOP: Hybrid Ant System for the Sequential Ordering Problem. Technical Report IDSIA-11-97, IDSIA, Lugano, Switzerland, 1997.

[76] L.M. Gambardella, E. Taillard, and G. Agazzi. MACS-VRPTW: A Multiple Ant Colony System For Vehicle Routing Problems With Time Windows. Technical report, IDSIA, Lugano, Switzerland, 1999.

[77] L.M. Gambardella, E.D. Taillard, and M. Dorigo. Ant Colonies for the QAP. Technical Report IDSIA-4-97, IDSIA, Lugano, Switzerland, 1997.

[78] Y. Ganjali and N. McKeown. Routing in a Highly Dynamic Topology. In *Proceedings of the Second Annual IEEE ComSoc SECON*, pages 164–175. IEEE Press, 2005.

[79] C. García-Martínez, O. Cordón, and F. Herrera. A Taxonomy and an Empirical Analysis of Multiple Objective Ant Colony Optimization Algorithms for the Bi-Criteria TSP. *European Journal of Operational Research*, 180(1):116–148, 2007.

[80] M. R. Garey and D. S. Johnson. *Computers and Intractability: A Guide to the Theory of NP-completeness*. W. H. Freeman, 1979.

[81] F. Glover and M. Laguna. Tabu Search. In C. Reeves, editor, *Modern Heuristic Techniques for Combinatorial Problems*, pages 70–151. Blackwell Scientific Publishing, 1993.

[82] A.J. Goldsmith and S.B. Wicker. Design Challenges for Energy-Constrained Ad Hoc Wireless Networks. *IEEE Wireless Communications Magazine*, 9(4):8–27, 2002.

[83] S. Goss, S. Aron, J.L. Deneubourg, and J.M. Pasteels. Self-Organized Shortcuts in the Argentine Ant. *Naturwissenschaften*, 76:579–581, 1989.

[84] P.P. Grasse. La Reconstruction du Noeud et les Coordinations Interindividuelles Chez Bellicositermes Natalensis et Cubiternes sp. La Theorie de la Stigmetrie: Essai d'Interpretation du Comportement des Termites Constructeur. Technical Report 6, 1959.

[85] M. Gravel, W. L. Price, and C. Gagné. Scheduling Continuous Casting of Aluminium Using A Multiple Objective Ant-Colony Optimization Meta-Heuristic. *European Journal of Operation Research*, 143(1):218–229, 2002.

[86] R.S. Gray. Soldiers, Agents and Wireless Networks: A Report on a Military Application. In *Proceedings of the Fifth International Conference and Exhibition on the Practical Application of Intelligent Agents and Multi-Agents*, 2000.

[87] M. Greef and A. P. Engelbrecht. Solving Dynamic Multi-Objective Problems with Vector Evaluated Particle Swarm Optimisation. In *IEEE Congress on Evolutionary Computation*, pages 2917–2924. IEEE Press, 2008.

[88] J. J. Grefenstette. Evolvability in Dynamic Fitness Landscapes, a Genetic Algorithm Approach. In *IEEE Congress on Evolutionary Computation*, pages 2031–2038. IEEE Press, 1999.

[89] S. Guan, Q. Chen, and W. Mo. Evolving Dynamic Multi-objective Optimisation Problems with Objective Replacement. *Artificial Intelligence Review*, 23(3):267–293, 2005.

[90] M. Guntsch and M. Middendorf. Pheromone Modification Strategies for Ant Algorithms Applied to Dynamic TSP. In *Proceedings of the Workshop on Applications of Evolutionary Computing*, pages 213–222, 2001.

[91] M. Guntsch and M. Middendorf. A Population Based Approach for ACO. In S. Cagnoni et al., editor, *Applications of Evolutionary Computing-EvoWorkshops*, pages 72–81. Springer-Verlag, 2002.

[92] M. Guntsch and M. Middendorf. Applying Population Based ACO to Dynamic Optimisation Problems. In *Proceedings of the Third International Workshop ANTS 2002*, pages 111–122. Springer-Verlag, 2003.

[93] M. Guntsch, M. Middendorf, and H. Schmeck. An Ant Colony Optimisation Approach to Dynamic TSP. In L. Spector et al., editor, *Genetic and Evolutionary Computation Conference*, pages 860–867. Morgan Kaufmann, 2001.

[94] N. Gupta and S. R. Das. Energy-aware On-demand Routing for Mobile Ad Hoc Networks. In *Proceedings of International Workshop in Distributed Computing*, pages 164–173, 2002.

[95] M.P. Hansen and A. Jaszkiewicz. Evaluating the Quality of Approximations to the Non-Dominated Set. Technical report, Technical University of Denmark, 1998.

[96] R. Hassin. Approximation Schemes for the Restricted Shortest Path Problem. *Mathematics of Operations Research*, 17(1):36–42, 1992.

[97] C. Hedrick. Routing Information Protocol. Internet Request for Comments RFC 1058. *IETF*, 1988.

[98] S. Hengwei and A. Shoichiro. An Agent-Based Approach to Routing in Communications Networks with Swarm Intelligence. *European Conference on Artificial Life*, 2801:716–723, 2003.

[99] T.S. Ho and K.C. Chen. Performance Analysis of IEEE 802.11 CSMA/CA Medium Access Control Protocol. In *Proceedings of IEEE PIMRC*, pages 407–411, 1996.

[100] M.O. Hofman, A. McGovern, and K.R. Whitebread. Mobile Agents on the Digital Battlefield. In *Proceedings of Second International Conference on AUTONOMOUS AGENTS*, pages 219–225, 1998.

[101] X. Hong, M. Gerla, G. Pei, and C. Chiang. A Group Mobility Model for Ad Hoc Wireless Networks. In *Proceedings of ACM/IEEE MSWiM99*, pages 53–60, 1999.

[102] X. Hu and R. Ebenhart. Multiobjective Optimization Using Dynamic Neighborhood Particle Swarm Optimization. In *Proceedings of the IEEE Congress on Evolutionary Computation*, volume 2, pages 1677–1681, 2002.

[103] C.L. Hwang, A.S.M. Masud, S.R. Paidy, and K. Yoon. *Multiple Objective Decision Making: Methods and Applications; A State of the Art Survey*. Springer, 1979.

[104] S. Iredi, D. Merkle, and M. Middendorf. Bi-criterion Optimisation with Multi Colony Ant Algorithms. In E. Zitzler et al., editor, *Evolutionary MultiCriterion Optimisation, First International Conference in LNCS*, volume 1993, pages 359–372. Springer-Verlag, 2001.

[105] G. Jayakumar and G. Gopinath. Ad Hoc Mobile Wireless Networks Routing Protocols - A Review. *Computer Sciences*, 3(8):574–582, 2007.

[106] Y. Jin and B. Sendhoff. Constructing Dynamic Optimisation Test Problems Using the Multi-objective Optimisation Concept. In *Proceedings of the EvoWorkshops*, pages 525–536. Springer-Verlag, 2004.

[107] D. Johnson and D. Maltz. Dynamic Source Routing in Ad Hoc Wireless Networks. In T. Imelinsky and H. Korth, editors, *Mobile Computing*, volume 353, pages 153–181. Kluwer Academic Publishers, 1996.

[108] D.S. Johnson. Approximation Algorithms for Combinatorial Problems. *Journal of Computer and System Sciences*, 23:256–278, 1974.

[109] C.E. Jones, K.M. Sivalingam, P. Agrawal, and J.C. Chen. A Survey of Energy Efficient Network Protocols for Wireless Networks. *Wireless Networks*, 7(4):343–358, 2001.

[110] D.A. Joseph, B.S. Manoj, and C.S.R. Murthy. Interoperability of Wi-Fi Hotspots and Cellular Networks. In *Proceedings of the 2nd ACM International Workshop on Wireless Mobile Applications and Services on WLAN Hotspots*, pages 127–136, 2004.

[111] S. Jung, N. Hundewale, and A. Zelikovsky. Energy Efficiency of Load Balancing in MANET Routing Protocols. In *Proceedings of the First ACIS International Workshop on Self-Assembling Wireless Networks*, pages 476–483. IEEE Press, 2005.

[112] K. Weicker. Performance Metrics for Dynamic Environments. In *Parallel Problem Solving from Nature - PPSN VII*, pages 64–73. Springer-Verlag, 2002.

[113] S. Kannan, T. Kalaikumaran, S. Karthik, and V.P. Arunachalam. Ant Colony Optimization for Routing in Mobile Ad-Hoc Networks. *International Journal of Software Computing*, 5(6):223–228, 2010.

[114] G. Kantor, S. Singh, R. Peterson, D. Rus, A. Das, V. Kumar, G. Pereira, and J. Spletzer. Distributed Search and Rescue with Robot and Sensor Teams. In *Proceedings of the 4th International Conference on Field and Service Robotics*, pages 529–538, 2003.

[115] K. Kar, M. Kodialam, T. Lakshman, and L. Tassiulas. Routing for Network Capacity Maximization in Energy-Constrained Ad Hoc Networks. In *Proceedings of IEEE INFOCOM*, pages 673–681, 2003.

[116] R. Kara, I. Ozcelik, and H. Ekiz. A New Routing Algorithm in MANETs: Position Based Hybrid Routing. *Scientific Research and Essays*, 5(3):328–338, 2010.

[117] D.K. Kim. A New Mobile Environment: Mobile Ad Hoc Networks (MANET). *IEEE Vehicular Technology Society News*, pages 29–35, 2003.

[118] S. Kirkpatrick, C.D. Gelatt Jr., and M.P. Vecchi. Optimisation by Simulated Annealing. *Science*, 220:671–680, 1983.

[119] J.D. Knowles. *Local-Search and Hybrid Evolutionary Algorithms for Pareto Optimisation*. PhD thesis, Department of Computer Science, The University of Reading, 2002.

[120] J.D. Knowles and D.W. Corne. Approximating the Non-dominated Front Using the Pareto Archived Evolution Strategy. *Evolutionary Computation*, 8(2):149–172, 2000.

[121] P. Korhonen. Multiple Objective Programming Support. Technical Report IIASA Report IR-98-010, 1998.

[122] J. Krajícek. *Bounded Arithmetic, Propositional Logic and Complexity Theory.* Cambridge University Press, 1995.

[123] M. K. J. Kumar and R.S. Rajesh. Performance Analysis of MANET Routing Protocols in Different Mobility Models. *International Journal of Computer Science and Network Security*, 9(2):22–29, 2009.

[124] M. K. Jeya Kumar and R.S. Rajesh. A Survey of MANET Routing Protocols in Mobility Models. *International Journal of Soft Computing*, 4(3):136–141, 2009.

[125] R. Kumar, V. Joshi, and V. Dhir. Performance Comparison of Routing Protocols in Mobile Ad Hoc Networks. *International Journal of Engineering Science and Technology*, 2(8):3494–3502, 2010.

[126] M. Laumanss, G. Rudolph, and H-P. Schwefel. Approximating the Pareto Set: Concepts, Diversity Issues and Performance Assessment. Technical report, University of Dortmund, Dortmund, Germany, 1999.

[127] E.L. Lawler, J.K. Lenstra, A.H.G. Rinnooy Kan, and D.B. Shmoys. *The Traveling Salesman Problem.* John Wiley, 1985.

[128] M.T.C. Lee, V. Tiwari, S. Malik, and M. Fujita. Power Analysis and Minimization Techniques for Embedded DSP Software. *IEEE Transactions on VLSI Systems*, pages 123–135, 1997.

[129] E. L. Lehmann. *Non Parametrics: Statistical Methods Based On Ranks.* Holden-Day San-Fransisco, California, 1975.

[130] F.T. Leighton and S. Rao. An Approximate Max-Flow Min-Cut Theorem for Uniform Multicommodity Flow Problems with Applications to Approximation Algorithms. In *IEEE Symposium on Foundations of Computer Science*, pages 422–431, 1988.

[131] L.Gu and J.A. Stankovic. Radio-Triggered Wake-Up for Wireless Sensor Networks. In *Proceedings of the 10th IEEE Real Time and Embedded Technology and Applications Symposium*, volume 29, pages 157–182, 2005.

[132] C. Liu and Y. Wang. A New Dynamic Multi-Objective Optimisation Evolutionary Algorithm. *International Journal of Innovative Computing, Information and Control*, 4(8):2087–2096, 2008.

[133] C. Lochert, B. Scheuermann, and M. Mauve. A Survey on Congestion Control for Mobile Ad-Hoc Networks. *Wiley Wireless Communication and Mobile Computing*, 7(5):655–676, 2007.

[134] M. López-Ibáñez and T. Stützle. The Impact of Design Choices of Multi-Objective Ant Colony Optimization Algorithms on Performance: An Experimental Study on the Biobjective TSP. In M. Pelikan and J. Branke, editors, *Proceedings of the Genetic and Evolutionary Computation Conference*, pages 71–78. ACM Press, 2010.

[135] A.K. Mackworth. Constraint Satisfaction. In S.C. Shapiro, editor, *Encyclopedia of Artificial Intelligence*, volume 1, pages 205–211, 1987.

[136] S.R. Madden, M.J. Franklin, J.M. Hellerstein, and W. Hong. TAG: A Tiny Aggregation Service for Ad Hoc Sensor Networks. In *Proceedings of 5th Symposium on Operating Systems Design and Implementation*, pages 131–146, 2002.

[137] A. Mainwaring, J. Polastre, R. Szewczyk, D. Culler, and J. Anderson. Wireless Sensor Networks for Habitat Monitoring. In *Proceedings of the First ACM International Workshop on Wireless Sensor Networks and Applications*, pages 88–97. ACM Press, 2002.

[138] M. H. Mamoun. A Novel Routing Algorithm for MANET. *International Journal of Electrical and Computer Sciences*, 10(2):9–12, 2009.

[139] M. H. Mamoun. A New Proactive Routing Algorithm for MANET. *International Journal of Academic Research*, 2(2):199–204, 2010.

[140] V. Maniezzo and A. Colorni. The Ant System Applied to the Quadratic Assignment Problem. *IEEE Transactions on Knowledge and Data Engineering*, 11(5):769–778, 1999.

[141] E.N. Marais. *The Soul of the Ant*. J.L. van Schaik, Pretoria, South Africa, fifth edition, 1948.

[142] C.E. Mariano and E. Morales. MOAQ an Ant-Q Algorithm for Multiple Objective Optimisation Problems. In W. Banzhaf and et al., editors, *Proceedings of the Genetic and Evolutionary Computation Conference*, volume 1, pages 894–901. Morgan Kaufmann, 1999.

[143] R.T. Marler and J.S. Arora. Survey of Multi-Objective Optimisation Methods for Engineering. *Structural and Multidisciplinary Optimisation*, 26:369–395, 2004.

[144] N. Mazhar. Energy Efficient Security in MANETs: A Comparison of Cryptographic and Artificial Immune Systems. *Pakistan Journal of Engineering and Applied Sciences*, 7:71–94, 2010.

[145] N. Mazhar and M. Farooq. A Sense of Danger: Dendritic Cells Inspired Artificial Immune System for Manet Security. In *Proceedings of the 10th Annual Conference on Genetic and Evolutionary Computation*, pages 63–70, 2008.

[146] M. Middendorf, F. Reichle, and H. Schmeck. Information Exhange in Multi Colony Ant Algorithms. In *Proceedings of IPDPS Workshops Future Generation Computer Systems*, pages 645–652, 2000.

[147] K.M. Miettinen. *Nonlinear Multi-objective Optimisation*. Kluwer Academic Publishers, Boston, Massachusetts, 1998.

[148] A. M. Mora, J.J.M. Guervós, P.A.C. Valdivieso, J.J.J. Laredo, and C. Cotta. Influence of Parameters on the Performance of a MOACO Algorithm for Solving the Bi-criteria Military Path-finding Problem. In *IEEE Congress on Evolutionary Computation*, pages 3507–3514. IEEE Press, 2008.

[149] R. Morrison. Performance Measurement in Dynamic Environments. In J. Branke, editor, *GECCO Workshop on Evolutionary Algorithms for Dynamic Optimisation*, pages 5–8, 2003.

[150] R.W. Morrison and K.A. De Jong. Measurement of Population Diversity. In *Artificial Evolution: Selected Papers of the 5th International Conference on Artificial Evolution*, pages 31–41. Springer-Verlag, 2002.

[151] N. R. Nielsen. The Allocation of Computing Resources Is Pricing the Answer? *Communications of the ACM*, 13(8):467–474, 1970.

[152] H. Osman and J.P. Kelly. *Meta-Heuristics: Theory and Applications.* Kluwer Academic Publishers, Norwell, Massachusetts, 1996.

[153] C. Papadimitriou and S. Vempala. On the Approximability of the Traveling Salesman Problem. In *Proceedings of the 32nd Annual ACM Symposium on Theory of Computing*, pages 126–133, 2000.

[154] C.H. Papadimitriou. *Computational Complexity.* Addison-Wesley, 1994.

[155] V. Pareto. *Cours D' Economie Politique, Volume I and II.* F. Rouge, Lausanne, 1896.

[156] V. Park and M. Corson. A Highly Adaptive Distributed Routing Algorithm for Mobile Wireless Networks. In *Proceedings of the IEEE Conference on Computer Communications*, pages 1405–1413, 1997.

[157] V. Park and M. Corson. Temporally-ordered Routing Algorithm (TORA): Version 1 Functional Specification. Internet-draft. *IETF*, July 2001.

[158] K. E. Parsopoulos, T. Bartz, and M. N. Vrahatis. Particle Swarm Optimizers For Pareto Optimization With Enhanced Archiving Techniques. In *Proceedings of the IEEE Congress on Evolutionary Computation*, pages 1780–1787, 2003.

[159] J.M. Pasteels, J.L. Deneubourg, and S. Goss. Self-Organization Mechanisms in Ant Societies (I): Trail Recruitment to Newly Discovered Food Sources. *Experientia Suppl., Journal of Insect Behavior*, 76:579–581, 1989.

[160] C. E. Perkins and P. Bhagwat. Highly Dynamic Destination-Sequenced Distance-Vector Routing (DSDV) for Mobile Computers. In *Proceedings of ACM SIGCOMM 94 Conference on Communications Architectures, Protocols and Applications*, pages 234–244. ACM Press, 1994.

[161] D. Pinto and B. Barán. Solving Multi-objective Multicast Routing Problem with a new Ant Colony Optimisation Approach. In *Proceeding of IFIP/ACM Latin-American Networking Conference*, pages 11–19, 2005.

[162] N. Pogkas, G.E. Karastergios, C.P. Antonopoulos, S. Koubias, and G. Papadopoulos. Architecture Design and Implementation of an Ad Hoc Network for Disaster Relief Operations. *Industrial Informatics, IEEE Transactions*, 3:63–72, 2007.

[163] D. Pong and T. Moors. The Impact of Random Waypoint Mobility on Infrastructure Wireless Networks. *International Journal of Wireless Information Networks*, 13:99–114, 2006.

[164] G.J. Pottie and W.J. Kaiser. Wireless Integrated Network Sensors. *Communications of the ACM*, 43(5):51–58, 2000.

[165] Q. Li and J. Aslam and D. Rus. Online Power-aware Routing in Wireless Ad-hoc Networks. In *Proceedings of MOBICOM*, pages 97–107, 2001.

[166] V. Raghunathan, C. Schurgers, S. Park, and M.B. Srivastava. Energy-aware Wireless Microsensor Networks. In *Proceedings of IEEE Signal Processing Magazine*, volume 19, pages 40–50, 2002.

[167] M.M. Raghuwanshi and O.G. Kakde. Survey on Multi-Objective Evolutionary and Real Coded Genetic Algorithms. In *Proceedings of the 8-th Asia Pacific Symposium on Intelligent and Evolutionary Systems*, pages 150–161, 2004.

[168] J. Raju and J.J. Garcia-Luna-Aceves. A Comparison of On-Demand and Table Driven Routing for Ad-Hoc Wireless Networks. In *IEEE International Conference on Communications*, pages 1702–1706, 2000.

[169] V. Ramos, C. Fernandes, and A.C. Rosa. Societal Memory and his Speed on Tracking Extrema over Dynamic Environments using Self-Regulatory Swarms. In *Proceedings of NISIS-05, 1st European Symposium on Nature Inspired Smart Information Systems*, 2005.

[170] T. Rappaport. *Wireless Communications: Principles and Practices*. Prentice Hall, 1996.

[171] T. Ray and K.M. Liew. A Swarm Metaphor For Multiobjective Design Optimization. *Engineering Optimization*, 34(2):141–153, 2002.

[172] D.J. Rosenkrantz, R.E. Stearns, and P.M. Lewis. An Analysis of Several Heuristics for the Traveling Salesman Problem. *SIAM Journal on Computing*, 6:563–581, 1977.

[173] E.M. Royer and C. Toh. A Review of Current Routing Protocols for Ad Hoc Mobile Wireless Networks. *IEEE Personal Communications*, pages 46–55, April 1999.

[174] M. I. M. Saad and Z. A. Zukarnain. Performance Analysis of Random-Based Mobility Models in MANET Routing Protocols. *European Journal of Scientific Research*, 32(4):444–454, 2009.

[175] S. Sahni. *Data Structures, Algorithms, and Applications in Java, 2nd Edition.* Silicon Press, NJ, 2005.

[176] S. Sarafijanovic and J. Y. Le Boudec. An Artificial Immune System Approach With Secondary Response for Misbehavior Detection in Mobile Ad Hoc Networks. *IEEE Transactions on Neural Networks*, 16(5):1076 – 1087, 2005.

[177] M. Schaerer and B. Barán. A Multi-Objective Ant Colony System For Vehicle Routing Problem With Time Windows. In *Proceedings of IASTED International Conference on Applied Informatics*, pages 97–102, 2003.

[178] R. Schoonderwoerd, O. Holland, and J. Bruten. Ant-Like Agents for Load Balancing in Telecommunications Networks. In *Proceedings of the First International Conference on Autonomous Agents*, pages 209–216. ACM Press, 1997.

[179] J.R. Schott. Fault Tolerant Design Using Single and Multicriteria Genetic Algorithm Optimisation. Master's thesis, Department of Aeronautics and Astronautics, Massachusetts Institute of Technology, Cambridge, Massachusetts, 1995.

[180] S. Sethi and S. K. Udgata. The Efficient Ant Routing Protocol for MANET. *International Journal on Computer Science and Engineering*, 2(7):2414–2420, 2010.

[181] R. C. Shah and J. Rabaey. Energy Aware Routing for Low Energy Ad Hoc Sensor Networks. In *Proceedings of IEEE Wireless Communications and Networking Conference*, pages 350–355, 2002.

[182] G. S. Sharvani, N. K. Cauvery, and T. Rangaswamy. Adaptive Routing Algorithm For MANET: Termite. *International Journal of Next-Generation Networks*, 1(1):38–43, 2009.

[183] S.T. Sheu, J. Chen, H.W. Tseng, and H.T. Chiang. A Safe Multiple Access-Rates Transmission (SMART) Scheme for IEEE 802.11 Wireless Networks. In *Proceedings of International Conference on Advanced Information Networking and Applications*, pages 172–175, 2003.

[184] S. Singh, C. Raghavendra, and J. Stepanek. Power-aware Broadcasting in Mobile Ad Hoc Networks. In *Proceedings of IEEE PIMRC*, 1999.

[185] S. Singh and C.S. Raghavendra. PAMAS – Power-Aware Multi-access Protocol with Signaling for Ad Hoc Networks. *ACM SIGCOMM Computer Communications Review*, 28(3):5–26, 1998.

[186] S. Singh, M. Woo, and C. Raghavendra. Power-Aware Routing in Mobile Ad Hoc Networks. In *Proceedings of International Conference on Mobile Computing and Networking*, pages 181–190, 1998.

[187] K. Sohrabi, J. Gao, V. Ailawadhi, and G.J. Pottie. Protocols for Self-organization of a Wireless Sensor Network. In *Proceedings of IEEE Personal Communications Magazine*, volume 7, pages 16–27, 2000.

[188] N. Srinivas and K. Deb. Multi-objective Optimisation using Non-dominated Sorting in Genetic Algorithms. *Evolutionary Computation*, 2(3):221–248, 1994.

[189] M. Stemm and R. H. Katz. Measuring and Reducing Energy Consumption of Network Interfaces in Hand-held Devices. *IEICE Transactions on Communications, Special Issue on Mobile Computing*, 80(8):1125–1131, 1997.

[190] E.H. Stergaard. Efficient Distributed Hormone Graph Gradients. *International Joint Conference on Artificial Intelligence*, pages 1489–1494, 2005.

[191] I. Stojmenovic and X. Lin. Power-aware Localized Routing in Wireless Networks. *IEEE Transactions on Parallel and Distributed Systems*, 12(11):1122–1133, 2001.

[192] T. Stützle. Iterated Local Search for the Flow Shop Problem. *Submitted to European Journal of Operational Research*, 1999.

[193] T. Stützle. *Local Search Algorithms for Combinatorial Problems–Analysis, Improvements, and New Applications*. PhD thesis, Darmstadt University of Technology, 1999.

[194] T. Stützle and H. Hoos. The MAX-MIN Ant System and Local Search for the Traveling Salesman Problem. In *Proceedings of the IEEE International Conference on Evolutionary Computation*, pages 309–314, 1997.

[195] T. Stützle and H. Hoos. MAX-MIN Ant System. *Future Generation Computer Systems*, 16(8):889–914, 2000.

[196] D. Subramanian, P. Druschel, and J. Chen. Ants and Reinforcement Learning: A Case Study in Routing in Dynamic Networks. In *Proceedings of International Joint Conference in Artificial Intelligence*, pages 832–838, 1997.

[197] R. Szewczyk, A. Mainwaring, J. Polastre, J. Anderson, and D. Culler. An Analysis of a Large Scale Habitat Monitoring Application. In *Proceedings of ACM SenSys*, pages 214–226, 2004.

[198] E.D. Taillard. FANT: Fast Ant System. Technical report, IDSIA, Lugano, Switzerland, 1998.

[199] E.D. Taillard and L.M. Gambardella. Adaptive Memories for the Quadratic Assignment Problem. Technical report, IDSIA, Lugano, Switzerland, 1997.

[200] H.O. Tan and I. Korpeoglu. Power Efficient Data Gathering and Aggregation in Wireless Sensor Networks. *SIGMOD Record*, 32(7):66–71, 2003.

[201] M.J. Taylor, R.C. Epper, and T. Tolman. State and Local Law Enforcement Wireless Communications and Interoperability: A Quantitative Analysis. *NCJ 168961*, 1998.

[202] V. Tiwari, S. Malik, and A. Wolfe. Power Analysis of Embedded Software: A First Step Towards Software Power Minimization. *IEEE Transactions on VLSI Systems*, pages 437–445, 1994.

[203] V. Tiwari, S. Malik, A. Wolfe, and M.T.C. Lee. Instruction Level Power Analysis and Optimisation of Software. *Journal of VLSI Signal Processing*, pages 1–18, 1996.

[204] J. A. Torkestani and M. R. Meybodi. Mobility-Based Multicast Routing Algorithm in Wireless Mobile Ad-Hoc Networks: A Learning Automata Approach. *Journal of Computer Communications*, 33(6):721–735, 2010.

[205] P. Toth and D. Vigo. *The Vehicle Routing Problem, chapter: An Overview of Vehicle Routing Problems*. SIAM, Society for Industrial and Applied Mathematics,Philadelphia, USA, 2000.

[206] T. Tran, B. Scheuermann, and M. Mauve. Detecting the Presence of Nodes in MANETs. In *Proceedings of Challenged Networks*, pages 43–50, 2007.

[207] K. Trojanowski and Z. Michalewicz. Searching for Optima in Non-stationary Environments. In *IEEE Congress on Evolutionary Computation*, pages 1843–1850. IEEE Press, 1999.

[208] D.A. Van Veldhuizen. *Multi-objective Evolutionary Algorithms: Classifications, Analyses, and New Innovations*. PhD thesis, Department of Electrical and Computer Engineering. Air Force Institute of Technology, Wright-Patterson AFB, Ohio, 1999.

[209] M.A.M. Vieira, C.N. Coelho. Jr., D.C. da Silva Jr., and J.M. da Mata. Survey On Wireless Sensor Network Devices. In *Emerging Technologies and Factory Automation. IEEE Conference*, pages 16–19, 2003.

[210] J. Wang, E. Osagie, P. Thulasiraman, and R. K. Thulasiram. HOPNET: A Hybrid Ant Colony Optimization Routing Algorithm for Mobile Ad Hoc Network. *Ad Hoc Networks*, 7:690–705, 2009.

[211] Y. Wang. Study on Energy Conservation in MANET. *Journal of Networks*, 5(6):708–715, 2010.

[212] K. Weicker and N. Weicker. On Evolutionary Strategy Optimization in Dynamic Environments. In *IEEE Congress on Evolutionary Computation*, pages 2039–2046. IEEE Press, 1999.

[213] D.J. White. Epsilon Efficiency. *Journal of Optimisation Theory and Applications*, 49(2):319–337, 1986.

[214] A. Woo and D. Culler. A Transmission Control Scheme for Media Access in Sensor Networks. In *Proceedings of the ACM/IEEE International Conference on Mobile Computing and Networking*, pages 221–235, 2001.

[215] X. Wu, H. R. Sadjadpour, and J. Garcia-Luna-Aceves. Link Lifetime as a Function of Node Mobility in MANETs With Restricted Mobility: Modeling and Applications. In *Modeling and Optimization in Mobile, Ad Hoc and Wireless Networks and Workshops. 5th International Symposium on WiOpt*, pages 1–10, 2007.

[216] X. Wu, H. Xu, H. R. Sadjadpour, and J.J Garcia-Luna-Aceves. Proactive or Reactive Routing: A Unified Analytical Framework in MANETs. In *Proceedings of IEEE Computer Communications and Networks*, pages 649–655, 2008.

[217] S. Xu and T. Saadawi. Does the IEEE 802.11 MAC Protocol Work Well in Multihop Wireless Ad Hoc Networks? *IEEE Communication Magazine*, June 2001.

[218] Q. Yang and S. Ding. Novel Algorithm to Calculate Hypervolume Indicator of Pareto Approximation Set. In *Proceedings of Advanced Intelligent Computing Theories and Applications. With Aspects of Theoretical and Methodological Issues, Third International Conference on Intelligent Computing*, volume 2, pages 235–244. Springer-Verlag, 2007.

[219] S. Yang. TORA, Correctness, Proofs and Model Checking. Master's thesis, Electrical and Computer Engineering Department, University of Maryland, December 2002.

[220] S. Yang and J.S. Baras. TORA, Verification, Proofs and Model Checking. In *Proceedings of WiOpt: Modeling and Optimisation in Mobile, AdHoc and Wireless Networks*, pages 3–5, 2003.

[221] W. Ye, J. Heidemann, and D. Estrin. An Energy-Efficient MAC Protocol for Wireless Sensor Networks. In *Proceedings of IEEE INFOCOM*, pages 1567–1576, 2002.

[222] J. Yen. Finding the k Shortest Loopless Path in a Network. *Management Science*, 17:712–716, 1971.

[223] E. Zitzler. *Evolutionary Algorithms for Multi-objective Optimisation.* PhD thesis, Swiss Federal Institute of Technology, Zurich, Switzerland, 1999.

[224] E. Zitzler, M. Laumanns, and S. Bleuler. A Tutorial on Evolutionary Multiobjective Optimisation. In X. Gandibleux, M. Sevaux, and K. Soerensen, editors, *Metaheuristics for Multi-objective Optimisation, Lecture Notes in Economics and Mathematical Systems*, volume 535, pages 3–38. Springer-Verlag, 2004.

[225] E. Zitzler, M. Laumanns, and L. Thiele. SPEA2: Improving the Strength Pareto Evolutionary Algorithm for Multi-Objective Optimisation. In *Proceedings of Evolutionary Methods for Design, Optimisation, and Control*, pages 19–26, 2002.

[226] E. Zitzler and L. Thiele. Multi-objective Evolutionary Algorithms: A Comparative Case Study and the Strength Pareto Approach. *IEEE Transactions on Evolutionary Computation*, 3(4):257–271, 1999.

[227] E. Zitzler, L. Thiele, and K. Deb. Comparison of Multi-Objective Evolutionary Algorithms:Empirical Results. *Evolutionary Computation*, 8(1):173–195, 2000.

[228] E. Zitzler, L. Thiele, M. Laumanns, C.M. Fonseca, and V.G. da Fonseca. Performance Assessment of Multi-objective Optimisers: An Analysis and Review. *IEEE Transactions on Evolutionary Computation*, 7(2):117–132, 2003.

Appendix A

Definition of Abbreviations

This appendix list abbreviations used in this thesis along with their explanations.

ACK : ACKnowledgement

ACO : Ant Colony Optimisation

ACS : Ant Colony System

ADC : Analogous to Digital Converter

ANSI : American National Standards Institute

AODV : Ad hoc On-demand Distance Vector

AP : Access Point

APC : AP Controller

ARQ : Automatic Repeat reQuest

ARQN : ARQ sequence Number

AS : Ant System

ASCII : American Standard Code for Information Interchange

ASP : Active Server Page

ATIM : Ad Hoc Traffic Indication Message

ATM : Asynchronous Transfer Mode

BSAMM : Boundless Simulation Area Mobility Model

BSC : Base Station Controller

BSS : Basic Service Set

CBR : Constant Bit Rate

CDM : Code Division Multiplexing

CDMA : Code Division Multiple Access

CDPD : Cellular Digital Packet Data

CMM : Column mobility model

CPU : Central Processing Unit

CRC : Cyclic Redundancy Check

CSMA : Carrier Sense Multiple Access

CSMA/CA : CSMA with Collision Avoidance

CSMA/CD : CSMA with Collision Detection

CSMM : City Section Mobility Model

CSP : Constraint Satisfaction Problem

CTS : Clear To Send

CW : Contention Window

DA : Destination Address

DAG : Directed Acyclic Graph

DCF : Distributed Coordination Function

DCS : Digital Cellular System

DNS : Domain Name System

DPSM : Dynamic power saving mechanism

DSDV : Destination Sequence Distance Vector

DSMA : Digital Sense Multiple Access

DSR : Dynamic Source Routing

DTMF : Dual Tone Multiple Frequency

DV : Distance Vector

EA : Evolutionary Algorithms

EC-MAC : Energy Conserving Medium Access Control

ECRMM : Exponential correlated random mobility model

EEMACOMC : Energy efficiency for mobile network using multi-objective ant colony optimisation, Multi-colony

EEMACOMH : Energy Efficiency for mobile network using multi-objective ant colony optimisation, Multi-heuristic

EEMACOMP : Energy Efficiency for mobile network using multi-objective ant colony optimisation, Multi-pheromone

EEMMASMH : Energy efficiency for mobile network using multi-objective MAX-MIN ant system optimisation, Multi-heuristic

EEMMASMP : Energy efficiency for mobile network using multi-objective MAX-MIN ant system optimisation, Multi-pheromone

EMO : Evolutionary Multi-objective Optimisation

ESS : Extended Service Set

FANT : Fast Ant System

FDM : Frequency Division Multiplexing

FDMA : Frequency Division Multiple Access

FEC : Forward Error Correction

FRTS : Future Request to Send

FSM : Frame Synchronisation Message

GMMM : Gauss-Markov Mobility Model

GPRS : General Packet Radio Service

GPS : Global Positioning System

IBSS : Independent Basic Service Set

IEEE : Institute of Electrical and Electronics Engineers

ILS : Iterated Local Search

IP : Internet Protocol

ISDN : Integrated Services Digital Network

ISO : International Organization for Standardization

LLC : Logical Link Control

MAC : Medium Access Control

MACA : Multiple Access with Collision Avoidance

MANET : Mobile Ad hoc NETwork

Mbps: Megabit per second

MMAS : Max-Min Ant System

MNC : Maximum Node Cost

MOACO : Multi-Objective Ant Colony Optimisation

MOEA : Multi-Objective Evolutionary Algorithms

MOGA: Multi-Objective Genetic Algorithm

MOO : Multi-Objective Optimisation

MOP : Multi-Objective Problem

MST : Minimum Spanning Trees

NCMM : Nomadic community mobility model

NPGA : Niched Pareto Genetic Algorithm

NSGA : Non-dominated Sorting Genetic Algorithm

OSI: Open Systems Interconnection

PAES : Pareto Archived Evolution Strategy

PAMAS : Power Aware Multi-Access Protocol

PCF : Point Coordination Function

PDN : Public Data Network

PDU : Protocol Data Unit

PEDAP : Power Efficient Data Gathering and Aggregation Protocol

PEDAP-PA : Power Efficient Data Gathering and Aggregation Protocol-Power Aware

PESA : Pareto Envelope-based Selection Algorithm

PESA-II : Pareto Envelope-based Selection Algorithm-II

PMM : Pursue mobility model

PSM : Protocol/Service Multiplexor

PSN : PDU Sequence Number

PSPDN : Public Switched Packet Data Network

PSTN : Public Switched Telephone Network

PVRWMM : A Probabilistic Version of the Random Walk Mobility Model

QAP : Quadratic Assignment Problem

RDMM: Random direction mobility model

RF : Radio Frequency

RPGM : Reference Point Group Mobility Model

RT : Radio Transceiver

RTR : Radio Transmission and Reception

RTS : Request To Send

RWMM :Random walk mobility model

RWPMM : Random waypoint mobility model

SA : Simulated Annealing

S-MAC : Sensors Medium Access Control

SMTTP : Single Machine Total Tardiness Problem

SPEA : Strength Pareto Evolutionary Algorithm

SPI: Serial Peripheral Interface

TBTT : Target Beacon Transmission Time

TCP : Transmission Control Protocol

TD-CDMA : Time Division-CDMA

TDD : Time Division Duplex

TDM : Time Division Multiplexing

TDMA : Time Division Multiple Access

T-MAC : Timeout Medium Access Control

TNP : Time to Network Partition

TS : Tabu search

TSP : Travelling Salesman Problem

UART : Universal Asynchronous Receiver Transmitter

UBR : Unspecified Bit Rate

UDP : User Datagram Protocol

VBR : Variable Bit Rate

VF : Variation Factor

VRS : Volcano Routing Scheme

WS : Wireless Sensor

WSN : Wireless Sensor Network

Appendix B

Definition of Symbols

This appendix list symbols used in this thesis along with their explanations.

Chapter 2: Energy Efficient Network Protocols for Mobile Ad-Hoc Networks

α_{max} : maximum angular change

$\mathbf{a}_{max}$: maximum acceleration

c_a : media dependent constant

c_p : clock period

$C_s(T_s)$: total edge weights in the spanning tree T_s

$c_{s,uw}$: weight of the edge (u, w)

d : distance travelled

d_s : maximum propagation delay among all pairs of nodes

d_{uw} : distance between node u and w

D_f : destination of the f-flow

e^r_{min} : minimum residual energy from all the nodes in a path

e^c_u : current energy of node u

e^m_u : energy needed by node u to transmit a message to its nearest neighbor

e^r_u : residual energy of node u

E : energy consumed by a program

E_u : initial energy of node u

E_{uw} : energy required to do a single-hop transmission from node u to node w

θ : the MN's direction

θx_t : random direction variable

$\bar{\theta}$: mean direction

$\Delta\theta$: change in direction

$G = (V, L)$: directed graph with nodes V and links between nodes, L

h_d : constant between 2 and 4

I_c : average current

$\kappa(u)$: fraction of node's u initial energy that has been used so far

N_c : number of clock cycles taken by a program

p_t : tuning parameter

$P(a, b)$: probability that a MN will go from state a to state b

P_u^f : potential associated with flow f at a given node u

P_o : average power

r_x : random offset of a MN, in direction x

r_y : random offset of a MN, in direction y

σ : constant for admission control

S_r : sending rate

t : time interval

$t_x^g(t)$: x position of a target

$t_y^g(t)$: y position of a target

Δt : time step

T_e : execution time of the program

T_s : spanning tree

$\mathbf{v}$: the MN's velocity

$\Delta\mathbf{v}$: change in velocity

v_s : supply voltage

v_{x_t} : random speed variable

$\bar{v}$: mean speed value

$\mathbf{v}_{max}$: maximum velocity

$\mathbf{x}_{j,i}(t)$: location of the i-th node in the j-th group at time t

$\mathbf{y}_{j,i}(t)$: reference location of the i-th node in the j-th group at time t

$\mathbf{z}_{j,i}(t)$: local displacement of the i-th node in the j-th group at time t

ζ : constant

Chapter 3: Combinatorial Optimisation and Ant Colony Optimisation Meta-heuristic

α: pheromone amplification coefficient

β: heuristic amplification coefficient

$f(x^k(t))$: lenght of the solution $x^k(t)$

h : bias to using pheromone deposits in the decision process

η_{ij} : heuristic preference of moving from node i to node j

n_k : number of ants

n_l : number of nodes in the candidate list

N_G : number of nodes

$N(\mathbf{x})$: neighbourhood of $\mathbf{x}$

$N_i^k(t)$: set of feasible nodes connected to node i, for ant k

L_m : number of ants that have used the lower branch

$p_{ij}^k(t)$: probability that ant k selects to move to node j from node i

$\hat{p}$: probability at which the best solution is constructed

$P_L(m)$: probability with which the $(m+1)$-th ant chooses the lower branch

$P_U(m)$: probability with which the $(m+1)$-th ant chooses the upper branch

Q : positive constant used to weight influence of f in solution quality calculation

r : random number

r_0 : tunable parameter to control exploration and exploitation

ρ : evaporation coefficient

ρ_l : evaporation coefficient governing local trail decay

$\Delta_{ij}(t)$: total amount of pheromone deposited by all ants on edge (i, j)

τ_0 : small positive constant

τ_{ij} : pheromone concentration on link (i, j)

τ_{min} : minimum allowed pheromone concentration

τ_{max} : maximum allowed pheromone concentration

U_m : number of ants that have used the upper branch

$x^k(t)$: solution found by ant k at time step t

$x^+(t)$: best tour since the beginning of the trial

$\tilde{x}(t)$: iteration-best solution found at time step t

$\hat{x}(t)$: global-best solution found at time step t

z : degree of attraction of an unexplored branch

Chapter 4: Multi-objective Optimisation

$\mathbf{x} \prec \mathbf{y}$: $\mathbf{x}$ strictly dominates $\mathbf{y}$

$\prec_n$: crowded comparison operator

$\#Col$: number of ant colonies

$\#\tau$: number of pheromone structures

B_i : compensation at busbar i

$c_c(i,j)$: changeover costs that has to be paid when j is the direct successor of i in a schedule.

c_{ij} : cost per bps of link (i,j)

C_j : completion time of job j in the current job sequence

c_m : centroid for objective f_m

d_i : Euclidian distance between i and nearest solution in the $P\mathcal{F}^*$

d_{ij} : propagation delay of link (i,j)

d_j^a : due date for job j

$\bar{d}$: mean of all d_i

ϵ : constant

f_d : density function

$\mathcal{F}$: feasible space

F_s : scalar function

$F_v(i)$: fitness value of i

g_m : inequality constraints

h_m : equality constraints

$i_{distance}$: crowding distance of solution i

i_{rank} : non-domination front rank of solution i

$\mathcal{I}$: non-dominated set

K : kernel function

λ_l : weighs the relative importance of the l-th objective

m_{best} : number of best ants in a colony

n_k : number of ants

n_o : number of objectives

n_x : dimension of the decision vector

$n_{\mathcal{PF}}$: number of solutions in the estimated Pareto front

N : number of vectors in the set of non-dominated solutions

N_G : number of nodes

N_{maxgen} : maximum number of generations

N_p : population size

$\mathcal{O}$: objective space

p_j : processing time for job j

P_0 : initial random population

P_s : Pareto set list for MOO power-aware problem

P^* : Pareto-optimal set, containing non-dominated position vectors

$P\mathcal{F}^*$: Pareto-optimal front containing non-dominated objective vectors

Q_0 : initial child population

R_t : combined population of parent and a child, at generation t

S : n_x dimensional search space

S_m : spread metric

$S_v(i)$: strenght value of i

t_{ij} : current traffic of link (i, j)

t_i^g : ideal value of objective i

$\mathbf{T}_k$: solution build by ant k

$T(s, N_r)$: multicast tree with source in s and a set of destinations N_r

V_i : actual voltage at busbar i

V_i^* : desired voltage at busbar i

x_{mj} : value of the objective f_m in the j-th non-dominated solution

$\mathbf{x}^*$: Pareto-optimal solution

$\mathcal{Z} = (\mathcal{Z}_1, \mathcal{Z}_2, ...)$: set of non-dominated fronts

Chapter 5: Dynamic Optimisation

γ_i : pheromone reset value for node i

d_{ij}^{η} : distance of node i to the nearest changed component j based on heuristic information

d_{ij}^{τ} : distance of node i to the nearest changed component j based on pheromone information

$\delta(t)$: time-dependent objective function

$L^{best}(t)$: best solution found up to iteration t

$L_W^{best}(t)$: best solution within the window W

$L_W^{worst}(t)$: worst solution within the window W

λ_E : strategy specific parameter

λ_R : strategy specific parameter

λ_τ : strategy specific parameter

n_c : number of changes of the fitness landscape during the run

n_I : number of iterations between environment changes

n_{PF} : number of solutions

n_r : number of runs

$\mathbf{x}^*(\mathbf{t})$: Pareto-optimal solution at time step t

Chapter 6: Multi-objective Optimisation Algorithms for Power-Aware Routing Metrics

c_{ij} : link cost for link (i, j)

$c^a(i, j)$: capacity of the edge (i, j)

γ_{ν_i} : variable proportionate to the nearest changed component j for objective EP

γ_{ξ_i} : variable proportionate to the nearest changed component j for objective TNP

γ_{π_i} : variable proportionate to the nearest changed component j for objective VF

γ_{ρ_i} : variable proportionate to the nearest changed component j for objective CP

γ_{ς_i} : variable proportionate to the nearest changed component j for objective MNC

$C_{n_i}(t)$: ratio of the total energy consumed up to time, t, over the initial energy, E_i

$e_i^e(t)$: total energy expended by node i so far

λ_ν : user-defined parameter which establish the importance of the objective EP in the search

λ_ξ : user-defined parameter which establish the importance of the objective TNP in the search

λ_π : user-defined parameter which establish the importance of the objective VF in the search

λ_ρ : user-defined parameter which establish the importance of the objective CP in the search

λ_ς : user-defined parameter which establish the importance of the objective MNC in the search

μ_L : average capacity for all edges L

n_{k_c} : number of ants for c colony

N_e : constant, the first N_e fittest individuals from population P_{t+1}

n_{ts} : number of time slices within the total simulation time

n_T : number of nodes in the solution T

n_{pT} : total number of packets from source s to destination D

$\eta_\nu(ij)$: heuristic desirability of the move from node i to node j associated with objective EP

$\eta_\xi(ij)$: heuristic desirability of the move from node i to node j associated with objective TNP

$\eta_\pi(ij)$: heuristic desirability of the move from node i to node j associated with objective VF

$\eta_\rho(ij)$: heuristic desirability of the move from node i to node j associated with objective CP

$\eta_\varsigma(ij)$: heuristic desirability of the move from node i to node j associated with objective MNC

P_{as} : maximum archive size

P_f : estimated Pareto set

P_G : global archive containing solutions from all the colonies in a specific iteration

R_g : radius from global centre

R : number of shortest path routes

R_i^p : residual power of a node i

$S_{T_{tot}}$: total simulation time

T_{N_p} : routing table with N_p paths

T_r : transmission range

T_{sm} : pause time/time before applying the mobility model

τ_{max_ν} : maximum allowed pheromone value for objective EP

τ_{max_ξ} : maximum allowed pheromone value for objective TNP

τ_{max_π} : maximum allowed pheromone value for objective VF

τ_{max_ρ} : maximum allowed pheromone value for objective CP

τ_{max_ς} : maximum allowed pheromone value for objective MNC

τ_{min_ν} : minimum allowed pheromone value for objective EP

τ_{min_ξ} : minimum allowed pheromone value for objective TNP

τ_{min_π} : minimum allowed pheromone value for objective VF

τ_{min_ρ} : minimum allowed pheromone value for objective CP

τ_{min_ς} : minimum allowed pheromone value for objective MNC

Chapter 7: Simulation and Empirical Analysis

P_a : approximation of the true Pareto front

$\bar{n}_{alg}$: average number of non-dominated solutions found by each algorithm

$\bar{\varrho}$: average value of the spacing metric

$\bar{\xi}$: average value of the hypervolume metric

n_{alg}^w : number of times that an algorithm has a better $\bar{n}_{alg}$ than the others, for each environment change

ϱ^w : number of times that an algorithm has a better $\bar{\varrho}$ than the others, for each environment change

ξ^w : number of times that an algorithm has a better $\bar{\xi}$ than the others, for each environment change

Appendix C

Definition of the Power-Aware Routing Problem

This appendix list symbols used in this thesis to formulate the multi-objective optimisation problem for power-aware routing metrics

$$
\begin{aligned}
V &: \textit{Set of nodes} \\
L &: \textit{Set of links} \\
G = (V, L) &: \textit{Directed graph} \\
(i, j) \in L &: \textit{Link from node } i \textit{ to node } j;\ i, j \in V. \\
E_{ij} &: \textit{The energy expenditure for unit flow transmission over the link } (i, j) \\
E_i &: \textit{Initial energy at the transmitting node } i \\
R_i &: \textit{Residual energy at the transmitting node } i \\
R_i^p &: \textit{Residual power of a node } i. \\
x_1, x_2, x_3 &: \textit{nonnegative weighting factors} \\
c_{ij} &: \textit{link cost for link } i, j \\
c_{ij} \textit{ is given by} &: c_{ij} = E_{ij}^{x1} E_i^{x2} R_i^{-x3} \\
d_{ij} &: \textit{Distance between the nodes } i \textit{ and } j \\
c_i &: \textit{cost of node } i,\ c_i = \frac{1}{R_i} \\
c^a(ij) &: \textit{Capacity of link } (i, j) \\
n_{pT} &: \textit{Number of packets for a request} \\
n_k &: \textit{Number of ants} \\
l_u &: \textit{Load of node } u \\
e_u^c &: \textit{Current energy of node } u
\end{aligned}
$$

n_T : *Number of nodes for path* T

$T(s, D)$: *path from source* s *to destination* $D = (n_1, n_2, ..., n_{n_T})$ *with* $s = n_1$ *and* $D = n_{n_T}$

T_r : *Transmission range*

z_i : *denotes the measured voltage (that gives a good indication of the energy used thus far)*

$0 < g(z_i) \leq 1.0$: *is the normalised remaining lifetime (or capacity) of the battery*

Appendix D

Control Parameter Tables

This appendix contains the results of the empirical analysis of the ant-based algorithms control parameters. The empirical analysis is done for all scenario combinations of 30 nodes, $T_{sm} \in \{1, 2, 3, 4, 5, 6\}$, and $R_g \in \{300, 500, 800\}$.
Tables D.1-D.3, D.4-D.6, D.7-D.9, D.10-D.12, D.13-D.15, and D.16-D.18 illustrate the influence of parameters β_ψ, r_0, ρ_l, ρ_g, α, and λ_E respectively, on the $\bar{n}_{alg}$, $\bar{\varrho}$ and $\bar{\xi}$ metrics.

Table D.1: Influence of parameter β_ψ on the $\bar{n}_{alg}$, $\bar{\varrho}$ and $\bar{\xi}$ metrics, for 30 nodes and $R_g = 300$

(a) $T_{sm} = 1$

β_ψ	$\mathcal{PF}$	$\bar{n}_{alg}$	$\bar{\varrho}$	$\bar{\xi}$
$\beta_\nu = 1.0$	$P_{EEMACOMP}$	50.38±5.89	0.213±0.024	45342.56±952.36
$\beta_\xi = 1.0$	$P_{EEMACOMH}$	48.21±5.22	0.221±0.027	44567.23±961.78
$\beta_\pi = 1.0$	$P_{EEMMASMP}$	53.41±5.14	0.218±0.029	44128.45±927.47
$\beta_\varrho = 1.0$	$P_{EEMMASMH}$	48.36±5.33	0.215±0.027	43567.38±966.96
$\beta_\varsigma = 1.0$	$P_{EEMACOMC}$	51.34±5.26	0.238±0.029	44528.09±975.72
$\beta_\nu = 3.0$	$P_{EEMACOMP}$	50.34±5.35	0.187±0.023	46873.32±946.23
$\beta_\xi = 3.0$	$P_{EEMACOMH}$	48.43±5.65	0.192±0.022	45568.27±957.32
$\beta_\pi = 3.0$	$P_{EEMMASMP}$	49.37±5.57	0.211±0.023	46785.32±953.23
$\beta_\varrho = 3.0$	$P_{EEMMASMH}$	48.54±5.45	0.186±0.024	47467.28±964.32
$\beta_\varsigma = 3.0$	$P_{EEMACOMC}$	51.37±5.63	0.188±0.021	47843.31±976.38
$\beta_\nu = 3.5$	$P_{EEMACOMP}$	84.67±4.49	0.053±0.008	62874.32±213.34
$\beta_\xi = 4.0$	$P_{EEMACOMH}$	82.35±4.46	0.054±0.008	62543.64±221.43
$\beta_\pi = 4.5$	$P_{EEMMASMP}$	79.65±4.74	0.057±0.009	62647.23±226.31
$\beta_\varrho = 4.0$	$P_{EEMMASMH}$	83.86±4.73	0.058±0.010	62568.22±236.74
$\beta_\varsigma = 5.0$	$P_{EEMACOMC}$	85.74±4.76	0.057±0.010	62657.82±223.52
$\beta_\nu = 4.5$	$P_{EEMACOMP}$	84.37±4.32	0.054±0.009	62676.43±202.41
$\beta_\xi = 5.0$	$P_{EEMACOMH}$	82.54±4.34	0.053±0.008	62217.32±213.52
$\beta_\pi = 3.5$	$P_{EEMMASMP}$	78.42±4.69	0.055±0.009	62542.43±203.43
$\beta_\varrho = 4.0$	$P_{EEMMASMH}$	82.64±4.54	0.057±0.009	62653.61±192.53
$\beta_\varsigma = 4.0$	$P_{EEMACOMC}$	84.67±4.63	0.056±0.009	62562.31±223.43
$\beta_\nu = 5.0$	$P_{EEMACOMP}$	83.76±4.46	0.052±0.008	62314.32±197.32
$\beta_\xi = 5.0$	$P_{EEMACOMH}$	79.32±4.56	0.050±0.008	62435.21±214.65
$\beta_\pi = 5.0$	$P_{EEMMASMP}$	76.32±4.89	0.051±0.009	62421.56±198.37
$\beta_\varrho = 5.0$	$P_{EEMMASMH}$	79.56±4.67	0.049±0.008	62652.27±187.43
$\beta_\varsigma = 5.0$	$P_{EEMACOMC}$	83.58±4.78	0.057±0.009	62467.48±215.76
$\beta_\nu = 7.0$	$P_{EEMACOMP}$	67.43±4.67	0.047±0.007	44673.36±934.24
$\beta_\xi = 7.0$	$P_{EEMACOMH}$	72.48±4.98	0.049±0.007	43456.22±956.76
$\beta_\pi = 7.0$	$P_{EEMMASMP}$	66.48±4.78	0.049±0.006	43467.83±946.32
$\beta_\varrho = 7.0$	$P_{EEMMASMH}$	72.74±4.54	0.047±0.006	44612.38±975.32
$\beta_\varsigma = 7.0$	$P_{EEMACOMC}$	72.45±4.47	0.055±0.007	44132.64±896.34

(b) $T_{sm} = 2$

β_ψ	$\mathcal{PF}$	$\bar{n}_{alg}$	$\bar{\varrho}$	$\bar{\xi}$
$\beta_\nu = 1.0$	$P_{EEMACOMP}$	54.67±5.13	0.186±0.022	47832.26±612.52
$\beta_\xi = 1.0$	$P_{EEMACOMH}$	47.32±5.32	0.176±0.022	46348.69±864.23
$\beta_\pi = 1.0$	$P_{EEMMASMP}$	54.76±5.21	0.195±0.024	46178.35±874.72
$\beta_\varrho = 1.0$	$P_{EEMMASMH}$	52.57±5.24	0.180±0.023	45674.86±849.78
$\beta_\varsigma = 1.0$	$P_{EEMACOMC}$	54.44±5.13	0.178±0.022	46234.12±875.92
$\beta_\nu = 3.0$	$P_{EEMACOMP}$	52.54±5.42	0.144±0.019	48765.24±896.38
$\beta_\xi = 3.0$	$P_{EEMACOMH}$	54.45±5.36	0.148±0.018	47654.34±876.36
$\beta_\pi = 3.0$	$P_{EEMMASMP}$	52.67±5.41	0.154±0.017	47654.38±887.56
$\beta_\varrho = 3.0$	$P_{EEMMASMH}$	56.21±5.32	0.158±0.016	48756.34±895.45
$\beta_\varsigma = 3.0$	$P_{EEMACOMC}$	57.24±5.12	0.153±0.017	48765.43±850.39
$\beta_\nu = 3.5$	$P_{EEMACOMP}$	87.32±3.68	0.039±0.007	62976.32±224.32
$\beta_\xi = 4.0$	$P_{EEMACOMH}$	85.21±3.68	0.042±0.007	62158.94±234.44
$\beta_\pi = 4.5$	$P_{EEMMASMP}$	82.43±3.59	0.040±0.007	62143.32±229.26
$\beta_\varrho = 4.0$	$P_{EEMMASMH}$	86.43±3.57	0.041±0.006	62234.65±242.76
$\beta_\varsigma = 5.0$	$P_{EEMACOMC}$	88.56±3.67	0.046±0.007	62214.32±226.83
$\beta_\nu = 4.5$	$P_{EEMACOMP}$	86.72±3.58	0.041±0.007	62645.76±223.24
$\beta_\xi = 5.0$	$P_{EEMACOMH}$	85.64±3.56	0.043±0.006	62228.56±217.57
$\beta_\pi = 3.5$	$P_{EEMMASMP}$	82.56±3.29	0.041±0.006	62147.89±212.28
$\beta_\varrho = 4.0$	$P_{EEMMASMH}$	86.32±3.67	0.042±0.007	62145.65±198.47
$\beta_\varsigma = 4.0$	$P_{EEMACOMC}$	85.21±3.76	0.043±0.008	62346.76±216.19
$\beta_\nu = 5.0$	$P_{EEMACOMP}$	86.73±3.24	0.038±0.006	62734.66±226.68
$\beta_\xi = 5.0$	$P_{EEMACOMH}$	85.43±3.78	0.042±0.007	62134.67±232.93
$\beta_\pi = 5.0$	$P_{EEMMASMP}$	78.43±4.14	0.042±0.008	62221.58±215.28
$\beta_\varrho = 5.0$	$P_{EEMMASMH}$	82.34±3.76	0.043±0.007	62352.25±197.47
$\beta_\varsigma = 5.0$	$P_{EEMACOMC}$	76.43±4.43	0.041±0.008	62367.44±232.19
$\beta_\nu = 7.0$	$P_{EEMACOMP}$	74.65±4.34	0.043±0.007	47432.65±938.36
$\beta_\xi = 7.0$	$P_{EEMACOMH}$	75.73±4.75	0.044±0.007	46783.43±949.27
$\beta_\pi = 7.0$	$P_{EEMMASMP}$	72.47±4.76	0.042±0.007	46754.28±938.68
$\beta_\varrho = 7.0$	$P_{EEMMASMH}$	75.83±4.37	0.043±0.006	46672.21±965.23
$\beta_\varsigma = 7.0$	$P_{EEMACOMC}$	74.86±4.25	0.041±0.006	46178.63±845.19

(c) $T_{sm} = 3$

β_ψ	$\mathcal{PF}$	$\bar{n}_{alg}$	$\bar{\varrho}$	$\bar{\xi}$
$\beta_\nu = 1.0$	$P_{EEMACOMP}$	56.78±4.32	0.157±0.015	49436.26±798.43
$\beta_\xi = 1.0$	$P_{EEMACOMH}$	52.23±4.56	0.146±0.015	48654.28±837.43
$\beta_\pi = 1.0$	$P_{EEMMASMP}$	56.32±4.76	0.161±0.017	48654.38±832.69
$\beta_\varrho = 1.0$	$P_{EEMMASMH}$	55.76±4.78	0.157±0.016	48685.36±826.79
$\beta_\varsigma = 1.0$	$P_{EEMACOMC}$	58.92±4.75	0.148±0.016	46678.54±823.56
$\beta_\nu = 3.0$	$P_{EEMACOMP}$	54.65±4.65	0.117±0.013	50343.32±765.34
$\beta_\xi = 3.0$	$P_{EEMACOMH}$	56.87±4.69	0.118±0.013	51345.65±768.45
$\beta_\pi = 3.0$	$P_{EEMMASMP}$	56.73±4.76	0.123±0.013	51346.76±765.38
$\beta_\varrho = 3.0$	$P_{EEMMASMH}$	57.85±4.65	0.126±0.014	51657.34±758.34
$\beta_\varsigma = 3.0$	$P_{EEMACOMC}$	58.34±4.67	0.127±0.014	52348.97±763.10
$\beta_\nu = 3.5$	$P_{EEMACOMP}$	89.45±3.47	0.036±0.006	63234.65±197.45
$\beta_\xi = 4.0$	$P_{EEMACOMH}$	88.12±3.48	0.037±0.007	62108.45±239.65
$\beta_\pi = 4.5$	$P_{EEMMASMP}$	87.32±3.87	0.034±0.005	62430.26±232.68
$\beta_\varrho = 4.0$	$P_{EEMMASMH}$	86.49±3.65	0.038±0.005	62450.32±238.46
$\beta_\varsigma = 5.0$	$P_{EEMACOMC}$	89.43±3.54	0.033±0.005	63346.65±187.58
$\beta_\nu = 4.5$	$P_{EEMACOMP}$	88.32±3.68	0.038±0.006	63245.67±237.54
$\beta_\xi = 5.0$	$P_{EEMACOMH}$	88.83±3.47	0.037±0.006	62128.90±226.78
$\beta_\pi = 3.5$	$P_{EEMMASMP}$	87.32±3.64	0.036±0.006	62234.56±224.67
$\beta_\varrho = 4.0$	$P_{EEMMASMH}$	88.42±3.59	0.037±0.007	62456.53±218.56
$\beta_\varsigma = 4.0$	$P_{EEMACOMC}$	87.43±3.43	0.033±0.006	63241.58±189.54
$\beta_\nu = 5.0$	$P_{EEMACOMP}$	88.65±3.85	0.037±0.005	63245.78±189.47
$\beta_\xi = 5.0$	$P_{EEMACOMH}$	87.32±3.65	0.037±0.006	62234.69±226.78
$\beta_\pi = 5.0$	$P_{EEMMASMP}$	88.34±3.89	0.038±0.007	62347.97±226.48
$\beta_\varrho = 5.0$	$P_{EEMMASMH}$	87.18±3.65	0.037±0.006	62569.35±225.54
$\beta_\varsigma = 5.0$	$P_{EEMACOMC}$	84.70±4.12	0.034±0.007	63257.89±196.37
$\beta_\nu = 7.0$	$P_{EEMACOMP}$	87.54±4.12	0.038±0.006	51679.32±785.43
$\beta_\xi = 7.0$	$P_{EEMACOMH}$	86.43±4.34	0.036±0.006	51125.43±754.23
$\beta_\pi = 7.0$	$P_{EEMMASMP}$	86.23±4.23	0.039±0.006	49765.43±784.53
$\beta_\varrho = 7.0$	$P_{EEMMASMH}$	82.46±4.12	0.037±0.005	48965.38±768.43
$\beta_\varsigma = 7.0$	$P_{EEMACOMC}$	84.78±4.32	0.034±0.005	49875.34±743.36

(d) $T_{sm} = 4$

β_ψ	$\mathcal{PF}$	$\bar{n}_{alg}$	$\bar{\varrho}$	$\bar{\xi}$
$\beta_\nu = 1.0$	$P_{EEMACOMP}$	58.54±4.32	0.136±0.014	52134.14±727.58
$\beta_\xi = 1.0$	$P_{EEMACOMH}$	56.32±4.56	0.131±0.014	51235.95±764.36
$\beta_\pi = 1.0$	$P_{EEMMASMP}$	57.73±4.76	0.134±0.015	49875.65±745.49
$\beta_\varrho = 1.0$	$P_{EEMMASMH}$	59.27±4.78	0.136±0.016	48765.86±734.56
$\beta_\varsigma = 1.0$	$P_{EEMACOMC}$	61.85±4.75	0.132±0.015	46678.54±732.45
$\beta_\nu = 3.0$	$P_{EEMACOMP}$	61.87±4.65	0.102±0.013	52785.36±674.53
$\beta_\xi = 3.0$	$P_{EEMACOMH}$	59.34±4.69	0.111±0.013	53456.25±687.32
$\beta_\pi = 3.0$	$P_{EEMMASMP}$	58.43±4.76	0.114±0.012	53456.78±638.56
$\beta_\varrho = 3.0$	$P_{EEMMASMH}$	61.54±4.65	0.112±0.012	54326.53±643.25
$\beta_\varsigma = 3.0$	$P_{EEMACOMC}$	61.68±4.67	0.117±0.012	54367.43±658.54
$\beta_\nu = 3.5$	$P_{EEMACOMP}$	95.47±1.47	0.033±0.005	63156.75±185.38
$\beta_\xi = 4.0$	$P_{EEMACOMH}$	98.35±1.14	0.035±0.006	62136.54±215.76
$\beta_\pi = 4.5$	$P_{EEMMASMP}$	96.84±1.37	0.030±0.004	62342.56±226.57
$\beta_\varrho = 4.0$	$P_{EEMMASMH}$	98.49±1.12	0.030±0.004	62269.09±234.56
$\beta_\varsigma = 5.0$	$P_{EEMACOMC}$	94.79±1.54	0.032±0.005	64356.43±185.43
$\beta_\nu = 4.5$	$P_{EEMACOMP}$	94.47±1.68	0.034±0.005	63096.54±198.65
$\beta_\xi = 5.0$	$P_{EEMACOMH}$	95.37±1.47	0.036±0.006	62132.34±223.73
$\beta_\pi = 3.5$	$P_{EEMMASMP}$	97.86±1.24	0.031±0.005	62326.78±216.74
$\beta_\varrho = 4.0$	$P_{EEMMASMH}$	96.44±1.39	0.032±0.005	62347.84±202.45
$\beta_\varsigma = 4.0$	$P_{EEMACOMC}$	95.34±1.45	0.029±0.004	64217.86±183.24
$\beta_\nu = 5.0$	$P_{EEMACOMP}$	96.74±1.45	0.033±0.005	63246.26±196.43
$\beta_\xi = 5.0$	$P_{EEMACOMH}$	95.45±1.65	0.032±0.006	62028.68±216.98
$\beta_\pi = 5.0$	$P_{EEMMASMP}$	94.24±1.69	0.034±0.006	62369.02±212.38
$\beta_\varrho = 5.0$	$P_{EEMMASMH}$	93.32±1.85	0.033±0.005	62346.32±218.65
$\beta_\varsigma = 5.0$	$P_{EEMACOMC}$	92.34±1.96	0.032±0.005	64341.56±185.73
$\beta_\nu = 7.0$	$P_{EEMACOMP}$	90.45±3.12	0.034±0.006	51467.65±643.67
$\beta_\xi = 7.0$	$P_{EEMACOMH}$	88.90±3.54	0.032±0.005	53457.32±689.02
$\beta_\pi = 7.0$	$P_{EEMMASMP}$	91.78±3.23	0.033±0.005	52368.65±654.32
$\beta_\varrho = 7.0$	$P_{EEMMASMH}$	90.37±3.10	0.034±0.004	50231.68±689.54
$\beta_\varsigma = 7.0$	$P_{EEMACOMC}$	89.45±3.32	0.030±0.004	52355.75±653.45

Table D.1: Influence of parameter β_ψ on the $\bar{n}_{alg}$, $\bar{\varrho}$ and $\bar{\xi}$ metrics, for 30 nodes and $R_g = 300$ (cont.)

(e) $T_{sm} = 5$

β_ψ	$\mathcal{PF}$	$\bar{n}_{alg}$	$\bar{\varrho}$	$\bar{\xi}$
$\beta_\nu = 1.0$	PEEMACOMP	60.34±3.60	0.117±0.011	52879.32±683.45
$\beta_\xi = 1.0$	PEEMACOMH	58.64±3.86	0.126±0.012	51786.43±678.54
$\beta_\pi = 1.0$	PEEMMASMP	58.65±3.86	0.126±0.012	50326.67±635.67
$\beta_\varrho = 1.0$	PEEMMASMH	60.32±3.47	0.133±0.013	50546.43±657.43
$\beta_\varsigma = 1.0$	PEEMACOMC	62.45±3.87	0.128±0.013	49647.54±643.54
$\beta_\nu = 3.0$	PEEMACOMP	63.45±3.58	0.096±0.010	53567.43±654.32
$\beta_\xi = 3.0$	PEEMACOMH	63.48±3.68	0.089±0.009	53345.89±537.89
$\beta_\pi = 3.0$	PEEMMASMP	61.37±3.88	0.094±0.010	54583.24±548.79
$\beta_\varrho = 3.0$	PEEMMASMH	63.68±3.56	0.092±0.011	54789.32±547.87
$\beta_\varsigma = 3.0$	PEEMACOMC	63.87±3.45	0.108±0.012	54786.54±547.86
$\beta_\nu = 3.5$	PEEMACOMP	97.43±1.68	0.028±0.002	63236.43±192.34
$\beta_\xi = 4.0$	PEEMACOMH	98.43±1.34	0.031±0.003	62096.56±217.65
$\beta_\pi = 4.5$	PEEMMASMP	97.65±1.54	0.029±0.003	62247.86±227.86
$\beta_\varrho = 4.0$	PEEMMASMH	98.78±1.76	0.029±0.003	62436.78±226.78
$\beta_\varsigma = 5.0$	PEEMACOMC	96.78±1.67	0.028±0.002	64786.54±176.54
$\beta_\nu = 4.5$	PEEMACOMP	97.65±1.74	0.027±0.002	63245.67±183.42
$\beta_\xi = 5.0$	PEEMACOMH	96.54±1.54	0.031±0.003	62158.65±216.54
$\beta_\pi = 3.5$	PEEMMASMP	96.78±1.76	0.030±0.003	62457.89±192.34
$\beta_\varrho = 4.0$	PEEMMASMH	97.98±1.67	0.030±0.003	62458.64±186.75
$\beta_\varsigma = 4.0$	PEEMACOMC	96.78±1.54	0.029±0.002	64658.54±175.67
$\beta_\nu = 5.0$	PEEMACOMP	97.86±1.89	0.026±0.002	62785.45±194.56
$\beta_\xi = 5.0$	PEEMACOMH	95.90±1.67	0.029±0.002	62216.54±209.63
$\beta_\pi = 5.0$	PEEMMASMP	98.64±1.35	0.028±0.002	62439.97±196.75
$\beta_\varrho = 5.0$	PEEMMASMH	96.43±1.67	0.029±0.003	62215.46±197.85
$\beta_\varsigma = 5.0$	PEEMACOMC	97.85±1.22	0.028±0.002	64217.87±176.54
$\beta_\nu = 7.0$	PEEMACOMP	90.45±4.12	0.028±0.002	52546.54±563.45
$\beta_\xi = 7.0$	PEEMACOMH	88.90±4.34	0.031±0.002	55748.75±579.35
$\beta_\pi = 7.0$	PEEMMASMP	91.78±4.23	0.028±0.002	53678.76±567.89
$\beta_\varrho = 7.0$	PEEMMASMH	90.37±4.12	0.029±0.003	52358.54±578.90
$\beta_\varsigma = 7.0$	PEEMACOMC	89.45±4.32	0.028±0.003	53687.54±543.87

(f) $T_{sm} = 6$

β_ψ	$\mathcal{PF}$	$\bar{n}_{alg}$	$\bar{\varrho}$	$\bar{\xi}$
$\beta_\nu = 1.0$	PEEMACOMP	62.48±2.78	0.089±0.010	54879.23±568.39
$\beta_\xi = 1.0$	PEEMACOMH	63.47±2.78	0.102±0.011	53568.65±589.26
$\beta_\pi = 1.0$	PEEMMASMP	62.47±2.68	0.113±0.011	53324.68±538.75
$\beta_\varrho = 1.0$	PEEMMASMH	64.54±2.46	0.115±0.012	55497.43±568.64
$\beta_\varsigma = 1.0$	PEEMACOMC	64.67±2.75	0.117±0.012	55665.78±589.43
$\beta_\nu = 3.0$	PEEMACOMP	63.89±2.48	0.087±0.009	56745.32±568.54
$\beta_\xi = 3.0$	PEEMACOMH	65.76±2.69	0.085±0.008	56453.23±575.68
$\beta_\pi = 3.0$	PEEMMASMP	64.68±2.84	0.082±0.007	56554.82±586.74
$\beta_\varrho = 3.0$	PEEMMASMH	64.79±2.58	0.081±0.008	57894.32±536.57
$\beta_\varsigma = 3.0$	PEEMACOMC	64.58±2.57	0.092±0.010	56778.45±556.90
$\beta_\nu = 3.5$	PEEMACOMP	98.75±0.42	0.028±0.002	63215.43±187.45
$\beta_\xi = 4.0$	PEEMACOMH	98.64±0.38	0.031±0.003	62226.53±209.84
$\beta_\pi = 4.5$	PEEMMASMP	98.65±0.52	0.028±0.002	62453.76±223.46
$\beta_\varrho = 4.0$	PEEMMASMH	98.67±0.51	0.027±0.002	62432.45±210.65
$\beta_\varsigma = 5.0$	PEEMACOMC	98.75±0.46	0.029±0.002	64879.07±186.74
$\beta_\nu = 4.5$	PEEMACOMP	98.41±0.57	0.027±0.002	63198.04±176.84
$\beta_\xi = 5.0$	PEEMACOMH	98.63±0.43	0.030±0.003	62137.64±196.74
$\beta_\pi = 3.5$	PEEMMASMP	97.84±0.58	0.031±0.003	62327.89±186.59
$\beta_\varrho = 4.0$	PEEMMASMH	98.75±0.58	0.029±0.002	62532.46±178.65
$\beta_\varsigma = 4.0$	PEEMACOMC	98.76±0.48	0.028±0.002	64784.56±168.54
$\beta_\nu = 5.0$	PEEMACOMP	98.75±0.45	0.028±0.002	63246.53±183.47
$\beta_\xi = 5.0$	PEEMACOMH	98.76±0.49	0.029±0.003	62068.65±187.08
$\beta_\pi = 5.0$	PEEMMASMP	98.75±0.52	0.028±0.002	62513.40±194.56
$\beta_\varrho = 5.0$	PEEMMASMH	97.83±0.47	0.028±0.003	62456.78±195.78
$\beta_\varsigma = 5.0$	PEEMACOMC	98.54±0.43	0.027±0.002	64479.65±185.60
$\beta_\nu = 7.0$	PEEMACOMP	94.58±1.28	0.030±0.003	55591.23±467.87
$\beta_\xi = 7.0$	PEEMACOMH	96.54±1.35	0.029±0.002	56489.78±487.98
$\beta_\pi = 7.0$	PEEMMASMP	96.78±1.41	0.031±0.002	55830.65±538.76
$\beta_\varrho = 7.0$	PEEMMASMH	94.56±1.34	0.028±0.003	54679.43±587.65
$\beta_\varsigma = 7.0$	PEEMACOMC	95.64±1.42	0.027±0.002	55892.36±564.38

Table D.2: Influence of parameter β_ψ on the $\bar{n}_{alg}$, $\bar{\varrho}$ and $\bar{\xi}$ metrics, for 30 nodes and $R_g = 500$

(a) $T_{sm} = 1$

β_ψ	$\mathcal{PF}$	$\bar{n}_{alg}$	$\bar{\varrho}$	$\bar{\xi}$
$\beta_\nu = 1.0$	$P_{EEMACOMP}$	48.32±5.59	0.235±0.024	44569.87±965.43
$\beta_\xi = 1.0$	$P_{EEMACOMH}$	46.34±5.71	0.242±0.024	42357.98±987.39
$\beta_\pi = 1.0$	$P_{EEMMASMP}$	48.64±5.63	0.229±0.023	42671.70±908.12
$\beta_\varrho = 1.0$	$P_{EEMMASMH}$	46.74±5.57	0.245±0.025	40178.68±957.52
$\beta_\varsigma = 1.0$	$P_{EEMACOMC}$	47.84±5.79	0.254±0.025	43678.12±945.68
$\beta_\nu = 3.0$	$P_{EEMACOMP}$	49.53±5.49	0.217±0.023	44568.93±938.50
$\beta_\xi = 3.0$	$P_{EEMACOMH}$	46.74±5.82	0.229±0.023	43476.90±929.02
$\beta_\pi = 3.0$	$P_{EEMMASMP}$	47.54±5.49	0.245±0.025	43412.96±949.25
$\beta_\varrho = 3.0$	$P_{EEMMASMH}$	45.32±5.67	0.221±0.022	44678.98±927.54
$\beta_\varsigma = 3.0$	$P_{EEMACOMC}$	47.21±5.83	0.246±0.024	43528.95±965.43
$\beta_\nu = 3.5$	$P_{EEMACOMP}$	80.57±4.27	0.062±0.008	63257.87±238.69
$\beta_\xi = 4.0$	$P_{EEMACOMH}$	76.53±4.31	0.065±0.009	63456.87±239.78
$\beta_\pi = 4.5$	$P_{EEMMASMP}$	73.57±4.37	0.064±0.008	63468.96±243.74
$\beta_\varrho = 4.0$	$P_{EEMMASMH}$	76.43±4.29	0.067±0.010	63578.98±239.39
$\beta_\varsigma = 5.0$	$P_{EEMACOMC}$	78.65±4.37	0.078±0.012	63412.96±243.29
$\beta_\nu = 4.5$	$P_{EEMACOMP}$	83.12±4.26	0.064±0.009	63689.09±238.20
$\beta_\xi = 5.0$	$P_{EEMACOMH}$	81.45±4.10	0.063±0.008	63578.95±258.93
$\beta_\pi = 3.5$	$P_{EEMMASMP}$	77.65±4.53	0.062±0.008	63689.02±232.78
$\beta_\varrho = 4.0$	$P_{EEMMASMH}$	78.61±4.34	0.069±0.010	63689.06±265.32
$\beta_\varsigma = 4.0$	$P_{EEMACOMC}$	80.43±4.26	0.076±0.011	63789.01±243.21
$\beta_\nu = 5.0$	$P_{EEMACOMP}$	79.54±4.39	0.060±0.007	63687.86±245.89
$\beta_\xi = 5.0$	$P_{EEMACOMH}$	78.78±4.38	0.063±0.008	63687.98±252.90
$\beta_\pi = 5.0$	$P_{EEMMASMP}$	79.68±4.48	0.062±0.008	63678.98±268.95
$\beta_\varrho = 5.0$	$P_{EEMMASMH}$	78.59±4.63	0.065±0.009	63768.38±234.78
$\beta_\varsigma = 5.0$	$P_{EEMACOMC}$	82.43±4.72	0.075±0.012	63768.47±246.85
$\beta_\nu = 7.0$	$P_{EEMACOMP}$	62.37±4.89	0.059±0.008	43483.85±977.58
$\beta_\xi = 7.0$	$P_{EEMACOMH}$	65.43±5.27	0.064±0.009	42568.87±948.69
$\beta_\pi = 7.0$	$P_{EEMMASMP}$	64.68±4.98	0.062±0.008	43578.89±967.74
$\beta_\varrho = 7.0$	$P_{EEMMASMH}$	67.54±4.67	0.065±0.008	42316.89±917.95
$\beta_\varsigma = 7.0$	$P_{EEMACOMC}$	67.43±4.75	0.075±0.009	42478.87±898.64

(b) $T_{sm} = 2$

β_ψ	$\mathcal{PF}$	$\bar{n}_{alg}$	$\bar{\varrho}$	$\bar{\xi}$
$\beta_\nu = 1.0$	$P_{EEMACOMP}$	51.23±5.38	0.201±0.022	46873.21±864.29
$\beta_\xi = 1.0$	$P_{EEMACOMH}$	49.47±5.81	0.228±0.023	44578.27±827.84
$\beta_\pi = 1.0$	$P_{EEMMASMP}$	49.54±5.37	0.217±0.022	44587.23±873.52
$\beta_\varrho = 1.0$	$P_{EEMMASMH}$	48.79±5.23	0.236±0.024	43568.26±827.48
$\beta_\varsigma = 1.0$	$P_{EEMACOMC}$	49.32±5.47	0.234±0.024	46237.53±824.56
$\beta_\nu = 3.0$	$P_{EEMACOMP}$	48.31±5.57	0.174±0.018	46587.32±857.48
$\beta_\xi = 3.0$	$P_{EEMACOMH}$	49.37±5.51	0.182±0.019	46542.76±837.21
$\beta_\pi = 3.0$	$P_{EEMMASMP}$	48.43±5.41	0.169±0.019	44528.43±853.28
$\beta_\varrho = 3.0$	$P_{EEMMASMH}$	49.42±5.38	0.186±0.019	46632.94±836.71
$\beta_\varsigma = 3.0$	$P_{EEMACOMC}$	48.31±5.49	0.158±0.018	44551.23±853.21
$\beta_\nu = 3.5$	$P_{EEMACOMP}$	84.59±3.84	0.050±0.007	63835.31±242.58
$\beta_\xi = 4.0$	$P_{EEMACOMH}$	82.45±3.78	0.054±0.008	63765.38±229.36
$\beta_\pi = 4.5$	$P_{EEMMASMP}$	85.32±3.74	0.052±0.008	63698.35±249.54
$\beta_\varrho = 4.0$	$P_{EEMMASMH}$	87.41±3.51	0.051±0.008	63854.32±232.35
$\beta_\varsigma = 5.0$	$P_{EEMACOMC}$	83.67±3.48	0.058±0.009	63764.28±231.56
$\beta_\nu = 4.5$	$P_{EEMACOMP}$	86.31±3.75	0.052±0.007	63785.34±242.78
$\beta_\xi = 5.0$	$P_{EEMACOMH}$	85.83±3.60	0.053±0.008	63875.32±229.51
$\beta_\pi = 3.5$	$P_{EEMMASMP}$	82.47±3.87	0.052±0.008	63865.31±243.76
$\beta_\varrho = 4.0$	$P_{EEMMASMH}$	83.68±3.74	0.050±0.008	63879.32±242.75
$\beta_\varsigma = 4.0$	$P_{EEMACOMC}$	84.59±3.67	0.057±0.009	63879.41±253.75
$\beta_\nu = 5.0$	$P_{EEMACOMP}$	83.76±3.87	0.051±0.007	63876.32±246.28
$\beta_\xi = 5.0$	$P_{EEMACOMH}$	82.47±3.60	0.050±0.007	63764.21±242.64
$\beta_\pi = 5.0$	$P_{EEMMASMP}$	82.39±3.59	0.053±0.008	63287.48±264.76
$\beta_\varrho = 5.0$	$P_{EEMMASMH}$	83.60±3.68	0.049±0.006	63872.46±231.64
$\beta_\varsigma = 5.0$	$P_{EEMACOMC}$	84.65±3.89	0.058±0.009	63897.36±227.85
$\beta_\nu = 7.0$	$P_{EEMACOMP}$	65.56±5.23	0.052±0.007	46783.21±847.32
$\beta_\xi = 7.0$	$P_{EEMACOMH}$	68.43±5.06	0.053±0.008	45612.67±816.93
$\beta_\pi = 7.0$	$P_{EEMMASMP}$	67.40±4.94	0.051±0.008	45783.54±814.54
$\beta_\varrho = 7.0$	$P_{EEMMASMH}$	68.72±4.28	0.050±0.007	45734.21±823.74
$\beta_\varsigma = 7.0$	$P_{EEMACOMC}$	69.03±4.43	0.056±0.008	46474.32±784.53

(c) $T_{sm} = 3$

β_ψ	$\mathcal{PF}$	$\bar{n}_{alg}$	$\bar{\varrho}$	$\bar{\xi}$
$\beta_\nu = 1.0$	$P_{EEMACOMP}$	53.42±5.28	0.178±0.017	48725.32±708.32
$\beta_\xi = 1.0$	$P_{EEMACOMH}$	52.31±5.41	0.203±0.018	47432.65±742.54
$\beta_\pi = 1.0$	$P_{EEMMASMP}$	52.34±5.26	0.202±0.017	46743.28±764.52
$\beta_\varrho = 1.0$	$P_{EEMMASMH}$	53.48±5.12	0.212±0.019	46734.19±791.36
$\beta_\varsigma = 1.0$	$P_{EEMACOMC}$	53.45±5.27	0.209±0.018	48684.32±754.18
$\beta_\nu = 3.0$	$P_{EEMACOMP}$	54.32±5.54	0.152±0.015	49321.32±758.32
$\beta_\xi = 3.0$	$P_{EEMACOMH}$	56.78±5.28	0.163±0.016	48987.54±798.43
$\beta_\pi = 3.0$	$P_{EEMMASMP}$	54.67±5.43	0.142±0.014	48743.12±783.21
$\beta_\varrho = 3.0$	$P_{EEMMASMH}$	53.68±5.42	0.158±0.015	49876.54±768.34
$\beta_\varsigma = 3.0$	$P_{EEMACOMC}$	52.78±5.21	0.147±0.015	44843.25±756.32
$\beta_\nu = 3.5$	$P_{EEMACOMP}$	87.43±3.65	0.045±0.006	64321.43±186.32
$\beta_\xi = 4.0$	$P_{EEMACOMH}$	86.87±3.52	0.048±0.006	64762.43±189.32
$\beta_\pi = 4.5$	$P_{EEMMASMP}$	87.32±3.42	0.049±0.007	64528.96±183.27
$\beta_\varrho = 4.0$	$P_{EEMMASMH}$	88.45±3.31	0.045±0.006	64876.32±168.32
$\beta_\varsigma = 5.0$	$P_{EEMACOMC}$	86.72±3.25	0.048±0.006	64326.54±179.34
$\beta_\nu = 4.5$	$P_{EEMACOMP}$	88.92±3.27	0.043±0.005	64679.03±189.43
$\beta_\xi = 5.0$	$P_{EEMACOMH}$	87.21±3.46	0.045±0.005	64328.54±183.46
$\beta_\pi = 3.5$	$P_{EEMMASMP}$	86.43±3.29	0.048±0.006	64578.21±197.32
$\beta_\varrho = 4.0$	$P_{EEMMASMH}$	85.87±3.45	0.046±0.006	64789.21±192.42
$\beta_\varsigma = 4.0$	$P_{EEMACOMC}$	87.62±3.32	0.047±0.006	64231.65±193.45
$\beta_\nu = 5.0$	$P_{EEMACOMP}$	86.73±3.61	0.045±0.004	64231.85±197.54
$\beta_\xi = 5.0$	$P_{EEMACOMH}$	85.82±3.42	0.047±0.006	64326.42±178.43
$\beta_\pi = 5.0$	$P_{EEMMASMP}$	86.74±3.32	0.048±0.006	64167.42±189.34
$\beta_\varrho = 5.0$	$P_{EEMMASMH}$	87.32±3.41	0.049±0.007	64231.42±185.32
$\beta_\varsigma = 5.0$	$P_{EEMACOMC}$	86.83±3.34	0.046±0.005	63897.36±194.32
$\beta_\nu = 7.0$	$P_{EEMACOMP}$	73.26±4.41	0.044±0.006	48653.23±749.85
$\beta_\xi = 7.0$	$P_{EEMACOMH}$	74.38±4.21	0.047±0.006	48864.28±738.21
$\beta_\pi = 7.0$	$P_{EEMMASMP}$	73.57±4.45	0.048±0.005	47632.13±732.51
$\beta_\varrho = 7.0$	$P_{EEMMASMH}$	72.65±4.21	0.046±0.006	48235.24±725.43
$\beta_\varsigma = 7.0$	$P_{EEMACOMC}$	73.31±4.13	0.047±0.006	47234.21±674.35

(d) $T_{sm} = 4$

β_ψ	$\mathcal{PF}$	$\bar{n}_{alg}$	$\bar{\varrho}$	$\bar{\xi}$
$\beta_\nu = 1.0$	$P_{EEMACOMP}$	56.32±4.65	0.154±0.015	51367.42±524.67
$\beta_\xi = 1.0$	$P_{EEMACOMH}$	54.52±4.76	0.168±0.017	51523.78±563.28
$\beta_\pi = 1.0$	$P_{EEMMASMP}$	55.21±4.86	0.174±0.016	51478.32±568.24
$\beta_\varrho = 1.0$	$P_{EEMMASMH}$	54.87±4.54	0.178±0.018	52367.81±537.82
$\beta_\varsigma = 1.0$	$P_{EEMACOMC}$	55.76±4.32	0.173±0.016	52418.34±572.36
$\beta_\nu = 3.0$	$P_{EEMACOMP}$	58.54±4.23	0.137±0.013	51764.34±528.54
$\beta_\xi = 3.0$	$P_{EEMACOMH}$	58.64±4.56	0.148±0.014	51378.41±548.39
$\beta_\pi = 3.0$	$P_{EEMMASMP}$	58.36±4.54	0.137±0.012	51378.78±537.27
$\beta_\varrho = 3.0$	$P_{EEMMASMH}$	57.33±4.79	0.142±0.013	52317.48±549.23
$\beta_\varsigma = 3.0$	$P_{EEMACOMC}$	57.64±4.37	0.141±0.013	48487.43±578.43
$\beta_\nu = 3.5$	$P_{EEMACOMP}$	91.32±1.23	0.043±0.004	64893.56±169.32
$\beta_\xi = 4.0$	$P_{EEMACOMH}$	92.54±1.28	0.044±0.005	64732.18±179.32
$\beta_\pi = 4.5$	$P_{EEMMASMP}$	92.45±1.52	0.044±0.005	64643.28±184.28
$\beta_\varrho = 4.0$	$P_{EEMMASMH}$	92.45±1.27	0.042±0.004	64743.28±165.87
$\beta_\varsigma = 5.0$	$P_{EEMACOMC}$	94.41±1.18	0.046±0.006	64769.32±167.32
$\beta_\nu = 4.5$	$P_{EEMACOMP}$	92.34±1.42	0.040±0.004	64784.39±179.32
$\beta_\xi = 5.0$	$P_{EEMACOMH}$	92.31±1.48	0.042±0.005	64328.54±167.42
$\beta_\pi = 3.5$	$P_{EEMMASMP}$	93.42±1.28	0.043±0.005	64652.81±158.36
$\beta_\varrho = 4.0$	$P_{EEMMASMH}$	91.24±1.59	0.043±0.005	64692.40±175.32
$\beta_\varsigma = 4.0$	$P_{EEMACOMC}$	92.84±1.56	0.046±0.006	64467.28±183.56
$\beta_\nu = 5.0$	$P_{EEMACOMP}$	92.45±1.42	0.041±0.004	64683.68±187.35
$\beta_\xi = 5.0$	$P_{EEMACOMH}$	93.56±1.69	0.043±0.005	64573.89±168.43
$\beta_\pi = 5.0$	$P_{EEMMASMP}$	94.31±1.58	0.044±0.004	64358.28±175.23
$\beta_\varrho = 5.0$	$P_{EEMMASMH}$	93.45±1.42	0.043±0.005	64487.29±168.34
$\beta_\varsigma = 5.0$	$P_{EEMACOMC}$	94.21±1.23	0.045±0.005	64468.37±176.26
$\beta_\nu = 7.0$	$P_{EEMACOMP}$	76.42±3.48	0.043±0.004	52678.38±548.84
$\beta_\xi = 7.0$	$P_{EEMACOMH}$	77.53±3.67	0.044±0.005	51278.39±532.65
$\beta_\pi = 7.0$	$P_{EEMMASMP}$	76.27±3.53	0.042±0.004	52689.30±548.27
$\beta_\varrho = 7.0$	$P_{EEMMASMH}$	75.43±3.67	0.043±0.005	52378.87±546.32
$\beta_\varsigma = 7.0$	$P_{EEMACOMC}$	77.25±3.45	0.046±0.005	51379.43±568.32

Table D.2: Influence of parameter β_ψ on the $\bar{n}_{alg}$, $\bar{\varrho}$ and $\bar{\xi}$ metrics, for 30 nodes and $R_g = 500$ (cont.)

(e) $T_{sm} = 5$

β_ψ	$\mathcal{PF}$	$\bar{n}_{alg}$	$\bar{\varrho}$	$\bar{\xi}$
$\beta_\nu = 1.0$	$\text{P}_{\text{EEMACOMP}}$	62.36±3.68	0.136±0.012	52468.32±462.63
$\beta_\xi = 1.0$	$\text{P}_{\text{EEMACOMH}}$	60.36±3.87	0.142±0.013	51679.43±478.32
$\beta_\pi = 1.0$	$\text{P}_{\text{EEMMASMP}}$	59.41±3.75	0.141±0.013	51743.28±482.46
$\beta_\varrho = 1.0$	$\text{P}_{\text{EEMMASMH}}$	58.95±3.68	0.138±0.012	53458.21±457.21
$\beta_\varsigma = 1.0$	$\text{P}_{\text{EEMACOMC}}$	58.45±3.64	0.139±0.012	53679.21±458.43
$\beta_\nu = 3.0$	$\text{P}_{\text{EEMACOMP}}$	60.43±3.59	0.113±0.011	53578.54±437.85
$\beta_\xi = 3.0$	$\text{P}_{\text{EEMACOMH}}$	61.69±3.53	0.121±0.011	53532.89±468.42
$\beta_\pi = 3.0$	$\text{P}_{\text{EEMMASMP}}$	62.78±3.67	0.116±0.010	52476.32±478.34
$\beta_\varrho = 3.0$	$\text{P}_{\text{EEMMASMH}}$	63.47±3.73	0.123±0.010	53648.21±437.84
$\beta_\varsigma = 3.0$	$\text{P}_{\text{EEMACOMC}}$	62.40±3.65	0.117±0.009	52678.32±462.74
$\beta_\nu = 3.5$	$\text{P}_{\text{EEMACOMP}}$	94.53±1.16	0.040±0.004	65135.84±162.48
$\beta_\xi = 4.0$	$\text{P}_{\text{EEMACOMH}}$	94.79±1.14	0.042±0.004	64876.35±160.34
$\beta_\pi = 4.5$	$\text{P}_{\text{EEMMASMP}}$	94.78±1.21	0.042±0.005	64967.43±168.36
$\beta_\varrho = 4.0$	$\text{P}_{\text{EEMMASMH}}$	94.76±1.13	0.043±0.004	64978.32±157.21
$\beta_\varsigma = 5.0$	$\text{P}_{\text{EEMACOMC}}$	95.67±1.02	0.044±0.005	64896.85±158.32
$\beta_\nu = 4.5$	$\text{P}_{\text{EEMACOMP}}$	95.28±1.32	0.041±0.004	64876.48±168.03
$\beta_\xi = 5.0$	$\text{P}_{\text{EEMACOMH}}$	96.73±1.28	0.042±0.005	64768.36±179.32
$\beta_\pi = 3.5$	$\text{P}_{\text{EEMMASMP}}$	95.67±1.28	0.041±0.004	64785.35±169.21
$\beta_\varrho = 4.0$	$\text{P}_{\text{EEMMASMH}}$	94.61±1.41	0.041±0.004	64895.54±175.32
$\beta_\varsigma = 4.0$	$\text{P}_{\text{EEMACOMC}}$	95.72±1.23	0.042±0.004	64869.45±178.42
$\beta_\nu = 5.0$	$\text{P}_{\text{EEMACOMP}}$	94.68±1.25	0.041±0.004	65130.74±185.74
$\beta_\xi = 5.0$	$\text{P}_{\text{EEMACOMH}}$	95.73±1.23	0.042±0.004	64768.32±162.69
$\beta_\pi = 5.0$	$\text{P}_{\text{EEMMASMP}}$	95.48±1.12	0.044±0.006	64673.40±172.68
$\beta_\varrho = 5.0$	$\text{P}_{\text{EEMMASMH}}$	94.68±1.03	0.041±0.004	64789.48±171.28
$\beta_\varsigma = 5.0$	$\text{P}_{\text{EEMACOMC}}$	96.71±1.02	0.041±0.005	64867.43±172.43
$\beta_\nu = 7.0$	$\text{P}_{\text{EEMACOMP}}$	78.43±2.96	0.042±0.005	53674.32±445.32
$\beta_\xi = 7.0$	$\text{P}_{\text{EEMACOMH}}$	78.32±2.68	0.041±0.004	54527.85±476.43
$\beta_\pi = 7.0$	$\text{P}_{\text{EEMMASMP}}$	78.35±2.89	0.041±0.004	54749.32±487.45
$\beta_\varrho = 7.0$	$\text{P}_{\text{EEMMASMH}}$	77.93±2.74	0.042±0.004	54638.32±478.45
$\beta_\varsigma = 7.0$	$\text{P}_{\text{EEMACOMC}}$	79.42±2.56	0.041±0.005	53689.32±468.47

(f) $T_{sm} = 6$

β_ψ	$\mathcal{PF}$	$\bar{n}_{alg}$	$\bar{\varrho}$	$\bar{\xi}$
$\beta_\nu = 1.0$	$\text{P}_{\text{EEMACOMP}}$	66.47±2.59	0.117±0.012	53470.53±354.72
$\beta_\xi = 1.0$	$\text{P}_{\text{EEMACOMH}}$	64.21±2.68	0.125±0.013	52548.54±381.43
$\beta_\pi = 1.0$	$\text{P}_{\text{EEMMASMP}}$	62.83±2.96	0.121±0.012	52876.49±378.43
$\beta_\varrho = 1.0$	$\text{P}_{\text{EEMMASMH}}$	64.89±2.86	0.119±0.011	54679.36±375.32
$\beta_\varsigma = 1.0$	$\text{P}_{\text{EEMACOMC}}$	64.56±2.75	0.123±0.011	55428.21±368.46
$\beta_\nu = 3.0$	$\text{P}_{\text{EEMACOMP}}$	65.32±2.73	0.087±0.010	55769.32±378.54
$\beta_\xi = 3.0$	$\text{P}_{\text{EEMACOMH}}$	64.75±2.54	0.086±0.008	54628.32±359.56
$\beta_\pi = 3.0$	$\text{P}_{\text{EEMMASMP}}$	66.48±2.95	0.092±0.009	53528.49±367.39
$\beta_\varrho = 3.0$	$\text{P}_{\text{EEMMASMH}}$	65.69±2.86	0.086±0.009	54619.43±376.39
$\beta_\varsigma = 3.0$	$\text{P}_{\text{EEMACOMC}}$	65.37±2.68	0.067±0.008	54783.91±387.43
$\beta_\nu = 3.5$	$\text{P}_{\text{EEMACOMP}}$	98.43±0.36	0.038±0.004	65132.56±173.24
$\beta_\xi = 4.0$	$\text{P}_{\text{EEMACOMH}}$	98.65±0.36	0.040±0.004	64917.65±166.43
$\beta_\pi = 4.5$	$\text{P}_{\text{EEMMASMP}}$	98.63±0.32	0.039±0.005	65108.41±172.54
$\beta_\varrho = 4.0$	$\text{P}_{\text{EEMMASMH}}$	98.32±0.28	0.039±0.005	64995.48±164.38
$\beta_\varsigma = 5.0$	$\text{P}_{\text{EEMACOMC}}$	97.63±0.35	0.040±0.005	65216.75±168.32
$\beta_\nu = 4.5$	$\text{P}_{\text{EEMACOMP}}$	97.85±0.38	0.039±0.005	65218.28±168.21
$\beta_\xi = 5.0$	$\text{P}_{\text{EEMACOMH}}$	98.43±0.42	0.041±0.005	64875.49±182.46
$\beta_\pi = 3.5$	$\text{P}_{\text{EEMMASMP}}$	97.54±0.39	0.039±0.004	64842.18±172.47
$\beta_\varrho = 4.0$	$\text{P}_{\text{EEMMASMH}}$	98.43±0.43	0.039±0.004	64978.42±179.21
$\beta_\varsigma = 4.0$	$\text{P}_{\text{EEMACOMC}}$	97.43±0.38	0.040±0.005	65237.65±164.28
$\beta_\nu = 5.0$	$\text{P}_{\text{EEMACOMP}}$	98.56±0.38	0.040±0.004	65174.29±174.53
$\beta_\xi = 5.0$	$\text{P}_{\text{EEMACOMH}}$	97.54±0.37	0.040±0.005	64875.34±157.42
$\beta_\pi = 5.0$	$\text{P}_{\text{EEMMASMP}}$	98.38±0.36	0.041±0.005	64843.76±164.86
$\beta_\varrho = 5.0$	$\text{P}_{\text{EEMMASMH}}$	96.94±0.34	0.039±0.004	64875.39±168.43
$\beta_\varsigma = 5.0$	$\text{P}_{\text{EEMACOMC}}$	98.45±0.32	0.038±0.005	65328.52±167.43
$\beta_\nu = 7.0$	$\text{P}_{\text{EEMACOMP}}$	82.54±1.70	0.039±0.005	55734.85±379.42
$\beta_\xi = 7.0$	$\text{P}_{\text{EEMACOMH}}$	84.53±1.59	0.039±0.004	56387.51±372.59
$\beta_\pi = 7.0$	$\text{P}_{\text{EEMMASMP}}$	82.38±1.48	0.040±0.005	55841.74±347.89
$\beta_\varrho = 7.0$	$\text{P}_{\text{EEMMASMH}}$	84.32±1.67	0.041±0.005	55874.32±386.42
$\beta_\varsigma = 7.0$	$\text{P}_{\text{EEMACOMC}}$	83.28±1.78	0.040±0.004	55278.32±365.74

Table D.3: Influence of parameter β_ψ on the $\bar{n}_{alg}$, $\bar{\varrho}$ and $\bar{\xi}$ metrics, for 30 nodes and $R_g = 800$

(a) $T_{sm} = 1$

β_ψ	$\mathcal{PF}$	$\bar{n}_{alg}$	$\bar{\varrho}$	$\bar{\xi}$
$\beta_\nu = 1.0$	$P_{EEMACOMP}$	44.65±5.92	0.264±0.027	42316.37±942.54
$\beta_\xi = 1.0$	$P_{EEMACOMH}$	41.68±5.97	0.278±0.028	41235.65±960.32
$\beta_\pi = 1.0$	$P_{EEMMASMP}$	45.78±6.12	0.247±0.026	41674.23±957.36
$\beta_\varrho = 1.0$	$P_{EEMMASMH}$	45.37±6.27	0.259±0.027	39123.45±976.21
$\beta_\varsigma = 1.0$	$P_{EEMACOMC}$	46.57±6.31	0.239±0.025	41345.43±967.32
$\beta_\nu = 3.0$	$P_{EEMACOMP}$	47.34±6.13	0.232±0.023	42456.21±939.42
$\beta_\xi = 3.0$	$P_{EEMACOMH}$	40.32±5.38	0.255±0.026	41326.48±942.65
$\beta_\pi = 3.0$	$P_{EEMMASMP}$	45.78±6.26	0.245±0.024	41267.74±953.48
$\beta_\varrho = 3.0$	$P_{EEMMASMH}$	44.12±6.23	0.234±0.023	41356.27±937.21
$\beta_\varsigma = 3.0$	$P_{EEMACOMC}$	43.56±5.97	0.257±0.026	42347.21±987.46
$\beta_\nu = 3.5$	$P_{EEMACOMP}$	77.43±3.82	0.121±0.013	62457.75±256.32
$\beta_\xi = 4.0$	$P_{EEMACOMH}$	51.38±5.68	0.158±0.021	62453.27±253.21
$\beta_\pi = 4.5$	$P_{EEMMASMP}$	76.84±3.75	0.118±0.012	62435.67±260.34
$\beta_\varrho = 4.0$	$P_{EEMMASMH}$	74.38±3.85	0.117±0.012	62456.87±263.52
$\beta_\varsigma = 5.0$	$P_{EEMACOMC}$	75.76±3.95	0.145±0.019	62121.45±264.32
$\beta_\nu = 4.5$	$P_{EEMACOMP}$	78.34±3.25	0.124±0.012	62347.21±268.32
$\beta_\xi = 5.0$	$P_{EEMACOMH}$	52.65±5.45	0.157±0.021	62413.67±276.32
$\beta_\pi = 3.5$	$P_{EEMMASMP}$	76.38±3.76	0.123±0.012	62437.12±265.32
$\beta_\varrho = 4.0$	$P_{EEMMASMH}$	73.76±3.98	0.120±0.013	62357.24±246.32
$\beta_\varsigma = 4.0$	$P_{EEMACOMC}$	75.83±3.68	0.147±0.019	62179.58±259.32
$\beta_\nu = 5.0$	$P_{EEMACOMP}$	76.48±3.79	0.123±0.013	62318.43±252.31
$\beta_\xi = 5.0$	$P_{EEMACOMH}$	49.36±5.62	0.160±0.020	62568.43±263.20
$\beta_\pi = 5.0$	$P_{EEMMASMP}$	72.57±3.87	0.124±0.013	62537.95±267.34
$\beta_\varrho = 5.0$	$P_{EEMMASMH}$	74.69±3.86	0.122±0.013	62457.32±252.43
$\beta_\varsigma = 5.0$	$P_{EEMACOMC}$	76.38±3.92	0.152±0.018	62168.65±258.43
$\beta_\nu = 7.0$	$P_{EEMACOMP}$	60.27±4.42	0.122±0.013	41357.43±921.54
$\beta_\xi = 7.0$	$P_{EEMACOMH}$	45.65±5.93	0.162±0.019	40235.42±907.43
$\beta_\pi = 7.0$	$P_{EEMMASMP}$	61.28±4.32	0.118±0.013	42315.32±975.75
$\beta_\varrho = 7.0$	$P_{EEMMASMH}$	63.67±4.42	0.117±0.012	41562.78±932.43
$\beta_\varsigma = 7.0$	$P_{EEMACOMC}$	62.67±4.46	0.147±0.017	41246.32±923.84

(b) $T_{sm} = 2$

β_ψ	$\mathcal{PF}$	$\bar{n}_{alg}$	$\bar{\varrho}$	$\bar{\xi}$
$\beta_\nu = 1.0$	$P_{EEMACOMP}$	44.75±5.23	0.242±0.024	44572.48±875.32
$\beta_\xi = 1.0$	$P_{EEMACOMH}$	38.27±4.78	0.258±0.026	42568.32±865.34
$\beta_\pi = 1.0$	$P_{EEMMASMP}$	44.37±5.78	0.229±0.023	44684.32±874.23
$\beta_\varrho = 1.0$	$P_{EEMMASMH}$	43.28±5.56	0.227±0.023	42168.38±891.25
$\beta_\varsigma = 1.0$	$P_{EEMACOMC}$	44.89±5.23	0.218±0.021	43451.56±864.29
$\beta_\nu = 3.0$	$P_{EEMACOMP}$	48.34±5.78	0.221±0.020	45628.92±875.43
$\beta_\xi = 3.0$	$P_{EEMACOMH}$	41.85±5.61	0.238±0.022	44567.38±859.32
$\beta_\pi = 3.0$	$P_{EEMMASMP}$	46.87±5.43	0.221±0.021	45672.49±867.32
$\beta_\varrho = 3.0$	$P_{EEMMASMH}$	46.38±5.74	0.216±0.019	43563.81±879.43
$\beta_\varsigma = 3.0$	$P_{EEMACOMC}$	46.39±5.53	0.236±0.023	44671.49±869.32
$\beta_\nu = 3.5$	$P_{EEMACOMP}$	80.43±2.56	0.101±0.014	63215.37±198.56
$\beta_\xi = 4.0$	$P_{EEMACOMH}$	44.65±5.34	0.162±0.017	63458.39±187.34
$\beta_\pi = 4.5$	$P_{EEMMASMP}$	79.54±2.79	0.106±0.012	63451.87±189.46
$\beta_\varrho = 4.0$	$P_{EEMMASMH}$	77.31±2.67	0.107±0.011	63486.83±196.36
$\beta_\varsigma = 5.0$	$P_{EEMACOMC}$	76.38±2.58	0.134±0.018	63151.78±197.34
$\beta_\nu = 4.5$	$P_{EEMACOMP}$	79.87±2.58	0.105±0.013	63268.54±185.64
$\beta_\xi = 5.0$	$P_{EEMACOMH}$	46.32±5.32	0.164±0.018	63478.85±179.54
$\beta_\pi = 3.5$	$P_{EEMMASMP}$	79.32±2.79	0.108±0.012	63679.36±193.45
$\beta_\varrho = 4.0$	$P_{EEMMASMH}$	76.86±2.48	0.106±0.011	63589.27±196.38
$\beta_\varsigma = 4.0$	$P_{EEMACOMC}$	77.43±2.58	0.132±0.018	63479.26±185.32
$\beta_\nu = 5.0$	$P_{EEMACOMP}$	78.65±2.58	0.103±0.012	63456.28±189.34
$\beta_\xi = 5.0$	$P_{EEMACOMH}$	45.21±5.23	0.161±0.017	63268.48±178.43
$\beta_\pi = 5.0$	$P_{EEMMASMP}$	77.54±2.76	0.107±0.012	63467.28±179.32
$\beta_\varrho = 5.0$	$P_{EEMMASMH}$	79.76±2.48	0.104±0.011	63542.67±168.04
$\beta_\varsigma = 5.0$	$P_{EEMACOMC}$	78.43±2.56	0.135±0.017	63417.43±185.39
$\beta_\nu = 7.0$	$P_{EEMACOMP}$	64.35±4.12	0.105±0.012	44576.32±823.45
$\beta_\xi = 7.0$	$P_{EEMACOMH}$	47.21±5.46	0.164±0.018	42478.32±826.74
$\beta_\pi = 7.0$	$P_{EEMMASMP}$	64.73±4.08	0.110±0.013	43578.31±858.32
$\beta_\varrho = 7.0$	$P_{EEMMASMH}$	63.89±4.25	0.103±0.011	44562.38±854.10
$\beta_\varsigma = 7.0$	$P_{EEMACOMC}$	63.78±4.13	0.132±0.016	44267.21±843.76

(c) $T_{sm} = 3$

β_ψ	$\mathcal{PF}$	$\bar{n}_{alg}$	$\bar{\varrho}$	$\bar{\xi}$
$\beta_\nu = 1.0$	$P_{EEMACOMP}$	47.43±5.32	0.213±0.019	46432.78±764.35
$\beta_\xi = 1.0$	$P_{EEMACOMH}$	42.87±5.67	0.224±0.021	45648.35±785.84
$\beta_\pi = 1.0$	$P_{EEMMASMP}$	48.32±5.59	0.213±0.020	45876.48±748.63
$\beta_\varrho = 1.0$	$P_{EEMMASMH}$	46.52±5.48	0.208±0.020	44675.39±743.56
$\beta_\varsigma = 1.0$	$P_{EEMACOMC}$	47.32±5.64	0.203±0.019	45673.28±785.32
$\beta_\nu = 3.0$	$P_{EEMACOMP}$	49.32±5.31	0.204±0.019	47845.21±754.28
$\beta_\xi = 3.0$	$P_{EEMACOMH}$	43.58±5.73	0.210±0.020	47641.09±765.36
$\beta_\pi = 3.0$	$P_{EEMMASMP}$	49.32±5.63	0.196±0.019	46539.27±785.34
$\beta_\varrho = 3.0$	$P_{EEMMASMH}$	48.31±5.47	0.189±0.018	46638.28±786.34
$\beta_\varsigma = 3.0$	$P_{EEMACOMC}$	48.65±5.31	0.175±0.018	46861.28±756.28
$\beta_\nu = 3.5$	$P_{EEMACOMP}$	87.23±2.37	0.090±0.013	64231.57±187.45
$\beta_\xi = 4.0$	$P_{EEMACOMH}$	61.32±4.87	0.117±0.015	64523.87±189.43
$\beta_\pi = 4.5$	$P_{EEMMASMP}$	85.64±2.68	0.092±0.014	64376.21±178.34
$\beta_\varrho = 4.0$	$P_{EEMMASMH}$	87.32±2.46	0.093±0.013	64231.76±172.72
$\beta_\varsigma = 5.0$	$P_{EEMACOMC}$	87.34±2.43	0.113±0.016	64326.75±178.43
$\beta_\nu = 4.5$	$P_{EEMACOMP}$	88.34±2.38	0.089±0.014	64532.62±183.35
$\beta_\xi = 5.0$	$P_{EEMACOMH}$	62.81±4.75	0.121±0.016	64325.66±189.12
$\beta_\pi = 3.5$	$P_{EEMMASMP}$	84.19±2.57	0.095±0.015	64512.64±190.32
$\beta_\varrho = 4.0$	$P_{EEMMASMH}$	85.23±2.42	0.097±0.015	64235.68±191.23
$\beta_\varsigma = 4.0$	$P_{EEMACOMC}$	86.31±2.43	0.116±0.015	64325.57±186.64
$\beta_\nu = 5.0$	$P_{EEMACOMP}$	88.74±2.21	0.093±0.013	64231.65±192.54
$\beta_\xi = 5.0$	$P_{EEMACOMH}$	63.71±4.73	0.123±0.016	64321.67±178.32
$\beta_\pi = 5.0$	$P_{EEMMASMP}$	87.43±2.45	0.097±0.013	64317.54±187.24
$\beta_\varrho = 5.0$	$P_{EEMMASMH}$	85.63±2.32	0.098±0.014	64326.64±172.43
$\beta_\varsigma = 5.0$	$P_{EEMACOMC}$	84.36±2.34	0.118±0.017	64587.21±185.39
$\beta_\nu = 7.0$	$P_{EEMACOMP}$	69.37±4.49	0.096±0.013	46367.21±734.23
$\beta_\xi = 7.0$	$P_{EEMACOMH}$	53.58±5.56	0.126±0.018	45427.34±768.34
$\beta_\pi = 7.0$	$P_{EEMMASMP}$	67.39±4.68	0.096±0.012	44532.76±758.32
$\beta_\varrho = 7.0$	$P_{EEMMASMH}$	66.37±4.47	0.095±0.012	44562.38±784.20
$\beta_\varsigma = 7.0$	$P_{EEMACOMC}$	64.75±4.32	0.116±0.017	45789.32±754.32

(d) $T_{sm} = 4$

β_ψ	$\mathcal{PF}$	$\bar{n}_{alg}$	$\bar{\varrho}$	$\bar{\xi}$
$\beta_\nu = 1.0$	$P_{EEMACOMP}$	52.43±4.23	0.178±0.018	48569.34±645.28
$\beta_\xi = 1.0$	$P_{EEMACOMH}$	43.48±4.54	0.186±0.017	47834.23±648.23
$\beta_\pi = 1.0$	$P_{EEMMASMP}$	51.67±4.32	0.202±0.019	47562.39±648.34
$\beta_\varrho = 1.0$	$P_{EEMMASMH}$	48.32±4.38	0.197±0.019	46739.32±648.23
$\beta_\varsigma = 1.0$	$P_{EEMACOMC}$	48.17±4.42	0.186±0.018	46893.58±657.21
$\beta_\nu = 3.0$	$P_{EEMACOMP}$	51.28±4.25	0.172±0.017	47987.34±674.23
$\beta_\xi = 3.0$	$P_{EEMACOMH}$	48.63±4.41	0.164±0.016	47876.23±679.24
$\beta_\pi = 3.0$	$P_{EEMMASMP}$	51.28±4.23	0.186±0.018	46876.32±648.23
$\beta_\varrho = 3.0$	$P_{EEMMASMH}$	51.67±4.31	0.188±0.018	47634.18±648.62
$\beta_\varsigma = 3.0$	$P_{EEMACOMC}$	52.48±4.27	0.162±0.017	47892.43±657.34
$\beta_\nu = 3.5$	$P_{EEMACOMP}$	90.24±1.78	0.080±0.008	65324.74±167.34
$\beta_\xi = 4.0$	$P_{EEMACOMH}$	48.79±4.34	0.145±0.015	64875.23±169.32
$\beta_\pi = 4.5$	$P_{EEMMASMP}$	90.24±1.67	0.083±0.008	65123.54±172.46
$\beta_\varrho = 4.0$	$P_{EEMMASMH}$	91.68±1.65	0.084±0.009	64897.32±182.34
$\beta_\varsigma = 5.0$	$P_{EEMACOMC}$	91.43±1.72	0.106±0.009	64875.93±164.67
$\beta_\nu = 4.5$	$P_{EEMACOMP}$	91.54±1.56	0.081±0.008	65134.26±157.21
$\beta_\xi = 5.0$	$P_{EEMACOMH}$	49.23±4.34	0.147±0.016	64587.21±186.39
$\beta_\pi = 3.5$	$P_{EEMMASMP}$	90.23±1.47	0.082±0.008	65236.28±175.31
$\beta_\varrho = 4.0$	$P_{EEMMASMH}$	90.45±1.38	0.083±0.009	64468.19±176.34
$\beta_\varsigma = 4.0$	$P_{EEMACOMC}$	89.38±1.42	0.107±0.009	64673.82±184.52
$\beta_\nu = 5.0$	$P_{EEMACOMP}$	91.54±1.35	0.079±0.008	65126.38±183.41
$\beta_\xi = 5.0$	$P_{EEMACOMH}$	48.25±4.45	0.151±0.016	64437.75±176.34
$\beta_\pi = 5.0$	$P_{EEMMASMP}$	91.32±1.36	0.083±0.008	65178.34±178.34
$\beta_\varrho = 5.0$	$P_{EEMMASMH}$	89.43±1.37	0.083±0.008	64258.54±164.28
$\beta_\varsigma = 5.0$	$P_{EEMACOMC}$	88.45±1.27	0.108±0.009	64731.84±163.58
$\beta_\nu = 7.0$	$P_{EEMACOMP}$	91.48±1.38	0.076±0.007	48356.75±623.58
$\beta_\xi = 7.0$	$P_{EEMACOMH}$	50.32±4.37	0.154±0.015	47834.28±628.56
$\beta_\pi = 7.0$	$P_{EEMMASMP}$	91.45±1.37	0.085±0.008	46735.18±684.32
$\beta_\varrho = 7.0$	$P_{EEMMASMH}$	87.23±1.42	0.087±0.009	46438.29±672.38
$\beta_\varsigma = 7.0$	$P_{EEMACOMC}$	92.42±1.48	0.109±0.010	46849.03±673.61

Table D.3: Influence of parameter β_ψ on the $\bar{n}_{alg}$, $\bar{\varrho}$ and $\bar{\xi}$ metrics, for 30 nodes and $R_g = 800$ (cont.)

(e) $T_{sm} = 5$

β_ψ	$\mathcal{PF}$	$\bar{n}_{alg}$	$\bar{\varrho}$	$\bar{\xi}$
$\beta_\nu = 1.0$	PEEMACOMP	56.89±3.78	0.153±0.016	51678.29±546.58
$\beta_\xi = 1.0$	PEEMACOMH	46.48±4.43	0.156±0.015	52368.21±548.28
$\beta_\pi = 1.0$	PEEMMASMP	54.87±3.65	0.180±0.018	50158.38±528.49
$\beta_\varrho = 1.0$	PEEMMASMH	57.59±3.58	0.165±0.017	48689.21±538.42
$\beta_\varsigma = 1.0$	PEEMACOMC	57.47±3.58	0.164±0.017	51674.39±538.27
$\beta_\nu = 3.0$	PEEMACOMP	56.28±3.68	0.134±0.014	52479.35±547.89
$\beta_\xi = 3.0$	PEEMACOMH	51.73±4.27	0.145±0.015	53478.94±538.91
$\beta_\pi = 3.0$	PEEMMASMP	57.38±3.48	0.157±0.016	52368.73±527.38
$\beta_\varrho = 3.0$	PEEMMASMH	57.43±3.84	0.143±0.015	52379.68±539.32
$\beta_\varsigma = 3.0$	PEEMACOMC	56.32±3.75	0.141±0.015	52198.48±528.84
$\beta_\nu = 3.5$	PEEMACOMP	94.35±1.54	0.076±0.007	65247.12±157.41
$\beta_\xi = 4.0$	PEEMACOMH	67.37±2.50	0.111±0.010	65108.26±162.37
$\beta_\pi = 4.5$	PEEMMASMP	95.21±1.45	0.080±0.008	65121.54±167.23
$\beta_\varrho = 4.0$	PEEMMASMH	94.78±1.53	0.078±0.008	64978.32±158.37
$\beta_\varsigma = 5.0$	PEEMACOMC	95.67±1.48	0.104±0.011	64984.32±148.27
$\beta_\nu = 4.5$	PEEMACOMP	94.68±1.62	0.078±0.007	65247.12±152.59
$\beta_\xi = 5.0$	PEEMACOMH	68.32±2.48	0.112±0.012	65141.58±176.32
$\beta_\pi = 3.5$	PEEMMASMP	95.68±1.68	0.081±0.008	65126.78±165.23
$\beta_\varrho = 4.0$	PEEMMASMH	94.38±1.64	0.080±0.008	64789.23±168.34
$\beta_\varsigma = 4.0$	PEEMACOMC	94.68±1.53	0.102±0.010	64853.68±178.31
$\beta_\nu = 5.0$	PEEMACOMP	93.68±1.57	0.074±0.008	65331.56±167.32
$\beta_\xi = 5.0$	PEEMACOMH	69.32±2.56	0.110±0.013	65135.61±165.32
$\beta_\pi = 5.0$	PEEMMASMP	95.78±1.47	0.078±0.007	65231.67±168.32
$\beta_\varrho = 5.0$	PEEMMASMH	94.67±1.48	0.078±0.007	65109.43±154.29
$\beta_\varsigma = 5.0$	PEEMACOMC	95.32±1.32	0.104±0.010	65123.56±153.28
$\beta_\nu = 7.0$	PEEMACOMP	92.63±1.42	0.074±0.008	52338.41±623.58
$\beta_\xi = 7.0$	PEEMACOMH	68.32±2.57	0.108±0.012	50279.32±538.35
$\beta_\pi = 7.0$	PEEMMASMP	93.87±1.48	0.081±0.007	50368.88±536.21
$\beta_\varrho = 7.0$	PEEMMASMH	92.59±1.47	0.082±0.008	48378.28±537.28
$\beta_\varsigma = 7.0$	PEEMACOMC	91.87±1.31	0.103±0.009	48765.46±543.61

(f) $T_{sm} = 6$

β_ψ	$\mathcal{PF}$	$\bar{n}_{alg}$	$\bar{\varrho}$	$\bar{\xi}$
$\beta_\nu = 1.0$	PEEMACOMP	57.12±3.47	0.132±0.014	53468.68±487.45
$\beta_\xi = 1.0$	PEEMACOMH	48.41±4.26	0.135±0.014	52367.94±475.27
$\beta_\pi = 1.0$	PEEMMASMP	57.46±3.54	0.147±0.016	52346.76±458.42
$\beta_\varrho = 1.0$	PEEMMASMH	58.94±3.43	0.146±0.016	51237.54±467.38
$\beta_\varsigma = 1.0$	PEEMACOMC	58.67±3.47	0.137±0.015	52678.45±438.73
$\beta_\nu = 3.0$	PEEMACOMP	58.34±3.62	0.127±0.013	53683.64±468.32
$\beta_\xi = 3.0$	PEEMACOMH	52.67±3.79	0.125±0.013	54328.38±472.39
$\beta_\pi = 3.0$	PEEMMASMP	58.43±3.45	0.131±0.014	53678.75±473.84
$\beta_\varrho = 3.0$	PEEMMASMH	59.43±3.12	0.132±0.014	53681.43±468.22
$\beta_\varsigma = 3.0$	PEEMACOMC	58.21±3.23	0.123±0.013	54128.62±438.50
$\beta_\nu = 3.5$	PEEMACOMP	96.78±0.41	0.073±0.006	65283.23±153.57
$\beta_\xi = 4.0$	PEEMACOMH	76.65±2.47	0.106±0.009	65139.49±157.28
$\beta_\pi = 4.5$	PEEMMASMP	96.32±0.48	0.078±0.007	65246.81±148.75
$\beta_\varrho = 4.0$	PEEMMASMH	95.78±0.47	0.079±0.008	65160.05±149.41
$\beta_\varsigma = 5.0$	PEEMACOMC	96.87±0.51	0.092±0.008	65237.17±146.18
$\beta_\nu = 4.5$	PEEMACOMP	97.45±0.35	0.074±0.007	65358.38±148.96
$\beta_\xi = 5.0$	PEEMACOMH	77.84±2.34	0.109±0.010	65185.33±154.32
$\beta_\pi = 3.5$	PEEMMASMP	97.54±0.25	0.080±0.008	65268.44±159.36
$\beta_\varrho = 4.0$	PEEMMASMH	95.68±0.47	0.078±0.007	65148.43±151.82
$\beta_\varsigma = 4.0$	PEEMACOMC	97.65±0.57	0.095±0.009	65206.66±159.43
$\beta_\nu = 5.0$	PEEMACOMP	97.54±0.27	0.075±0.007	65368.24±151.26
$\beta_\xi = 5.0$	PEEMACOMH	78.11±2.67	0.106±0.010	65247.48±148.53
$\beta_\pi = 5.0$	PEEMMASMP	96.54±0.66	0.076±0.007	65369.17±151.48
$\beta_\varrho = 5.0$	PEEMMASMH	95.67±0.49	0.079±0.007	65369.32±152.48
$\beta_\varsigma = 5.0$	PEEMACOMC	97.82±0.58	0.097±0.009	65138.49±156.99
$\beta_\nu = 7.0$	PEEMACOMP	94.43±1.37	0.073±0.007	54163.47±543.73
$\beta_\xi = 7.0$	PEEMACOMH	73.19±2.78	0.107±0.010	52479.76±547.54
$\beta_\pi = 7.0$	PEEMMASMP	93.92±1.52	0.075±0.007	52689.43±549.21
$\beta_\varrho = 7.0$	PEEMMASMH	92.45±1.36	0.078±0.008	47864.57±568.32
$\beta_\varsigma = 7.0$	PEEMACOMC	93.78±1.31	0.098±0.010	47894.22±563.89

Table D.4: Influence of parameter r_0 on the $\bar{n}_{alg}$, $\bar{\varrho}$ and $\bar{\xi}$ metrics, for 30 nodes and $R_g = 300$

(a) $T_{sm} = 1$

r_0	$\mathcal{PF}$	$\bar{n}_{alg}$	$\bar{\varrho}$	$\bar{\xi}$
0.1	P$_{\text{EEMACOMP}}$	58.32±5.23	0.216±0.021	45123.28±1211.21
	P$_{\text{EEMACOMH}}$	55.17±6.23	0.238±0.023	43234.19±1326.15
	P$_{\text{EEMACOMC}}$	52.29±6.48	0.272±0.025	46156.21±1129.75
0.3	P$_{\text{EEMACOMP}}$	61.35±4.26	0.176±0.015	47657.56±1123.69
	P$_{\text{EEMACOMH}}$	58.87±5.76	0.197±0.017	45864.43±1178.28
	P$_{\text{EEMACOMC}}$	54.38±5.97	0.251±0.023	48234.76±1031.65
0.5	P$_{\text{EEMACOMP}}$	86.28±1.36	0.062±0.005	59649.56± 823.69
	P$_{\text{EEMACOMH}}$	83.75±1.34	0.065±0.006	58284.28± 864.32
	P$_{\text{EEMACOMC}}$	82.38±1.97	0.067±0.006	55127.83± 776.23
0.7	P$_{\text{EEMACOMP}}$	89.72±1.02	0.067±0.006	58124.34± 975.87
	P$_{\text{EEMACOMH}}$	87.65±1.03	0.069±0.006	59658.24± 675.21
	P$_{\text{EEMACOMC}}$	87.72±1.57	0.073±0.007	54354.12± 855.12
0.9	P$_{\text{EEMACOMP}}$	91.75±1.34	0.082±0.007	54287.38± 876.82
	P$_{\text{EEMACOMH}}$	88.23±1.65	0.079±0.008	53129.12± 995.34
	P$_{\text{EEMACOMC}}$	87.97±1.12	0.079±0.007	52876.21± 954.12

(b) $T_{sm} = 2$

r_0	$\mathcal{PF}$	$\bar{n}_{alg}$	$\bar{\varrho}$	$\bar{\xi}$
0.1	P$_{\text{EEMACOMP}}$	64.21±4.12	0.149±0.016	45123.28±1165.13
	P$_{\text{EEMACOMH}}$	60.28±3.89	0.198±0.018	46234.12±1026.45
	P$_{\text{EEMACOMC}}$	59.34±4.25	0.223±0.022	48234.15±1089.43
0.3	P$_{\text{EEMACOMP}}$	68.23±3.12	0.134±0.013	48123.24±1024.12
	P$_{\text{EEMACOMH}}$	63.45±4.16	0.153±0.015	46987.23±1054.23
	P$_{\text{EEMACOMC}}$	66.13±3.26	0.178±0.013	49134.73±1012.34
0.5	P$_{\text{EEMACOMP}}$	92.12±1.12	0.058±0.005	57876.43± 834.12
	P$_{\text{EEMACOMH}}$	90.12±1.12	0.063±0.005	58724.45± 812.33
	P$_{\text{EEMACOMC}}$	89.28±1.27	0.061±0.006	58827.14± 761.41
0.7	P$_{\text{EEMACOMP}}$	95.24 ±0.89	0.062±0.006	58824.12± 946.56
	P$_{\text{EEMACOMH}}$	90.43±0.98	0.068±0.007	57239.15± 667.21
	P$_{\text{EEMACOMC}}$	91.34±1.02	0.065±0.006	56431.12± 765.13
0.9	P$_{\text{EEMACOMP}}$	93.84±0.76	0.071±0.006	56128.13± 898.83
	P$_{\text{EEMACOMH}}$	89.11±1.02	0.073±0.007	55321.26± 965.12
	P$_{\text{EEMACOMC}}$	89.12±1.05	0.074±0.006	54132.15± 875.11

(c) $T_{sm} = 3$

r_0	$\mathcal{PF}$	$\bar{n}_{alg}$	$\bar{\varrho}$	$\bar{\xi}$
0.1	P$_{\text{EEMACOMP}}$	85.23±1.23	0.028±0.005	48234.35± 897.56
	P$_{\text{EEMACOMH}}$	80.35±1.69	0.032±0.006	51167.54± 896.37
	P$_{\text{EEMACOMC}}$	76.12±2.12	0.031±0.006	52342.28± 897.45
0.3	P$_{\text{EEMACOMP}}$	86.34±1.06	0.030±0.006	52347.32±1012.23
	P$_{\text{EEMACOMH}}$	82.87±1.23	0.034±0.007	49258.87±1017.85
	P$_{\text{EEMACOMC}}$	84.18±1.18	0.037±0.005	53276.34± 987.23
0.5	P$_{\text{EEMACOMP}}$	96.19±0.89	0.032±0.003	62345.17± 342.67
	P$_{\text{EEMACOMH}}$	94.24±1.04	0.035±0.003	62126.65± 342.43
	P$_{\text{EEMACOMC}}$	92.45±1.08	0.034±0.004	61897.24± 376.43
0.7	P$_{\text{EEMACOMP}}$	98.32±0.81	0.039±0.005	61763.28± 432.17
	P$_{\text{EEMACOMH}}$	96.67±0.91	0.042±0.006	61348.68± 327.56
	P$_{\text{EEMACOMC}}$	93.38±0.99	0.043±0.006	60897.74± 467.36
0.9	P$_{\text{EEMACOMP}}$	94.83±0.76	0.048±0.008	58321.46± 459.31
	P$_{\text{EEMACOMH}}$	92.45±0.83	0.062±0.009	57387.54± 543.26
	P$_{\text{EEMACOMC}}$	90.89±0.89	0.065±0.008	56428.43± 543.35

(d) $T_{sm} = 4$

r_0	$\mathcal{PF}$	$\bar{n}_{alg}$	$\bar{\varrho}$	$\bar{\xi}$
0.1	P$_{\text{EEMACOMP}}$	99.34±0.14	0.025±0.002	56235.43±687.43
	P$_{\text{EEMACOMH}}$	99.45±0.18	0.029±0.003	57832.12±567.23
	P$_{\text{EEMACOMC}}$	99.34±0.21	0.026±0.003	58432.25±563.21
0.3	P$_{\text{EEMACOMP}}$	98.89±0.87	0.028±0.003	56886.31±761.26
	P$_{\text{EEMACOMH}}$	97.87±1.03	0.030±0.004	59112.21±623.75
	P$_{\text{EEMACOMC}}$	98.32±1.07	0.027±0.005	59124.41±682.65
0.5	P$_{\text{EEMACOMP}}$	99.89±0.07	0.029±0.003	63126.26±298.12
	P$_{\text{EEMACOMH}}$	98.76±1.14	0.031±0.003	62234.67±307.21
	P$_{\text{EEMACOMC}}$	99.43±0.38	0.027±0.002	64123.32±187.23
0.7	P$_{\text{EEMACOMP}}$	99.21±0.45	0.038±0.005	63654.21±321.21
	P$_{\text{EEMACOMH}}$	98.97±0.67	0.040±0.005	62312.35±235.65
	P$_{\text{EEMACOMC}}$	99.25±0.63	0.041±0.006	63897.45±256.32
0.9	P$_{\text{EEMACOMP}}$	96.87±0.93	0.045±0.008	60123.34±378.54
	P$_{\text{EEMACOMH}}$	96.56±0.87	0.048±0.010	61234.32±231.33
	P$_{\text{EEMACOMC}}$	97.78±1.25	0.057±0.010	58765.34±431.29

(e) $T_{sm} = 5$

r_0	$\mathcal{PF}$	$\bar{n}_{alg}$	$\bar{\varrho}$	$\bar{\xi}$
0.1	P$_{\text{EEMACOMP}}$	99.42±0.17	0.024±0.002	56198.78±679.53
	P$_{\text{EEMACOMH}}$	99.64±0.13	0.028±0.004	57832.12±558.98
	P$_{\text{EEMACOMC}}$	99.57±0.12	0.026±0.003	58532.67±560.76
0.3	P$_{\text{EEMACOMP}}$	99.81±0.16	0.026±0.003	56897.34±743.21
	P$_{\text{EEMACOMH}}$	99.78±0.15	0.029±0.004	59123.13±617.45
	P$_{\text{EEMACOMC}}$	98.99±0.59	0.026±0.004	59123.41±676.46
0.5	P$_{\text{EEMACOMP}}$	99.67±0.28	0.026±0.002	63561.36±264.39
	P$_{\text{EEMACOMH}}$	99.45±0.46	0.030±0.004	62247.56±275.34
	P$_{\text{EEMACOMC}}$	99.76±0.04	0.026±0.002	65234.12± 97.24
0.7	P$_{\text{EEMACOMP}}$	99.26±0.37	0.036±0.004	63654.43±302.13
	P$_{\text{EEMACOMH}}$	99.78±0.08	0.038±0.006	62415.45±212.34
	P$_{\text{EEMACOMC}}$	99.64±0.06	0.039±0.005	63912.34±203.31
0.9	P$_{\text{EEMACOMP}}$	99.75±0.07	0.045±0.008	60896.12±371.23
	P$_{\text{EEMACOMH}}$	99.76±0.06	0.048±0.010	61431.34±212.38
	P$_{\text{EEMACOMC}}$	99.68±0.12	0.057±0.010	59249.23±397.32

(f) $T_{sm} = 6$

r_0	$\mathcal{PF}$	$\bar{n}_{alg}$	$\bar{\varrho}$	$\bar{\xi}$
0.1	P$_{\text{EEMACOMP}}$	99.65±0.12	0.024±0.003	56987.24±613.65
	P$_{\text{EEMACOMH}}$	99.78±0.09	0.027±0.003	58182.41±521.45
	P$_{\text{EEMACOMC}}$	99.86±0.02	0.025±0.003	59326.48±489.49
0.3	P$_{\text{EEMACOMP}}$	99.88±0.02	0.026±0.002	56896.32±761.26
	P$_{\text{EEMACOMH}}$	99.89±0.01	0.028±0.004	59123.12±623.75
	P$_{\text{EEMACOMC}}$	99.98±0.01	0.027±0.003	59123.41±682.65
0.5	P$_{\text{EEMACOMP}}$	99.90±0.02	0.026±0.002	63673.29±264.25
	P$_{\text{EEMACOMH}}$	99.68±0.07	0.027±0.003	62345.12±219.28
	P$_{\text{EEMACOMC}}$	99.81±0.05	0.025±0.002	63592.15± 87.34
0.7	P$_{\text{EEMACOMP}}$	99.83±0.07	0.033±0.005	63687.32±276.12
	P$_{\text{EEMACOMH}}$	99.82±0.09	0.034±0.005	62234.23±201.21
	P$_{\text{EEMACOMC}}$	99.78±0.07	0.036±0.006	63943.21±178.32
0.9	P$_{\text{EEMACOMP}}$	99.82±0.03	0.041±0.007	60993.49±389.45
	P$_{\text{EEMACOMH}}$	99.79±0.04	0.044±0.009	61431.87±209.21
	P$_{\text{EEMACOMC}}$	99.84±0.03	0.050±0.009	59789.67±334.98

Table D.5: Influence of parameter r_0 on the $\bar{n}_{alg}$, $\bar{\varrho}$ and $\bar{\xi}$ metrics, for 30 nodes and $R_g = 500$

(a) $T_{sm} = 1$

r_0	$\mathcal{PF}$	$\bar{n}_{alg}$	$\bar{\varrho}$	ξ
0.1	P$_{\text{EEMACOMP}}$	56.23±6.14	0.227±0.025	46234.96±1236.24
	P$_{\text{EEMACOMH}}$	54.19±6.38	0.259±0.027	45534.36±1298.32
	P$_{\text{EEMACOMC}}$	51.67±6.68	0.279±0.029	48342.32±1129.75
0.3	P$_{\text{EEMACOMP}}$	60.12±4.49	0.192±0.016	49765.32±1139.31
	P$_{\text{EEMACOMH}}$	55.43±5.89	0.204±0.016	46743.46±1145.32
	P$_{\text{EEMACOMC}}$	52.32±6.32	0.264±0.022	49876.87±1012.61
0.5	P$_{\text{EEMACOMP}}$	96.43±1.03	0.062±0.006	63843.61±321.24
	P$_{\text{EEMACOMH}}$	94.65±1.26	0.064±0.008	63875.32±349.38
	P$_{\text{EEMACOMC}}$	96.39±1.05	0.074±0.008	62784.56±356.26
0.7	P$_{\text{EEMACOMP}}$	97.65±0.89	0.078±0.007	59234.74±621.74
	P$_{\text{EEMACOMH}}$	96.56±1.01	0.079±0.009	58421.32±666.23
	P$_{\text{EEMACOMC}}$	97.36±1.02	0.082±0.009	56389.32±701.32
0.9	P$_{\text{EEMACOMP}}$	93.34±1.23	0.089±0.009	56235.42±654.23
	P$_{\text{EEMACOMH}}$	92.32±1.25	0.082±0.011	55981.21±674.21
	P$_{\text{EEMACOMC}}$	90.61±1.30	0.084±0.013	54238.27±687.32

(b) $T_{sm} = 2$

r_0	$\mathcal{PF}$	$\bar{n}_{alg}$	$\bar{\varrho}$	ξ
0.1	P$_{\text{EEMACOMP}}$	62.11±4.59	0.168±0.015	46239.37±1053.24
	P$_{\text{EEMACOMH}}$	58.23±3.98	0.234±0.019	48341.65±1012.32
	P$_{\text{EEMACOMC}}$	57.21±4.76	0.243±0.024	49431.43±1074.21
0.3	P$_{\text{EEMACOMP}}$	67.12±3.19	0.149±0.019	49763.46±1013.34
	P$_{\text{EEMACOMH}}$	62.36±4.36	0.165±0.017	48754.25±1034.27
	P$_{\text{EEMACOMC}}$	64.28±3.69	0.184±0.019	49986.24±1003.65
0.5	P$_{\text{EEMACOMP}}$	95.35±1.09	0.047±0.006	63639.29±254.29
	P$_{\text{EEMACOMH}}$	94.22±1.02	0.050±0.006	64567.65±223.76
	P$_{\text{EEMACOMC}}$	96.43±0.96	0.053±0.008	63730.62±261.23
0.7	P$_{\text{EEMACOMP}}$	96.25±1.15	0.076±0.013	58598.45±431.23
	P$_{\text{EEMACOMH}}$	94.09±1.05	0.072±0.011	57123.32±436.43
	P$_{\text{EEMACOMC}}$	93.89±1.17	0.068±0.009	56428.23±452.31
0.9	P$_{\text{EEMACOMP}}$	92.34±0.87	0.078±0.012	58238.27±496.23
	P$_{\text{EEMACOMH}}$	91.23±1.28	0.076±0.011	57431.38±654.28
	P$_{\text{EEMACOMC}}$	91.38±1.28	0.079±0.012	56458.49±658.90

(c) $T_{sm} = 3$

r_0	$\mathcal{PF}$	$\bar{n}_{alg}$	$\bar{\varrho}$	ξ
0.1	P$_{\text{EEMACOMP}}$	82.34±1.45	0.041±0.005	50234.76±867.32
	P$_{\text{EEMACOMH}}$	78.76±1.78	0.036±0.004	53568.98±865.32
	P$_{\text{EEMACOMC}}$	75.14±2.14	0.034±0.005	53476.28±854.27
0.3	P$_{\text{EEMACOMP}}$	84.76±1.28	0.042±0.006	54127.54±895.64
	P$_{\text{EEMACOMH}}$	81.83±1.43	0.041±0.005	52378.74±934.21
	P$_{\text{EEMACOMC}}$	83.12±1.22	0.039±0.005	55274.71±953.43
0.5	P$_{\text{EEMACOMP}}$	94.54±0.94	0.042±0.005	65325.63±154.78
	P$_{\text{EEMACOMH}}$	94.69±1.13	0.041±0.006	65378.32±162.84
	P$_{\text{EEMACOMC}}$	93.42±1.17	0.040±0.006	65673.82±175.24
0.7	P$_{\text{EEMACOMP}}$	97.98±0.23	0.044±0.008	64512.65±248.54
	P$_{\text{EEMACOMH}}$	95.46±0.45	0.043±0.007	64256.27±234.63
	P$_{\text{EEMACOMC}}$	92.45±0.57	0.040±0.006	63459.29±257.38
0.9	P$_{\text{EEMACOMP}}$	92.65±0.79	0.046±0.009	60342.11±345.35
	P$_{\text{EEMACOMH}}$	91.78±0.87	0.058±0.012	59472.12±389.32
	P$_{\text{EEMACOMC}}$	90.65±1.16	0.061±0.013	59765.23±397.45

(d) $T_{sm} = 4$

r_0	$\mathcal{PF}$	$\bar{n}_{alg}$	$\bar{\varrho}$	ξ
0.1	P$_{\text{EEMACOMP}}$	98.12±0.25	0.032±0.002	58234.34±634.21
	P$_{\text{EEMACOMH}}$	97.13±0.24	0.033±0.003	59876.26±583.76
	P$_{\text{EEMACOMC}}$	97.34±0.28	0.030±0.002	59128.45±524.23
0.3	P$_{\text{EEMACOMP}}$	97.83±0.82	0.034±0.003	58983.24±687.12
	P$_{\text{EEMACOMH}}$	97.57±1.17	0.034±0.003	60862.42±568.23
	P$_{\text{EEMACOMC}}$	97.64±1.37	0.032±0.002	61347.68±547.89
0.5	P$_{\text{EEMACOMP}}$	98.86±0.45	0.038±0.004	64897.34±265.37
	P$_{\text{EEMACOMH}}$	99.27±0.17	0.043±0.005	64523.46±289.31
	P$_{\text{EEMACOMC}}$	98.96±0.43	0.046±0.005	65236.24±167.27
0.7	P$_{\text{EEMACOMP}}$	98.14±0.64	0.041±0.004	63865.23±196.78
	P$_{\text{EEMACOMH}}$	98.24±0.62	0.046±0.005	62896.48±227.34
	P$_{\text{EEMACOMC}}$	98.64±0.57	0.048±0.008	63985.34±223.47
0.9	P$_{\text{EEMACOMP}}$	95.75±1.03	0.053±0.007	61325.87±282.56
	P$_{\text{EEMACOMH}}$	95.72±1.23	0.062±0.006	61657.12±264.24
	P$_{\text{EEMACOMC}}$	96.34±1.39	0.067±0.007	60321.56±368.43

(e) $T_{sm} = 5$

r_0	$\mathcal{PF}$	$\bar{n}_{alg}$	$\bar{\varrho}$	ξ
0.1	P$_{\text{EEMACOMP}}$	99.80±0.06	0.028±0.003	58145.25±647.23
	P$_{\text{EEMACOMH}}$	99.72±0.07	0.029±0.004	58754.23±517.28
	P$_{\text{EEMACOMC}}$	99.65±0.15	0.027±0.003	59846.26±543.76
0.3	P$_{\text{EEMACOMP}}$	99.92±0.06	0.032±0.005	58754.38±712.35
	P$_{\text{EEMACOMH}}$	99.82±0.09	0.034±0.006	59876.26±617.45
	P$_{\text{EEMACOMC}}$	99.12±0.08	0.036±0.007	59976.39±643.43
0.5	P$_{\text{EEMACOMP}}$	99.86±0.28	0.036±0.006	65147.76±145.13
	P$_{\text{EEMACOMH}}$	99.48±0.36	0.040±0.007	65432.67±172.34
	P$_{\text{EEMACOMC}}$	99.70±0.13	0.042±0.008	65435.14±99.86
0.7	P$_{\text{EEMACOMP}}$	99.43±0.34	0.042±0.008	64567.81±231.21
	P$_{\text{EEMACOMH}}$	99.83±0.09	0.045±0.008	64541.26±216.31
	P$_{\text{EEMACOMC}}$	99.72±0.08	0.044±0.009	64125.36±213.24
0.9	P$_{\text{EEMACOMP}}$	99.85±0.06	0.052±0.012	62312.26±293.24
	P$_{\text{EEMACOMH}}$	99.87±0.06	0.057±0.014	62456.28±228.65
	P$_{\text{EEMACOMC}}$	99.88±0.06	0.064±0.015	61387.37±304.18

(f) $T_{sm} = 6$

r_0	$\mathcal{PF}$	$\bar{n}_{alg}$	$\bar{\varrho}$	ξ
0.1	P$_{\text{EEMACOMP}}$	99.90±0.01	0.027±0.002	58123.43±516.37
	P$_{\text{EEMACOMH}}$	99.92±0.02	0.028±0.003	59282.39±503.68
	P$_{\text{EEMACOMC}}$	99.99±0.01	0.028±0.003	59835.76±496.52
0.3	P$_{\text{EEMACOMP}}$	99.93±0.03	0.030±0.003	58126.39±524.42
	P$_{\text{EEMACOMH}}$	99.94±0.01	0.031±0.003	59581.18±512.32
	P$_{\text{EEMACOMC}}$	99.90±0.01	0.033±0.004	59765.36±534.27
0.5	P$_{\text{EEMACOMP}}$	99.94±0.03	0.035±0.004	65238.56±154.23
	P$_{\text{EEMACOMH}}$	99.79±0.04	0.037±0.004	65276.89±152.31
	P$_{\text{EEMACOMC}}$	99.83±0.04	0.036±0.005	65394.26±123.54
0.7	P$_{\text{EEMACOMP}}$	99.67±0.09	0.040±0.006	63876.35±223.41
	P$_{\text{EEMACOMH}}$	99.63±0.11	0.045±0.007	62784.43±213.41
	P$_{\text{EEMACOMC}}$	99.56±0.12	0.047±0.008	63978.27±147.23
0.9	P$_{\text{EEMACOMP}}$	99.73±0.03	0.051±0.008	61239.58±325.26
	P$_{\text{EEMACOMH}}$	99.72±0.03	0.054±0.009	61674.89±288.45
	P$_{\text{EEMACOMC}}$	99.80±0.02	0.062±0.010	59893.72±328.86

Table D.6: Influence of parameter r_0 on the $\bar{n}_{alg}$, $\bar{\varrho}$ and $\bar{\xi}$ metrics, for 30 nodes and $R_g = 800$

(a) $T_{sm} = 1$

r_0	$\mathcal{PF}$	$\bar{n}_{alg}$	$\bar{\varrho}$	$\bar{\xi}$
0.1	P$_{\text{EEMACOMP}}$	43.12±4.12	0.257±0.022	44123.34±1248.68
	P$_{\text{EEMACOMH}}$	34.76±5.23	0.278±0.024	43126.32±1305.34
	P$_{\text{EEMACOMC}}$	44.36±4.56	0.286±0.023	46651.67±1158.65
0.3	P$_{\text{EEMACOMP}}$	46.57±4.87	0.217±0.020	46238.52±1146.31
	P$_{\text{EEMACOMH}}$	38.24±6.03	0.232±0.021	44297.42±1167.29
	P$_{\text{EEMACOMC}}$	48.98±5.34	0.204±0.020	47147.65±1065.21
0.5	P$_{\text{EEMACOMP}}$	96.31±0.86	0.116±0.014	63573.38±363.25
	P$_{\text{EEMACOMH}}$	62.34±3.01	0.153±0.017	63743.85±356.38
	P$_{\text{EEMACOMC}}$	96.85±0.87	0.144±0.015	62341.52±387.41
0.7	P$_{\text{EEMACOMP}}$	96.87±0.84	0.135±0.015	56128.39±628.39
	P$_{\text{EEMACOMH}}$	61.28±3.06	0.176±0.018	56217.42±675.84
	P$_{\text{EEMACOMC}}$	96.84±0.91	0.163±0.017	57120.43±613.61
0.9	P$_{\text{EEMACOMP}}$	90.54±1.25	0.139±0.014	55742.67±658.54
	P$_{\text{EEMACOMH}}$	58.32±2.36	0.173±0.018	56236.28±689.45
	P$_{\text{EEMACOMC}}$	89.45±1.45	0.165±0.019	53760.31±698.42

(b) $T_{sm} = 2$

r_0	$\mathcal{PF}$	$\bar{n}_{alg}$	$\bar{\varrho}$	$\bar{\xi}$
0.1	P$_{\text{EEMACOMP}}$	45.25±4.49	0.235±0.021	44123.76±1076.45
	P$_{\text{EEMACOMH}}$	36.19±3.88	0.256±0.022	46237.57±1042.74
	P$_{\text{EEMACOMC}}$	46.63±4.77	0.264±0.024	47891.46±1097.63
0.3	P$_{\text{EEMACOMP}}$	52.98±3.65	0.189±0.019	49123.62±1021.53
	P$_{\text{EEMACOMH}}$	38.85±4.80	0.205±0.023	48124.74±1042.52
	P$_{\text{EEMACOMC}}$	61.37±3.98	0.198±0.016	48342.38±1023.53
0.5	P$_{\text{EEMACOMP}}$	95.43±1.32	0.094±0.008	63436.89±265.73
	P$_{\text{EEMACOMH}}$	47.67±1.89	0.152±0.012	64194.75±212.53
	P$_{\text{EEMACOMC}}$	97.28±1.32	0.129±0.009	63456.68±282.48
0.7	P$_{\text{EEMACOMP}}$	97.38±1.24	0.112±0.012	57428.85±542.53
	P$_{\text{EEMACOMH}}$	46.67±1.87	0.162±0.014	58024.76±548.59
	P$_{\text{EEMACOMC}}$	97.58±1.32	0.143±0.011	56197.76±567.89
0.9	P$_{\text{EEMACOMP}}$	92.27±1.32	0.104±0.014	56743.91±598.96
	P$_{\text{EEMACOMH}}$	46.28±1.28	0.158±0.013	57101.56±587.43
	P$_{\text{EEMACOMC}}$	91.38±1.28	0.138±0.011	56142.53±579.21

(c) $T_{sm} = 3$

r_0	$\mathcal{PF}$	$\bar{n}_{alg}$	$\bar{\varrho}$	$\bar{\xi}$
0.1	P$_{\text{EEMACOMP}}$	80.34±1.25	0.078±0.010	50142.09±887.31
	P$_{\text{EEMACOMH}}$	70.32±1.86	0.103±0.012	52386.48±884.29
	P$_{\text{EEMACOMC}}$	73.70±1.98	0.101±0.012	52568.36±867.32
0.3	P$_{\text{EEMACOMP}}$	82.79±1.18	0.081±0.010	53127.59±907.23
	P$_{\text{EEMACOMH}}$	72.74±1.47	0.108±0.010	51124.78±948.49
	P$_{\text{EEMACOMC}}$	82.45±1.28	0.106±0.010	53682.68±964.18
0.5	P$_{\text{EEMACOMP}}$	92.72±0.76	0.089±0.008	64897.65±164.73
	P$_{\text{EEMACOMH}}$	75.78±1.34	0.117±0.010	64161.46±168.31
	P$_{\text{EEMACOMC}}$	90.43±1.05	0.111±0.009	64678.54±189.52
0.7	P$_{\text{EEMACOMP}}$	98.27±0.17	0.098±0.009	62893.56±267.71
	P$_{\text{EEMACOMH}}$	73.43±1.51	0.138±0.012	62784.23±245.76
	P$_{\text{EEMACOMC}}$	97.84±0.62	0.123±0.011	62172.58±268.81
0.9	P$_{\text{EEMACOMP}}$	95.89±0.73	0.126±0.011	60194.33±367.30
	P$_{\text{EEMACOMH}}$	71.67±1.95	0.148±0.012	58634.87±395.44
	P$_{\text{EEMACOMC}}$	90.12±1.12	0.135±0.012	58025.76±403.29

(d) $T_{sm} = 4$

r_0	$\mathcal{PF}$	$\bar{n}_{alg}$	$\bar{\varrho}$	$\bar{\xi}$
0.1	P$_{\text{EEMACOMP}}$	82.33±1.16	0.065±0.004	51421.08±815.23
	P$_{\text{EEMACOMH}}$	45.12±1.76	0.096±0.011	52876.62±835.75
	P$_{\text{EEMACOMC}}$	74.81±1.84	0.081±0.009	52879.57±843.19
0.3	P$_{\text{EEMACOMP}}$	84.56±1.03	0.068±0.006	53864.62±863.28
	P$_{\text{EEMACOMH}}$	46.52±1.62	0.100±0.013	51671.49±931.76
	P$_{\text{EEMACOMC}}$	83.56±1.28	0.096±0.013	53783.18±918.38
0.5	P$_{\text{EEMACOMP}}$	98.67±0.64	0.078±0.009	65154.39±142.75
	P$_{\text{EEMACOMH}}$	50.34±1.61	0.103±0.013	65329.01±158.29
	P$_{\text{EEMACOMC}}$	98.65±0.72	0.105±0.011	65874.84±163.90
0.7	P$_{\text{EEMACOMP}}$	97.89±0.13	0.098±0.009	63162.30±178.23
	P$_{\text{EEMACOMH}}$	50.03±1.68	0.124±0.015	63812.28±164.23
	P$_{\text{EEMACOMC}}$	97.97±0.32	0.116±0.013	63976.23±168.13
0.9	P$_{\text{EEMACOMP}}$	96.12±0.70	0.112±0.010	61328.76±367.30
	P$_{\text{EEMACOMH}}$	47.48±2.13	0.137±0.015	59205.19±395.44
	P$_{\text{EEMACOMC}}$	92.61±1.23	0.130±0.013	58785.54±403.29

(e) $T_{sm} = 5$

r_0	$\mathcal{PF}$	$\bar{n}_{alg}$	$\bar{\varrho}$	$\bar{\xi}$
0.1	P$_{\text{EEMACOMP}}$	84.42±1.23	0.062±0.005	52241.12±764.27
	P$_{\text{EEMACOMH}}$	56.55±1.87	0.097±0.010	52985.93±798.45
	P$_{\text{EEMACOMC}}$	76.76±1.42	0.088±0.009	53129.52±754.18
0.3	P$_{\text{EEMACOMP}}$	86.45±1.01	0.066±0.006	54198.37±812.54
	P$_{\text{EEMACOMH}}$	58.89±1.84	0.101±0.011	52468.65±902.36
	P$_{\text{EEMACOMC}}$	85.58±1.12	0.099±0.010	54513.76±846.37
0.5	P$_{\text{EEMACOMP}}$	98.87±0.31	0.068±0.007	65253.36±134.76
	P$_{\text{EEMACOMH}}$	68.23±1.54	0.102±0.010	65367.28±146.78
	P$_{\text{EEMACOMC}}$	98.83±0.32	0.103±0.010	65886.36±154.67
0.7	P$_{\text{EEMACOMP}}$	96.86±0.63	0.074±0.007	63329.53±169.24
	P$_{\text{EEMACOMH}}$	65.23±1.74	0.107± 0.011	63883.34±166.28
	P$_{\text{EEMACOMC}}$	96.62±0.67	0.109±0.011	63998.29±162.67
0.9	P$_{\text{EEMACOMP}}$	97.23±0.62	0.070±0.007	61678.43±345.56
	P$_{\text{EEMACOMH}}$	64.42±1.86	0.110±0.012	59987.14±378.27
	P$_{\text{EEMACOMC}}$	94.67±1.01	0.113±0.013	59326.83±382.88

(f) $T_{sm} = 6$

r_0	$\mathcal{PF}$	$\bar{n}_{alg}$	$\bar{\varrho}$	$\bar{\xi}$
0.1	P$_{\text{EEMACOMP}}$	86.32±1.16	0.060±0.005	53441.17±715.76
	P$_{\text{EEMACOMH}}$	64.56±1.65	0.094±0.012	53142.56±767.43
	P$_{\text{EEMACOMC}}$	79.84±1.37	0.082±0.008	53897.43±735.36
0.3	P$_{\text{EEMACOMP}}$	89.76±0.97	0.064±0.005	56321.43±765.23
	P$_{\text{EEMACOMH}}$	67.43±1.65	0.100±0.009	54568.23±679.43
	P$_{\text{EEMACOMC}}$	88.75±1.03	0.087±0.008	58376.21±627.47
0.5	P$_{\text{EEMACOMP}}$	99.90±0.05	0.068±0.005	65731.34±132.56
	P$_{\text{EEMACOMH}}$	77.90±1.32	0.101±0.009	65302.24±138.21
	P$_{\text{EEMACOMC}}$	99.82±0.06	0.088±0.008	65285.43±146.27
0.7	P$_{\text{EEMACOMP}}$	98.83±0.08	0.076±0.006	63473.17±156.72
	P$_{\text{EEMACOMH}}$	75.34±1.45	0.108±0.011	63912.45±161.45
	P$_{\text{EEMACOMC}}$	97.85±0.13	0.097±0.009	64087.43±143.82
0.9	P$_{\text{EEMACOMP}}$	97.23±0.34	0.065±0.006	62061.43±327.31
	P$_{\text{EEMACOMH}}$	64.42±1.67	0.097±0.009	60129.65±356.73
	P$_{\text{EEMACOMC}}$	94.67±0.97	0.086±0.010	60459.37±362.78

Table D.7: Influence of parameter ρ_l on the $\bar{n}_{alg}$, $\bar{\varrho}$ and $\bar{\xi}$ metrics, for 30 nodes and $R_g = 300$

(a) $T_{sm} = 1$

ρ_l	$\mathcal{PF}$	$\bar{n}_{alg}$	$\bar{\varrho}$	ξ
0.1	P$_{\text{EEMACOMP}}$	55.34±5.12	0.203±0.021	44683.37±1237.31
	P$_{\text{EEMACOMH}}$	52.43±6.13	0.218±0.027	42478.34±1359.27
	P$_{\text{EEMACOMC}}$	50.67±6.22	0.248±0.022	45678.26±1198.47
0.3	P$_{\text{EEMACOMP}}$	60.59±4.02	0.163±0.012	48976.09±1179.18
	P$_{\text{EEMACOMH}}$	56.47±4.98	0.183±0.014	46390.56±1272.47
	P$_{\text{EEMACOMC}}$	52.69±5.16	0.224±0.020	49346.21±1078.43
0.5	P$_{\text{EEMACOMP}}$	93.59±1.09	0.065±0.006	62549.20± 210.37
	P$_{\text{EEMACOMH}}$	92.45±1.16	0.063±0.005	61843.22± 222.67
	P$_{\text{EEMACOMC}}$	91.75±1.21	0.062±0.007	62734.23± 185.48
0.7	P$_{\text{EEMACOMP}}$	87.62±1.06	0.060±0.006	62139.56± 187.25
	P$_{\text{EEMACOMH}}$	85.69±1.11	0.064±0.007	61372.73± 231.45
	P$_{\text{EEMACOMC}}$	87.12±1.12	0.063±0.007	63719.63± 145.62
0.9	P$_{\text{EEMACOMP}}$	84.24±1.28	0.096±0.008	50165.23± 887.41
	P$_{\text{EEMACOMH}}$	86.38±1.22	0.087±0.008	52345.78± 934.26
	P$_{\text{EEMACOMC}}$	86.72±1.17	0.088±0.009	53485.26± 976.25

(b) $T_{sm} = 2$

ρ_l	$\mathcal{PF}$	$\bar{n}_{alg}$	$\bar{\varrho}$	ξ
0.1	P$_{\text{EEMACOMP}}$	60.45±3.99	0.188±0.017	45893.24±1102.12
	P$_{\text{EEMACOMH}}$	61.34±3.65	0.205±0.019	46673.28±1003.37
	P$_{\text{EEMACOMC}}$	57.48±4.12	0.214±0.025	48657.27±1067.23
0.3	P$_{\text{EEMACOMP}}$	66.34±2.65	0.142±0.015	49985.34±1013.45
	P$_{\text{EEMACOMH}}$	61.32±3.69	0.162±0.016	48987.58±1034.63
	P$_{\text{EEMACOMC}}$	64.37±3.12	0.171±0.018	49896.47±1024.63
0.5	P$_{\text{EEMACOMP}}$	94.47±1.02	0.040±0.006	62984.23± 249.31
	P$_{\text{EEMACOMH}}$	90.38±1.15	0.039±0.006	61575.23± 275.52
	P$_{\text{EEMACOMC}}$	91.32±1.35	0.044±0.007	63473.28± 214.71
0.7	P$_{\text{EEMACOMP}}$	94.27±0.69	0.038±0.004	63243.56± 187.45
	P$_{\text{EEMACOMH}}$	91.82±0.85	0.040±0.005	61187.53± 197.37
	P$_{\text{EEMACOMC}}$	90.26±0.87	0.043±0.005	63385.32± 124.84
0.9	P$_{\text{EEMACOMP}}$	91.63±0.83	0.076±0.007	54127.83± 612.43
	P$_{\text{EEMACOMH}}$	85.28±1.07	0.078±0.007	55873.63± 603.45
	P$_{\text{EEMACOMC}}$	85.69±1.08	0.081±0.008	53486.28± 624.47

(c) $T_{sm} = 3$

ρ_l	$\mathcal{PF}$	$\bar{n}_{alg}$	$\bar{\varrho}$	ξ
0.1	P$_{\text{EEMACOMP}}$	72.29±2.54	0.167±0.015	47468.49±1043.32
	P$_{\text{EEMACOMH}}$	73.45±2.43	0.186±0.017	48654.12± 973.52
	P$_{\text{EEMACOMC}}$	68.64±2.05	0.194±0.021	47643.15±1023.54
0.3	P$_{\text{EEMACOMP}}$	79.32±2.34	0.122±0.012	50237.54± 926.32
	P$_{\text{EEMACOMH}}$	74.56±2.67	0.135±0.013	49675.32± 963.28
	P$_{\text{EEMACOMC}}$	76.63±3.03	0.162±0.015	51254.52± 912.74
0.5	P$_{\text{EEMACOMP}}$	96.53±0.49	0.033±0.002	63421.43± 236.41
	P$_{\text{EEMACOMH}}$	94.31±0.45	0.036±0.004	61142.32± 312.42
	P$_{\text{EEMACOMC}}$	91.74±0.89	0.035±0.003	63372.15± 238.21
0.7	P$_{\text{EEMACOMP}}$	95.12±0.53	0.037±0.002	62134.63± 237.83
	P$_{\text{EEMACOMH}}$	92.52±0.74	0.040±0.003	60287.16± 257.48
	P$_{\text{EEMACOMC}}$	92.24±0.76	0.041±0.003	62315.36± 223.64
0.9	P$_{\text{EEMACOMP}}$	92.89±0.83	0.070±0.006	56367.32± 532.16
	P$_{\text{EEMACOMH}}$	88.84±1.07	0.071±0.006	57342.75± 523.63
	P$_{\text{EEMACOMC}}$	87.73±1.08	0.076±0.008	55634.27± 546.72

(d) $T_{sm} = 4$

ρ_l	$\mathcal{PF}$	$\bar{n}_{alg}$	$\bar{\varrho}$	ξ
0.1	P$_{\text{EEMACOMP}}$	84.65±2.34	0.132±0.012	50238.42±1043.32
	P$_{\text{EEMACOMH}}$	83.89±2.37	0.151±0.017	50123.52± 962.53
	P$_{\text{EEMACOMC}}$	89.85±2.13	0.153±0.016	48532.19±1023.54
0.3	P$_{\text{EEMACOMP}}$	81.32±2.13	0.114±0.011	51429.73± 875.34
	P$_{\text{EEMACOMH}}$	86.87±2.43	0.126±0.011	50873.28± 879.45
	P$_{\text{EEMACOMC}}$	80.63±2.67	0.139±0.013	52389.29± 861.38
0.5	P$_{\text{EEMACOMP}}$	98.43±0.38	0.029±0.002	63428.52± 167.29
	P$_{\text{EEMACOMH}}$	96.84±0.42	0.033±0.003	62314.53± 173.59
	P$_{\text{EEMACOMC}}$	94.76±0.43	0.030±0.003	63753.41± 165.25
0.7	P$_{\text{EEMACOMP}}$	96.72±0.47	0.034±0.002	62236.73± 194.23
	P$_{\text{EEMACOMH}}$	94.41±0.52	0.038±0.003	60574.29± 223.56
	P$_{\text{EEMACOMC}}$	93.28±0.61	0.036±0.002	62639.29± 196.49
0.9	P$_{\text{EEMACOMP}}$	93.56±0.66	0.065±0.006	58894.29± 438.09
	P$_{\text{EEMACOMH}}$	89.94±0.87	0.063±0.005	58674.39± 476.28
	P$_{\text{EEMACOMC}}$	89.43±0.86	0.067±0.007	56879.34± 487.19

(e) $T_{sm} = 5$

ρ_l	$\mathcal{PF}$	$\bar{n}_{alg}$	$\bar{\varrho}$	ξ
0.1	P$_{\text{EEMACOMP}}$	93.24±0.92	0.075±0.009	55287.12±612.39
	P$_{\text{EEMACOMH}}$	94.38±0.93	0.086±0.010	56289.33±605.28
	P$_{\text{EEMACOMC}}$	94.36±0.81	0.096±0.012	56498.39±606.34
0.3	P$_{\text{EEMACOMP}}$	90.49±1.62	0.046±0.007	58723.29±484.03
	P$_{\text{EEMACOMH}}$	92.21±1.34	0.059±0.008	57128.83±497.23
	P$_{\text{EEMACOMC}}$	92.47±1.58	0.068±0.009	56294.29±538.28
0.5	P$_{\text{EEMACOMP}}$	99.99±0.03	0.027±0.002	63484.56±138.28
	P$_{\text{EEMACOMH}}$	99.99±0.04	0.028±0.002	62226.38±174.28
	P$_{\text{EEMACOMC}}$	99.99±0.03	0.026±0.002	64138.39±132.38
0.7	P$_{\text{EEMACOMP}}$	98.97±0.32	0.027±0.002	62873.28±184.29
	P$_{\text{EEMACOMH}}$	97.76±0.47	0.030±0.003	61348.06±209.36
	P$_{\text{EEMACOMC}}$	98.87±0.29	0.024±0.002	63102.37±167.28
0.9	P$_{\text{EEMACOMP}}$	96.48±0.45	0.045±0.005	60342.11±217.38
	P$_{\text{EEMACOMH}}$	97.52±0.39	0.037±0.005	61238.40±227.38
	P$_{\text{EEMACOMC}}$	96.85±0.23	0.046±0.006	61469.03±267.28

(f) $T_{sm} = 6$

ρ_l	$\mathcal{PF}$	$\bar{n}_{alg}$	$\bar{\varrho}$	ξ
0.1	P$_{\text{EEMACOMP}}$	94.23±1.02	0.070±0.009	54376.53±873.23
	P$_{\text{EEMACOMH}}$	93.76±1.03	0.076±0.010	53276.37±892.73
	P$_{\text{EEMACOMC}}$	97.63±0.89	0.084±0.010	52156.89±912.32
0.3	P$_{\text{EEMACOMP}}$	93.25±1.03	0.040±0.008	55897.32±782.37
	P$_{\text{EEMACOMH}}$	96.34±0.92	0.055±0.010	54562.38±794.52
	P$_{\text{EEMACOMC}}$	97.42±0.97	0.063±0.012	53896.31±822.57
0.5	P$_{\text{EEMACOMP}}$	99.99±0.04	0.026±0.002	63456.29±169.48
	P$_{\text{EEMACOMH}}$	99.99±0.05	0.027±0.003	62296.32±196.49
	P$_{\text{EEMACOMC}}$	99.99±0.02	0.026±0.002	63767.29±172.31
0.7	P$_{\text{EEMACOMP}}$	98.86±0.36	0.027±0.002	62576.34±196.74
	P$_{\text{EEMACOMH}}$	98.87±0.43	0.026±0.003	60867.29±217.45
	P$_{\text{EEMACOMC}}$	98.58±0.26	0.024±0.002	62832.27±198.93
0.9	P$_{\text{EEMACOMP}}$	96.45±0.45	0.043±0.003	59132.34±234.73
	P$_{\text{EEMACOMH}}$	97.93±0.39	0.035±0.003	59675.23±239.02
	P$_{\text{EEMACOMC}}$	98.38±0.23	0.044±0.004	58739.28±324.53

Table D.8: Influence of parameter ρ_l on the $\bar{n}_{alg}$, $\bar{\varrho}$ and $\bar{\xi}$ metrics, for 30 nodes and $R_g = 500$

(a) $T_{sm} = 1$

ρ_l	$\mathcal{PF}$	$\bar{n}_{alg}$	$\bar{\varrho}$	ξ
0.1	P$_{\text{EEMACOMP}}$	57.24±4.38	0.214±0.023	48425.14±1028.39
	P$_{\text{EEMACOMH}}$	55.32±5.30	0.229±0.029	47542.46±1145.29
	P$_{\text{EEMACOMC}}$	51.34±5.29	0.257±0.024	49428.31±1112.41
0.3	P$_{\text{EEMACOMP}}$	62.31±4.01	0.187±0.014	53276.28± 943.28
	P$_{\text{EEMACOMH}}$	56.23±4.36	0.194±0.016	49763.29± 995.24
	P$_{\text{EEMACOMC}}$	52.61±5.06	0.232±0.020	52376.29± 968.38
0.5	P$_{\text{EEMACOMP}}$	94.29±1.13	0.063±0.006	63378.20± 224.29
	P$_{\text{EEMACOMH}}$	88.98±1.17	0.062±0.006	62268.38± 229.10
	P$_{\text{EEMACOMC}}$	87.11±1.18	0.078±0.008	63965.32± 213.60
0.7	P$_{\text{EEMACOMP}}$	93.28±0.96	0.062±0.005	63489.29± 156.39
	P$_{\text{EEMACOMH}}$	89.24±0.98	0.065±0.007	62318.39± 197.30
	P$_{\text{EEMACOMC}}$	88.39±1.02	0.076±0.008	64231.72± 143.10
0.9	P$_{\text{EEMACOMP}}$	87.29±1.15	0.098±0.011	54519.21± 843.56
	P$_{\text{EEMACOMH}}$	86.49±1.17	0.086±0.009	55289.16± 861.28
	P$_{\text{EEMACOMC}}$	86.98±1.18	0.085±0.009	56534.29± 824.49

(b) $T_{sm} = 2$

ρ_l	$\mathcal{PF}$	$\bar{n}_{alg}$	$\bar{\varrho}$	ξ
0.1	P$_{\text{EEMACOMP}}$	65.38±3.99	0.193±0.019	50476.29±976.23
	P$_{\text{EEMACOMH}}$	64.29±3.65	0.209±0.019	51289.38±964.23
	P$_{\text{EEMACOMC}}$	59.18±4.12	0.202±0.026	53287.38±943.27
0.3	P$_{\text{EEMACOMP}}$	71.28±2.65	0.154±0.017	54673.28± 942.32
	P$_{\text{EEMACOMH}}$	67.39±3.69	0.173±0.018	56987.29± 854.25
	P$_{\text{EEMACOMC}}$	69.28±3.12	0.182±0.019	53278.29±947.43
0.5	P$_{\text{EEMACOMP}}$	97.65±0.63	0.049±0.008	63986.23±247.45
	P$_{\text{EEMACOMH}}$	96.49±0.79	0.048±0.008	64289.39±232.65
	P$_{\text{EEMACOMC}}$	98.37±0.53	0.056±0.009	64612.48±217.45
0.7	P$_{\text{EEMACOMP}}$	98.27±0.26	0.048±0.007	64378.28±132.46
	P$_{\text{EEMACOMH}}$	97.39±0.28	0.050±0.007	64231.29±126.39
	P$_{\text{EEMACOMC}}$	96.49±0.68	0.055±0.008	64538.29±122.84
0.9	P$_{\text{EEMACOMP}}$	93.47±0.76	0.079±0.007	58156.28±534.23
	P$_{\text{EEMACOMH}}$	88.32±1.02	0.082±0.007	58249.42±537.49
	P$_{\text{EEMACOMC}}$	85.85±1.01	0.084±0.008	56754.48±527.30

(c) $T_{sm} = 3$

ρ_l	$\mathcal{PF}$	$\bar{n}_{alg}$	$\bar{\varrho}$	ξ
0.1	P$_{\text{EEMACOMP}}$	70.34±2.58	0.186±0.016	55342.31±436.35
	P$_{\text{EEMACOMH}}$	71.43±2.51	0.197±0.018	56349.29±423.72
	P$_{\text{EEMACOMC}}$	65.39±2.26	0.199±0.020	54892.36±437.89
0.3	P$_{\text{EEMACOMP}}$	76.78±2.43	0.146±0.013	58765.36±379.28
	P$_{\text{EEMACOMH}}$	75.58±2.87	0.164±0.013	58764.28±389.45
	P$_{\text{EEMACOMC}}$	74.28±3.12	0.178±0.014	61368.48±342.71
0.5	P$_{\text{EEMACOMP}}$	96.28±0.47	0.042±0.002	63856.29±265.29
	P$_{\text{EEMACOMH}}$	94.34±0.48	0.046±0.003	62489.49±248.49
	P$_{\text{EEMACOMC}}$	95.71±0.92	0.047±0.003	64128.23±217.39
0.7	P$_{\text{EEMACOMP}}$	93.48±0.55	0.040±0.002	62562.39±227.38
	P$_{\text{EEMACOMH}}$	91.48±0.73	0.042±0.002	62340.57±227.43
	P$_{\text{EEMACOMC}}$	91.89±0.72	0.043±0.003	62873.29±243.23
0.9	P$_{\text{EEMACOMP}}$	92.12±0.75	0.076±0.005	59127.85±387.36
	P$_{\text{EEMACOMH}}$	88.13±1.02	0.078±0.005	61378.27±363.81
	P$_{\text{EEMACOMC}}$	86.38±1.01	0.079±0.007	60321.76±338.29

(d) $T_{sm} = 4$

ρ_l	$\mathcal{PF}$	$\bar{n}_{alg}$	$\bar{\varrho}$	ξ
0.1	P$_{\text{EEMACOMP}}$	81.43±2.38	0.152±0.014	58245.56±532.54
	P$_{\text{EEMACOMH}}$	81.62±2.39	0.165±0.018	57845.39±523.58
	P$_{\text{EEMACOMC}}$	86.27±2.16	0.173±0.018	56398.29±611.26
0.3	P$_{\text{EEMACOMP}}$	80.16±2.19	0.126±0.013	59783.21±267.39
	P$_{\text{EEMACOMH}}$	84.68±2.48	0.135±0.012	58321.34±246.38
	P$_{\text{EEMACOMC}}$	78.38±2.69	0.148±0.015	60341.38±234.56
0.5	P$_{\text{EEMACOMP}}$	97.29±0.39	0.040±0.003	64211.52±126.39
	P$_{\text{EEMACOMH}}$	95.93±0.44	0.046±0.004	64287.29±125.67
	P$_{\text{EEMACOMC}}$	93.28±0.47	0.048±0.004	64231.76±123.56
0.7	P$_{\text{EEMACOMP}}$	94.28±0.49	0.037±0.002	63128.45±174.29
	P$_{\text{EEMACOMH}}$	92.34±0.56	0.039±0.003	62657.12±209.31
	P$_{\text{EEMACOMC}}$	92.46±0.64	0.039±0.003	63105.58±175.30
0.9	P$_{\text{EEMACOMP}}$	92.47±0.68	0.074±0.006	59873.28±358.20
	P$_{\text{EEMACOMH}}$	89.13±0.89	0.078±0.007	59765.39±386.29
	P$_{\text{EEMACOMC}}$	89.12±0.89	0.079±0.007	58768.34±376.20

(e) $T_{sm} = 5$

ρ_l	$\mathcal{PF}$	$\bar{n}_{alg}$	$\bar{\varrho}$	ξ
0.1	P$_{\text{EEMACOMP}}$	86.34±1.56	0.081±0.009	59134.28±387.31
	P$_{\text{EEMACOMH}}$	85.29±1.67	0.087±0.011	59629.22±376.23
	P$_{\text{EEMACOMC}}$	87.26±1.74	0.098±0.014	58987.34±386.29
0.3	P$_{\text{EEMACOMP}}$	88.21±0.87	0.056±0.007	60235.39±332.45
	P$_{\text{EEMACOMH}}$	88.76±0.86	0.064±0.007	60341.67±334.74
	P$_{\text{EEMACOMC}}$	89.12±0.79	0.075±0.009	61329.45±317.29
0.5	P$_{\text{EEMACOMP}}$	99.99±0.02	0.038±0.002	63897.34±113.52
	P$_{\text{EEMACOMH}}$	99.99±0.02	0.043±0.003	64126.67±164.29
	P$_{\text{EEMACOMC}}$	99.99±0.02	0.042±0.003	64435.34±143.19
0.7	P$_{\text{EEMACOMP}}$	96.64±0.33	0.034±0.003	62436.37±164.28
	P$_{\text{EEMACOMH}}$	95.34±0.49	0.035±0.003	61283.17±187.39
	P$_{\text{EEMACOMC}}$	96.35±0.29	0.029±0.002	63451.38±174.28
0.9	P$_{\text{EEMACOMP}}$	95.89±0.46	0.049±0.006	61204.25±189.28
	P$_{\text{EEMACOMH}}$	96.34±0.43	0.046±0.006	61654.29±185.28
	P$_{\text{EEMACOMC}}$	96.73±0.24	0.049±0.007	61859.14±187.28

(f) $T_{sm} = 6$

ρ_l	$\mathcal{PF}$	$\bar{n}_{alg}$	$\bar{\varrho}$	ξ
0.1	P$_{\text{EEMACOMP}}$	93.17±1.06	0.074±0.010	60124.32±432.11
	P$_{\text{EEMACOMH}}$	93.13±1.05	0.082±0.011	58491.67±539.03
	P$_{\text{EEMACOMC}}$	97.14±0.92	0.093±0.012	59247.38±543.85
0.3	P$_{\text{EEMACOMP}}$	92.35±1.07	0.054±0.006	60975.12±332.81
	P$_{\text{EEMACOMH}}$	96.39±0.94	0.060±0.007	59728.34±396.58
	P$_{\text{EEMACOMC}}$	96.26±0.99	0.067±0.008	58347.98±354.67
0.5	P$_{\text{EEMACOMP}}$	99.99±0.02	0.037±0.003	65123.45±146.76
	P$_{\text{EEMACOMH}}$	99.99±0.02	0.040±0.004	64598.26±175.73
	P$_{\text{EEMACOMC}}$	99.99±0.02	0.038 ±0.003	64897.16±134.76
0.7	P$_{\text{EEMACOMP}}$	97.15±0.39	0.034±0.003	63785.26±186.39
	P$_{\text{EEMACOMH}}$	97.12±0.46	0.032±0.002	61349.39±187.32
	P$_{\text{EEMACOMC}}$	98.13±0.28	0.029±0.002	63412.90±165.28
0.9	P$_{\text{EEMACOMP}}$	97.12±0.48	0.049±0.006	60245.21±224.65
	P$_{\text{EEMACOMH}}$	98.23±0.43	0.047±0.006	60276.54±228.48
	P$_{\text{EEMACOMC}}$	98.16±0.24	0.042±0.007	59875.20±315.68

Table D.9: Influence of parameter ρ_l on the $\bar{n}_{alg}$, $\bar{\varrho}$ and $\bar{\xi}$ metrics, for 30 nodes and $R_g = 800$

(a) $T_{sm} = 1$

ρ_l	$\mathcal{PF}$	$\bar{n}_{alg}$	$\bar{\varrho}$	ξ
0.1	P$_{\text{EEMACOMP}}$	50.23±4.87	0.245±0.025	46327.43±1067.12
	P$_{\text{EEMACOMH}}$	38.23±6.78	0.246±0.027	46528.31±1178.34
	P$_{\text{EEMACOMC}}$	43.56±5.45	0.287±0.028	47623.63±1137.20
0.3	P$_{\text{EEMACOMP}}$	57.23±4.83	0.223±0.019	52387.41± 964.29
	P$_{\text{EEMACOMH}}$	43.51±6.34	0.213±0.018	47392.09± 996.62
	P$_{\text{EEMACOMC}}$	43.27±5.59	0.249±0.023	50230.71± 979.45
0.5	P$_{\text{EEMACOMP}}$	89.46±1.45	0.126±0.017	62345.26± 248.39
	P$_{\text{EEMACOMH}}$	52.45±2.45	0.152±0.019	61327.87± 269.29
	P$_{\text{EEMACOMC}}$	86.35±1.53	0.147±0.018	62391.34± 236.51
0.7	P$_{\text{EEMACOMP}}$	90.45±0.99	0.117±0.016	62315.36± 168.30
	P$_{\text{EEMACOMH}}$	56.21±1.78	0.154±0.018	61651.67± 199.97
	P$_{\text{EEMACOMC}}$	85.37±1.24	0.145±0.017	62316.76± 165.38
0.9	P$_{\text{EEMACOMP}}$	85.23±1.37	0.145±0.017	52341.67± 867.25
	P$_{\text{EEMACOMH}}$	52.45±1.46	0.167±0.019	53720.56± 887.34
	P$_{\text{EEMACOMC}}$	82.37±1.40	0.154±0.018	54592.46± 865.29

(b) $T_{sm} = 2$

ρ_l	$\mathcal{PF}$	$\bar{n}_{alg}$	$\bar{\varrho}$	ξ
0.1	P$_{\text{EEMACOMP}}$	61.34±2.76	0.234±0.023	50416.83±983.12
	P$_{\text{EEMACOMH}}$	34.45±3.69	0.228±0.022	50598.30±915.84
	P$_{\text{EEMACOMC}}$	56.47±2.68	0.224±0.023	52783.62±937.75
0.3	P$_{\text{EEMACOMP}}$	67.45±1.87	0.168±0.018	53247.83±869.23
	P$_{\text{EEMACOMH}}$	36.12±3.87	0.197±0.021	55127.84±854.25
	P$_{\text{EEMACOMC}}$	66.31±2.34	0.198±0.022	52134.74±875.84
0.5	P$_{\text{EEMACOMP}}$	95.42±1.21	0.097±0.010	63687.36±157.23
	P$_{\text{EEMACOMH}}$	45.56±2.35	0.152±0.014	64165.67±135.28
	P$_{\text{EEMACOMC}}$	96.23±1.23	0.130±0.012	64151.75±147.82
0.7	P$_{\text{EEMACOMP}}$	96.34±0.67	0.094±0.009	64132.87±138.43
	P$_{\text{EEMACOMH}}$	46.56±2.38	0.150±0.013	64124.36±128.38
	P$_{\text{EEMACOMC}}$	94.28±0.97	0.132±0.012	64256.97±137.83
0.9	P$_{\text{EEMACOMP}}$	92.45±0.98	0.123±0.012	58102.65±524.47
	P$_{\text{EEMACOMH}}$	44.59±1.57	0.154±0.014	58168.35±557.85
	P$_{\text{EEMACOMC}}$	82.67±1.13	0.143±0.014	56637.19±548.29

(c) $T_{sm} = 3$

ρ_l	$\mathcal{PF}$	$\bar{n}_{alg}$	$\bar{\varrho}$	ξ
0.1	P$_{\text{EEMACOMP}}$	67.39±2.89	0.198±0.020	55894.10±413.45
	P$_{\text{EEMACOMH}}$	60.29±3.28	0.215±0.021	56764.20±428.40
	P$_{\text{EEMACOMC}}$	61.34±2.57	0.216±0.022	56230.41±457.12
0.3	P$_{\text{EEMACOMP}}$	72.76±2.68	0.165±0.016	60356.76±365.20
	P$_{\text{EEMACOMH}}$	67.23±3.56	0.187±0.018	60345.56±374.12
	P$_{\text{EEMACOMC}}$	72.45±2.87	0.194±0.021	61846.27±367.20
0.5	P$_{\text{EEMACOMP}}$	94.29±0.68	0.089±0.009	64389.29±167.34
	P$_{\text{EEMACOMH}}$	75.37±1.87	0.117±0.011	64298.57±178.27
	P$_{\text{EEMACOMC}}$	94.29±0.62	0.112±0.013	64129.34±176.27
0.7	P$_{\text{EEMACOMP}}$	91.45±0.85	0.082±0.008	63978.12±242.19
	P$_{\text{EEMACOMH}}$	70.32±1.26	0.109±0.011	62875.23±267.48
	P$_{\text{EEMACOMC}}$	90.65±0.76	0.105±0.011	63216.75±237.28
0.9	P$_{\text{EEMACOMP}}$	92.12±0.89	0.114±0.010	61268.47±289.47
	P$_{\text{EEMACOMH}}$	72.45±1.25	0.126±0.013	62346.63±275.28
	P$_{\text{EEMACOMC}}$	84.27±1.08	0.129±0.014	62561.37±256.29

(d) $T_{sm} = 4$

ρ_l	$\mathcal{PF}$	$\bar{n}_{alg}$	$\bar{\varrho}$	ξ
0.1	P$_{\text{EEMACOMP}}$	74.29±3.45	0.187±0.016	59754.25±523.42
	P$_{\text{EEMACOMH}}$	40.23±5.28	0.198±0.021	58673.88±523.65
	P$_{\text{EEMACOMC}}$	72.45±3.76	0.184±0.020	56498.49±634.29
0.3	P$_{\text{EEMACOMP}}$	77.43±2.46	0.164±0.018	60158.48±287.39
	P$_{\text{EEMACOMH}}$	43.42±4.78	0.162±0.018	59438.29±267.69
	P$_{\text{EEMACOMC}}$	75.32±3.75	0.137±0.017	60856.27±267.84
0.5	P$_{\text{EEMACOMP}}$	96.34±0.56	0.074±0.007	65237.29±112.54
	P$_{\text{EEMACOMH}}$	50.24±3.89	0.140±0.009	64012.46±122.59
	P$_{\text{EEMACOMC}}$	94.29±0.78	0.105±0.008	64784.57±117.45
0.7	P$_{\text{EEMACOMP}}$	93.64±0.87	0.067±0.004	63538.35±165.24
	P$_{\text{EEMACOMH}}$	48.45±0.76	0.126±0.008	62896.56±164.37
	P$_{\text{EEMACOMC}}$	90.34±0.84	0.083±0.007	63784.39±145.22
0.9	P$_{\text{EEMACOMP}}$	91.07±0.68	0.087±0.007	59675.32±278.34
	P$_{\text{EEMACOMH}}$	45.62±0.89	0.129±0.009	59347.84±267.93
	P$_{\text{EEMACOMC}}$	87.34±0.89	0.098±0.008	58986.67±297.48

(e) $T_{sm} = 5$

ρ_l	$\mathcal{PF}$	$\bar{n}_{alg}$	$\bar{\varrho}$	ξ
0.1	P$_{\text{EEMACOMP}}$	94.26±0.75	0.134±0.013	59843.25±297.45
	P$_{\text{EEMACOMH}}$	61.27±1.48	0.148±0.014	59834.76±285.36
	P$_{\text{EEMACOMC}}$	96.74±0.76	0.124±0.012	59876.30±227.69
0.3	P$_{\text{EEMACOMP}}$	98.54±0.56	0.125±0.012	60654.23±245.76
	P$_{\text{EEMACOMH}}$	64.27±1.43	0.138±0.013	60453.28±243.76
	P$_{\text{EEMACOMC}}$	98.67±0.46	0.127±0.011	61456.76±231.45
0.5	P$_{\text{EEMACOMP}}$	99.45±0.03	0.074±0.006	65142.45±109.50
	P$_{\text{EEMACOMH}}$	70.21±1.14	0.108±0.008	64984.21±128.59
	P$_{\text{EEMACOMC}}$	99.23±0.03	0.103±0.008	64793.24±124.53
0.7	P$_{\text{EEMACOMP}}$	98.14±0.35	0.065±0.004	62865.23±164.28
	P$_{\text{EEMACOMH}}$	66.34±1.46	0.089±0.007	61563.20±178.36
	P$_{\text{EEMACOMC}}$	98.27±0.32	0.096±0.007	63851.34±145.67
0.9	P$_{\text{EEMACOMP}}$	97.89±0.46	0.089±0.008	61673.87±182.41
	P$_{\text{EEMACOMH}}$	63.28±1.93	0.098±0.009	61874.30±178.37
	P$_{\text{EEMACOMC}}$	98.73±0.24	0.099±0.009	61812.67±176.34

(f) $T_{sm} = 6$

ρ_l	$\mathcal{PF}$	$\bar{n}_{alg}$	$\bar{\varrho}$	ξ
0.1	P$_{\text{EEMACOMP}}$	91.15±1.08	0.116±0.011	60867.92±387.29
	P$_{\text{EEMACOMH}}$	92.48±1.07	0.122±0.012	59786.20±419.34
	P$_{\text{EEMACOMC}}$	96.30±0.87	0.117±0.011	60589.20±396.16
0.3	P$_{\text{EEMACOMP}}$	91.87±1.06	0.107±0.010	60909.34±304.65
	P$_{\text{EEMACOMH}}$	95.18±0.91	0.103±0.011	59989.45±376.43
	P$_{\text{EEMACOMC}}$	95.22±0.93	0.116±0.012	59876.63±346.72
0.5	P$_{\text{EEMACOMP}}$	99.53±0.02	0.070±0.006	65133.28±115.67
	P$_{\text{EEMACOMH}}$	99.52±0.02	0.101±0.008	65237.75±104.67
	P$_{\text{EEMACOMC}}$	99.29±0.03	0.089±0.007	65162.58±112.68
0.7	P$_{\text{EEMACOMP}}$	96.87±0.32	0.057±0.005	63972.49±142.58
	P$_{\text{EEMACOMH}}$	96.03±0.41	0.076±0.006	61859.85±125.67
	P$_{\text{EEMACOMC}}$	97.37±0.29	0.079±0.006	63653.86±143.67
0.9	P$_{\text{EEMACOMP}}$	95.23±0.42	0.078±0.009	60879.34±213.67
	P$_{\text{EEMACOMH}}$	96.25±0.37	0.106±0.011	60867.45±222.79
	P$_{\text{EEMACOMC}}$	96.89±0.27	0.092±0.010	59932.05±276.38

Table D.10: Influence of parameter ρ_g on the $\bar{n}_{alg}$, $\bar{\varrho}$ and $\bar{\xi}$ metrics, for 30 nodes and $R_g = 300$

(a) $T_{sm} = 1$

ρ_g	$\mathcal{PF}$	$\bar{n}_{alg}$	$\bar{\varrho}$	$\bar{\xi}$
0.1	P$_{\text{EEMACOMP}}$	53.21±5.89	0.212±0.023	44785.23±1242.54
	P$_{\text{EEMACOMH}}$	51.45±6.78	0.214±0.026	42564.32±1323.65
	P$_{\text{EEMMASMP}}$	56.28±6.91	0.213±0.029	42368.65±1324.58
	P$_{\text{EEMMASMH}}$	51.52±6.62	0.210±0.028	42468.45±1368.29
	P$_{\text{EEMACOMC}}$	54.68±6.35	0.240±0.024	45783.59±1284.92
0.3	P$_{\text{EEMACOMP}}$	62.78±4.67	0.160±0.014	49102.46±1164.27
	P$_{\text{EEMACOMH}}$	58.97±5.39	0.174±0.013	46450.67±1237.86
	P$_{\text{EEMMASMP}}$	56.49±5.28	0.143±0.012	46463.54±1245.63
	P$_{\text{EEMMASMH}}$	58.56±5.36	0.175±0.013	46563.41±1256.23
	P$_{\text{EEMACOMC}}$	54.54±5.43	0.212±0.021	49673.43±1065.28
0.5	P$_{\text{EEMACOMP}}$	84.97±1.53	0.061±0.006	60684.53± 346.37
	P$_{\text{EEMACOMH}}$	85.87±1.78	0.062±0.005	59974.87± 343.85
	P$_{\text{EEMMASMP}}$	86.85±1.43	0.063±0.004	59765.39± 343.85
	P$_{\text{EEMMASMH}}$	87.56±1.57	0.064±0.005	59749.76± 356.86
	P$_{\text{EEMACOMC}}$	88.43±1.54	0.070±0.006	56863.47± 397.67
0.7	P$_{\text{EEMACOMP}}$	88.61±1.12	0.056±0.005	62348.62± 192.54
	P$_{\text{EEMACOMH}}$	87.38±1.15	0.061±0.006	61537.83± 242.75
	P$_{\text{EEMMASMP}}$	84.29±1.16	0.060±0.005	61458.77± 246.84
	P$_{\text{EEMMASMH}}$	86.89±1.16	0.062±0.006	61683.42± 247.85
	P$_{\text{EEMACOMC}}$	87.54±1.14	0.060±0.008	63741.48± 148.38
0.9	P$_{\text{EEMACOMP}}$	86.36±1.32	0.091±0.007	50365.45± 897.65
	P$_{\text{EEMACOMH}}$	86.89±1.24	0.082±0.007	52729.12± 845.34
	P$_{\text{EEMMASMP}}$	85.29±1.21	0.081±0.009	52483.81± 947.41
	P$_{\text{EEMMASMH}}$	88.23±1.25	0.082±0.008	52279.01± 948.01
	P$_{\text{EEMACOMC}}$	84.32±1.19	0.085±0.008	53625.45± 982.38

(b) $T_{sm} = 2$

ρ_g	$\mathcal{PF}$	$\bar{n}_{alg}$	$\bar{\varrho}$	$\bar{\xi}$
0.1	P$_{\text{EEMACOMP}}$	63.29±4.21	0.188±0.016	45583.13±1096.23
	P$_{\text{EEMACOMH}}$	63.58±3.82	0.196±0.017	46583.40±1024.97
	P$_{\text{EEMMASMP}}$	64.29±3.63	0.187±0.017	46279.83±1045.79
	P$_{\text{EEMMASMH}}$	63.89±3.82	0.184±0.016	46784.57±1042.65
	P$_{\text{EEMACOMC}}$	59.49±4.39	0.150±0.022	48871.39±1045.09
0.3	P$_{\text{EEMACOMP}}$	67.39±2.87	0.141±0.013	50167.94±1025.35
	P$_{\text{EEMACOMH}}$	64.38±3.89	0.156±0.014	49531.64±1025.65
	P$_{\text{EEMMASMP}}$	62.57±3.94	0.158±0.014	49238.78±1015.75
	P$_{\text{EEMMASMH}}$	64.54±3.64	0.149±0.015	49436.78±1024.76
	P$_{\text{EEMACOMC}}$	65.29±3.26	0.165±0.016	49916.74±1012.57
0.5	P$_{\text{EEMACOMP}}$	93.23±1.46	0.052±0.005	61268.01± 336.86
	P$_{\text{EEMACOMH}}$	88.89±1.43	0.057±0.005	61362.39± 313.64
	P$_{\text{EEMMASMP}}$	89.35±1.28	0.058±0.006	61235.85± 323.89
	P$_{\text{EEMMASMH}}$	89.10±1.32	0.057±0.005	60898.74± 307.64
	P$_{\text{EEMACOMC}}$	87.78±1.48	0.058±0.005	58763.83± 346.76
0.7	P$_{\text{EEMACOMP}}$	95.29±0.71	0.037±0.005	63452.74± 168.38
	P$_{\text{EEMACOMH}}$	91.98±0.97	0.038±0.005	61246.78± 178.38
	P$_{\text{EEMMASMP}}$	92.58±0.92	0.036±0.005	61379.76± 169.53
	P$_{\text{EEMMASMH}}$	92.81±0.92	0.037±0.005	61542.74± 187.84
	P$_{\text{EEMACOMC}}$	91.68±0.91	0.040±0.004	63427.64± 135.74
0.9	P$_{\text{EEMACOMP}}$	93.87±0.91	0.072±0.006	54237.93± 567.24
	P$_{\text{EEMACOMH}}$	86.38±1.12	0.074±0.007	55974.83± 578.64
	P$_{\text{EEMMASMP}}$	87.43±1.16	0.075±0.006	55958.81± 594.85
	P$_{\text{EEMMASMH}}$	87.47±1.21	0.075±0.007	56412.87± 584.68
	P$_{\text{EEMACOMC}}$	86.91±1.23	0.078±0.007	53684.59± 567.96

(c) $T_{sm} = 3$

ρ_g	$\mathcal{PF}$	$\bar{n}_{alg}$	$\bar{\varrho}$	$\bar{\xi}$
0.1	P$_{\text{EEMACOMP}}$	74.29±2.65	0.163±0.013	47674.68±1024.58
	P$_{\text{EEMACOMH}}$	73.89±2.62	0.182±0.015	48784.46± 965.90
	P$_{\text{EEMMASMP}}$	74.21±2.54	0.181±0.015	48874.37± 958.85
	P$_{\text{EEMMASMP}}$	74.72±2.67	0.182±0.016	48784.75± 965.85
	P$_{\text{EEMACOMC}}$	69.45±2.13	0.192±0.022	47852.54±1012.78
0.3	P$_{\text{EEMACOMP}}$	79.86±2.45	0.120±0.010	50452.87± 912.85
	P$_{\text{EEMACOMH}}$	75.59±2.76	0.131±0.011	49872.76± 987.94
	P$_{\text{EEMMASMP}}$	75.32±2.81	0.132±0.012	49873.67± 985.95
	P$_{\text{EEMMASMH}}$	74.89±2.82	0.136±0.011	49876.86± 996.28
	P$_{\text{EEMACOMC}}$	76.67±3.12	0.167±0.013	51469.86± 942.67
0.5	P$_{\text{EEMACOMP}}$	96.84±0.56	0.032±0.002	63562.67± 223.48
	P$_{\text{EEMACOMH}}$	94.78±0.57	0.034±0.003	61413.78± 302.34
	P$_{\text{EEMMASMP}}$	95.67±0.58	0.033±0.003	61345.56± 269.89
	P$_{\text{EEMMASMH}}$	95.48±0.68	0.032±0.004	61456.74± 289.98
	P$_{\text{EEMACOMC}}$	98.46±0.96	0.034±0.003	63467.75± 226.86
0.7	P$_{\text{EEMACOMP}}$	95.64±0.68	0.031±0.002	63254.76± 227.64
	P$_{\text{EEMACOMH}}$	93.49±0.82	0.033±0.003	61467.64± 238.89
	P$_{\text{EEMMASMP}}$	93.67±0.84	0.033±0.004	61427.53± 268.98
	P$_{\text{EEMMASMH}}$	94.63±0.82	0.035±0.003	61452.34± 286.42
	P$_{\text{EEMACOMC}}$	92.24±0.83	0.040±0.003	62438.56± 232.84
0.9	P$_{\text{EEMACOMP}}$	93.78±0.86	0.068±0.005	56684.76± 525.65
	P$_{\text{EEMACOMH}}$	89.26±1.16	0.067±0.006	57684.87± 542.98
	P$_{\text{EEMMASMP}}$	89.34±1.18	0.069±0.005	57764.89± 527.83
	P$_{\text{EEMMASMH}}$	89.63±1.16	0.067±0.005	57765.95± 545.95
	P$_{\text{EEMACOMC}}$	88.82±1.15	0.072±0.007	55874.65± 556.96

(d) $T_{sm} = 4$

ρ_g	$\mathcal{PF}$	$\bar{n}_{alg}$	$\bar{\varrho}$	$\bar{\xi}$
0.1	P$_{\text{EEMACOMP}}$	85.87±2.56	0.131±0.011	50458.95±1024.64
	P$_{\text{EEMACOMH}}$	84.65±2.67	0.148±0.015	50457.43± 963.87
	P$_{\text{EEMMASMP}}$	84.75±2.68	0.149±0.015	50348.93± 967.85
	P$_{\text{EEMMASMH}}$	84.83±2.78	0.145±0.015	50456.28± 993.69
	P$_{\text{EEMACOMC}}$	90.21±2.98	0.148±0.014	48894.27±1014.85
0.3	P$_{\text{EEMACOMP}}$	82.53±2.56	0.112±0.010	51653.84± 856.83
	P$_{\text{EEMACOMH}}$	87.97±2.67	0.124±0.012	51206.36± 847.96
	P$_{\text{EEMMASMP}}$	88.34±2.67	0.122±0.013	51208.36± 857.48
	P$_{\text{EEMMASMH}}$	88.91±2.58	0.125±0.013	50927.84± 857.79
	P$_{\text{EEMACOMC}}$	82.53±2.84	0.137±0.012	52563.28± 842.69
0.5	P$_{\text{EEMACOMP}}$	98.64±0.63	0.027±0.003	63652.74± 149.59
	P$_{\text{EEMACOMH}}$	97.83±0.65	0.033±0.003	62348.94± 165.85
	P$_{\text{EEMMASMP}}$	98.43±0.64	0.030±0.003	62648.83± 163.47
	P$_{\text{EEMMASMH}}$	97.54±0.62	0.032±0.003	62651.84± 187.34
	P$_{\text{EEMACOMC}}$	95.74±0.54	0.028±0.002	63851.28± 147.86
0.7	P$_{\text{EEMACOMP}}$	98.47±0.51	0.029±0.002	63461.86± 184.76
	P$_{\text{EEMACOMH}}$	96.85±0.57	0.032±0.003	62673.96± 212.78
	P$_{\text{EEMMASMP}}$	96.38±0.58	0.033±0.003	62759.39± 217.95
	P$_{\text{EEMMASMH}}$	96.42±0.51	0.033±0.003	62712.84± 224.97
	P$_{\text{EEMACOMC}}$	94.28±0.64	0.030±0.002	63845.83± 179.86
0.9	P$_{\text{EEMACOMP}}$	94.74±0.69	0.061±0.005	58912.59± 412.49
	P$_{\text{EEMACOMH}}$	90.37±0.89	0.061±0.005	58851.68± 456.75
	P$_{\text{EEMMASMP}}$	90.52±0.88	0.065±0.005	58879.48± 453.98
	P$_{\text{EEMMASMH}}$	90.31±0.89	0.059±0.005	58827.78± 446.85
	P$_{\text{EEMACOMC}}$	89.88±0.84	0.068±0.006	56912.67± 456.37

(e) $T_{sm} = 5$

ρ_g	$\mathcal{PF}$	$\bar{n}_{alg}$	$\bar{\varrho}$	$\bar{\xi}$
0.1	P$_{\text{EEMACOMP}}$	98.52±0.55	0.077±0.009	55468.75± 602.23
	P$_{\text{EEMACOMH}}$	97.41±0.66	0.088±0.012	56369.85± 616.11
	P$_{\text{EEMMASMP}}$	97.84±0.65	0.082±0.012	56378.84± 623.54
	P$_{\text{EEMMASMH}}$	97.95±0.66	0.081±0.010	56469.84± 624.76
	P$_{\text{EEMACOMC}}$	98.64±0.78	0.092±0.013	56672.65± 628.45
0.3	P$_{\text{EEMACOMP}}$	98.84±0.66	0.045±0.008	58853.48± 458.27
	P$_{\text{EEMACOMH}}$	99.76±0.37	0.062±0.009	57349.81± 486.24
	P$_{\text{EEMMASMP}}$	99.32±0.35	0.057±0.008	57269.78± 457.53
	P$_{\text{EEMMASMH}}$	99.64±0.37	0.056±0.007	57471.87± 467.84
	P$_{\text{EEMACOMC}}$	98.73±0.62	0.064±0.008	56412.36± 528.85
0.5	P$_{\text{EEMACOMP}}$	99.99±0.01	0.026±0.002	63625.85± 145.28
	P$_{\text{EEMACOMH}}$	99.99±0.01	0.029±0.002	62368.73± 165.76
	P$_{\text{EEMMASMP}}$	99.98±0.01	0.028±0.002	62479.98± 169.52
	P$_{\text{EEMMASMH}}$	99.99±0.01	0.027±0.002	62538.74± 178.49
	P$_{\text{EEMACOMC}}$	99.98±0.02	0.027±0.002	64113.18± 145.87
0.7	P$_{\text{EEMACOMP}}$	98.91±0.34	0.027±0.002	63838.92± 165.39
	P$_{\text{EEMACOMH}}$	98.67±0.49	0.030±0.003	62416.62± 201.23
	P$_{\text{EEMMASMP}}$	98.43±0.52	0.027±0.002	62412.37± 214.45
	P$_{\text{EEMMASMH}}$	98.85±0.53	0.028±0.002	62376.73± 202.27
	P$_{\text{EEMACOMC}}$	99.35±0.34	0.025±0.002	64362.61± 156.64
0.9	P$_{\text{EEMACOMP}}$	98.89±0.52	0.046±0.004	60450.39± 212.36
	P$_{\text{EEMACOMH}}$	98.87±0.46	0.038±0.004	61348.27± 212.27
	P$_{\text{EEMMASMP}}$	98.75±0.46	0.039±0.004	61328.56± 213.78
	P$_{\text{EEMMASMH}}$	98.87±0.43	0.036±0.004	61327.68± 212.49
	P$_{\text{EEMACOMC}}$	99.31±0.31	0.048±0.005	61579.37± 245.22

(f) $T_{sm} = 6$

ρ_g	$\mathcal{PF}$	$\bar{n}_{alg}$	$\bar{\varrho}$	$\bar{\xi}$
0.1	P$_{\text{EEMACOMP}}$	98.37±1.23	0.105±0.013	54412.73± 873.23
	P$_{\text{EEMACOMH}}$	98.76±1.21	0.123±0.013	53348.54± 892.73
	P$_{\text{EEMMASMP}}$	97.83±1.17	0.120±0.014	53351.75± 892.73
	P$_{\text{EEMMASMH}}$	98.62±1.17	0.124±0.014	53345.48± 892.73
	P$_{\text{EEMACOMC}}$	98.83±0.93	0.136±0.014	52187.38± 912.32
0.3	P$_{\text{EEMACOMP}}$	99.53±1.12	0.069±0.008	55936.76± 782.37
	P$_{\text{EEMACOMH}}$	99.72±0.95	0.088±0.009	54675.85± 794.52
	P$_{\text{EEMMASMP}}$	99.29±0.94	0.087±0.009	54653.73± 794.52
	P$_{\text{EEMMASMH}}$	99.72±0.95	0.084±0.009	54587.64± 794.52
	P$_{\text{EEMACOMC}}$	99.83±0.99	0.087±0.010	53913.43± 822.57
0.5	P$_{\text{EEMACOMP}}$	99.98±0.02	0.029±0.002	63516.38± 169.48
	P$_{\text{EEMACOMH}}$	99.99±0.01	0.033±0.003	62247.68± 196.49
	P$_{\text{EEMMASMP}}$	99.97±0.01	0.031±0.002	62327.75± 196.49
	P$_{\text{EEMMASMH}}$	99.99±0.01	0.032±0.003	62368.48± 196.49
	P$_{\text{EEMACOMC}}$	99.99±0.01	0.028±0.002	63869.54± 172.31
0.7	P$_{\text{EEMACOMP}}$	99.64±0.39	0.029±0.002	63646.74± 196.74
	P$_{\text{EEMACOMH}}$	99.97±0.48	0.031±0.003	62946.73± 217.45
	P$_{\text{EEMMASMP}}$	99.91±0.47	0.032±0.003	62953.63± 224.61
	P$_{\text{EEMMASMH}}$	99.98±0.47	0.031±0.002	62934.74± 213.08
	P$_{\text{EEMACOMC}}$	99.74±0.29	0.026±0.002	63912.69± 198.93
0.9	P$_{\text{EEMACOMP}}$	99.92±0.48	0.053±0.004	59345.58± 234.73
	P$_{\text{EEMACOMH}}$	98.42±0.42	0.041±0.005	59697.79± 239.02
	P$_{\text{EEMMASMP}}$	99.38±0.45	0.042±0.004	59696.48± 239.02
	P$_{\text{EEMMASMH}}$	98.31±0.45	0.045±0.004	59874.75± 239.02
	P$_{\text{EEMACOMC}}$	98.74±0.26	0.059±0.005	58854.85± 324.53

Table D.11: Influence of parameter ρ_g on the $\bar{n}_{alg}$, $\bar{\varrho}$ and $\bar{\xi}$ metrics, for 30 nodes and $R_g = 500$

(a) $T_{sm} = 1$

ρ_g	$\mathcal{PF}$	$\bar{n}_{alg}$	$\bar{\varrho}$	$\bar{\xi}$
0.1	$P_{EEMACOMP}$	58.36±4.57	0.202±0.021	48524.76±1012.65
	$P_{EEMACOMH}$	57.54±5.67	0.212±0.026	47674.96±1123.45
	$P_{EEMMASMP}$	56.86±5.32	0.214±0.025	47543.64±1124.57
	$P_{EEMMASMH}$	58.58±5.42	0.209±0.022	47653.63±1118.53
	$P_{EEMACOMC}$	53.26±4.87	0.237±0.027	49532.64±1102.39
0.3	$P_{EEMACOMP}$	63.48±4.78	0.168±0.013	53348.89± 924.57
	$P_{EEMACOMH}$	57.67±4.13	0.175±0.014	49766.45±1027.65
	$P_{EEMMASMP}$	56.78±4.26	0.172±0.014	49543.26±1056.54
	$P_{EEMMASMH}$	57.38±4.42	0.179±0.015	49875.47±1037.89
	$P_{EEMACOMC}$	53.87±4.79	0.213±0.022	52568.84± 947.65
0.5	$P_{EEMACOMP}$	85.67±1.37	0.068±0.005	61573.57± 313.24
	$P_{EEMACOMH}$	86.23±1.68	0.067±0.006	59878.53± 335.68
	$P_{EEMMASMP}$	85.73±1.43	0.071±0.006	59997.63± 311.24
	$P_{EEMMASMH}$	86.47±1.35	0.074±0.007	59986.47± 354.35
	$P_{EEMACOMC}$	84.12±1.25	0.082±0.008	58964.47± 354.36
0.7	$P_{EEMACOMP}$	93.59±0.87	0.062±0.004	63556.75± 146.74
	$P_{EEMACOMH}$	90.32±0.92	0.068±0.006	62146.63± 178.67
	$P_{EEMMASMP}$	90.49±0.59	0.067±0.007	62674.32± 174.32
	$P_{EEMMASMH}$	90.37±0.87	0.062±0.007	62456.64± 169.75
	$P_{EEMACOMC}$	89.89±0.95	0.077±0.008	64143.54± 113.56
0.9	$P_{EEMACOMP}$	89.35±1.10	0.096±0.010	55642.15± 764.32
	$P_{EEMACOMH}$	87.83±1.12	0.084±0.008	55376.53± 757.54
	$P_{EEMMASMP}$	87.52±1.13	0.083±0.008	55857.98± 774.35
	$P_{EEMMASMH}$	87.31±1.12	0.087±0.009	55436.97± 743.46
	$P_{EEMACOMC}$	87.88±1.15	0.082±0.008	56798.95± 724.73

(b) $T_{sm} = 2$

ρ_g	$\mathcal{PF}$	$\bar{n}_{alg}$	$\bar{\varrho}$	$\bar{\xi}$
0.1	$P_{EEMACOMP}$	66.34±3.76	0.183±0.019	50675.53±965.43
	$P_{EEMACOMH}$	66.82±3.43	0.187±0.024	51347.75±946.29
	$P_{EEMMASMP}$	65.28±3.37	0.198±0.023	51564.64±947.25
	$P_{EEMMASMH}$	66.72±3.39	0.196±0.023	51346.54±946.29
	$P_{EEMACOMC}$	61.28±4.04	0.187±0.024	53567.64±956.53
0.3	$P_{EEMACOMP}$	71.79±2.45	0.145±0.016	54674.46±923.53
	$P_{EEMACOMH}$	68.36±3.47	0.157±0.017	56947.64±845.42
	$P_{EEMMASMP}$	67.89±3.38	0.162±0.017	57322.56±845.63
	$P_{EEMMASMH}$	67.74±3.35	0.162±0.018	57423.49±875.43
	$P_{EEMACOMC}$	70.85±3.05	0.168±0.019	54325.53±912.54
0.5	$P_{EEMACOMP}$	93.87±0.76	0.063±0.007	62432.54±313.47
	$P_{EEMACOMH}$	90.58±0.86	0.064±0.007	61654.76±327.84
	$P_{EEMMASMP}$	90.46±0.84	0.067±0.008	61546.87±343.58
	$P_{EEMMASMH}$	90.48±0.86	0.066±0.008	61489.56±348.53
	$P_{EEMACOMC}$	90.74±0.83	0.069±0.008	60986.54±337.53
0.7	$P_{EEMACOMP}$	98.74±0.22	0.049±0.006	64328.35±133.25
	$P_{EEMACOMH}$	97.73±0.27	0.054±0.007	64211.31±145.32
	$P_{EEMMASMP}$	98.64±0.25	0.053±0.006	64228.84±132.76
	$P_{EEMMASMH}$	98.36±0.26	0.052±0.007	64223.12±129.75
	$P_{EEMACOMC}$	97.39±0.28	0.056±0.007	64453.21±122.84
0.9	$P_{EEMACOMP}$	94.57±0.72	0.077±0.008	58137.64±525.46
	$P_{EEMACOMH}$	89.26±0.87	0.084±0.009	58362.26±556.36
	$P_{EEMMASMP}$	89.32±0.74	0.081±0.008	58753.32±524.36
	$P_{EEMMASMH}$	89.48±0.36	0.080±0.008	58458.64±527.65
	$P_{EEMACOMC}$	87.23±0.78	0.082±0.008	56873.25±512.65

(c) $T_{sm} = 3$

ρ_g	$\mathcal{PF}$	$\bar{n}_{alg}$	$\bar{\varrho}$	$\bar{\xi}$
0.1	$P_{EEMACOMP}$	72.46±2.43	0.164±0.014	55453.27±437.54
	$P_{EEMACOMH}$	73.58±2.52	0.186±0.016	56567.32±415.43
	$P_{EEMMASMP}$	72.57±2.48	0.185±0.016	56864.32±421.64
	$P_{EEMMASMH}$	71.84±2.53	0.186±0.017	56347.27±443.25
	$P_{EEMACOMC}$	66.79±2.78	0.189±0.018	55632.24±431.87
0.3	$P_{EEMACOMP}$	77.43±2.36	0.137±0.012	58875.32±367.45
	$P_{EEMACOMH}$	75.89±2.56	0.162±0.014	58986.43±392.36
	$P_{EEMMASMP}$	75.72±2.59	0.160±0.013	58975.23±358.53
	$P_{EEMMASMH}$	76.73±2.67	0.158±0.013	58865.43±348.09
	$P_{EEMACOMC}$	74.69±2.78	0.167±0.014	61654.32±327.85
0.5	$P_{EEMACOMP}$	96.12±0.39	0.043±0.003	63475.24±279.75
	$P_{EEMACOMH}$	94.79±0.42	0.047±0.004	62175.43±267.54
	$P_{EEMMASMP}$	95.90±0.44	0.045±0.003	62284.56±268.94
	$P_{EEMMASMH}$	92.79±0.56	0.044±0.003	62489.49±267.54
	$P_{EEMACOMC}$	96.31±0.40	0.048±0.005	64028.23±234.72
0.7	$P_{EEMACOMP}$	92.58±0.58	0.042±0.002	63675.43±235.87
	$P_{EEMACOMH}$	92.67±0.61	0.044±0.002	62532.25±246.54
	$P_{EEMMASMP}$	92.78±0.65	0.047±0.004	62765.43±245.89
	$P_{EEMMASMH}$	92.98±0.68	0.046±0.003	62450.46±223.67
	$P_{EEMACOMC}$	92.37±0.75	0.048±0.004	63965.43±228.85
0.9	$P_{EEMACOMP}$	93.58±0.73	0.079±0.006	59765.43±378.54
	$P_{EEMACOMH}$	89.48±0.87	0.076±0.005	61353.32±314.68
	$P_{EEMMASMP}$	89.27±0.79	0.076±0.005	61343.62±321.35
	$P_{EEMMASMH}$	89.38±0.84	0.073±0.004	61576.64±326.87
	$P_{EEMACOMC}$	87.84±0.74	0.082±0.006	60543.32±346.75

(d) $T_{sm} = 4$

ρ_g	$\mathcal{PF}$	$\bar{n}_{alg}$	$\bar{\varrho}$	$\bar{\xi}$
0.1	$P_{EEMACOMP}$	82.69±2.25	0.148±0.014	58486.76±517.65
	$P_{EEMACOMH}$	81.78±2.36	0.152±0.017	57965.35±513.45
	$P_{EEMMASMP}$	82.46±2.19	0.156±0.017	57354.54±525.43
	$P_{EEMMASMH}$	83.48±2.39	0.158±0.018	58236.54±496.39
	$P_{EEMACOMC}$	87.82±1.97	0.162±0.018	56543.21±605.58
0.3	$P_{EEMACOMP}$	82.36±2.14	0.123±0.012	59764.32±276.54
	$P_{EEMACOMH}$	85.98±2.37	0.125±0.011	58287.54±276.54
	$P_{EEMMASMP}$	86.34±2.42	0.137±0.013	58345.43±265.43
	$P_{EEMMASMH}$	87.02±2.52	0.132±0.013	58574.32±274.37
	$P_{EEMACOMC}$	79.56±2.37	0.144±0.015	60564.26±247.78
0.5	$P_{EEMACOMP}$	98.35±0.33	0.042±0.003	64202.65±115.75
	$P_{EEMACOMH}$	96.78±0.52	0.048±0.005	64157.54±124.83
	$P_{EEMMASMP}$	96.43±0.56	0.046±0.004	64231.76±121.28
	$P_{EEMMASMH}$	96.78±0.48	0.047±0.004	64210.43±117.84
	$P_{EEMACOMC}$	95.37±0.57	0.050±0.005	64256.34±118.32
0.7	$P_{EEMACOMP}$	95.38±0.56	0.037±0.002	64124.23±162.18
	$P_{EEMACOMH}$	93.58±0.78	0.039±0.003	64342.54±178.56
	$P_{EEMMASMP}$	94.67±0.63	0.042±0.005	64342.25±186.59
	$P_{EEMMASMH}$	93.87±0.74	0.045±0.005	64273.45±187.29
	$P_{EEMACOMC}$	93.58±0.58	0.039±0.004	64165.54±158.48
0.9	$P_{EEMACOMP}$	93.74±0.64	0.072±0.006	59765.43±346.59
	$P_{EEMACOMH}$	90.56±0.63	0.067±0.004	62753.24±198.48
	$P_{EEMMASMP}$	90.47±0.64	0.065±0.004	62264.13±204.39
	$P_{EEMMASMH}$	90.49±0.92	0.078±0.006	59986.43±338.77
	$P_{EEMACOMC}$	89.69±0.86	0.074±0.006	58975.43±367.58

(e) $T_{sm} = 5$

ρ_g	$\mathcal{PF}$	$\bar{n}_{alg}$	$\bar{\varrho}$	$\bar{\xi}$
0.1	$P_{EEMACOMP}$	90.58±0.74	0.080±0.009	59256.84±357.39
	$P_{EEMACOMH}$	91.38±0.83	0.083±0.012	59874.32±386.46
	$P_{EEMMASMP}$	91.74±0.81	0.084±0.012	60132.25±398.48
	$P_{EEMMASMH}$	90.74±0.82	0.085±0.013	59986.54±386.39
	$P_{EEMACOMC}$	91.89±0.81	0.093±0.014	59543.21±392.48
0.3	$P_{EEMACOMP}$	92.87±0.62	0.053±0.006	60435.43±352.38
	$P_{EEMACOMH}$	92.23±0.68	0.061±0.007	60653.33±347.72
	$P_{EEMMASMP}$	90.85±0.72	0.062±0.007	60674.24±365.83
	$P_{EEMMASMH}$	91.95±0.58	0.062±0.008	60653.25±363.82
	$P_{EEMACOMC}$	90.59±0.74	0.071±0.008	61543.36±337.73
0.5	$P_{EEMACOMP}$	99.98±0.02	0.038±0.003	63764.35±110.93
	$P_{EEMACOMH}$	99.99±0.01	0.048±0.005	64053.42±153.28
	$P_{EEMMASMP}$	99.98±0.02	0.047±0.004	64112.32±172.17
	$P_{EEMMASMH}$	99.99±0.01	0.046±0.004	64145.65±159.48
	$P_{EEMACOMC}$	99.97±0.02	0.043±0.003	64234.56±137.48
0.7	$P_{EEMACOMP}$	97.89±0.32	0.036±0.003	63687.68±156.28
	$P_{EEMACOMH}$	96.65±0.39	0.038±0.004	64146.54±167.59
	$P_{EEMMASMP}$	96.89±0.45	0.037±0.004	64278.54±178.45
	$P_{EEMMASMH}$	95.35±0.46	0.039±0.004	64249.56±178.37
	$P_{EEMACOMC}$	96.70±0.32	0.032±0.002	64367.13±167.48
0.9	$P_{EEMACOMP}$	96.98±0.43	0.048±0.005	61342.63±167.26
	$P_{EEMACOMH}$	97.65±0.40	0.044±0.005	61764.36±164.84
	$P_{EEMMASMP}$	97.49±0.37	0.045±0.005	61784.35±162.86
	$P_{EEMMASMH}$	97.30±0.36	0.048±0.006	61875.43±168.32
	$P_{EEMACOMC}$	96.50±0.26	0.052±0.007	61986.65±163.28

(f) $T_{sm} = 6$

ρ_g	$\mathcal{PF}$	$\bar{n}_{alg}$	$\bar{\varrho}$	$\bar{\xi}$
0.1	$P_{EEMACOMP}$	94.46±0.97	0.103±0.014	60245.56±413.45
	$P_{EEMACOMH}$	93.57±0.87	0.113±0.014	58654.36±518.64
	$P_{EEMMASMP}$	93.79±0.97	0.123±0.015	58674.35±527.53
	$P_{EEMMASMH}$	94.74±0.98	0.122±0.015	58689.38±568.54
	$P_{EEMACOMC}$	97.89±0.94	0.138±0.016	59567.32±568.26
0.3	$P_{EEMACOMP}$	92.45±0.97	0.074±0.008	60943.46±315.46
	$P_{EEMACOMH}$	96.44±0.87	0.087±0.010	59875.43±413.95
	$P_{EEMMASMP}$	97.48±0.78	0.086±0.010	59874.28±417.74
	$P_{EEMMASMH}$	96.85±0.86	0.087±0.011	59778.03±424.67
	$P_{EEMACOMC}$	97.93±0.95	0.092±0.012	58467.27±385.43
0.5	$P_{EEMACOMP}$	99.98±0.02	0.038±0.003	65025.35±138.65
	$P_{EEMACOMH}$	99.97±0.02	0.042±0.004	64297.54±158.64
	$P_{EEMMASMP}$	99.98±0.02	0.041±0.004	64325.31±154.92
	$P_{EEMMASMH}$	99.99±0.01	0.041±0.004	64257.43±165.73
	$P_{EEMACOMC}$	99.99±0.01	0.039±0.003	64449.23±146.54
0.7	$P_{EEMACOMP}$	97.78±0.32	0.036±0.003	63579.65±167.41
	$P_{EEMACOMH}$	96.49±0.43	0.035±0.003	64278.17±175.73
	$P_{EEMMASMP}$	96.63±0.41	0.037±0.004	64476.73±173.28
	$P_{EEMMASMH}$	96.69±0.40	0.036±0.003	64173.18±168.85
	$P_{EEMACOMC}$	98.78±0.23	0.033±0.003	64317.67±161.84
0.9	$P_{EEMACOMP}$	97.36±0.35	0.062±0.005	60367.64±234.56
	$P_{EEMACOMH}$	97.87±0.36	0.054±0.005	60546.76±243.45
	$P_{EEMMASMP}$	97.94±0.37	0.058±0.006	60458.46±232.57
	$P_{EEMMASMH}$	98.32±0.32	0.059±0.006	60368.65±226.76
	$P_{EEMACOMC}$	98.89±0.36	0.068±0.007	59975.45±327.65

Table D.12: Influence of parameter ρ_g on the $\bar{n}_{alg}$, $\bar{\varrho}$ and $\bar{\xi}$ metrics, for 30 nodes and $R_g = 800$

(a) $T_{sm} = 1$

ρ_g	$\mathcal{PF}$	$\bar{n}_{alg}$	$\bar{\varrho}$	$\bar{\xi}$
0.1	PEEMACOMP	51.47±4.89	0.193±0.023	46157.89±875.48
	PEEMACOMH	40.32±5.56	0.215±0.024	46326.74±843.21
	PEEMMASMP	51.57±4.71	0.195±0.022	45923.46±824.58
	PEEMMASMH	52.67±4.82	0.192±0.021	46165.78±893.27
	PEEMACOMC	53.45±4.63	0.208±0.023	47124.68±845.37
0.3	PEEMACOMP	60.39±2.69	0.172±0.018	53467.67±423.45
	PEEMACOMH	43.21±3.28	0.196±0.020	51568.78±420.47
	PEEMMASMP	62.36±2.58	0.171±0.017	53678.49±389.34
	PEEMMASMH	63.78±2.56	0.173±0.017	54267.75±367.23
	PEEMACOMC	64.78±2.32	0.184±0.018	53678.59±312.67
0.5	PEEMACOMP	80.43±2.43	0.158±0.016	61576.23±278.45
	PEEMACOMH	47.21±2.78	0.182±0.018	60345.67±347.87
	PEEMMASMP	82.34±1.98	0.156±0.015	60987.36±356.89
	PEEMMASMH	80.23±2.13	0.151±0.014	61203.67±289.56
	PEEMACOMC	82.56±2.12	0.166±0.018	61342.67±275.79
0.7	PEEMACOMP	91.50±1.23	0.115±0.012	63768.23±162.45
	PEEMACOMH	58.68±1.86	0.153±0.016	63867.12±156.34
	PEEMMASMP	93.18±0.95	0.113±0.012	63784.37±158.43
	PEEMMASMH	91.36±1.17	0.116±0.013	64106.23±145.37
	PEEMACOMC	93.27±0.89	0.143±0.014	62897.45±167.45
0.9	PEEMACOMP	87.34±1.32	0.142±0.014	56345.54±632.34
	PEEMACOMH	52.67±2.34	0.168±0.016	55267.43±643.27
	PEEMMASMP	89.45±0.94	0.135±0.013	57389.28±648.48
	PEEMMASMH	87.45±1.23	0.138±0.013	58489.54±568.23
	PEEMACOMC	99.56±0.96	0.140±0.014	57231.65±598.32

(b) $T_{sm} = 2$

ρ_g	$\mathcal{PF}$	$\bar{n}_{alg}$	$\bar{\varrho}$	$\bar{\xi}$
0.1	PEEMACOMP	60.43±5.89	0.193±0.029	50125.54±962.35
	PEEMACOMH	34.13±8.65	0.239±0.035	51267.35±972.34
	PEEMMASMP	61.45±6.34	0.201±0.032	51568.56±973.15
	PEEMMASMH	60.37±6.78	0.197±0.030	51345.78±916.26
	PEEMACOMC	59.75±6.43	0.202±0.031	51267.78±946.32
0.3	PEEMACOMP	72.34±4.56	0.152±0.019	53412.45±862.34
	PEEMACOMH	34.26±8.12	0.196±0.031	54528.54±876.54
	PEEMMASMP	72.45±5.13	0.147±0.019	54461.24±778.32
	PEEMMASMH	68.23±5.67	0.154±0.020	53764.83±896.32
	PEEMACOMC	71.38±5.27	0.175±0.025	53674.78±845.46
0.5	PEEMACOMP	91.23±0.67	0.115±0.016	61368.34±359.27
	PEEMACOMH	40.12±6.79	0.162±0.026	61658.38±378.13
	PEEMMASMP	91.31±1.13	0.114±0.017	61578.37±358.12
	PEEMMASMH	85.32±3.42	0.113±0.016	61679.28±397.21
	PEEMACOMC	92.38±1.23	0.148±0.019	61267.28±392.35
0.7	PEEMACOMP	96.38±0.57	0.095±0.008	64963.58±180.65
	PEEMACOMH	46.76±6.69	0.154±0.023	64643.84±181.34
	PEEMMASMP	95.34±0.48	0.102±0.015	64764.39±183.87
	PEEMMASMH	90.48±0.72	0.104±0.015	64998.64±184.76
	PEEMACOMC	97.12±0.42	0.134±0.017	64326.75±198.85
0.9	PEEMACOMP	92.14±0.78	0.116±0.015	58687.12±210.56
	PEEMACOMH	42.36±7.76	0.173±0.025	64643.84±234.56
	PEEMMASMP	90.31±0.57	0.117±0.015	64764.39±247.96
	PEEMMASMH	85.31±3.78	0.123±0.016	64998.64±235.61
	PEEMACOMC	92.56±1.24	0.152±0.019	64326.75±246.75

(c) $T_{sm} = 3$

ρ_g	$\mathcal{PF}$	$\bar{n}_{alg}$	$\bar{\varrho}$	$\bar{\xi}$
0.1	PEEMACOMP	66.45±5.13	0.197±0.026	55142.48±835.67
	PEEMACOMH	35.61±8.23	0.221±0.032	55897.26±832.45
	PEEMMASMP	65.47±6.16	0.178±0.030	55897.38±845.23
	PEEMMASMH	64.78±6.47	0.176±0.028	55789.16±834.58
	PEEMACOMC	63.13±6.73	0.180±0.028	55789.38±864.14
0.3	PEEMACOMP	73.45±4.56	0.150±0.018	58235.56±735.78
	PEEMACOMH	36.12±8.12	0.192±0.028	59745.38±736.56
	PEEMMASMP	73.46±5.13	0.145±0.017	59237.48±757.86
	PEEMMASMH	69.89±5.67	0.152±0.018	59657.37±763.28
	PEEMACOMC	72.48±5.27	0.171±0.022	58467.29±784.43
0.5	PEEMACOMP	98.58±0.46	0.082±0.008	64987.34±212.54
	PEEMACOMH	77.87±5.13	0.116±0.011	64786.43±214.89
	PEEMMASMP	97.38±0.46	0.092±0.010	64879.45±217.86
	PEEMMASMH	95.69±0.67	0.089±0.009	64987.48±223.78
	PEEMACOMC	97.89±0.43	0.110±0.010	65022.45±201.74
0.7	PEEMACOMP	91.34±1.34	0.082±0.008	64657.28±232.45
	PEEMACOMH	69.37±5.67	0.108±0.010	64734.12±245.27
	PEEMMASMP	90.45±1.68	0.090±0.010	64847.28±246.28
	PEEMMASMH	89.34±1.76	0.087±0.008	64827.67±253.27
	PEEMACOMC	91.58±1.67	0.105±0.010	65136.68±227.84
0.9	PEEMACOMP	75.23±5.26	0.116±0.012	61231.24±321.25
	PEEMACOMH	64.25±6.75	0.127±0.013	61324.32±342.45
	PEEMMASMP	74.32±5.68	0.114±0.013	62123.58±346.67
	PEEMMASMH	74.58±5.89	0.113±0.012	62356.67±356.17
	PEEMACOMC	73.58±5.87	0.128±0.014	62542.46±368.32

(d) $T_{sm} = 4$

ρ_g	$\mathcal{PF}$	$\bar{n}_{alg}$	$\bar{\varrho}$	$\bar{\xi}$
0.1	PEEMACOMP	74.23±5.01	0.190±0.024	59754.23±632.45
	PEEMACOMH	43.48±7.83	0.196±0.030	58654.39±675.34
	PEEMMASMP	71.27±5.28	0.189±0.027	59648.28±674.27
	PEEMMASMH	72.34±5.78	0.186±0.026	58795.48±694.26
	PEEMACOMC	69.28±5.72	0.187±0.027	59756.76±693.09
0.3	PEEMACOMP	77.32±4.83	0.150±0.016	60145.63±609.23
	PEEMACOMH	42.35±8.09	0.192±0.025	60126.65±578.95
	PEEMMASMP	76.74±4.78	0.145±0.016	58643.27±623.46
	PEEMMASMH	76.43±4.87	0.152±0.017	59643.28±643.12
	PEEMACOMC	77.54±4.79	0.171±0.021	59856.20±620.54
0.5	PEEMACOMP	97.75±0.34	0.075±0.006	65135.76±148.45
	PEEMACOMH	49.78±3.76	0.143±0.011	64876.59±154.79
	PEEMMASMP	96.54±0.42	0.083±0.007	65237.89±165.89
	PEEMMASMH	94.35±0.54	0.084±0.007	65210.76±163.56
	PEEMACOMC	98.95±0.45	0.106±0.009	64897.04±172.68
0.7	PEEMACOMP	93.56±2.12	0.068±0.008	65215.43±212.34
	PEEMACOMH	47.57±7.29	0.124±0.010	64678.27±235.37
	PEEMMASMP	92.35±1.76	0.067±0.010	65368.34±218.35
	PEEMMASMH	87.36±1.78	0.066±0.008	65418.48±215.31
	PEEMACOMC	90.68±1.13	0.086±0.010	64245.54±247.78
0.9	PEEMACOMP	76.26±6.13	0.087±0.012	56237.84±432.27
	PEEMACOMH	43.67±8.12	0.128±0.013	56231.37±456.78
	PEEMMASMP	76.28±6.16	0.087±0.013	57643.27±467.37
	PEEMMASMH	75.38±6.78	0.089±0.012	57634.25±487.37
	PEEMACOMC	77.81±6.12	0.099±0.014	57248.39±487.43

(e) $T_{sm} = 5$

ρ_g	$\mathcal{PF}$	$\bar{n}_{alg}$	$\bar{\varrho}$	$\bar{\xi}$
0.1	PEEMACOMP	94.34±1.12	0.135±0.024	59743.25±614.54
	PEEMACOMH	60.67±6.23	0.150±0.030	59124.34±676.85
	PEEMMASMP	94.32±1.21	0.134±0.027	59547.28±687.94
	PEEMMASMH	93.76±1.07	0.136±0.026	59765.27±686.12
	PEEMACOMC	95.29±0.89	0.127±0.027	59158.68±675.65
0.3	PEEMACOMP	97.13±0.65	0.125±0.027	60234.56±658.34
	PEEMACOMH	64.45±7.12	0.137±0.028	60346.76±634.52
	PEEMMASMP	98.67±0.22	0.128±0.027	58764.38±645.68
	PEEMMASMH	98.87±0.27	0.126±0.026	59786.45±657.38
	PEEMACOMC	97.89±0.38	0.125±0.029	59976.40±643.12
0.5	PEEMACOMP	99.65±0.37	0.075±0.012	65126.89±157.45
	PEEMACOMH	70.09±4.12	0.109±0.018	64997.65±167.32
	PEEMMASMP	99.13±0.35	0.076±0.013	65321.67±158.23
	PEEMMASMH	96.38±0.74	0.078±0.014	65213.78±142.54
	PEEMACOMC	99.34±0.29	0.104±0.018	65132.86±164.32
0.7	PEEMACOMP	98.12±1.07	0.066±0.009	65257.62±233.46
	PEEMACOMH	65.78±6.78	0.092±0.011	64789.32±286.54
	PEEMMASMP	97.23±1.23	0.068±0.011	65297.41±226.23
	PEEMMASMH	96.21±1.41	0.068±0.011	65179.45±238.12
	PEEMACOMC	96.53±1.23	0.092±0.013	65248.87±227.49
0.9	PEEMACOMP	77.12±6.03	0.088±0.012	57368.65±412.45
	PEEMACOMH	64.32±7.86	0.098±0.014	56334.77±435.67
	PEEMMASMP	77.93±6.36	0.087±0.014	57748.63±446.64
	PEEMMASMH	77.29±6.46	0.089±0.014	57564.25±427.74
	PEEMACOMC	78.85±6.36	0.101±0.015	57347.89±438.42

(f) $T_{sm} = 6$

ρ_g	$\mathcal{PF}$	$\bar{n}_{alg}$	$\bar{\varrho}$	$\bar{\xi}$
0.1	PEEMACOMP	93.35±1.56	0.127±0.022	60654.24±512.46
	PEEMACOMH	61.46±6.67	0.134±0.027	60124.45±532.65
	PEEMMASMP	93.47±1.31	0.133±0.026	60123.34±545.63
	PEEMMASMH	90.77±1.01	0.132±0.025	60127.38±578.38
	PEEMACOMC	93.27±0.67	0.158±0.031	60126.38±568.27
0.3	PEEMACOMP	94.89±0.47	0.108±0.015	60786.34±542.67
	PEEMACOMH	62.78±7.78	0.104±0.016	60765.38±576.38
	PEEMMASMP	93.93±0.38	0.111±0.017	60876.34±548.97
	PEEMMASMH	91.37±0.32	0.123±0.018	60765.38±568.27
	PEEMACOMC	97.28±0.39	0.116±0.017	60856.32±638.91
0.5	PEEMACOMP	99.42±0.24	0.074±0.009	65235.74±165.89
	PEEMACOMH	76.44±5.12	0.104±0.015	65243.78±188.76
	PEEMMASMP	99.47±0.23	0.076±0.008	65345.87±167.85
	PEEMMASMH	95.75±0.32	0.077±0.007	65358.96±156.89
	PEEMACOMC	99.43±0.28	0.090±0.011	65234.85±178.90
0.7	PEEMACOMP	96.45±1.13	0.067±0.009	65367.84±258.48
	PEEMACOMH	67.38±6.87	0.093±0.012	65174.29±267.39
	PEEMMASMP	96.38±1.15	0.069±0.012	65276.38±244.12
	PEEMMASMH	92.58±1.38	0.070±0.012	65186.56±272.46
	PEEMACOMC	94.28±1.26	0.091±0.015	65289.98±265.67
0.9	PEEMACOMP	78.28±5.78	0.097±0.013	60135.78±445.76
	PEEMACOMH	65.59±7.46	0.102±0.016	58976.36±448.76
	PEEMMASMP	79.26±6.15	0.098±0.016	58765.93±465.89
	PEEMMASMH	78.32±6.32	0.098±0.016	59478.58±437.83
	PEEMACOMC	76.29±6.28	0.117±0.018	60368.85±468.38

Table D.13: Influence of parameter α on the $\bar{n}_{alg}$, $\bar{\varrho}$ and $\bar{\xi}$ metrics, for 30 nodes and $R_g = 300$

(a) $T_{sm} = 1$

α	$\mathcal{PF}$	$\bar{n}_{alg}$	$\bar{\varrho}$	$\bar{\xi}$
1.00	$P_{EEMMASMP}$	86.23±1.56	0.054±0.007	44326.65±1231.15
	$P_{EEMMASMH}$	87.67±1.47	0.052±0.008	47234.57±1234.16
1.50	$P_{EEMMASMP}$	88.36±1.14	0.048±0.006	59234.45± 479.34
	$P_{EEMMASMH}$	86.38±1.13	0.049±0.007	59379.23± 523.43
2.00	$P_{EEMMASMP}$	89.35±1.03	0.058±0.006	58345.67± 667.87
	$P_{EEMMASMH}$	87.25±1.35	0.062±0.006	57453.65± 723.56
2.50	$P_{EEMMASMP}$	90.21±0.56	0.078±0.007	59135.51± 673.26
	$P_{EEMMASMH}$	90.14±0.58	0.082±0.008	57256.53± 723.45
3.00	$P_{EEMMASMP}$	57.56±4.31	0.078±0.008	45124.34± 865.32
	$P_{EEMMASMH}$	58.91±4.21	0.076±0.008	46432.32± 867.35
3.50	$P_{EEMMASMP}$	55.48±4.24	0.082±0.008	43257.82± 874.53
	$P_{EEMMASMH}$	57.76±4.38	0.079±0.008	44267.81± 874.27

(b) $T_{sm} = 2$

α	$\mathcal{PF}$	$\bar{n}_{alg}$	$\bar{\varrho}$	$\bar{\xi}$
1.00	$P_{EEMMASMP}$	91.35±1.21	0.052±0.007	46456.38±1131.45
	$P_{EEMMASMH}$	90.68±1.26	0.054±0.007	49589.28±1078.81
1.50	$P_{EEMMASMP}$	88.43±0.99	0.040±0.006	60341.45± 643.31
	$P_{EEMMASMH}$	89.45±1.13	0.042±0.006	58743.24± 675.63
2.00	$P_{EEMMASMP}$	91.57±0.83	0.053±0.006	60834.47± 682.34
	$P_{EEMMASMH}$	92.67±1.27	0.054±0.007	59234.45± 673.35
2.50	$P_{EEMMASMP}$	91.45±0.95	0.076±0.008	61324.89± 674.21
	$P_{EEMMASMH}$	91.89±1.14	0.075±0.007	59242.43± 639.39
3.00	$P_{EEMMASMP}$	64.45±3.89	0.076±0.008	46745.98± 732.19
	$P_{EEMMASMH}$	63.89±3.75	0.078±0.008	46879.23± 753.96
3.50	$P_{EEMMASMP}$	66.43±3.37	0.079±0.008	45789.74± 779.90
	$P_{EEMMASMH}$	66.45±3.56	0.085±0.009	44789.37± 765.89

(c) $T_{sm} = 3$

α	$\mathcal{PF}$	$\bar{n}_{alg}$	$\bar{\varrho}$	$\bar{\xi}$
1.00	$P_{EEMMASMP}$	93.37±0.67	0.036±0.003	47654.78±1011.25
	$P_{EEMMASMH}$	90.53±0.83	0.035±0.003	49789.48±1023.65
1.50	$P_{EEMMASMP}$	89.56±0.87	0.033±0.002	61678.38± 354.21
	$P_{EEMMASMH}$	90.78±1.09	0.034±0.003	60345.43± 387.43
2.00	$P_{EEMMASMP}$	92.87±0.78	0.033±0.003	60934.24± 467.21
	$P_{EEMMASMH}$	93.87±1.16	0.032±0.002	60327.48± 486.21
2.50	$P_{EEMMASMP}$	92.56±0.92	0.058±0.008	61871.54± 321.43
	$P_{EEMMASMH}$	91.78±1.11	0.061±0.007	60673.65± 321.46
3.00	$P_{EEMMASMP}$	65.85±3.65	0.062±0.006	48754.32± 632.34
	$P_{EEMMASMH}$	64.76±3.59	0.071±0.007	49124.65± 645.21
3.50	$P_{EEMMASMP}$	68.45±3.43	0.072±0.007	47123.64± 723.54
	$P_{EEMMASMH}$	67.87±3.78	0.079±0.008	46543.76± 745.65

(d) $T_{sm} = 4$

α	$\mathcal{PF}$	$\bar{n}_{alg}$	$\bar{\varrho}$	$\bar{\xi}$
1.00	$P_{EEMMASMP}$	94.79±0.64	0.030±0.002	48694.23±689.32
	$P_{EEMMASMH}$	92.68±0.79	0.031±0.002	50346.65±679.43
1.50	$P_{EEMMASMP}$	91.67±0.92	0.031±0.002	61875.54±332.65
	$P_{EEMMASMH}$	91.64±1.02	0.032±0.002	60984.27±375.42
2.00	$P_{EEMMASMP}$	92.81±0.73	0.033±0.003	61324.67±364.67
	$P_{EEMMASMH}$	93.65±1.11	0.030±0.002	60985.64±389.43
2.50	$P_{EEMMASMP}$	93.86±0.87	0.054±0.006	61934.17±312.45
	$P_{EEMMASMH}$	92.67±1.05	0.054±0.007	61456.76±314.78
3.00	$P_{EEMMASMP}$	67.51±3.57	0.058±0.007	49427.75±623.56
	$P_{EEMMASMH}$	66.87±3.43	0.068±0.007	49843.67±645.71
3.50	$P_{EEMMASMP}$	72.43±3.34	0.067±0.008	48764.36±703.41
	$P_{EEMMASMH}$	75.65±3.57	0.076±0.008	48521.72±713.65

(e) $T_{sm} = 5$

α	$\mathcal{PF}$	$\bar{n}_{alg}$	$\bar{\varrho}$	$\bar{\xi}$
1.00	$P_{EEMMASMP}$	96.54±0.54	0.028±0.002	49875.23±598.43
	$P_{EEMMASMH}$	94.52±0.65	0.030±0.002	52345.93±587.21
1.50	$P_{EEMMASMP}$	94.59±0.48	0.029±0.002	61975.84±321.45
	$P_{EEMMASMH}$	95.61±0.37	0.030±0.002	62148.45±335.76
2.00	$P_{EEMMASMP}$	94.51±0.45	0.030±0.003	62153.28±301.62
	$P_{EEMMASMH}$	95.78±0.39	0.028±0.002	61997.32±321.68
2.50	$P_{EEMMASMP}$	94.16±0.46	0.045±0.005	61989.34±324.74
	$P_{EEMMASMH}$	93.85±0.42	0.042±0.005	61769.43±316.82
3.00	$P_{EEMMASMP}$	70.52±3.32	0.051±0.006	51279.67±598.34
	$P_{EEMMASMH}$	68.67±3.12	0.059±0.007	50898.58±612.46
3.50	$P_{EEMMASMP}$	73.69±2.85	0.061±0.007	48895.42±640.23
	$P_{EEMMASMH}$	77.84±2.77	0.072±0.008	48943.52±632.68

(f) $T_{sm} = 6$

α	$\mathcal{PF}$	$\bar{n}_{alg}$	$\bar{\varrho}$	$\bar{\xi}$
1.00	$P_{EEMMASMP}$	97.32±0.44	0.027±0.002	50128.93±547.58
	$P_{EEMMASMH}$	96.27±0.58	0.029±0.002	53257.74±537.74
1.50	$P_{EEMMASMP}$	99.21±0.13	0.028±0.002	62143.65±214.43
	$P_{EEMMASMH}$	97.82±0.27	0.029±0.002	62159.53±197.84
2.00	$P_{EEMMASMP}$	98.72±0.15	0.029±0.002	62358.28±217.53
	$P_{EEMMASMH}$	98.12±0.17	0.029±0.002	62108.34±228.53
2.50	$P_{EEMMASMP}$	95.46±0.26	0.039±0.004	62346.27±237.84
	$P_{EEMMASMH}$	96.62±0.23	0.040±0.004	61985.53±267.84
3.00	$P_{EEMMASMP}$	74.63±2.56	0.049±0.005	53276.45±532.54
	$P_{EEMMASMH}$	70.83±2.87	0.055±0.006	52356.43±523.12
3.50	$P_{EEMMASMP}$	75.42±2.65	0.060±0.006	48895.42±640.23
	$P_{EEMMASMH}$	73.54±2.34	0.068±0.006	48943.52±632.68

Table D.14: Influence of parameter α on the $\bar{n}_{alg}$, $\bar{\varrho}$ and $\bar{\xi}$ metrics, for 30 nodes and $R_g = 500$

(a) $T_{sm} = 1$

α	$\mathcal{PF}$	$\bar{n}_{alg}$	$\bar{\varrho}$	$\bar{\xi}$
1.00	$P_{EEMMASMP}$	85.21±1.69	0.063±0.008	42457.65±935.59
	$P_{EEMMASMH}$	83.26±1.75	0.067±0.009	45127.78±897.77
1.50	$P_{EEMMASMP}$	82.67±1.54	0.064±0.008	58764.23±498.27
	$P_{EEMMASMH}$	82.84±1.35	0.063±0.007	58653.13±516.68
2.00	$P_{EEMMASMP}$	85.12±1.42	0.088±0.009	58234.87±531.65
	$P_{EEMMASMH}$	82.38±1.34	0.082±0.009	58321.78±543.82
2.50	$P_{EEMMASMP}$	90.54±0.91	0.126±0.011	58247.80±542.76
	$P_{EEMMASMH}$	90.76±0.87	0.137±0.013	57379.21±562.68
3.00	$P_{EEMMASMP}$	53.87±4.39	0.135±0.012	43217.75±987.49
	$P_{EEMMASMH}$	52.82±4.54	0.138±0.012	44673.12±886.32
3.50	$P_{EEMMASMP}$	52.43±4.47	0.132±0.013	42368.93±932.56
	$P_{EEMMASMH}$	51.76±4.76	0.145±0.014	42368.75±942.58

(b) $T_{sm} = 2$

α	$\mathcal{PF}$	$\bar{n}_{alg}$	$\bar{\varrho}$	$\bar{\xi}$
1.00	$P_{EEMMASMP}$	86.32±1.31	0.052±0.006	45378.97±785.43
	$P_{EEMMASMH}$	85.47±1.43	0.051±0.004	46734.48±768.34
1.50	$P_{EEMMASMP}$	83.86±1.23	0.053±0.005	63367.34±225.67
	$P_{EEMMASMH}$	84.21±1.12	0.051±0.004	63876.43±227.54
2.00	$P_{EEMMASMP}$	87.86±1.41	0.049±0.004	63216.25±248.65
	$P_{EEMMASMH}$	84.56±1.23	0.048±0.004	63425.71±246.58
2.50	$P_{EEMMASMP}$	92.34±0.87	0.087±0.006	63256.76±245.65
	$P_{EEMMASMH}$	92.76±0.78	0.118±0.011	63245.56±231.43
3.00	$P_{EEMMASMP}$	56.34±4.12	0.121±0.011	46758.34±752.32
	$P_{EEMMASMH}$	54.67±4.23	0.124±0.012	48654.23±768.34
3.50	$P_{EEMMASMP}$	54.76±4.36	0.124±0.013	44354.76±837.32
	$P_{EEMMASMH}$	53.98±4.23	0.132±0.013	44567.28±876.23

(c) $T_{sm} = 3$

α	$\mathcal{PF}$	$\bar{n}_{alg}$	$\bar{\varrho}$	$\bar{\xi}$
1.00	$P_{EEMMASMP}$	88.31±1.27	0.047±0.005	48126.43±675.43
	$P_{EEMMASMH}$	88.32±1.34	0.046±0.004	48765.32±658.32
1.50	$P_{EEMMASMP}$	86.32±1.28	0.045±0.004	63786.32±187.45
	$P_{EEMMASMH}$	87.32±1.17	0.045±0.003	63997.32±189.54
2.00	$P_{EEMMASMP}$	89.97±1.14	0.046±0.004	64217.43±164.32
	$P_{EEMMASMH}$	86.74±1.23	0.044±0.003	63974.32±167.34
2.50	$P_{EEMMASMP}$	94.65±0.64	0.071±0.006	63546.27±175.35
	$P_{EEMMASMH}$	95.87±0.67	0.102±0.008	63754.32±198.76
3.00	$P_{EEMMASMP}$	59.32±3.79	0.085±0.008	49324.65±657.32
	$P_{EEMMASMH}$	58.76±3.98	0.096±0.009	49876.24±657.43
3.50	$P_{EEMMASMP}$	58.54±4.05	0.102±0.011	46786.43±823.34
	$P_{EEMMASMH}$	56.12±4.13	0.112±0.012	46782.34±835.27

(d) $T_{sm} = 4$

α	$\mathcal{PF}$	$\bar{n}_{alg}$	$\bar{\varrho}$	$\bar{\xi}$
1.00	$P_{EEMMASMP}$	89.38±1.21	0.044±0.004	50326.67±546.38
	$P_{EEMMASMH}$	90.37±1.25	0.044±0.004	50268.45±569.23
1.50	$P_{EEMMASMP}$	87.35±1.14	0.046±0.004	63456.32±183.17
	$P_{EEMMASMH}$	89.32±1.16	0.045±0.003	63765.78±182.34
2.00	$P_{EEMMASMP}$	91.23±1.01	0.045±0.004	64129.54±185.23
	$P_{EEMMASMH}$	88.76±1.12	0.043±0.004	63795.21±187.21
2.50	$P_{EEMMASMP}$	96.67±0.53	0.065±0.006	64231.58±178.27
	$P_{EEMMASMH}$	97.43±0.56	0.097±0.009	64258.21±174.32
3.00	$P_{EEMMASMP}$	64.38±3.63	0.078±0.008	51478.38±578.32
	$P_{EEMMASMH}$	62.24±3.77	0.085±0.008	51789.25±578.32
3.50	$P_{EEMMASMP}$	62.48±3.87	0.097±0.010	48765.38±732.24
	$P_{EEMMASMH}$	69.23±3.49	0.096±0.011	48654.34±765.32

(e) $T_{sm} = 5$

α	$\mathcal{PF}$	$\bar{n}_{alg}$	$\bar{\varrho}$	$\bar{\xi}$
1.00	$P_{EEMMASMP}$	92.69±1.13	0.043±0.005	51356.86±535.86
	$P_{EEMMASMH}$	90.93±1.24	0.042±0.004	50786.78±556.84
1.50	$P_{EEMMASMP}$	89.74±1.76	0.044±0.004	63765.97±186.28
	$P_{EEMMASMH}$	91.53±0.78	0.045±0.005	63869.86±187.93
2.00	$P_{EEMMASMP}$	93.46±0.75	0.043±0.004	63976.49±190.23
	$P_{EEMMASMH}$	89.89±0.78	0.043±0.004	63975.34±192.45
2.50	$P_{EEMMASMP}$	98.98±0.49	0.070±0.007	64127.86±176.92
	$P_{EEMMASMH}$	98.74±0.46	0.094±0.009	64138.28±179.74
3.00	$P_{EEMMASMP}$	66.83±3.68	0.082±0.008	52347.86±548.94
	$P_{EEMMASMH}$	64.74±3.67	0.088±0.009	52478.54±546.73
3.50	$P_{EEMMASMP}$	65.75±3.58	0.095±0.010	49875.39±708.86
	$P_{EEMMASMH}$	71.68±3.37	0.102±0.010	49745.75±714.58

(f) $T_{sm} = 6$

α	$\mathcal{PF}$	$\bar{n}_{alg}$	$\bar{\varrho}$	$\bar{\xi}$
1.00	$P_{EEMMASMP}$	94.83±0.87	0.041±0.004	52568.85±587.61
	$P_{EEMMASMH}$	96.67±0.76	0.042±0.004	51865.27±559.32
1.50	$P_{EEMMASMP}$	94.97±0.63	0.042±0.005	64987.43±191.57
	$P_{EEMMASMH}$	95.54±0.56	0.042±0.005	65132.12±183.68
2.00	$P_{EEMMASMP}$	98.37±0.41	0.040±0.004	65234.58±175.68
	$P_{EEMMASMH}$	93.47±0.63	0.039±0.004	65210.58±174.27
2.50	$P_{EEMMASMP}$	99.17±0.34	0.072±0.008	64237.82±173.58
	$P_{EEMMASMH}$	98.94±0.32	0.090±0.009	64565.34±172.47
3.00	$P_{EEMMASMP}$	71.23±3.58	0.076±0.008	53563.82±579.34
	$P_{EEMMASMH}$	69.41±3.47	0.081±0.009	53642.48±587.45
3.50	$P_{EEMMASMP}$	69.74±3.34	0.087±0.010	50874.28±618.39
	$P_{EEMMASMH}$	76.93±3.57	0.096±0.011	50684.23±674.32

Table D.15: Influence of parameter α on the $\bar{n}_{alg}$, $\bar{\varrho}$ and $\bar{\xi}$ metrics, for 30 nodes and $R_g = 800$

(a) $T_{sm} = 1$

α	$\mathcal{PF}$	$\bar{n}_{alg}$	$\bar{\varrho}$	$\bar{\xi}$
1.00	$P_{EEMMASMP}$	81.31±1.45	0.117±0.015	40235.76±958.27
	$P_{EEMMASMH}$	82.87±1.37	0.120±0.015	43468.97±934.28
1.50	$P_{EEMMASMP}$	86.34±1.46	0.115±0.014	57685.29±538.27
	$P_{EEMMASMH}$	84.84±1.47	0.114±0.015	57743.29±529.43
2.00	$P_{EEMMASMP}$	84.10±1.48	0.116±0.014	57639.73±528.53
	$P_{EEMMASMH}$	80.12±1.59	0.117±0.013	57497.28±563.19
2.50	$P_{EEMMASMP}$	88.43±0.98	0.149±0.018	58754.27±562.49
	$P_{EEMMASMH}$	83.31±0.93	0.156±0.018	55126.43±576.26
3.00	$P_{EEMMASMP}$	50.34±4.63	0.142±0.018	40237.87±958.23
	$P_{EEMMASMH}$	48.53±4.68	0.145±0.019	42579.42±897.36
3.50	$P_{EEMMASMP}$	48.26±4.69	0.151±0.020	41368.28±965.29
	$P_{EEMMASMH}$	47.83±4.87	0.168±0.022	40489.38±976.32

(b) $T_{sm} = 2$

α	$\mathcal{PF}$	$\bar{n}_{alg}$	$\bar{\varrho}$	$\bar{\xi}$
1.00	$P_{EEMMASMP}$	84.41±1.56	0.103±0.012	42348.86±895.28
	$P_{EEMMASMH}$	83.75±1.59	0.105±0.013	44876.74±875.29
1.50	$P_{EEMMASMP}$	88.63±1.40	0.101±0.012	59564.20±486.73
	$P_{EEMMASMH}$	85.87±1.45	0.104±0.014	59764.32±487.63
2.00	$P_{EEMMASMP}$	86.82±1.42	0.099±0.012	59754.63±487.93
	$P_{EEMMASMH}$	81.87±1.56	0.103±0.012	58965.38±498.49
2.50	$P_{EEMMASMP}$	89.76±0.85	0.138±0.019	59458.32±524.87
	$P_{EEMMASMH}$	86.23±0.87	0.137±0.018	57278.94±512.65
3.00	$P_{EEMMASMP}$	53.67±4.53	0.136±0.018	42459.05±879.39
	$P_{EEMMASMH}$	49.87±4.54	0.141±0.018	43268.74±856.83
3.50	$P_{EEMMASMP}$	51.67±4.45	0.143±0.020	42568.94±985.84
	$P_{EEMMASMH}$	53.89±4.67	0.162±0.021	41764.98±974.92

(c) $T_{sm} = 3$

α	$\mathcal{PF}$	$\bar{n}_{alg}$	$\bar{\varrho}$	$\bar{\xi}$
1.00	$P_{EEMMASMP}$	86.19±1.84	0.090±0.012	43785.93±765.39
	$P_{EEMMASMH}$	88.39±1.78	0.092±0.013	45672.95±784.29
1.50	$P_{EEMMASMP}$	91.63±1.02	0.091±0.012	62568.83±379.74
	$P_{EEMMASMH}$	90.57±1.13	0.088±0.012	62853.05±368.97
2.00	$P_{EEMMASMP}$	92.76±0.91	0.088±0.012	62348.95±378.94
	$P_{EEMMASMH}$	92.12±0.95	0.089±0.011	62452.97±364.27
2.50	$P_{EEMMASMP}$	92.57±0.96	0.115±0.017	63109.98±427.98
	$P_{EEMMASMH}$	91.79±0.98	0.126±0.018	62341.98±438.92
3.00	$P_{EEMMASMP}$	53.68±4.49	0.118±0.017	43569.09±764.92
	$P_{EEMMASMH}$	50.87±4.37	0.136±0.018	45785.94±785.53
3.50	$P_{EEMMASMP}$	51.86±4.34	0.127±0.018	43658.86±875.34
	$P_{EEMMASMH}$	52.98±4.23	0.143±0.019	43875.92±867.43

(d) $T_{sm} = 4$

α	$\mathcal{PF}$	$\bar{n}_{alg}$	$\bar{\varrho}$	$\bar{\xi}$
1.00	$P_{EEMMASMP}$	91.64±1.11	0.083±0.011	45347.37±674.32
	$P_{EEMMASMH}$	90.43±1.24	0.082±0.011	46783.58±687.54
1.50	$P_{EEMMASMP}$	94.26±0.98	0.084±0.010	63124.56±347.28
	$P_{EEMMASMH}$	92.15±1.04	0.081±0.011	63321.54±358.39
2.00	$P_{EEMMASMP}$	94.87±0.93	0.084±0.012	63427.65±347.38
	$P_{EEMMASMH}$	94.24±0.91	0.084±0.012	63214.45±337.48
2.50	$P_{EEMMASMP}$	93.21±0.92	0.110±0.016	63435.63±345.76
	$P_{EEMMASMH}$	92.32±0.96	0.113±0.017	63256.53±398.43
3.00	$P_{EEMMASMP}$	57.23±4.21	0.112±0.017	45673.27±687.43
	$P_{EEMMASMH}$	54.45±4.14	0.123±0.018	46876.34±675.34
3.50	$P_{EEMMASMP}$	54.87±4.23	0.121±0.017	44567.32±835.63
	$P_{EEMMASMH}$	55.23±4.06	0.124±0.017	44563.28±813.45

(e) $T_{sm} = 5$

α	$\mathcal{PF}$	$\bar{n}_{alg}$	$\bar{\varrho}$	$\bar{\xi}$
1.00	$P_{EEMMASMP}$	94.54±0.69	0.077±0.008	50238.32±628.13
	$P_{EEMMASMH}$	95.76±0.64	0.076±0.008	49683.42±614.57
1.50	$P_{EEMMASMP}$	99.15±0.53	0.076±0.008	65236.21±187.58
	$P_{EEMMASMH}$	95.78±0.67	0.075±0.007	65214.54±175.32
2.00	$P_{EEMMASMP}$	99.32±0.16	0.078±0.008	65341.36±174.47
	$P_{EEMMASMH}$	96.32±0.38	0.078±0.008	65139.32±178.32
2.50	$P_{EEMMASMP}$	99.13±0.14	0.097±0.014	65231.65±175.23
	$P_{EEMMASMH}$	96.31±0.63	0.102±0.015	65237.74±176.34
3.00	$P_{EEMMASMP}$	62.87±3.37	0.106±0.015	49864.32±664.21
	$P_{EEMMASMH}$	61.49±3.26	0.110±0.017	49742.32±654.38
3.50	$P_{EEMMASMP}$	59.43±3.47	0.111±0.015	48632.93±669.23
	$P_{EEMMASMH}$	60.43±3.32	0.112±0.016	49743.27±667.34

(f) $T_{sm} = 6$

α	$\mathcal{PF}$	$\bar{n}_{alg}$	$\bar{\varrho}$	$\bar{\xi}$
1.00	$P_{EEMMASMP}$	98.41±0.49	0.078±0.009	48653.23±668.25
	$P_{EEMMASMH}$	96.64±0.46	0.077±0.009	47845.57±623.56
1.50	$P_{EEMMASMP}$	99.23±0.53	0.076±0.008	64235.76±268.43
	$P_{EEMMASMH}$	96.17±0.78	0.075±0.008	64357.78±242.58
2.00	$P_{EEMMASMP}$	99.45±0.38	0.078±0.008	64567.21±249.32
	$P_{EEMMASMH}$	97.12±0.65	0.077±0.009	64565.87±246.53
2.50	$P_{EEMMASMP}$	99.53±0.43	0.103±0.015	64265.76±238.65
	$P_{EEMMASMH}$	96.89±0.75	0.108±0.016	64567.23±216.74
3.00	$P_{EEMMASMP}$	63.56±3.78	0.109±0.017	48754.23±675.32
	$P_{EEMMASMH}$	61.83±3.57	0.114±0.017	47965.23±685.78
3.50	$P_{EEMMASMP}$	62.92±3.54	0.112±0.016	46743.27±693.26
	$P_{EEMMASMH}$	62.32±3.65	0.115±0.016	47853.32±693.26

Table D.16: Influence of parameter λ_E on the $\bar{n}_{alg}$, $\bar{\varrho}$ and $\bar{\xi}$ metrics, for 30 nodes and $R_g = 300$

(a) $T_{sm} = 1$

λ_E	$\mathcal{PF}$	$\bar{n}_{alg}$	$\bar{\varrho}$	$\bar{\xi}$
$\lambda_E = 2.0$	$P_{EEMACOMP}$	45.17±6.48	0.227±0.026	38238.38±989.21
	$P_{EEMACOMH}$	44.69±6.93	0.238±0.028	37128.43±978.32
	$P_{EEMMASMP}$	47.68±6.58	0.248±0.029	35359.78±947.39
	$P_{EEMMASMH}$	46.59±6.69	0.259±0.028	38589.56±949.16
	$P_{EEMACOMC}$	47.38±6.75	0.267±0.031	37431.34±968.32
$\lambda_E = 4.0$	$P_{EEMACOMP}$	83.12±4.83	0.056±0.009	61567.32±228.31
	$P_{EEMACOMH}$	81.43±4.58	0.057±0.009	62568.43±243.78
	$P_{EEMMASMP}$	76.69±5.11	0.060±0.009	62749.21±238.10
	$P_{EEMMASMH}$	83.59±4.98	0.062±0.010	61895.23±229.42
	$P_{EEMACOMC}$	82.58±4.76	0.059±0.011	62458.29±225.62
$\lambda_E = 6.0$	$P_{EEMACOMP}$	83.48±4.75	0.055±0.009	61897.32±283.20
	$P_{EEMACOMH}$	84.59±4.58	0.056±0.009	62678.21±264.28
	$P_{EEMMASMP}$	80.32±4.73	0.061±0.010	62456.21±247.21
	$P_{EEMMASMH}$	80.38±4.68	0.062±0.011	62134.67±241.67
	$P_{EEMACOMC}$	81.84±4.72	0.063±0.011	62348.21±243.46
$\lambda_E = 8.0$	$P_{EEMACOMP}$	50.36±6.23	0.235±0.027	41268.32±987.51
	$P_{EEMACOMH}$	48.41±6.09	0.268±0.029	41468.43±967.39
	$P_{EEMMASMP}$	49.48±6.14	0.258±0.028	40234.76±989.32
	$P_{EEMMASMH}$	51.32±6.26	0.231±0.026	38235.56±976.31
	$P_{EEMACOMC}$	50.42±6.28	0.259±0.030	44132.64±924.67

(b) $T_{sm} = 2$

λ_E	$\mathcal{PF}$	$\bar{n}_{alg}$	$\bar{\varrho}$	$\bar{\xi}$
$\lambda_E = 2.0$	$P_{EEMACOMP}$	51.54±5.35	0.198±0.023	43127.34±834.56
	$P_{EEMACOMH}$	49.21±5.58	0.196±0.024	42347.11±832.57
	$P_{EEMMASMP}$	52.68±5.29	0.214±0.026	41346.21±864.28
	$P_{EEMMASMH}$	51.64±5.79	0.203±0.023	42347.31±838.23
	$P_{EEMACOMC}$	51.32±5.37	0.189±0.023	44247.31±879.31
$\lambda_E = 4.0$	$P_{EEMACOMP}$	86.28±3.23	0.043±0.008	62128.42±236.27
	$P_{EEMACOMH}$	84.23±3.47	0.044±0.007	62245.26±256.28
	$P_{EEMMASMP}$	83.78±3.29	0.042±0.008	62253.38±236.20
	$P_{EEMMASMH}$	84.61±3.38	0.043±0.006	62348.21±242.67
	$P_{EEMACOMC}$	86.78±3.84	0.048±0.007	62357.21±238.41
$\lambda_E = 6.0$	$P_{EEMACOMP}$	85.28±3.28	0.044±0.007	62856.31±235.28
	$P_{EEMACOMH}$	86.41±3.95	0.046±0.008	62236.18±238.31
	$P_{EEMMASMP}$	84.79±3.30	0.041±0.007	62241.69±236.40
	$P_{EEMMASMH}$	87.32±3.37	0.040±0.007	62217.74±248.31
	$P_{EEMACOMC}$	87.59±3.20	0.047±0.008	62248.21±238.31
$\lambda_E = 8.0$	$P_{EEMACOMP}$	52.86±5.21	0.181±0.023	44827.39±725.58
	$P_{EEMACOMH}$	49.41±5.46	0.184±0.024	43148.36±853.28
	$P_{EEMMASMP}$	52.79±5.39	0.187±0.024	44269.31±867.31
	$P_{EEMMASMH}$	53.89±5.20	0.183±0.023	42168.23±856.30
	$P_{EEMACOMC}$	55.28±5.38	0.194±0.025	44568.25±848.21

(c) $T_{sm} = 3$

λ_E	$\mathcal{PF}$	$\bar{n}_{alg}$	$\bar{\varrho}$	$\bar{\xi}$
$\lambda_E = 2.0$	$P_{EEMACOMP}$	52.35±4.39	0.168±0.016	46278.38±823.57
	$P_{EEMACOMH}$	51.58±4.31	0.167±0.016	45723.59±812.68
	$P_{EEMMASMP}$	52.47±4.57	0.172±0.018	44689.26±847.75
	$P_{EEMMASMH}$	54.68±4.83	0.163±0.017	45749.24±839.33
	$P_{EEMACOMC}$	55.31±4.47	0.162±0.015	44568.27±848.31
$\lambda_E = 4.0$	$P_{EEMACOMP}$	87.32±3.28	0.039±0.007	63258.43±185.32
	$P_{EEMACOMH}$	88.37±3.29	0.038±0.007	62314.27±226.21
	$P_{EEMMASMP}$	87.48±3.74	0.036±0.006	62336.39±246.78
	$P_{EEMMASMH}$	86.68±3.61	0.039±0.007	62352.68±254.78
	$P_{EEMACOMC}$	89.78±3.63	0.034±0.005	63216.79±186.36
$\lambda_E = 6.0$	$P_{EEMACOMP}$	89.68±3.78	0.038±0.007	63252.78±194.56
	$P_{EEMACOMH}$	88.48±3.52	0.037±0.007	62127.65±248.21
	$P_{EEMMASMP}$	88.53±3.73	0.035±0.006	62387.21±245.29
	$P_{EEMMASMH}$	87.69±3.63	0.040±0.007	62379.42±249.35
	$P_{EEMACOMC}$	89.67±3.61	0.035±0.006	63258.85±197.34
$\lambda_E = 8.0$	$P_{EEMACOMP}$	53.58±4.46	0.162±0.016	46436.74±842.37
	$P_{EEMACOMH}$	51.49±4.67	0.151±0.015	46478.24±846.31
	$P_{EEMMASMP}$	52.46±4.73	0.162±0.017	47347.28±825.67
	$P_{EEMMASMH}$	54.69±4.71	0.163±0.017	46389.25±838.38
	$P_{EEMACOMC}$	57.28±4.76	0.155±0.016	45780.23±837.81

(d) $T_{sm} = 4$

λ_E	$\mathcal{PF}$	$\bar{n}_{alg}$	$\bar{\varrho}$	$\bar{\xi}$
$\lambda_E = 2.0$	$P_{EEMACOMP}$	56.31±3.54	0.124±0.014	48267.21±756.23
	$P_{EEMACOMH}$	54.78±3.48	0.127±0.014	47864.23±769.32
	$P_{EEMMASMP}$	55.38±3.89	0.113±0.013	48479.31±758.31
	$P_{EEMMASMH}$	57.39±3.56	0.118±0.013	47438.21±776.49
	$P_{EEMACOMC}$	57.45±3.48	0.126±0.014	47268.37±764.54
$\lambda_E = 4.0$	$P_{EEMACOMP}$	97.32±2.67	0.036±0.005	63023.41±196.32
	$P_{EEMACOMH}$	97.21±2.45	0.037±0.005	62245.64±224.54
	$P_{EEMMASMP}$	96.28±2.63	0.032±0.004	62136.29±236.73
	$P_{EEMMASMH}$	97.59±2.47	0.031±0.004	62224.52±238.38
	$P_{EEMACOMC}$	95.38±2.43	0.033±0.004	64238.21±198.37
$\lambda_E = 6.0$	$P_{EEMACOMP}$	95.38±2.57	0.036±0.006	63231.43±192.37
	$P_{EEMACOMH}$	97.32±2.48	0.034±0.005	62245.20±223.47
	$P_{EEMMASMP}$	97.73±2.64	0.035±0.004	62237.43±221.68
	$P_{EEMMASMH}$	97.69±2.53	0.032±0.004	62236.32±216.38
	$P_{EEMACOMC}$	96.18±2.64	0.033±0.004	64239.32±174.62
$\lambda_E = 8.0$	$P_{EEMACOMP}$	56.32±3.43	0.124±0.013	50235.53±746.32
	$P_{EEMACOMH}$	53.28±3.52	0.116±0.012	49189.32±784.25
	$P_{EEMMASMP}$	54.58±3.47	0.128±0.014	48752.31±787.25
	$P_{EEMMASMH}$	57.32±3.67	0.122±0.013	48358.61±768.42
	$P_{EEMACOMC}$	56.36±3.58	0.118±0.012	45489.31±742.52

(e) $T_{sm} = 5$

λ_E	$\mathcal{PF}$	$\bar{n}_{alg}$	$\bar{\varrho}$	$\bar{\xi}$
$\lambda_E = 2.0$	$P_{EEMACOMP}$	57.27±3.45	0.105±0.011	50458.13±664.37
	$P_{EEMACOMH}$	56.63±3.67	0.113±0.012	48736.32±657.32
	$P_{EEMMASMP}$	57.43±3.64	0.112±0.011	49843.34±658.21
	$P_{EEMMASMH}$	58.74±3.58	0.114±0.012	50258.16±646.72
	$P_{EEMACOMC}$	59.35±3.69	0.116±0.012	47637.89±659.28
$\lambda_E = 4.0$	$P_{EEMACOMP}$	98.32±1.49	0.029±0.002	63125.78±198.41
	$P_{EEMACOMH}$	98.75±1.56	0.031±0.003	62152.34±212.38
	$P_{EEMMASMP}$	97.89±1.58	0.030±0.003	62049.21±216.38
	$P_{EEMMASMH}$	98.43±1.49	0.028±0.002	62137.43±217.39
	$P_{EEMACOMC}$	97.32±1.57	0.029±0.002	64128.34±172.48
$\lambda_E = 6.0$	$P_{EEMACOMP}$	96.48±1.54	0.030±0.003	63102.31±178.36
	$P_{EEMACOMH}$	97.40±1.39	0.030±0.003	62126.37±211.38
	$P_{EEMMASMP}$	97.72±1.58	0.028±0.002	62138.37±212.79
	$P_{EEMMASMH}$	98.58±1.43	0.029±0.002	62257.32±222.38
	$P_{EEMACOMC}$	97.39±1.66	0.030±0.003	64458.32±192.27
$\lambda_E = 8.0$	$P_{EEMACOMP}$	60.23±3.47	0.103±0.010	52678.48±656.28
	$P_{EEMACOMH}$	59.87±3.65	0.114±0.012	51887.45±668.32
	$P_{EEMMASMP}$	58.43±3.83	0.102±0.010	52568.32±672.19
	$P_{EEMMASMH}$	61.42±3.64	0.117±0.012	53468.29±647.28
	$P_{EEMACOMC}$	61.89±3.68	0.121±0.013	50328.52±648.26

(f) $T_{sm} = 6$

λ_E	$\mathcal{PF}$	$\bar{n}_{alg}$	$\bar{\varrho}$	$\bar{\xi}$
$\lambda_E = 2.0$	$P_{EEMACOMP}$	59.32±3.62	0.102±0.010	53878.32±632.27
	$P_{EEMACOMH}$	60.24±3.55	0.104±0.010	51736.48±634.68
	$P_{EEMMASMP}$	61.38±3.49	0.110±0.011	50648.25±618.36
	$P_{EEMMASMH}$	62.48±3.52	0.109±0.011	52868.37±636.42
	$P_{EEMACOMC}$	62.49±3.48	0.112±0.011	52438.68±647.29
$\lambda_E = 4.0$	$P_{EEMACOMP}$	98.58±1.48	0.028±0.002	63234.69±192.26
	$P_{EEMACOMH}$	98.63±1.52	0.030±0.003	62252.45±216.59
	$P_{EEMMASMP}$	98.38±1.53	0.030±0.003	62149.31±222.37
	$P_{EEMMASMH}$	98.92±1.48	0.028±0.003	62236.28±227.94
	$P_{EEMACOMC}$	97.59±1.48	0.022±0.002	62160.32±228.39
$\lambda_E = 6.0$	$P_{EEMACOMP}$	97.62±1.53	0.030±0.003	63148.45±187.53
	$P_{EEMACOMH}$	97.52±1.42	0.028±0.002	62221.46±234.17
	$P_{EEMMASMP}$	98.63±1.46	0.028±0.002	62248.29±227.35
	$P_{EEMMASMH}$	98.86±1.48	0.029±0.003	62237.28±232.67
	$P_{EEMACOMC}$	97.76±1.43	0.029±0.003	62369.31±236.48
$\lambda_E = 8.0$	$P_{EEMACOMP}$	60.45±3.38	0.097±0.010	53569.31±556.32
	$P_{EEMACOMH}$	62.38±3.42	0.098±0.011	52848.42±573.28
	$P_{EEMMASMP}$	62.38±3.58	0.088±0.009	53739.24±562.59
	$P_{EEMMASMH}$	64.67±3.37	0.092±0.008	53894.16±548.28
	$P_{EEMACOMC}$	63.69±3.34	0.108±0.011	53269.31±538.38

Table D.17: Influence of parameter λ_E on the $\bar{n}_{alg}$, $\bar{\varrho}$ and $\bar{\xi}$ metrics, for 30 nodes and $R_g = 500$

(a) $T_{sm} = 1$

λ_E	$\mathcal{PF}$	$\bar{n}_{alg}$	$\bar{\varrho}$	$\bar{\xi}$
$\lambda_E = 2.0$	$P_{EEMACOMP}$	42.37±6.46	0.245±0.028	35328.32±985.34
	$P_{EEMACOMH}$	42.39±6.76	0.254±0.029	36348.21±964.32
	$P_{EEMMASMP}$	44.52±6.45	0.268±0.030	34689.32±988.37
	$P_{EEMMASMH}$	42.78±6.38	0.286±0.032	36328.27±953.28
	$P_{EEMACOMC}$	45.40±6.72	0.272±0.032	34581.74±975.35
$\lambda_E = 4.0$	$P_{EEMACOMP}$	80.49±4.63	0.067±0.011	63579.58±198.27
	$P_{EEMACOMH}$	79.85±4.79	0.066±0.012	63589.37±196.36
	$P_{EEMMASMP}$	75.26±5.14	0.068±0.011	63589.46±186.32
	$P_{EEMMASMH}$	79.28±4.98	0.067±0.012	63729.48±208.83
	$P_{EEMACOMC}$	79.37±4.79	0.076±0.013	63689.21±205.58
$\lambda_E = 6.0$	$P_{EEMACOMP}$	78.19±4.97	0.068±0.012	63521.68±195.68
	$P_{EEMACOMH}$	79.38±4.73	0.067±0.011	63689.32±187.43
	$P_{EEMMASMP}$	81.25±4.56	0.069±0.012	63658.31±196.37
	$P_{EEMMASMH}$	80.29±4.52	0.066±0.012	63479.31±186.33
	$P_{EEMACOMC}$	81.75±4.74	0.078±0.013	63479.35±192.48
$\lambda_E = 8.0$	$P_{EEMACOMP}$	47.47±6.35	0.242±0.029	38236.82±986.34
	$P_{EEMACOMH}$	48.83±6.48	0.273±0.031	36279.38±998.26
	$P_{EEMMASMP}$	47.18±6.48	0.262±0.030	38269.27±968.37
	$P_{EEMMASMH}$	46.27±6.56	0.246±0.029	34279.32±989.12
	$P_{EEMACOMC}$	47.45±6.78	0.267±0.031	37378.36±974.38

(b) $T_{sm} = 2$

λ_E	$\mathcal{PF}$	$\bar{n}_{alg}$	$\bar{\varrho}$	$\bar{\xi}$
$\lambda_E = 2.0$	$P_{EEMACOMP}$	49.32±5.74	0.225±0.024	40237.35±857.32
	$P_{EEMACOMH}$	48.48±5.73	0.235±0.025	41459.38±847.39
	$P_{EEMMASMP}$	50.39±5.69	0.228±0.025	40269.28±874.37
	$P_{EEMMASMH}$	48.39±5.85	0.221±0.023	40159.74±857.24
	$P_{EEMACOMC}$	50.28±5.75	0.198±0.021	41359.38±846.48
$\lambda_E = 4.0$	$P_{EEMACOMP}$	85.38±3.47	0.046±0.008	64236.18±186.32
	$P_{EEMACOMH}$	83.12±3.75	0.049±0.008	64279.54±185.29
	$P_{EEMMASMP}$	84.88±3.53	0.050±0.009	64287.53±194.32
	$P_{EEMMASMH}$	85.23±3.38	0.048±0.007	64798.32±185.29
	$P_{EEMACOMC}$	85.38±3.76	0.055±0.009	64689.23±178.43
$\lambda_E = 6.0$	$P_{EEMACOMP}$	86.53±3.57	0.047±0.008	64689.32±183.27
	$P_{EEMACOMH}$	85.38±3.76	0.049±0.008	64538.26±195.29
	$P_{EEMMASMP}$	85.43±3.67	0.052±0.009	64769.32±193.36
	$P_{EEMMASMH}$	86.85±3.67	0.050±0.008	64678.36±198.48
	$P_{EEMACOMC}$	86.76±3.38	0.056±0.009	64537.28±184.29
$\lambda_E = 8.0$	$P_{EEMACOMP}$	49.32±5.75	0.198±0.024	44827.39±824.76
	$P_{EEMACOMH}$	50.68±5.48	0.203±0.025	43148.36±834.57
	$P_{EEMMASMP}$	51.38±5.54	0.199±0.024	44269.31±856.28
	$P_{EEMMASMH}$	48.35±5.47	0.204±0.025	42168.23±848.37
	$P_{EEMACOMC}$	50.45±5.46	0.216±0.026	44568.25±859.16

(c) $T_{sm} = 3$

λ_E	$\mathcal{PF}$	$\bar{n}_{alg}$	$\bar{\varrho}$	$\bar{\xi}$
$\lambda_E = 2.0$	$P_{EEMACOMP}$	52.67±5.22	0.176±0.018	43247.17±875.23
	$P_{EEMACOMH}$	52.89±5.26	0.183±0.018	42547.25±878.41
	$P_{EEMMASMP}$	53.69±5.14	0.186±0.018	42379.31±876.39
	$P_{EEMMASMH}$	53.75±4.95	0.184±0.017	41469.34±864.79
	$P_{EEMACOMC}$	54.89±4.97	0.165±0.016	42689.42±869.29
$\lambda_E = 4.0$	$P_{EEMACOMP}$	86.42±3.58	0.043±0.007	64128.43±192.34
	$P_{EEMACOMH}$	86.29±3.69	0.046±0.007	64279.41±179.32
	$P_{EEMMASMP}$	87.97±3.84	0.046±0.006	64479.69±186.38
	$P_{EEMMASMH}$	87.39±3.82	0.045±0.006	64589.31±189.27
	$P_{EEMACOMC}$	88.36±3.74	0.050±0.007	64268.31±184.28
$\lambda_E = 6.0$	$P_{EEMACOMP}$	87.47±3.82	0.044±0.006	64316.48±198.32
	$P_{EEMACOMH}$	87.53±3.73	0.045±0.007	64582.63±186.30
	$P_{EEMMASMP}$	88.89±3.69	0.046±0.006	64689.24±180.38
	$P_{EEMMASMH}$	88.25±3.85	0.045±0.007	64269.51±193.60
	$P_{EEMACOMC}$	87.93±3.73	0.052±0.007	64693.28±185.32
$\lambda_E = 8.0$	$P_{EEMACOMP}$	50.32±5.38	0.174±0.016	43580.21±874.19
	$P_{EEMACOMH}$	50.37±5.19	0.171±0.016	43689.32±869.38
	$P_{EEMMASMP}$	51.46±5.28	0.184±0.017	43474.19±840.85
	$P_{EEMMASMH}$	52.68±5.23	0.185±0.018	45270.31±858.71
	$P_{EEMACOMC}$	56.13±4.89	0.179±0.017	44528.81±859.26

(d) $T_{sm} = 4$

λ_E	$\mathcal{PF}$	$\bar{n}_{alg}$	$\bar{\varrho}$	$\bar{\xi}$
$\lambda_E = 2.0$	$P_{EEMACOMP}$	53.78±3.74	0.129±0.016	46379.31±787.37
	$P_{EEMACOMH}$	52.96±3.69	0.138±0.017	46628.39±774.62
	$P_{EEMMASMP}$	54.68±3.95	0.127±0.014	44784.02±779.26
	$P_{EEMMASMH}$	56.89±3.74	0.125±0.013	45279.26±764.28
	$P_{EEMACOMC}$	57.38±3.80	0.132±0.014	44479.37±759.31
$\lambda_E = 4.0$	$P_{EEMACOMP}$	96.78±1.85	0.040±0.006	64268.41±187.31
	$P_{EEMACOMH}$	95.29±1.75	0.044±0.006	62989.23±212.74
	$P_{EEMMASMP}$	96.88±1.84	0.044±0.006	63456.81±194.36
	$P_{EEMMASMH}$	95.59±1.85	0.045±0.005	63579.26±196.38
	$P_{EEMACOMC}$	96.84±1.78	0.048±0.007	64138.31±195.28
$\lambda_E = 6.0$	$P_{EEMACOMP}$	97.12±1.95	0.041±0.005	64258.35±181.48
	$P_{EEMACOMH}$	96.24±1.79	0.043±0.006	63897.31±192.69
	$P_{EEMMASMP}$	97.32±1.68	0.044±0.006	63158.36±185.38
	$P_{EEMMASMH}$	97.20±1.84	0.046±0.006	62236.32±187.28
	$P_{EEMACOMC}$	97.23±1.79	0.047±0.007	64239.39±178.37
$\lambda_E = 8.0$	$P_{EEMACOMP}$	53.78±3.63	0.135±0.015	48259.37±779.31
	$P_{EEMACOMH}$	54.68±3.68	0.126±0.013	47289.41±796.28
	$P_{EEMMASMP}$	54.76±3.75	0.137±0.014	46280.35±775.27
	$P_{EEMMASMH}$	53.28±3.84	0.131±0.013	46685.21±783.19
	$P_{EEMACOMC}$	54.60±3.92	0.125±0.012	44682.30±734.68

(e) $T_{sm} = 5$

λ_E	$\mathcal{PF}$	$\bar{n}_{alg}$	$\bar{\varrho}$	$\bar{\xi}$
$\lambda_E = 2.0$	$P_{EEMACOMP}$	56.51±3.76	0.123±0.012	53673.29±578.35
	$P_{EEMACOMH}$	55.78±3.84	0.126±0.013	52459.31±589.37
	$P_{EEMMASMP}$	54.74±3.86	0.121±0.012	54389.31±595.68
	$P_{EEMMASMH}$	57.39±3.89	0.118±0.012	53258.16±574.29
	$P_{EEMACOMC}$	58.29±3.73	0.131±0.013	55865.32±583.19
$\lambda_E = 4.0$	$P_{EEMACOMP}$	97.35±1.58	0.038±0.004	64317.45±176.35
	$P_{EEMACOMH}$	97.84±1.69	0.043±0.005	64578.87±185.48
	$P_{EEMMASMP}$	98.12±1.46	0.042±0.004	64268.38±187.43
	$P_{EEMMASMH}$	98.26±1.45	0.041±0.004	64789.42±195.39
	$P_{EEMACOMC}$	97.59±1.53	0.042±0.005	64247.39±192.36
$\lambda_E = 6.0$	$P_{EEMACOMP}$	97.69±1.62	0.039±0.004	64345.28±186.32
	$P_{EEMACOMH}$	98.84±1.45	0.042±0.005	64679.13±178.37
	$P_{EEMMASMP}$	97.93±1.60	0.041±0.004	64639.21±176.43
	$P_{EEMMASMH}$	98.78±1.48	0.042±0.005	64529.43±182.58
	$P_{EEMACOMC}$	98.49±1.62	0.043±0.005	64779.52±187.41
$\lambda_E = 8.0$	$P_{EEMACOMP}$	57.32±3.59	0.123±0.012	52689.31±548.37
	$P_{EEMACOMH}$	56.83±3.87	0.126±0.012	52367.64±548.31
	$P_{EEMMASMP}$	57.59±3.88	0.117±0.011	52784.21±569.32
	$P_{EEMMASMH}$	58.30±3.83	0.120±0.011	54689.32±579.31
	$P_{EEMACOMC}$	59.32±3.72	0.132±0.013	54563.21±583.27

(f) $T_{sm} = 6$

λ_E	$\mathcal{PF}$	$\bar{n}_{alg}$	$\bar{\varrho}$	$\bar{\xi}$
$\lambda_E = 2.0$	$P_{EEMACOMP}$	58.32±3.76	0.113±0.011	55638.29±484.27
	$P_{EEMACOMH}$	58.54±3.69	0.118±0.012	53589.38±499.31
	$P_{EEMMASMP}$	60.82±3.65	0.119±0.012	52468.17±516.74
	$P_{EEMMASMH}$	61.34±3.69	0.114±0.011	53589.12±487.59
	$P_{EEMACOMC}$	60.42±3.74	0.125±0.012	54681.37±472.83
$\lambda_E = 4.0$	$P_{EEMACOMP}$	98.89±1.38	0.038±0.003	64237.69±185.31
	$P_{EEMACOMH}$	98.76±1.37	0.039±0.004	64512.78±186.23
	$P_{EEMMASMP}$	98.59±1.42	0.041±0.003	64562.73±189.37
	$P_{EEMMASMH}$	98.98±1.36	0.040±0.003	64282.21±184.73
	$P_{EEMACOMC}$	98.98±1.45	0.041±0.003	64897.13±194.27
$\lambda_E = 6.0$	$P_{EEMACOMP}$	98.37±1.44	0.039±0.003	64561.27±184.28
	$P_{EEMACOMH}$	98.48±1.41	0.040±0.004	64628.35±185.24
	$P_{EEMMASMP}$	98.87±1.40	0.041±0.003	64678.27±184.36
	$P_{EEMMASMH}$	98.95±1.35	0.042±0.004	64528.31±171.64
	$P_{EEMACOMC}$	98.85±1.41	0.038±0.003	64896.42±183.68
$\lambda_E = 8.0$	$P_{EEMACOMP}$	59.58±3.48	0.105±0.011	55678.23±437.59
	$P_{EEMACOMH}$	61.58±3.49	0.106±0.012	56238.30±427.31
	$P_{EEMMASMP}$	61.47±3.61	0.097±0.009	54751.73±467.31
	$P_{EEMMASMH}$	62.73±3.57	0.098±0.009	54518.47±475.38
	$P_{EEMACOMC}$	62.86±3.53	0.114±0.012	54369.53±482.44

Table D.18: Influence of parameter λ_E on the $\bar{n}_{alg}$, $\bar{\varrho}$ and $\bar{\xi}$ metrics, for 30 nodes and $R_g = 800$

(a) $T_{sm} = 1$

λ_E	$\mathcal{PF}$	$\bar{n}_{alg}$	$\bar{\varrho}$	$\bar{\xi}$
$\lambda_E = 2.0$	$P_{EEMACOMP}$	40.32±6.67	0.262±0.029	38967.05±876.94
	$P_{EEMACOMH}$	35.56±7.45	0.312±0.032	39080.56±857.84
	$P_{EEMMASMP}$	41.35±6.41	0.275±0.031	37946.08±859.75
	$P_{EEMMASMH}$	40.25±6.58	0.267±0.030	38460.84±843.94
	$P_{EEMACOMC}$	38.73±6.44	0.297±0.031	37960.48±857.04
$\lambda_E = 4.0$	$P_{EEMACOMP}$	78.37±4.59	0.122±0.013	63739.40±214.97
	$P_{EEMACOMH}$	55.24±5.64	0.162±0.018	63489.95±235.96
	$P_{EEMMASMP}$	75.32±4.67	0.118±0.014	63749.94±247.38
	$P_{EEMMASMH}$	74.57±4.43	0.120±0.013	63974.05±232.69
	$P_{EEMACOMC}$	73.68±4.48	0.114±0.012	62589.08±242.74
$\lambda_E = 6.0$	$P_{EEMACOMP}$	78.32±4.63	0.120±0.013	63634.70±224.85
	$P_{EEMACOMH}$	56.32±5.60	0.161±0.019	63583.58±234,93
	$P_{EEMMASMP}$	77.32±4.62	0.116±0.015	63685.48±217.92
	$P_{EEMMASMH}$	74.56±4.53	0.123±0.013	63907.37±218.84
	$P_{EEMACOMC}$	73.28±4.72	0.112±0.013	62689.04±248.39
$\lambda_E = 8.0$	$P_{EEMACOMP}$	44.35±6.13	0.253±0.029	40346.89±827.32
	$P_{EEMACOMH}$	38.52±7.28	0.287±0.032	38956.58±845.83
	$P_{EEMMASMP}$	44.28±6.34	0.266±0.031	39705.45±848.03
	$P_{EEMMASMH}$	43.12±6.35	0.252±0.028	37584.48±874.38
	$P_{EEMACOMC}$	44.70±6.36	0.278±0.031	38570.74±864.59

(b) $T_{sm} = 2$

λ_E	$\mathcal{PF}$	$\bar{n}_{alg}$	$\bar{\varrho}$	$\bar{\xi}$
$\lambda_E = 2.0$	$P_{EEMACOMP}$	47.21±5.23	0.236±0.024	43469.21±762.39
	$P_{EEMACOMH}$	36.32±6.41	0.247±0.025	44579.27±739.31
	$P_{EEMMASMP}$	47.21±5.32	0.238±0.024	41379.38±770.23
	$P_{EEMMASMH}$	45.28±5.42	0.222±0.022	42369.48±739.36
	$P_{EEMACOMC}$	47.31±5.47	0.242±0.024	42479.28±748.31
$\lambda_E = 4.0$	$P_{EEMACOMP}$	84.28±3.53	0.096±0.010	64451.85±182.58
	$P_{EEMACOMH}$	45.69±4.36	0.152±0.016	64528.37±178.35
	$P_{EEMMASMP}$	82.75±3.62	0.106±0.012	64387.31±189.49
	$P_{EEMMASMH}$	80.23±3.58	0.104±0.012	64873.27±182.32
	$P_{EEMACOMC}$	83.68±3.41	0.132±0.014	64134.69±197.48
$\lambda_E = 6.0$	$P_{EEMACOMP}$	86.98±3.47	0.098±0.010	64704.32±180.51
	$P_{EEMACOMH}$	46.89±6.57	0.153±0.017	64548.32±184.29
	$P_{EEMMASMP}$	83.78±3.48	0.107±0.013	64684.71±184.08
	$P_{EEMMASMH}$	80.73±3.62	0.103±0.012	64370.26±186.03
	$P_{EEMACOMC}$	85.95±3.62	0.130±0.015	64268.28±178.71
$\lambda_E = 8.0$	$P_{EEMACOMP}$	47.86±5.48	0.209±0.024	46480.31±734.94
	$P_{EEMACOMH}$	38.85±6.38	0.247±0.026	45268.37±794.62
	$P_{EEMMASMP}$	51.51±5.29	0.209±0.022	45379.21±785.37
	$P_{EEMMASMH}$	47.06±5.52	0.233±0.024	44269.32±792.04
	$P_{EEMACOMC}$	50.74±5.36	0.238±0.024	46391.38±738.58

(c) $T_{sm} = 3$

λ_E	$\mathcal{PF}$	$\bar{n}_{alg}$	$\bar{\varrho}$	$\bar{\xi}$
$\lambda_E = 2.0$	$P_{EEMACOMP}$	49.31±5.46	0.192±0.019	45438.75±745.07
	$P_{EEMACOMH}$	45.62±5.83	0.224±0.022	44792.08±739.04
	$P_{EEMMASMP}$	50.38±5.36	0.207±0.020	43697.74±748.31
	$P_{EEMMASMH}$	51.63±5.12	0.205±0.020	44689.29±749.62
	$P_{EEMACOMC}$	52.70±4.98	0.214±0.021	43793.83±763.07
$\lambda_E = 4.0$	$P_{EEMACOMP}$	83.67±3.63	0.088±0.015	64876.37±174.29
	$P_{EEMACOMH}$	75.36±3.84	0.117±0.018	64697.39±178.34
	$P_{EEMMASMP}$	84.68±3.62	0.089±0.015	64868.36±173.05
	$P_{EEMMASMH}$	84.18±3.69	0.088±0.016	64894.28±172.85
	$P_{EEMACOMC}$	85.82±3.57	0.110±0.013	64749.28±176.83
$\lambda_E = 6.0$	$P_{EEMACOMP}$	85.28±3.48	0.089±0.016	64853.20±174.93
	$P_{EEMACOMH}$	76.39±3.86	0.120±0.017	64749.78±179.23
	$P_{EEMMASMP}$	86.38±3.32	0.088±0.015	64759.39±176.81
	$P_{EEMMASMH}$	84.31±3.64	0.088±0.016	64997.48±167.03
	$P_{EEMACOMC}$	86.84±3.25	0.109±0.012	64865.38±174.82
$\lambda_E = 8.0$	$P_{EEMACOMP}$	48.29±5.48	0.182±0.018	46893.03±745.03
	$P_{EEMACOMH}$	44.28±5.63	0.205±0.019	45803.67±779.28
	$P_{EEMMASMP}$	47.59±5.49	0.192±0.018	47941.06±786.85
	$P_{EEMMASMH}$	48.27±5.58	0.192±0.018	48077.49±715.94
	$P_{EEMACOMC}$	47.38±5.38	0.197±0.019	46830.74±749.26

(d) $T_{sm} = 4$

λ_E	$\mathcal{PF}$	$\bar{n}_{alg}$	$\bar{\varrho}$	$\bar{\xi}$
$\lambda_E = 2.0$	$P_{EEMACOMP}$	50.63±3.82	0.126±0.017	48428.79±674.32
	$P_{EEMACOMH}$	44.85±4.23	0.179±0.019	48739.28±684.29
	$P_{EEMMASMP}$	51.05±3.73	0.132±0.017	46894.32±693.23
	$P_{EEMMASMH}$	52.83±3.69	0.137±0.016	47598.25±674.25
	$P_{EEMACOMC}$	52.39±3.62	0.157±0.017	46830.42±694.32
$\lambda_E = 4.0$	$P_{EEMACOMP}$	95.28±0.73	0.076±0.008	64479.32±182.31
	$P_{EEMACOMH}$	50.27±3.58	0.142±0.018	64529.69±186.48
	$P_{EEMMASMP}$	94.87±0.94	0.083±0.009	64986.36±187.28
	$P_{EEMMASMH}$	91.86±1.36	0.084±0.009	64993.37±186.19
	$P_{EEMACOMC}$	97.52±0.72	0.107±0.010	64769.41±182.37
$\lambda_E = 6.0$	$P_{EEMACOMP}$	95.83±0.87	0.077±0.008	64453.28±185.27
	$P_{EEMACOMH}$	49.95±3.61	0.140±0.018	64389.21±183.28
	$P_{EEMMASMP}$	95.83±0.90	0.083±0.009	64279.32±182.69
	$P_{EEMMASMH}$	92.94±1.26	0.081±0.009	64587.27±185.17
	$P_{EEMACOMC}$	96.82±0.72	0.104±0.009	64247.73±183.28
$\lambda_E = 8.0$	$P_{EEMACOMP}$	51.84±3.84	0.143±0.018	49637.20±648.29
	$P_{EEMACOMH}$	44.79±4.83	0.157±0.020	49641.05±639.48
	$P_{EEMMASMP}$	51.58±3.77	0.144±0.018	48528.26±674.98
	$P_{EEMMASMH}$	50.74±3.96	0.146±0.018	47287.19±683.28
	$P_{EEMACOMC}$	51.48±3.83	0.152±0.019	46729.37±697.36

(e) $T_{sm} = 5$

λ_E	$\mathcal{PF}$	$\bar{n}_{alg}$	$\bar{\varrho}$	$\bar{\xi}$
$\lambda_E = 2.0$	$P_{EEMACOMP}$	52.48±3.85	0.135±0.014	55731.73±468.24
	$P_{EEMACOMH}$	45.37±4.65	0.153±0.015	54672.18±478.23
	$P_{EEMMASMP}$	52.74±3.87	0.132±0.013	56792.36±486.37
	$P_{EEMMASMH}$	53.63±3.73	0.134±0.013	54527.27±487.74
	$P_{EEMACOMC}$	53.75±3.61	0.156±0.015	56984.58±483.84
$\lambda_E = 4.0$	$P_{EEMACOMP}$	96.32±0.26	0.074±0.011	64784.27±164.32
	$P_{EEMACOMH}$	70.32±1.89	0.109±0.015	64768.38±168.28
	$P_{EEMMASMP}$	97.34±0.28	0.078±0.011	64468.28±172.63
	$P_{EEMMASMH}$	94.78±0.35	0.079±0.012	64974.27±168.37
	$P_{EEMACOMC}$	97.87±0.27	0.103±0.014	64684.72±171.73
$\lambda_E = 6.0$	$P_{EEMACOMP}$	96.34±0.28	0.072±0.011	64572.73±174.28
	$P_{EEMACOMH}$	70.34±1.73	0.107±0.014	64884.28±172.48
	$P_{EEMMASMP}$	96.73±0.32	0.076±0.009	64854.18±169.24
	$P_{EEMMASMH}$	95.73±0.35	0.076±0.009	64764.48±172.69
	$P_{EEMACOMC}$	97.78±0.26	0.103±0.014	64875.21±171.38
$\lambda_E = 8.0$	$P_{EEMACOMP}$	56.23±3.74	0.135±0.016	54761.85±452.84
	$P_{EEMACOMH}$	51.67±4.81	0.152±0.018	53582.83±468.24
	$P_{EEMMASMP}$	55.42±3.92	0.128±0.016	54783.49±458.58
	$P_{EEMMASMH}$	56.48±3.88	0.125±0.016	54894.52±460.47
	$P_{EEMACOMC}$	56.41±3.89	0.137±0.017	54783.49±462.74

(f) $T_{sm} = 6$

λ_E	$\mathcal{PF}$	$\bar{n}_{alg}$	$\bar{\varrho}$	$\bar{\xi}$
$\lambda_E = 2.0$	$P_{EEMACOMP}$	58.46±3.74	0.118±0.012	57348.29±368.93
	$P_{EEMACOMH}$	51.31±4.12	0.136±0.015	56538.29±379.32
	$P_{EEMMASMP}$	59.37±3.85	0.124±0.014	55682.49±369.36
	$P_{EEMMASMH}$	56.65±3.79	0.123±0.013	55789.24±387.43
	$P_{EEMACOMC}$	58.37±3.72	0.131±0.014	56389.20±374.73
$\lambda_E = 4.0$	$P_{EEMACOMP}$	99.23±0.08	0.072±0.008	64989.21±181.49
	$P_{EEMACOMH}$	78.32±2.12	0.102±0.011	64526.48±182.48
	$P_{EEMMASMP}$	99.34±0.13	0.076±0.008	64579.25±182.38
	$P_{EEMMASMH}$	96.14±0.22	0.077±0.008	64869.37±179.26
	$P_{EEMACOMC}$	98.79±0.15	0.092±0.009	64784.23±178.36
$\lambda_E = 6.0$	$P_{EEMACOMP}$	98.77±0.13	0.072±0.008	64897.35±178.42
	$P_{EEMACOMH}$	77.83±2.31	0.103±0.011	64863.28±174.79
	$P_{EEMMASMP}$	99.64±0.16	0.078±0.008	64759.26±175.28
	$P_{EEMMASMH}$	95.76±0.28	0.077±0.008	64529.28±172.38
	$P_{EEMACOMC}$	98.95±0.17	0.091±0.010	64975.36±174.38
$\lambda_E = 8.0$	$P_{EEMACOMP}$	58.23±3.57	0.119±0.013	57842.79±377.39
	$P_{EEMACOMH}$	52.48±3.78	0.138±0.015	57841.79±377.73
	$P_{EEMMASMP}$	60.26±3.53	0.125±0.013	58847.28±364.28
	$P_{EEMMASMH}$	61.84±3.42	0.126±0.013	56793.26±388.27
	$P_{EEMACOMC}$	60.84±3.47	0.132±0.014	56729.39±389.54

Appendix E

Control Parameter Graphs

This appendix contains FluxViz graphs to visualise the results of the empirical analysis of the ant-based algorithm control parameters, for all scenario combinations of 30 nodes, $T_{sm} \in \{1, 2, 3, 4, 5, 6\}$, and $R_g \in \{300, 500, 800\}$.

Figures E.1-E.15 visualise the influence of β_ψ on the $\bar{n}_{alg}$, $\bar{\varrho}$ and $\bar{\xi}$ metrics for all the proposed ACO algorithms, based on the results of Tables D.1-D.3. Figures E.16-E.24 visualise the influence of r_0 on the $\bar{n}_{alg}$, $\bar{\varrho}$ and $\bar{\xi}$ metrics for the EEMACOMP, EEMACOMH, and EEMACOMC algorithms, based on the results of Tables D.4-D.6. Figures E.25-E.33 visualise the influence of ρ_l on the $\bar{n}_{alg}$, $\bar{\varrho}$ and $\bar{\xi}$ metrics for the EEMACOMP, EEMACOMH, and EEMACOMC algorithms, based on the results of Tables D.7-D.9. Figures E.34-E.48 visualise the influence of ρ_g on the $\bar{n}_{alg}$, $\bar{\varrho}$ and $\bar{\xi}$ metrics for all the proposed ACO algorithms, based on the results of Tables D.10-D.12. Figures E.49-E.54 visualise the influence of α on the $\bar{n}_{alg}$, $\bar{\varrho}$ and $\bar{\xi}$ metrics for the EEMMASMP and EEMMASMH algorithms, based on the results of Tables D.13-D.15 and Figures E.55-E.69 visualise the influence of λ_E on the $\bar{n}_{alg}$, $\bar{\varrho}$ and $\bar{\xi}$ metrics for all the proposed ACO algorithms, based on the results of Tables D.16-D.18.

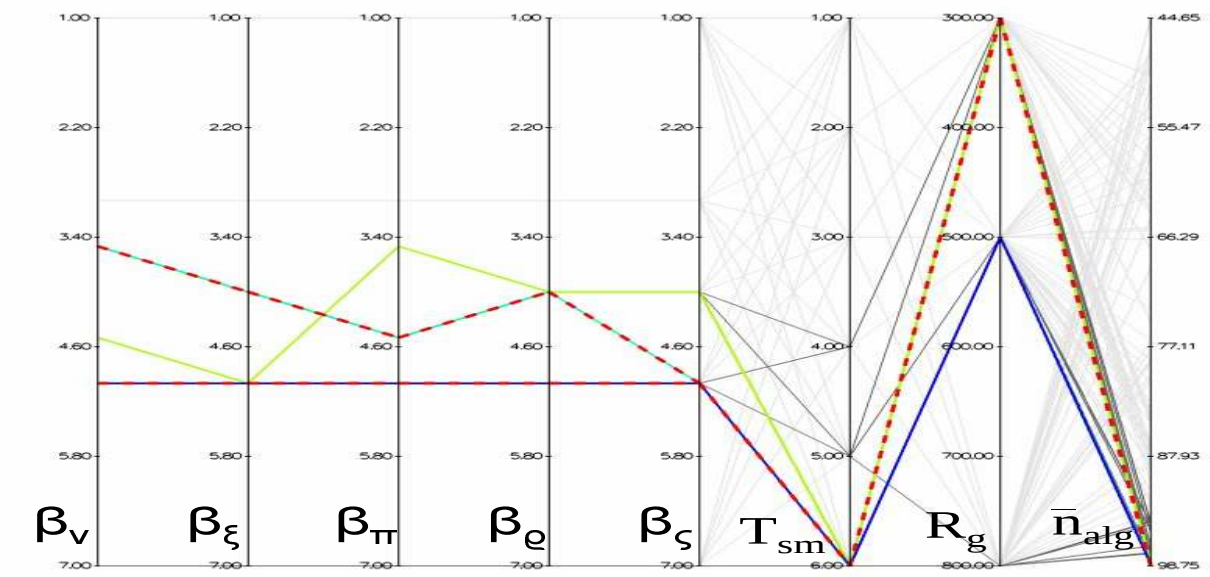

Figure E.1: Influence of β_ψ on the $\bar{n}_{alg}$ metric for EEMACOMP

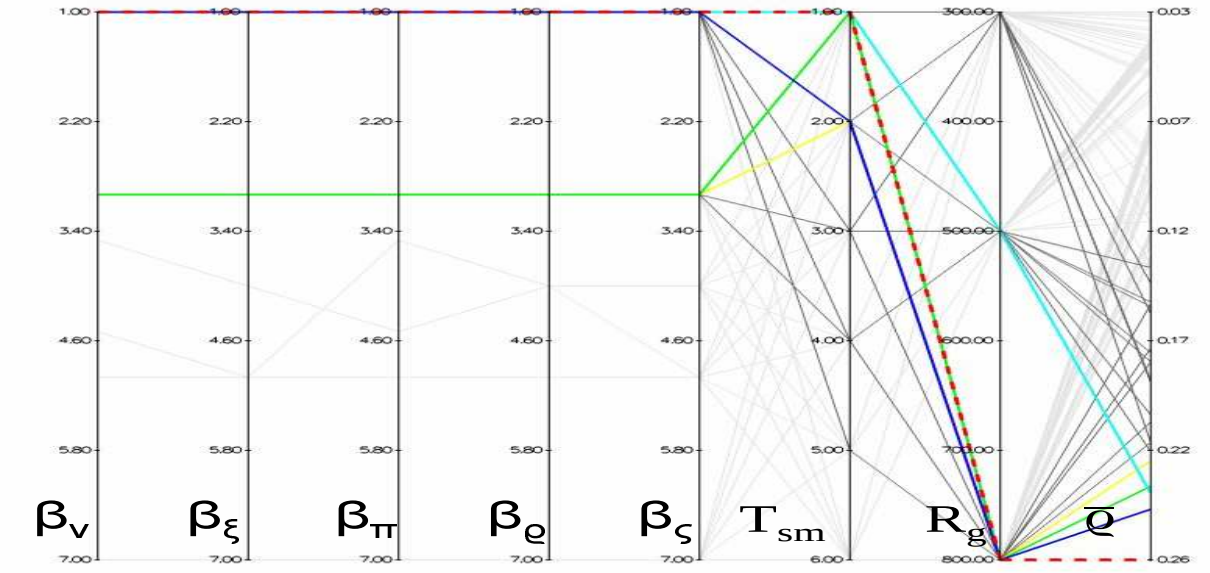

Figure E.2: Influence of β_ψ on the $\bar{\varrho}$ metric for EEMACOMP

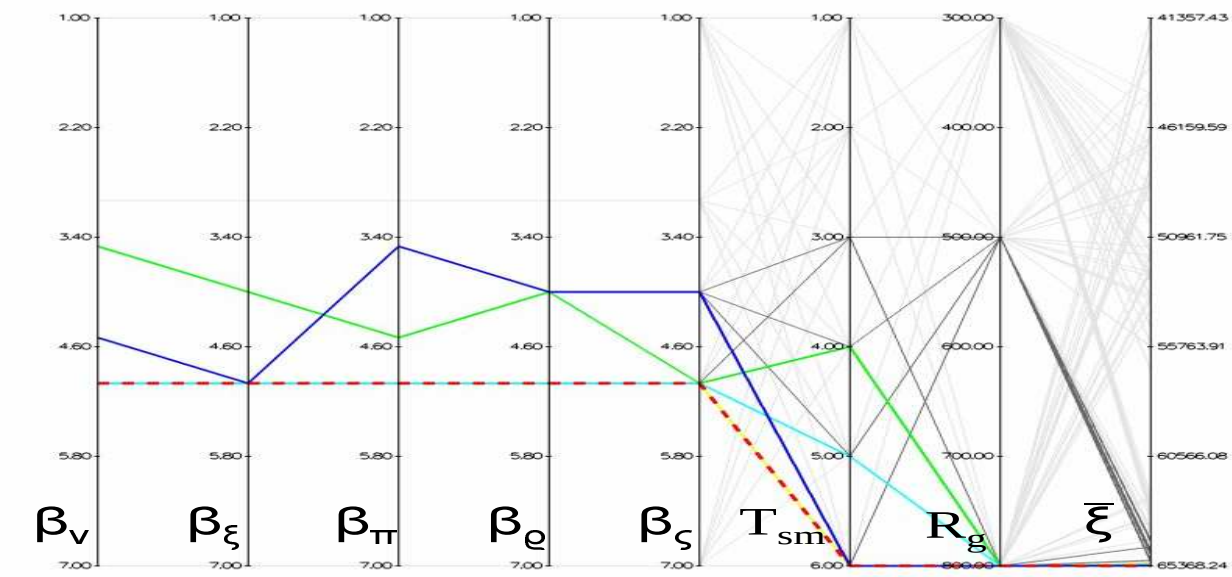

Figure E.3: Influence of β_ψ on the $\bar{\xi}$ metric for EEMACOMP

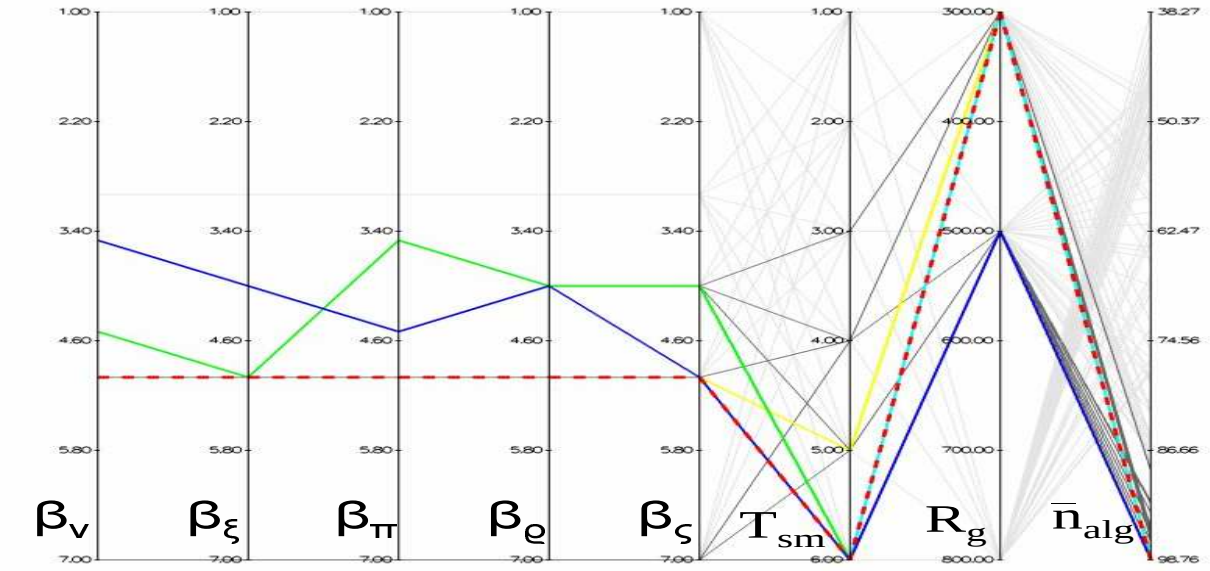

Figure E.4: Influence of β_ψ on the $\bar{n}_{alg}$ metric for EEMACOMH

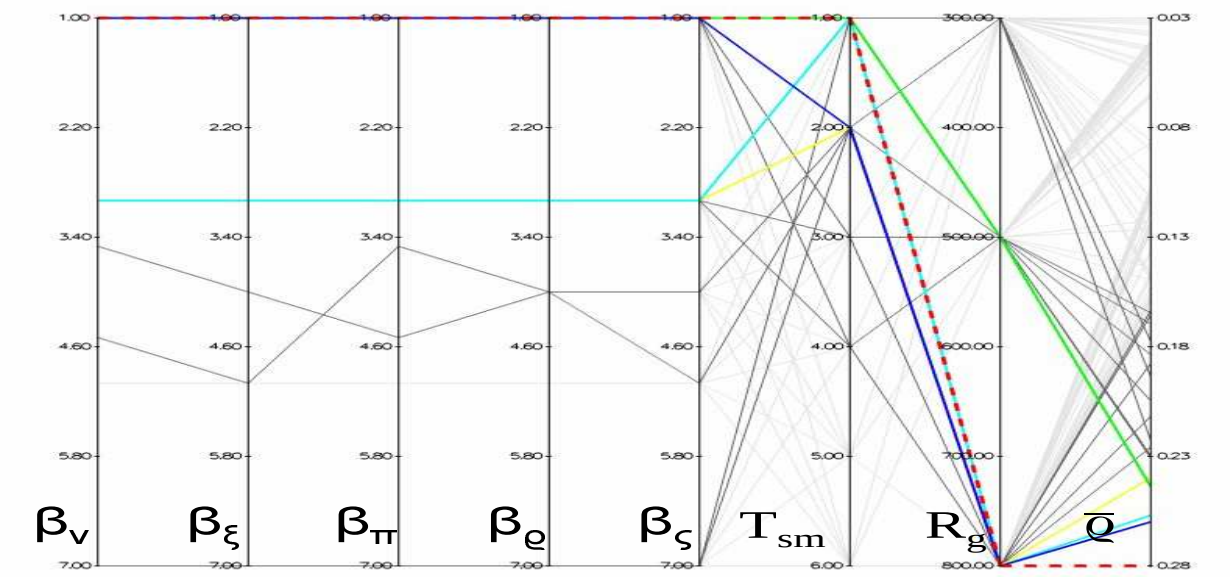

Figure E.5: Influence of β_ψ on the $\bar{\varrho}$ metric for EEMACOMH

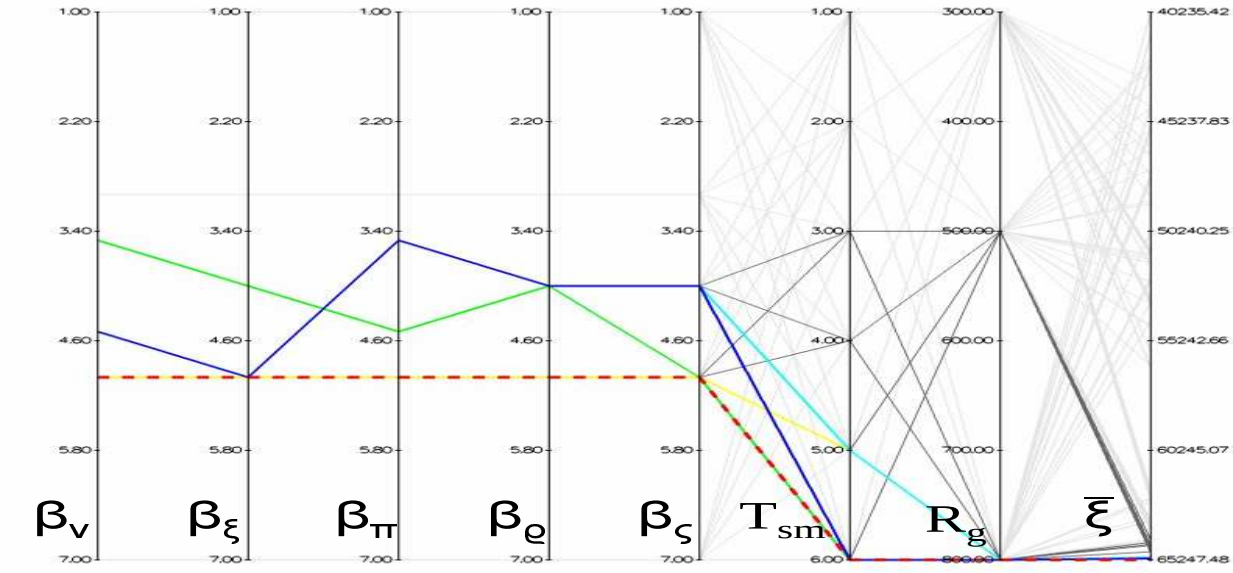

Figure E.6: Influence of β_ψ on the $\bar{\xi}$ metric for EEMACOMH

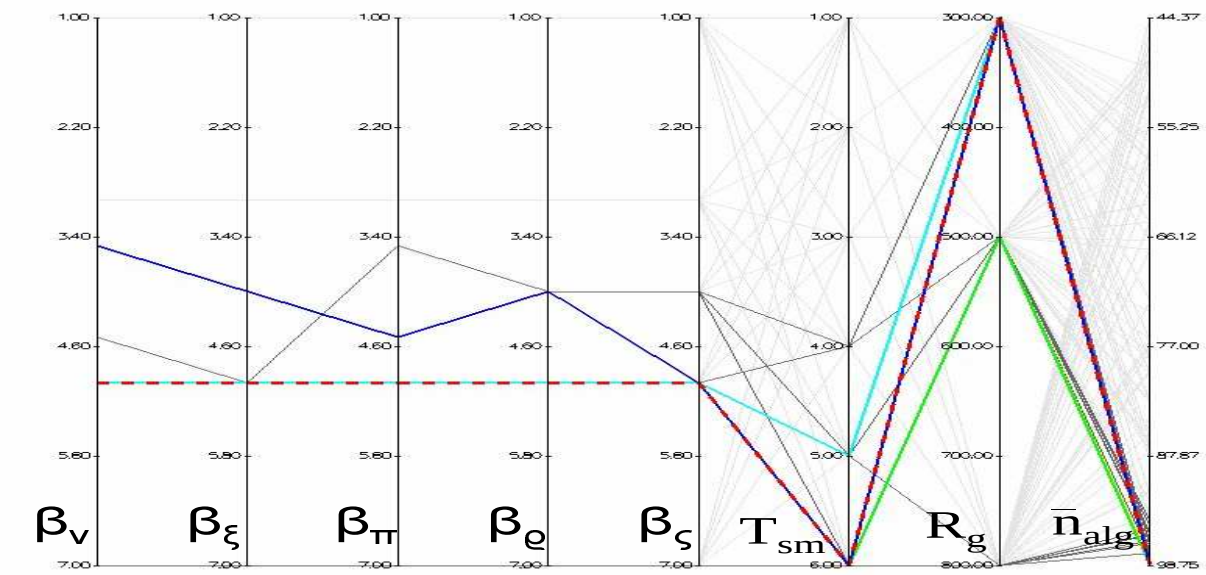

Figure E.7: Influence of β_ψ on the $\bar{n}_{alg}$ metric for EEMMASMP

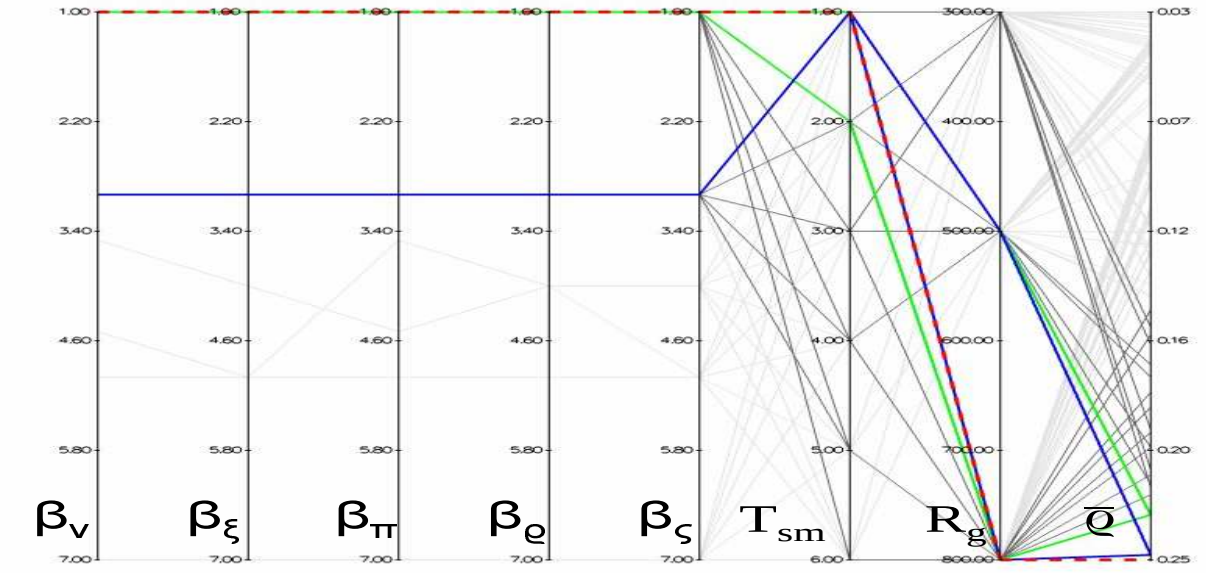

Figure E.8: Influence of β_ψ on the $\bar{\varrho}$ metric for EEMMASMP

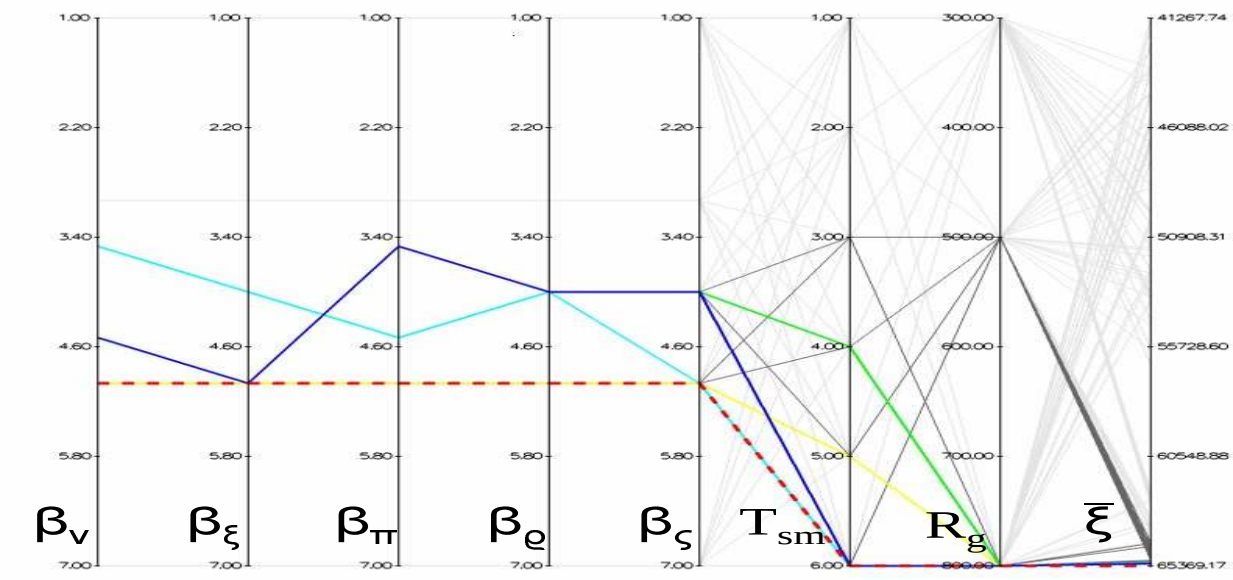

Figure E.9: Influence of β_ψ on the $\bar{\xi}$ metric for EEMMASMP

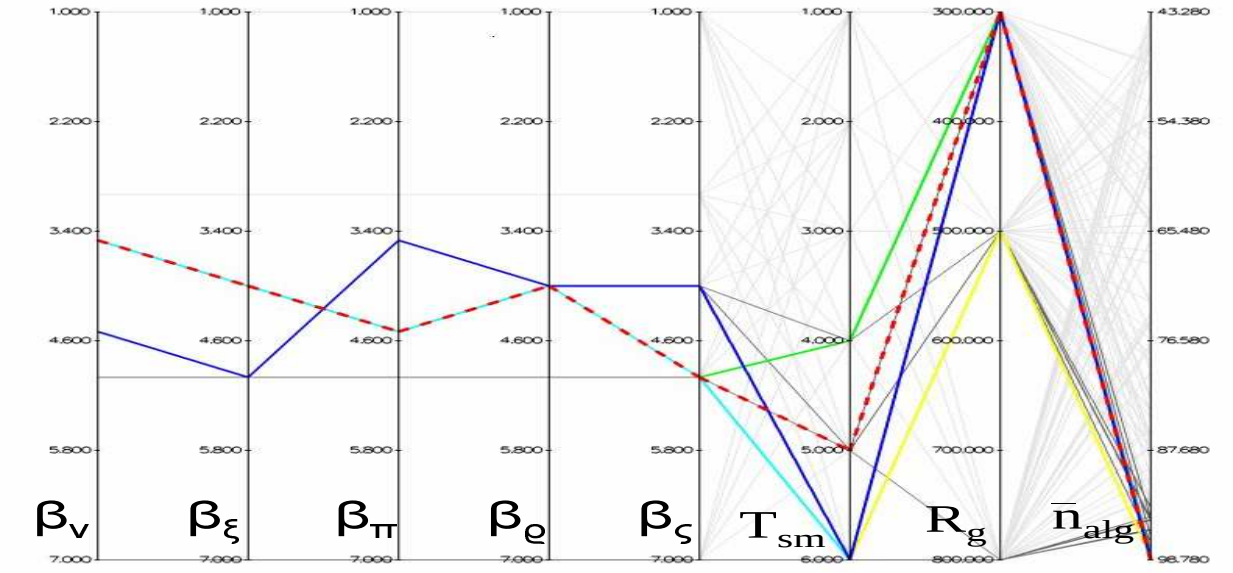

Figure E.10: Influence of β_ψ on the $\bar{n}_{alg}$ metric for EEMMASMH

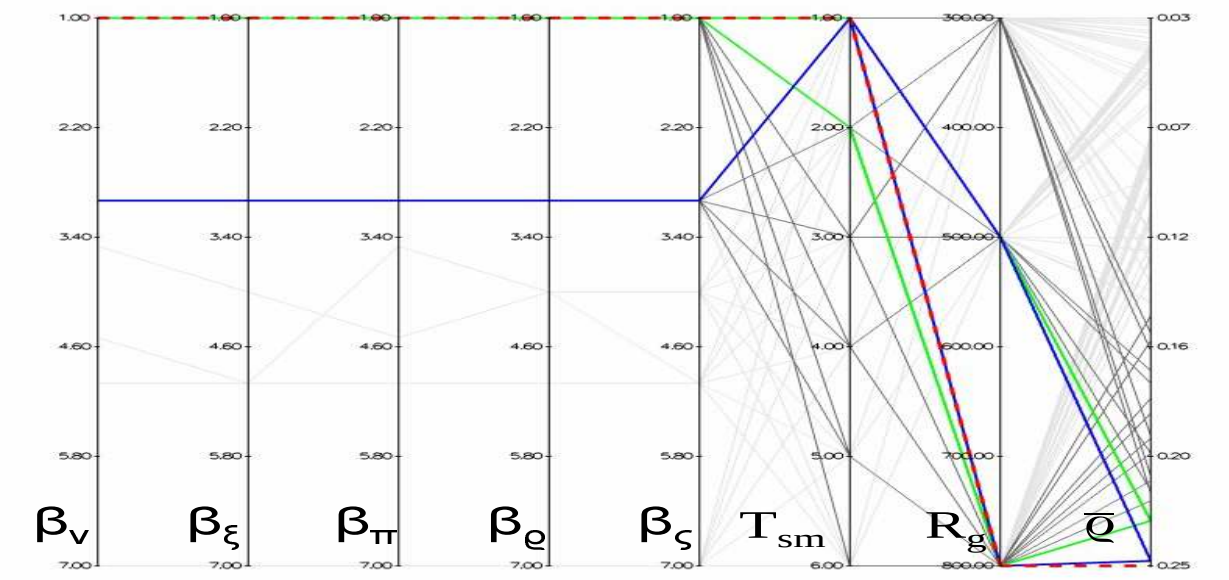

Figure E.11: Influence of β_ψ on the $\bar{\varrho}$ metric for EEMMASMH

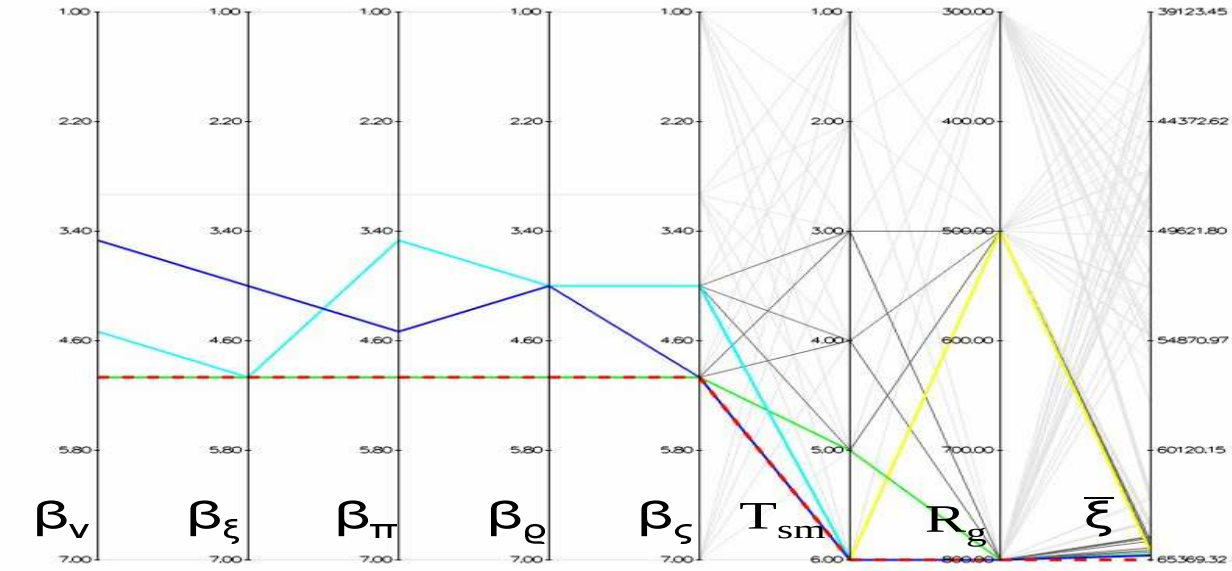

Figure E.12: Influence of β_ψ on the $\bar{\xi}$ metric for EEMMASMH

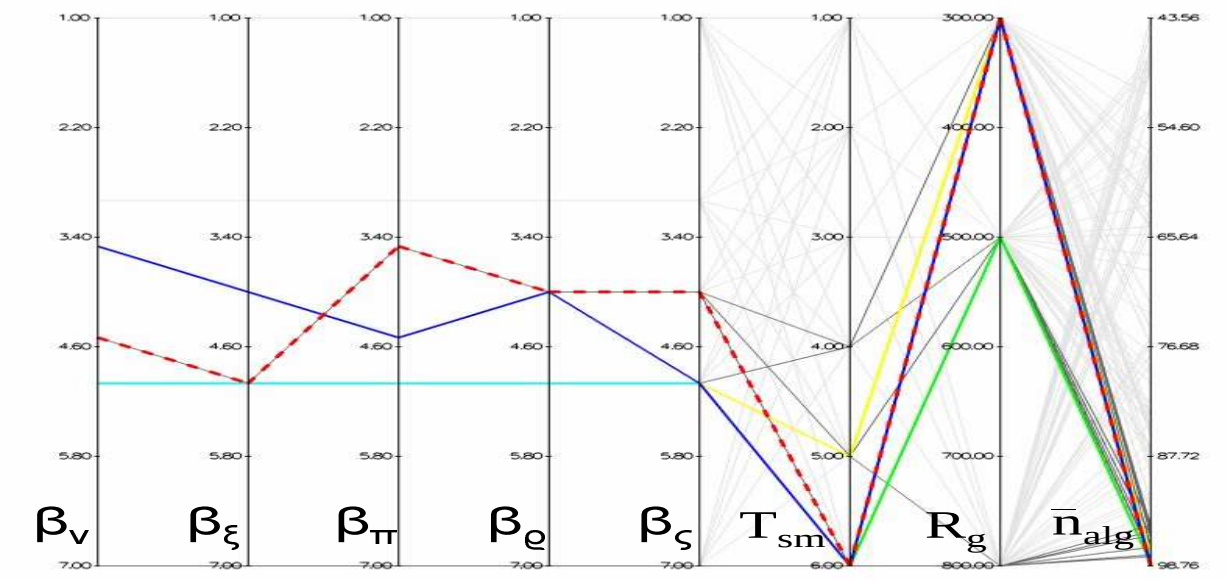

Figure E.13: Influence of β_ψ on the $\bar{n}_{alg}$ metric for EEMACOMC

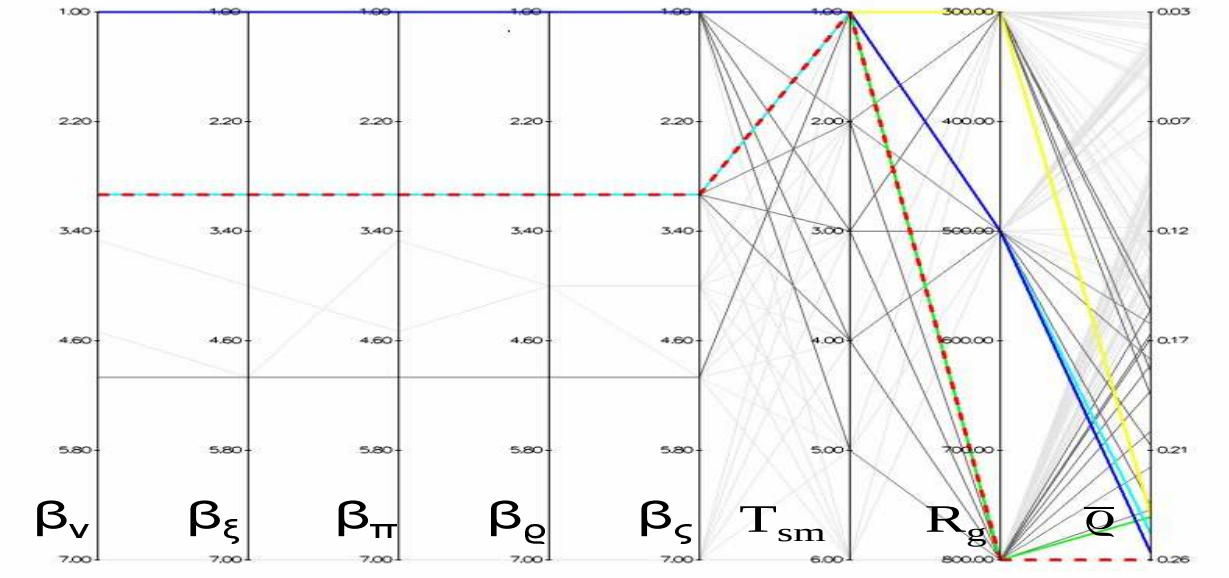

Figure E.14: Influence of β_ψ on the $\bar{\varrho}$ metric for EEMACOMC

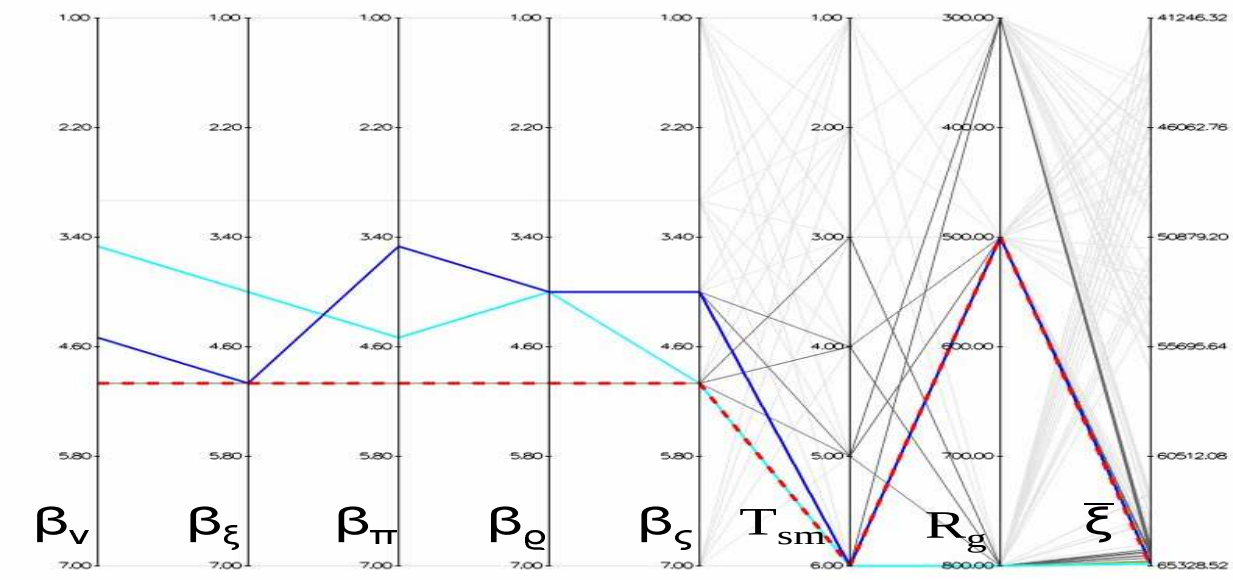

Figure E.15: Influence of β_ψ on the $\bar{\xi}$ metric for EEMACOMC

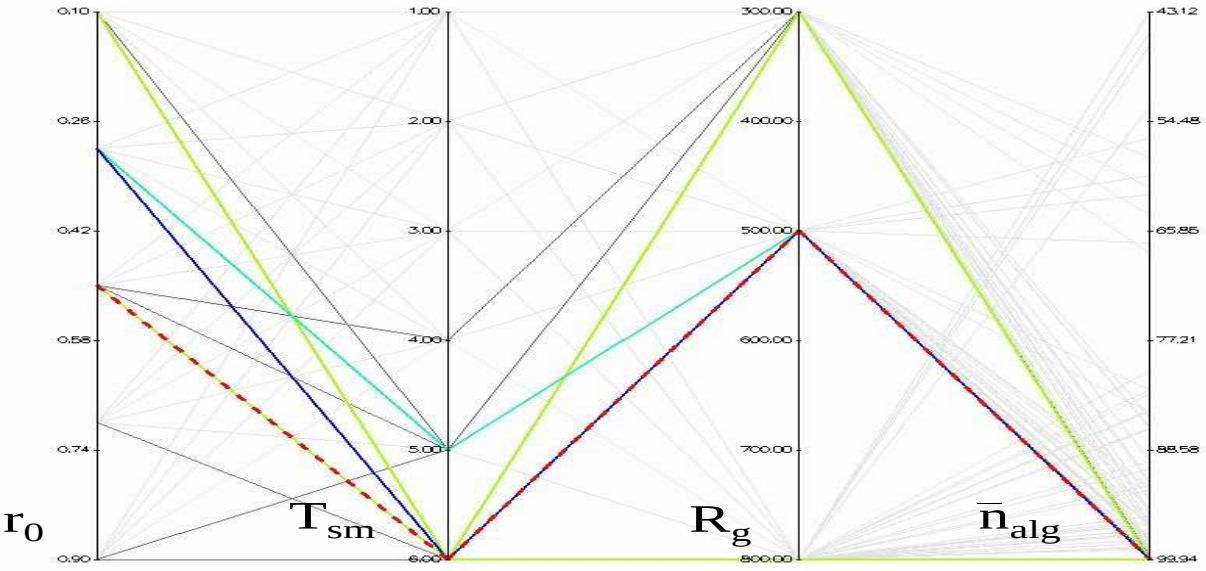

Figure E.16: Influence of r_0 on the $\bar{n}_{alg}$ metric for EEMACOMP

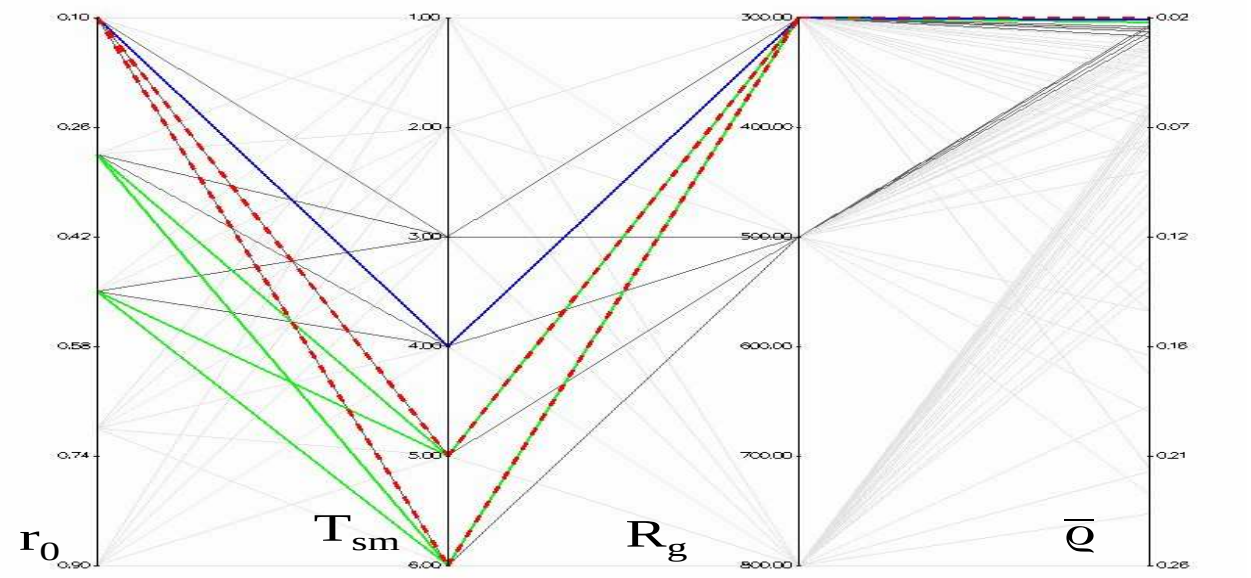

Figure E.17: Influence of r_0 on the $\bar{\varrho}$ metric for EEMACOMP

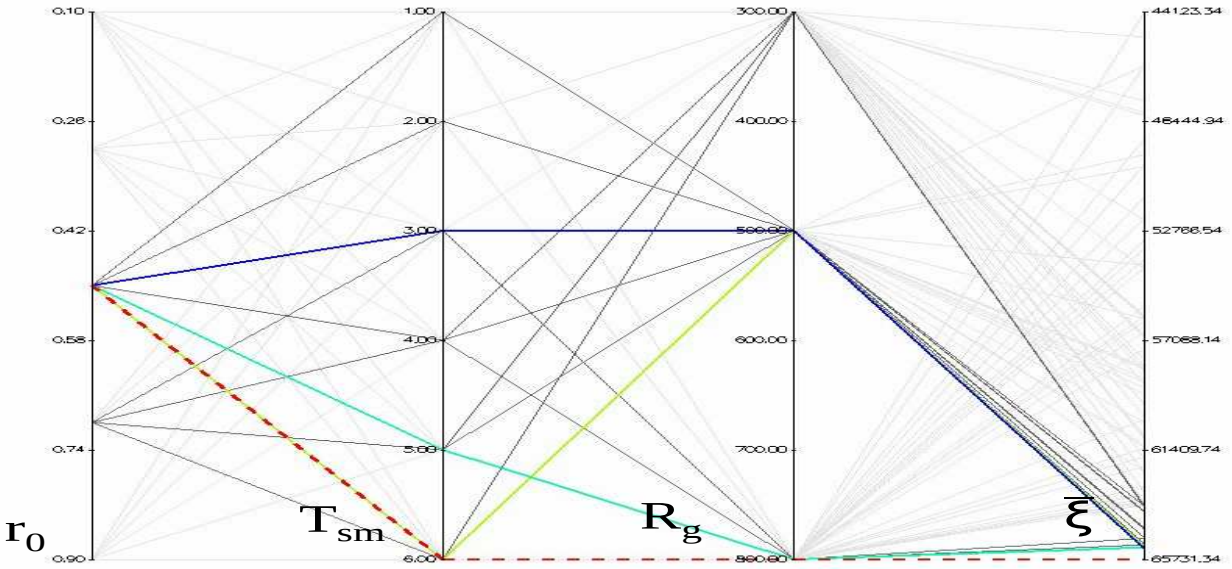

Figure E.18: Influence of r_0 on the $\bar{\xi}$ metric for EEMACOMP

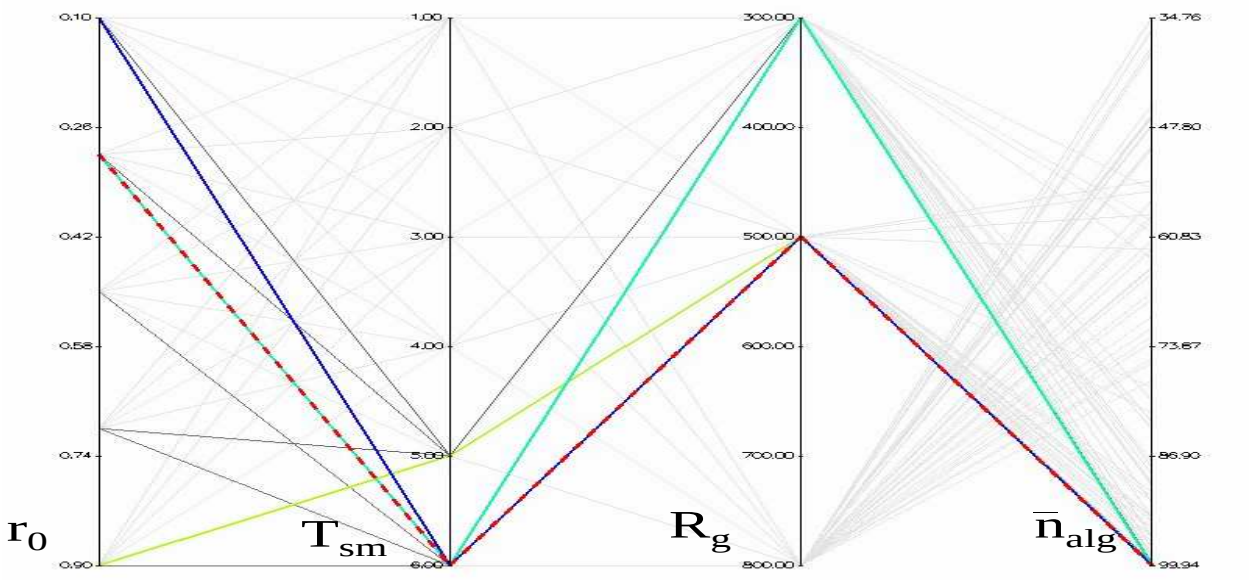

Figure E.19: Influence of r_0 on the $\bar{n}_{alg}$ metric for EEMACOMH

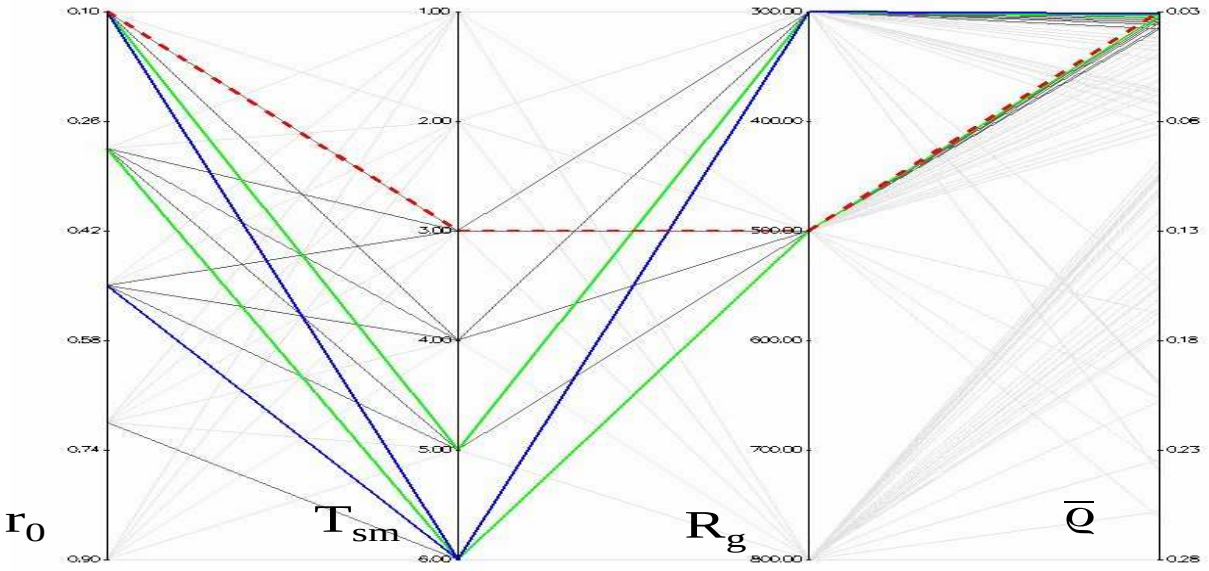

Figure E.20: Influence of r_0 on the $\bar{\varrho}$ metric for EEMACOMH

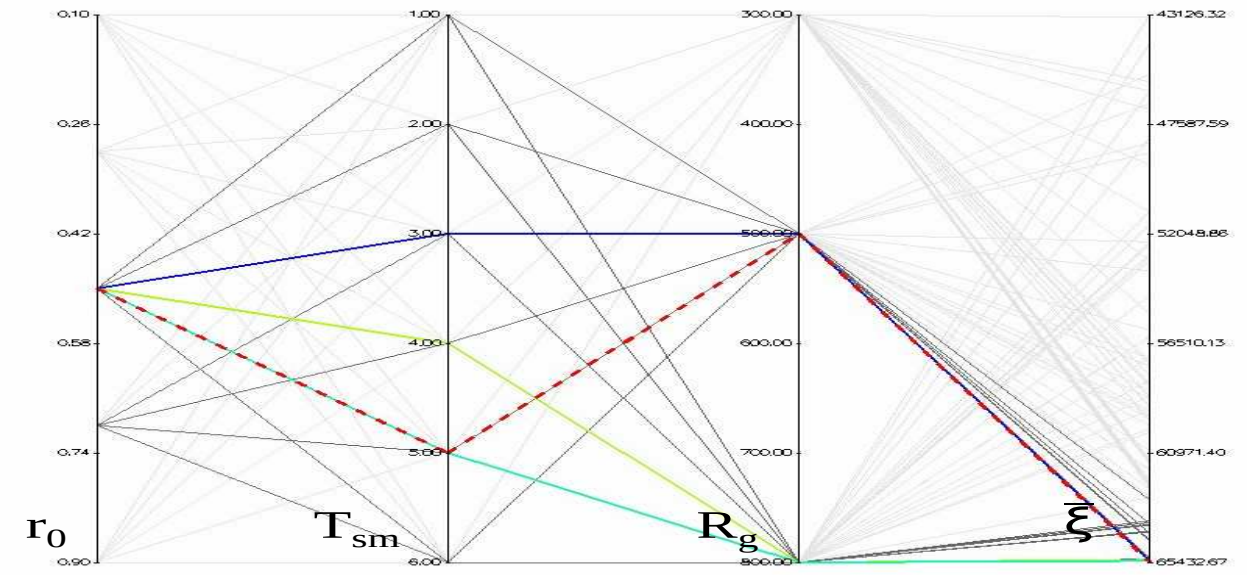

Figure E.21: Influence of r_0 on the $\bar{\xi}$ metric for EEMACOMH

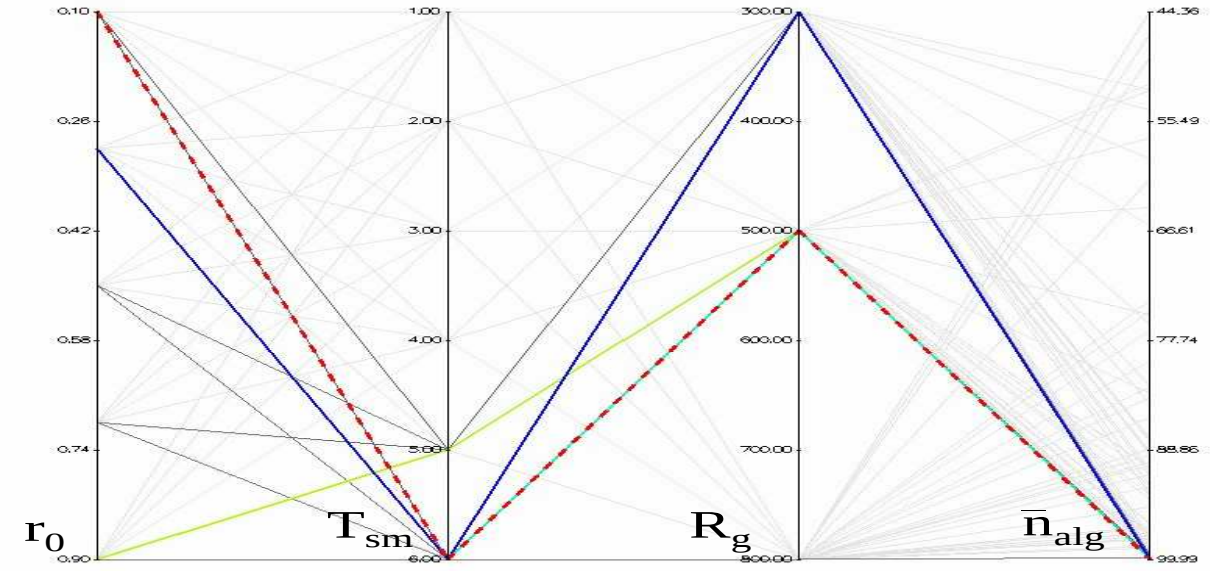

Figure E.22: Influence of r_0 on the $\bar{n}_{alg}$ metric for EEMACOMC

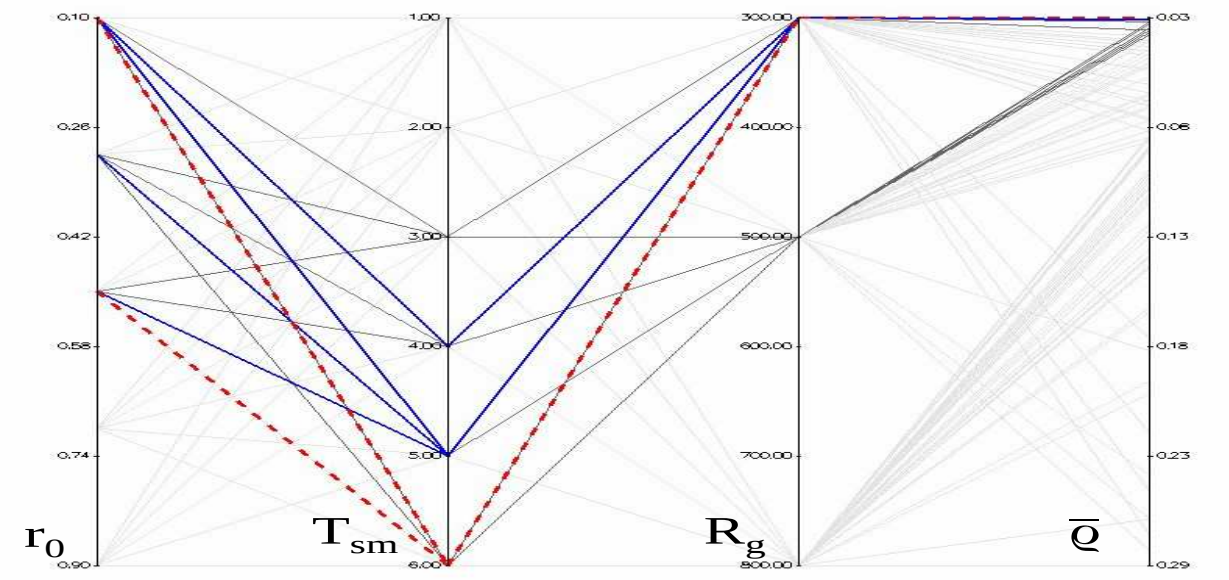

Figure E.23: Influence of r_0 on the $\bar{\varrho}$ metric for EEMACOMC

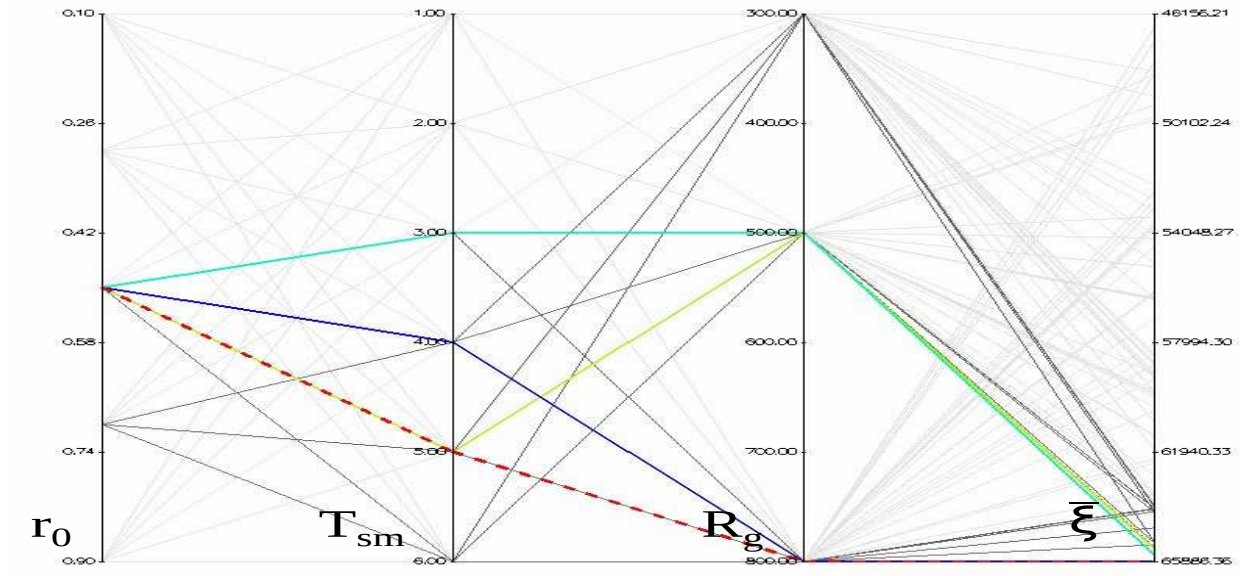

Figure E.24: Influence of r_0 on the $\bar{\xi}$ metric for EEMACOMC

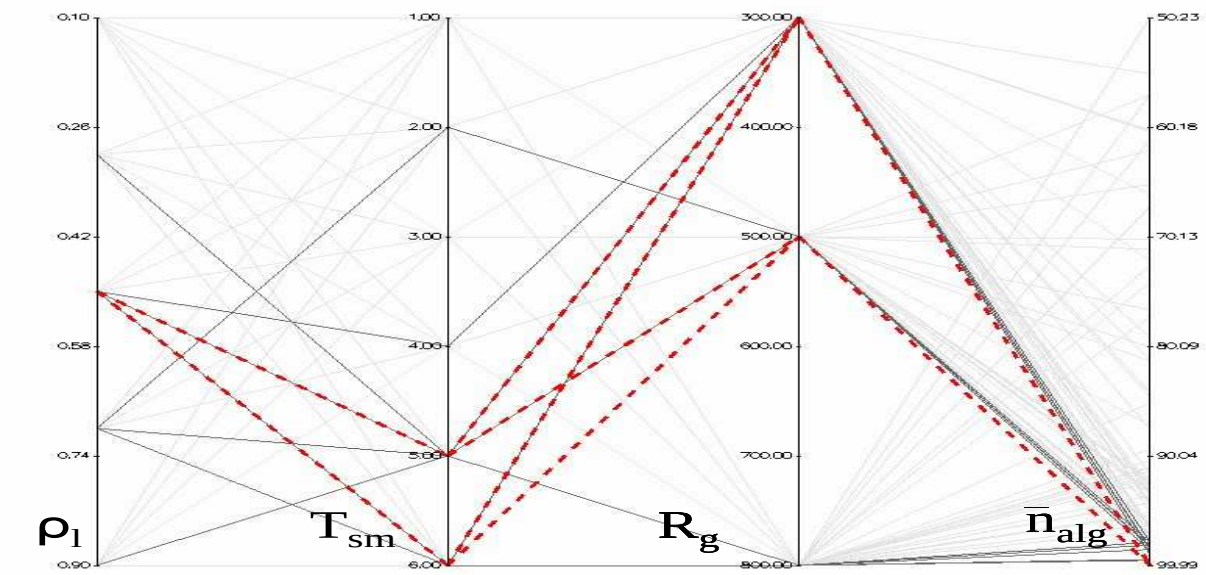

Figure E.25: Influence of ρ_l on the $\bar{n}_{alg}$ metric for EEMACOMP

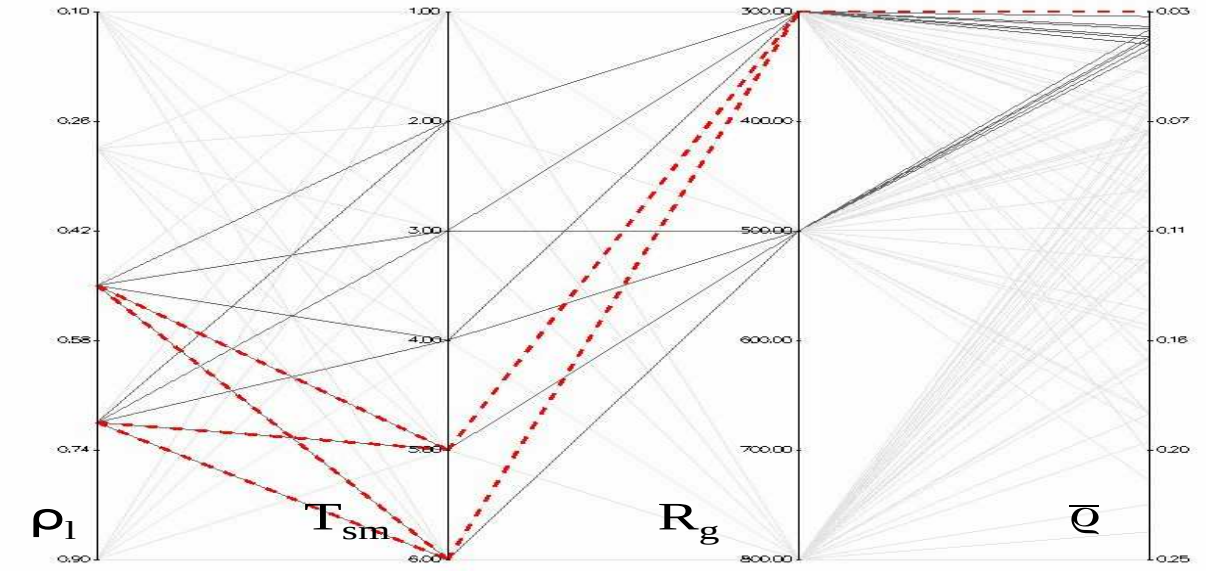

Figure E.26: Influence of ρ_l on the $\bar{\varrho}$ metric for EEMACOMP

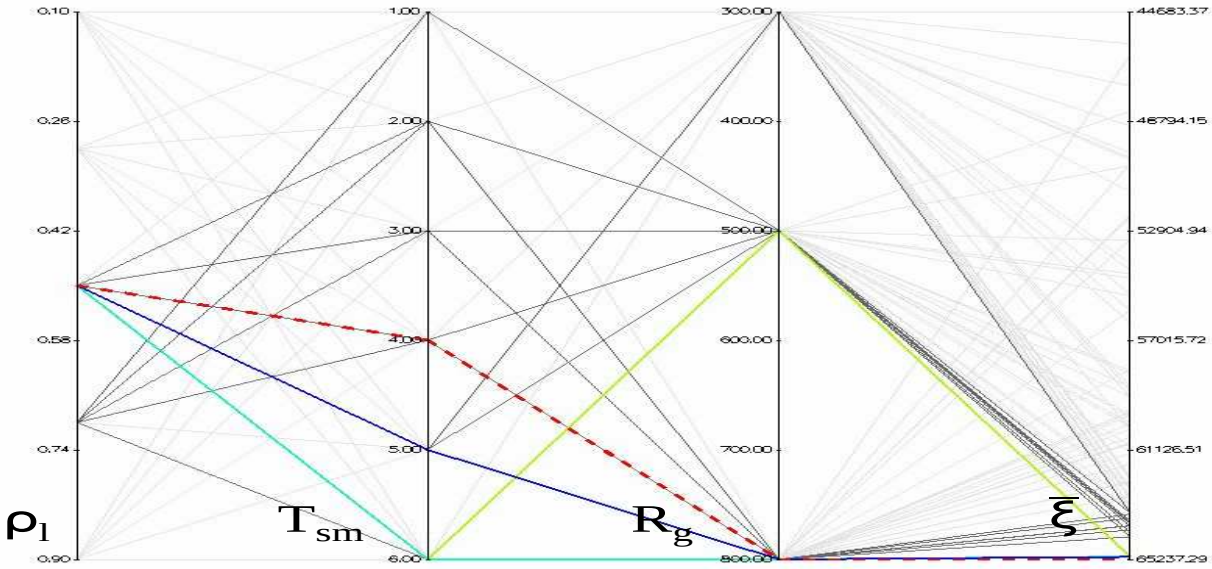

Figure E.27: Influence of ρ_l on the $\bar{\xi}$ metric for EEMACOMP

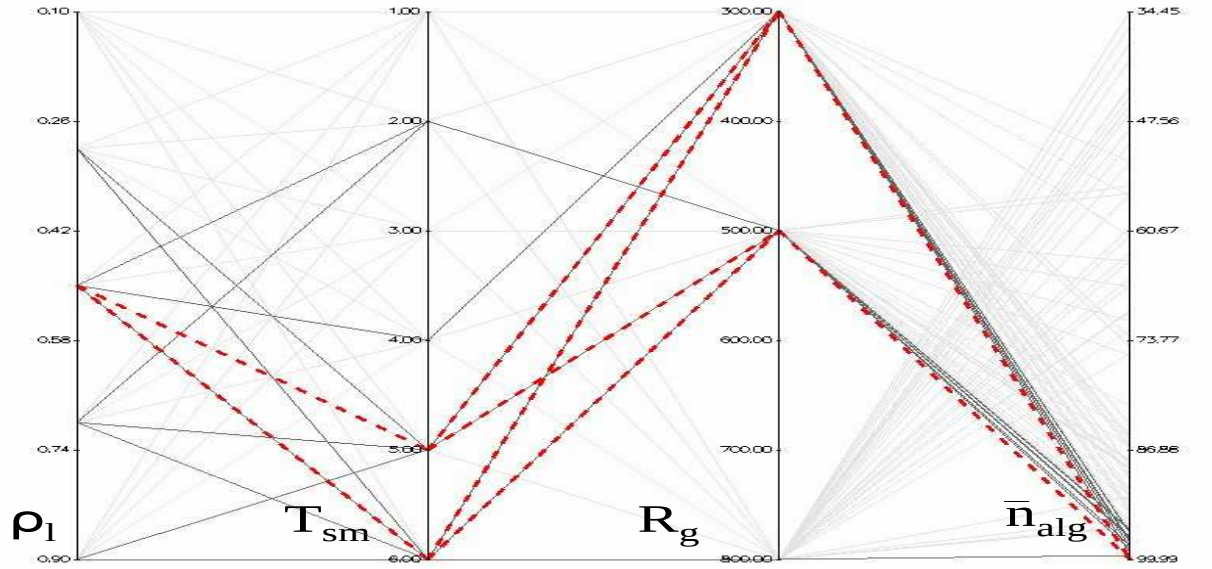

Figure E.28: Influence of ρ_l on the $\bar{n}_{alg}$ metric for EEMACOMH

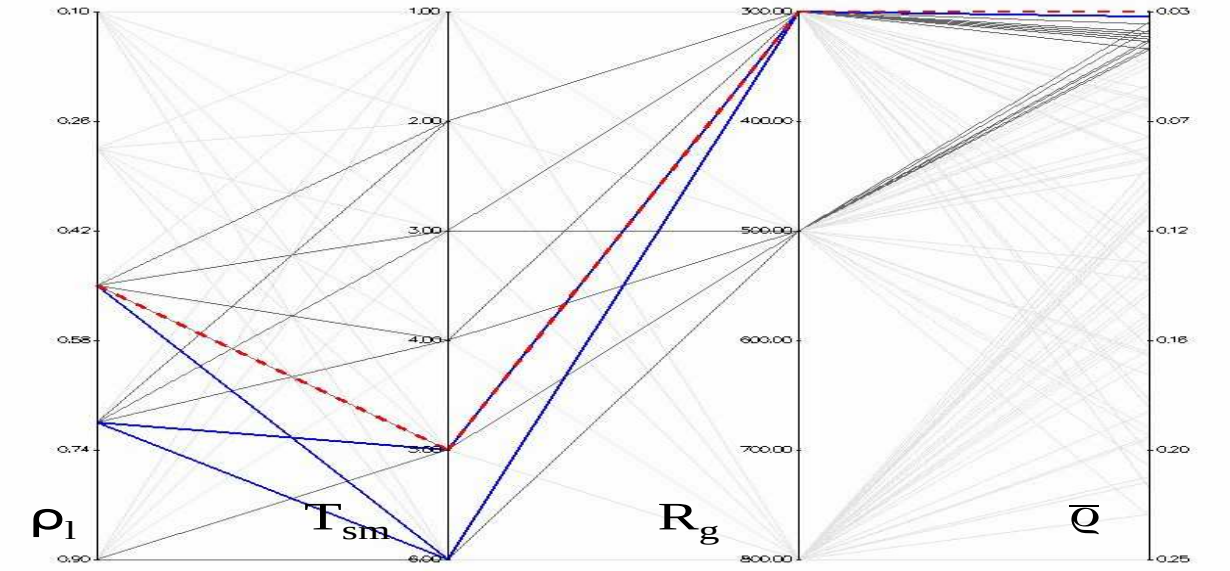

Figure E.29: Influence of ρ_l on the $\bar{\varrho}$ metric for EEMACOMH

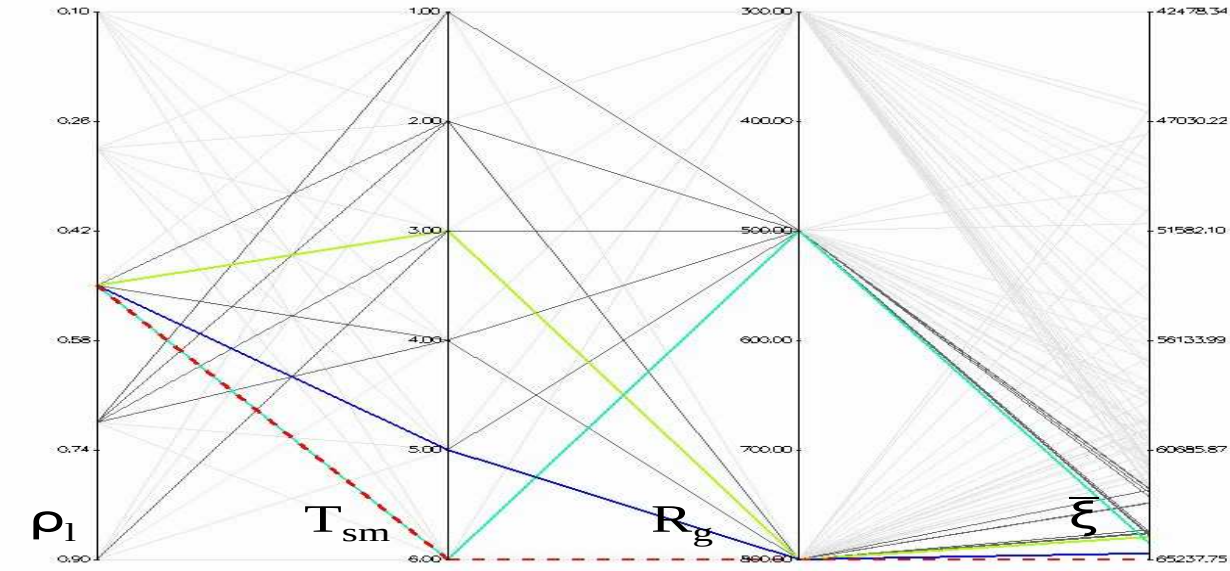

Figure E.30: Influence of ρ_l on the $\bar{\xi}$ metric for EEMACOMH

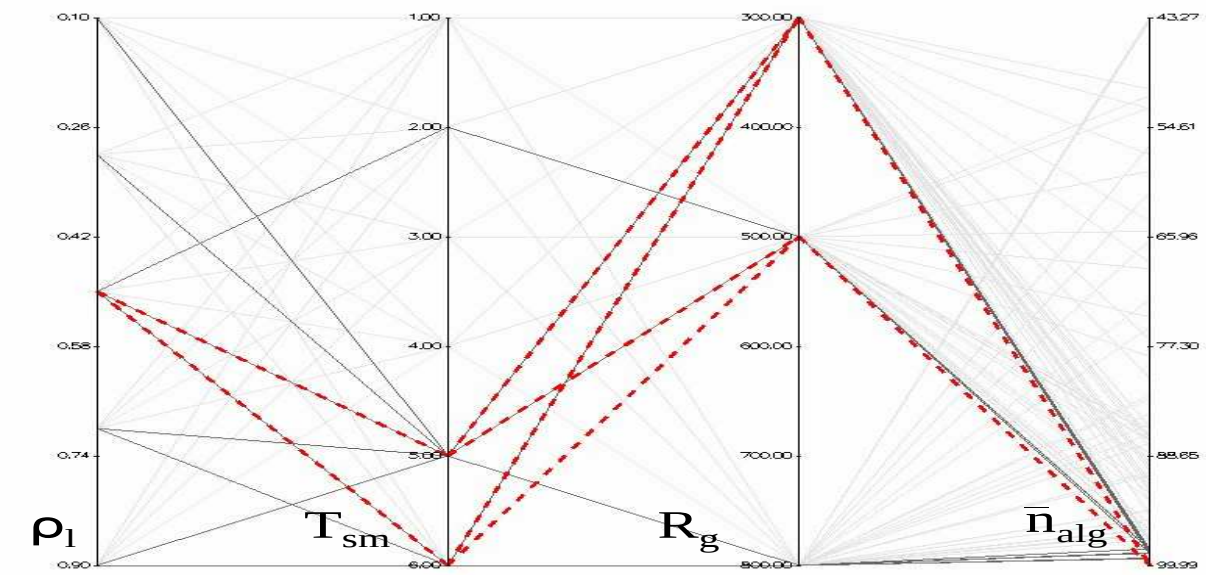

Figure E.31: Influence of ρ_l on the $\bar{n}_{alg}$ metric for EEMACOMC

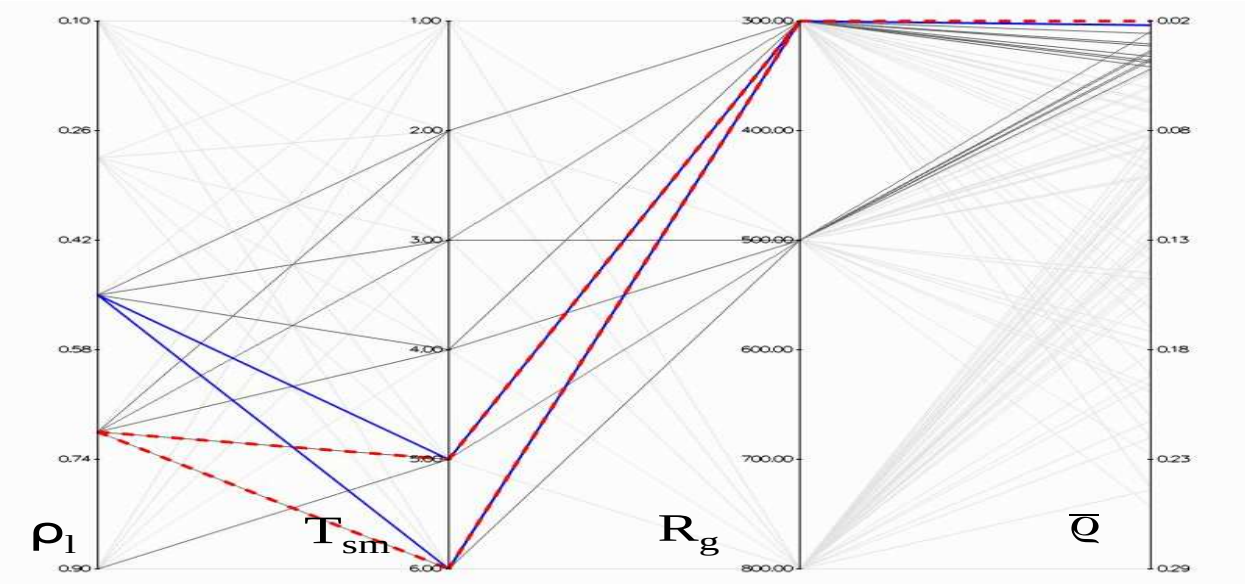

Figure E.32: Influence of ρ_l on the $\bar{\varrho}$ metric for EEMACOMC

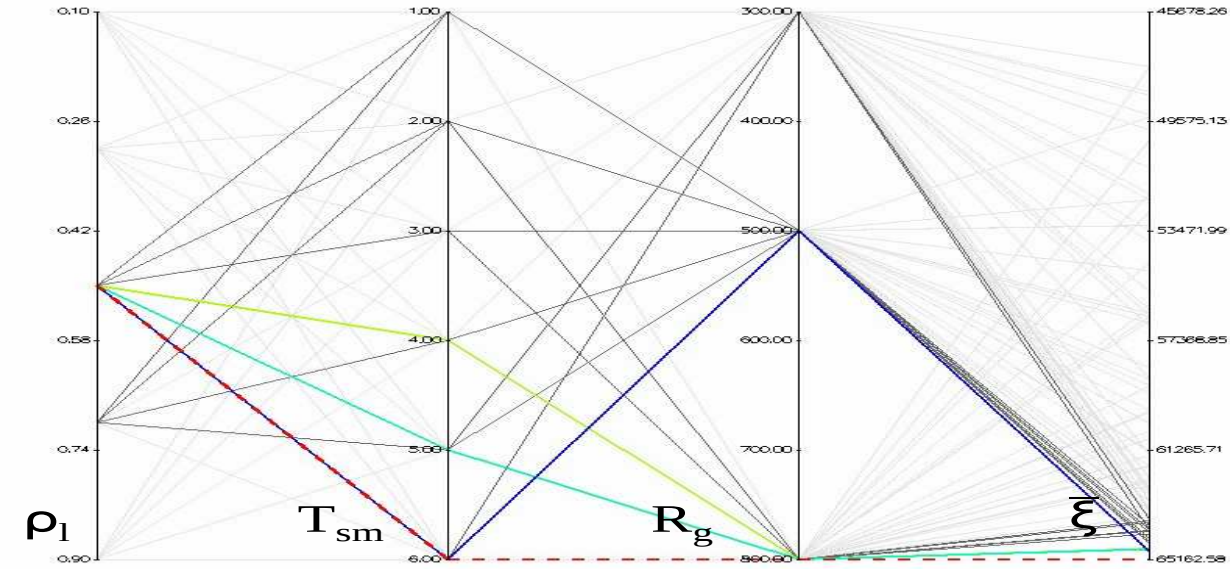

Figure E.33: Influence of ρ_l on the $\bar{\xi}$ metric for EEMACOMC

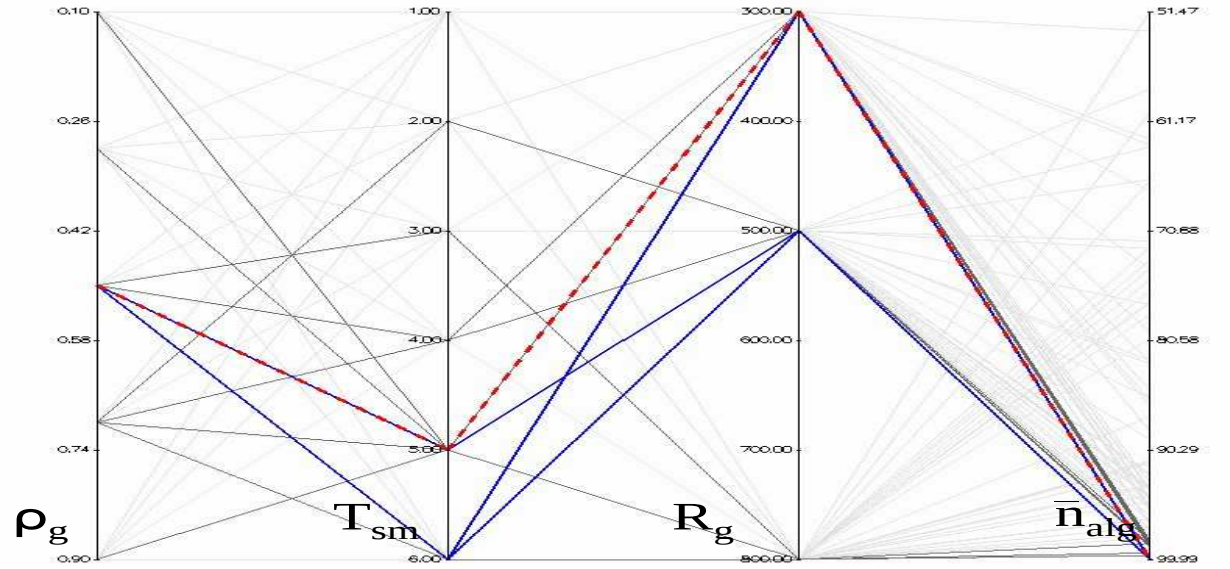

Figure E.34: Influence of ρ_g on the $\bar{n}_{alg}$ metric for EEMACOMP

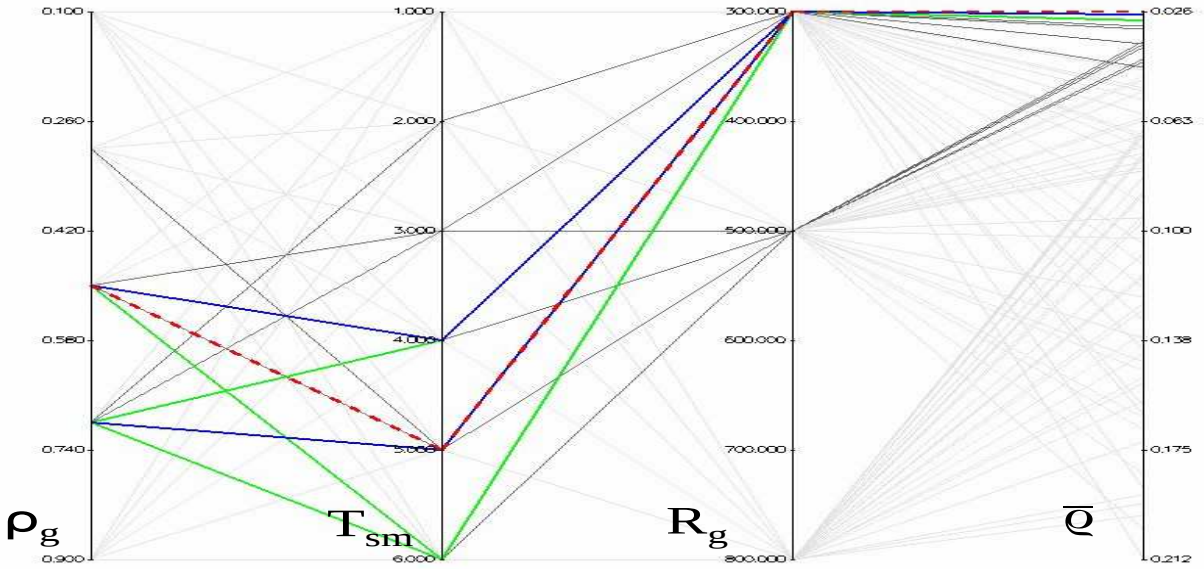

Figure E.35: Influence of ρ_g on the $\bar{\varrho}$ metric for EEMACOMP

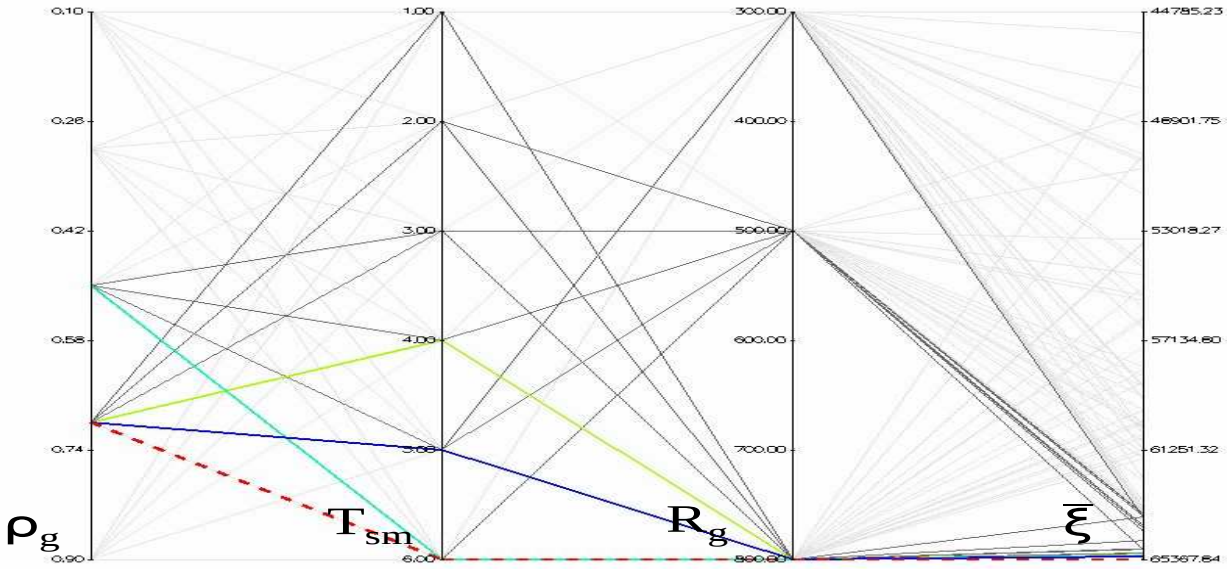

Figure E.36: Influence of ρ_g on the $\bar{\xi}$ metric for EEMACOMP

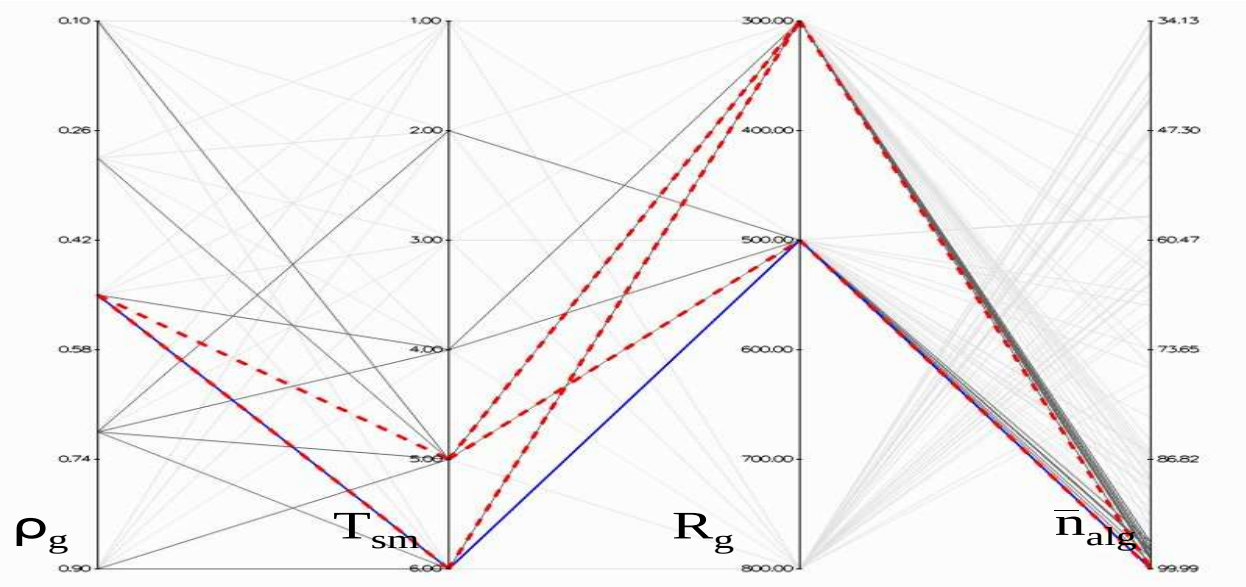

Figure E.37: Influence of ρ_g on the $\bar{n}_{alg}$ metric for EEMACOMH

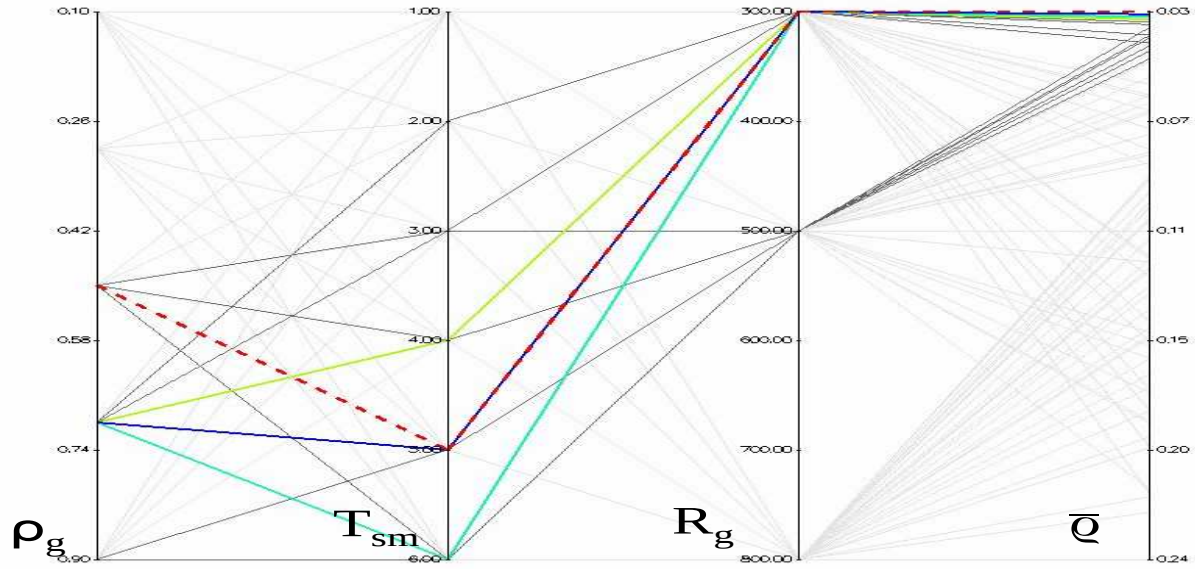

Figure E.38: Influence of ρ_g on the $\bar{\varrho}$ metric for EEMACOMH

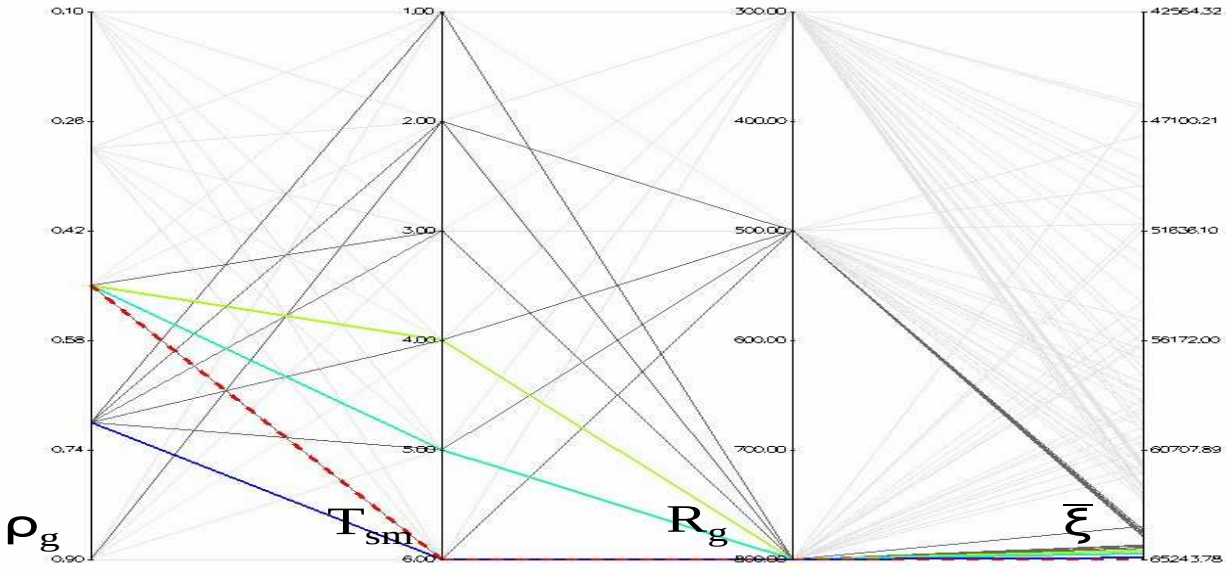

Figure E.39: Influence of ρ_g on the $\bar{\xi}$ metric for EEMACOMH

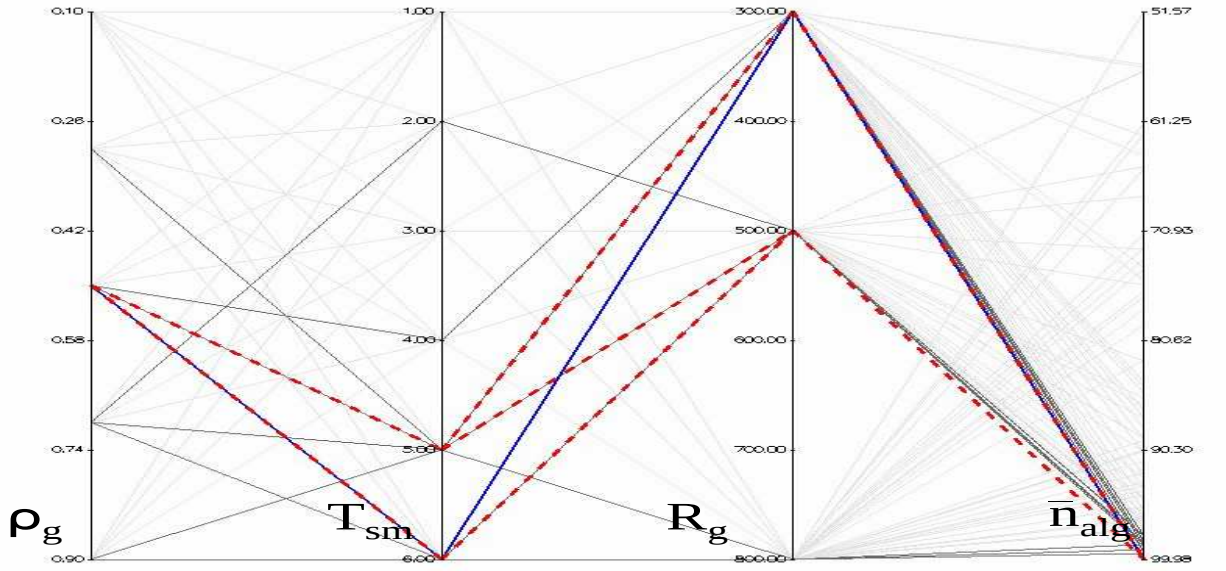

Figure E.40: Influence of ρ_g on the $\bar{n}_{alg}$ metric for EEMMASMP

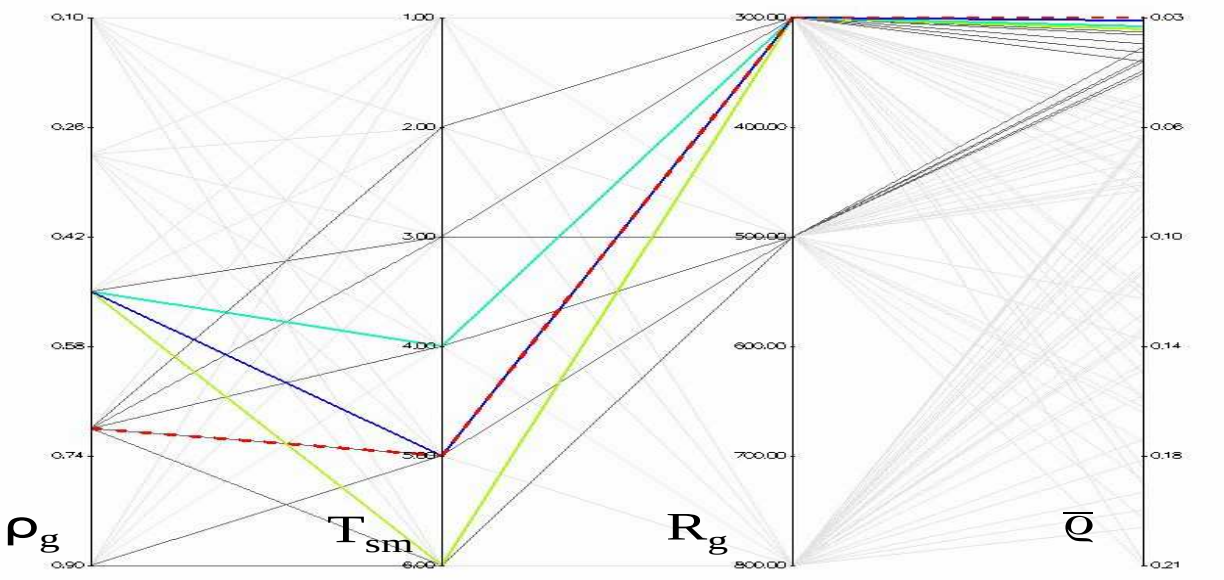

Figure E.41: Influence of ρ_g on the $\bar{\varrho}$ metric for EEMMASMP

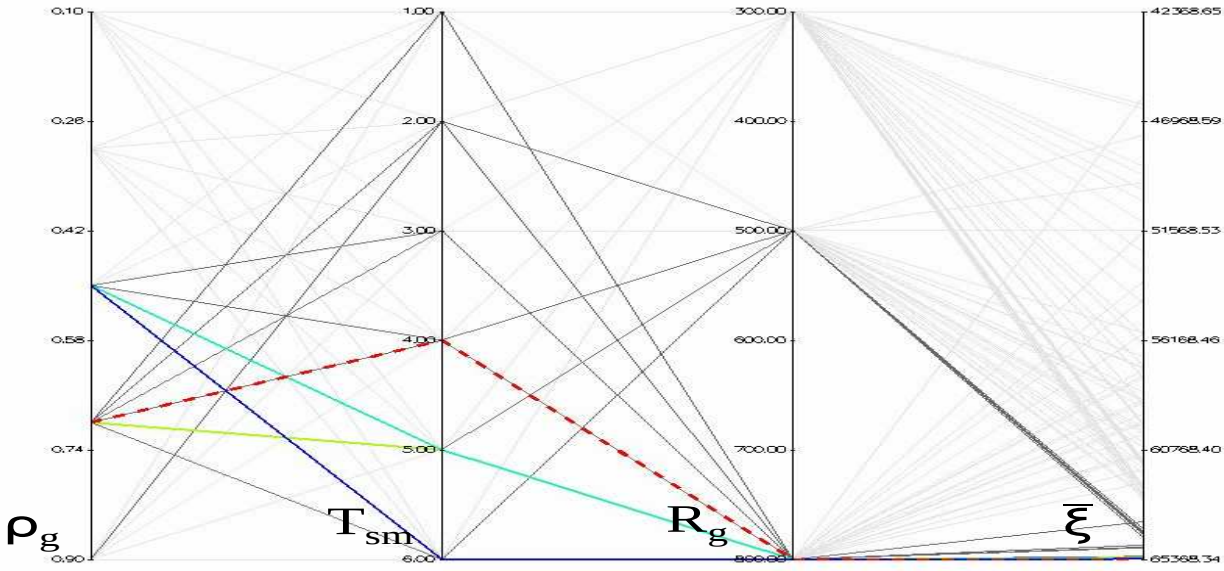

Figure E.42: Influence of ρ_g on the $\bar{\xi}$ metric for EEMMASMP

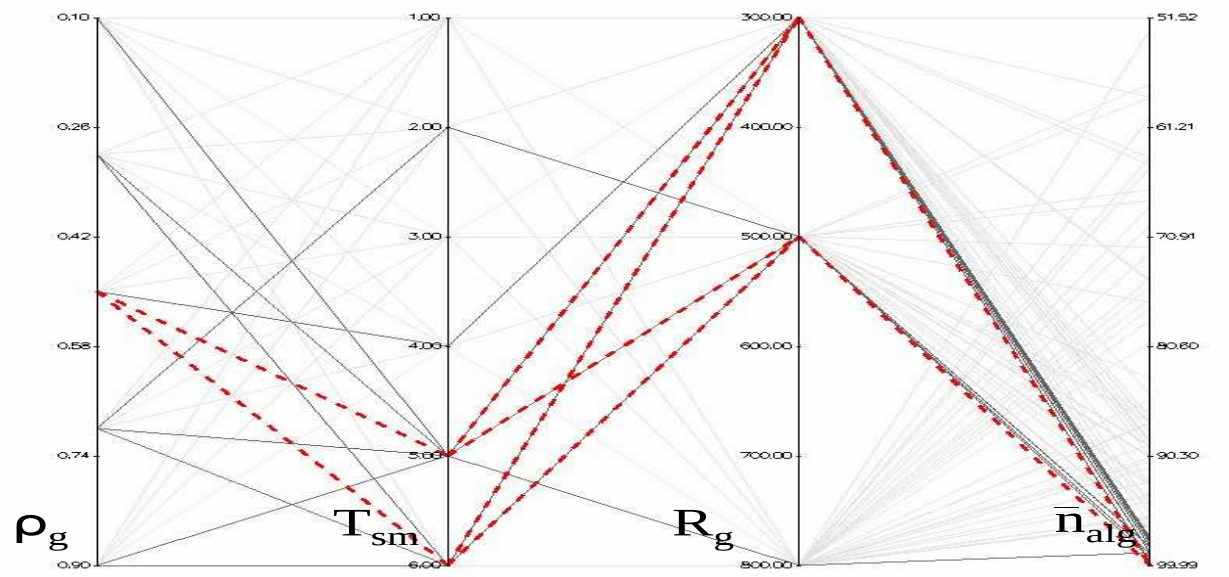

Figure E.43: Influence of ρ_g on the $\bar{n}_{alg}$ metric for EEMMASMH

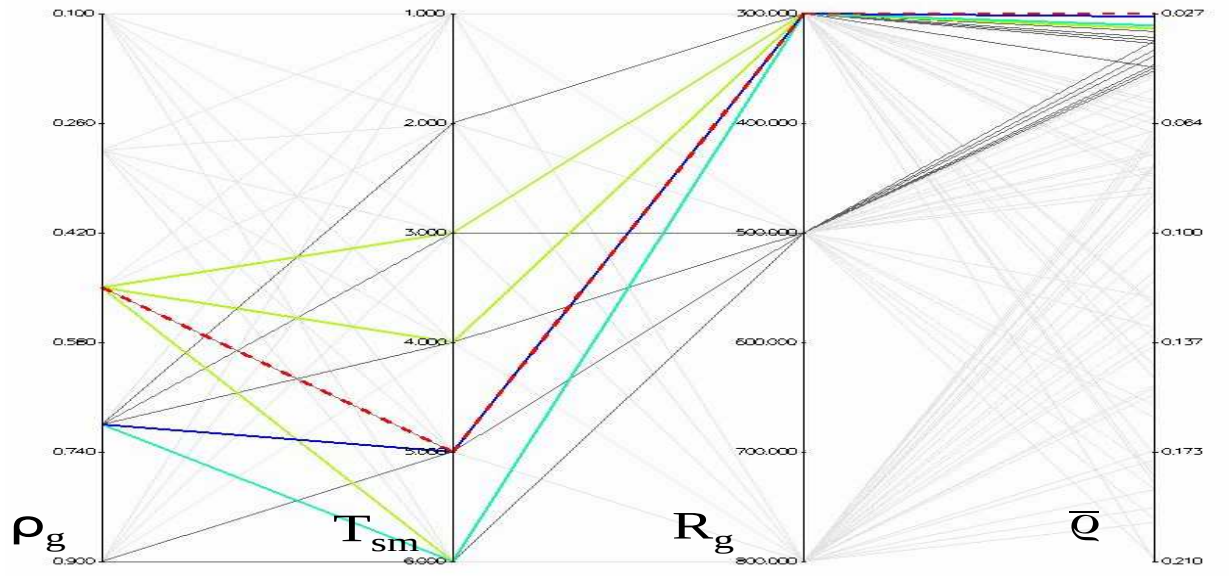

Figure E.44: Influence of ρ_g on the $\bar{\varrho}$ metric for EEMMASMH

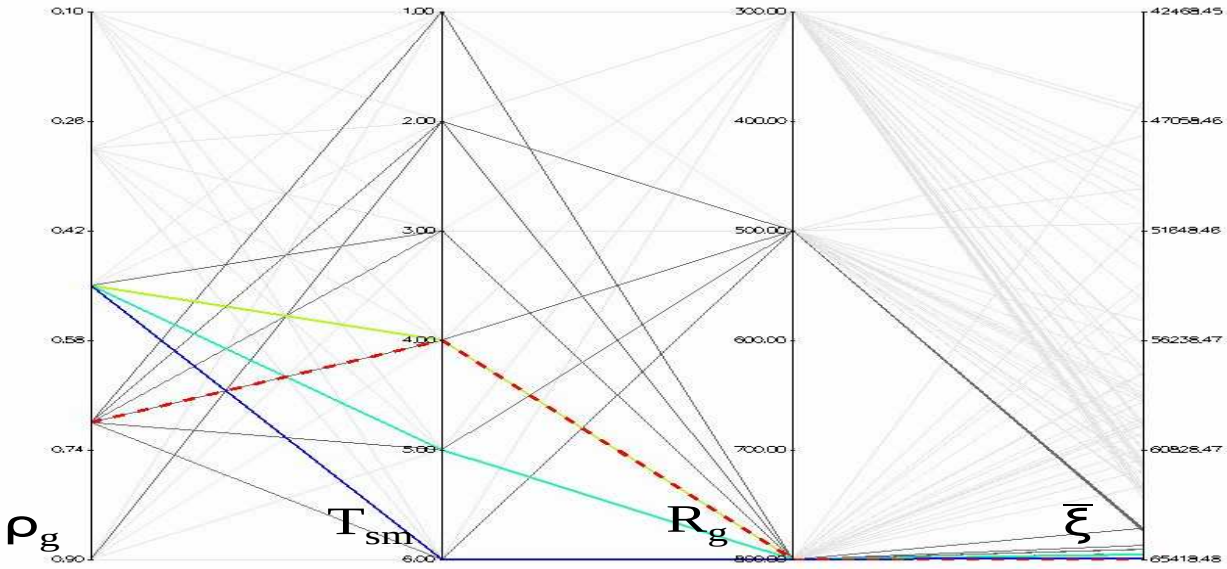

Figure E.45: Influence of ρ_g on the $\bar{\xi}$ metric for EEMMASMH

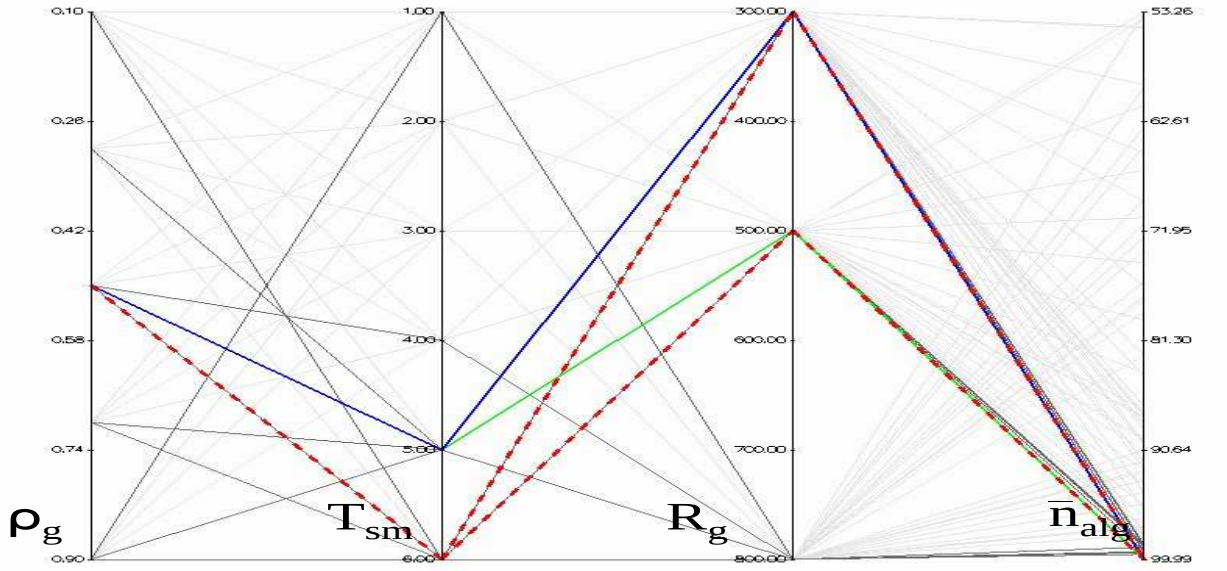

Figure E.46: Influence of ρ_g on the $\bar{n}_{alg}$ metric for EEMACOMC

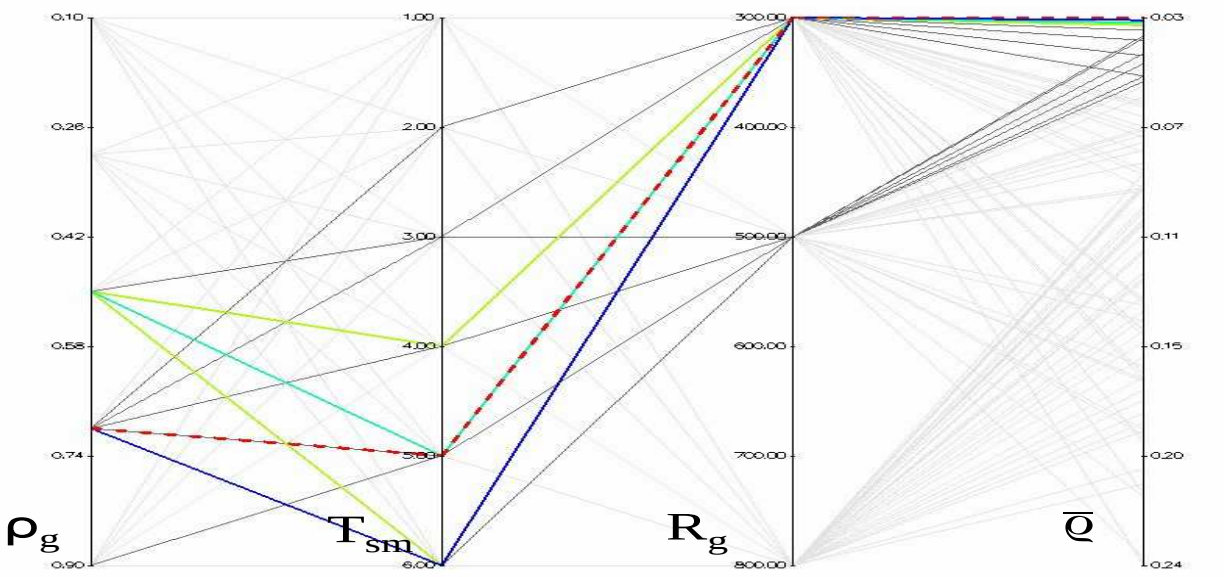

Figure E.47: Influence of ρ_g on the $\bar{\varrho}$ metric for EEMACOMC

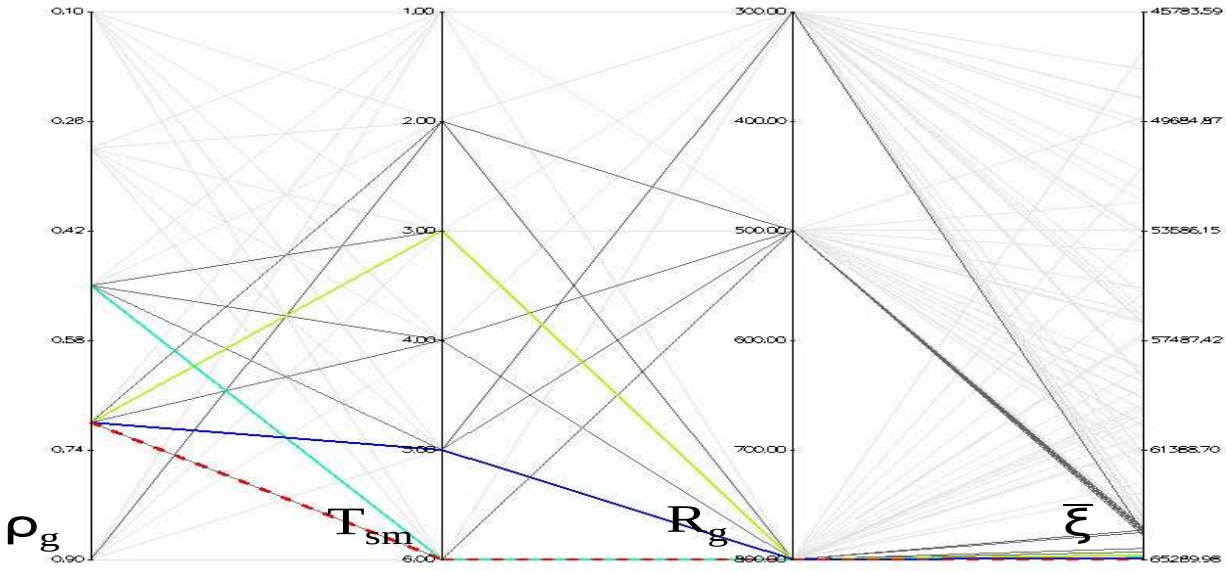

Figure E.48: Influence of ρ_g on the $\bar{\xi}$ metric for EEMACOMC

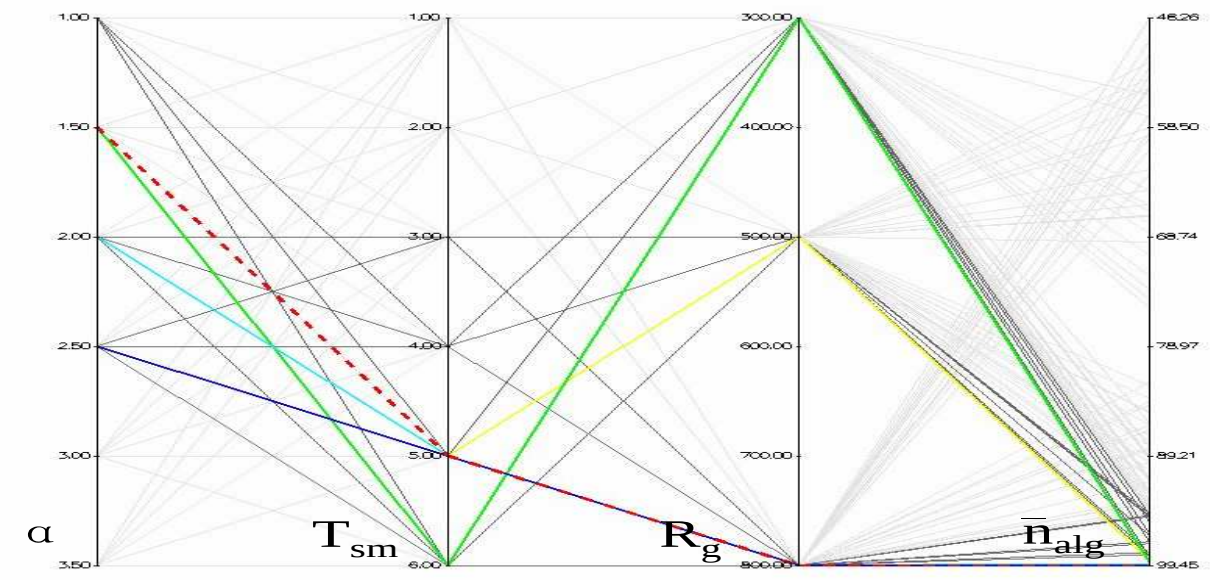

Figure E.49: Influence of α on the $\bar{n}_{alg}$ metric for EEMMASMP

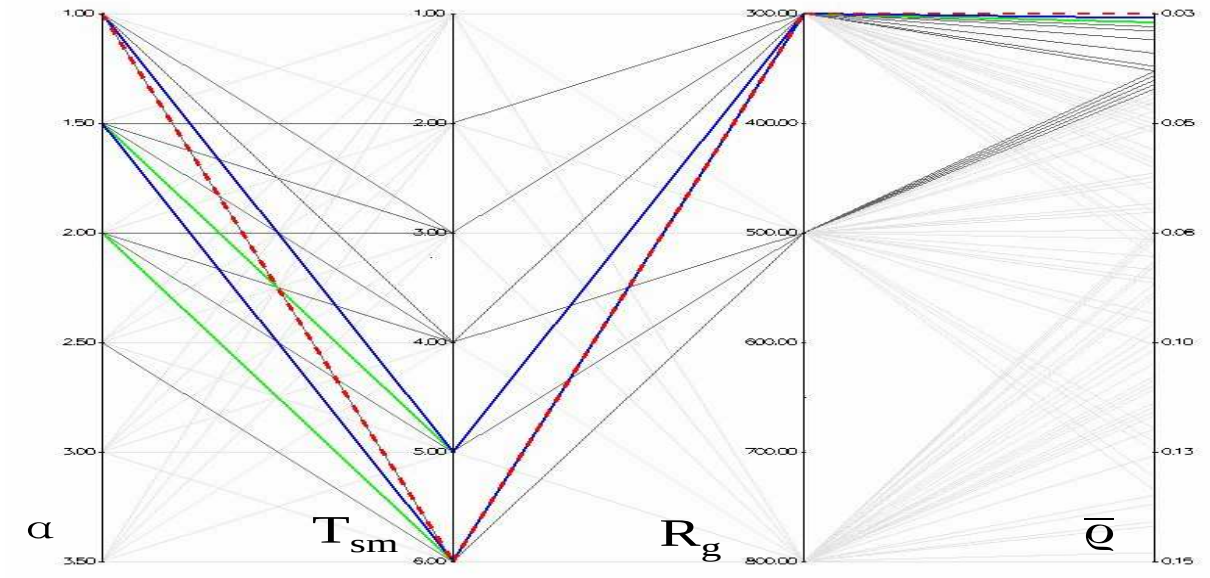

Figure E.50: Influence of α on the $\bar{\varrho}$ metric for EEMMASMP

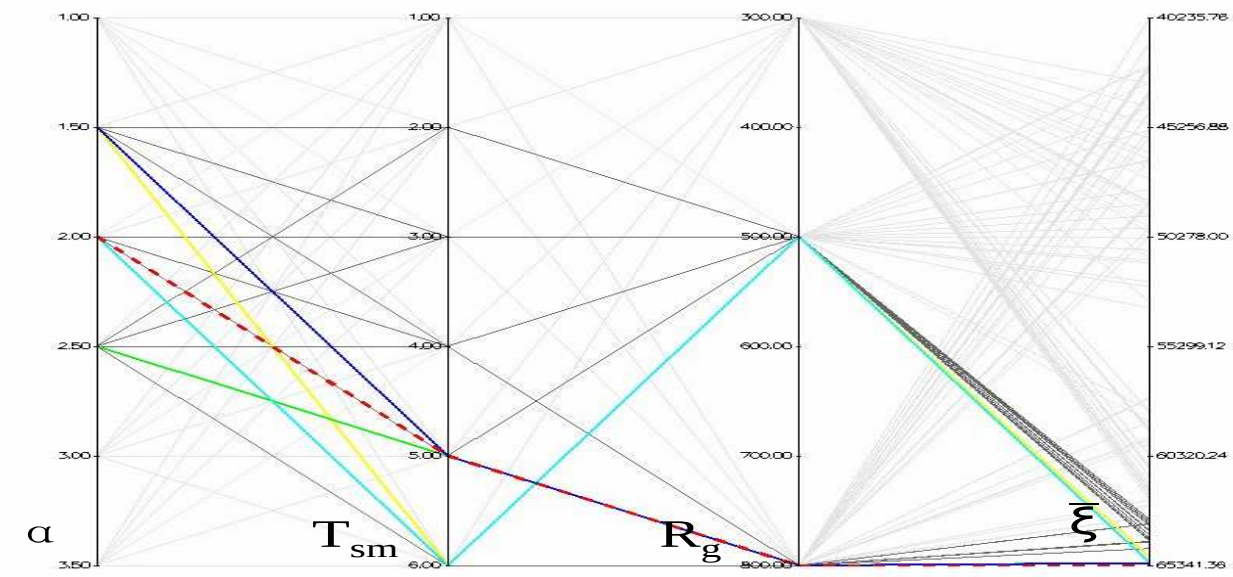

Figure E.51: Influence of α on the $\bar{\xi}$ metric for EEMMASMP

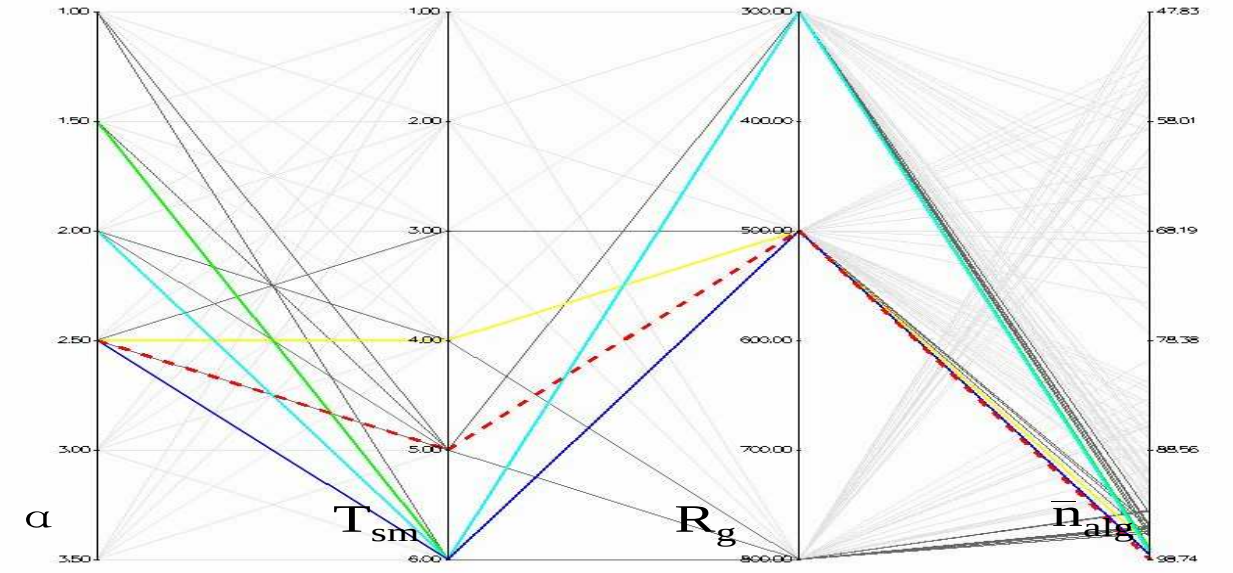

Figure E.52: Influence of α on the $\bar{n}_{alg}$ metric for EEMMASMH

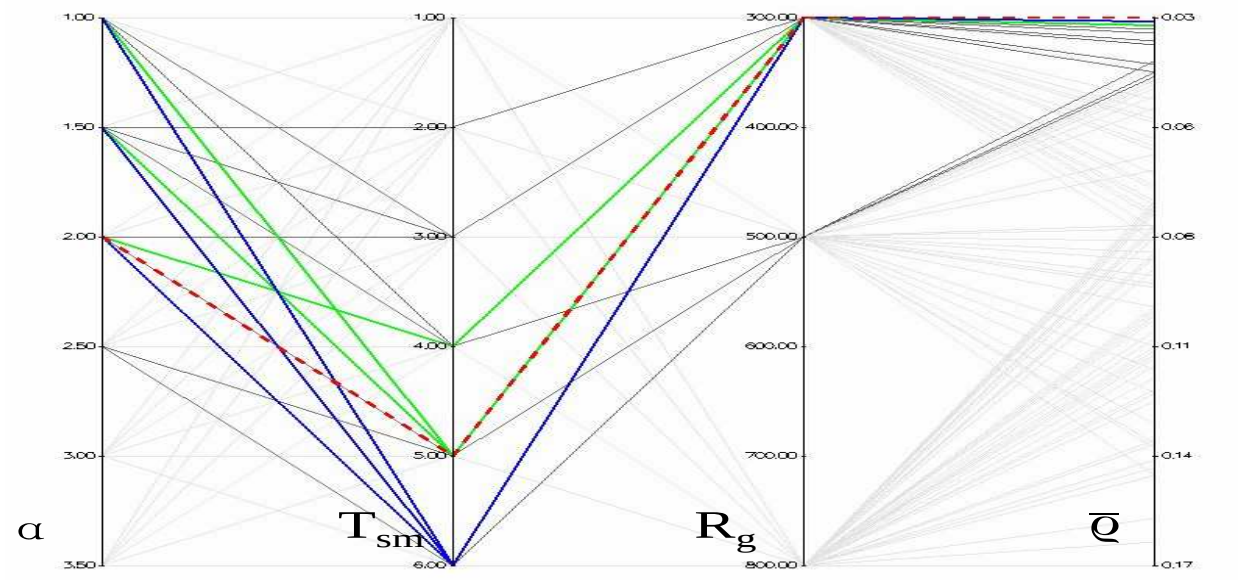

Figure E.53: Influence of α on the $\bar{\varrho}$ metric for EEMMASMH

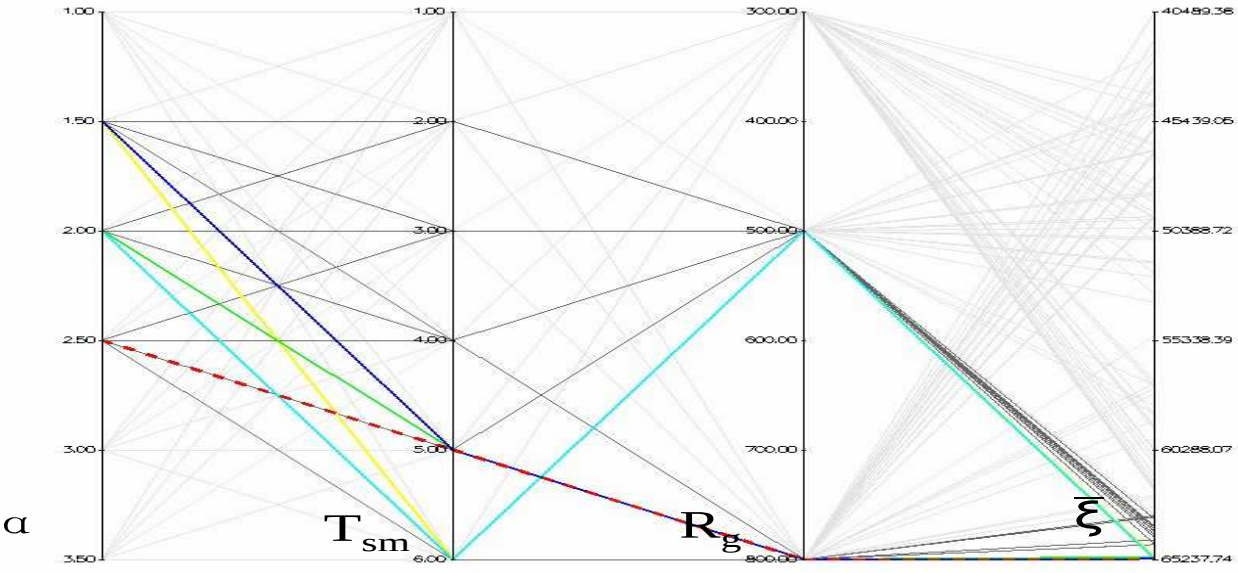

Figure E.54: Influence of α on the $\bar{\xi}$ metric for EEMMASMH

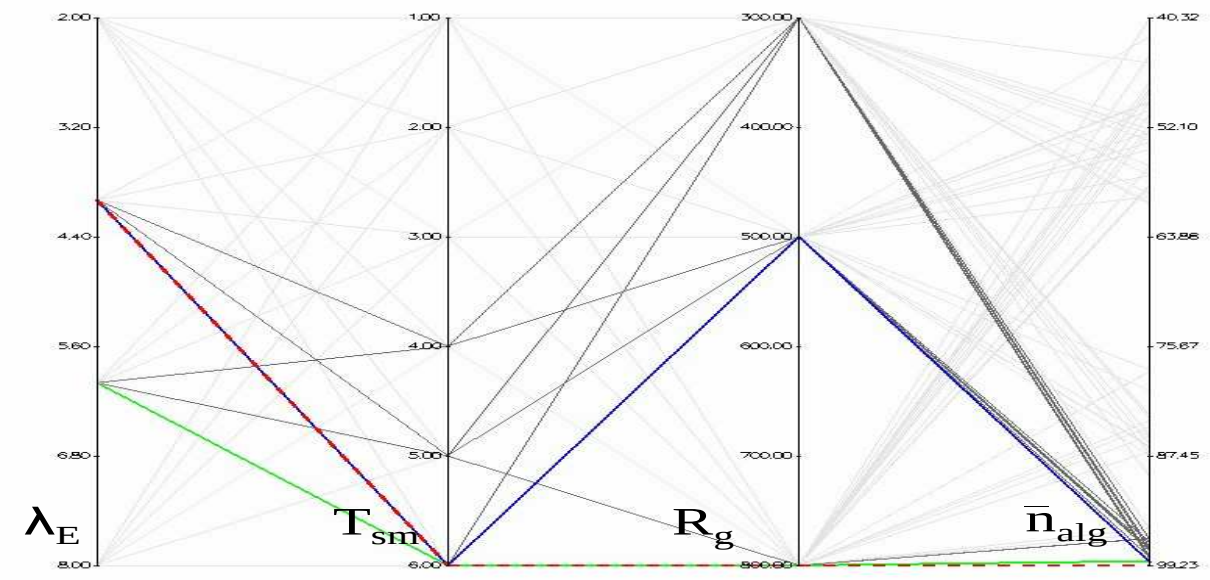

Figure E.55: Influence of λ_E on the $\bar{n}_{alg}$ metric for EEMACOMP

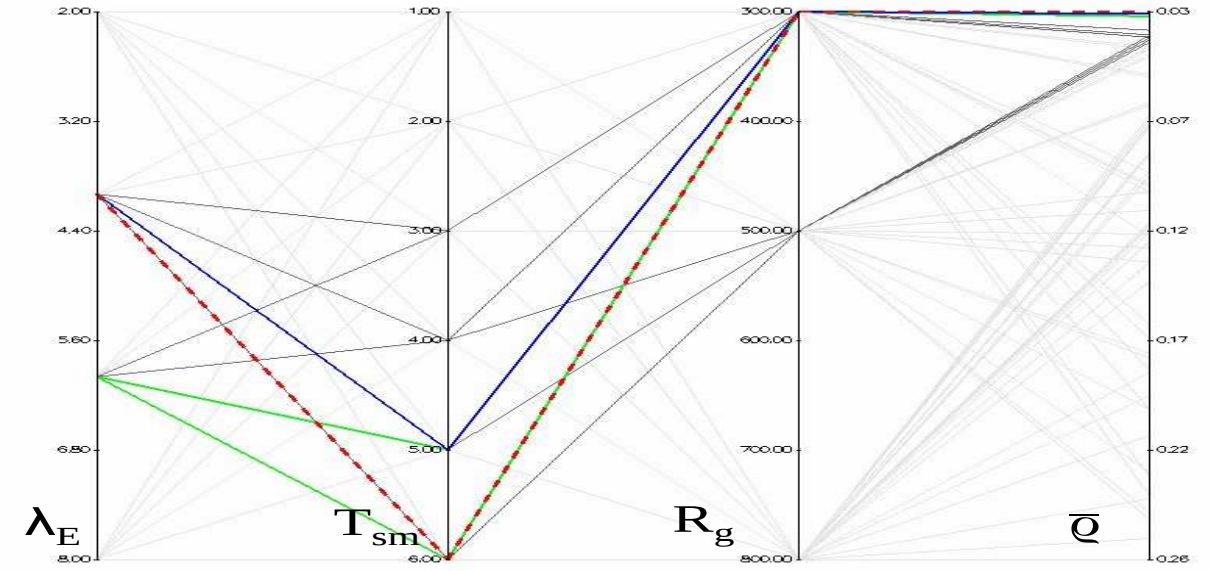

Figure E.56: Influence of λ_E on the $\bar{\varrho}$ metric for EEMACOMP

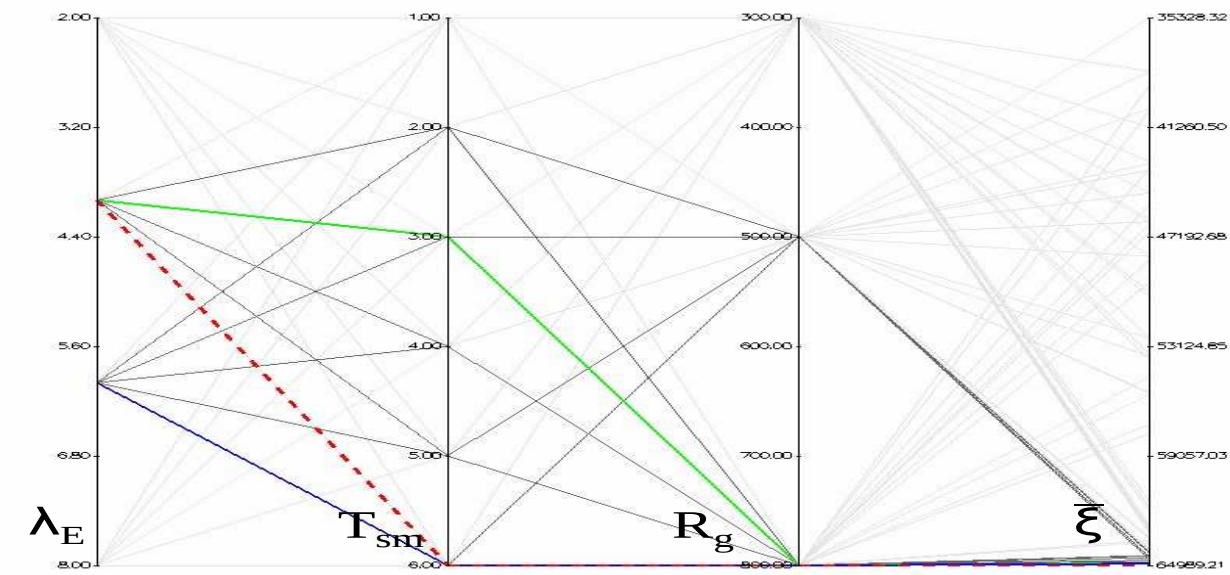

Figure E.57: Influence of λ_E on the $\bar{\xi}$ metric for EEMACOMP

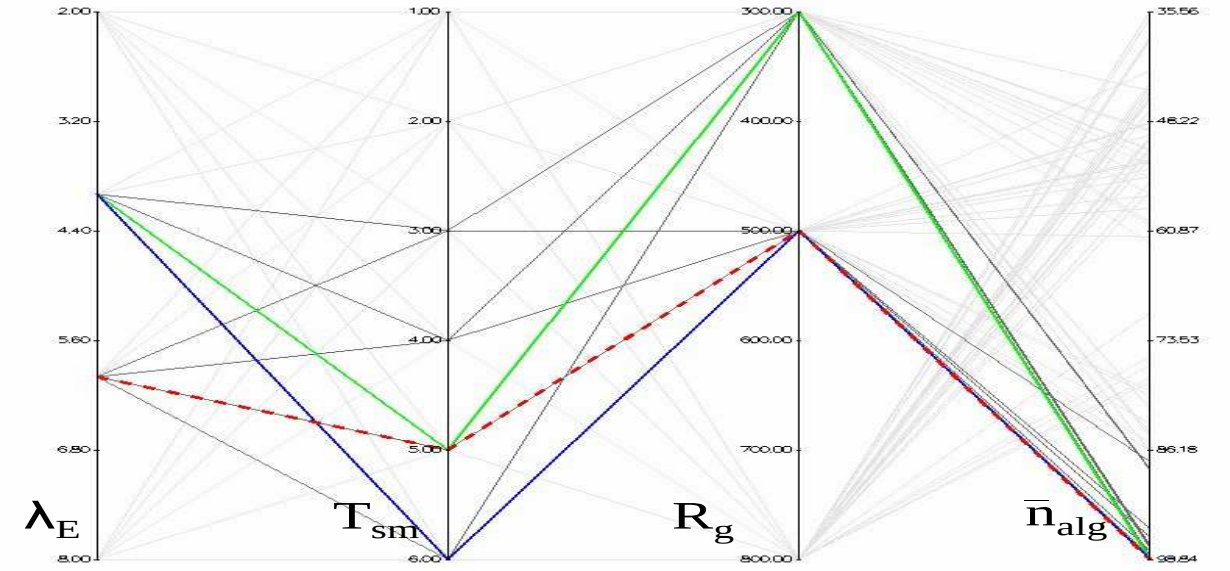

Figure E.58: Influence of λ_E on the $\bar{n}_{alg}$ metric for EEMACOMH

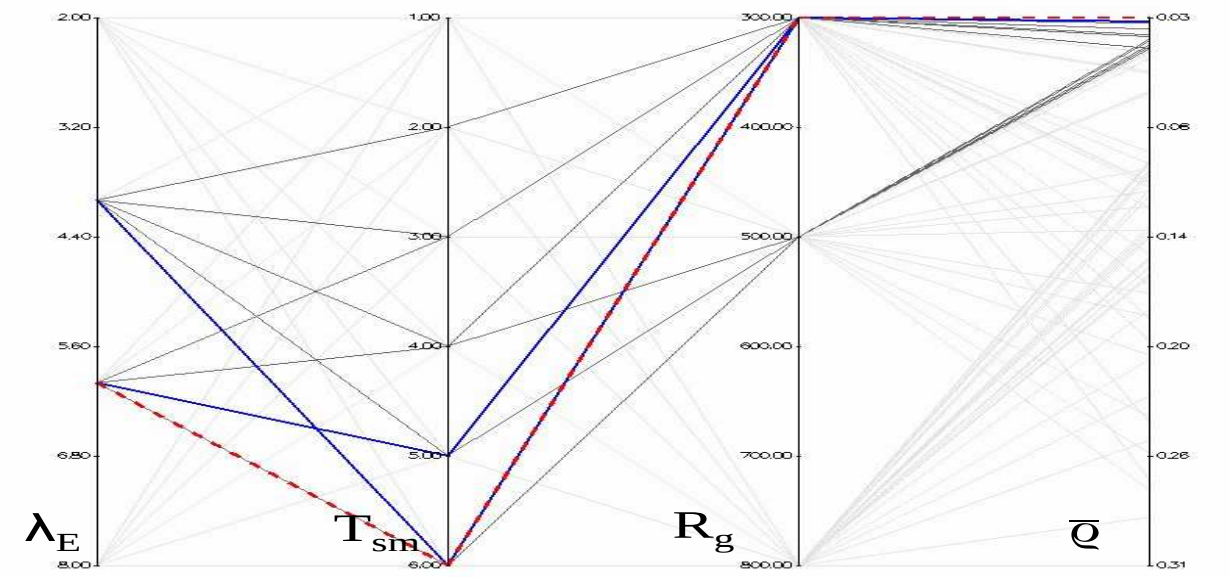

Figure E.59: Influence of λ_E on the $\bar{\varrho}$ metric for EEMACOMH

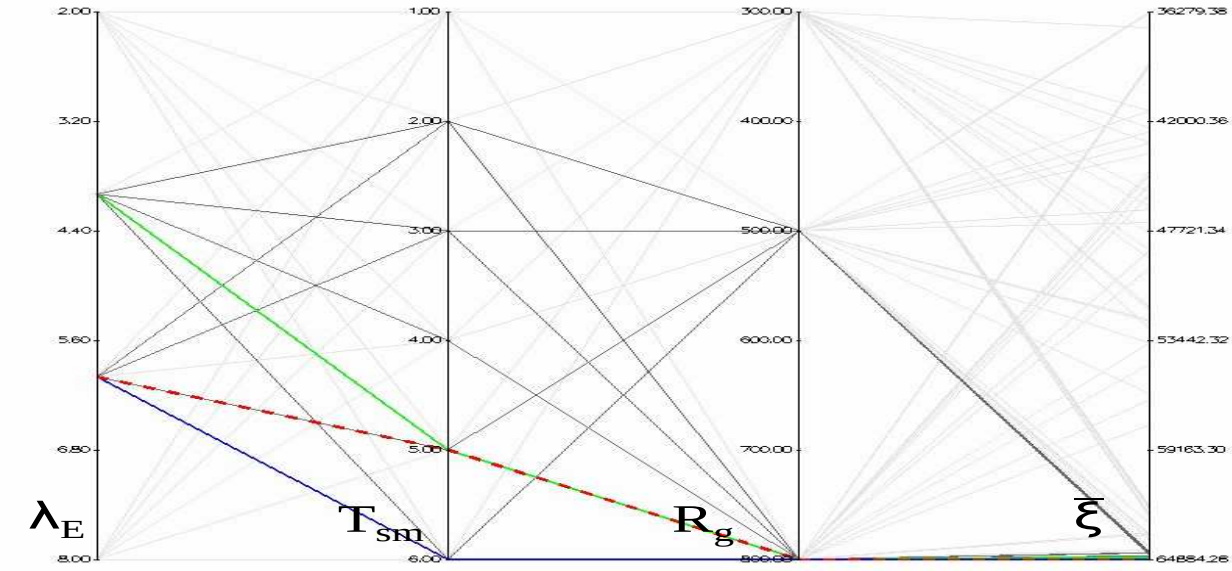

Figure E.60: Influence of λ_E on the $\bar{\xi}$ metric for EEMACOMH

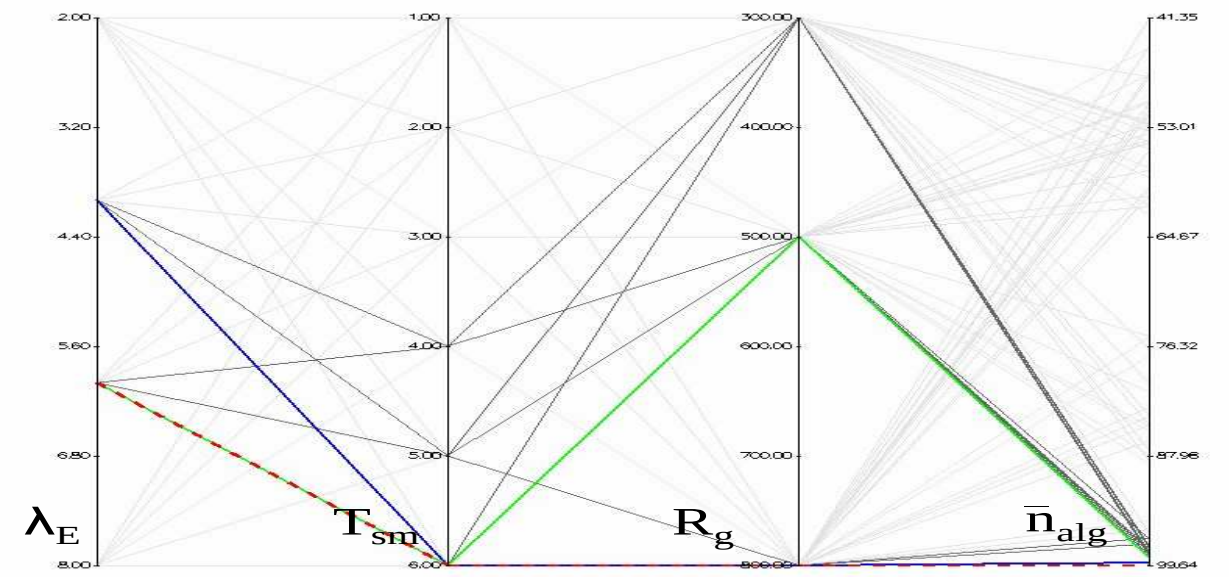

Figure E.61: Influence of λ_E on the $\bar{n}_{alg}$ metric for EEMMASMP

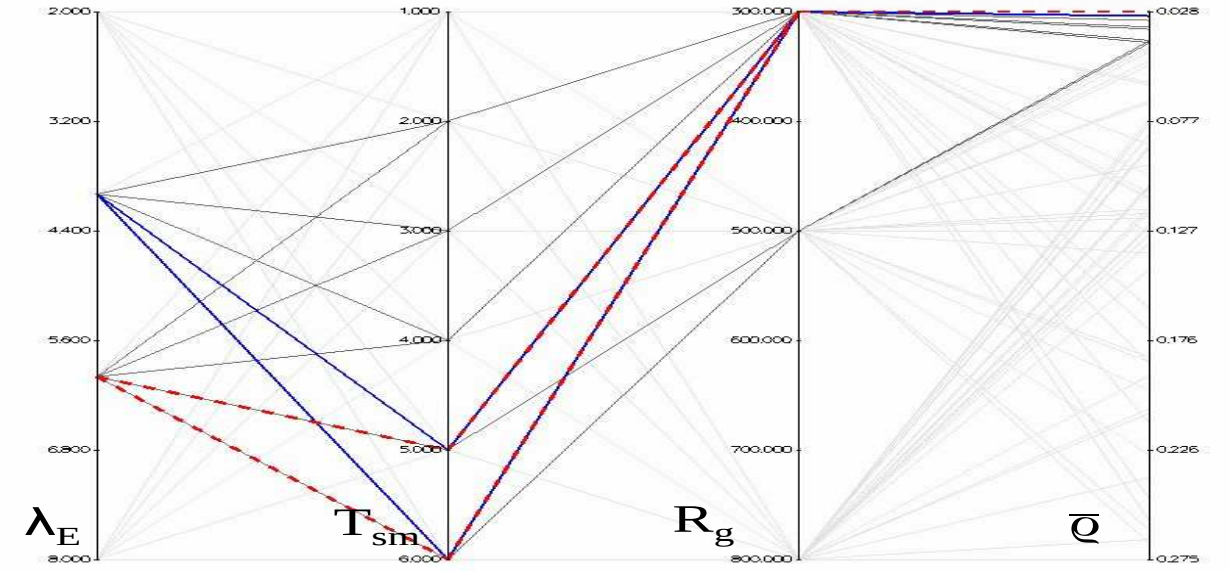

Figure E.62: Influence of λ_E on the $\bar{\varrho}$ metric for EEMMASMP

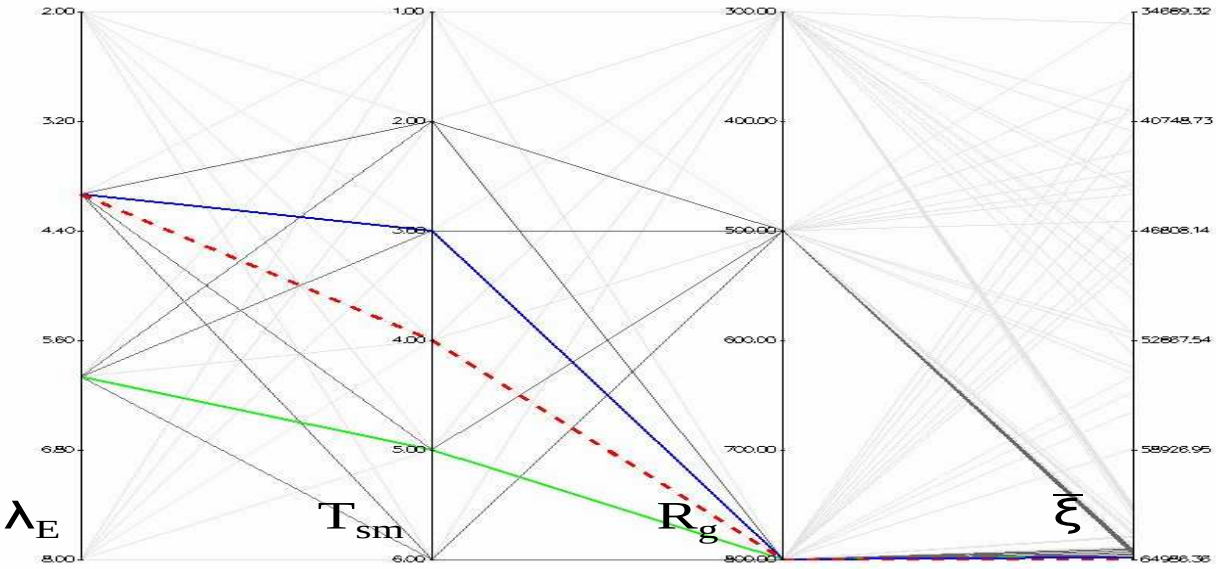

Figure E.63: Influence of λ_E on the $\bar{\xi}$ metric for EEMMASMP

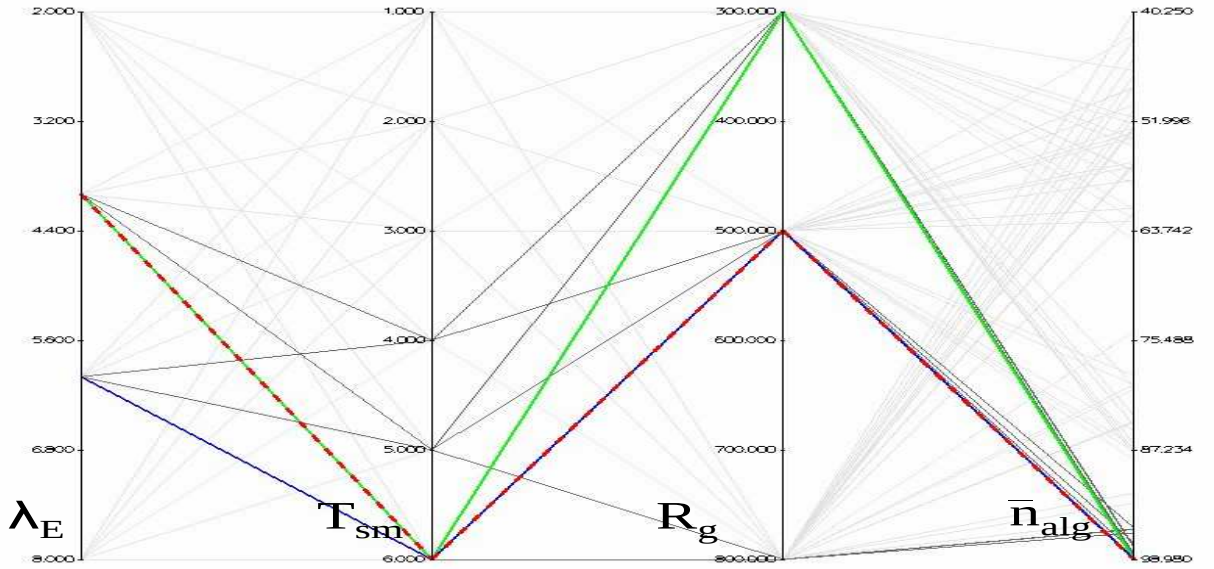

Figure E.64: Influence of λ_E on the $\bar{n}_{alg}$ metric for EEMMASMH

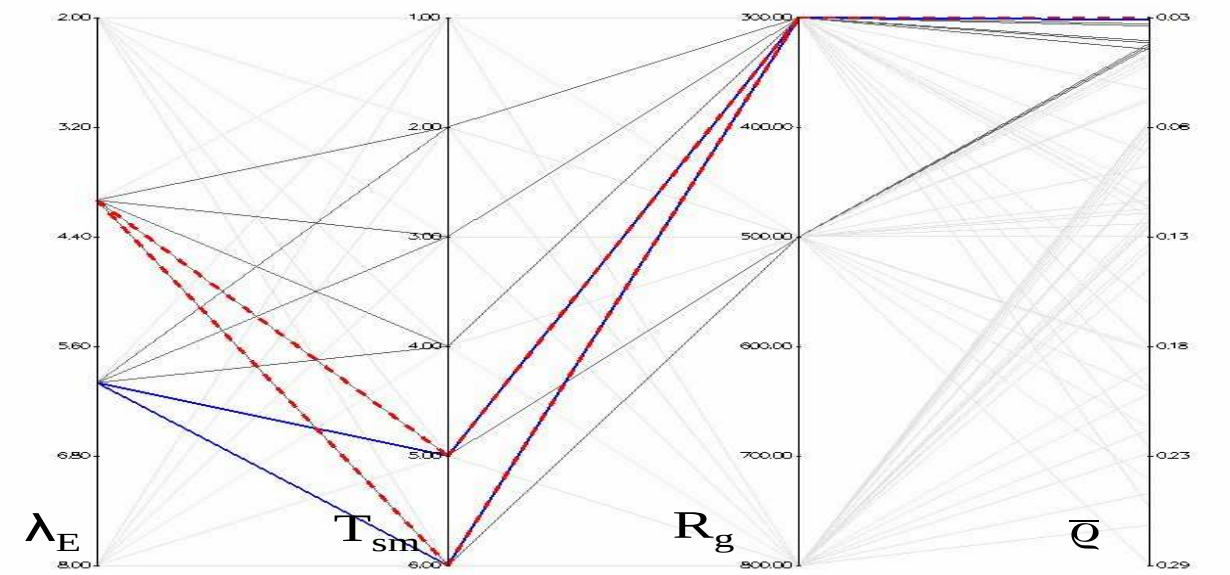

Figure E.65: Influence of λ_E on the $\bar{\varrho}$ metric for EEMMASMH

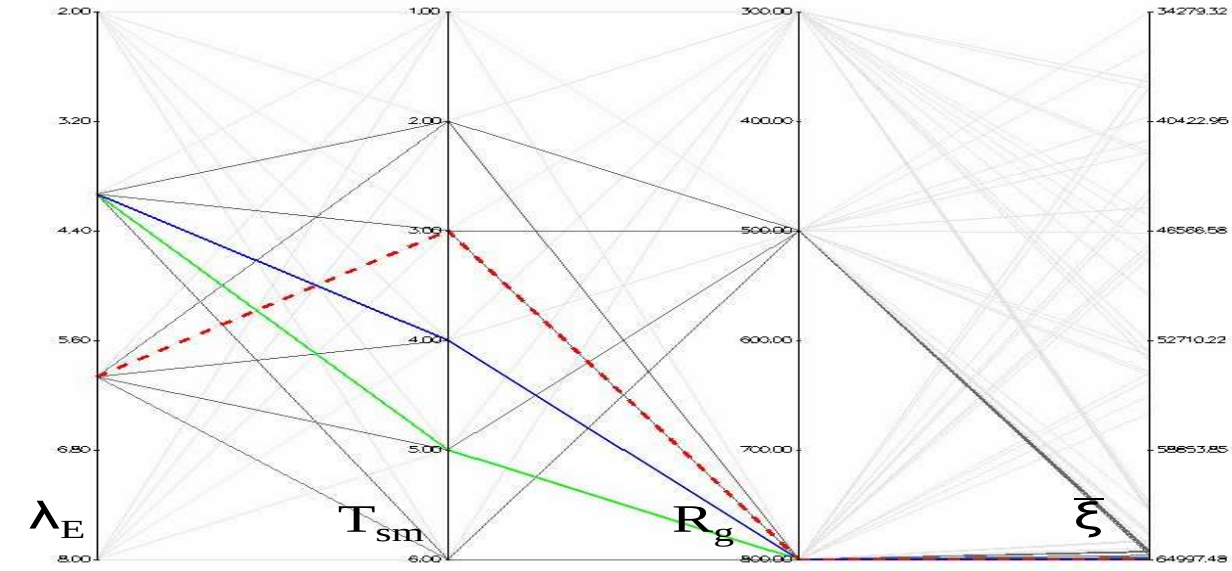

Figure E.66: Influence of λ_E on the $\bar{\xi}$ metric for EEMMASMH

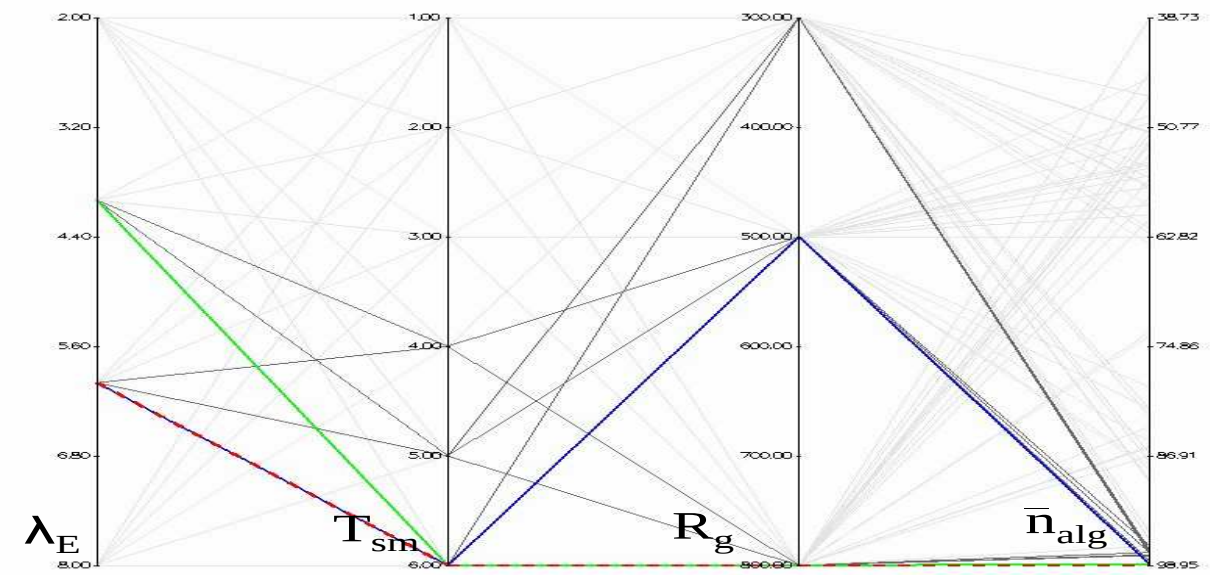

Figure E.67: Influence of λ_E on the $\bar{n}_{alg}$ metric for EEMACOMC

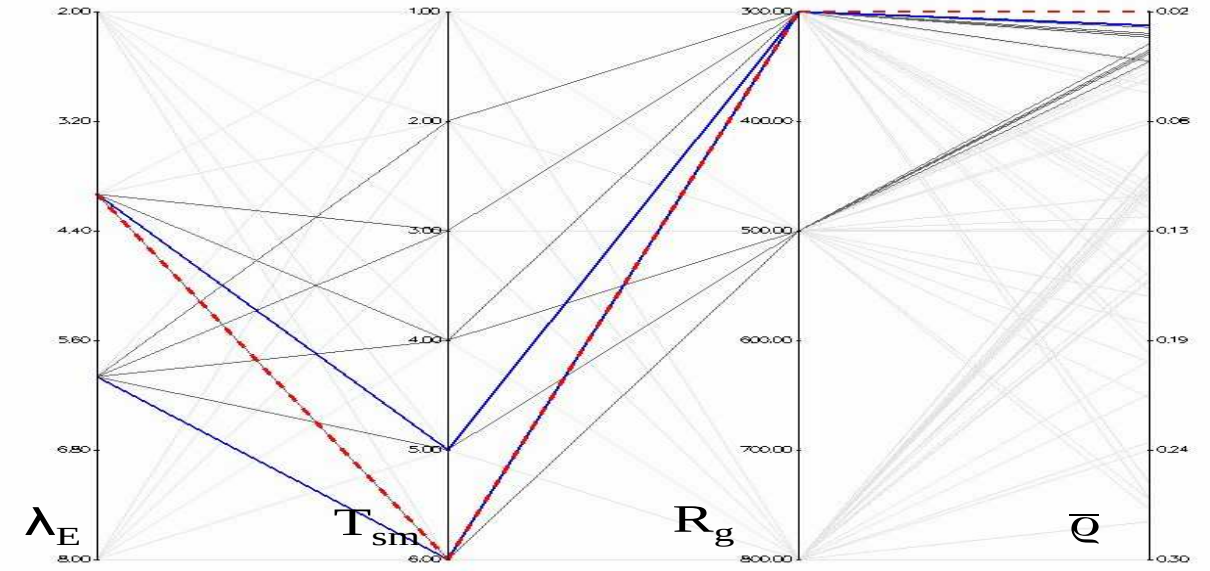

Figure E.68: Influence of λ_E on the $\bar{\varrho}$ metric for EEMACOMC

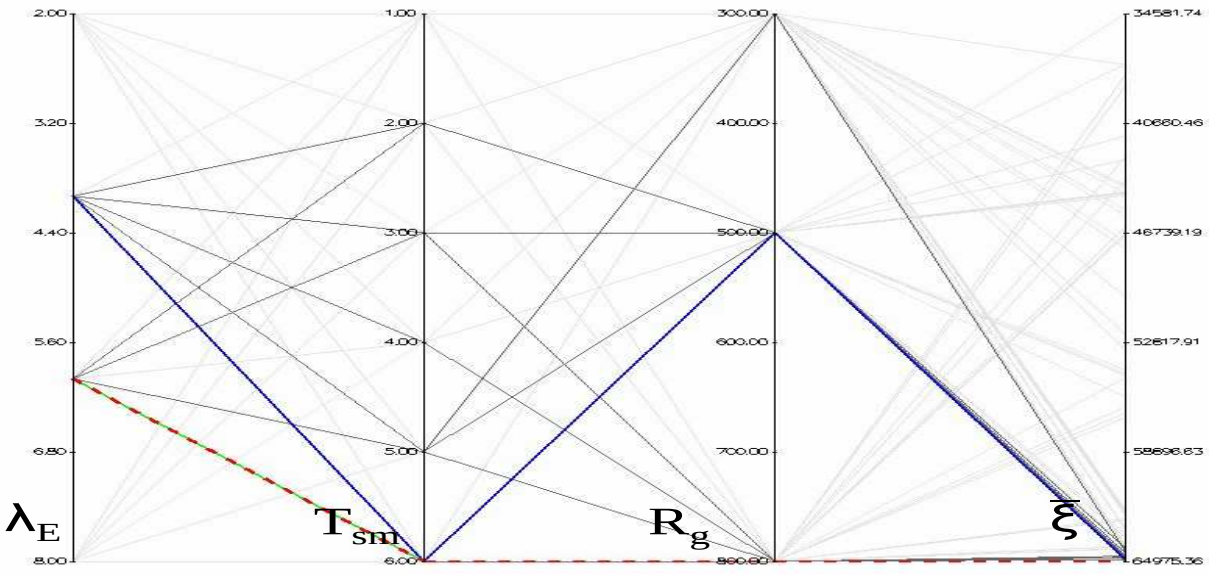

Figure E.69: Influence of λ_E on the $\bar{\xi}$ metric for EEMACOMC

Appendix F

Algorithms Results for Different Scenarios

This appendix contains the results obtained from the execution of EEMACOMP, EEMACOMH, EEMMASMP, EEMMASMH, EEMACOMC, and NSGA-II-MPA algorithms. Each table represents the results of the execution for each algorithm, for a specific scenario. The results of a total of 54 scenarios, generated as listed in Table 7.2 were presented.

Table F.1: Scenario 1a: $N_G = 30$, $T_{sm} = 1$, $R_g = 300$

$\mathcal{PF}$	$\bar{n}_{alg}$	CI	n^w_{alg}	$\bar{\varrho}$	CI	ϱ^w	ξ	CI	ξ^w	rank
$P_{EEMACOMP}$	99.90 ± 0.46	0.174	0	0.041 ± 0.007	0.003	3	63224.486 ± 267.890	101.730	0	4
$P_{EEMACOMH}$	99.01 ± 3.18	1.209	0	0.045 ± 0.007	0.003	0	62092.989 ± 226.056	85.844	0	5
$P_{EEMMASMP}$	99.98 ± 0.04	0.015	5	0.044 ± 0.006	0.002	0	62296.492 ± 233.573	88.699	0	3
$P_{EEMMASMH}$	99.82 ± 0.74	0.280	0	0.044 ± 0.007	0.003	0	62327.805 ± 229.138	87.015	0	5
$P_{EEMACOMC}$	99.99 ± 0.01	0.003	10	0.053 ± 0.011	0.004	0	64314.165 ± 235.574	89.459	120	1
$P_{NSGA-II-MPA}$	63.33 ± 8.78	3.336	0	0.035 ± 0.013	0.005	117	56870.433 ± 603.268	229.089	0	2

Table F.2: Scenario 1b: $N_G = 30$, $T_{sm} = 2$, $R_g = 300$

$\mathcal{PF}$	$\bar{n}_{alg}$	CI	n^w_{alg}	$\bar{\varrho}$	CI	ϱ^w	ξ	CI	ξ^w	rank
$P_{EEMACOMP}$	99.99 ± 0.01	0.004	0	0.032 ± 0.005	0.002	0	63565.719 ± 176.532	67.038	0	5
$P_{EEMACOMH}$	99.95 ± 0.08	0.029	0	0.036 ± 0.005	0.002	0	62211.133 ± 189.257	71.870	0	5
$P_{EEMMASMP}$	99.99 ± 0.01	0.004	1	0.034 ± 0.005	0.002	0	62392.343 ± 181.858	69.060	0	3
$P_{EEMMASMH}$	99.99 ± 0.01	0.003	0	0.034 ± 0.005	0.002	1	62428.696 ± 157.554	59.831	0	3
$P_{EEMACOMC}$	99.99 ± 0.01	0.005	0	0.037 ± 0.006	0.002	0	64688.689 ± 126.121	47.894	60	1
$P_{NSGA-II-MPA}$	67.49 ± 4.75	1.802	0	0.026 ± 0.007	0.003	59	55614.676 ± 519.436	197.254	0	2

Table F.3: Scenario 1c: $N_G = 30$, $T_{sm} = 3$, $R_g = 300$

$\mathcal{PF}$	$\bar{n}_{alg}$	CI	n^w_{alg}	$\bar{\varrho}$	CI	ϱ^w	ξ	CI	ξ^w	rank
$P_{EEMACOMP}$	99.99 ± 0.02	0.006	0	0.031 ± 0.006	0.002	0	63544.068 ± 161.976	61.510	0	4
$P_{EEMACOMH}$	99.99 ± 0.02	0.009	0	0.034 ± 0.005	0.002	0	62274.447 ± 164.946	62.638	0	4
$P_{EEMMASMP}$	99.99 ± 0.01	0.006	0	0.032 ± 0.005	0.002	0	62570.899 ± 169.698	64.442	0	4
$P_{EEMMASMH}$	100.00 ± 0.01	0.005	0	0.032 ± 0.006	0.002	1	62620.186 ± 193.859	73.617	0	3
$P_{EEMACOMC}$	100.00 ± 0.00	0.002	0	0.033 ± 0.007	0.003	0	64891.575 ± 113.712	43.182	40	1
$P_{NSGA-II-MPA}$	69.73 ± 3.58	1.359	0	0.026 ± 0.008	0.003	39	55185.113 ± 380.058	144.326	0	2

Table F.4: Scenario 1d: $N_G = 30$, $T_{sm} = 4$, $R_g = 300$

$\mathcal{PF}$	$\bar{n}_{alg}$	CI	n^w_{alg}	$\bar{\varrho}$	CI	ϱ^w	ξ	CI	ξ^w	rank
$P_{EEMACOMP}$	99.99 ± 0.02	0.006	0	0.027 ± 0.002	0.001	0	63506.710 ± 162.595	61.745	0	4
$P_{EEMACOMH}$	99.98 ± 0.03	0.010	0	0.030 ± 0.003	0.001	0	62157.398 ± 189.768	72.064	0	4
$P_{EEMMASMP}$	99.99 ± 0.02	0.007	0	0.028 ± 0.002	0.001	1	62491.748 ± 164.565	62.493	0	3
$P_{EEMMASMH}$	99.98 ± 0.03	0.010	0	0.028 ± 0.003	0.001	0	62548.683 ± 132.324	50.250	0	4
$P_{EEMACOMC}$	100.00 ± 0.01	0.005	0	0.027 ± 0.003	0.001	0	64966.841 ± 95.356	36.211	30	1
$P_{NSGA-II-MPA}$	68.40 ± 3.38	1.284	0	0.022 ± 0.004	0.002	29	54799.546 ± 349.731	132.809	0	2

Table F.5: Scenario 1e: $N_G = 30$, $T_{sm} = 5$, $R_g = 300$

$\mathcal{PF}$	$\bar{n}_{alg}$	CI	n^w_{alg}	$\bar{\varrho}$	CI	ϱ^w	ξ	CI	ξ^w	rank
$P_{EEMACOMP}$	99.99 ± 0.03	0.012	0	0.026 ± 0.002	0.001	0	63653.053 ± 181.660	68.985	0	4
$P_{EEMACOMH}$	99.98 ± 0.03	0.010	0	0.029 ± 0.003	0.001	0	62291.449 ± 174.384	66.222	0	4
$P_{EEMMASMP}$	99.99 ± 0.02	0.008	0	0.027 ± 0.002	0.001	0	62606.987 ± 101.707	38.623	0	4
$P_{EEMMASMH}$	99.99 ± 0.02	0.009	0	0.027 ± 0.002	0.001	1	62644.622 ± 109.402	41.545	0	3
$P_{EEMACOMC}$	100.00 ± 0.01	0.004	0	0.025 ± 0.003	0.001	0	65083.452 ± 82.395	31.289	24	1
$P_{NSGA-II-MPA}$	68.64 ± 3.21	1.218	0	0.021 ± 0.003	0.001	23	54743.463 ± 371.421	141.046	0	2

Table F.6: Scenario 1f: $N_G = 30$, $T_{sm} = 6$, $R_g = 300$

$\mathcal{PF}$	$\bar{n}_{alg}$	CI	n^w_{alg}	$\bar{\varrho}$	CI	ϱ^w	ξ	CI	ξ^w	rank
$P_{EEMACOMP}$	99.99 ± 0.02	0.007	0	0.026 ± 0.003	0.001	0	63568.844 ± 178.857	67.920	0	4
$P_{EEMACOMH}$	99.97 ± 0.04	0.016	0	0.028 ± 0.002	0.001	0	62232.058 ± 211.322	80.249	0	4
$P_{EEMMASMP}$	99.99 ± 0.02	0.009	0	0.026 ± 0.003	0.001	0	62585.621 ± 151.951	57.703	0	4
$P_{EEMMASMH}$	99.99 ± 0.02	0.007	0	0.026 ± 0.003	0.001	1	62645.141 ± 169.564	64.391	0	3
$P_{EEMACOMC}$	99.99 ± 0.02	0.006	0	0.026 ± 0.003	0.001	1	65034.690 ± 111.904	42.495	20	1
$P_{NSGA-II-MPA}$	69.41 ± 2.15	0.816	0	0.022 ± 0.004	0.002	18	54680.648 ± 367.682	139.626	0	2

Table F.7: Scenario 2a: $N_G = 30$, $T_{sm} = 1$, $R_g = 500$

$\mathcal{PF}$	$\bar{n}_{alg}$	CI	n^w_{alg}	$\bar{\varrho}$	CI	ϱ^w	ξ	CI	ξ^w	rank
$P_{EEMACOMP}$	99.99 ± 0.01	0.005	5	0.058 ± 0.012	0.005	54	65226.872 ± 263.451	100.045	9	1
$P_{EEMACOMH}$	99.19 ± 1.40	0.533	0	0.062 ± 0.015	0.006	6	65120.907 ± 269.432	102.316	4	5
$P_{EEMMASMP}$	99.99 ± 0.01	0.004	4	0.059 ± 0.011	0.004	43	65181.359 ± 249.229	94.644	20	2
$P_{EEMMASMH}$	99.95 ± 0.14	0.055	2	0.061 ± 0.011	0.004	16	65230.484 ± 255.296	96.948	35	4
$P_{EEMACOMC}$	99.99 ± 0.02	0.006	1	0.073 ± 0.012	0.005	1	65235.356 ± 201.804	76.634	52	3
$P_{NSGA-II-MPA}$	34.62 ± 10.30	3.913	0	0.071 ± 0.041	0.016	0	58325.611 ± 1226.224	465.655	0	6

Table F.8: Scenario 2b: $N_G = 30$, $T_{sm} = 2$, $R_g = 500$

$\mathcal{PF}$	$\bar{n}_{alg}$	CI	n^w_{alg}	$\bar{\varrho}$	CI	ϱ^w	ξ	CI	ξ^w	rank
$P_{EEMACOMP}$	99.99 ± 0.01	0.004	0	0.045 ± 0.009	0.003	31	65515.194 ± 167.296	63.530	13	1
$P_{EEMACOMH}$	99.97 ± 0.03	0.013	1	0.048 ± 0.007	0.003	7	65275.753 ± 257.623	97.831	0	5
$P_{EEMMASMP}$	99.99 ± 0.01	0.005	0	0.047 ± 0.006	0.002	9	65383.847 ± 258.138	98.027	4	4
$P_{EEMMASMH}$	100.00 ± 0.01	0.004	1	0.046 ± 0.007	0.003	13	65404.545 ± 270.217	102.614	10	3
$P_{EEMACOMC}$	99.99 ± 0.02	0.007	0	0.053 ± 0.009	0.003	0	65606.504 ± 140.949	53.525	33	2
$P_{NSGA-II-MPA}$	38.35 ± 10.92	4.145	0	0.056 ± 0.022	0.008	0	56729.359 ± 1082.743	411.168	0	6

Table F.9: Scenario 2c: $N_G = 30$, $T_{sm} = 3$, $R_g = 500$

$\mathcal{PF}$	$\bar{n}_{alg}$	CI	n^w_{alg}	$\bar{\varrho}$	CI	ϱ^w	ξ	CI	ξ^w	rank
$P_{EEMACOMP}$	99.99 ± 0.01	0.005	0	0.040 ± 0.006	0.002	29	65546.819 ± 143.534	54.507	6	1
$P_{EEMACOMH}$	99.98 ± 0.02	0.008	0	0.044 ± 0.008	0.003	1	65132.242 ± 205.670	78.103	0	5
$P_{EEMMASMP}$	99.99 ± 0.01	0.005	0	0.043 ± 0.006	0.002	6	65328.468 ± 204.463	77.644	0	3
$P_{EEMMASMH}$	100.00 ± 0.01	0.004	0	0.043 ± 0.007	0.003	4	65322.738 ± 219.420	83.324	0	4
$P_{EEMACOMC}$	99.99 ± 0.02	0.007	0	0.045 ± 0.004	0.001	0	65781.230 ± 112.204	42.609	34	2
$P_{NSGA-II-MPA}$	40.08 ± 8.05	3.058	0	0.050 ± 0.017	0.006	0	55849.097 ± 1056.987	401.388	0	6

Table F.10: Scenario 2d: $N_G = 30$, $T_{sm} = 4$, $R_g = 500$

$\mathcal{PF}$	$\bar{n}_{alg}$	CI	n^w_{alg}	$\bar{\varrho}$	CI	ϱ^w	ξ	CI	ξ^w	rank
$P_{EEMACOMP}$	99.99 ± 0.03	0.010	0	0.038 ± 0.004	0.001	28	65125.553 ± 237.599	90.227	0	2
$P_{EEMACOMH}$	99.61 ± 0.21	0.081	0	0.042 ± 0.005	0.002	1	64730.302 ± 276.602	105.039	0	3
$P_{EEMMASMP}$	100.00 ± 0.01	0.005	0	0.041 ± 0.005	0.002	1	64927.279 ± 214.315	81.385	0	3
$P_{EEMMASMH}$	99.99 ± 0.03	0.011	0	0.041 ± 0.005	0.002	0	64999.946 ± 254.636	96.697	0	5
$P_{EEMACOMC}$	99.99 ± 0.02	0.009	0	0.045 ± 0.005	0.002	0	65783.826 ± 122.137	46.381	30	1
$P_{NSGA-II-MPA}$	37.51 ± 8.74	3.319	0	0.056 ± 0.020	0.008	0	55655.191 ± 1070.395	406.479	0	5

Table F.11: Scenario 2e: $N_G = 30$, $T_{sm} = 5$, $R_g = 500$

$\mathcal{PF}$	$\bar{n}_{alg}$	CI	n^w_{alg}	$\bar{\varrho}$	CI	ϱ^w	ξ	CI	ξ^w	rank
$P_{EEMACOMP}$	99.99 ± 0.02	0.008	0	0.036 ± 0.005	0.002	18	65617.854 ± 168.297	63.910	0	2
$P_{EEMACOMH}$	99.99 ± 0.02	0.008	0	0.041 ± 0.005	0.002	0	65145.065 ± 266.484	101.197	0	5
$P_{EEMMASMP}$	100.00 ± 0.01	0.005	0	0.040 ± 0.007	0.003	3	65344.205 ± 205.927	78.200	0	3
$P_{EEMMASMH}$	100.00 ± 0.02	0.006	0	0.040 ± 0.005	0.002	1	65316.900 ± 207.545	78.815	0	4
$P_{EEMACOMC}$	99.98 ± 0.03	0.012	0	0.040 ± 0.009	0.003	2	65966.720 ± 143.414	54.461	24	1
$P_{NSGA-II-MPA}$	38.40 ± 8.95	3.400	0	0.056 ± 0.022	0.009	0	55630.706 ± 1023.066	388.506	0	5

Table F.12: Scenario 2f: $N_G = 30$, $T_{sm} = 6$, $R_g = 500$

$\mathcal{PF}$	$\bar{n}_{alg}$	CI	n^w_{alg}	$\bar{\varrho}$	CI	ϱ^w	ξ	CI	ξ^w	rank
$P_{EEMACOMP}$	99.99 ± 0.02	0.007	0	0.036 ± 0.005	0.002	14	65484.216 ± 147.404	55.976	0	2
$P_{EEMACOMH}$	99.99 ± 0.02	0.007	0	0.039 ± 0.008	0.003	0	65075.075 ± 216.256	82.122	0	3
$P_{EEMMASMP}$	99.99 ± 0.02	0.008	0	0.039 ± 0.006	0.002	0	65324.222 ± 186.415	70.790	0	3
$P_{EEMMASMH}$	100.00 ± 0.01	0.003	0	0.038 ± 0.006	0.002	0	65374.224 ± 215.049	81.664	0	3
$P_{EEMACOMC}$	99.98 ± 0.04	0.013	0	0.037 ± 0.003	0.001	6	65984.503 ± 105.847	40.195	20	1
$P_{NSGA-II-MPA}$	38.14 ± 6.74	2.560	0	0.057 ± 0.019	0.007	0	55545.986 ± 914.529	347.290	0	3

Table F.13: Scenario 3a: $N_G = 30$, $T_{sm} = 1$, $R_g = 800$

$\mathcal{PF}$	$\bar{n}_{alg}$	CI	n^w_{alg}	$\bar{\varrho}$	CI	ϱ^w	ξ	CI	ξ^w	rank
$P_{EEMACOMP}$	94.69 ± 4.28	1.626	6	0.114 ± 0.021	0.008	28	64001.298 ± 1414.019	536.969	23	4
$P_{EEMACOMH}$	62.99 ± 5.77	2.191	0	0.150 ± 0.017	0.007	0	64034.460 ± 1198.534	455.140	0	6
$P_{EEMMASMP}$	99.41 ± 0.44	0.168	21	0.112 ± 0.015	0.006	50	64171.344 ± 1224.235	464.899	19	2
$P_{EEMMASMH}$	95.04 ± 3.77	1.430	9	0.114 ± 0.011	0.004	42	64240.559 ± 1131.037	429.508	56	1
$P_{EEMACOMC}$	99.70 ± 0.10	0.038	73	0.140 ± 0.021	0.008	0	63131.522 ± 2180.916	828.196	0	3
$P_{NSGA-II-MPA}$	10.91 ± 2.18	0.827	0	0.648 ± 0.804	0.305	0	73608.534 ± 18301.648	6949.995	22	5

Table F.14: Scenario 3b: $N_G = 30$, $T_{sm} = 2$, $R_g = 800$

$\mathcal{PF}$	$\bar{n}_{alg}$	CI	n^w_{alg}	$\bar{\varrho}$	CI	ϱ^w	ξ	CI	ξ^w	rank
$P_{EEMACOMP}$	97.33 ± 1.84	0.699	11	0.093 ± 0.014	0.005	43	65057.395 ± 662.695	251.657	31	1
$P_{EEMACOMH}$	48.72 ± 4.03	1.530	0	0.149 ± 0.019	0.007	0	64744.536 ± 487.665	185.189	0	6
$P_{EEMMASMP}$	96.90 ± 0.84	0.319	0	0.099 ± 0.014	0.005	9	64984.261 ± 526.431	199.911	1	4
$P_{EEMMASMH}$	92.59 ± 3.71	1.407	0	0.102 ± 0.014	0.005	8	65018.660 ± 480.622	182.515	24	3
$P_{EEMACOMC}$	99.16 ± 0.31	0.118	49	0.128 ± 0.017	0.007	0	64552.590 ± 809.187	307.286	0	2
$P_{NSGA-II-MPA}$	11.50 ± 2.30	0.875	0	0.336 ± 0.037	0.014	0	64672.183 ± 299.427	113.706	4	5

Table F.15: Scenario 3c: $N_G = 30$, $T_{sm} = 3$, $R_g = 800$

$\mathcal{PF}$	$\bar{n}_{alg}$	CI	n^w_{alg}	$\bar{\varrho}$	CI	ϱ^w	ξ	CI	ξ^w	rank
$P_{EEMACOMP}$	99.85 ± 0.14	0.054	4	0.086 ± 0.016	0.006	13	65629.139 ± 265.796	100.935	39	1
$P_{EEMACOMH}$	78.10 ± 5.92	2.248	0	0.114 ± 0.019	0.007	0	65128.423 ± 231.488	87.907	0	5
$P_{EEMMASMP}$	99.77 ± 0.13	0.048	5	0.087 ± 0.010	0.004	8	65546.599 ± 212.285	80.615	1	3
$P_{EEMMASMH}$	98.06 ± 0.15	0.057	5	0.086 ± 0.011	0.004	19	65544.757 ± 238.916	90.728	0	2
$P_{EEMACOMC}$	99.90 ± 0.10	0.038	14	0.108 ± 0.015	0.006	0	65242.358 ± 222.482	84.487	0	3
$P_{NSGA-II-MPA}$	12.27 ± 2.16	0.820	0	0.327 ± 0.043	0.016	0	64696.133 ± 152.603	57.951	0	5

Table F.16: Scenario 3d: $N_G = 30$, $T_{sm} = 4$, $R_g = 800$

$\mathcal{PF}$	$\bar{n}_{alg}$	CI	n^w_{alg}	$\bar{\varrho}$	CI	ϱ^w	ξ	CI	ξ^w	rank
$P_{EEMACOMP}$	99.13 ± 0.26	0.098	6	0.074 ± 0.008	0.003	20	65495.200 ± 147.854	56.147	29	1
$P_{EEMACOMH}$	51.07 ± 4.78	1.816	0	0.139 ± 0.024	0.009	0	64988.903 ± 186.441	70.801	0	5
$P_{EEMMASMP}$	97.34 ± 0.49	0.187	4	0.080 ± 0.009	0.003	6	65405.510 ± 159.005	60.382	1	3
$P_{EEMMASMH}$	96.10 ± 0.72	0.273	2	0.081 ± 0.011	0.004	4	65397.152 ± 161.211	61.219	0	4
$P_{EEMACOMC}$	99.07 ± 0.24	0.091	13	0.102 ± 0.011	0.004	0	65161.206 ± 175.899	66.797	0	2
$P_{NSGA-II-MPA}$	12.07 ± 2.18	0.828	0	0.335 ± 0.046	0.018	0	64609.478 ± 155.420	59.020	0	5

Table F.17: Scenario 3e: $N_G = 30$, $T_{sm} = 5$, $R_g = 800$

$\mathcal{PF}$	$\bar{n}_{alg}$	CI	n^w_{alg}	$\bar{\varrho}$	CI	ϱ^w	ξ	CI	ξ^w	rank
$P_{EEMACOMP}$	99.92 ± 0.08	0.031	4	0.072 ± 0.013	0.005	14	65491.333 ± 154.719	58.754	17	1
$P_{EEMACOMH}$	71.58 ± 5.62	2.133	0	0.106 ± 0.019	0.007	0	65142.655 ± 154.383	58.626	0	5
$P_{EEMMASMP}$	99.92 ± 0.09	0.033	3	0.075 ± 0.007	0.003	2	65430.145 ± 151.300	57.456	2	4
$P_{EEMMASMH}$	96.89 ± 0.16	0.062	1	0.076 ± 0.009	0.003	8	65411.462 ± 144.077	54.713	3	2
$P_{EEMACOMC}$	99.76 ± 0.19	0.072	8	0.101 ± 0.019	0.007	0	65377.718 ± 220.545	83.751	2	3
$P_{NSGA-II-MPA}$	12.13 ± 2.54	0.963	0	0.344 ± 0.049	0.019	0	64617.781 ± 134.993	51.263	0	5

Table F.18: Scenario 3f: $N_G = 30$, $T_{sm} = 6$, $R_g = 800$

$\mathcal{PF}$	$\bar{n}_{alg}$	CI	n^w_{alg}	$\bar{\varrho}$	CI	ϱ^w	$\bar{\xi}$	CI	ξ^w	rank
$P_{EEMACOMP}$	99.93 ± 0.09	0.033	3	0.071 ± 0.011	0.004	11	65779.387 ± 147.350	55.956	20	1
$P_{EEMACOMH}$	79.73 ± 5.16	1.959	0	0.102 ± 0.015	0.006	0	65317.919 ± 238.452	90.551	0	5
$P_{EEMMASMP}$	99.90 ± 0.13	0.048	2	0.075 ± 0.008	0.003	3	65664.166 ± 141.667	53.797	0	3
$P_{EEMMASMH}$	96.66 ± 0.25	0.094	5	0.076 ± 0.007	0.003	6	65659.230 ± 142.055	53.945	0	2
$P_{EEMACOMC}$	99.93 ± 0.10	0.040	5	0.089 ± 0.011	0.004	0	65383.320 ± 169.117	64.222	0	3
$P_{NSGA-II-MPA}$	12.68 ± 1.86	0.706	0	0.327 ± 0.026	0.010	0	64572.612 ± 165.208	62.737	0	5

Table F.19: Scenario 4a: $N_G = 100$, $T_{sm} = 1$, $R_g = 300$

$\mathcal{PF}$	$\bar{n}_{alg}$	CI	n^w_{alg}	$\bar{\varrho}$	CI	ϱ^w	$\bar{\xi}$	CI	ξ^w	rank
$P_{EEMACOMP}$	97.49 ± 6.58	2.497	118	0.031 ± 0.007	0.003	114	60767.397 ± 641.430	243.581	32	1
$P_{EEMACOMH}$	49.48 ± 18.62	7.070	0	0.060 ± 0.014	0.005	0	59463.509 ± 932.029	353.935	0	6
$P_{EEMMASMP}$	93.30 ± 11.89	4.514	0	0.039 ± 0.009	0.004	1	60679.108 ± 681.288	258.717	0	5
$P_{EEMMASMH}$	90.23 ± 13.43	5.099	2	0.040 ± 0.011	0.004	1	60711.591 ± 698.380	265.208	1	4
$P_{EEMACOMC}$	88.02 ± 10.31	3.914	0	0.037 ± 0.007	0.003	4	60278.843 ± 759.165	288.291	1	3
$P_{NSGA-II-MPA}$	25.44 ± 10.98	4.170	0	0.237 ± 0.078	0.030	0	62051.618 ± 1288.137	489.166	86	2

Table F.20: Scenario 4b: $N_G = 100$, $T_{sm} = 2$, $R_g = 300$

$\mathcal{PF}$	$\bar{n}_{alg}$	CI	n^w_{alg}	$\bar{\varrho}$	CI	ϱ^w	$\bar{\xi}$	CI	ξ^w	rank
$P_{EEMACOMP}$	99.97 ± 0.04	0.014	47	0.023 ± 0.004	0.002	59	61684.110 ± 263.857	100.199	39	1
$P_{EEMACOMH}$	59.65 ± 16.82	6.389	0	0.047 ± 0.009	0.003	0	60582.562 ± 435.989	165.565	0	6
$P_{EEMMASMP}$	99.52 ± 0.98	0.373	2	0.030 ± 0.007	0.003	0	61505.116 ± 289.649	109.993	0	3
$P_{EEMMASMH}$	97.44 ± 2.26	0.857	1	0.032 ± 0.008	0.003	0	61515.673 ± 304.920	115.793	1	3
$P_{EEMACOMC}$	97.34 ± 4.47	1.699	0	0.032 ± 0.012	0.005	1	61251.689 ± 446.044	169.384	0	5
$P_{NSGA-II-MPA}$	35.68 ± 14.93	5.671	0	0.217 ± 0.097	0.037	0	61231.443 ± 1012.577	384.523	20	2

Table F.21: Scenario 4c: $N_G = 100$, $T_{sm} = 3$, $R_g = 300$

$\mathcal{PF}$	$\bar{n}_{alg}$	CI	n^w_{alg}	$\bar{\varrho}$	CI	ϱ^w	$\bar{\xi}$	CI	ξ^w	rank
$P_{EEMACOMP}$	99.98 ± 0.03	0.012	8	0.018 ± 0.002	0.001	39	61926.924 ± 181.857	69.059	40	1
$P_{EEMACOMH}$	75.45 ± 14.40	5.468	0	0.038 ± 0.006	0.002	0	61074.074 ± 384.329	145.948	0	5
$P_{EEMMASMP}$	99.95 ± 0.09	0.036	2	0.024 ± 0.004	0.001	0	61816.187 ± 206.793	78.529	0	4
$P_{EEMMASMH}$	97.73 ± 0.14	0.054	5	0.026 ± 0.004	0.001	0	61802.234 ± 234.342	88.991	0	2
$P_{EEMACOMC}$	99.70 ± 0.79	0.301	2	0.024 ± 0.004	0.002	1	61734.794 ± 278.649	105.816	0	3
$P_{NSGA-II-MPA}$	44.72 ± 14.29	5.428	0	0.165 ± 0.067	0.026	0	60308.215 ± 955.849	362.981	0	5

Table F.22: Scenario 4d: $N_G = 100$, $T_{sm} = 4$, $R_g = 300$

$\mathcal{PF}$	$\bar{n}_{alg}$	CI	n^w_{alg}	$\bar{\varrho}$	CI	ϱ^w	$\bar{\xi}$	CI	ξ^w	rank
$P_{EEMACOMP}$	99.98 ± 0.03	0.010	12	0.019 ± 0.004	0.002	27	61948.178 ± 190.681	72.411	29	1
$P_{EEMACOMH}$	71.71 ± 16.65	6.321	0	0.039 ± 0.007	0.003	0	61054.009 ± 357.629	135.808	0	5
$P_{EEMMASMP}$	99.89 ± 0.27	0.103	3	0.023 ± 0.005	0.002	0	61807.696 ± 212.408	80.661	0	3
$P_{EEMMASMH}$	96.92 ± 0.56	0.211	2	0.024 ± 0.004	0.002	0	61814.092 ± 212.300	80.620	1	2
$P_{EEMACOMC}$	99.76 ± 0.48	0.181	0	0.022 ± 0.002	0.001	3	61688.167 ± 289.308	109.864	0	3
$P_{NSGA-II-MPA}$	43.28 ± 14.74	5.596	0	0.188 ± 0.076	0.029	0	60668.669 ± 977.903	371.356	0	5

Table F.23: Scenario 4e: $N_G = 100$, $T_{sm} = 5$, $R_g = 300$

$\mathcal{PF}$	$\bar{n}_{alg}$	CI	n^w_{alg}	$\bar{\varrho}$	CI	ϱ^w	$\bar{\xi}$	CI	ξ^w	rank
$P_{EEMACOMP}$	99.99 ± 0.03	0.013	2	0.017 ± 0.003	0.001	24	62059.323 ± 183.441	69.661	23	1
$P_{EEMACOMH}$	77.88 ± 12.32	4.680	0	0.036 ± 0.007	0.003	0	61224.766 ± 284.764	108.138	0	4
$P_{EEMMASMP}$	99.97 ± 0.05	0.020	0	0.022 ± 0.003	0.001	0	61884.880 ± 200.674	76.205	0	4
$P_{EEMMASMH}$	96.32 ± 0.18	0.070	1	0.026 ± 0.004	0.002	0	61869.871 ± 205.383	77.993	0	3
$P_{EEMACOMC}$	99.82 ± 0.41	0.157	0	0.021 ± 0.002	0.001	0	61837.894 ± 271.395	103.061	1	2
$P_{NSGA-II-MPA}$	41.24 ± 16.47	6.256	0	0.206 ± 0.097	0.037	0	60573.137 ± 798.495	303.226	0	4

Table F.24: Scenario 4f: $N_G = 100$, $T_{sm} = 6$, $R_g = 300$

$\mathcal{PF}$	$\bar{n}_{alg}$	CI	n^w_{alg}	$\bar{\varrho}$	CI	ϱ^w	$\bar{\xi}$	CI	ξ^w	rank
$P_{EEMACOMP}$	99.99 ± 0.02	0.007	3	0.015 ± 0.003	0.001	20	62023.971 ± 173.217	65.778	20	1
$P_{EEMACOMH}$	77.76 ± 11.65	4.423	0	0.033 ± 0.007	0.003	0	61177.929 ± 258.965	98.341	0	3
$P_{EEMMASMP}$	99.98 ± 0.04	0.016	0	0.019 ± 0.003	0.001	0	61890.620 ± 201.835	76.646	0	3
$P_{EEMMASMH}$	95.59 ± 0.14	0.052	0	0.023 ± 0.003	0.001	0	61870.458 ± 190.483	72.335	0	3
$P_{EEMACOMC}$	99.95 ± 0.08	0.030	0	0.020 ± 0.002	0.001	0	61786.033 ± 227.451	86.374	0	3
$P_{NSGA-II-MPA}$	44.31 ± 14.71	5.586	0	0.188 ± 0.077	0.029	0	60534.065 ± 624.689	237.224	0	2

Table F.25: Scenario 5a: $N_G = 100$, $T_{sm} = 1$, $R_g = 500$

$\mathcal{PF}$	$\bar{n}_{alg}$	CI	n^w_{alg}	$\bar{\varrho}$	CI	ϱ^w	$\bar{\xi}$	CI	ξ^w	rank
$P_{EEMACOMP}$	94.53 ± 9.51	3.611	56	0.047 ± 0.008	0.003	119	60709.700 ± 981.508	372.725	70	1
$P_{EEMACOMH}$	47.57 ± 18.58	7.055	0	0.096 ± 0.032	0.012	0	58818.263 ± 985.701	374.317	0	5
$P_{EEMMASMP}$	94.75 ± 9.25	3.511	61	0.061 ± 0.010	0.004	0	60576.821 ± 777.649	295.310	2	2
$P_{EEMMASMH}$	92.40 ± 11.00	4.177	2	0.061 ± 0.022	0.008	1	60465.880 ± 789.736	299.900	1	4
$P_{EEMACOMC}$	78.79 ± 16.81	6.382	0	0.063 ± 0.015	0.006	0	60499.958 ± 890.883	338.310	0	5
$P_{NSGA-II-MPA}$	51.53 ± 14.69	5.580	0	0.099 ± 0.070	0.026	0	60083.048 ± 1612.485	612.336	47	3

Table F.26: Scenario 5b: $N_G = 100$, $T_{sm} = 2$, $R_g = 500$

$\mathcal{PF}$	$\bar{n}_{alg}$	CI	n^w_{alg}	$\bar{\varrho}$	CI	ϱ^w	$\bar{\xi}$	CI	ξ^w	rank
$P_{EEMACOMP}$	99.48 ± 1.32	0.500	34	0.036 ± 0.005	0.002	59	61651.210 ± 677.703	257.356	52	1
$P_{EEMACOMH}$	67.85 ± 17.96	6.819	0	0.065 ± 0.017	0.006	0	59580.938 ± 843.767	320.418	0	5
$P_{EEMMASMP}$	99.14 ± 2.27	0.863	13	0.047 ± 0.006	0.002	0	61250.944 ± 659.970	250.622	2	2
$P_{EEMMASMH}$	97.23 ± 3.34	1.268	6	0.048 ± 0.008	0.003	1	61235.382 ± 635.453	241.311	1	3
$P_{EEMACOMC}$	91.60 ± 11.59	4.400	0	0.047 ± 0.008	0.003	0	61409.163 ± 722.389	274.325	5	4
$P_{NSGA-II-MPA}$	62.93 ± 11.06	4.200	0	0.063 ± 0.039	0.015	0	58489.752 ± 1437.332	545.822	0	5

Table F.27: Scenario 5c: $N_G = 100$, $T_{sm} = 3$, $R_g = 500$

$\mathcal{PF}$	$\bar{n}_{alg}$	CI	n^w_{alg}	$\bar{\varrho}$	CI	ϱ^w	$\bar{\xi}$	CI	ξ^w	rank
$P_{EEMACOMP}$	98.74 ± 3.27	1.241	36	0.034 ± 0.005	0.002	38	61716.716 ± 419.716	159.386	39	1
$P_{EEMACOMH}$	45.07 ± 13.03	4.949	0	0.067 ± 0.011	0.004	0	59371.538 ± 724.454	275.109	0	5
$P_{EEMMASMP}$	97.13 ± 4.57	1.737	3	0.042 ± 0.010	0.004	0	61190.523 ± 477.902	181.482	0	3
$P_{EEMMASMH}$	94.67 ± 6.12	2.323	1	0.044 ± 0.006	0.002	1	61200.155 ± 504.360	191.529	1	2
$P_{EEMACOMC}$	84.33 ± 11.22	4.259	0	0.044 ± 0.005	0.002	0	61313.928 ± 545.723	207.237	0	5
$P_{NSGA-II-MPA}$	64.12 ± 10.24	3.890	0	0.064 ± 0.042	0.016	1	58209.978 ± 1306.440	496.116	0	4

Table F.28: Scenario 5d: $N_G = 100$, $T_{sm} = 4$, $R_g = 500$

$\mathcal{PF}$	$\bar{n}_{alg}$	CI	n^w_{alg}	$\bar{\varrho}$	CI	ϱ^w	$\bar{\xi}$	CI	ξ^w	rank
$P_{EEMACOMP}$	99.94 ± 0.07	0.028	9	0.029 ± 0.003	0.001	30	62177.310 ± 278.901	105.912	29	1
$P_{EEMACOMH}$	66.07 ± 14.56	5.529	0	0.057 ± 0.011	0.004	0	59980.010 ± 541.183	205.513	0	4
$P_{EEMMASMP}$	99.93 ± 0.12	0.047	6	0.037 ± 0.004	0.002	0	61674.493 ± 282.908	107.433	0	2
$P_{EEMMASMH}$	96.91 ± 0.18	0.070	3	0.040 ± 0.003	0.001	0	61613.815 ± 274.259	104.149	1	3
$P_{EEMACOMC}$	94.84 ± 7.03	2.671	0	0.038 ± 0.004	0.002	0	61693.781 ± 407.696	154.821	0	4
$P_{NSGA-II-MPA}$	67.49 ± 5.73	2.174	0	0.053 ± 0.025	0.010	0	57864.309 ± 1064.516	404.247	0	4

Table F.29: Scenario 5e: $N_G = 100$, $T_{sm} = 5$, $R_g = 500$

$\mathcal{PF}$	$\bar{n}_{alg}$	CI	n^w_{alg}	$\bar{\varrho}$	CI	ϱ^w	$\bar{\xi}$	CI	ξ^w	rank
$P_{EEMACOMP}$	99.91 ± 0.13	0.050	4	0.028 ± 0.002	0.001	24	62324.560 ± 277.373	105.332	23	1
$P_{EEMACOMH}$	69.79 ± 13.49	5.122	0	0.054 ± 0.011	0.004	0	60058.741 ± 424.982	161.386	0	4
$P_{EEMMASMP}$	99.86 ± 0.31	0.117	5	0.038 ± 0.005	0.002	0	61790.100 ± 318.713	121.030	0	3
$P_{EEMMASMH}$	96.08 ± 0.37	0.139	6	0.040 ± 0.005	0.002	0	61706.344 ± 318.672	121.015	1	2
$P_{EEMACOMC}$	96.76 ± 4.47	1.699	0	0.039 ± 0.005	0.002	0	61734.661 ± 368.194	139.820	0	4
$P_{NSGA-II-MPA}$	68.13 ± 3.92	1.489	0	0.048 ± 0.020	0.008	0	57600.732 ± 1039.846	394.878	0	4

Table F.30: Scenario 5f: $N_G = 100$, $T_{sm} = 6$, $R_g = 500$

$\mathcal{PF}$	$\bar{n}_{alg}$	CI	n^w_{alg}	$\bar{\varrho}$	CI	ϱ^w	$\bar{\xi}$	CI	ξ^w	rank
$P_{EEMACOMP}$	99.88 ± 0.39	0.148	6	0.027 ± 0.002	0.001	20	62397.835 ± 344.081	130.664	20	1
$P_{EEMACOMH}$	70.14 ± 17.50	6.646	0	0.047 ± 0.009	0.003	0	60103.994 ± 633.657	240.630	0	4
$P_{EEMMASMP}$	99.80 ± 0.57	0.218	1	0.033 ± 0.004	0.002	0	61816.394 ± 386.216	146.664	0	3
$P_{EEMMASMH}$	95.34 ± 0.42	0.160	4	0.040 ± 0.004	0.002	0	61719.687 ± 460.593	174.909	0	2
$P_{EEMACOMC}$	94.90 ± 7.76	2.947	0	0.036 ± 0.006	0.002	0	61839.904 ± 518.148	196.765	0	4
$P_{NSGA-II-MPA}$	67.31 ± 6.85	2.600	0	0.055 ± 0.032	0.012	0	57782.114 ± 1099.095	417.378	0	4

Table F.31: Scenario 6a: $N_G = 100$, $T_{sm} = 1$, $R_g = 800$

$\mathcal{PF}$	$\bar{n}_{alg}$	CI	n^w_{alg}	$\bar{\varrho}$	CI	ϱ^w	$\bar{\xi}$	CI	ξ^w	rank
$P_{EEMACOMP}$	49.76 ± 7.60	2.888	63	0.101 ± 0.014	0.005	0	63966.209 ± 239.094	90.795	4	3
$P_{EEMACOMH}$	17.87 ± 1.97	0.747	0	0.141 ± 0.027	0.010	0	63092.267 ± 469.712	178.372	0	4
$P_{EEMMASMP}$	45.36 ± 6.69	2.542	0	0.102 ± 0.013	0.005	0	63802.972 ± 284.920	108.198	0	4
$P_{EEMMASMH}$	37.76 ± 6.23	2.366	0	0.111 ± 0.017	0.007	0	63743.410 ± 334.980	127.208	0	4
$P_{EEMACOMC}$	46.63 ± 7.77	2.949	55	0.145 ± 0.026	0.010	0	64132.040 ± 218.203	82.862	67	2
$P_{NSGA-II-MPA}$	39.99 ± 4.14	1.571	2	0.066 ± 0.015	0.006	120	63723.083 ± 668.519	253.868	49	1

Table F.32: Scenario 6b: $N_G = 100$, $T_{sm} = 2$, $R_g = 800$

$\mathcal{PF}$	$\bar{n}_{alg}$	CI	n^w_{alg}	$\bar{\varrho}$	CI	ϱ^w	$\bar{\xi}$	CI	ξ^w	rank
$P_{EEMACOMP}$	70.35 ± 11.25	4.273	57	0.067 ± 0.006	0.002	9	64222.008 ± 410.147	155.752	0	1
$P_{EEMACOMH}$	19.54 ± 3.58	1.360	0	0.109 ± 0.018	0.007	0	62811.829 ± 524.574	199.205	0	4
$P_{EEMMASMP}$	52.48 ± 9.25	3.513	0	0.082 ± 0.008	0.003	0	63657.375 ± 356.806	135.496	0	4
$P_{EEMMASMH}$	49.32 ± 9.27	3.522	0	0.081 ± 0.009	0.003	0	63592.264 ± 408.145	154.992	0	4
$P_{EEMACOMC}$	49.79 ± 9.64	3.661	1	0.125 ± 0.025	0.010	0	64552.145 ± 224.790	85.363	60	2
$P_{NSGA-II-MPA}$	44.33 ± 2.90	1.100	2	0.056 ± 0.009	0.003	51	63066.698 ± 589.824	223.984	0	3

Table F.33: Scenario 6c: $N_G = 100$, $T_{sm} = 3$, $R_g = 800$

$\mathcal{PF}$	$\bar{n}_{alg}$	CI	n^w_{alg}	$\bar{\varrho}$	CI	ϱ^w	$\bar{\xi}$	CI	ξ^w	rank
$P_{EEMACOMP}$	83.52 ± 5.96	2.265	40	0.057 ± 0.008	0.003	8	64377.146 ± 324.728	123.315	0	1
$P_{EEMACOMH}$	21.44 ± 2.07	0.785	0	0.096 ± 0.016	0.006	0	62801.812 ± 557.635	211.760	0	4
$P_{EEMMASMP}$	58.83 ± 6.17	2.344	0	0.070 ± 0.010	0.004	0	63719.011 ± 314.813	119.549	0	4
$P_{EEMMASMH}$	57.77 ± 5.95	2.259	0	0.072 ± 0.008	0.003	0	63736.318 ± 356.174	135.256	0	4
$P_{EEMACOMC}$	52.75 ± 8.59	3.261	0	0.116 ± 0.020	0.008	0	64776.202 ± 297.890	113.123	40	2
$P_{NSGA-II-MPA}$	45.09 ± 2.97	1.126	0	0.052 ± 0.011	0.004	32	62842.974 ± 425.018	161.399	0	3

Table F.34: Scenario 6d: $N_G = 100$, $T_{sm} = 4$, $R_g = 800$

$\mathcal{PF}$	$\bar{n}_{alg}$	CI	n^w_{alg}	$\bar{\varrho}$	CI	ϱ^w	$\bar{\xi}$	CI	ξ^w	rank
$P_{EEMACOMP}$	88.91 ± 5.12	1.946	30	0.054 ± 0.007	0.003	12	64408.502 ± 333.447	126.625	0	1
$P_{EEMACOMH}$	21.50 ± 2.42	0.919	0	0.093 ± 0.021	0.008	0	62719.980 ± 425.522	161.591	0	4
$P_{EEMMASMP}$	60.10 ± 5.38	2.043	0	0.071 ± 0.009	0.003	0	63729.103 ± 363.186	137.919	0	4
$P_{EEMMASMH}$	63.17 ± 7.47	2.838	0	0.071 ± 0.008	0.003	0	63776.172 ± 412.075	156.484	0	4
$P_{EEMACOMC}$	51.06 ± 7.59	2.880	0	0.113 ± 0.019	0.007	0	64852.175 ± 254.121	96.502	30	2
$P_{NSGA-II-MPA}$	43.60 ± 2.54	0.966	0	0.055 ± 0.014	0.005	18	62682.837 ± 431.736	163.951	0	3

Table F.35: Scenario 6e: $N_G = 100$, $T_{sm} = 5$, $R_g = 800$

$\mathcal{PF}$	$\bar{n}_{alg}$	CI	n^w_{alg}	$\bar{\varrho}$	CI	ϱ^w	$\bar{\xi}$	CI	ξ^w	rank
$P_{EEMACOMP}$	97.41 ± 1.83	0.695	23	0.051 ± 0.008	0.003	16	64694.801 ± 305.435	115.988	0	1
$P_{EEMACOMH}$	27.80 ± 3.85	1.462	0	0.085 ± 0.018	0.007	0	62955.198 ± 394.722	149.895	0	5
$P_{EEMMASMP}$	77.58 ± 9.38	3.562	0	0.063 ± 0.008	0.003	0	64064.886 ± 315.961	119.985	0	5
$P_{EEMMASMH}$	83.74 ± 9.15	3.474	1	0.065 ± 0.009	0.003	1	64302.477 ± 356.163	135.252	0	4
$P_{EEMACOMC}$	66.10 ± 9.08	3.447	0	0.099 ± 0.013	0.005	0	65124.118 ± 247.699	94.063	24	2
$P_{NSGA-II-MPA}$	44.81 ± 2.54	0.964	0	0.054 ± 0.014	0.005	7	62688.714 ± 428.186	162.602	0	3

Table F.36: Scenario 6f: $N_G = 100$, $T_{sm} = 6$, $R_g = 800$

$\mathcal{PF}$	$\bar{n}_{alg}$	CI	n^w_{alg}	$\bar{\varrho}$	CI	ϱ^w	$\bar{\xi}$	CI	ξ^w	rank
$P_{EEMACOMP}$	98.35 ± 1.71	0.649	19	0.046 ± 0.005	0.002	13	64816.358 ± 324.336	123.166	0	1
$P_{EEMACOMH}$	30.25 ± 4.11	1.561	0	0.078 ± 0.012	0.005	0	63037.767 ± 456.105	173.205	0	5
$P_{EEMMASMP}$	81.69 ± 8.01	3.041	0	0.057 ± 0.006	0.002	0	64133.585 ± 329.989	125.312	0	5
$P_{EEMMASMH}$	90.11 ± 5.77	2.190	1	0.060 ± 0.006	0.002	2	64401.268 ± 313.081	118.892	0	4
$P_{EEMACOMC}$	71.83 ± 10.60	4.026	0	0.097 ± 0.014	0.005	0	65167.685 ± 219.785	83.463	20	2
$P_{NSGA-II-MPA}$	45.46 ± 2.59	0.984	0	0.051 ± 0.010	0.004	5	62698.708 ± 402.134	152.709	0	3

Table F.37: Scenario 7a: $N_G = 300$, $T_{sm} = 1$, $R_g = 300$

$\mathcal{PF}$	$\bar{n}_{alg}$	CI	n^w_{alg}	$\bar{\varrho}$	CI	ϱ^w	$\bar{\xi}$	CI	ξ^w	rank
$P_{EEMACOMP}$	93.04 ± 5.98	2.272	118	0.070 ± 0.011	0.004	114	59664.151 ± 817.604	310.483	0	1
$P_{EEMACOMH}$	55.69 ± 15.85	6.020	0	0.116 ± 0.022	0.008	0	58365.149 ± 1338.723	508.376	0	6
$P_{EEMMASMP}$	83.60 ± 9.50	3.608	0	0.081 ± 0.014	0.005	3	59098.923 ± 1124.492	427.022	0	3
$P_{EEMMASMH}$	78.12 ± 12.14	4.609	1	0.088 ± 0.014	0.005	0	58932.512 ± 1047.305	397.711	0	5
$P_{EEMACOMC}$	78.70 ± 11.56	4.391	0	0.090 ± 0.017	0.007	1	60895.836 ± 663.018	251.779	120	2
$P_{NSGA-II-MPA}$	41.79 ± 6.96	2.641	1	0.126 ± 0.037	0.014	2	55946.879 ± 845.442	321.054	0	3

Table F.38: Scenario 7b: $N_G = 300$, $T_{sm} = 2$, $R_g = 300$

$\mathcal{PF}$	$\bar{n}_{alg}$	CI	n^w_{alg}	$\bar{\varrho}$	CI	ϱ^w	$\bar{\xi}$	CI	ξ^w	rank
$P_{EEMACOMP}$	98.26 ± 1.09	0.415	60	0.057 ± 0.007	0.003	57	60744.233 ± 701.076	266.231	0	1
$P_{EEMACOMH}$	54.51 ± 12.58	4.778	0	0.107 ± 0.017	0.006	0	59134.469 ± 1211.763	460.163	0	5
$P_{EEMMASMP}$	91.20 ± 5.40	2.050	0	0.070 ± 0.010	0.004	0	60135.895 ± 678.887	257.805	0	5
$P_{EEMMASMH}$	85.95 ± 7.65	2.905	0	0.070 ± 0.011	0.004	2	60004.429 ± 727.168	276.140	0	3
$P_{EEMACOMC}$	86.81 ± 7.31	2.775	0	0.074 ± 0.009	0.003	0	61624.241 ± 514.635	195.431	60	2
$P_{NSGA-II-MPA}$	47.93 ± 6.57	2.495	0	0.101 ± 0.023	0.009	1	57023.982 ± 614.058	233.187	0	4

Table F.39: Scenario 7c: $N_G = 300$, $T_{sm} = 3$, $R_g = 300$

$\mathcal{PF}$	$\bar{n}_{alg}$	CI	n^w_{alg}	$\bar{\varrho}$	CI	ϱ^w	$\bar{\xi}$	CI	ξ^w	rank
$P_{EEMACOMP}$	99.01 ± 0.74	0.282	39	0.053 ± 0.005	0.002	39	60833.889 ± 603.457	229.161	0	1
$P_{EEMACOMH}$	58.28 ± 12.14	4.609	0	0.096 ± 0.012	0.005	0	59270.084 ± 1200.147	455.752	0	5
$P_{EEMMASMP}$	94.08 ± 4.04	1.535	0	0.063 ± 0.009	0.003	0	60381.056 ± 705.074	267.750	0	5
$P_{EEMMASMH}$	89.50 ± 6.73	2.556	1	0.069 ± 0.008	0.003	0	60385.598 ± 910.002	345.570	0	3
$P_{EEMACOMC}$	89.82 ± 5.01	1.902	0	0.069 ± 0.007	0.003	0	61955.239 ± 413.362	156.973	40	2
$P_{NSGA-II-MPA}$	54.78 ± 4.96	1.884	0	0.089 ± 0.017	0.007	1	57707.289 ± 846.618	321.501	0	3

Table F.40: Scenario 7d: $N_G = 300$, $T_{sm} = 4$, $R_g = 300$

$\mathcal{PF}$	$\bar{n}_{alg}$	CI	nns	ρ	CI	nsp	ξ	CI	nhy	rank
$P_{EEMACOMP}$	99.51 ± 0.69	0.263	29	0.049 ± 0.004	0.002	27	61362.221 ± 583.576	221.611	0	1
$P_{EEMACOMH}$	61.48 ± 11.41	4.331	0	0.090 ± 0.012	0.005	0	59652.101 ± 962.851	365.640	0	5
$P_{EEMMASMP}$	96.38 ± 2.10	0.798	0	0.056 ± 0.006	0.002	2	60695.994 ± 730.138	277.268	0	3
$P_{EEMMASMH}$	92.91 ± 4.42	1.680	1	0.063 ± 0.006	0.002	1	60657.401 ± 705.691	267.984	0	3
$P_{EEMACOMC}$	92.94 ± 4.00	1.520	0	0.066 ± 0.006	0.002	0	62310.982 ± 326.953	124.160	30	2
$P_{NSGA-II-MPA}$	56.15 ± 4.17	1.585	0	0.086 ± 0.012	0.005	0	57993.635 ± 618.046	234.701	0	5

Table F.41: Scenario 7e: $N_G = 300$, $T_{sm} = 5$, $R_g = 300$

$\mathcal{PF}$	$\bar{n}_{alg}$	CI	n^w_{alg}	$\bar{\varrho}$	CI	ϱ^w	$\bar{\xi}$	CI	ξ^w	rank
$P_{EEMACOMP}$	99.72 ± 0.23	0.088	24	0.047 ± 0.005	0.002	23	61310.428 ± 684.846	260.068	0	1
$P_{EEMACOMH}$	61.82 ± 11.87	4.508	0	0.090 ± 0.014	0.005	0	59550.839 ± 1205.634	457.836	0	4
$P_{EEMMASMP}$	96.97 ± 0.92	0.349	0	0.057 ± 0.007	0.003	0	60885.171 ± 651.764	247.505	0	4
$P_{EEMMASMH}$	93.70 ± 3.04	1.153	0	0.063 ± 0.008	0.003	0	60799.321 ± 742.919	282.121	0	4
$P_{EEMACOMC}$	94.73 ± 2.77	1.052	0	0.063 ± 0.007	0.003	0	62121.522 ± 368.008	139.750	24	2
$P_{NSGA-II-MPA}$	57.11 ± 4.31	1.637	0	0.084 ± 0.018	0.007	1	58166.765 ± 494.275	187.699	0	3

Table F.42: Scenario 7f: $N_G = 300$, $T_{sm} = 6$, $R_g = 300$

$\mathcal{PF}$	$\bar{n}_{alg}$	CI	n^w_{alg}	$\bar{\varrho}$	CI	ϱ^w	$\bar{\xi}$	CI	ξ^w	rank
$P_{EEMACOMP}$	99.77 ± 0.18	0.066	15	0.047 ± 0.005	0.002	18	61453.252 ± 515.557	195.781	0	1
$P_{EEMACOMH}$	64.31 ± 8.84	3.359	0	0.086 ± 0.013	0.005	0	59624.352 ± 1108.043	420.776	0	6
$P_{EEMMASMP}$	97.26 ± 0.52	0.199	2	0.057 ± 0.007	0.003	0	61127.984 ± 601.689	228.490	0	4
$P_{EEMMASMH}$	94.51 ± 1.10	0.419	2	0.062 ± 0.007	0.003	1	60694.849 ± 758.565	288.063	0	3
$P_{EEMACOMC}$	96.04 ± 1.72	0.653	0	0.062 ± 0.006	0.002	0	62292.129 ± 341.366	129.633	20	2
$P_{NSGA-II-MPA}$	57.44 ± 4.29	1.629	0	0.085 ± 0.018	0.007	1	58260.458 ± 547.242	207.813	0	5

Table F.43: Scenario 8a: $N_G = 300$, $T_{sm} = 1$, $R_g = 500$

$\mathcal{PF}$	$\bar{n}_{alg}$	CI	n^w_{alg}	$\bar{\varrho}$	CI	ϱ^w	$\bar{\xi}$	CI	ξ^w	rank
$P_{EEMACOMP}$	57.73 ± 9.90	3.759	119	0.106 ± 0.013	0.005	118	59920.766 ± 726.594	275.922	0	1
$P_{EEMACOMH}$	30.13 ± 5.41	2.053	0	0.191 ± 0.025	0.009	0	57008.681 ± 1295.680	492.030	0	5
$P_{EEMMASMP}$	47.69 ± 7.94	3.014	0	0.126 ± 0.021	0.008	1	59349.600 ± 842.997	320.125	0	4
$P_{EEMMASMH}$	44.55 ± 8.13	3.086	1	0.139 ± 0.029	0.011	1	59158.660 ± 808.495	307.024	0	3
$P_{EEMACOMC}$	48.00 ± 8.15	3.096	0	0.139 ± 0.019	0.007	0	60049.206 ± 641.399	243.569	0	5
$P_{NSGA-II-MPA}$	20.46 ± 2.97	1.127	0	0.265 ± 0.036	0.014	0	64489.940 ± 804.127	305.365	120	2

Table F.44: Scenario 8b: $N_G = 300$, $T_{sm} = 2$, $R_g = 500$

$\mathcal{PF}$	$\bar{n}_{alg}$	CI	n^w_{alg}	$\bar{\varrho}$	CI	ϱ^w	$\bar{\xi}$	CI	ξ^w	rank
$P_{EEMACOMP}$	56.48 ± 9.23	3.506	59	0.099 ± 0.016	0.006	58	60475.012 ± 649.481	246.639	0	1
$P_{EEMACOMH}$	28.44 ± 5.56	2.110	0	0.177 ± 0.025	0.009	0	57370.244 ± 1110.111	421.561	0	5
$P_{EEMMASMP}$	44.34 ± 6.94	2.634	0	0.121 ± 0.019	0.007	1	59858.127 ± 785.103	298.141	0	4
$P_{EEMMASMH}$	42.37 ± 8.36	3.174	1	0.135 ± 0.021	0.008	1	59535.577 ± 859.987	326.577	0	3
$P_{EEMACOMC}$	46.25 ± 7.19	2.729	0	0.126 ± 0.018	0.007	0	60600.033 ± 447.278	169.853	0	5
$P_{NSGA-II-MPA}$	22.78 ± 4.19	1.590	0	0.251 ± 0.028	0.011	0	64926.835 ± 398.208	151.218	60	2

Table F.45: Scenario 8c: $N_G = 300$, $T_{sm} = 3$, $R_g = 500$

$\mathcal{PF}$	$\bar{n}_{alg}$	CI	n^w_{alg}	$\bar{\varrho}$	CI	ϱ^w	$\bar{\xi}$	CI	ξ^w	rank
$P_{EEMACOMP}$	65.50 ± 12.17	4.622	39	0.087 ± 0.013	0.005	39	61097.779 ± 584.252	221.868	0	1
$P_{EEMACOMH}$	30.20 ± 5.08	1.928	0	0.173 ± 0.020	0.008	0	57665.954 ± 1015.658	385.693	0	4
$P_{EEMMASMP}$	50.63 ± 8.67	3.292	0	0.115 ± 0.037	0.014	0	60559.718 ± 693.155	263.223	0	4
$P_{EEMMASMH}$	46.66 ± 9.57	3.636	1	0.122 ± 0.017	0.006	1	60147.474 ± 745.628	283.150	0	3
$P_{EEMACOMC}$	48.00 ± 7.94	3.016	0	0.116 ± 0.022	0.008	0	60969.451 ± 508.311	193.030	0	4
$P_{NSGA-II-MPA}$	22.93 ± 3.95	1.502	0	0.260 ± 0.027	0.010	0	64903.466 ± 217.519	82.602	40	2

Table F.46: Scenario 8d: $N_G = 300$, $T_{sm} = 4$, $R_g = 500$

$\mathcal{PF}$	$\bar{n}_{alg}$	CI	n^w_{alg}	$\bar{\varrho}$	CI	ϱ^w	$\bar{\xi}$	CI	ξ^w	rank
$P_{EEMACOMP}$	68.56 ± 8.41	3.194	29	0.078 ± 0.008	0.003	29	61270.011 ± 471.914	179.208	0	1
$P_{EEMACOMH}$	30.50 ± 4.38	1.664	0	0.171 ± 0.017	0.006	0	57855.751 ± 900.304	341.888	0	4
$P_{EEMMASMP}$	53.40 ± 6.43	2.442	0	0.105 ± 0.020	0.008	0	60902.062 ± 487.941	185.294	0	4
$P_{EEMMASMH}$	49.46 ± 7.41	2.815	1	0.116 ± 0.012	0.004	1	60419.280 ± 589.481	223.853	0	3
$P_{EEMACOMC}$	53.36 ± 7.65	2.904	0	0.109 ± 0.015	0.006	0	61248.190 ± 346.946	131.752	0	4
$P_{NSGA-II-MPA}$	24.30 ± 3.95	1.500	0	0.260 ± 0.026	0.010	0	64803.937 ± 186.757	70.920	30	2

Table F.47: Scenario 8e: $N_G = 300$, $T_{sm} = 5$, $R_g = 500$

$\mathcal{PF}$	$\bar{n}_{alg}$	CI	n^w_{alg}	$\bar{\varrho}$	CI	ϱ^w	$\bar{\xi}$	CI	ξ^w	rank
$P_{EEMACOMP}$	71.88 ± 10.71	4.069	23	0.077 ± 0.015	0.006	23	61379.528 ± 492.537	187.039	0	1
$P_{EEMACOMH}$	31.02 ± 4.26	1.619	0	0.164 ± 0.020	0.007	0	57910.109 ± 1204.360	457.352	0	4
$P_{EEMMASMP}$	53.98 ± 7.82	2.971	0	0.097 ± 0.019	0.007	0	61146.303 ± 535.447	203.334	0	4
$P_{EEMMASMH}$	49.03 ± 9.02	3.426	1	0.106 ± 0.017	0.007	1	60546.164 ± 672.581	255.410	0	3
$P_{EEMACOMC}$	54.58 ± 9.08	3.450	0	0.106 ± 0.014	0.005	0	61458.694 ± 338.349	128.487	0	4
$P_{NSGA-II-MPA}$	22.41 ± 3.84	1.458	0	0.259 ± 0.023	0.009	0	64684.148 ± 469.194	178.175	24	2

Table F.48: Scenario 8f: $N_G = 300$, $T_{sm} = 6$, $R_g = 500$

$\mathcal{PF}$	$\bar{n}_{alg}$	CI	n^w_{alg}	$\bar{\varrho}$	CI	ϱ^w	$\bar{\xi}$	CI	ξ^w	rank
$P_{EEMACOMP}$	86.12 ± 5.06	1.921	19	0.068 ± 0.011	0.004	19	61913.483 ± 406.288	154.287	0	1
$P_{EEMACOMH}$	35.75 ± 4.20	1.594	0	0.152 ± 0.020	0.008	0	58739.849 ± 679.759	258.136	0	4
$P_{EEMMASMP}$	63.01 ± 4.72	1.793	0	0.091 ± 0.016	0.006	0	61552.664 ± 363.220	137.932	0	4
$P_{EEMMASMH}$	58.56 ± 4.73	1.797	1	0.111 ± 0.024	0.009	1	61103.759 ± 441.805	167.774	0	3
$P_{EEMACOMC}$	64.24 ± 7.35	2.793	0	0.089 ± 0.010	0.004	0	61737.664 ± 219.503	83.356	0	4
$P_{NSGA-II-MPA}$	21.37 ± 4.27	1.620	0	0.271 ± 0.028	0.011	0	64744.982 ± 132.848	50.449	20	2

Table F.49: Scenario 9a: $N_G = 300$, $T_{sm} = 1$, $R_g = 800$

$\mathcal{PF}$	$\bar{n}_{alg}$	CI	n^w_{alg}	$\bar{\varrho}$	CI	ϱ^w	$\bar{\xi}$	CI	ξ^w	rank
$P_{EEMACOMP}$	19.90 ± 2.38	0.903	0	0.187 ± 0.025	0.010	5	49998.628 ± 1503.670	571.014	0	2
$P_{EEMACOMH}$	12.40 ± 1.71	0.650	0	0.296 ± 0.041	0.016	0	44856.393 ± 1623.950	616.690	0	4
$P_{EEMMASMP}$	16.28 ± 1.73	0.657	0	0.209 ± 0.023	0.009	0	48540.331 ± 1094.242	415.535	0	4
$P_{EEMMASMH}$	14.79 ± 1.68	0.639	0	0.225 ± 0.029	0.011	2	47568.622 ± 1660.751	630.665	0	3
$P_{EEMACOMC}$	14.37 ± 1.87	0.709	0	0.246 ± 0.037	0.014	0	50765.209 ± 1246.919	473.514	0	4
$P_{NSGA-II-MPA}$	26.87 ± 3.17	1.203	120	0.148 ± 0.025	0.009	113	58532.224 ± 916.999	348.228	120	1

Table F.50: Scenario 9b: $N_G = 300$, $T_{sm} = 2$, $R_g = 800$

$\mathcal{PF}$	$\bar{n}_{alg}$	CI	n^w_{alg}	$\bar{\varrho}$	CI	ϱ^w	$\bar{\xi}$	CI	ξ^w	rank
$P_{EEMACOMP}$	20.43 ± 3.20	1.216	2	0.176 ± 0.022	0.008	3	51058.473 ± 1205.798	457.898	0	2
$P_{EEMACOMH}$	12.49 ± 1.32	0.500	0	0.284 ± 0.039	0.015	0	45387.773 ± 1578.853	599.565	0	4
$P_{EEMMASMP}$	16.51 ± 2.35	0.891	0	0.209 ± 0.037	0.014	1	49824.905 ± 1304.895	495.530	0	3
$P_{EEMMASMH}$	14.31 ± 1.98	0.751	0	0.214 ± 0.027	0.010	0	48500.839 ± 1543.321	586.072	0	4
$P_{EEMACOMC}$	14.69 ± 2.13	0.809	0	0.229 ± 0.029	0.011	0	51500.682 ± 1137.012	431.777	0	4
$P_{NSGA-II-MPA}$	23.64 ± 2.80	1.062	58	0.148 ± 0.029	0.011	56	60058.894 ± 535.292	203.275	60	1

Table F.51: Scenario 9c: $N_G = 300$, $T_{sm} = 3$, $R_g = 800$

$\mathcal{PF}$	$\bar{n}_{alg}$	CI	n^w_{alg}	$\bar{\varrho}$	CI	ϱ^w	$\bar{\xi}$	CI	ξ^w	rank
$P_{EEMACOMP}$	24.53 ± 3.42	1.299	35	0.156 ± 0.021	0.008	18	52374.117 ± 788.967	299.608	0	2
$P_{EEMACOMH}$	13.36 ± 1.47	0.560	0	0.251 ± 0.024	0.009	0	45869.401 ± 1662.672	631.395	0	5
$P_{EEMMASMP}$	19.71 ± 2.20	0.835	1	0.170 ± 0.016	0.006	7	51680.217 ± 983.538	373.495	0	3
$P_{EEMMASMH}$	16.49 ± 2.34	0.888	1	0.196 ± 0.026	0.010	0	50509.870 ± 1215.758	461.680	0	4
$P_{EEMACOMC}$	15.84 ± 2.61	0.991	0	0.205 ± 0.033	0.013	0	52969.544 ± 834.896	317.049	0	5
$P_{NSGA-II-MPA}$	21.35 ± 2.27	0.862	3	0.164 ± 0.024	0.009	15	61001.573 ± 430.931	163.645	40	1

Table F.52: Scenario 9d: $N_G = 300$, $T_{sm} = 4$, $R_g = 800$

$\mathcal{PF}$	$\bar{n}_{alg}$	CI	n^w_{alg}	$\bar{\varrho}$	CI	ϱ^w	$\bar{\xi}$	CI	ξ^w	rank
$P_{EEMACOMP}$	25.84 ± 3.88	1.472	28	0.146 ± 0.019	0.007	18	52801.550 ± 1032.938	392.255	0	1
$P_{EEMACOMH}$	13.69 ± 1.42	0.539	0	0.261 ± 0.044	0.017	0	46294.130 ± 1514.349	575.069	0	4
$P_{EEMMASMP}$	19.49 ± 3.01	1.141	1	0.171 ± 0.024	0.009	1	51326.327 ± 1189.155	451.578	0	3
$P_{EEMMASMH}$	16.91 ± 2.10	0.796	0	0.192 ± 0.029	0.011	0	50389.864 ± 1739.927	660.732	0	4
$P_{EEMACOMC}$	16.05 ± 2.37	0.899	0	0.195 ± 0.034	0.013	0	53072.900 ± 1251.343	475.194	0	4
$P_{NSGA-II-MPA}$	21.43 ± 2.22	0.842	1	0.154 ± 0.022	0.009	11	61174.784 ± 383.731	145.721	30	2

Table F.53: Scenario 9e: $N_G = 300$, $T_{sm} = 5$, $R_g = 800$

$\mathcal{PF}$	$\bar{n}_{alg}$	CI	n^w_{alg}	$\bar{\varrho}$	CI	ϱ^w	$\bar{\xi}$	CI	ξ^w	rank
$P_{EEMACOMP}$	25.49 ± 4.02	1.527	21	0.146 ± 0.024	0.009	17	53088.762 ± 1097.656	416.832	0	1
$P_{EEMACOMH}$	13.68 ± 1.86	0.706	0	0.265 ± 0.052	0.020	0	46410.901 ± 1824.780	692.955	0	4
$P_{EEMMASMP}$	20.37 ± 2.48	0.942	2	0.163 ± 0.015	0.006	4	51953.859 ± 743.169	282.216	0	3
$P_{EEMMASMH}$	16.92 ± 2.20	0.836	0	0.186 ± 0.030	0.012	0	50803.910 ± 1415.343	537.472	0	4
$P_{EEMACOMC}$	17.48 ± 2.72	1.034	0	0.201 ± 0.031	0.012	0	53250.626 ± 823.638	312.774	0	4
$P_{NSGA-II-MPA}$	19.11 ± 1.91	0.725	1	0.175 ± 0.026	0.010	3	61664.790 ± 427.184	162.222	24	2

Table F.54: Scenario 9f: $N_G = 300$, $T_{sm} = 6$, $R_g = 800$

$\mathcal{PF}$	$\bar{n}_{alg}$	CI	n^w_{alg}	$\bar{\varrho}$	CI	ϱ^w	$\bar{\xi}$	CI	ξ^w	rank
$P_{EEMACOMP}$	37.32 ± 5.34	2.029	18	0.115 ± 0.014	0.005	17	54929.165 ± 778.742	295.725	0	1
$P_{EEMACOMH}$	16.71 ± 1.97	0.748	0	0.219 ± 0.036	0.014	0	47976.933 ± 1287.187	488.805	0	6
$P_{EEMMASMP}$	30.40 ± 4.41	1.675	0	0.136 ± 0.014	0.006	2	53865.025 ± 736.264	279.594	0	3
$P_{EEMMASMH}$	23.64 ± 3.30	1.253	1	0.160 ± 0.019	0.007	1	52832.253 ± 726.900	276.038	0	3
$P_{EEMACOMC}$	22.17 ± 3.13	1.189	1	0.170 ± 0.026	0.010	0	55091.131 ± 808.302	306.950	0	5
$P_{NSGA-II-MPA}$	19.40 ± 2.48	0.940	0	0.165 ± 0.030	0.011	0	61614.645 ± 268.340	101.901	20	2

Appendix G

Illustration of the Influence of Change Frequency and Change Severity on the Performance Metrics

This appendix presents a three dimension graphs to illustrate the influence of change frequency, T_{sm}, and change severity, R_g, on the performance metrics, $\bar{n}_{alg}$, $\bar{\varrho}$, and $\bar{\xi}$ for different number of nodes.

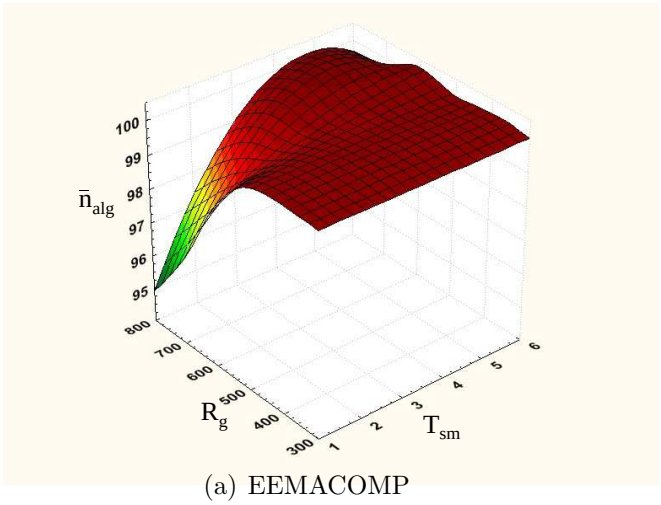

(a) EEMACOMP

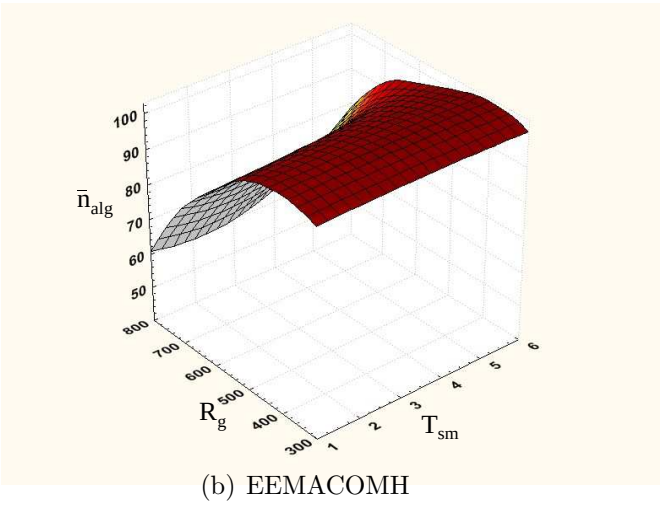

(b) EEMACOMH

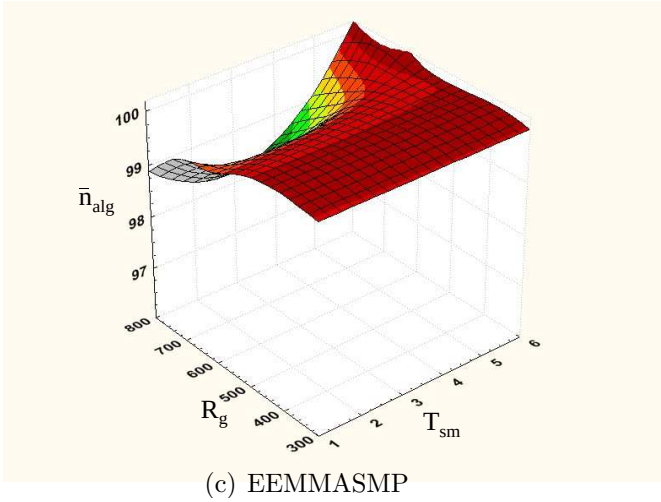

(c) EEMMASMP

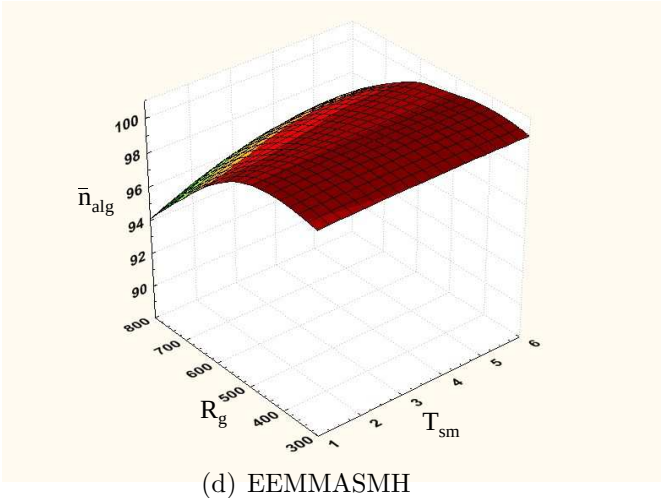

(d) EEMMASMH

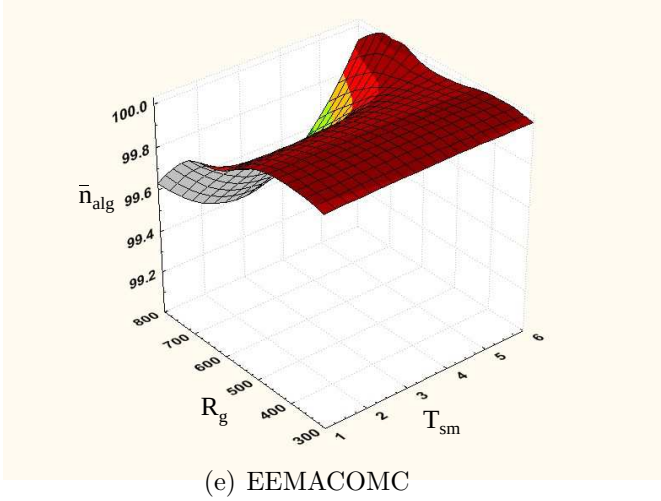

(e) EEMACOMC

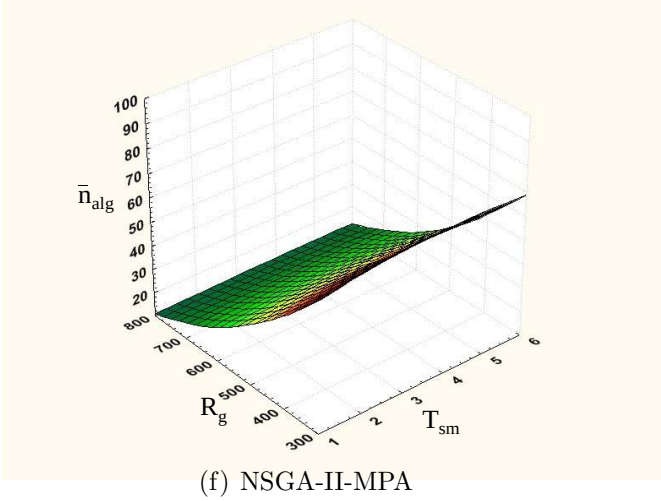

(f) NSGA-II-MPA

Figure G.1: Influence of R_g and T_{sm} on the $\bar{n}_{alg}$ metric for $N_G = 30$

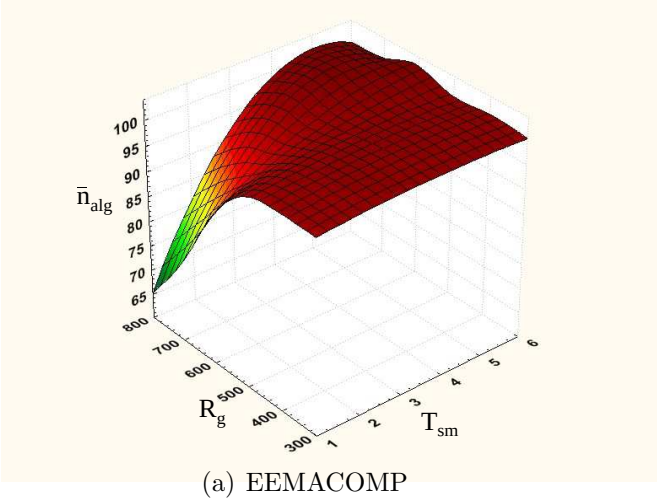

(a) EEMACOMP

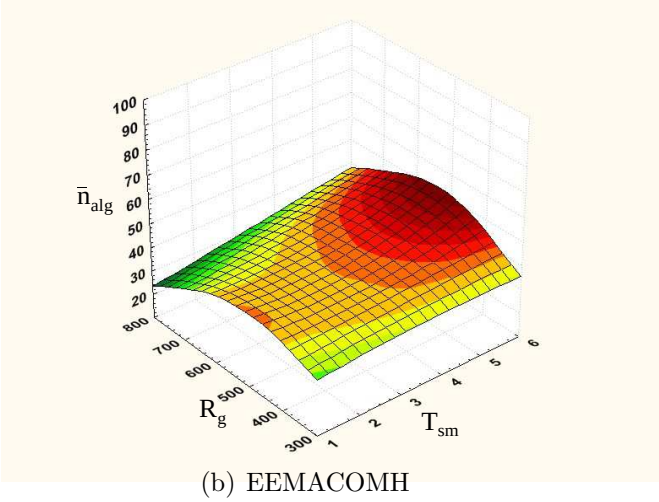

(b) EEMACOMH

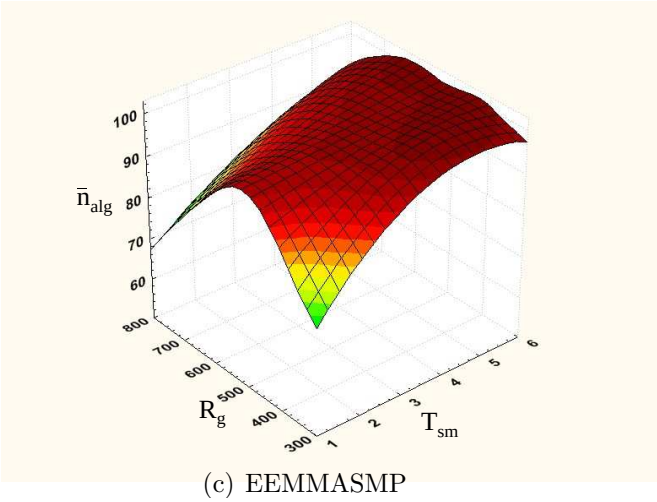

(c) EEMMASMP

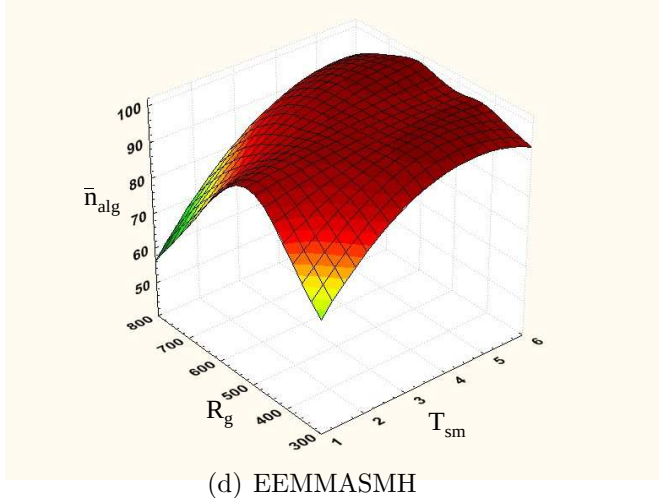

(d) EEMMASMH

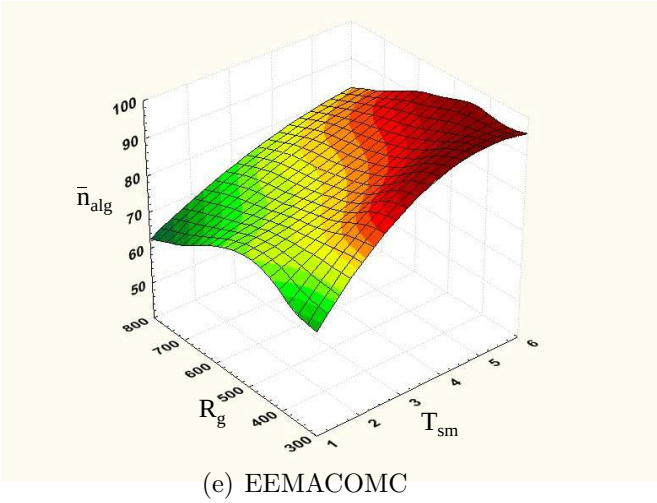

(e) EEMACOMC

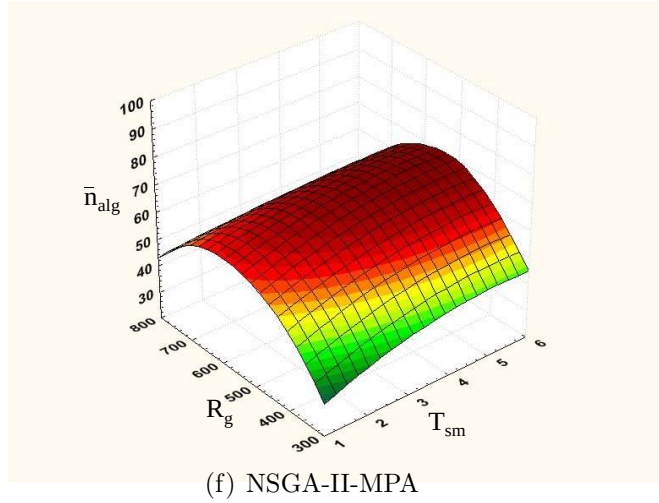

(f) NSGA-II-MPA

Figure G.2: Influence of R_g and T_{sm} on the $\bar{n}_{alg}$ metric for $N_G = 100$

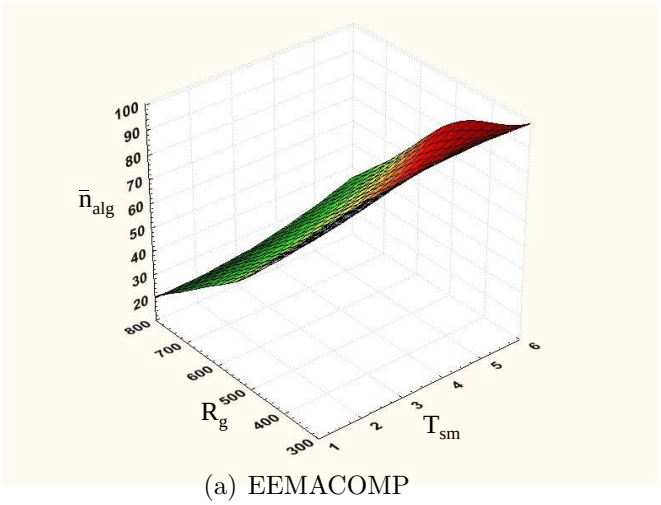

(a) EEMACOMP

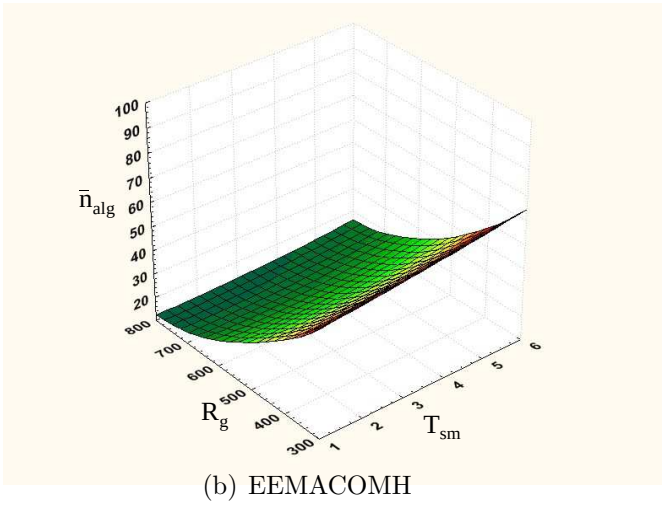

(b) EEMACOMH

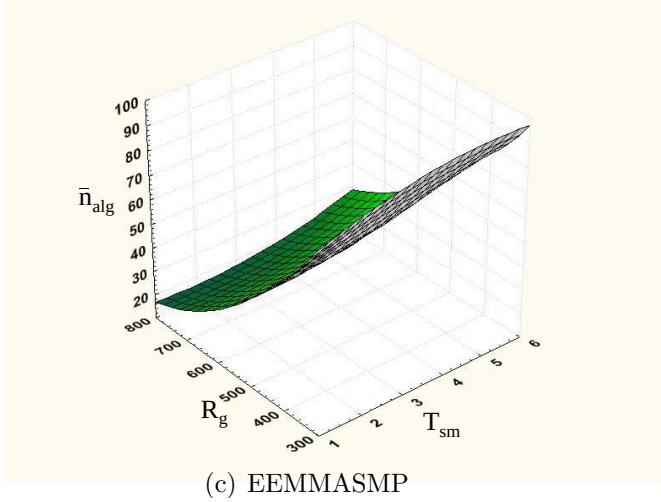

(c) EEMMASMP

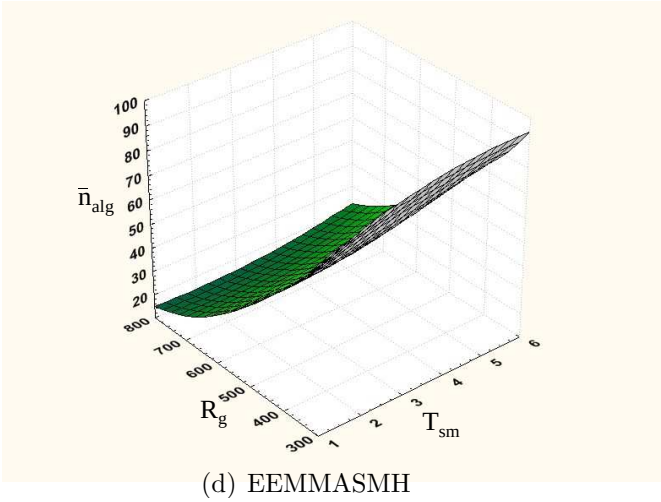

(d) EEMMASMH

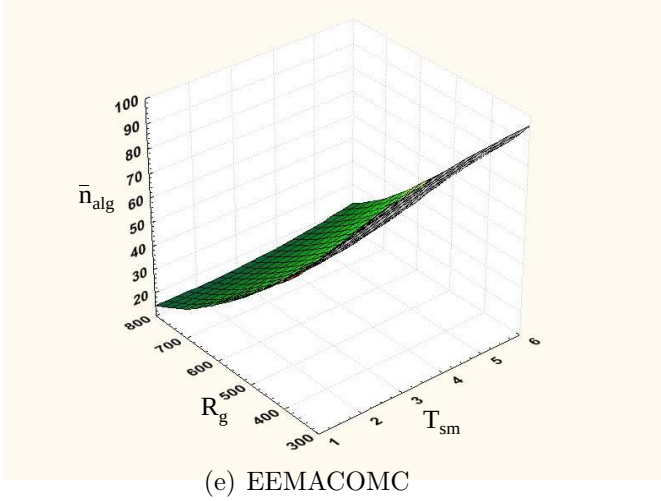

(e) EEMACOMC

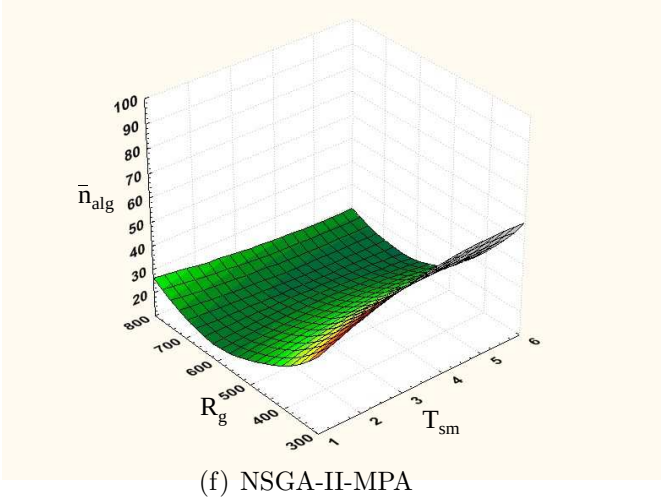

(f) NSGA-II-MPA

Figure G.3: Influence of R_g and T_{sm} on the $\bar{n}_{alg}$ metric for $N_G = 300$

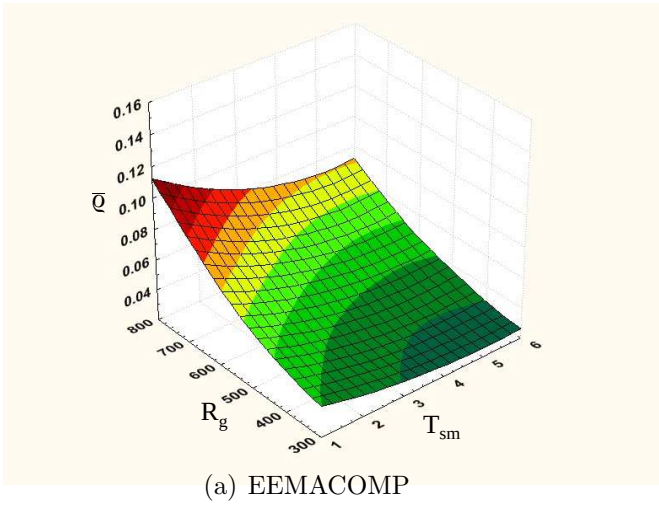

(a) EEMACOMP

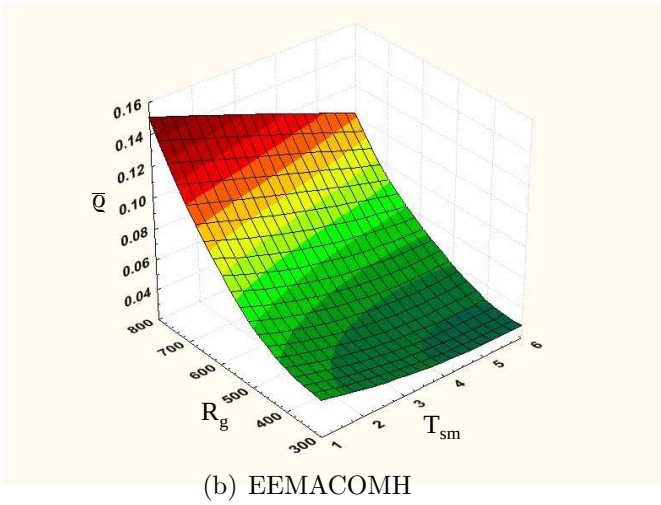

(b) EEMACOMH

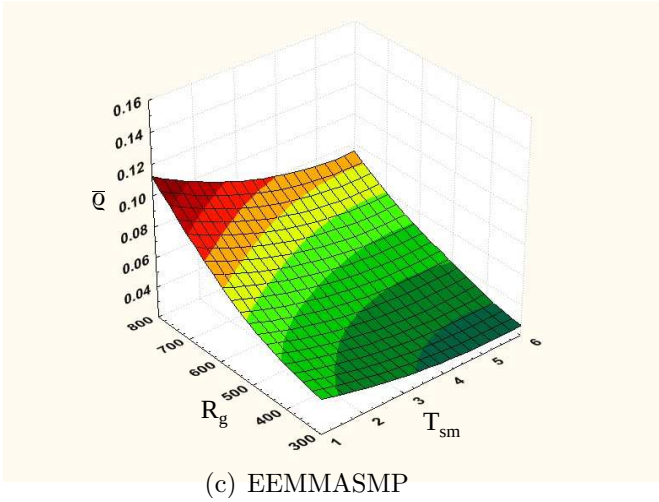

(c) EEMMASMP

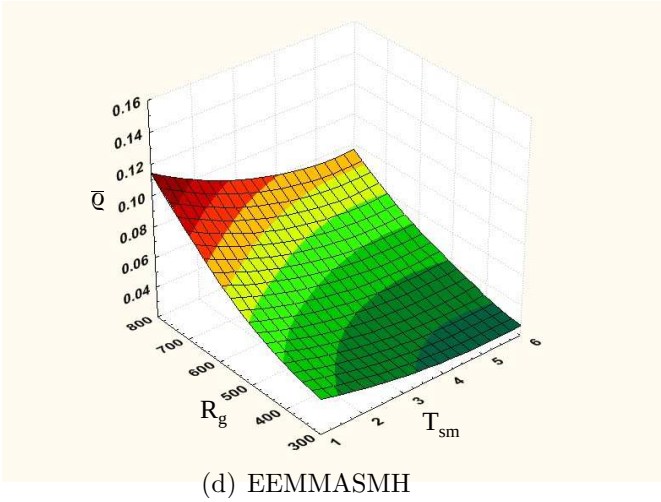

(d) EEMMASMH

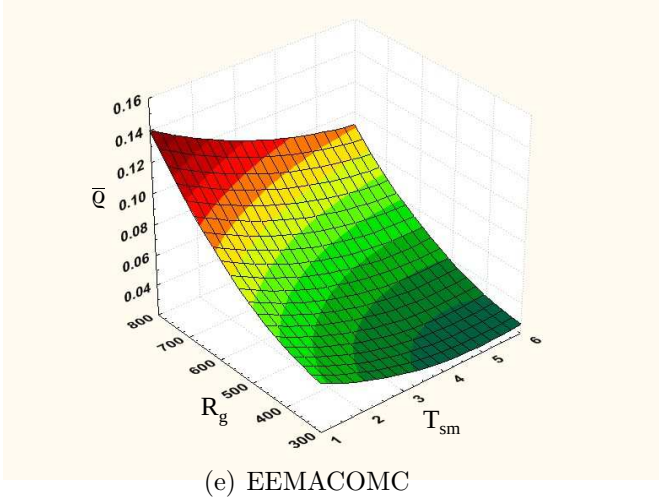

(e) EEMACOMC

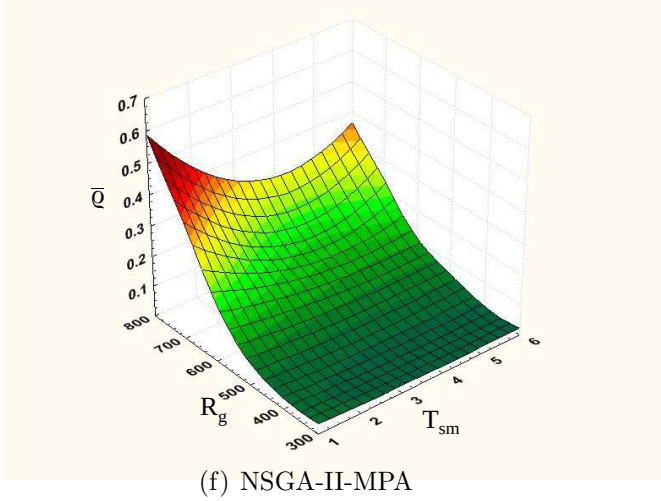

(f) NSGA-II-MPA

Figure G.4: Influence of R_g and T_{sm} on the $\bar{\varrho}$ metric for $N_G = 30$

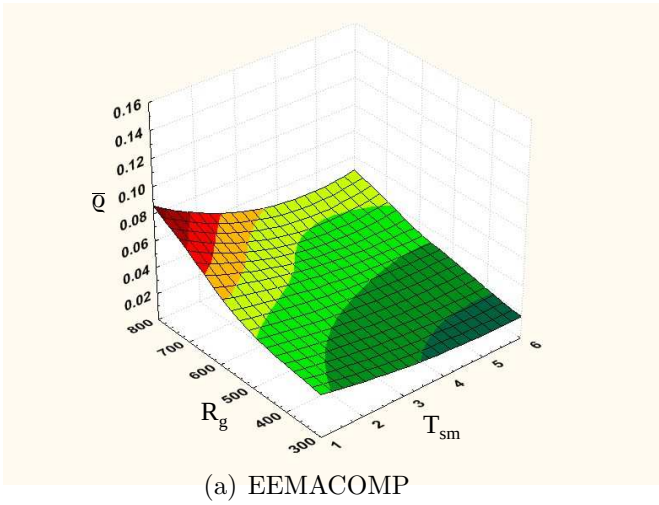

(a) EEMACOMP

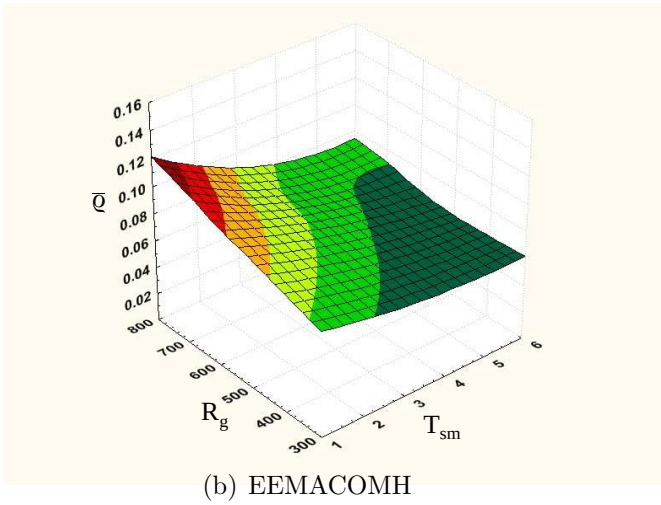

(b) EEMACOMH

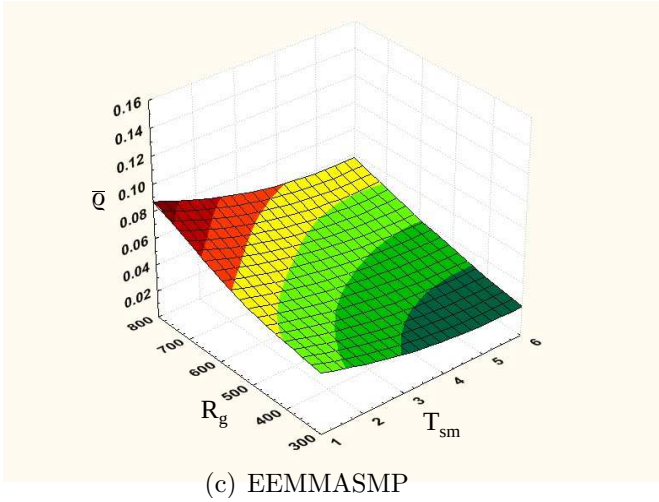

(c) EEMMASMP

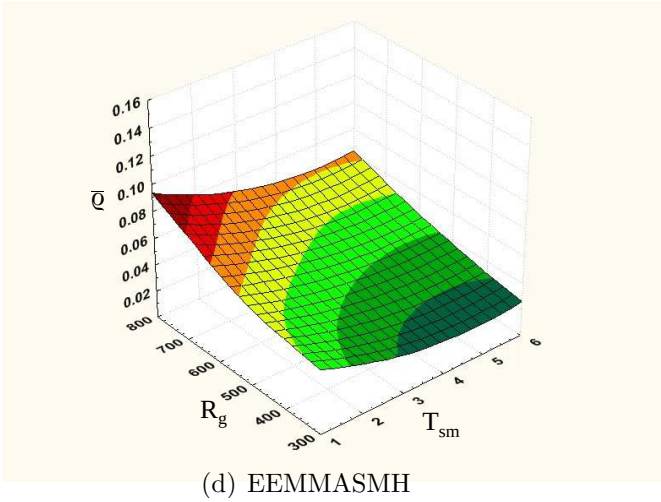

(d) EEMMASMH

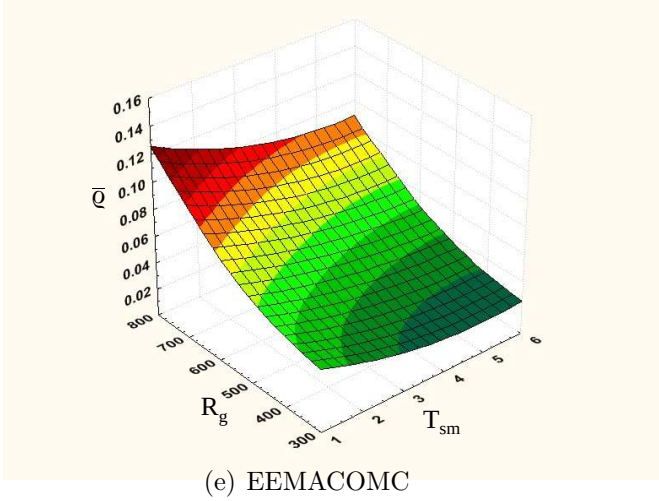

(e) EEMACOMC

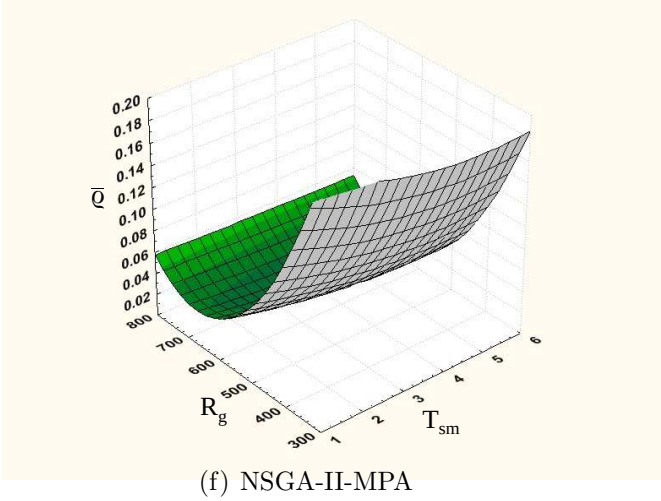

(f) NSGA-II-MPA

Figure G.5: Influence of R_g and T_{sm} on the $\bar{\varrho}$ metric for $N_G = 100$

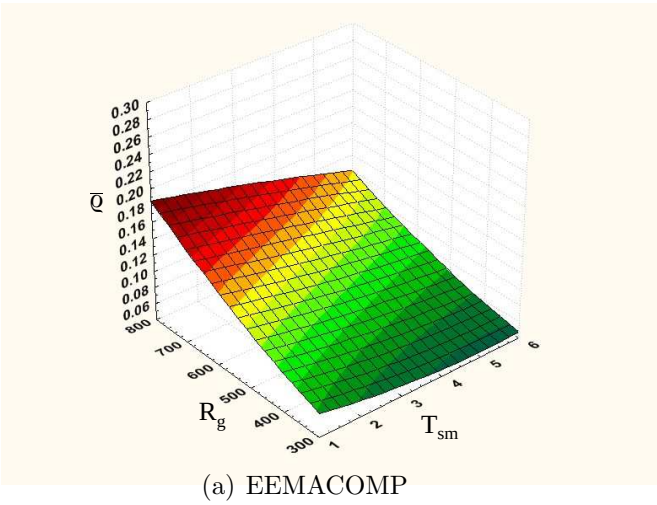

(a) EEMACOMP

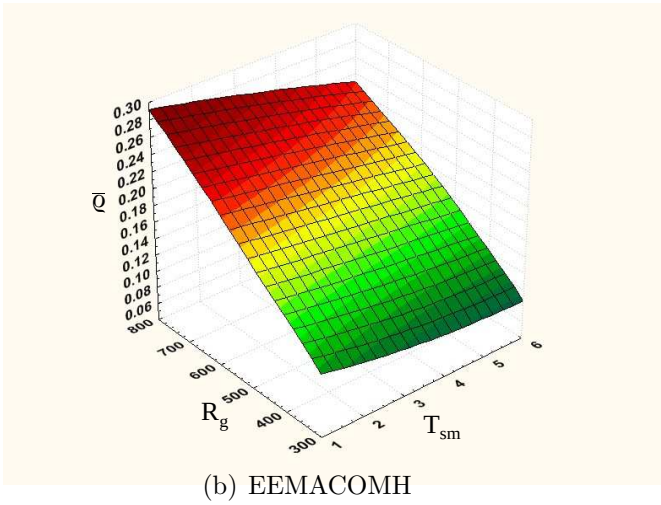

(b) EEMACOMH

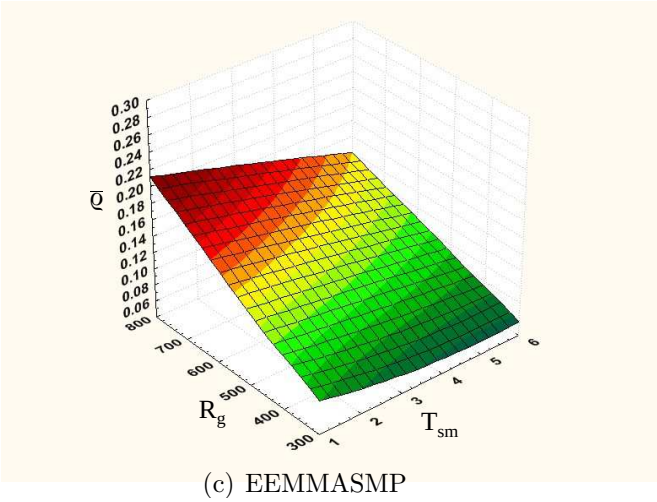

(c) EEMMASMP

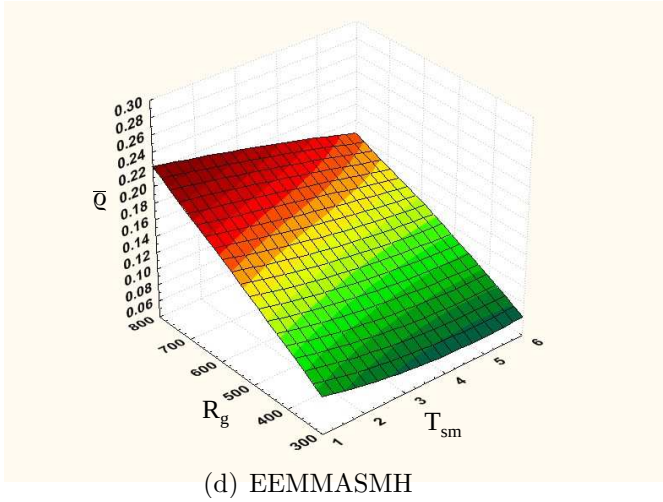

(d) EEMMASMH

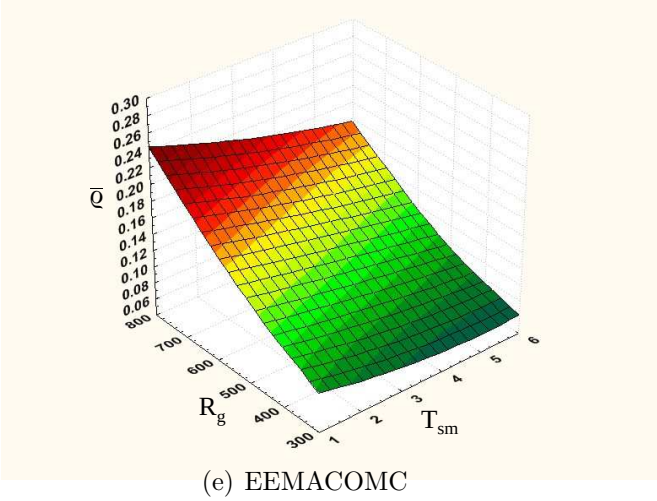

(e) EEMACOMC

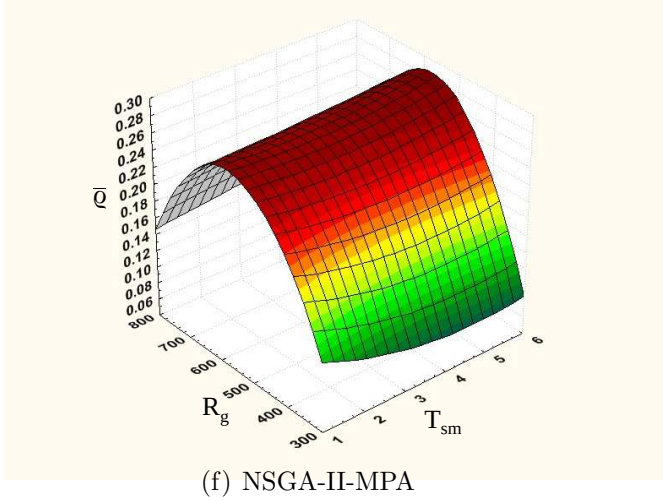

(f) NSGA-II-MPA

Figure G.6: Influence of R_g and T_{sm} on the $\bar{\varrho}$ metric for $N_G = 300$

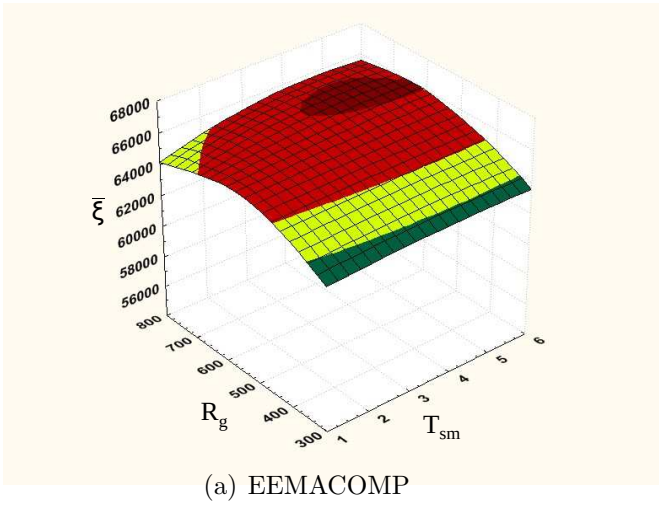

(a) EEMACOMP

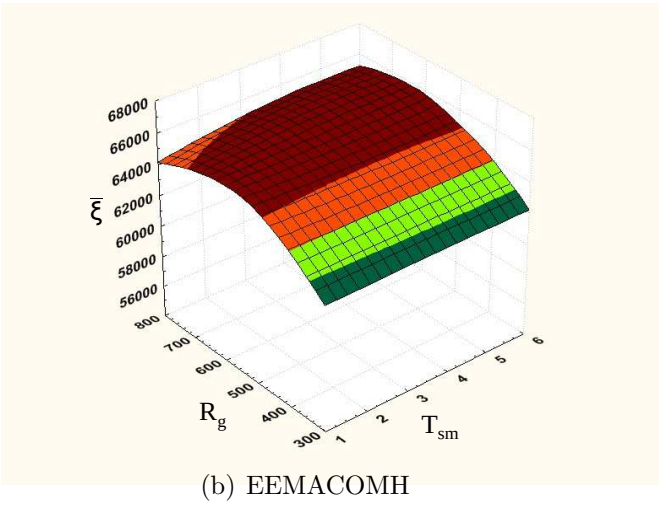

(b) EEMACOMH

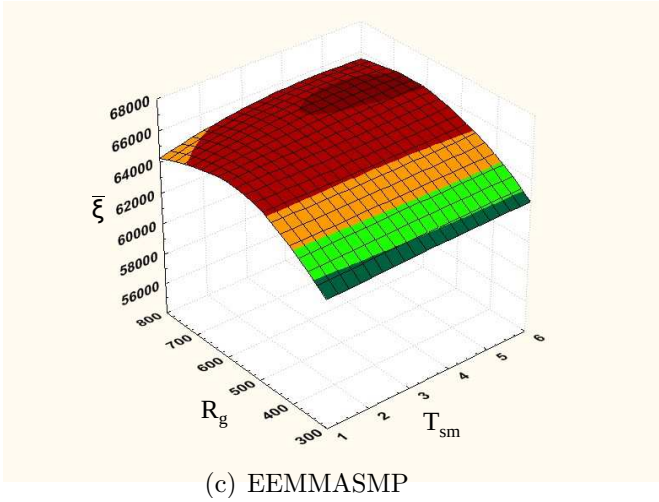

(c) EEMMASMP

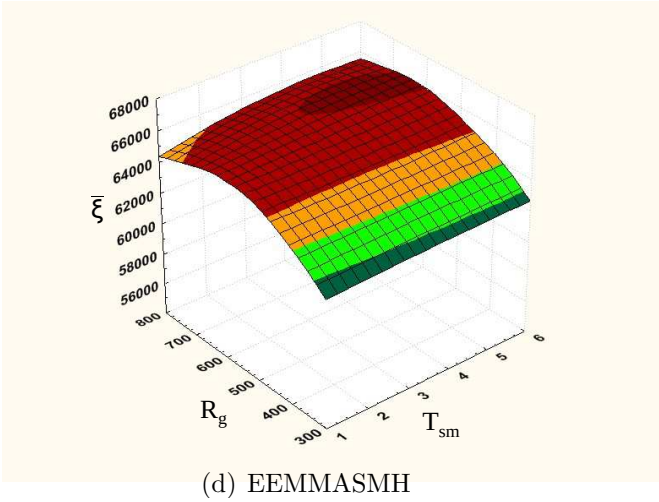

(d) EEMMASMH

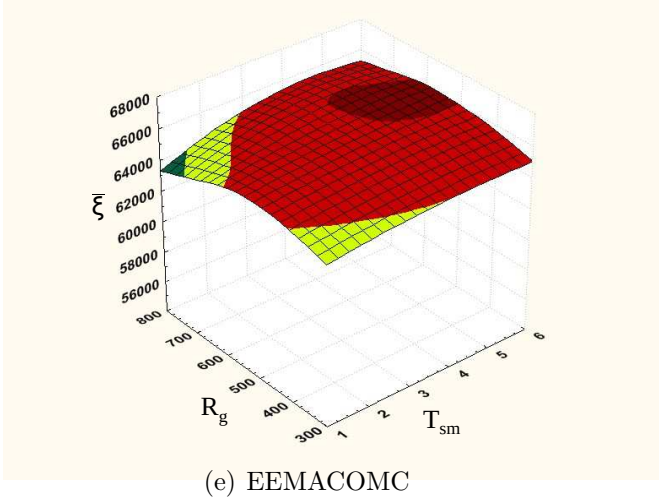

(e) EEMACOMC

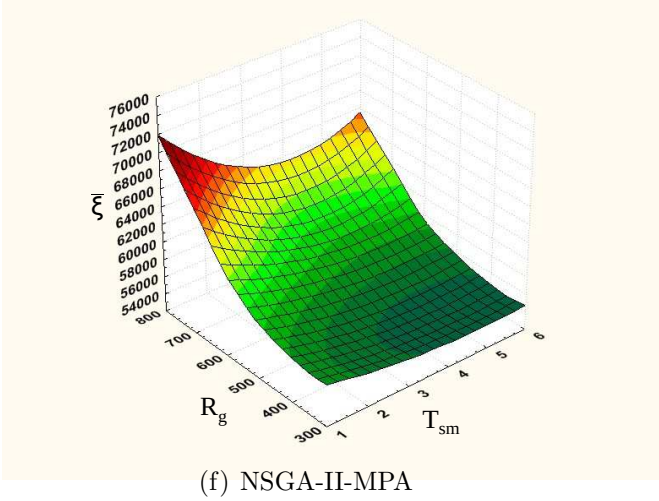

(f) NSGA-II-MPA

Figure G.7: Influence of R_g and T_{sm} on the $\bar{\xi}$ metric for $N_G = 30$

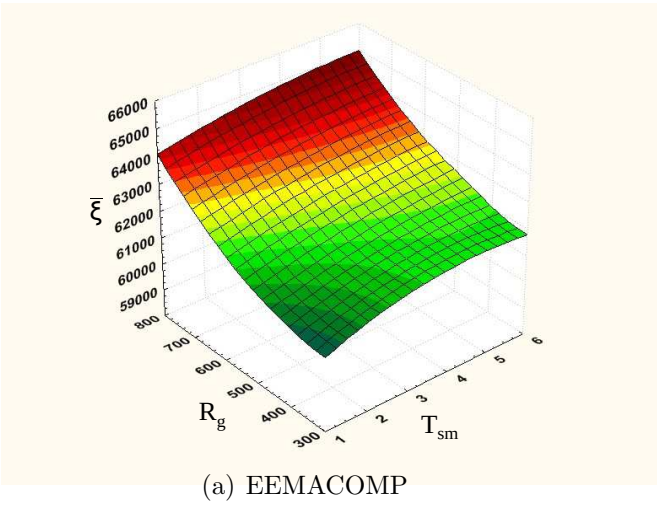

(a) EEMACOMP

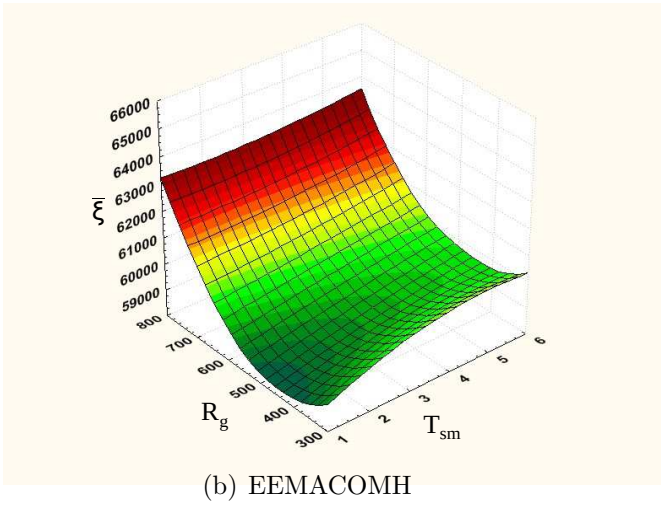

(b) EEMACOMH

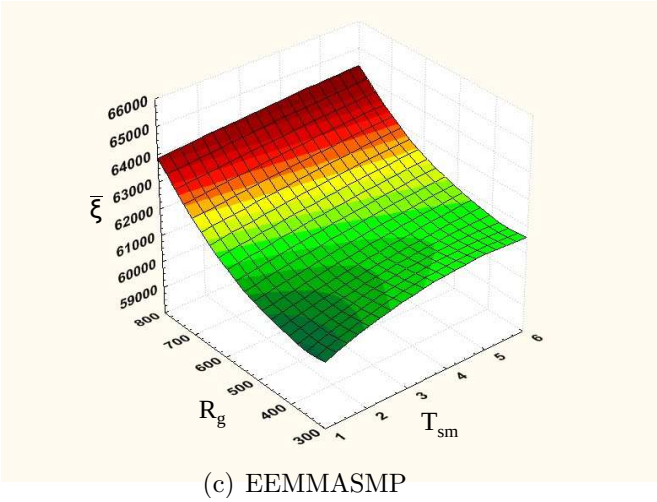

(c) EEMMASMP

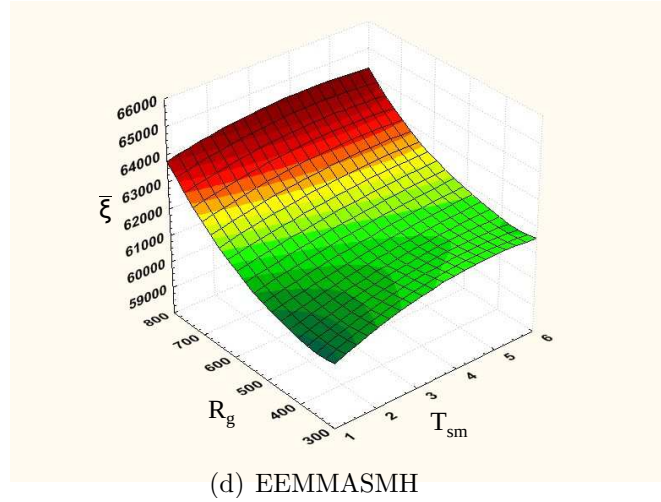

(d) EEMMASMH

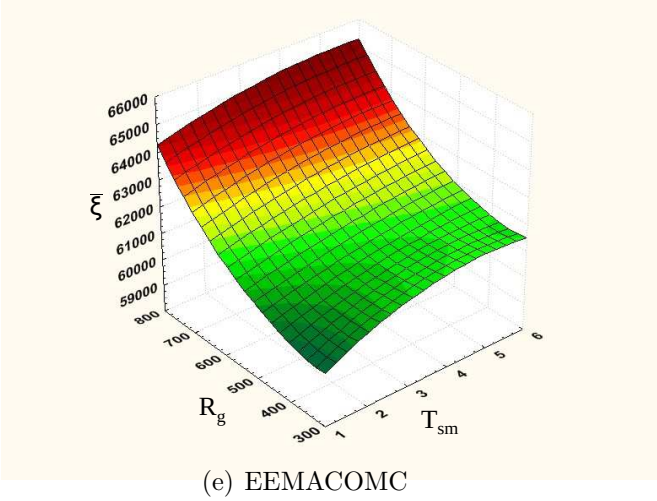

(e) EEMACOMC

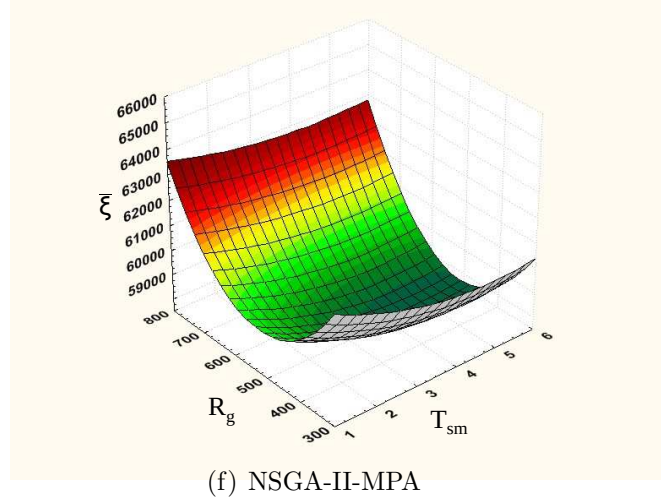

(f) NSGA-II-MPA

Figure G.8: Influence of R_g and T_{sm} on the $\bar{\xi}$ metric for $N_G = 100$

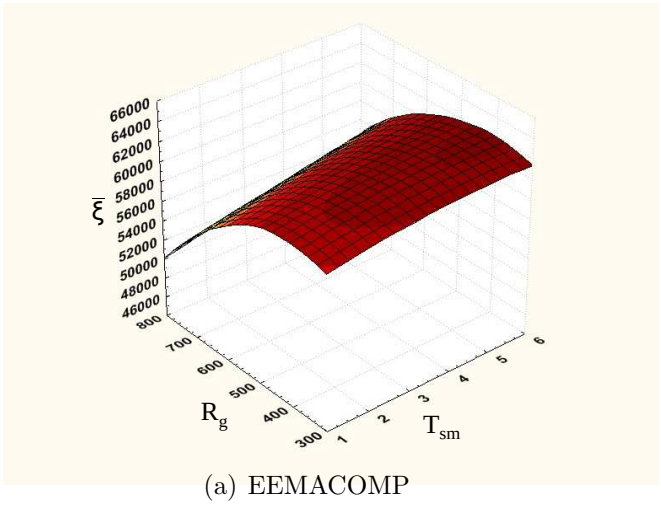

(a) EEMACOMP

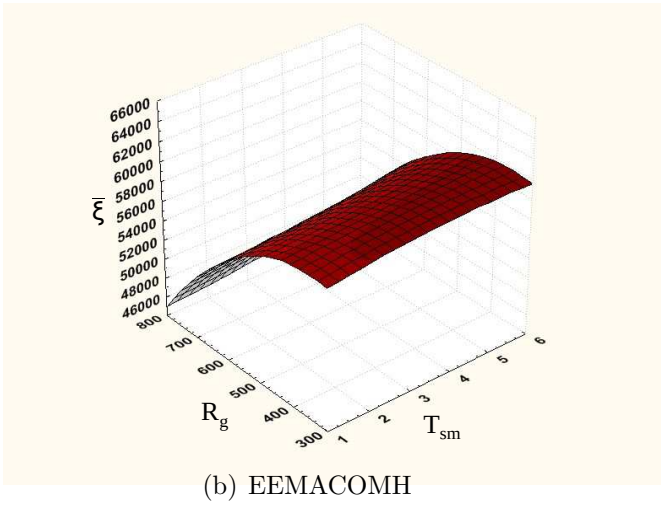

(b) EEMACOMH

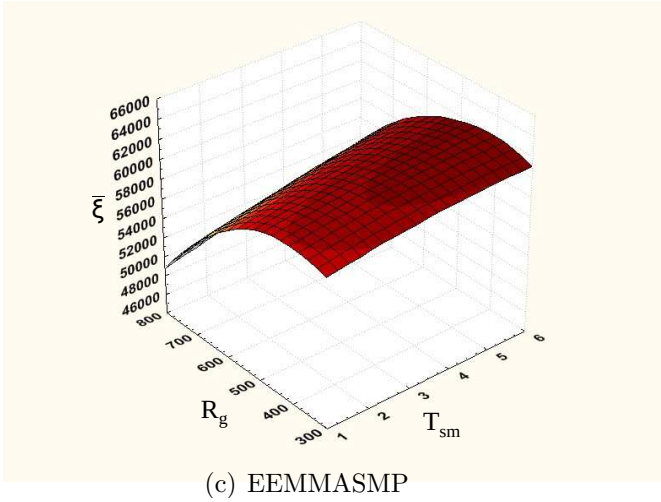

(c) EEMMASMP

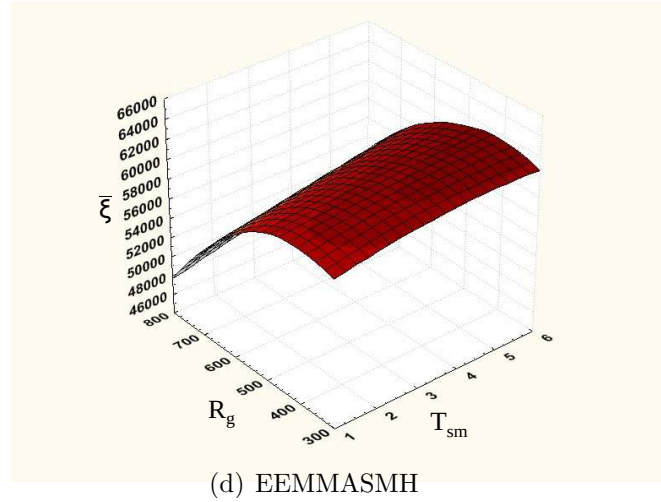

(d) EEMMASMH

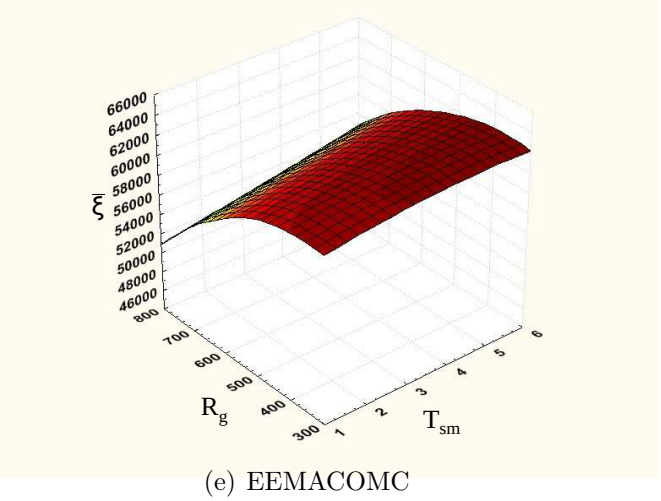

(e) EEMACOMC

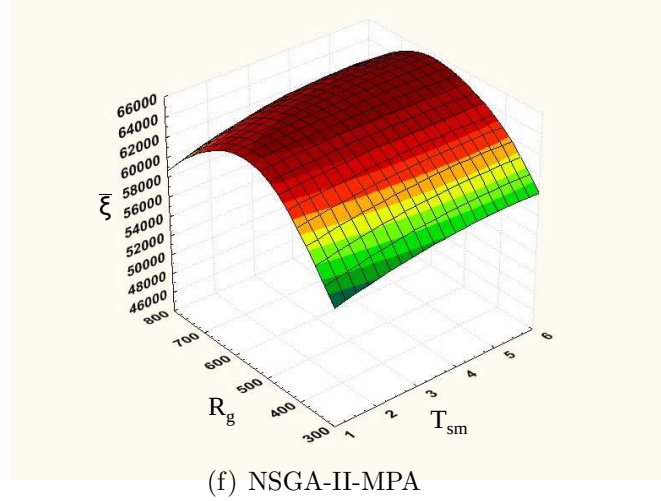

(f) NSGA-II-MPA

Figure G.9: Influence of R_g and T_{sm} on the $\bar{\xi}$ metric for $N_G = 300$

Appendix H

Results of the Mann-Whitney U Test

This appendix contains the results of the Mann-Whitney U test for each pair of algorithms to be compared. Results are visualised using the FluxViz graphs. Each graph contains 4 axis. The first axis represents the change frequency, T_{sm}, the second axis represents the change severity, R_g, and the third axis represents the number of nodes, N_G. The last axis represents the results of the Mann-Whitney U test one for each of the T_{sm}, R_g and N_G combinations. Each combination corresponds to a specific scenario. If the result of the Mann-Whitney U test for each scenario has the value of zero then there is no significant difference between the two algorithms to be compared. The symbol "$\approx$" is displayed next to the value of zero. If the result of the Mann-Whitney U test has the value of one then the first algorithm is significantly better than the second algorithm for the specific scenario. The symbol "$>$" is displayed next to the value of one.

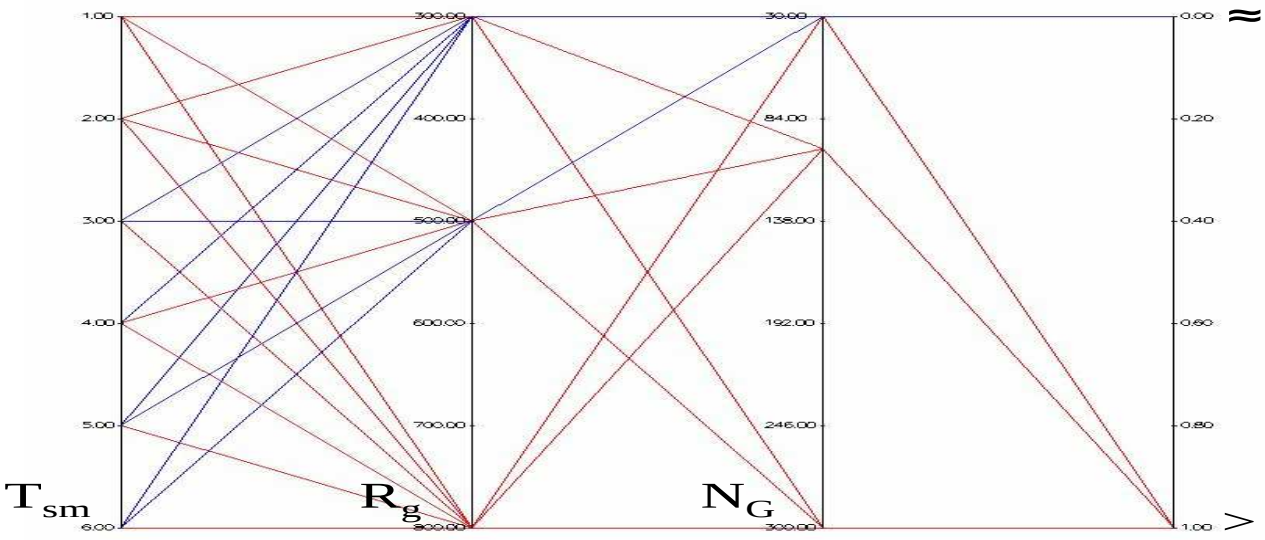

Figure H.1: Comparing the EEMACOMP against the EEMACOMH algorithm with regard to the $\bar{n}_{alg}$ metric using the Mann-Whitney U test

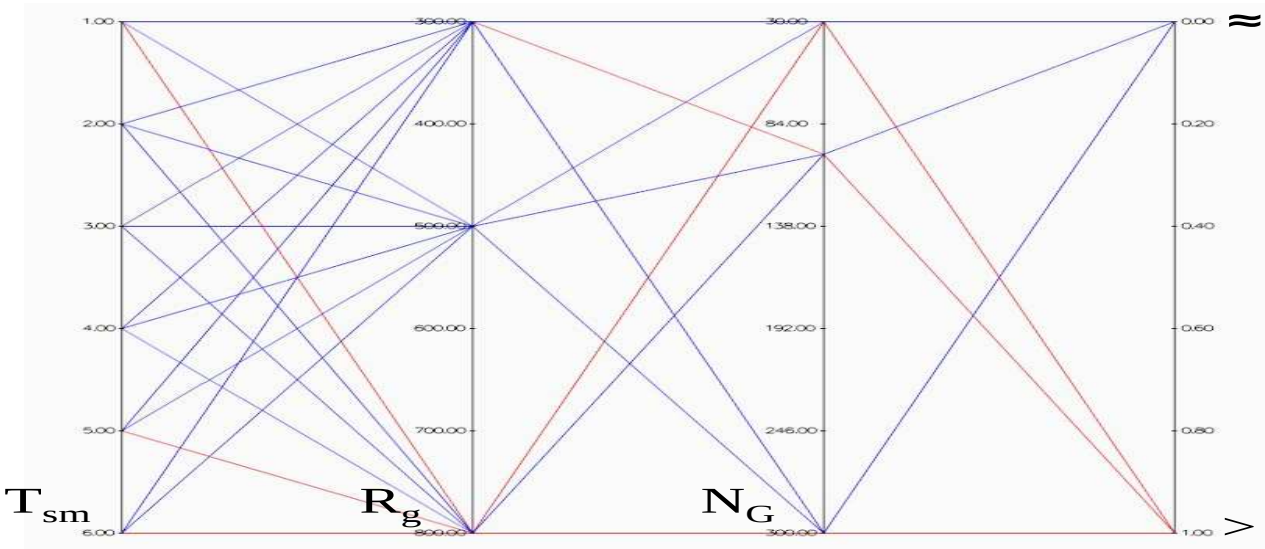

Figure H.2: Comparing the EEMMASMP against the EEMMASMH algorithm with regard to the $\bar{n}_{alg}$ metric using the Mann-Whitney U test

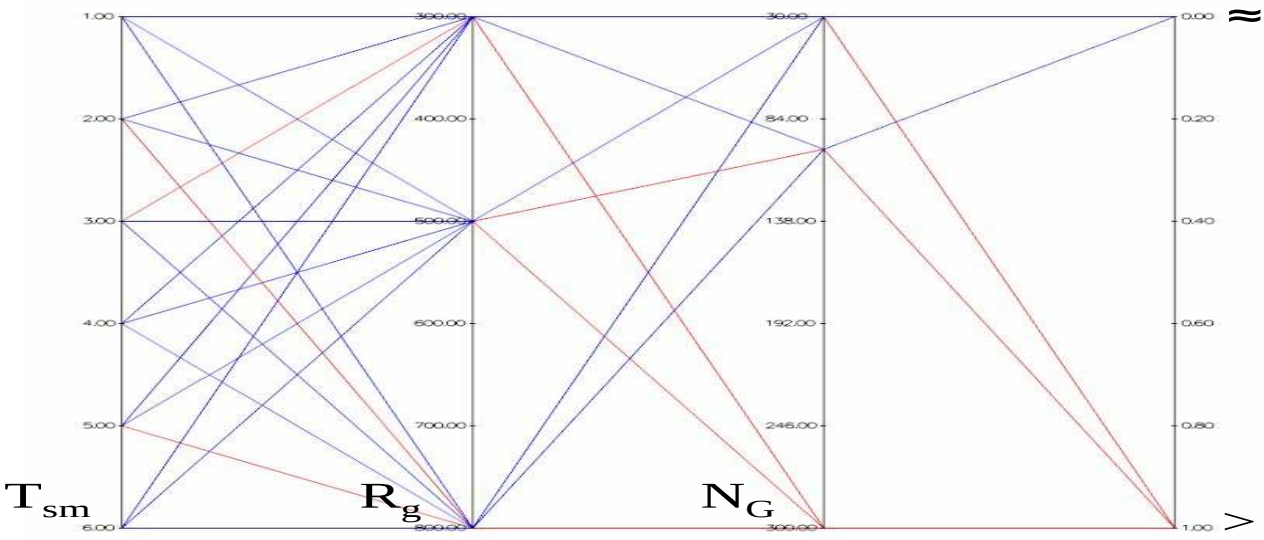

Figure H.3: Comparing the EEMACOMP against the EEMACOMC algorithm with regard to the $\bar{n}_{alg}$ metric using the Mann-Whitney U test

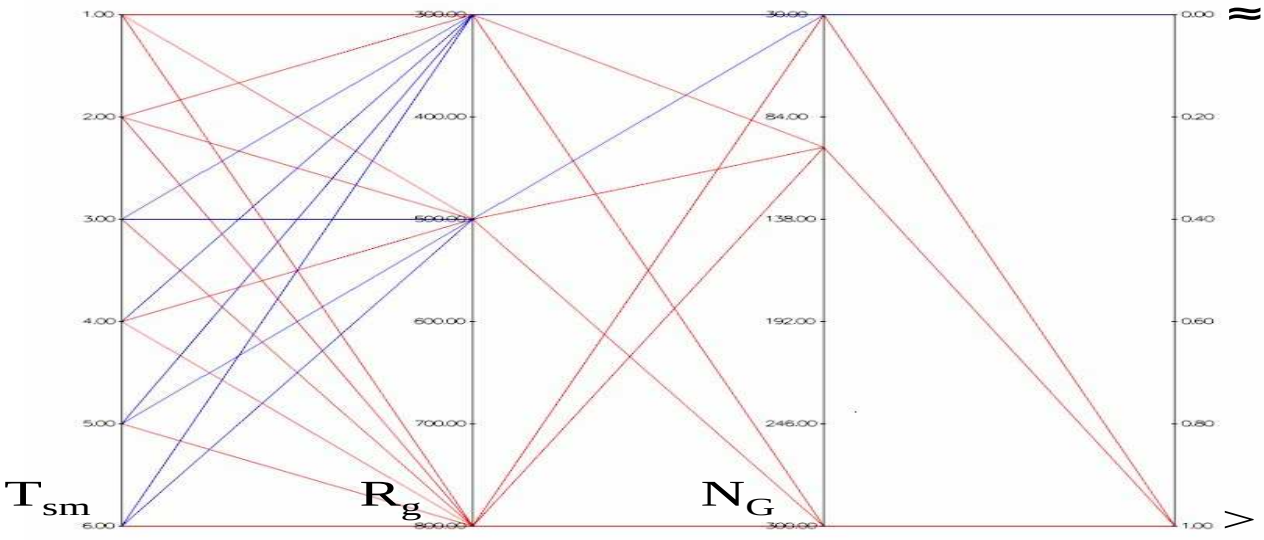

Figure H.4: Comparing the EEMACOMC against the EEMACOMH algorithm with regard to the $\bar{n}_{alg}$ metric using the Mann-Whitney U test

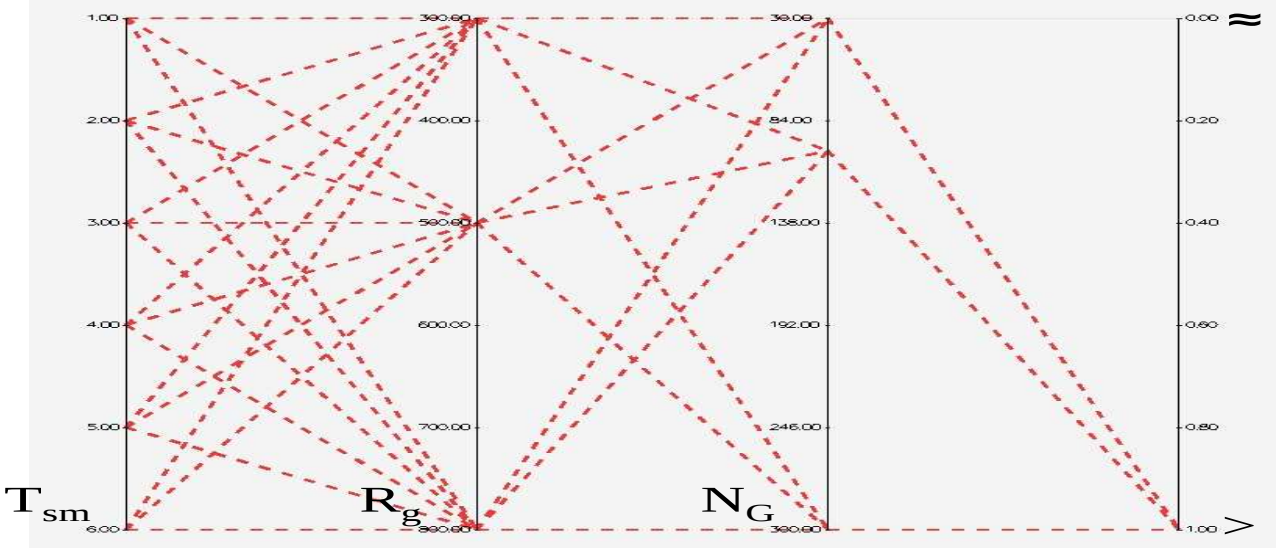

Figure H.5: Comparing the EEMACOMP against the NSGA-II-MPA algorithm with regard to the $\bar{n}_{alg}$ metric using the Mann-Whitney U test

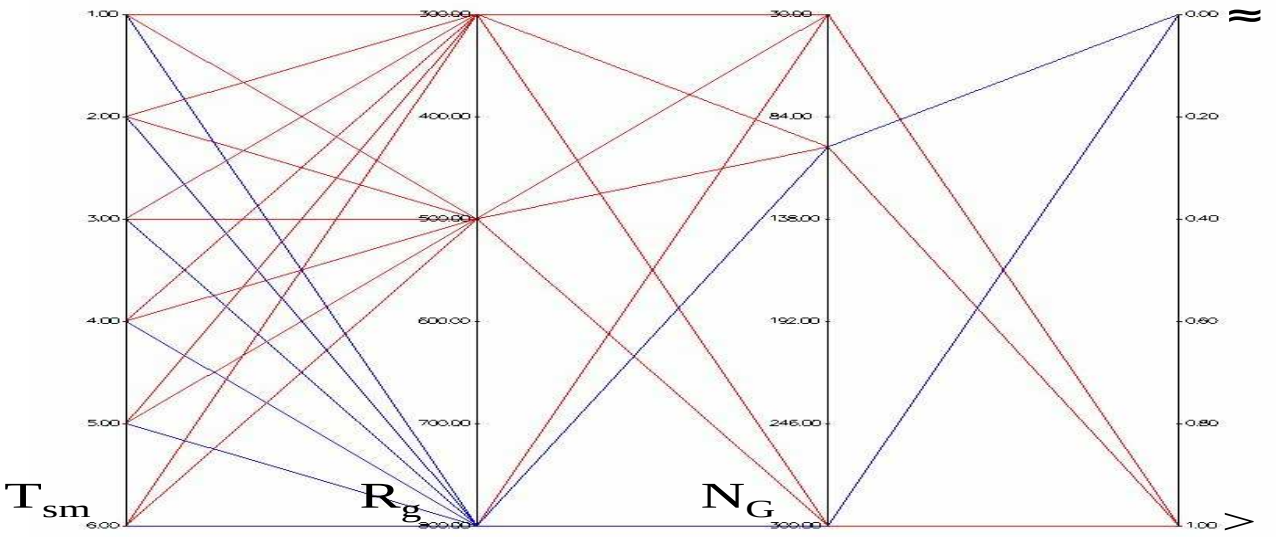

Figure H.6: Comparing the EEMACOMH against the NSGA-II-MPA algorithm with regard to the $\bar{n}_{alg}$ metric using the Mann-Whitney U test

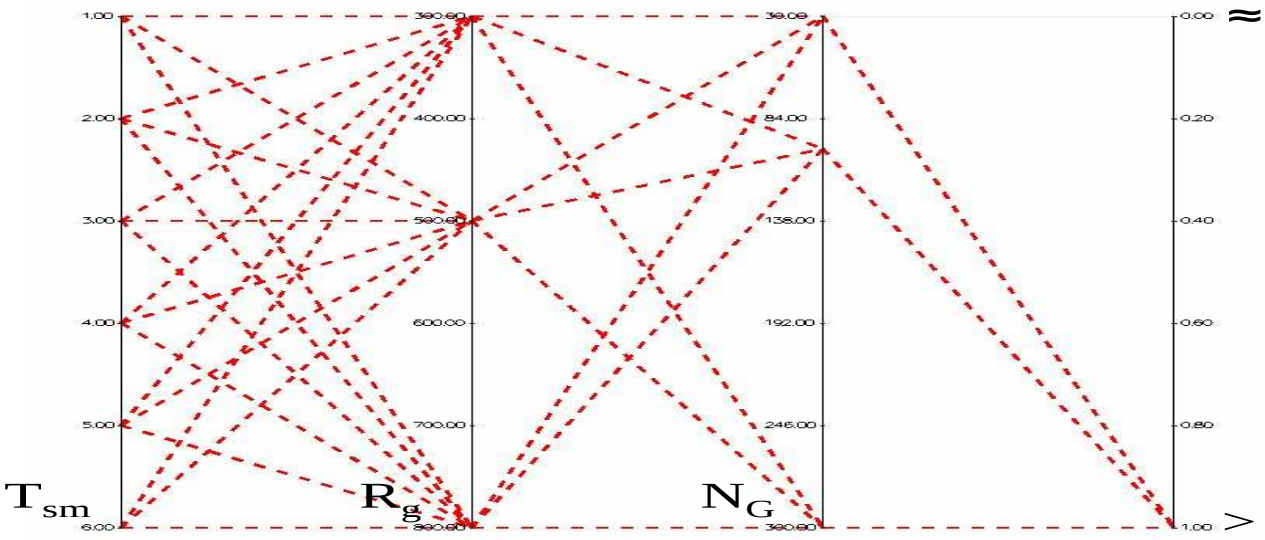

Figure H.7: Comparing the EEMMASMP against the NSGA-II-MPA algorithm with regard to the $\bar{n}_{alg}$ metric using the Mann-Whitney U test

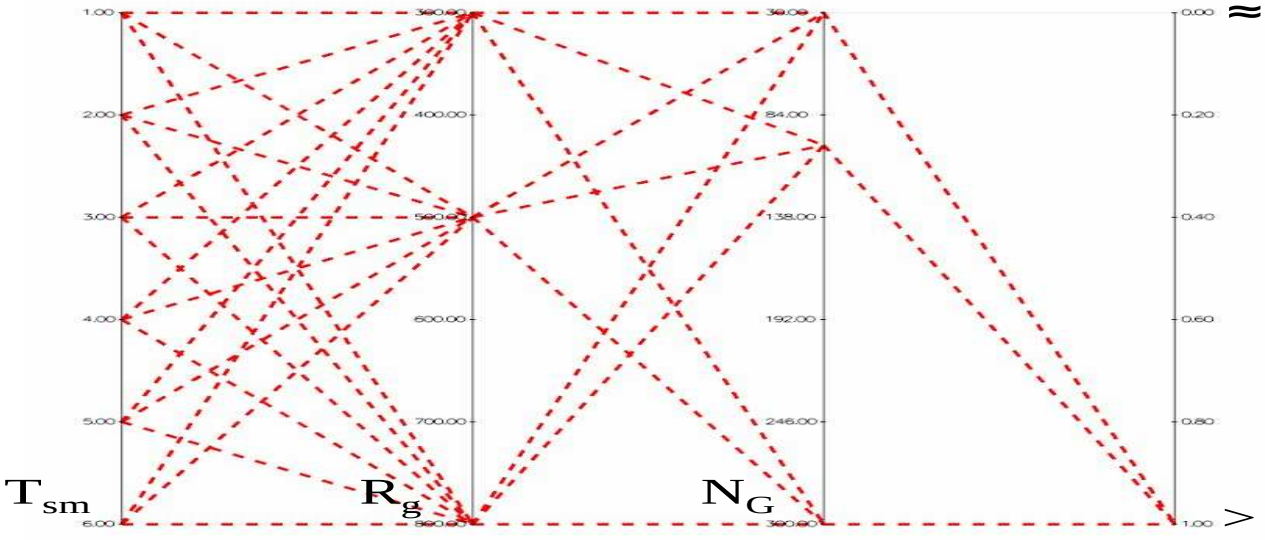

Figure H.8: Comparing the EEMMASMH against the NSGA-II-MPA algorithm with regard to the $\bar{n}_{alg}$ metric using the Mann-Whitney U test

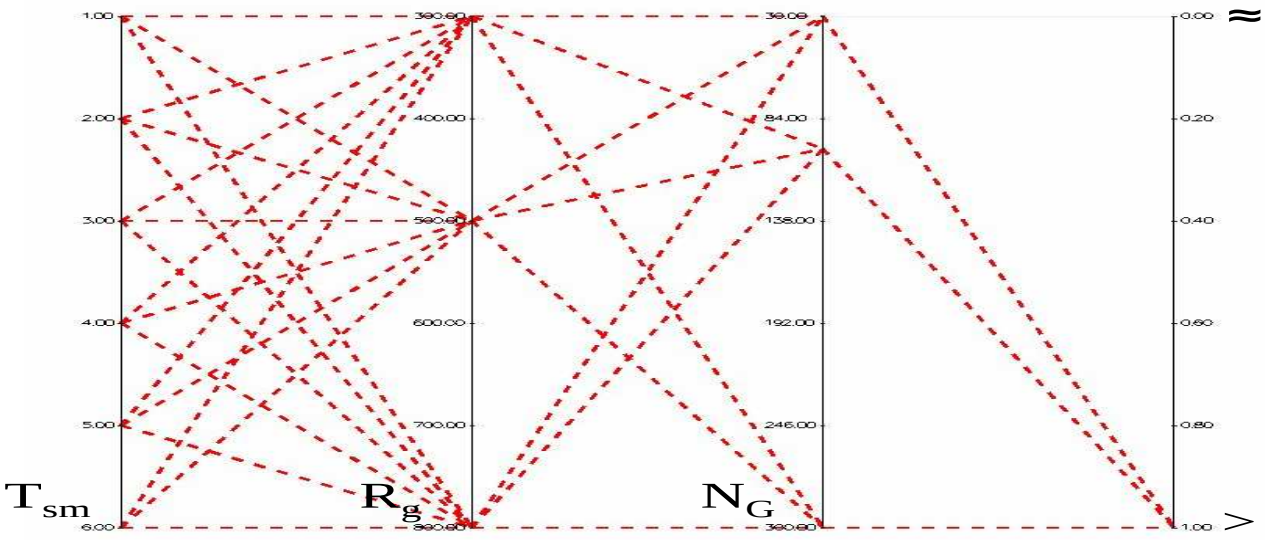

Figure H.9: Comparing the EEMACOMC against the NSGA-II-MPA algorithm with regard to the $\bar{n}_{alg}$ metric using the Mann-Whitney U test

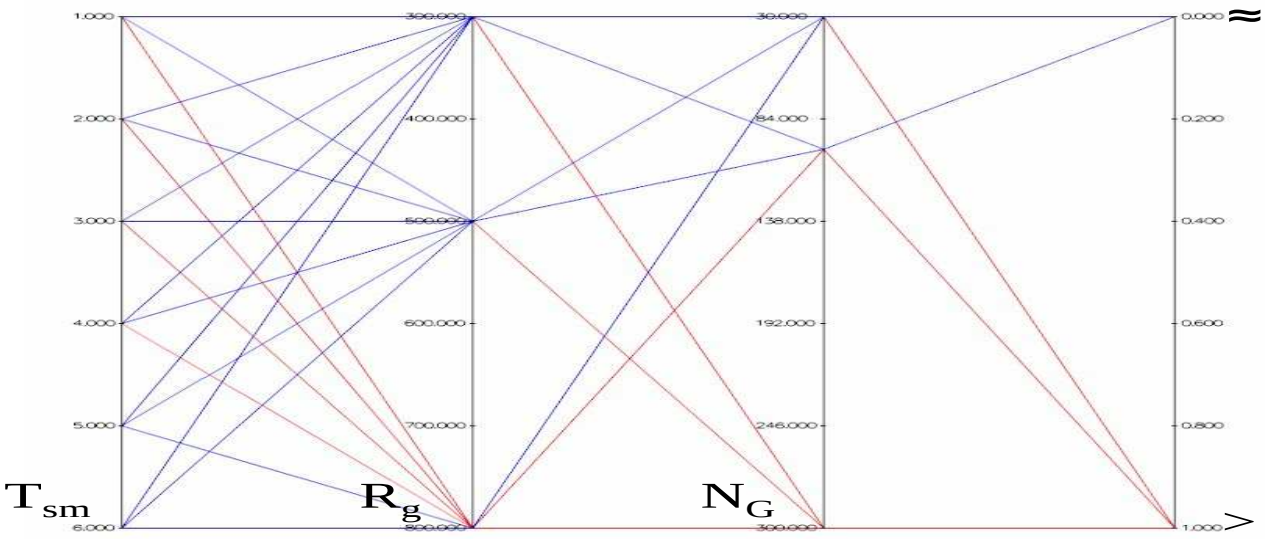

Figure H.10: Comparing the EEMACOMP against the EEMMASMP algorithm with regard to the $\bar{n}_{alg}$ metric using the Mann-Whitney U test

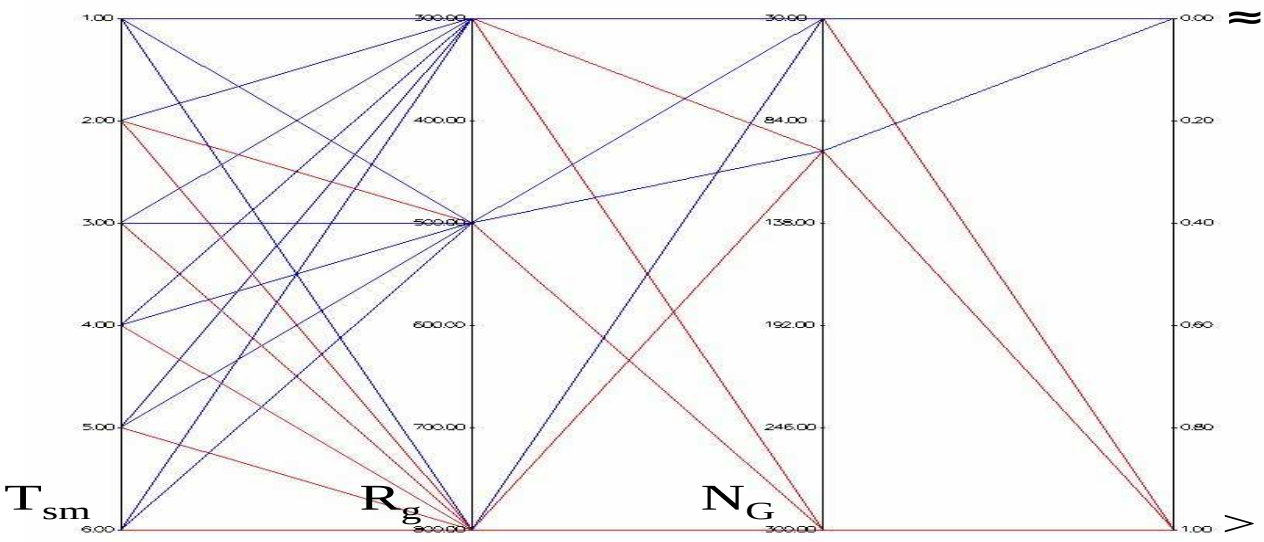

Figure H.11: Comparing the EEMACOMP against the EEMMASMH algorithm with regard to the $\bar{n}_{alg}$ metric using the Mann-Whitney U test

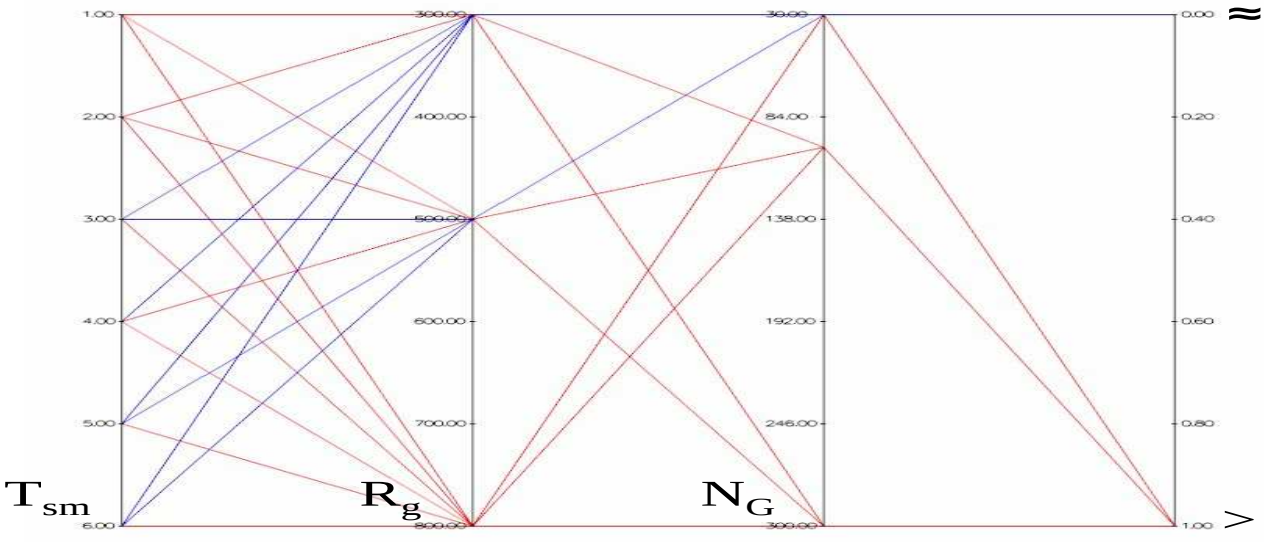

Figure H.12: Comparing the EEMMASMH against the EEMACOMH algorithm with regard to the $\bar{n}_{alg}$ metric using the Mann-Whitney U test

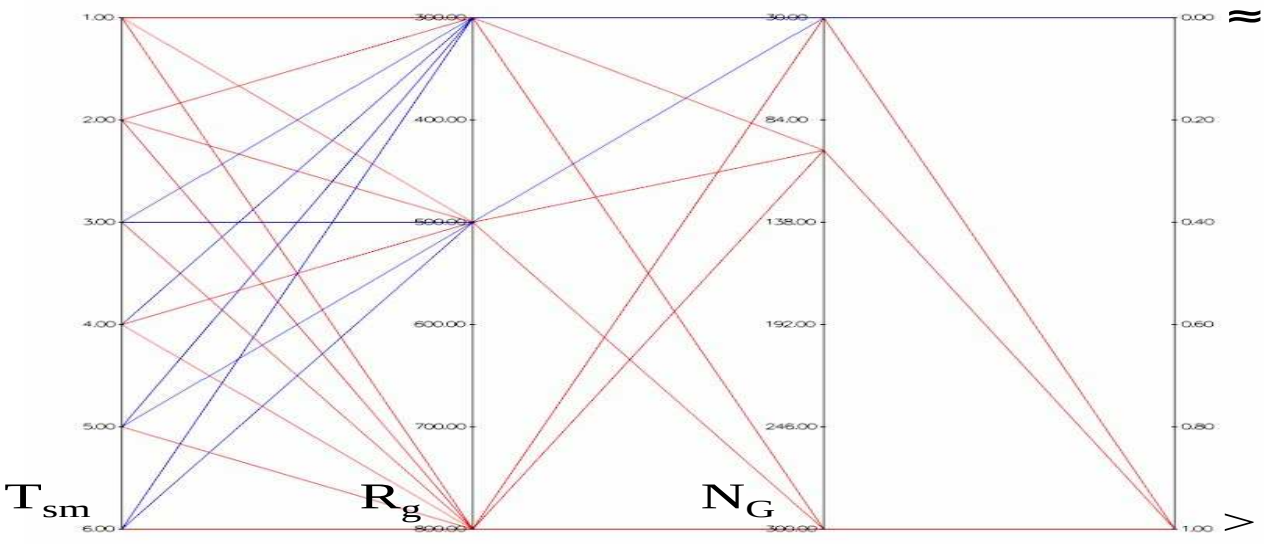

Figure H.13: Comparing the EEMMASMP against the EEMACOMH algorithm with regard to the $\bar{n}_{alg}$ metric using the Mann-Whitney U test

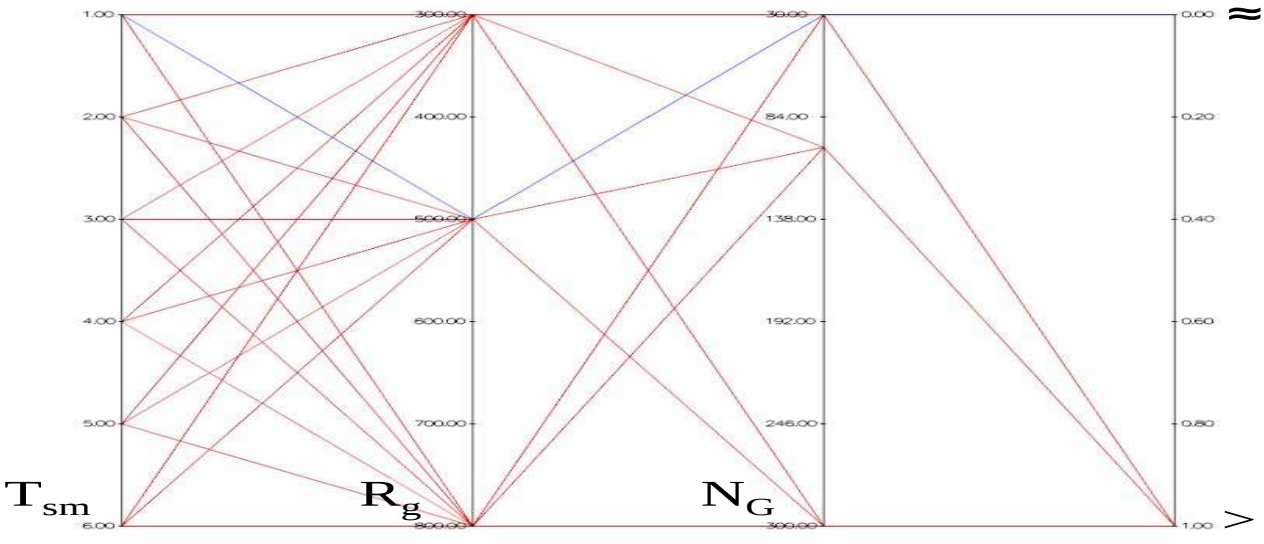

Figure H.14: Comparing the EEMACOMP against the EEMACOMH algorithm with regard to the $\bar{\varrho}$ metric using the Mann-Whitney U test

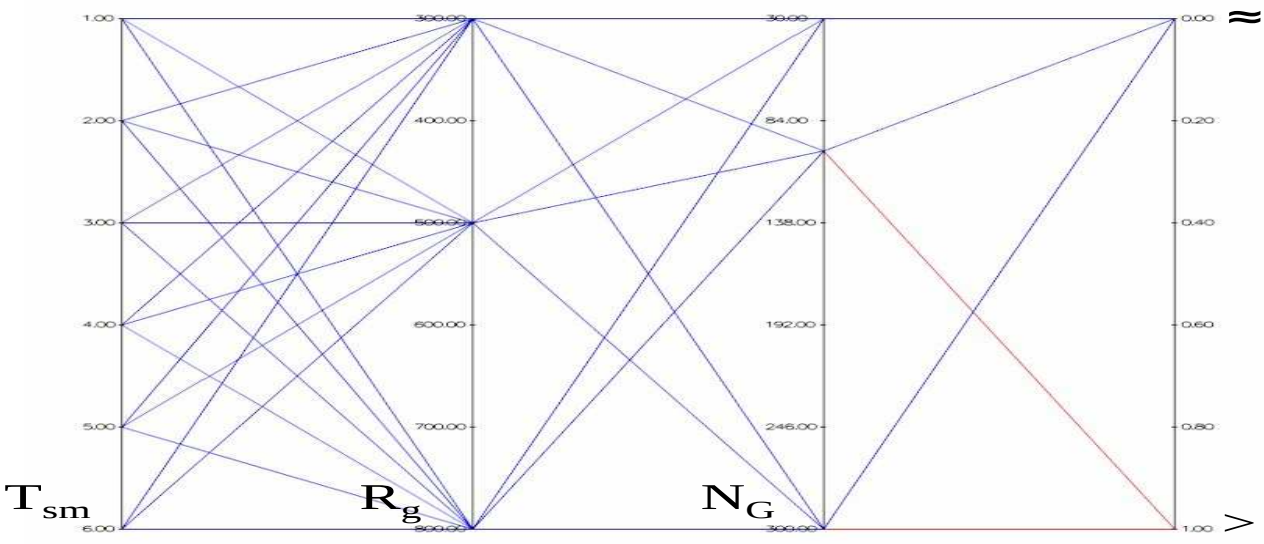

Figure H.15: Comparing the EEMMASMP against the EEMMASMH algorithm with regard to the $\bar{\varrho}$ metric using the Mann-Whitney U test

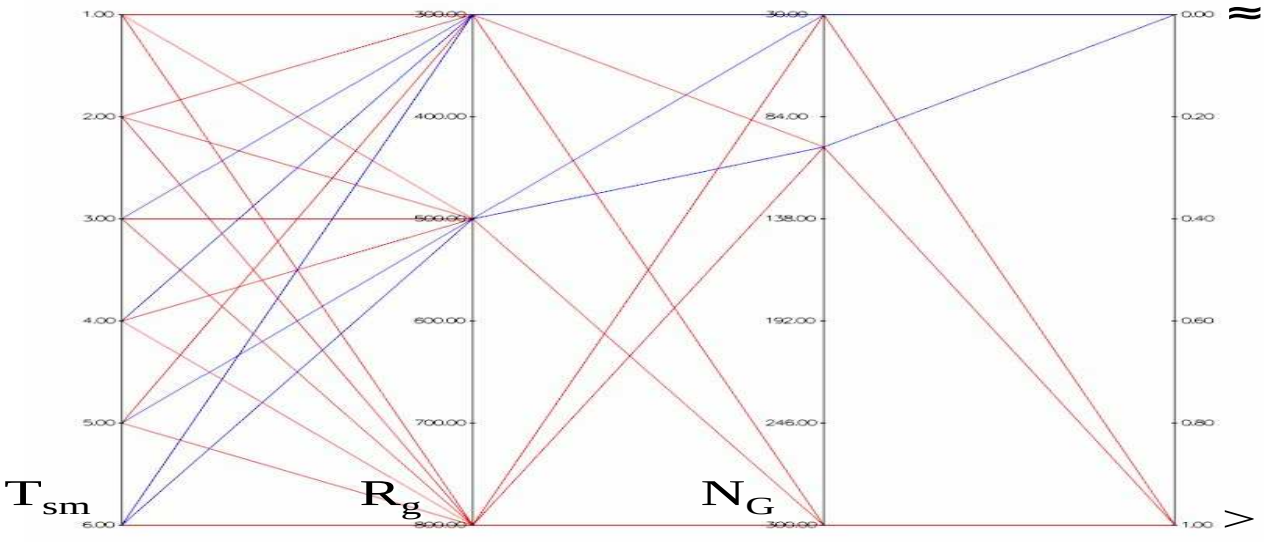

Figure H.16: Comparing the EEMACOMP against the EEMACOMC algorithm with regard to the $\bar{\varrho}$ metric using the Mann-Whitney U test

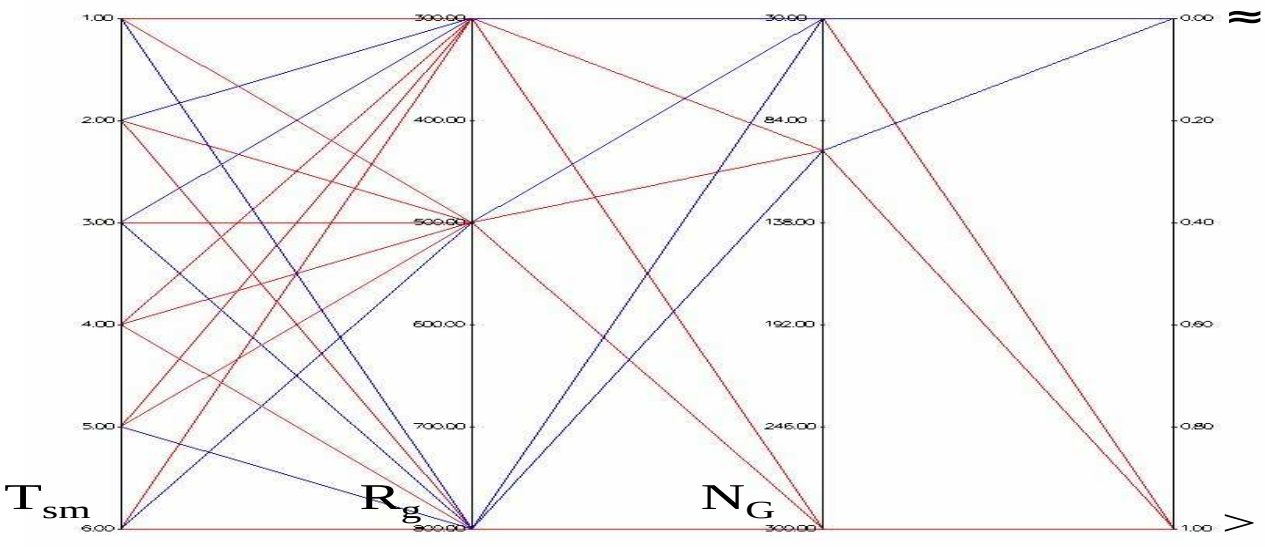

Figure H.17: Comparing the EEMACOMC against the EEMACOMH algorithm with regard to the $\bar{\varrho}$ metric using the Mann-Whitney U test

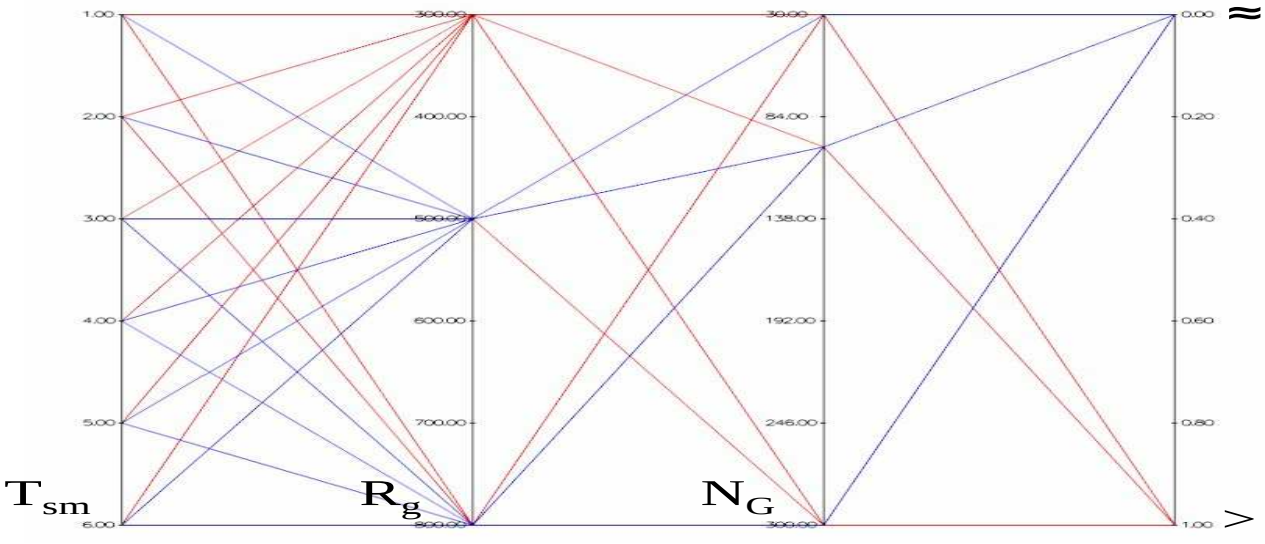

Figure H.18: Comparing the EEMACOMP against the NSGA-II-MPA algorithm with regard to the $\bar{\varrho}$ metric using the Mann-Whitney U test

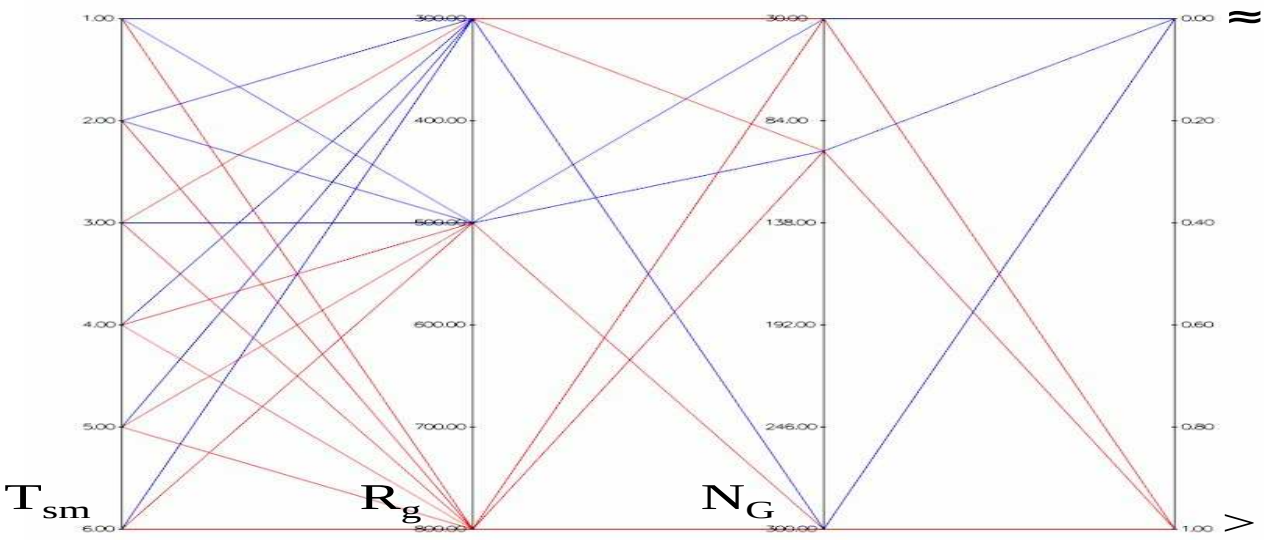

Figure H.19: Comparing the EEMACOMH against the NSGA-II-MPA algorithm with regard to the $\bar{\varrho}$ metric using the Mann-Whitney U test

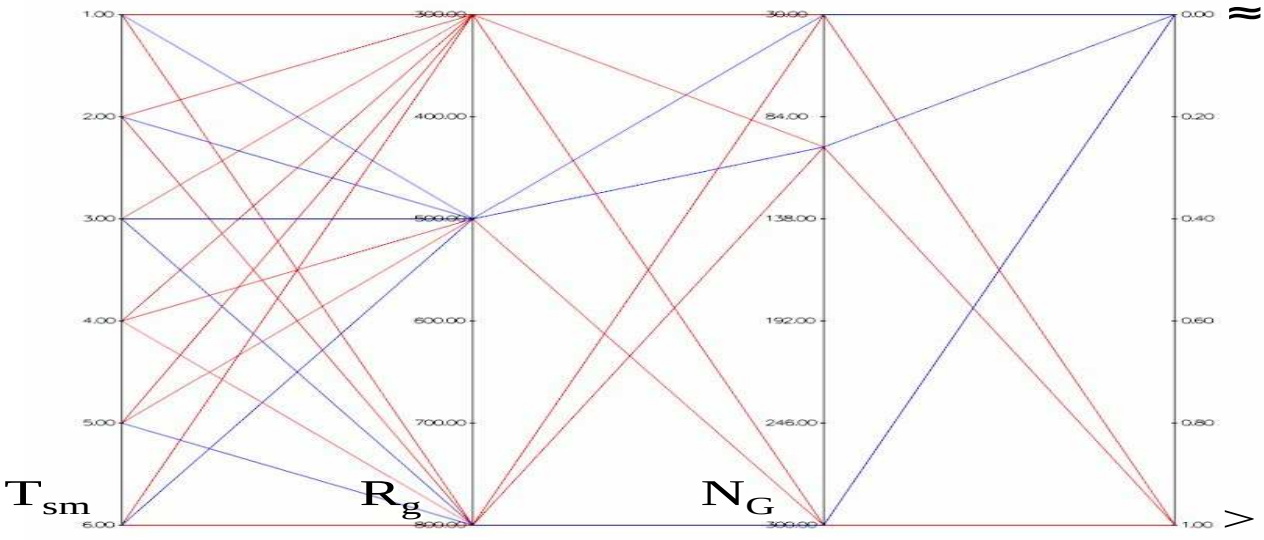

Figure H.20: Comparing the EEMMASMP against the NSGA-II-MPA algorithm with regard to the $\bar{\varrho}$ metric using the Mann-Whitney U test

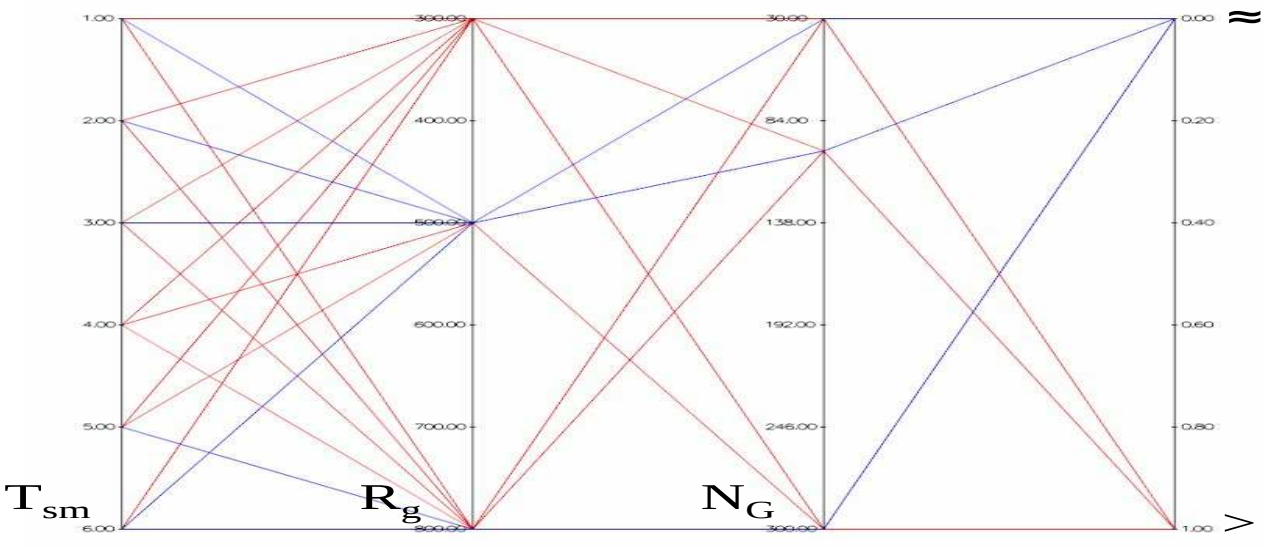

Figure H.21: Comparing the EEMMASMH against the NSGA-II-MPA algorithm with regard to the $\bar{\varrho}$ metric using the Mann-Whitney U test

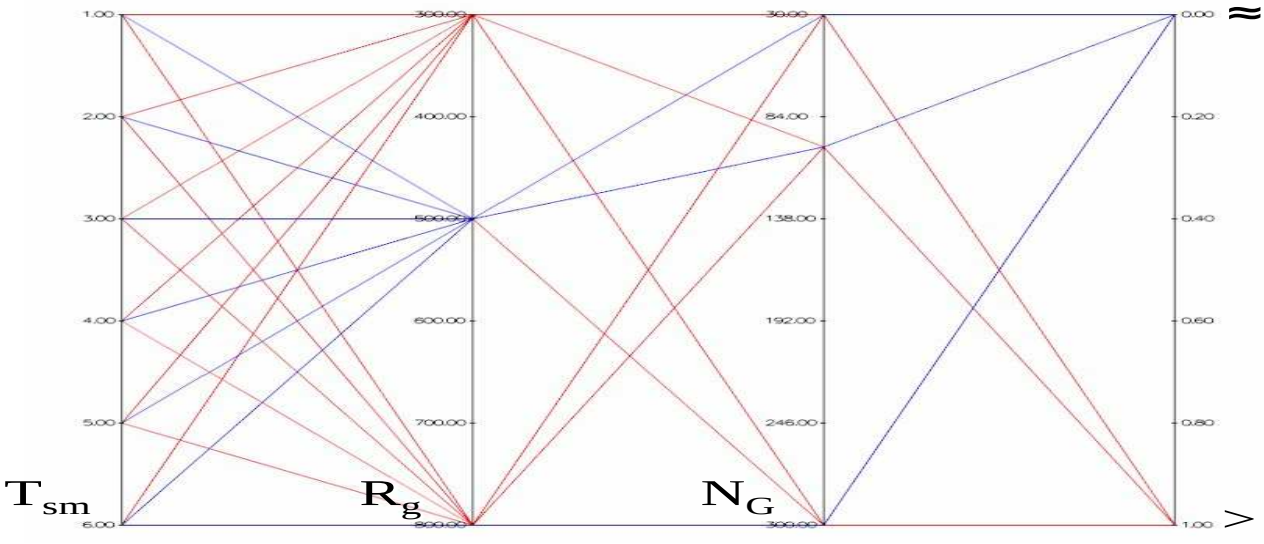

Figure H.22: Comparing the EEMACOMC against the NSGA-II-MPA algorithm with regard to the $\bar{\varrho}$ metric using the Mann-Whitney U test

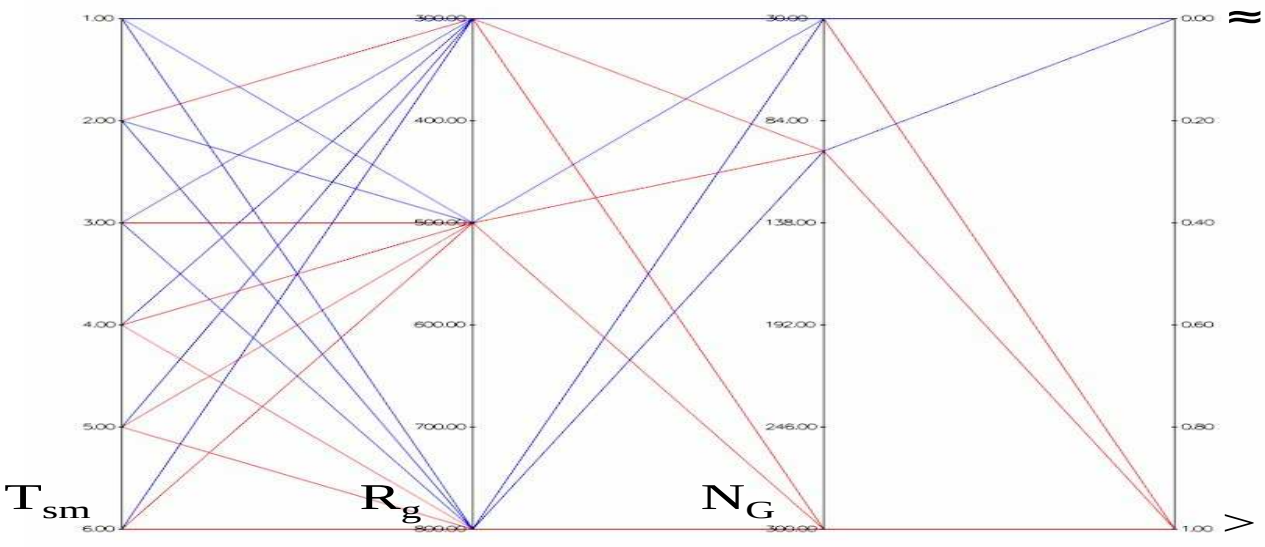

Figure H.23: Comparing the EEMACOMP against the EEMMASMP algorithm with regard to the $\bar{\varrho}$ metric using the Mann-Whitney U test

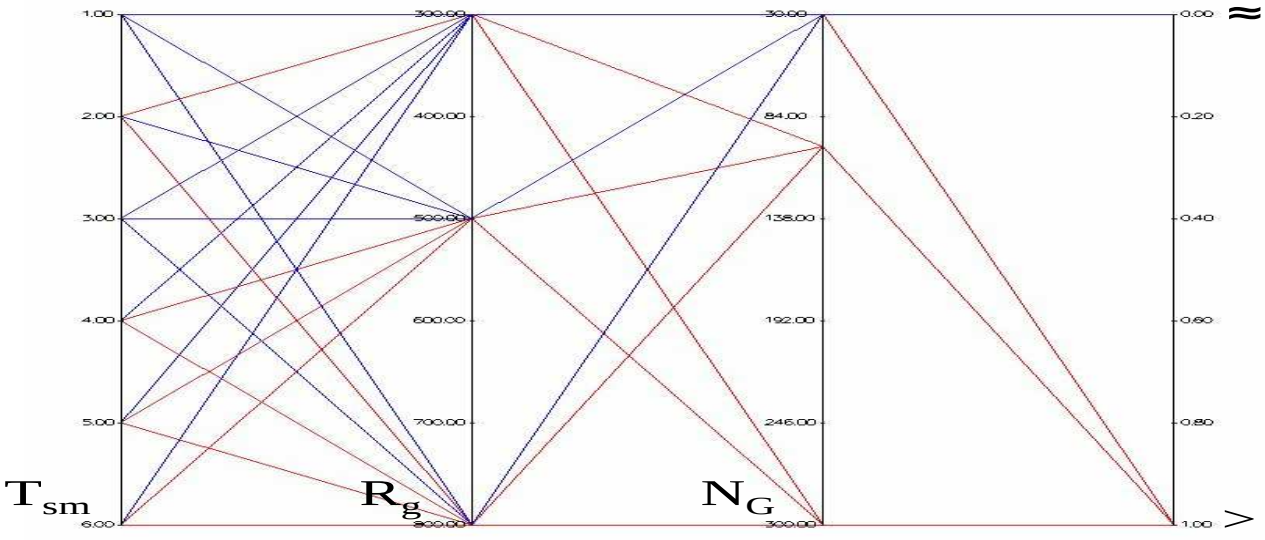

Figure H.24: Comparing the EEMACOMP against the EEMMASMH algorithm with regard to the $\bar{\varrho}$ metric using the Mann-Whitney U test

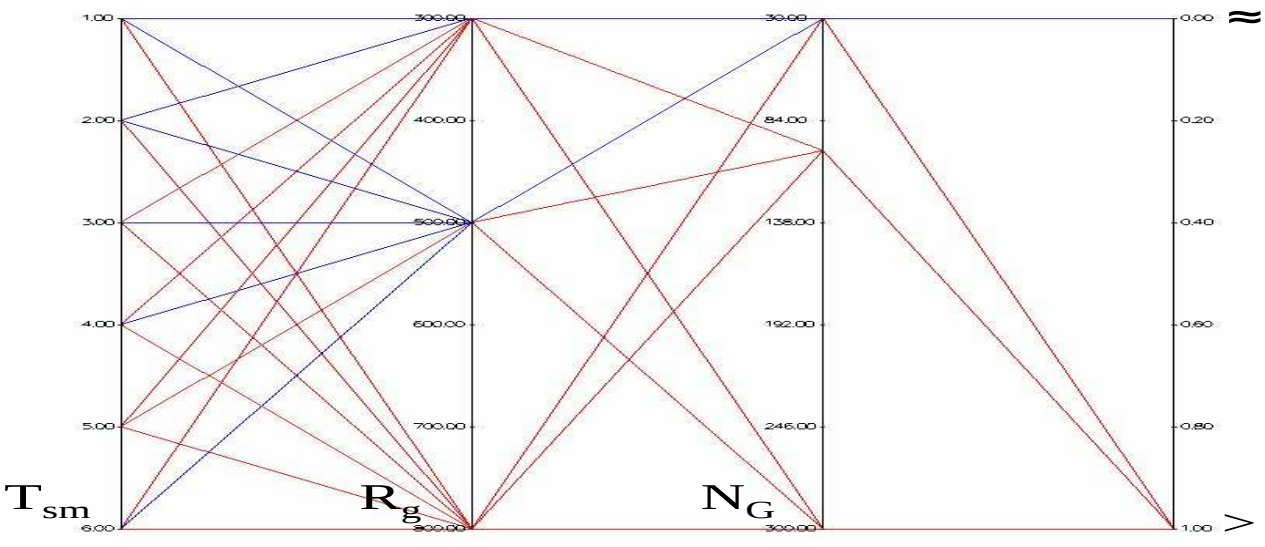

Figure H.25: Comparing the EEMMASMP against the EEMACOMH algorithm with regard to the $\bar{\varrho}$ metric using the Mann-Whitney U test

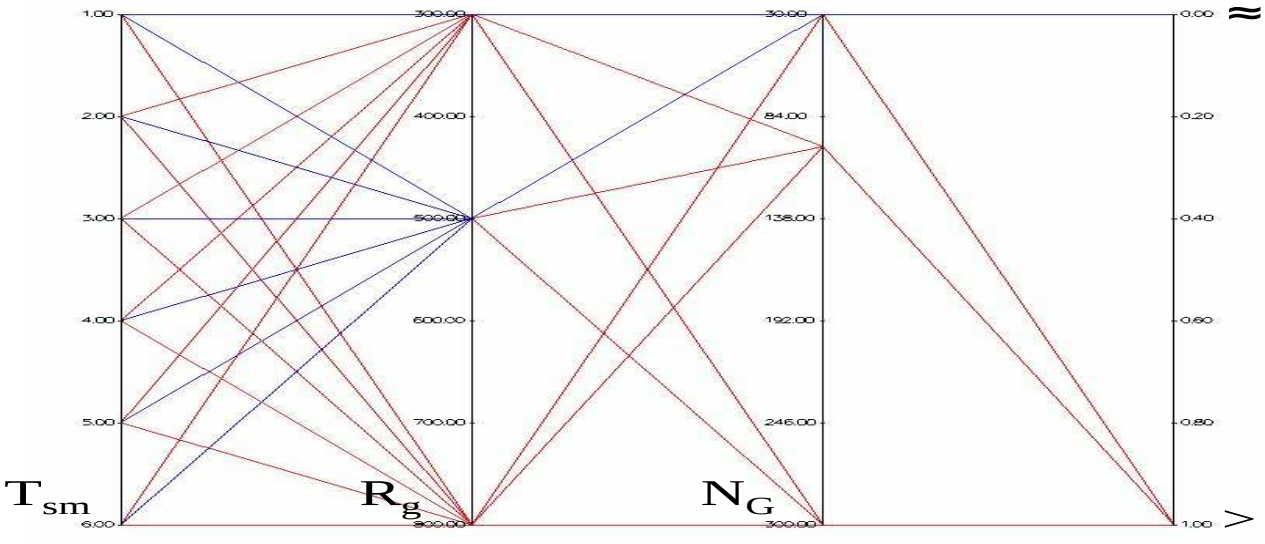

Figure H.26: Comparing the EEMMASMH against the EEMACOMH algorithm with regard to the $\bar{\varrho}$ metric using the Mann-Whitney U test

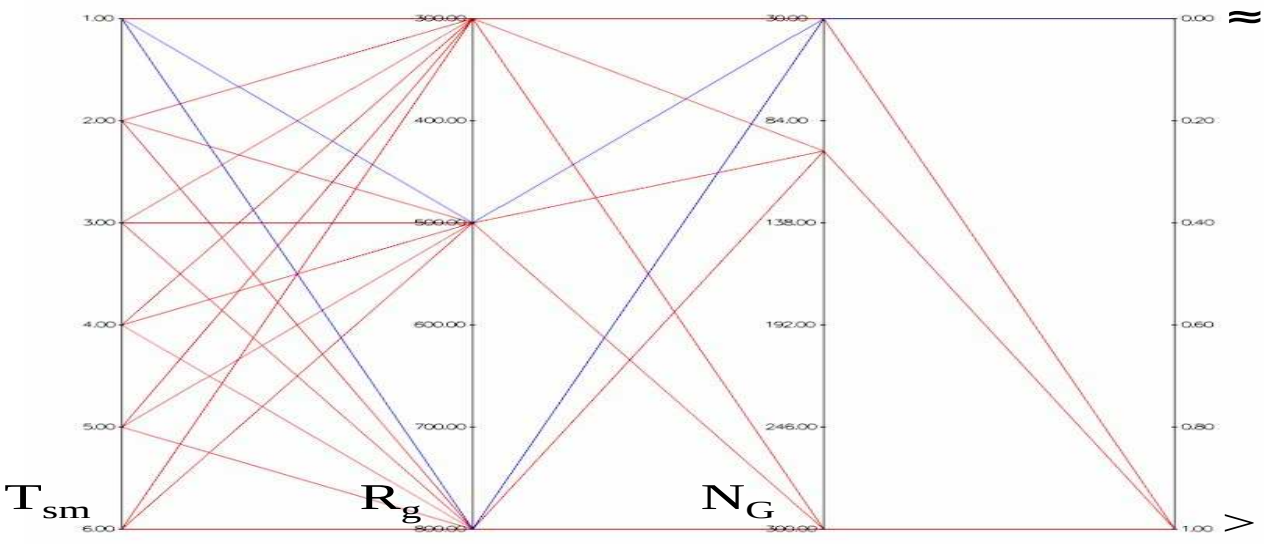

Figure H.27: Comparing the EEMACOMP against the EEMACOMH algorithm with regard to the $\bar{\xi}$ metric using the Mann-Whitney U test

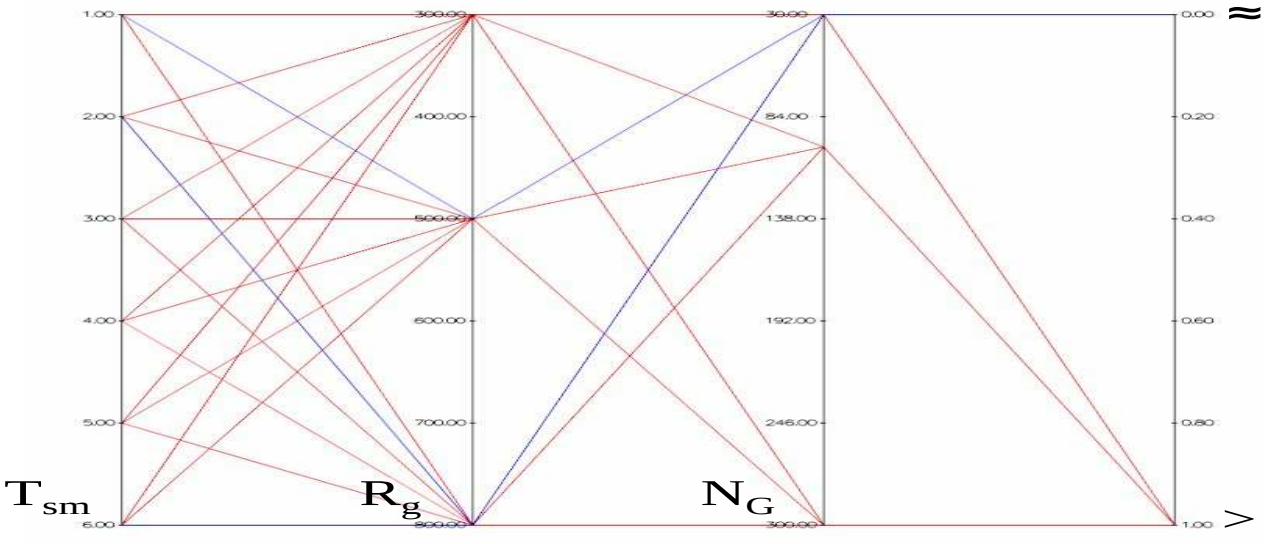

Figure H.28: Comparing the EEMACOMC against the EEMACOMH algorithm with regard to the $\bar{\xi}$ metric using the Mann-Whitney U test

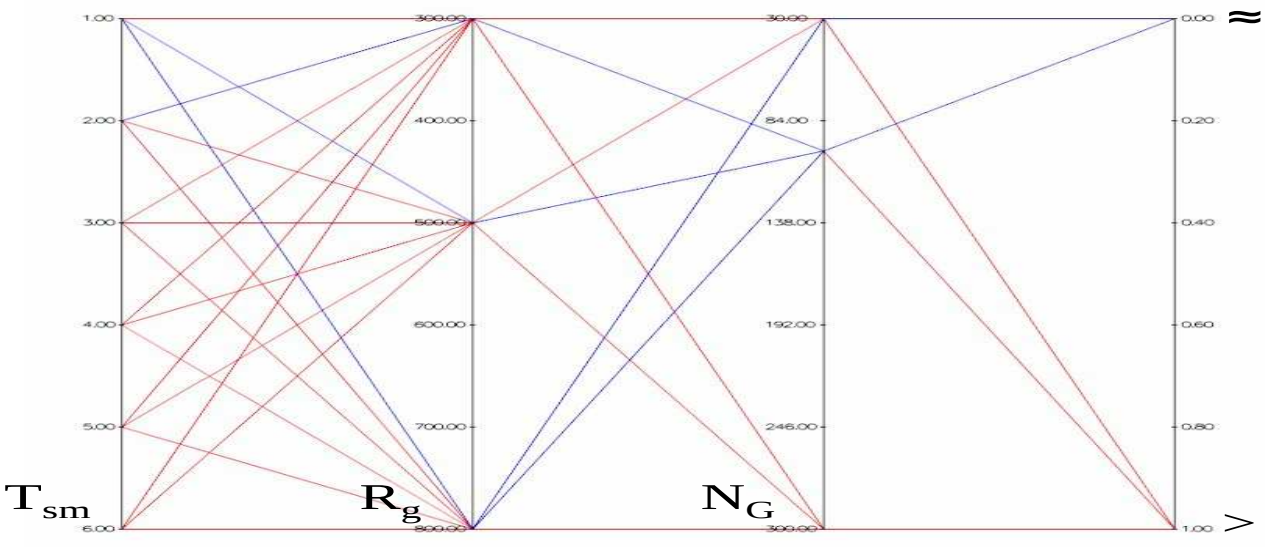

Figure H.29: Comparing the EEMACOMP against the NSGA-II-MPA algorithm with regard to the $\bar{\xi}$ metric using the Mann-Whitney U test

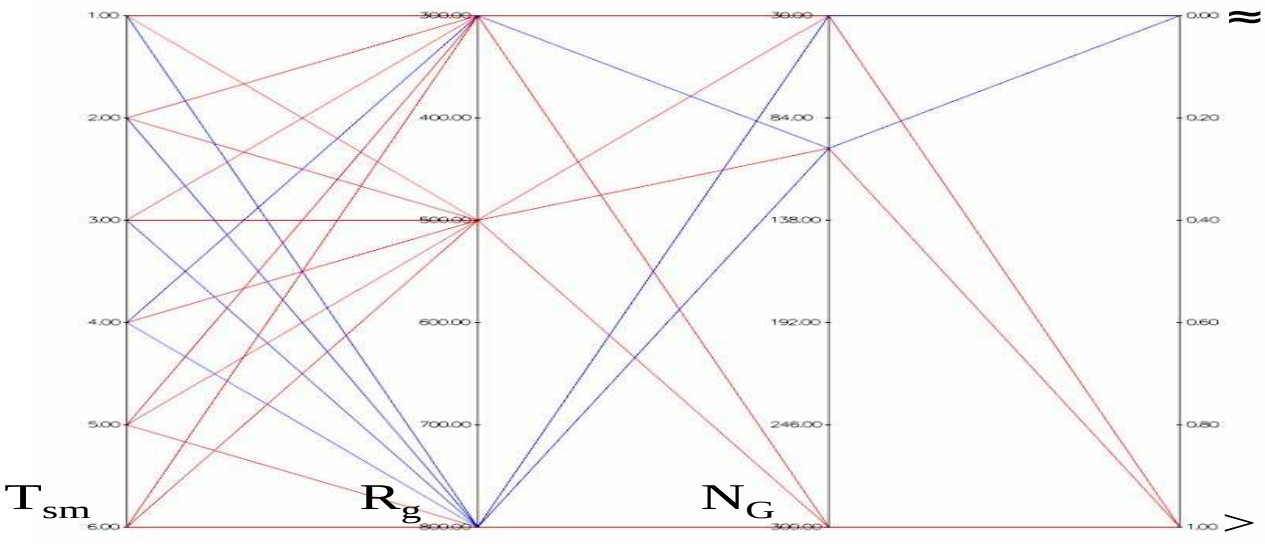

Figure H.30: Comparing the EEMACOMH against the NSGA-II-MPA algorithm with regard to the $\bar{\xi}$ metric using the Mann-Whitney U test

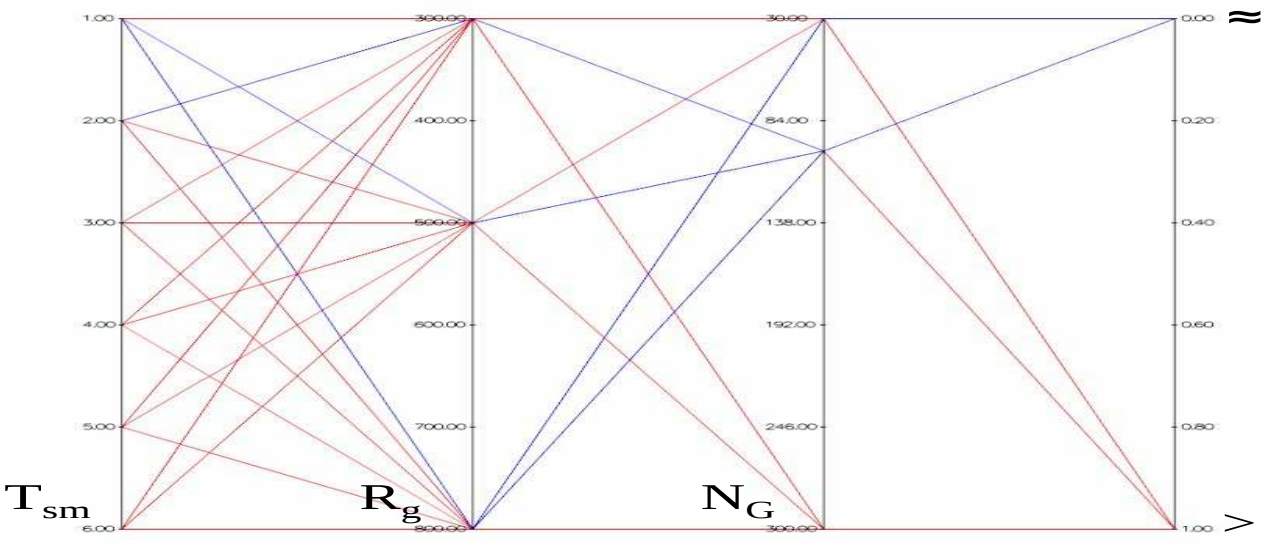

Figure H.31: Comparing the EEMMASMP against the NSGA-II-MPA algorithm with regard to the $\bar{\xi}$ metric using the Mann-Whitney U test

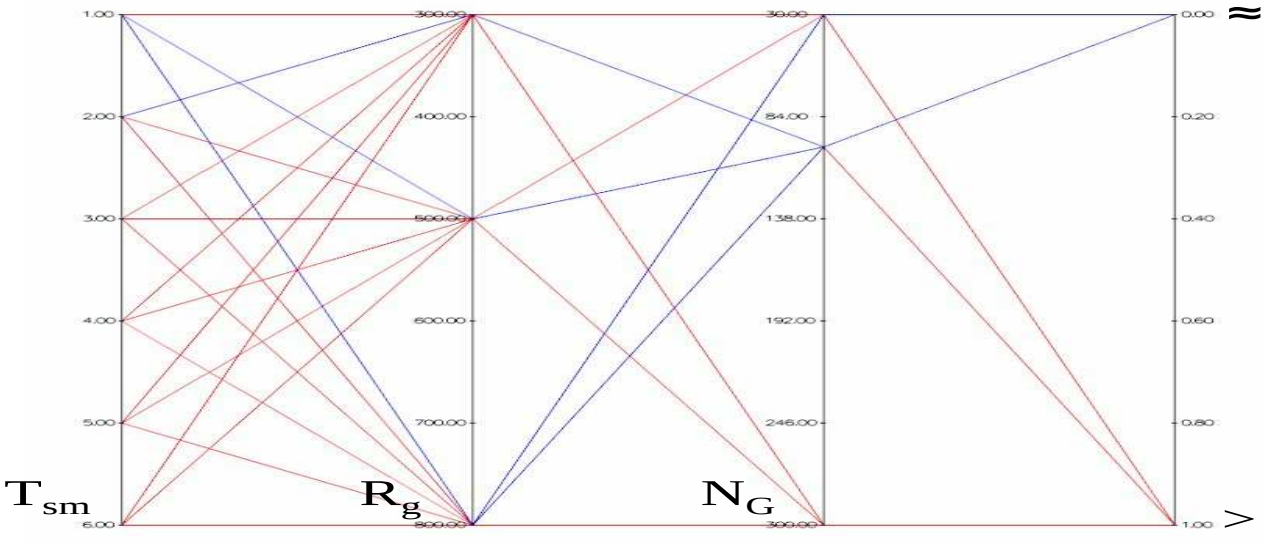

Figure H.32: Comparing the EEMMASMH against the NSGA-II-MPA algorithm with regard to the $\bar{\xi}$ metric using the Mann-Whitney U test

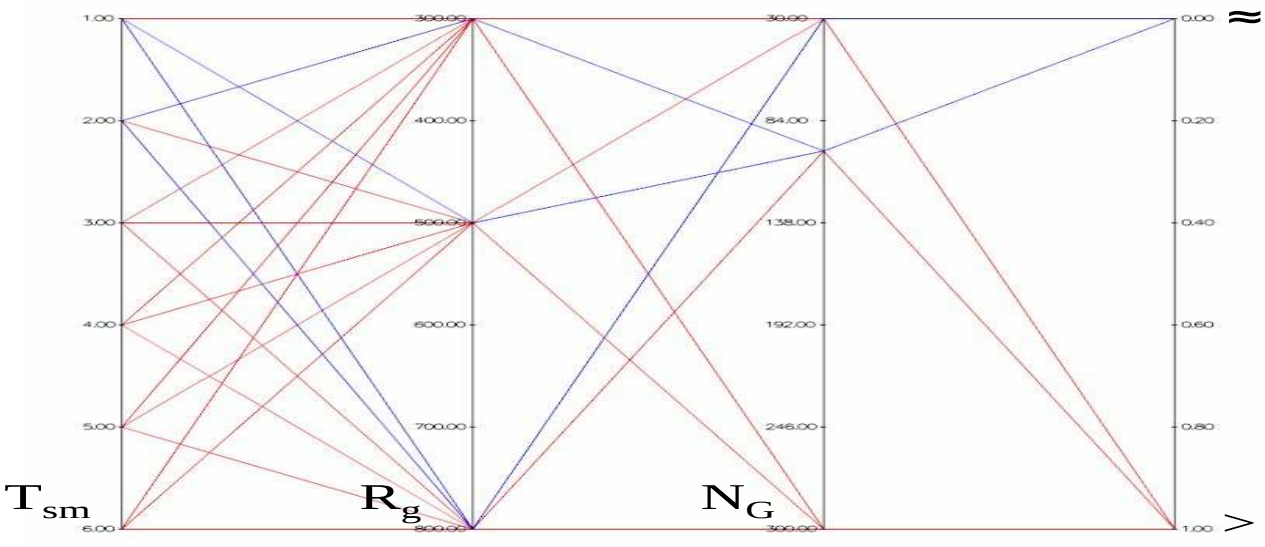

Figure H.33: Comparing the EEMACOMC against the NSGA-II-MPA algorithm with regard to the $\bar{\xi}$ metric using the Mann-Whitney U test

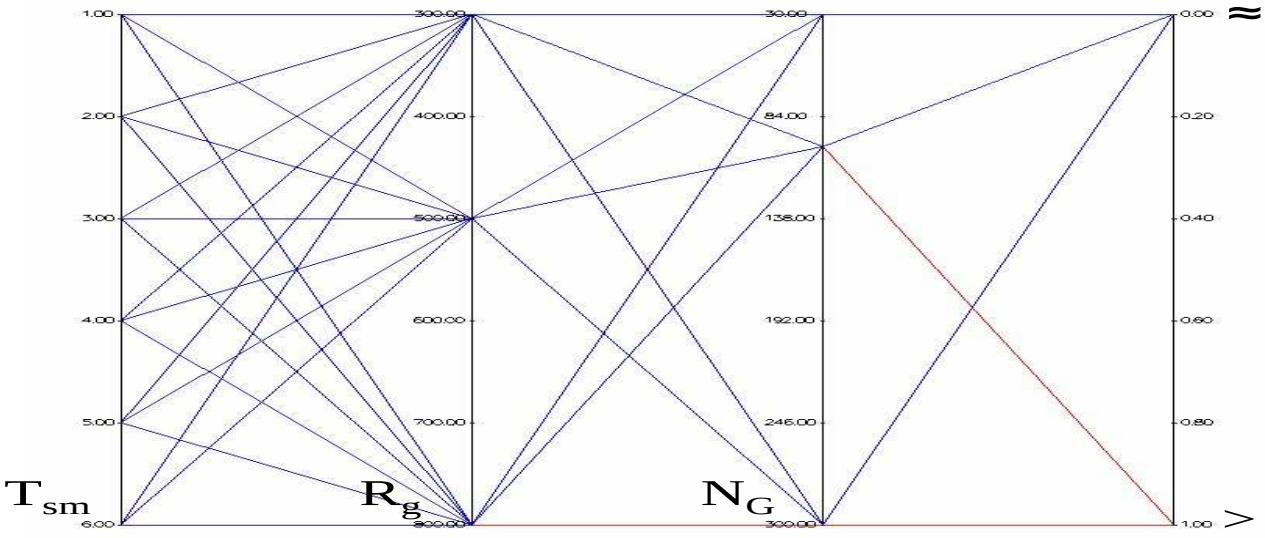

Figure H.34: Comparing the EEMMASMP against the EEMMASMH algorithm with regard to the $\bar{\xi}$ metric using the Mann-Whitney U test

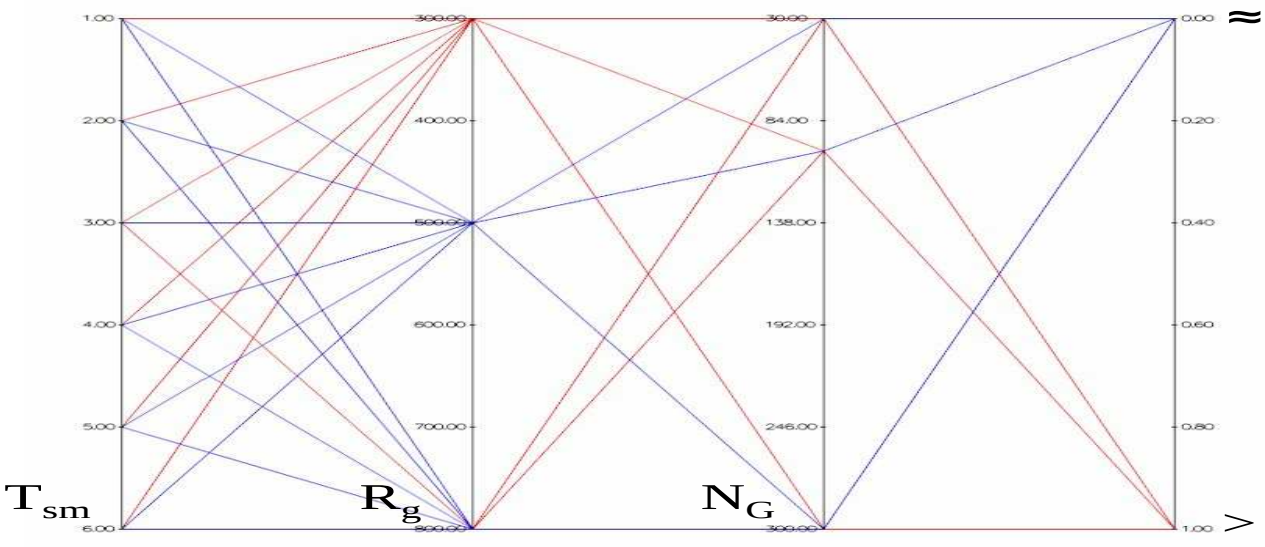

Figure H.35: Comparing the EEMACOMP against the EEMACOMC algorithm with regard to the $\bar{\xi}$ metric using the Mann-Whitney U test

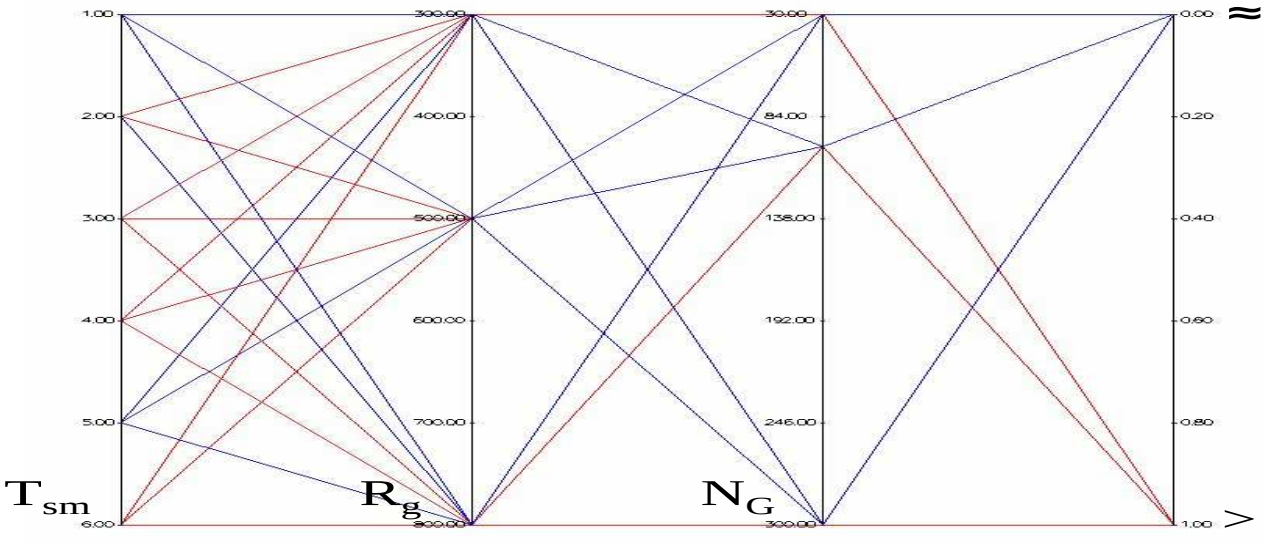

Figure H.36: Comparing the EEMACOMP against the EEMMASMP algorithm with regard to the $\bar{\xi}$ metric using the Mann-Whitney U test

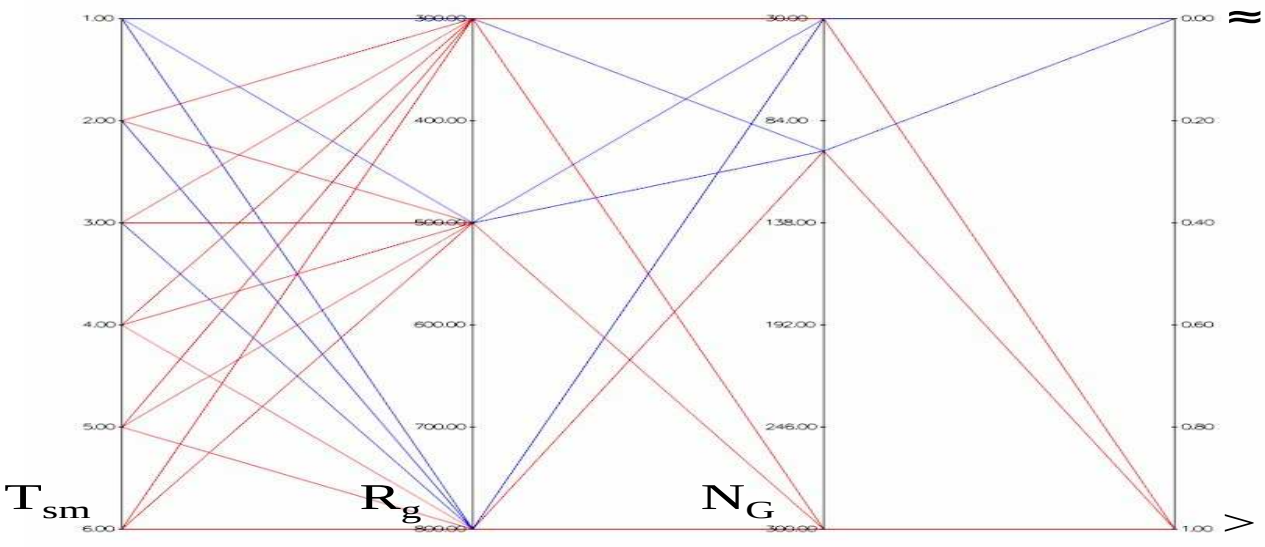

Figure H.37: Comparing the EEMACOMP against the EEMMASMH algorithm with regard to the $\bar{\xi}$ metric using the Mann-Whitney U test

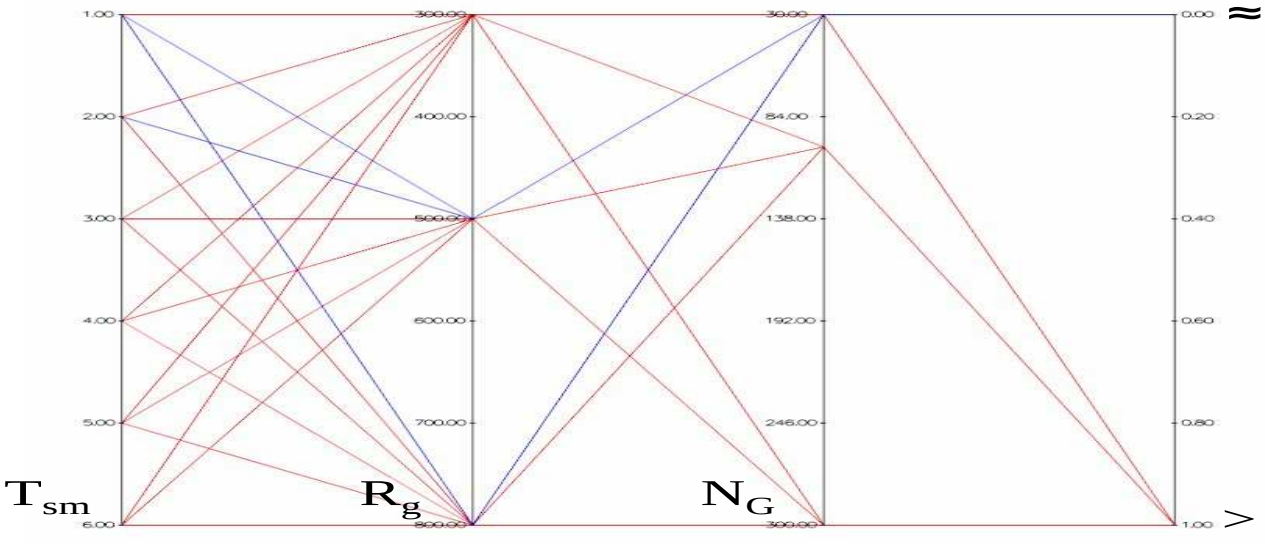

Figure H.38: Comparing the EEMMASMH against the EEMACOMH algorithm with regard to the $\bar{\xi}$ metric using the Mann-Whitney U test

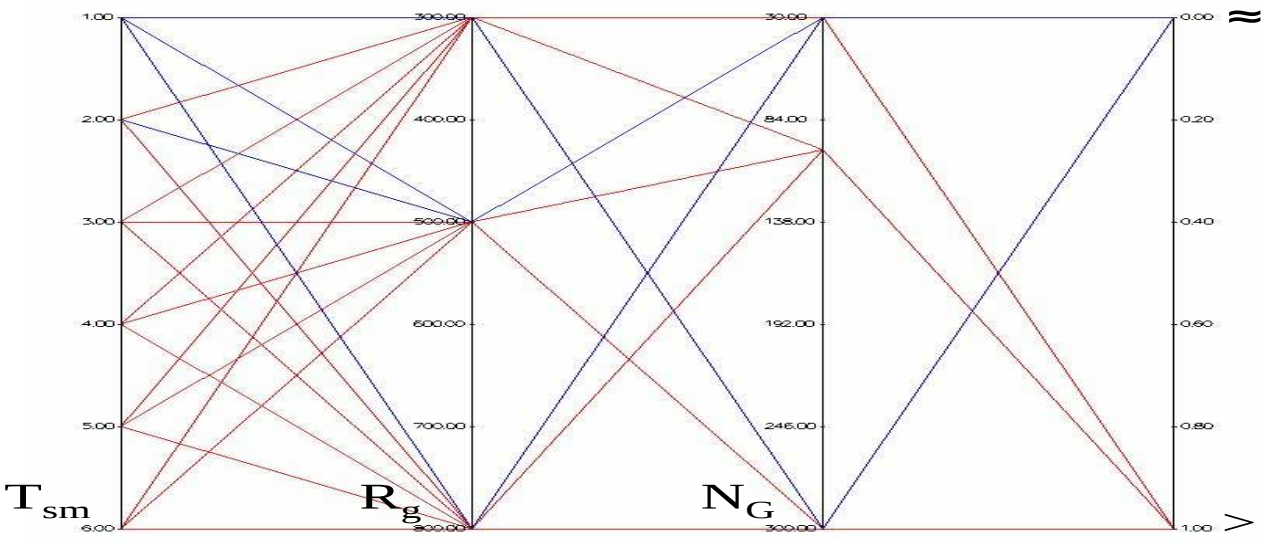

Figure H.39: Comparing the EEMMASMP against the EEMACOMH algorithm with regard to the $\bar{\xi}$ metric using the Mann-Whitney U test

Appendix I

Optimisation Criteria Results

This appendix summarises the values of each objective function for each algorithm EEMACOMP, EEMACOMH, EEMMASMP, EEMMASMH, EEMACOMC, and NSGA-II-MPA and for each scenario.

Table I.1: EP objective: $N_G = 30$, $R_g = 300$

$\mathcal{PF}$	T_{sm}					
	1	2	3	4	5	6
$P_{EEMACOMP}$	2.99±0.19	3.04±0.19	3.05±0.16	3.06±0.16	3.10±0.15	3.07±0.14
$P_{EEMACOMH}$	2.68±0.12	2.71±0.12	2.71±0.11	2.70±0.11	2.74±0.11	2.70±0.10
$P_{EEMMASMP}$	2.76±0.13	2.79±0.13	2.79±0.11	2.80±0.12	2.82±0.11	2.80±0.10
$P_{EEMMASMH}$	2.79±0.13	2.81±0.13	2.80±0.12	2.81±0.12	2.84±0.11	2.82±0.11
$P_{EEMACOMC}$	4.16±0.27	4.01±0.23	3.95±0.17	3.94±0.13	3.94±0.15	3.90±0.12
$P_{NSGA-II-MPA}$	1.84±0.12	1.78±0.09	1.73±0.07	1.72±0.07	1.72±0.06	1.71±0.06

Table I.2: EP objective: $N_G = 30$, $R_g = 500$

$\mathcal{PF}$	T_{sm}					
	1	2	3	4	5	6
$P_{EEMACOMP}$	4.11±0.42	4.00±0.27	4.03±0.24	3.71±0.25	4.10±0.25	3.90±0.20
$P_{EEMACOMH}$	3.71±0.34	3.58±0.22	3.58±0.21	3.24±0.17	3.60±0.21	3.46±0.15
$P_{EEMMASMP}$	3.64±0.33	3.57±0.19	3.56±0.18	3.36±0.19	3.59±0.18	3.59±0.17
$P_{EEMMASMH}$	3.66±0.33	3.59±0.22	3.58±0.19	3.39±0.19	3.60±0.18	3.63±0.19
$P_{EEMACOMC}$	5.76±0.46	5.50±0.34	5.49±0.36	5.48±0.36	5.38±0.33	5.30±0.36
$P_{NSGA-II-MPA}$	1.93±0.18	1.82±0.11	1.79±0.09	1.78±0.09	1.76±0.07	1.74±0.06

Table I.3: EP objective: $N_G = 30$, $R_g = 800$

$\mathcal{PF}$	T_{sm}					
	1	2	3	4	5	6
$P_{EEMACOMP}$	5.79±0.66	6.01±0.45	6.34±0.37	6.05±0.35	6.21±0.43	6.42±0.37
$P_{EEMACOMH}$	5.41±0.39	5.29±0.44	5.47±0.29	5.27±0.29	5.39±0.26	5.56±0.26
$P_{EEMMASMP}$	5.64±0.41	5.56±0.31	5.78±0.30	5.55±0.26	5.60±0.29	5.79±0.28
$P_{EEMMASMH}$	5.50±0.40	5.50±0.31	5.81±0.30	5.55±0.30	5.57±0.30	5.85±0.29
$P_{EEMACOMC}$	8.63±0.77	8.60±0.75	8.67±0.66	8.62±0.66	8.67±0.65	8.57±0.59
$P_{NSGA-II-MPA}$	2.95±0.32	2.91±0.24	2.82±0.18	2.80±0.14	2.79±0.13	2.79±0.13

Table I.4: EP objective: $N_G = 100$, $R_g = 300$

$\mathcal{PF}$	T_{sm}					
	1	2	3	4	5	6
$P_{EEMACOMP}$	4.57±0.33	4.55±0.24	4.47±0.21	4.52±0.18	4.50±0.17	4.50±0.14
$P_{EEMACOMH}$	4.72±0.55	4.69±0.40	4.56±0.39	4.66±0.34	4.65±0.31	4.67±0.31
$P_{EEMMASMP}$	4.37±0.32	4.44±0.23	4.41±0.19	4.47±0.16	4.47±0.16	4.47±0.15
$P_{EEMMASMH}$	4.37±0.38	4.45±0.28	4.43±0.29	4.49±0.27	4.51±0.31	4.52±0.30
$P_{EEMACOMC}$	4.25±0.42	4.31±0.24	4.32±0.20	4.38±0.17	4.40±0.18	4.39±0.15
$P_{NSGA-II-MPA}$	2.15±0.20	2.13±0.16	2.11±0.16	2.11±0.15	2.11±0.17	2.14±0.15

Table I.5: EP objective: $N_G = 100$, $R_g = 500$

$\mathcal{PF}$	T_{sm}					
	1	2	3	4	5	6
$P_{EEMACOMP}$	3.78±0.38	3.85±0.36	3.68±0.31	3.75±0.31	3.78±0.31	3.76±0.29
$P_{EEMACOMH}$	3.35±0.63	3.09±0.40	3.31±0.51	3.13±0.37	3.09±0.31	3.07±0.37
$P_{EEMMASMP}$	3.40±0.30	3.48±0.26	3.28±0.28	3.46±0.28	3.49±0.26	3.45±0.27
$P_{EEMMASMH}$	3.43±0.34	3.55±0.32	3.36±0.37	3.54±0.37	3.54±0.37	3.62±0.36
$P_{EEMACOMC}$	3.57±0.52	3.59±0.38	3.39±0.29	3.46±0.31	3.50±0.30	3.49±0.26
$P_{NSGA-II-MPA}$	2.05±0.14	2.03±0.11	2.01±0.09	2.00±0.08	2.00±0.08	1.99±0.09

Table I.6: EP objective: $N_G = 100$, $R_g = 800$

$\mathcal{PF}$	T_{sm}					
	1	2	3	4	5	6
$P_{EEMACOMP}$	3.45±0.34	3.64±0.33	3.65±0.29	3.71±0.30	3.99±0.29	4.04±0.27
$P_{EEMACOMH}$	2.79±0.37	2.73±0.27	2.64±0.24	2.64±0.23	2.71±0.25	2.70±0.21
$P_{EEMMASMP}$	3.16±0.29	3.21±0.29	3.21±0.27	3.27±0.29	3.43±0.25	3.43±0.27
$P_{EEMMASMH}$	3.13±0.31	3.20±0.26	3.19±0.23	3.31±0.26	3.65±0.24	3.67±0.22
$P_{EEMACOMC}$	5.12±0.53	5.48±0.52	5.53±0.46	5.59±0.53	5.89±0.51	6.00±0.46
$P_{NSGA-II-MPA}$	2.53±0.19	2.47±0.13	2.38±0.08	2.38±0.09	2.39±0.09	2.36±0.08

Table I.7: EP objective: $N_G = 300$, $R_g = 300$

$\mathcal{PF}$	T_{sm}					
	1	2	3	4	5	6
$P_{EEMACOMP}$	19.25±2.44	19.27±2.01	19.19±1.98	18.64±1.93	18.95±1.84	18.92±1.62
$P_{EEMACOMH}$	20.08±4.16	21.68±3.89	21.80±3.76	21.64±3.63	22.47±3.71	22.14±3.25
$P_{EEMMASMP}$	19.59±2.51	19.64±1.98	19.53±1.96	19.25±1.71	19.36±1.60	19.14±1.33
$P_{EEMMASMH}$	19.67±2.71	19.53±2.26	19.40±2.53	19.16±2.59	19.29±2.43	19.24±2.80
$P_{EEMACOMC}$	15.20±2.13	14.96±1.64	14.83±1.57	14.78±1.41	14.92±1.20	14.77±1.12
$P_{NSGA-II-MPA}$	2.85±0.21	2.85±0.19	2.95±0.16	2.91±0.14	2.91±0.16	2.90±0.14

Table I.8: EP objective: $N_G = 300$, $R_g = 500$

$\mathcal{PF}$	T_{sm}					
	1	2	3	4	5	6
$P_{EEMACOMP}$	14.58±2.69	15.59±2.54	15.08±2.24	14.91±2.28	14.93±2.33	14.50±1.98
$P_{EEMACOMH}$	19.13±4.86	21.92±4.63	22.22±4.30	22.31±4.50	23.10±4.48	22.22±3.78
$P_{EEMMASMP}$	15.90±2.92	17.53±2.81	17.32±2.30	16.96±2.16	17.34±2.33	16.38±1.85
$P_{EEMMASMH}$	16.46±3.38	18.02±3.63	17.59±3.58	17.63±3.99	17.64±4.08	16.80±4.12
$P_{EEMACOMC}$	13.25±2.56	14.44±2.52	14.16±2.17	13.78±2.07	13.97±2.21	13.12±1.99
$P_{NSGA-II-MPA}$	2.71±0.22	2.81±0.16	2.83±0.12	2.80±0.12	2.81±0.12	2.85±0.12

Table I.9: EP objective: $N_G = 300$, $R_g = 800$

$\mathcal{PF}$	T_{sm}					
	1	2	3	4	5	6
$P_{EEMACOMP}$	18.86±3.83	18.96±3.61	17.75±2.87	17.49±2.98	17.26±2.84	15.45±2.22
$P_{EEMACOMH}$	27.20±6.73	28.53±6.95	27.18±6.14	27.27±5.87	27.84±5.98	25.43±4.89
$P_{EEMMASMP}$	21.33±4.43	21.43±4.20	19.87±3.71	20.24±3.73	19.95±3.47	17.63±2.56
$P_{EEMMASMH}$	22.84±5.04	22.97±5.36	21.54±5.23	21.57±5.63	21.15±6.62	18.59±6.99
$P_{EEMACOMC}$	18.56±4.37	19.23±4.10	17.55±3.28	17.40±3.65	17.40±2.98	15.51±2.55
$P_{NSGA-II-MPA}$	4.16±0.28	4.19±0.24	4.12±0.26	4.13±0.20	4.17±0.23	4.18±0.21

Table I.10: TNP objective: $N_G = 30$, $R_g = 300$

$\mathcal{PF}$	T_{sm}					
	1	2	3	4	5	6
$P_{EEMACOMP}$	0.0018±0.0002	0.0016±0.0001	0.0016±0.0001	0.0016±0.0001	0.0016±0.0001	0.0016±0.0000
$P_{EEMACOMH}$	0.0018±0.0002	0.0016±0.0001	0.0016±0.0001	0.0016±0.0001	0.0016±0.0001	0.0016±0.0001
$P_{EEMMASMP}$	0.0017±0.0002	0.0016±0.0001	0.0016±0.0001	0.0016±0.0001	0.0016±0.0001	0.0015±0.0001
$P_{EEMMASMH}$	0.0017±0.0002	0.0016±0.0001	0.0016±0.0001	0.0016±0.0001	0.0015±0.0001	0.0015±0.0001
$P_{EEMACOMC}$	0.0017±0.0001	0.0017±0.0001	0.0016±0.0001	0.0016±0.0000	0.0016±0.0000	0.0016±0.0000
$P_{NSGA-II-MPA}$	0.0015±0.0002	0.0014±0.0001	0.0014±0.0001	0.0013±0.0001	0.0013±0.0001	0.0013±0.0000

Table I.11: TNP objective: $N_G = 30$, $R_g = 500$

$\mathcal{PF}$	T_{sm}					
	1	2	3	4	5	6
$P_{EEMACOMP}$	0.0028±0.0005	0.0025±0.0002	0.0024±0.0002	0.0024±0.0002	0.0023±0.0001	0.0024±0.0001
$P_{EEMACOMH}$	0.0029±0.0004	0.0026±0.0002	0.0026±0.0001	0.0025±0.0001	0.0025±0.0001	0.0024±0.0001
$P_{EEMMASMP}$	0.0028±0.0004	0.0026±0.0002	0.0025±0.0001	0.0025±0.0001	0.0025±0.0001	0.0025±0.0001
$P_{EEMMASMH}$	0.0028±0.0004	0.0026±0.0002	0.0025±0.0001	0.0025±0.0001	0.0025±0.0001	0.0025±0.0001
$P_{EEMACOMC}$	0.0027±0.0002	0.0025±0.0001	0.0025±0.0001	0.0025±0.0001	0.0024±0.0001	0.0024±0.0001
$P_{NSGA-II-MPA}$	0.0020±0.0005	0.0017±0.0002	0.0017±0.0002	0.0017±0.0001	0.0017±0.0001	0.0016±0.0001

Table I.12: TNP objective: $N_G = 30$, $R_g = 800$

$\mathcal{PF}$	T_{sm}					
	1	2	3	4	5	6
$P_{EEMACOMP}$	0.0064±0.0016	0.0057±0.0009	0.0053±0.0006	0.0051±0.0006	0.0047±0.0005	0.0049±0.0006
$P_{EEMACOMH}$	0.0067±0.0018	0.0060±0.0009	0.0054±0.0005	0.0053±0.0005	0.0049±0.0003	0.0050±0.0003
$P_{EEMMASMP}$	0.0064±0.0017	0.0056±0.0009	0.0051±0.0006	0.0050±0.0005	0.0046±0.0004	0.0047±0.0004
$P_{EEMMASMH}$	0.0063±0.0016	0.0055±0.0008	0.0051±0.0006	0.0050±0.0005	0.0046±0.0004	0.0047±0.0004
$P_{EEMACOMC}$	0.0045±0.0005	0.0043±0.0003	0.0043±0.0003	0.0042±0.0003	0.0039±0.0002	0.0042±0.0003
$P_{NSGA-II-MPA}$	0.0860±0.0840	0.0051±0.0017	0.0042±0.0008	0.0041±0.0006	0.0039±0.0005	0.0038±0.0004

Table I.13: TNP objective: $N_G = 100$, $R_g = 300$

$\mathcal{PF}$	T_{sm}					
	1	2	3	4	5	6
$P_{EEMACOMP}$	0.0014±0.0001	0.0013±0.0001	0.0013±0.0000	0.0013±0.0000	0.0013±0.0000	0.0013±0.0000
$P_{EEMACOMH}$	0.0016±0.0002	0.0014±0.0001	0.0014±0.0001	0.0014±0.0001	0.0013±0.0000	0.0013±0.0000
$P_{EEMMASMP}$	0.0014±0.0001	0.0013±0.0001	0.0013±0.0000	0.0013±0.0000	0.0013±0.0000	0.0013±0.0000
$P_{EEMMASMH}$	0.0014±0.0001	0.0013±0.0001	0.0013±0.0001	0.0013±0.0001	0.0013±0.0001	0.0013±0.0001
$P_{EEMACOMC}$	0.0015±0.0002	0.0014±0.0001	0.0014±0.0001	0.0014±0.0001	0.0013±0.0000	0.0013±0.0000
$P_{NSGA-II-MPA}$	0.0119±0.4545	0.0022±0.0008	0.0017±0.0003	0.0018±0.0004	0.0018±0.0004	0.0017±0.0003

Table I.14: TNP objective: $N_G = 100$, $R_g = 500$

$\mathcal{PF}$	T_{sm}					
	1	2	3	4	5	6
$P_{EEMACOMP}$	0.0016±0.0002	0.0016±0.0002	0.0015±0.0001	0.0015±0.0001	0.0015±0.0001	0.0015±0.0001
$P_{EEMACOMH}$	0.0018±0.0002	0.0016±0.0002	0.0016±0.0001	0.0016±0.0001	0.0015±0.0001	0.0015±0.0001
$P_{EEMMASMP}$	0.0016±0.0002	0.0015±0.0001	0.0015±0.0001	0.0015±0.0001	0.0015±0.0001	0.0015±0.0001
$P_{EEMMASMH}$	0.0016±0.0002	0.0015±0.0001	0.0015±0.0001	0.0015±0.0001	0.0015±0.0001	0.0015±0.0001
$P_{EEMACOMC}$	0.0018±0.0002	0.0017±0.0002	0.0016±0.0001	0.0016±0.0001	0.0016±0.0001	0.0016±0.0001
$P_{NSGA-II-MPA}$	0.0022±0.0077	0.0016±0.0003	0.0015±0.0002	0.0015±0.0001	0.0015±0.0001	0.0015±0.0001

Table I.15: TNP objective: $N_G = 100$, $R_g = 800$

$\mathcal{PF}$	T_{sm}					
	1	2	3	4	5	6
$P_{EEMACOMP}$	0.0031±0.0004	0.0029±0.0003	0.0028±0.0002	0.0027±0.0002	0.0028±0.0002	0.0027±0.0002
$P_{EEMACOMH}$	0.0033±0.0004	0.0030±0.0003	0.0028±0.0002	0.0028±0.0002	0.0027±0.0002	0.0027±0.0001
$P_{EEMMASMP}$	0.0031±0.0003	0.0029±0.0002	0.0027±0.0002	0.0027±0.0001	0.0027±0.0001	0.0027±0.0001
$P_{EEMMASMH}$	0.0031±0.0004	0.0029±0.0002	0.0027±0.0002	0.0027±0.0002	0.0027±0.0002	0.0027±0.0001
$P_{EEMACOMC}$	0.0038±0.0003	0.0037±0.0002	0.0035±0.0001	0.0035±0.0001	0.0035±0.0002	0.0035±0.0001
$P_{NSGA-II-MPA}$	0.0028±0.0004	0.0026±0.0002	0.0025±0.0001	0.0025±0.0001	0.0025±0.0001	0.0024±0.0001

Table I.16: TNP objective: $N_G = 300$, $R_g = 300$

$\mathcal{PF}$	T_{sm}					
	1	2	3	4	5	6
$P_{EEMACOMP}$	0.0012±0.0001	0.0012±0.0000	0.0011±0.0000	0.0011±0.0000	0.0011±0.0000	0.0011±0.0000
$P_{EEMACOMH}$	0.0013±0.0001	0.0013±0.0001	0.0012±0.0000	0.0012±0.0000	0.0012±0.0000	0.0012±0.0000
$P_{EEMMASMP}$	0.0012±0.0000	0.0012±0.0000	0.0011±0.0000	0.0011±0.0000	0.0011±0.0000	0.0011±0.0000
$P_{EEMMASMH}$	0.0012±0.0001	0.0012±0.0000	0.0012±0.0000	0.0011±0.0001	0.0011±0.0001	0.0011±0.0001
$P_{EEMACOMC}$	0.0013±0.0001	0.0012±0.0000	0.0012±0.0000	0.0012±0.0000	0.0012±0.0000	0.0012±0.0000
$P_{NSGA-II-MPA}$	0.0018±0.0005	0.0016±0.0002	0.0015±0.0002	0.0014±0.0001	0.0014±0.0001	0.0014±0.0001

Table I.17: TNP objective: $N_G = 300$, $R_g = 500$

$\mathcal{PF}$	T_{sm}					
	1	2	3	4	5	6
$P_{EEMACOMP}$	0.0014±0.0001	0.0014±0.0001	0.0013±0.0001	0.0013±0.0001	0.0013±0.0001	0.0013±0.0000
$P_{EEMACOMH}$	0.0016±0.0002	0.0016±0.0002	0.0016±0.0002	0.0015±0.0001	0.0016±0.0002	0.0015±0.0002
$P_{EEMMASMP}$	0.0014±0.0001	0.0014±0.0001	0.0013±0.0000	0.0013±0.0000	0.0013±0.0000	0.0013±0.0000
$P_{EEMMASMH}$	0.0014±0.0001	0.0014±0.0001	0.0014±0.0001	0.0014±0.0001	0.0014±0.0001	0.0013±0.0001
$P_{EEMACOMC}$	0.0015±0.0001	0.0015±0.0001	0.0015±0.0001	0.0015±0.0001	0.0015±0.0001	0.0014±0.0001
$P_{NSGA-II-MPA}$	0.0042±0.0027	0.0027±0.0008	0.0024±0.0004	0.0023±0.0003	0.0023±0.0003	0.0022±0.0003

Table I.18: TNP objective: $N_G = 300$, $R_g = 800$

$\mathcal{PF}$	T_{sm}					
	1	2	3	4	5	6
$P_{EEMACOMP}$	0.0020±0.0002	0.0019±0.0002	0.0018±0.0001	0.0018±0.0001	0.0018±0.0001	0.0017±0.0001
$P_{EEMACOMH}$	0.0025±0.0003	0.0024±0.0003	0.0023±0.0003	0.0023±0.0002	0.0022±0.0002	0.0022±0.0002
$P_{EEMMASMP}$	0.0020±0.0002	0.0020±0.0001	0.0019±0.0001	0.0019±0.0001	0.0018±0.0001	0.0018±0.0001
$P_{EEMMASMH}$	0.0021±0.0002	0.0020±0.0002	0.0019±0.0001	0.0019±0.0002	0.0019±0.0002	0.0018±0.0002
$P_{EEMACOMC}$	0.0024±0.0002	0.0023±0.0002	0.0022±0.0002	0.0021±0.0002	0.0021±0.0002	0.0020±0.0001
$P_{NSGA-II-MPA}$	0.0049±0.0010	0.0044±0.0006	0.0043±0.0006	0.0042±0.0005	0.0043±0.0006	0.0042±0.0006

Table I.19: VNP objective: $N_G = 30$, $R_g = 300$

$\mathcal{PF}$	T_{sm}					
	1	2	3	4	5	6
$P_{EEMACOMP}$	108.10±6.46	110.91±5.39	112.53±4.46	112.24±3.57	112.09±3.88	113.13±2.93
$P_{EEMACOMH}$	113.66±6.21	117.24±4.80	118.96±3.93	118.89±2.83	118.71±3.08	119.69±2.35
$P_{EEMMASMP}$	112.59±6.16	115.70±4.89	117.40±4.11	117.09±3.18	117.02±3.40	117.87±2.53
$P_{EEMMASMH}$	112.31±6.37	115.43±4.94	117.21±4.22	116.94±3.16	116.78±3.38	117.58±2.51
$P_{EEMACOMC}$	90.67±6.65	95.73±5.54	98.05±4.36	98.36±3.21	98.94±3.33	99.75±2.68
$P_{NSGA-II-MPA}$	134.02±10.59	141.11±6.91	145.06±5.40	145.95±4.32	146.53±4.33	147.30±3.75

Table I.20: VNP objective: $N_G = 30$, $R_g = 500$

$\mathcal{PF}$	T_{sm}					
	1	2	3	4	5	6
$P_{EEMACOMP}$	83.60±8.03	88.39±4.44	89.48±3.72	91.67±4.82	89.75±3.37	90.85±3.48
$P_{EEMACOMH}$	83.81±8.65	90.16±4.77	91.87±3.82	94.43±4.67	92.75±3.52	94.07±3.23
$P_{EEMMASMP}$	87.70±7.77	91.77±4.28	92.93±3.58	94.85±4.45	93.33±3.29	93.05±3.01
$P_{EEMMASMH}$	87.33±8.05	91.82±4.24	93.06±3.47	94.69±4.34	93.28±3.13	92.69±3.36
$P_{EEMACOMC}$	67.67±6.13	73.01±4.35	74.57±4.81	73.03±4.44	76.97±3.75	77.42±3.76
$P_{NSGA-II-MPA}$	126.29±11.08	134.26±6.34	137.05±5.46	138.41±4.46	138.94±3.58	139.91±3.46

Table I.21: VNP objective: $N_G = 30$, $R_g = 800$

$\mathcal{PF}$	T_{sm}					
	1	2	3	4	5	6
$P_{EEMACOMP}$	79.72±15.02	74.19±13.71	74.02±12.39	72.01±12.55	72.55±12.62	69.33±11.01
$P_{EEMACOMH}$	78.85±12.66	78.44±12.07	67.41±7.60	72.48±9.20	66.56±8.56	63.58±7.14
$P_{EEMMASMP}$	79.17±13.93	73.49±13.24	73.30±10.97	71.07±11.67	70.74±11.58	69.49±10.33
$P_{EEMMASMH}$	76.36±13.58	70.87±11.50	71.60±10.65	70.62±12.93	73.37±11.79	68.00±9.89
$P_{EEMACOMC}$	54.91±9.10	53.07±6.33	57.80±7.85	55.47±6.77	56.42±7.35	58.03±7.69
$P_{NSGA-II-MPA}$	113.15±22.97	106.48±14.44	105.87±9.37	109.76±11.97	105.53±7.64	107.30±8.22

Table I.22: VNP objective: $N_G = 100$, $R_g = 300$

	T_{sm}					
$\mathcal{PF}$	1	2	3	4	5	6
$P_{EEMACOMP}$	85.02±6.10	83.95±4.37	84.97±3.83	83.76±3.12	84.08±3.00	83.73±2.66
$P_{EEMACOMH}$	91.30±7.59	87.06±5.61	85.78±5.45	84.39±4.99	83.74±4.58	82.78±4.65
$P_{EEMMASMP}$	87.58±6.10	85.17±4.09	85.84±3.65	84.52±2.88	84.66±2.89	84.39±2.63
$P_{EEMMASMH}$	88.09±5.78	85.54±4.09	85.96±3.68	84.76±3.12	84.78±3.23	84.47±2.87
$P_{EEMACOMC}$	92.17±6.11	88.69±4.85	87.87±3.82	86.63±2.73	86.34±2.95	86.07±2.47
$P_{NSGA-II-MPA}$	118.54±13.32	124.89±8.47	129.26±5.64	129.68±5.78	130.83±5.63	130.96±5.24

Table I.23: VNP objective: $N_G = 100$, $R_g = 500$

	T_{sm}					
$\mathcal{PF}$	1	2	3	4	5	6
$P_{EEMACOMP}$	103.59±5.40	104.14±3.86	104.73±4.08	103.72±3.87	103.49±3.27	103.37±3.07
$P_{EEMACOMH}$	118.22±5.91	119.04±4.14	119.38±4.90	119.73±4.34	120.16±3.02	119.47±3.43
$P_{EEMMASMP}$	107.90±4.61	108.33±3.36	110.67±3.48	108.72±3.47	108.56±2.91	108.36±2.77
$P_{EEMMASMH}$	108.11±4.49	108.03±3.35	110.22±3.49	108.19±3.61	108.28±3.19	107.81±3.08
$P_{EEMACOMC}$	105.14±5.41	104.41±3.79	106.48±3.32	105.93±4.00	105.58±3.15	105.47±3.04
$P_{NSGA-II-MPA}$	120.06±11.35	127.65±7.50	130.26±5.68	131.94±4.03	132.33±3.97	133.21±4.40

Table I.24: VNP objective: $N_G = 100$, $R_g = 800$

	T_{sm}					
$\mathcal{PF}$	1	2	3	4	5	6
$P_{EEMACOMP}$	83.78±8.00	83.86±7.42	86.17±5.70	85.33±5.82	83.34±4.35	83.88±4.08
$P_{EEMACOMH}$	99.07±12.52	102.94±11.51	107.01±9.25	107.31±9.25	104.19±8.06	104.64±7.24
$P_{EEMMASMP}$	87.75±8.80	91.04±7.60	93.86±6.11	93.71±5.98	89.65±4.64	89.86±4.44
$P_{EEMMASMH}$	89.66±8.79	91.59±9.01	93.88±7.35	92.89±8.12	87.98±8.40	88.18±8.58
$P_{EEMACOMC}$	63.80±8.35	66.19±7.91	69.01±7.77	69.80±6.69	67.61±6.96	66.78±5.36
$P_{NSGA-II-MPA}$	97.34±7.90	100.57±5.66	105.18±4.03	104.85±4.48	104.84±3.89	106.40±3.81

Table I.25: VNP objective: $N_G = 300$, $R_g = 300$

	T_{sm}					
$\mathcal{PF}$	1	2	3	4	5	6
$P_{EEMACOMP}$	36.37±5.36	34.53±4.65	33.36±3.95	34.48±4.50	33.47±4.32	33.42±4.26
$P_{EEMACOMH}$	42.67±6.45	38.45±5.65	36.07±4.72	35.33±4.88	33.85±4.49	33.42±4.56
$P_{EEMMASMP}$	35.75±4.97	33.03±3.50	31.99±3.01	32.29±2.99	31.74±2.82	31.75±2.48
$P_{EEMMASMH}$	36.34±4.67	33.85±3.39	32.89±3.16	33.20±2.92	32.70±2.74	32.50±2.50
$P_{EEMACOMC}$	45.39±5.07	42.62±3.95	41.48±3.46	41.27±3.48	40.16±2.99	40.12±3.09
$P_{NSGA-II-MPA}$	119.89±16.36	116.80±9.58	114.37±8.87	113.77±6.63	113.71±6.16	113.65±5.58

Table I.26: VNP objective: $N_G = 300$, $R_g = 500$

	T_{sm}					
$\mathcal{PF}$	1	2	3	4	5	6
$P_{EEMACOMP}$	58.39±7.40	55.22±6.48	53.78±5.40	52.15±5.83	51.69±5.52	50.86±5.05
$P_{EEMACOMH}$	69.95±9.15	64.73±8.64	61.26±7.30	58.97±7.01	57.71±7.11	55.71±6.25
$P_{EEMMASMP}$	56.12±6.32	53.21±5.01	51.98±4.39	51.02±3.66	50.51±3.89	50.27±3.67
$P_{EEMMASMH}$	57.07±6.12	55.20±5.71	53.43±4.23	52.36±4.16	52.31±4.59	52.09±3.73
$P_{EEMACOMC}$	67.50±6.72	64.57±5.20	62.93±5.05	62.78±4.48	62.85±4.48	61.63±4.33
$P_{NSGA-II-MPA}$	106.86±12.57	102.19±7.11	103.40±5.26	105.41±5.21	105.22±4.09	104.76±3.22

Table I.27: VNP objective: $N_G = 300$, $R_g = 800$

	T_{sm}					
$\mathcal{PF}$	1	2	3	4	5	6
$P_{EEMACOMP}$	95.20±7.57	90.53±8.03	85.94±6.58	85.22±7.00	83.13±6.38	80.44±6.45
$P_{EEMACOMH}$	112.43±9.39	108.35±9.40	104.05±8.82	101.90±8.34	99.25±8.61	96.59±7.85
$P_{EEMMASMP}$	92.01±6.48	90.39±6.14	86.76±5.59	86.35±5.52	84.35±5.21	82.33±4.60
$P_{EEMMASMH}$	94.65±6.84	91.93±6.76	89.43±5.92	89.22±6.54	88.11±6.24	85.95±6.64
$P_{EEMACOMC}$	99.21±6.94	97.30±6.57	94.25±6.92	93.16±5.77	93.49±6.15	89.33±5.10
$P_{NSGA-II-MPA}$	95.84±12.89	102.66±12.83	104.40±12.81	109.51±12.47	107.60±12.36	111.38±12.81

Table I.28: CP objective: $N_G = 30$, $R_g = 300$

	T_{sm}					
$\mathcal{PF}$	1	2	3	4	5	6
$P_{EEMACOMP}$	0.013±0.001	0.013±0.001	0.014±0.001	0.014±0.001	0.014±0.001	0.014±0.001
$P_{EEMACOMH}$	0.012±0.001	0.012±0.001	0.012±0.001	0.012±0.001	0.013±0.000	0.012±0.001
$P_{EEMMASMP}$	0.012±0.001	0.013±0.001	0.013±0.001	0.013±0.001	0.013±0.001	0.013±0.000
$P_{EEMMASMH}$	0.012±0.001	0.013±0.001	0.013±0.001	0.013±0.001	0.013±0.001	0.013±0.001
$P_{EEMACOMC}$	0.017±0.001	0.017±0.001	0.017±0.000	0.017±0.001	0.017±0.001	0.017±0.000
$P_{NSGA-II-MPA}$	0.009±0.001	0.009±0.000	0.009±0.000	0.009±0.000	0.009±0.000	0.009±0.000

Table I.29: CP objective: $N_G = 30$, $R_g = 500$

	T_{sm}					
$\mathcal{PF}$	1	2	3	4	5	6
$P_{EEMACOMP}$	0.012±0.001	0.012±0.001	0.012±0.001	0.011±0.001	0.012±0.001	0.012±0.001
$P_{EEMACOMH}$	0.011±0.000	0.010±0.000	0.010±0.000	0.010±0.000	0.011±0.000	0.010±0.000
$P_{EEMMASMP}$	0.011±0.000	0.010±0.000	0.010±0.000	0.010±0.000	0.011±0.000	0.011±0.000
$P_{EEMMASMH}$	0.011±0.000	0.011±0.000	0.011±0.000	0.010±0.000	0.011±0.000	0.011±0.000
$P_{EEMACOMC}$	0.017±0.001	0.016±0.001	0.016±0.001	0.016±0.001	0.016±0.001	0.015±0.001
$P_{NSGA-II-MPA}$	0.009±0.001	0.008±0.001	0.008±0.001	0.008±0.001	0.008±0.001	0.008±0.001

Table I.30: CP objective: $N_G = 30$, $R_g = 800$

	T_{sm}					
$\mathcal{PF}$	1	2	3	4	5	6
$P_{EEMACOMP}$	0.011±0.001	0.010±0.000	0.011±0.001	0.011±0.000	0.011±0.001	0.011±0.001
$P_{EEMACOMH}$	0.010±0.001	0.009±0.001	0.009±0.000	0.009±0.000	0.010±0.000	0.009±0.000
$P_{EEMMASMP}$	0.011±0.001	0.010±0.000	0.010±0.000	0.010±0.000	0.010±0.000	0.010±0.000
$P_{EEMMASMH}$	0.010±0.001	0.010±0.000	0.010±0.000	0.010±0.000	0.010±0.000	0.010±0.000
$P_{EEMACOMC}$	0.019±0.002	0.018±0.001	0.017±0.001	0.017±0.001	0.018±0.001	0.017±0.001
$P_{NSGA-II-MPA}$	0.066±3.068	0.008±0.001	0.008±0.001	0.008±0.000	0.008±0.000	0.008±0.000

Table I.31: CP objective: $N_G = 100$, $R_g = 300$

	T_{sm}					
$\mathcal{PF}$	1	2	3	4	5	6
$P_{EEMACOMP}$	0.025±0.002	0.025±0.001	0.025±0.001	0.025±0.001	0.025±0.001	0.025±0.001
$P_{EEMACOMH}$	0.025±0.003	0.026±0.002	0.025±0.002	0.026±0.002	0.026±0.002	0.026±0.002
$P_{EEMMASMP}$	0.024±0.002	0.025±0.001	0.025±0.001	0.025±0.001	0.025±0.001	0.025±0.001
$P_{EEMMASMH}$	0.024±0.002	0.025±0.002	0.025±0.001	0.025±0.001	0.025±0.001	0.025±0.001
$P_{EEMACOMC}$	0.022±0.002	0.023±0.002	0.023±0.001	0.023±0.001	0.024±0.001	0.024±0.001
$P_{NSGA-II-MPA}$	0.016±0.341	0.010±0.002	0.011±0.002	0.010±0.002	0.010±0.002	0.011±0.002

Table I.32: CP objective: $N_G = 100$, $R_g = 500$

	T_{sm}					
$\mathcal{PF}$	1	2	3	4	5	6
$P_{EEMACOMP}$	0.019±0.002	0.019±0.002	0.019±0.002	0.019±0.002	0.019±0.001	0.019±0.001
$P_{EEMACOMH}$	0.016±0.003	0.015±0.002	0.016±0.003	0.016±0.002	0.016±0.002	0.015±0.002
$P_{EEMMASMP}$	0.017±0.002	0.017±0.001	0.017±0.001	0.018±0.001	0.018±0.001	0.018±0.001
$P_{EEMMASMH}$	0.017±0.002	0.018±0.002	0.017±0.002	0.018±0.002	0.018±0.002	0.019±0.002
$P_{EEMACOMC}$	0.016±0.002	0.017±0.002	0.016±0.001	0.016±0.001	0.017±0.001	0.016±0.001
$P_{NSGA-II-MPA}$	0.010±0.006	0.010±0.001	0.010±0.001	0.010±0.001	0.010±0.001	0.010±0.001

Table I.33: CP objective: $N_G = 100$, $R_g = 800$

	T_{sm}					
$\mathcal{PF}$	1	2	3	4	5	6
$P_{EEMACOMP}$	0.010±0.001	0.010±0.001	0.010±0.000	0.010±0.000	0.011±0.001	0.011±0.000
$P_{EEMACOMH}$	0.008±0.001	0.008±0.001	0.008±0.001	0.008±0.000	0.008±0.001	0.008±0.000
$P_{EEMMASMP}$	0.009±0.001	0.009±0.001	0.009±0.001	0.010±0.001	0.010±0.001	0.010±0.001
$P_{EEMMASMH}$	0.009±0.001	0.009±0.001	0.009±0.001	0.010±0.001	0.010±0.001	0.011±0.001
$P_{EEMACOMC}$	0.012±0.002	0.013±0.002	0.013±0.002	0.013±0.002	0.014±0.002	0.014±0.002
$P_{NSGA-II-MPA}$	0.008±0.000	0.008±0.000	0.008±0.000	0.008±0.000	0.008±0.000	0.008±0.000

Table I.34: CP objective: $N_G = 300$, $R_g = 300$

$\mathcal{PF}$	T_{sm}					
	1	2	3	4	5	6
$P_{EEMACOMP}$	0.117±0.015	0.117±0.012	0.117±0.012	0.113±0.012	0.115±0.011	0.115±0.010
$P_{EEMACOMH}$	0.121±0.025	0.131±0.024	0.132±0.023	0.131±0.022	0.136±0.023	0.134±0.020
$P_{EEMMASMP}$	0.120±0.015	0.120±0.012	0.119±0.012	0.117±0.010	0.118±0.010	0.117±0.008
$P_{EEMMASMH}$	0.120±0.017	0.119±0.014	0.118±0.015	0.117±0.016	0.118±0.015	0.117±0.017
$P_{EEMACOMC}$	0.091±0.013	0.090±0.010	0.089±0.010	0.089±0.009	0.090±0.007	0.089±0.007
$P_{NSGA-II-MPA}$	0.014±0.002	0.015±0.002	0.016±0.001	0.016±0.001	0.016±0.001	0.016±0.001

Table I.35: CP objective: $N_G = 300$, $R_g = 500$

$\mathcal{PF}$	T_{sm}					
	1	2	3	4	5	6
$P_{EEMACOMP}$	0.085±0.016	0.091±0.015	0.088±0.013	0.087±0.014	0.087±0.014	0.085±0.012
$P_{EEMACOMH}$	0.108±0.029	0.125±0.028	0.128±0.026	0.129±0.027	0.133±0.027	0.129±0.023
$P_{EEMMASMP}$	0.093±0.017	0.103±0.017	0.101±0.014	0.099±0.013	0.102±0.014	0.096±0.011
$P_{EEMMASMH}$	0.096±0.020	0.105±0.021	0.103±0.021	0.103±0.024	0.103±0.024	0.098±0.024
$P_{EEMACOMC}$	0.074±0.015	0.081±0.015	0.080±0.013	0.077±0.012	0.079±0.013	0.074±0.012
$P_{NSGA-II-MPA}$	0.012±0.002	0.012±0.001	0.012±0.001	0.012±0.001	0.012±0.001	0.013±0.001

Table I.36: CP objective: $N_G = 300$, $R_g = 800$

$\mathcal{PF}$	T_{sm}					
	1	2	3	4	5	6
$P_{EEMACOMP}$	0.098±0.021	0.099±0.020	0.094±0.016	0.093±0.017	0.092±0.016	0.083±0.013
$P_{EEMACOMH}$	0.137±0.036	0.145±0.038	0.140±0.034	0.142±0.033	0.146±0.034	0.134±0.028
$P_{EEMMASMP}$	0.111±0.024	0.112±0.023	0.104±0.021	0.106±0.021	0.105±0.019	0.093±0.014
$P_{EEMMASMH}$	0.119±0.027	0.120±0.029	0.113±0.028	0.113±0.031	0.111±0.036	0.098±0.037
$P_{EEMACOMC}$	0.088±0.022	0.092±0.021	0.084±0.017	0.083±0.019	0.083±0.016	0.075±0.014
$P_{NSGA-II-MPA}$	0.011±0.001	0.011±0.001	0.011±0.001	0.011±0.001	0.011±0.001	0.011±0.001

Table I.37: MNC objective: $N_G = 30$, $R_g = 300$

$\mathcal{PF}$	T_{sm}					
	1	2	3	4	5	6
$P_{EEMACOMP}$	2.604±0.889	1.835±0.460	1.600±0.335	1.467±0.263	1.395±0.223	1.323±0.179
$P_{EEMACOMH}$	2.494±0.814	1.747±0.419	1.587±0.319	1.421±0.244	1.368±0.211	1.292±0.164
$P_{EEMMASMP}$	2.701±0.947	1.919±0.493	1.616±0.329	1.531±0.294	1.453±0.257	1.353±0.208
$P_{EEMMASMH}$	2.701±0.937	1.921±0.495	1.605±0.349	1.499±0.286	1.410±0.228	1.358±0.205
$P_{EEMACOMC}$	3.633±1.558	2.466±0.802	1.964±0.557	1.675±0.365	1.460±0.280	1.497±0.277
$P_{NSGA-II-MPA}$	1.076±0.022	1.084±0.021	1.088±0.018	1.078±0.025	1.084±0.022	1.084±0.022

Table I.38: MNC objective: $N_G = 30$, $R_g = 500$

$\mathcal{PF}$	T_{sm}					
	1	2	3	4	5	6
$P_{EEMACOMP}$	3.141±1.179	2.089±0.584	1.759±0.407	1.553±0.306	1.547±0.295	1.417±0.222
$P_{EEMACOMH}$	2.913±1.063	1.920±0.505	1.711±0.395	1.489±0.277	1.415±0.233	1.365±0.202
$P_{EEMMASMP}$	2.975±1.119	2.058±0.562	1.752±0.406	1.570±0.312	1.500±0.268	1.410±0.234
$P_{EEMMASMH}$	2.957±1.091	2.046±0.550	1.689±0.385	1.555±0.311	1.497±0.265	1.445±0.248
$P_{EEMACOMC}$	4.914±2.267	3.122±1.154	2.389±0.813	1.862±0.457	1.660±0.392	1.674±0.362
$P_{NSGA-II-MPA}$	1.115±0.030	1.111±0.021	1.112±0.022	1.090±0.021	1.105±0.030	1.103±0.030

Table I.39: MNC objective: $N_G = 30$, $R_g = 800$

$\mathcal{PF}$	T_{sm}					
	1	2	3	4	5	6
$P_{EEMACOMP}$	3.988±1.619	2.613±0.812	2.118±0.571	1.877±0.445	1.706±0.330	1.663±0.341
$P_{EEMACOMH}$	3.919±1.473	2.492±0.787	2.346±0.698	1.983±0.516	1.792±0.422	1.829±0.435
$P_{EEMMASMP}$	4.168±1.687	2.813±0.887	2.301±0.662	2.075±0.531	1.855±0.429	1.791±0.431
$P_{EEMMASMH}$	4.217±1.740	2.858±0.925	2.207±0.667	2.023±0.508	1.816±0.389	1.824±0.425
$P_{EEMACOMC}$	7.024±3.452	4.441±1.855	3.201±1.244	2.596±0.816	2.137±0.631	2.059±0.562
$P_{NSGA-II-MPA}$	1.303±0.231	1.236±0.058	1.237±0.049	1.234±0.057	1.246±0.065	1.231±0.054

Table I.40: MNC objective: $N_G = 100$, $R_g = 300$

	T_{sm}					
$\mathcal{PF}$	1	2	3	4	5	6
$P_{EEMACOMP}$	1.953±0.497	1.528±0.255	1.378±0.183	1.309±0.145	1.257±0.120	1.229±0.108
$P_{EEMACOMH}$	2.070±0.528	1.614±0.275	1.457±0.197	1.388±0.165	1.329±0.143	1.284±0.119
$P_{EEMMASMP}$	2.229±0.605	1.731±0.356	1.530±0.261	1.451±0.215	1.371±0.182	1.310±0.147
$P_{EEMMASMH}$	2.211±0.589	1.737±0.369	1.528±0.260	1.431±0.203	1.367±0.176	1.341±0.151
$P_{EEMACOMC}$	2.139±0.569	1.714±0.349	1.517±0.254	1.391±0.188	1.356±0.174	1.287±0.138
$P_{NSGA-II-MPA}$	1.179±0.070	1.153±0.056	1.140±0.029	1.143±0.037	1.146±0.044	1.138±0.038

Table I.41: MNC objective: $N_G = 100$, $R_g = 500$

	T_{sm}					
$\mathcal{PF}$	1	2	3	4	5	6
$P_{EEMACOMP}$	2.409±0.773	1.841±0.443	1.591±0.300	1.479±0.245	1.417±0.218	1.363±0.184
$P_{EEMACOMH}$	2.319±0.670	1.829±0.414	1.632±0.320	1.477±0.231	1.430±0.218	1.350±0.176
$P_{EEMMASMP}$	2.720±0.904	2.037±0.560	1.703±0.373	1.580±0.320	1.524±0.298	1.424±0.236
$P_{EEMMASMH}$	2.682±0.866	2.042±0.564	1.724±0.381	1.584±0.306	1.510±0.282	1.452±0.231
$P_{EEMACOMC}$	2.488±0.799	1.924±0.529	1.631±0.314	1.485±0.243	1.435±0.234	1.372±0.188
$P_{NSGA-II-MPA}$	1.129±0.034	1.129±0.019	1.123±0.023	1.121±0.021	1.114±0.025	1.111±0.024

Table I.42: MNC objective: $N_G = 100$, $R_g = 800$

	T_{sm}					
$\mathcal{PF}$	1	2	3	4	5	6
$P_{EEMACOMP}$	3.645±1.382	2.520±0.784	2.095±0.571	1.849±0.419	1.701±0.369	1.618±0.337
$P_{EEMACOMH}$	3.031±1.100	2.056±0.568	1.826±0.414	1.626±0.328	1.536±0.290	1.497±0.270
$P_{EEMMASMP}$	3.612±1.457	2.508±0.836	1.984±0.521	1.804±0.425	1.739±0.401	1.595±0.340
$P_{EEMMASMH}$	3.359±1.292	2.406±0.762	1.980±0.570	1.758±0.420	1.746±0.393	1.749±0.394
$P_{EEMACOMC}$	5.147±2.514	3.393±1.388	2.608±0.951	2.026±0.606	2.013±0.576	1.914±0.509
$P_{NSGA-II-MPA}$	1.099±0.019	1.140±0.024	1.129±0.024	1.126±0.034	1.128±0.028	1.132±0.034

Table I.43: MNC objective: $N_G = 300$, $R_g = 300$

	T_{sm}					
$\mathcal{PF}$	1	2	3	4	5	6
$P_{EEMACOMP}$	2.514±0.739	1.824±0.382	1.613±0.274	1.466±0.212	1.393±0.180	1.334±0.156
$P_{EEMACOMH}$	2.669±0.771	1.948±0.409	1.727±0.301	1.607±0.256	1.525±0.224	1.469±0.214
$P_{EEMMASMP}$	3.026±1.006	2.215±0.601	1.794±0.378	1.656±0.309	1.557±0.266	1.459±0.224
$P_{EEMMASMH}$	2.992±0.971	2.185±0.606	1.821±0.409	1.622±0.286	1.566±0.268	1.490±0.223
$P_{EEMACOMC}$	2.580±0.823	1.899±0.429	1.638±0.318	1.466±0.208	1.390±0.179	1.372±0.175
$P_{NSGA-II-MPA}$	2.083±0.595	1.574±0.287	1.417±0.192	1.329±0.144	1.277±0.116	1.248±0.101

Table I.44: MNC objective: $N_G = 300$, $R_g = 500$

	T_{sm}					
$\mathcal{PF}$	1	2	3	4	5	6
$P_{EEMACOMP}$	2.318±0.604	1.791±0.343	1.576±0.250	1.473±0.203	1.396±0.168	1.327±0.137
$P_{EEMACOMH}$	2.504±0.667	1.959±0.400	1.728±0.294	1.618±0.242	1.554±0.223	1.463±0.187
$P_{EEMMASMP}$	2.860±0.878	2.184±0.574	1.773±0.363	1.616±0.280	1.546±0.261	1.430±0.196
$P_{EEMMASMH}$	2.859±0.861	2.171±0.580	1.810±0.390	1.629±0.285	1.562±0.257	1.439±0.191
$P_{EEMACOMC}$	2.482±0.731	1.890±0.427	1.646±0.308	1.484±0.210	1.389±0.170	1.352±0.160
$P_{NSGA-II-MPA}$	1.284±0.258	1.199±0.065	1.190±0.030	1.177±0.030	1.181±0.039	1.174±0.034

Table I.45: MNC objective: $N_G = 300$, $R_g = 800$

	T_{sm}					
$\mathcal{PF}$	1	2	3	4	5	6
$P_{EEMACOMP}$	2.894±0.824	2.163±0.492	1.814±0.330	1.645±0.254	1.554±0.211	1.416±0.167
$P_{EEMACOMH}$	3.225±1.001	2.425±0.599	1.992±0.419	1.810±0.312	1.716±0.282	1.558±0.217
$P_{EEMMASMP}$	3.526±1.134	2.510±0.669	2.014±0.444	1.819±0.339	1.680±0.287	1.499±0.209
$P_{EEMMASMH}$	3.628±1.189	2.614±0.721	2.087±0.465	1.882±0.373	1.737±0.300	1.546±0.216
$P_{EEMACOMC}$	3.216±1.008	2.341±0.593	1.921±0.405	1.775±0.322	1.646±0.266	1.478±0.193
$P_{NSGA-II-MPA}$	3.348±1.254	2.430±0.755	1.968±0.506	1.789±0.395	1.625±0.323	1.594±0.283

Appendix J

Illustration of the Influence of Change Frequency, Change Severity, and Number of Nodes on the Optimisation Criteria

This appendix presents FluxViz graphs to illustrate the influence of change frequency, T_{sm} and change severity, R_g, on the EP, TNP, VNP, CP and MNC optimisation criteria for different number of nodes, N_G. Figures J.1-J.3 visualise the influence of T_{sm} and R_g on the EP criterion based on the results of Tables I.1-I.9. Figures J.4-J.6 visualise the influence of T_{sm} and R_g on the TNP criterion based on the results of Tables I.10-I.18. Figures J.7-J.9 visualise the influence of T_{sm} and R_g on the VNP criterion based on the results of Tables I.19-I.27. Figures J.10-J.12 illustrate the influence of T_{sm} and R_g on the CP criterion based on the results of Tables I.28-I.36, while Figures J.13-J.15 visualise the influence of T_{sm} and R_g on the MNC criterion based on the results of Tables I.37-I.45.

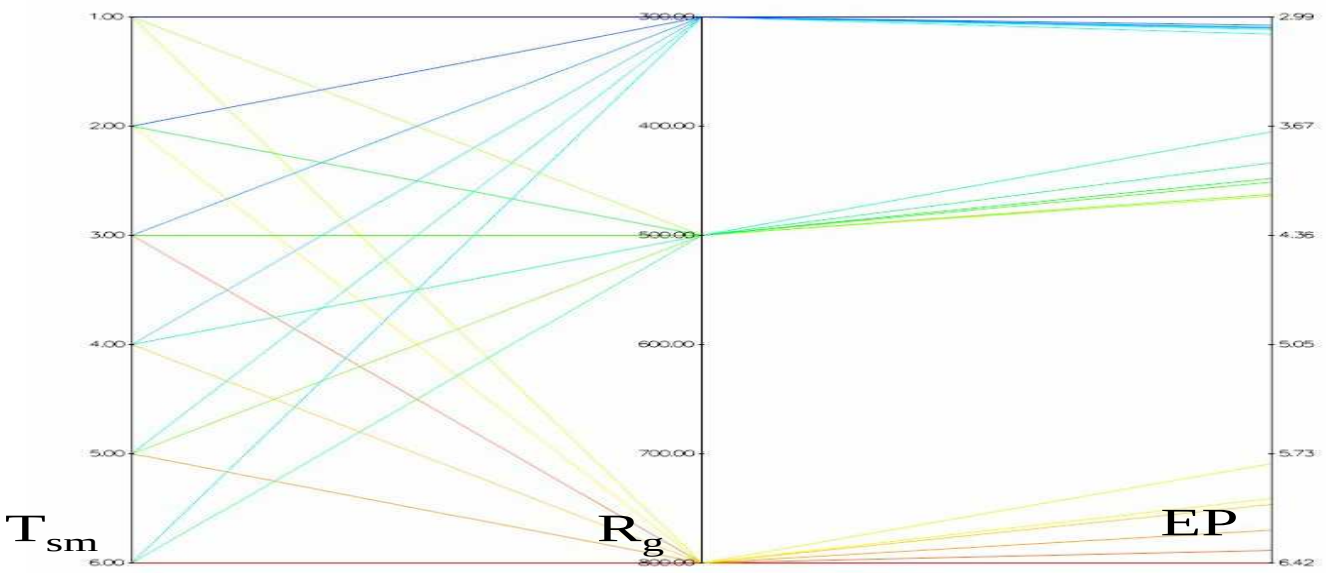

(a) EEMACOMP

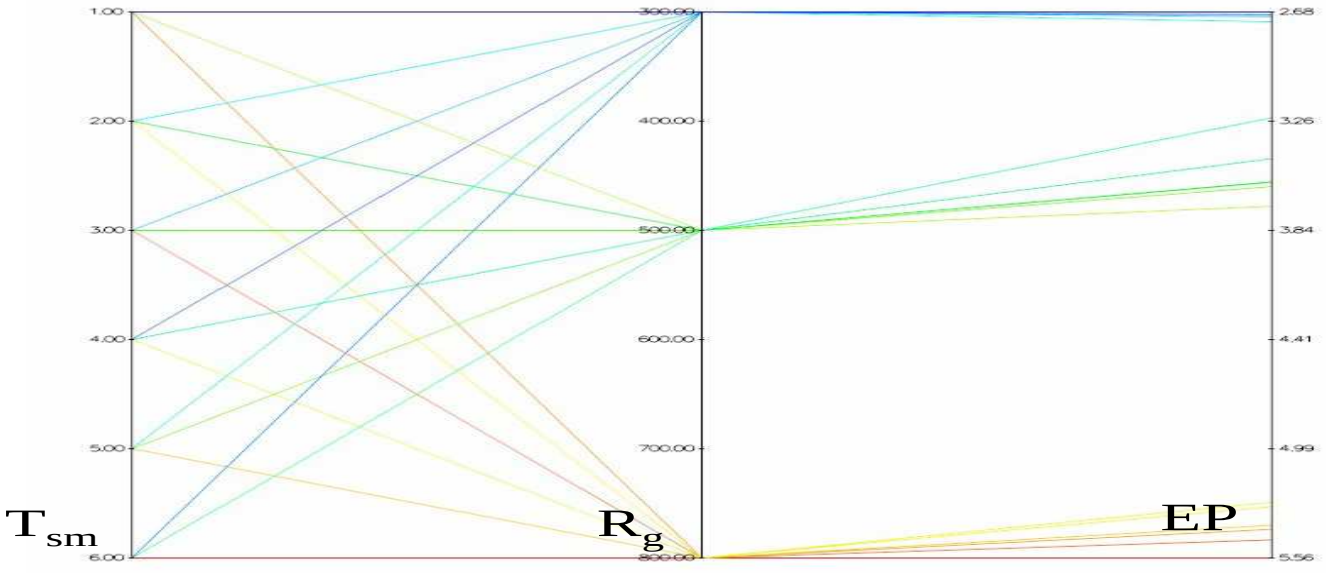

(b) EEMACOMH

Figure J.1: Influence of R_g and T_{sm} on the EP objective for $N_G = 30$

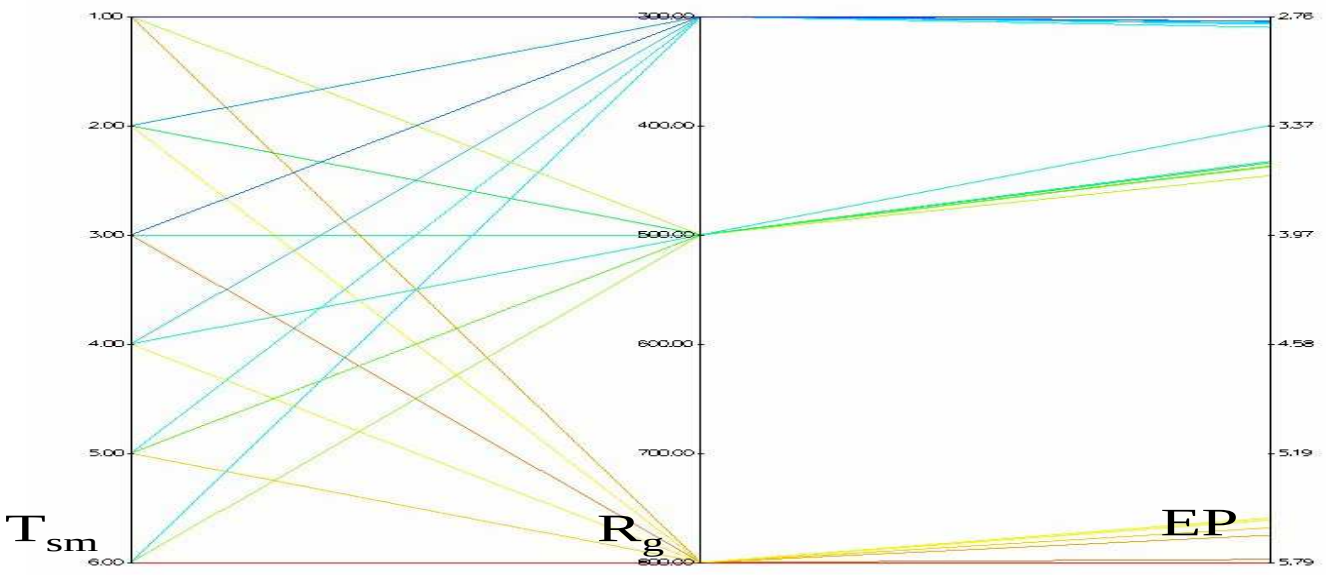

(c) EEMMASMP

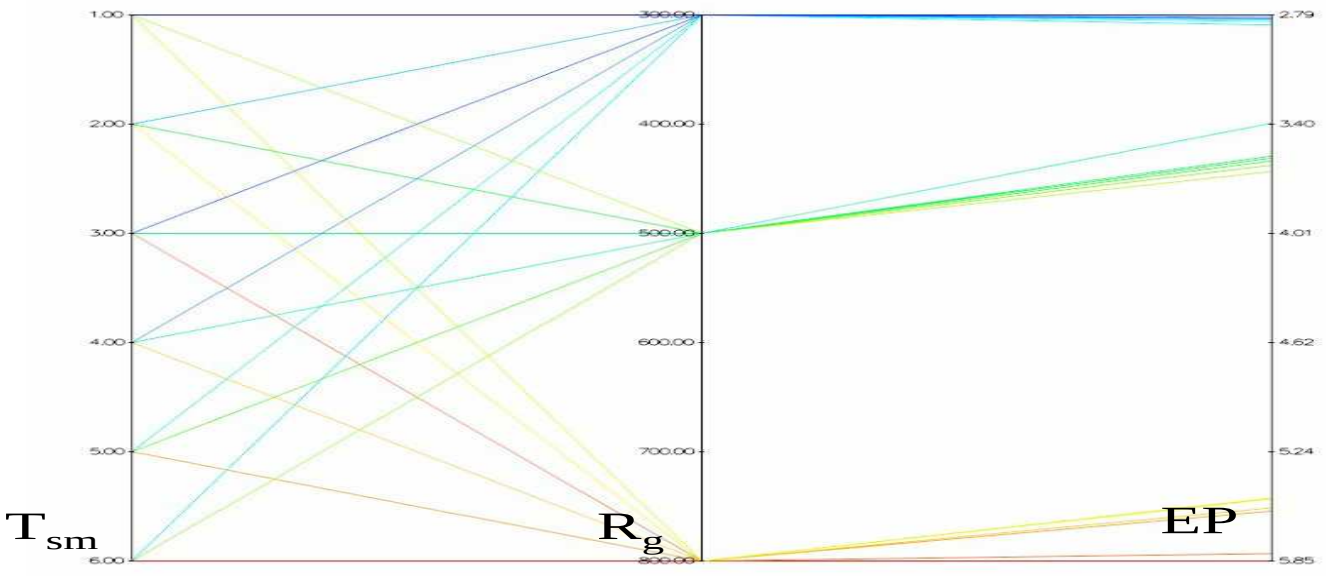

(d) EEMMASMH

Figure J.1: Influence of R_g and T_{sm} on the EP objective for $N_G = 30$ (cont.)

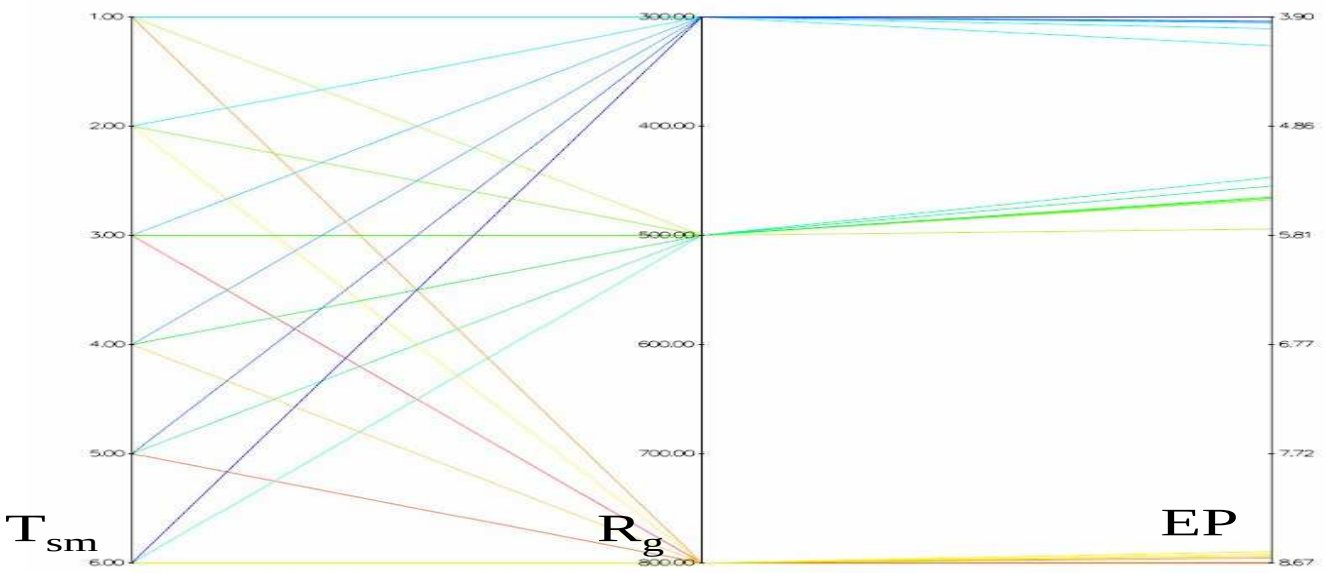

(e) EEMACOMC

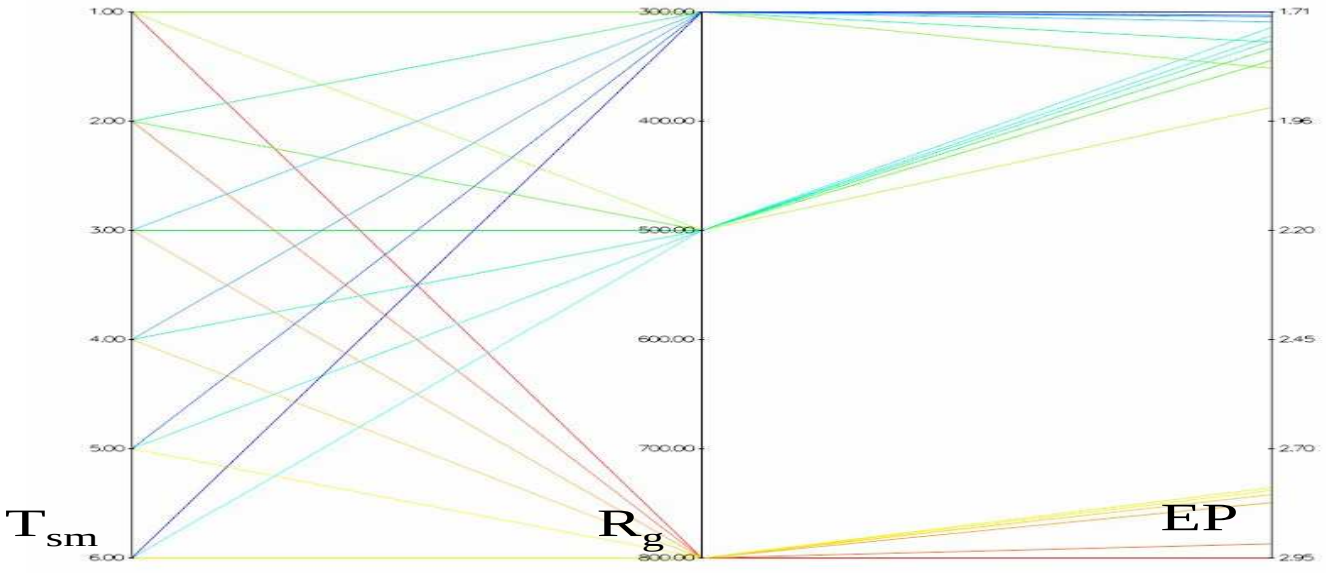

(f) NSGA-II-MPA

Figure J.1: Influence of R_g and T_{sm} on the EP objective for $N_G = 30$ (cont.)

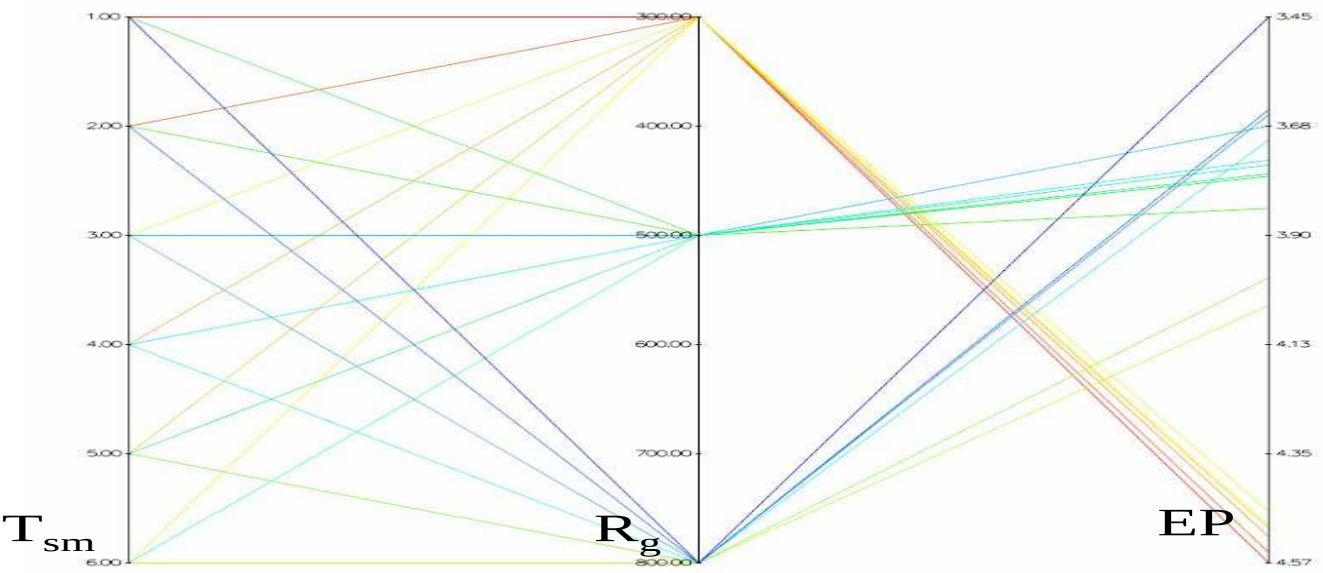

(a) EEMACOMP

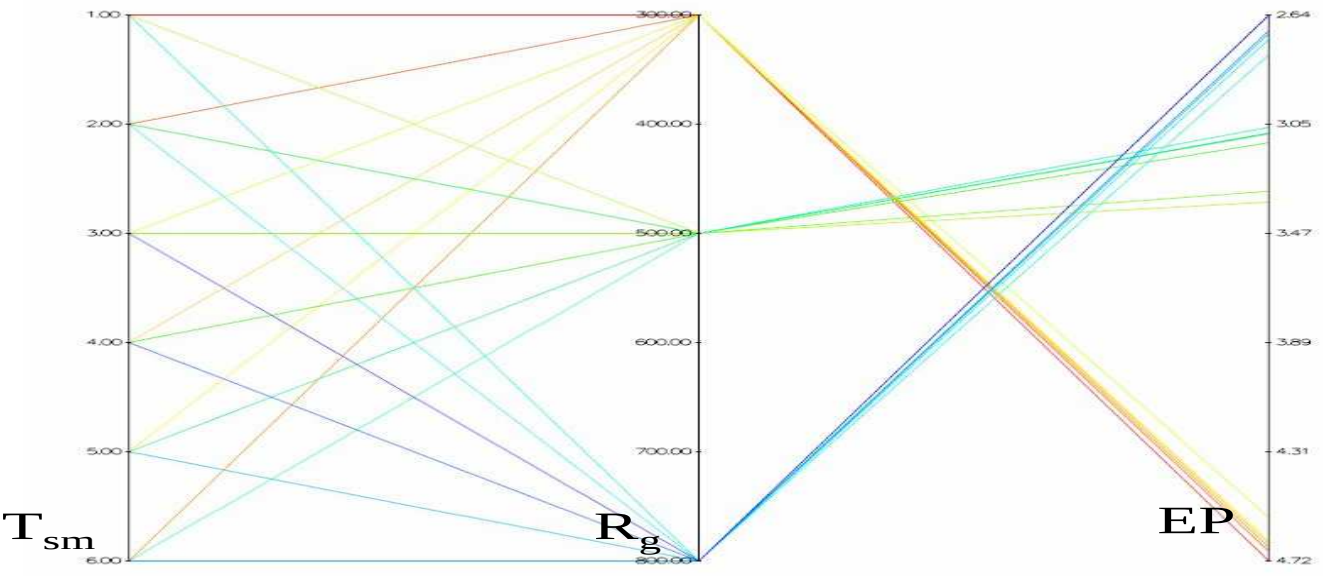

(b) EEMACOMH

Figure J.2: Influence of R_g and T_{sm} on the EP objective for $N_G = 100$

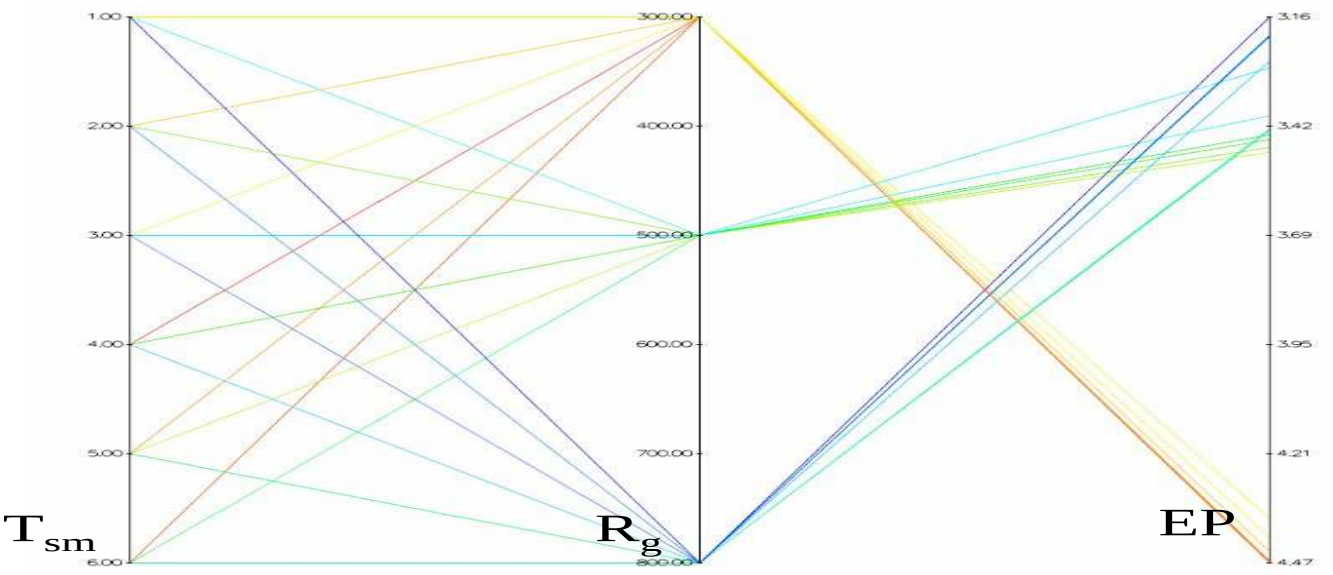

(c) EEMMASMP

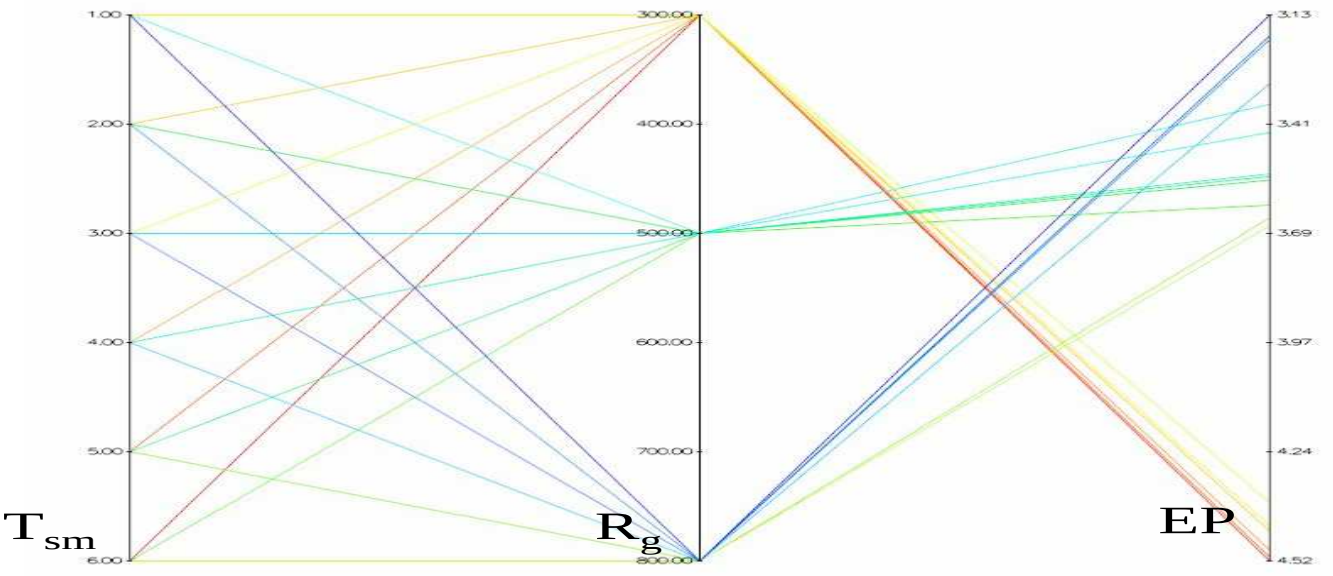

(d) EEMMASMH

Figure J.2: Influence of R_g and T_{sm} on the EP objective for $N_G = 100$ (cont.)

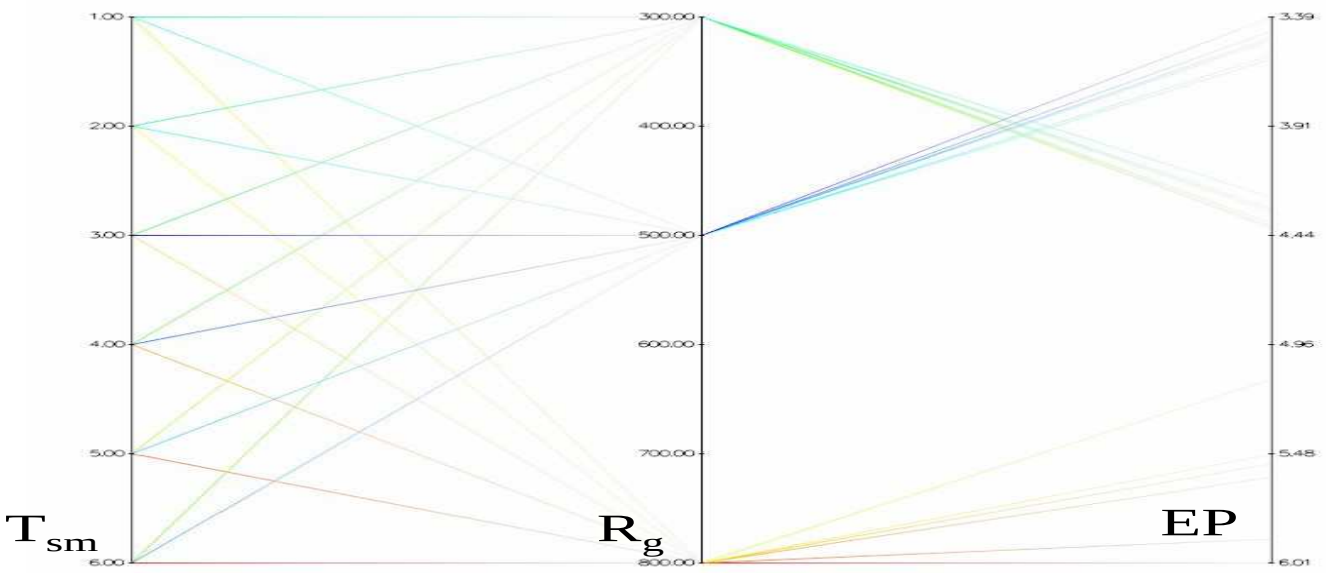

(e) EEMACOMC

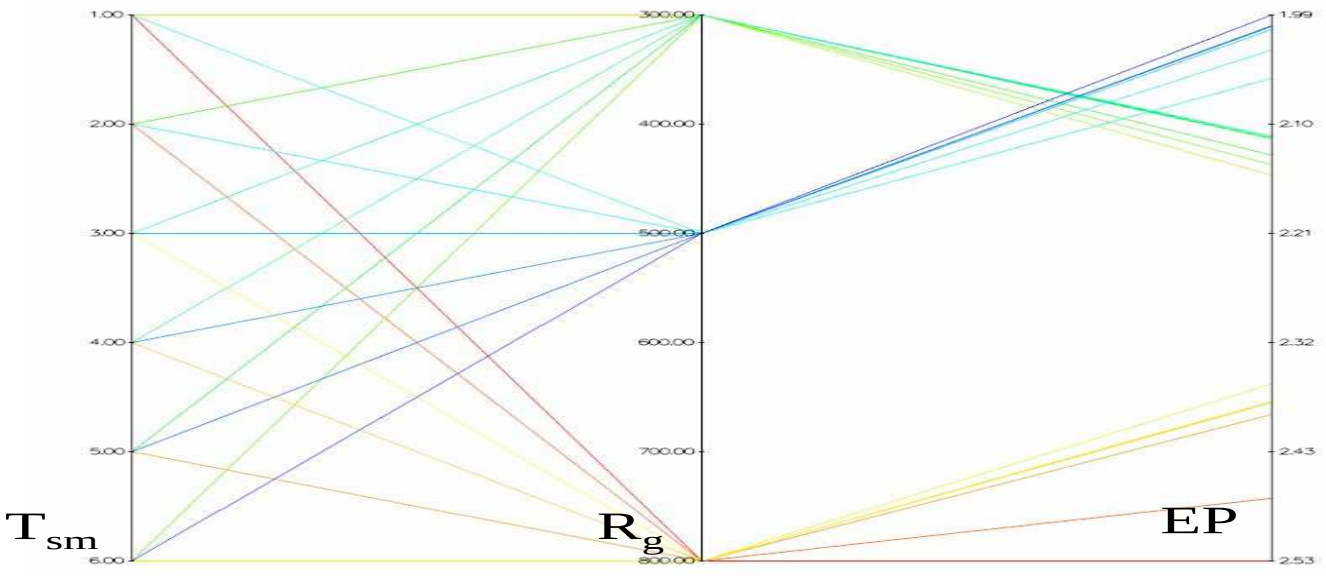

(f) NSGA-II-MPA

Figure J.2: Influence of R_g and T_{sm} on the EP objective for $N_G = 100$ (cont.)

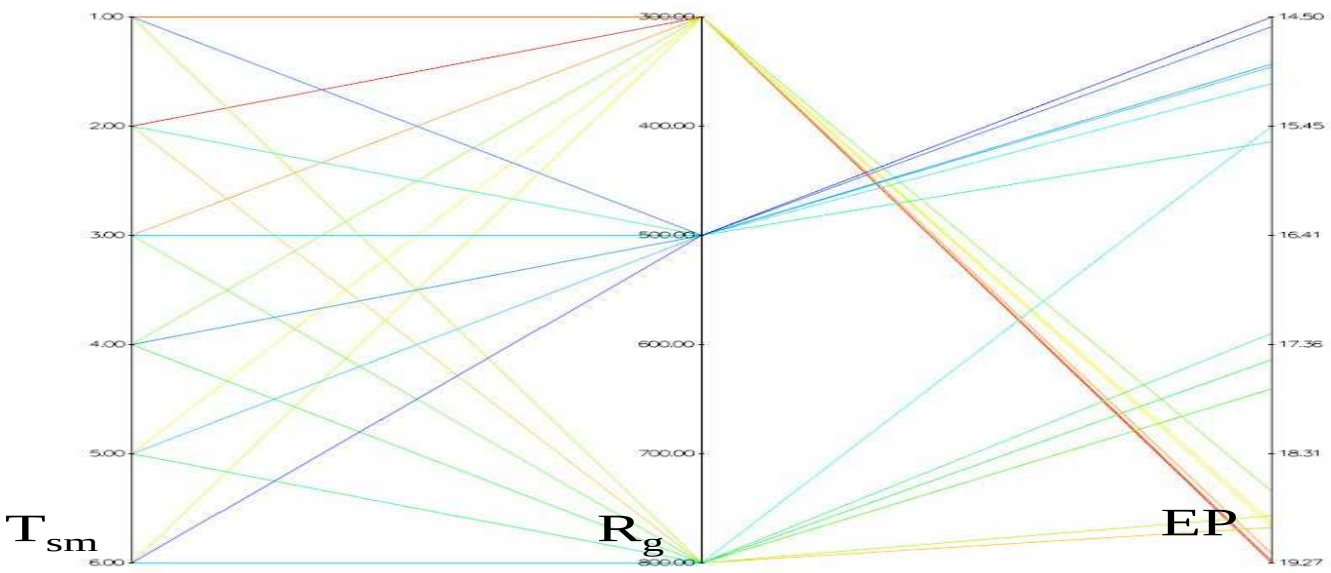

(a) EEMACOMP

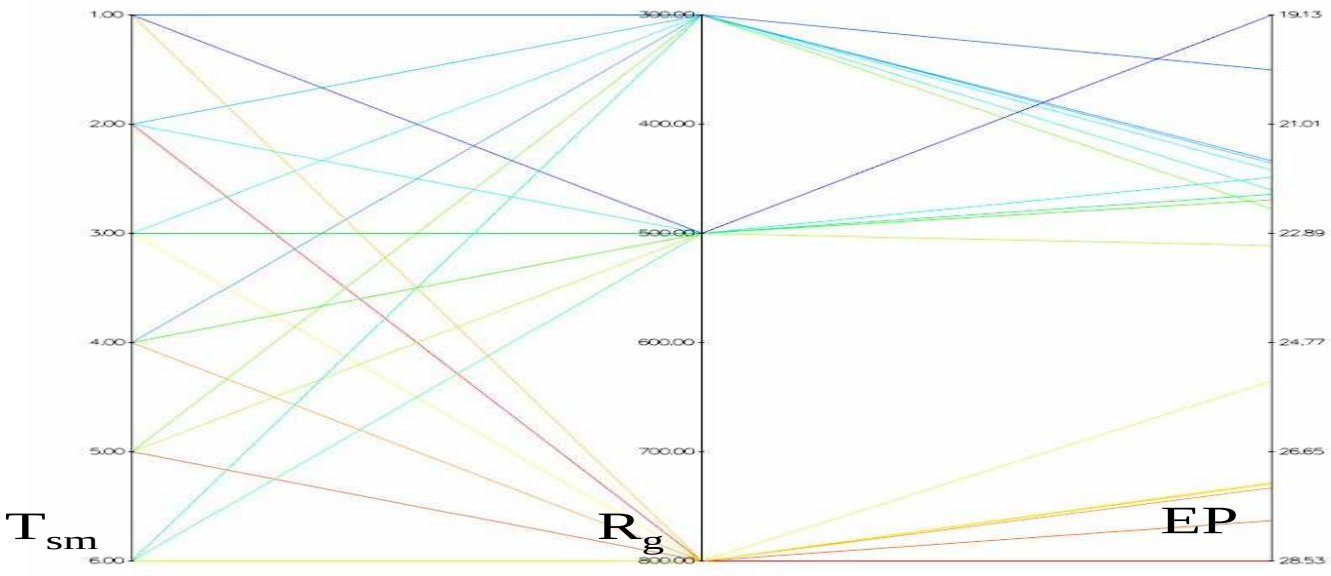

(b) EEMACOMH

Figure J.3: Influence of R_g and T_{sm} on the EP objective for $N_G = 300$

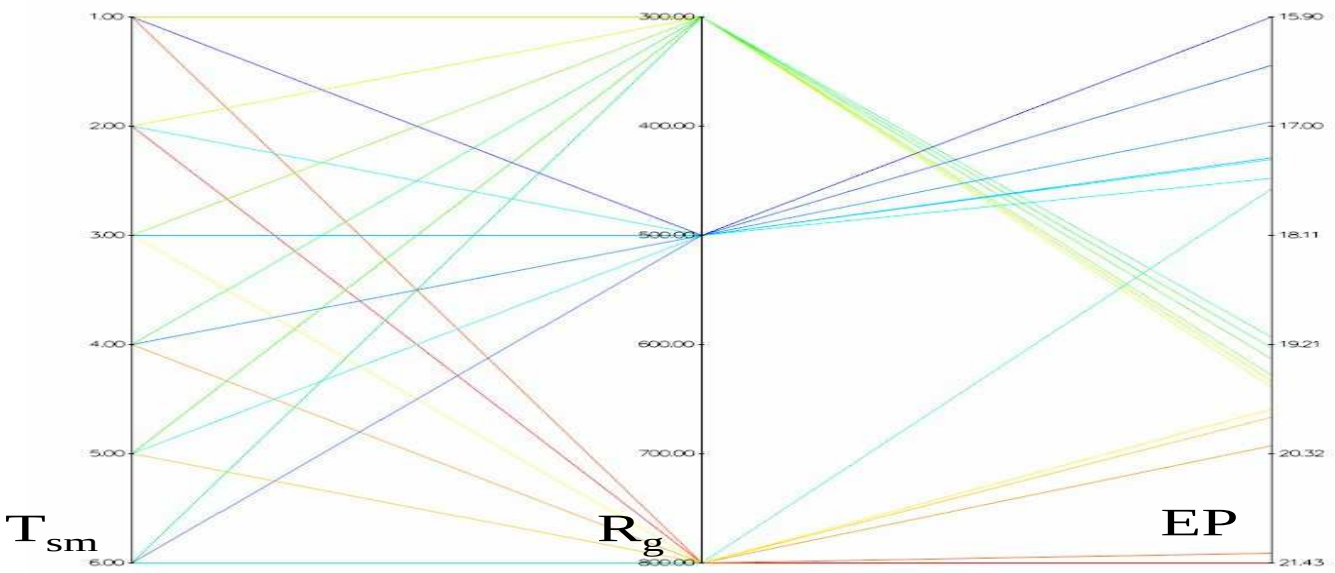

(c) EEMMASMP

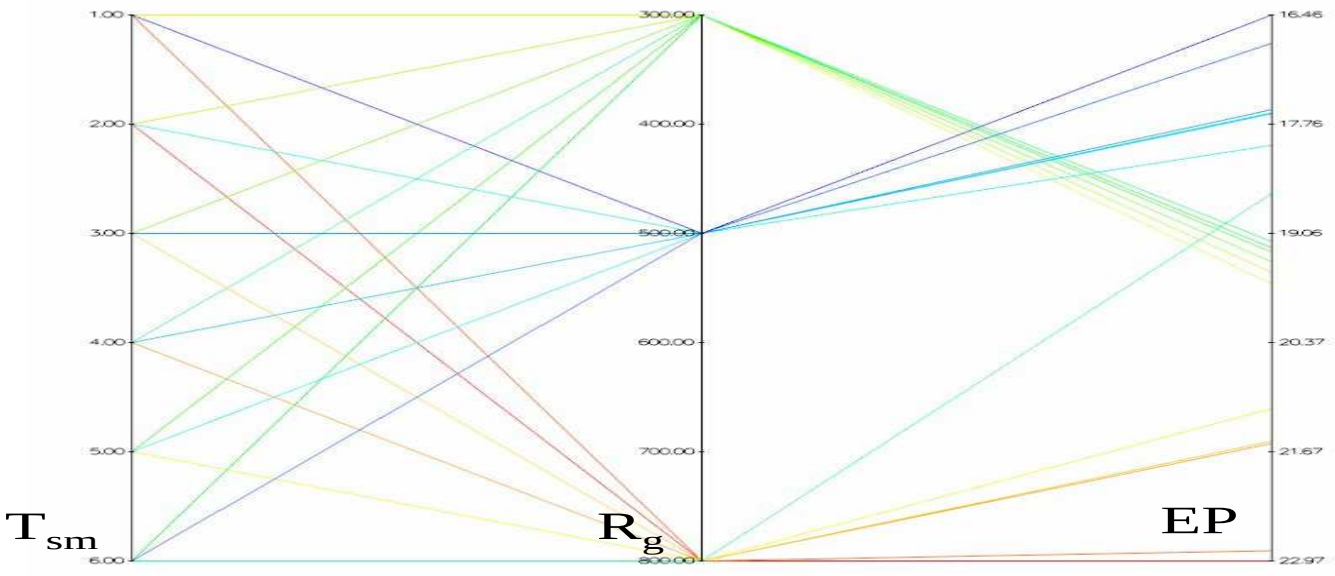

(d) EEMMASMH

Figure J.3: Influence of R_g and T_{sm} on the EP objective for $N_G = 300$ (cont.)

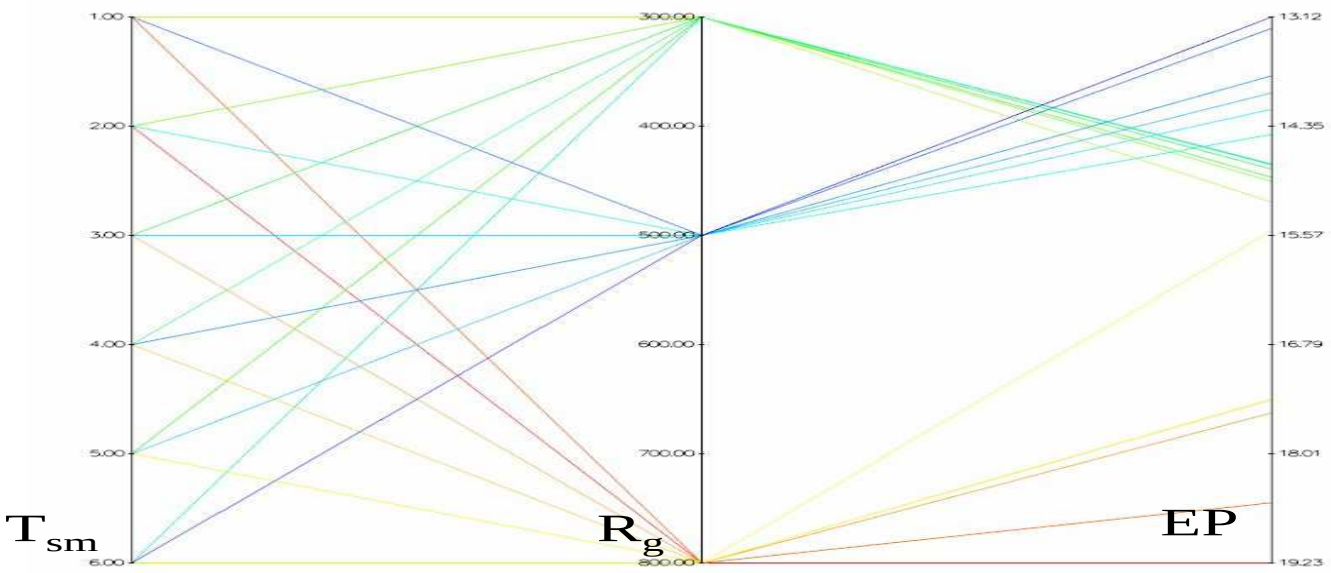

(e) EEMACOMC

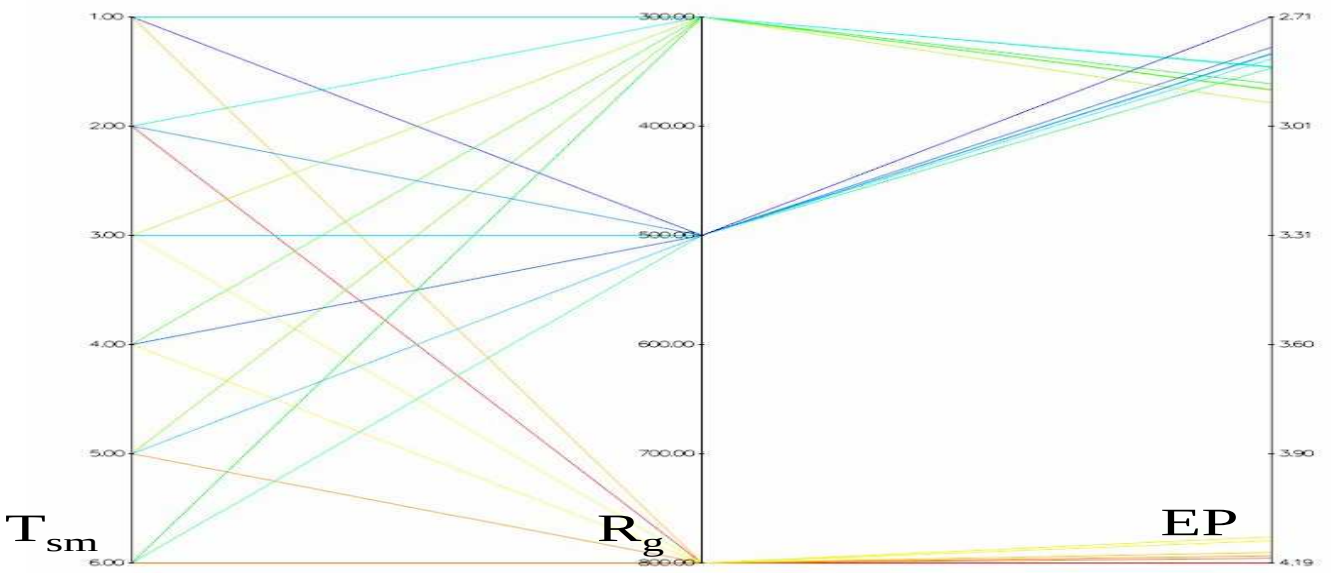

(f) NSGA-II-MPA

Figure J.3: Influence of R_g and T_{sm} on the EP objective for $N_G = 300$ (cont.)

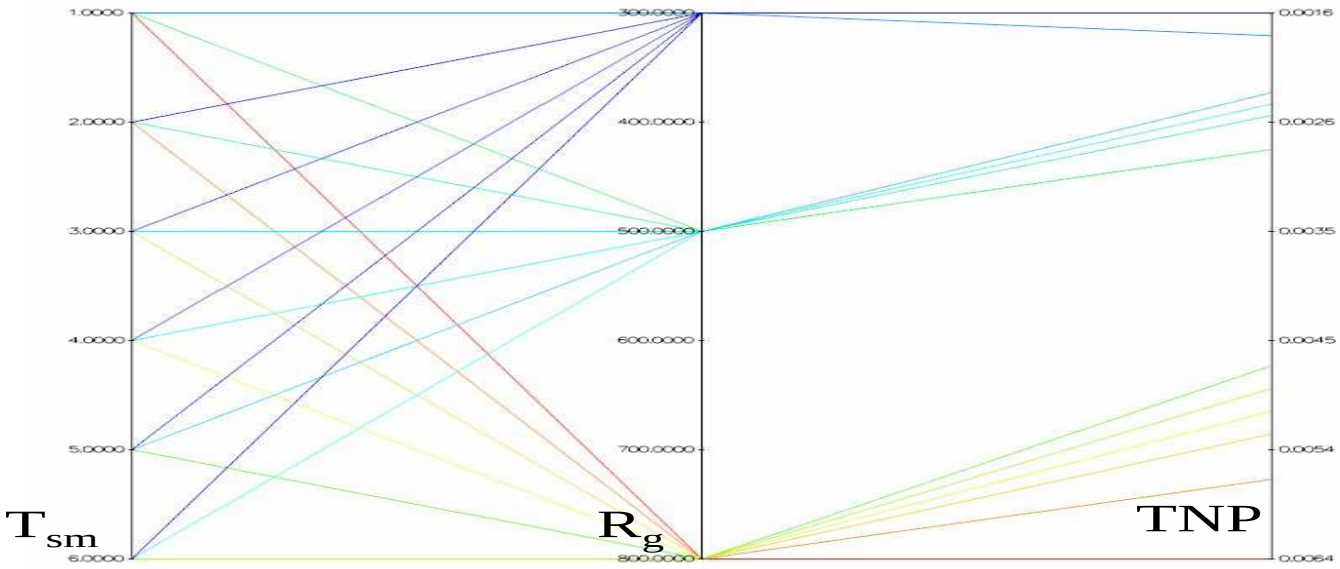

(a) EEMACOMP

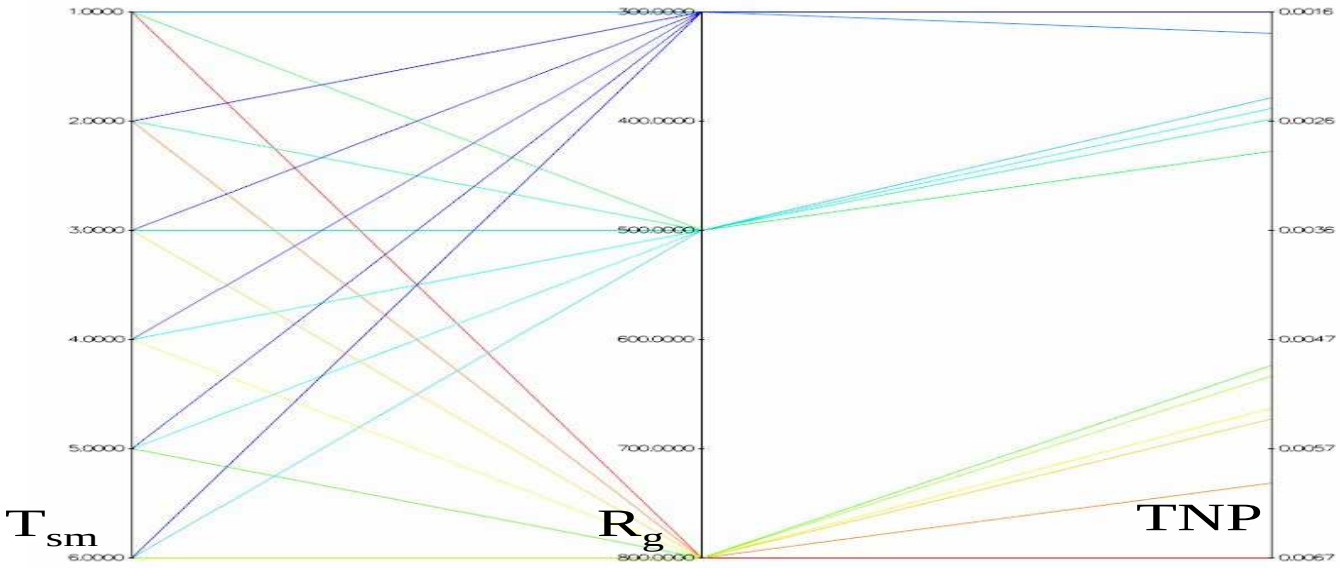

(b) EEMACOMH

Figure J.4: Influence of R_g and T_{sm} on the TNP objective for $N_G = 30$

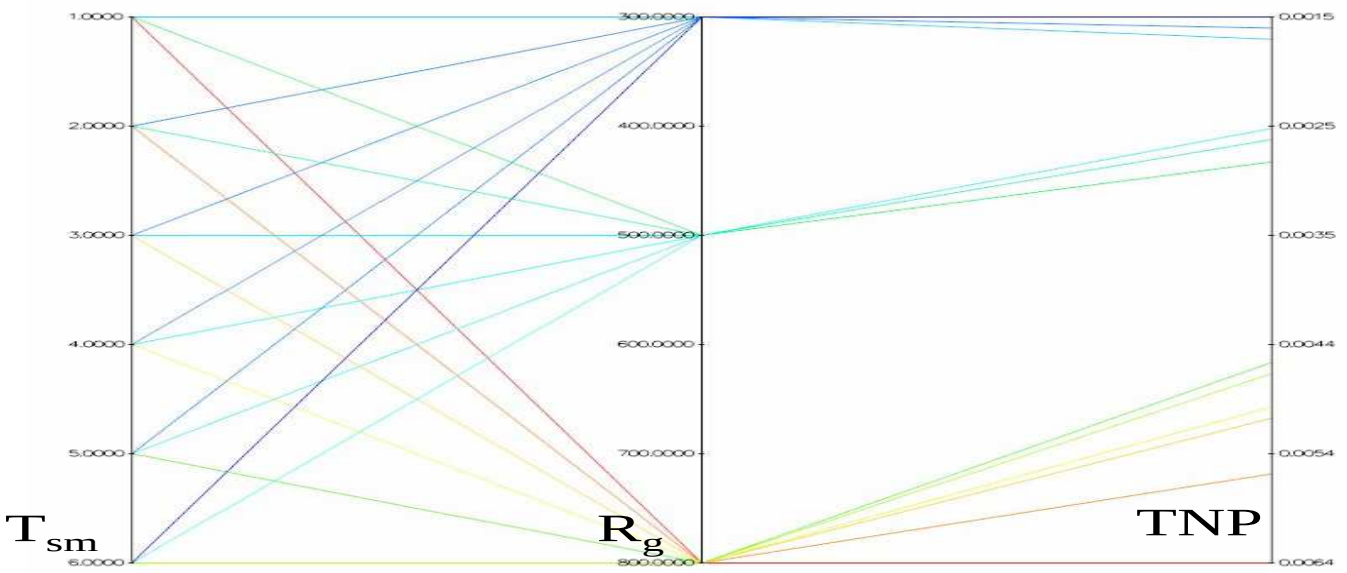

(c) EEMMASMP

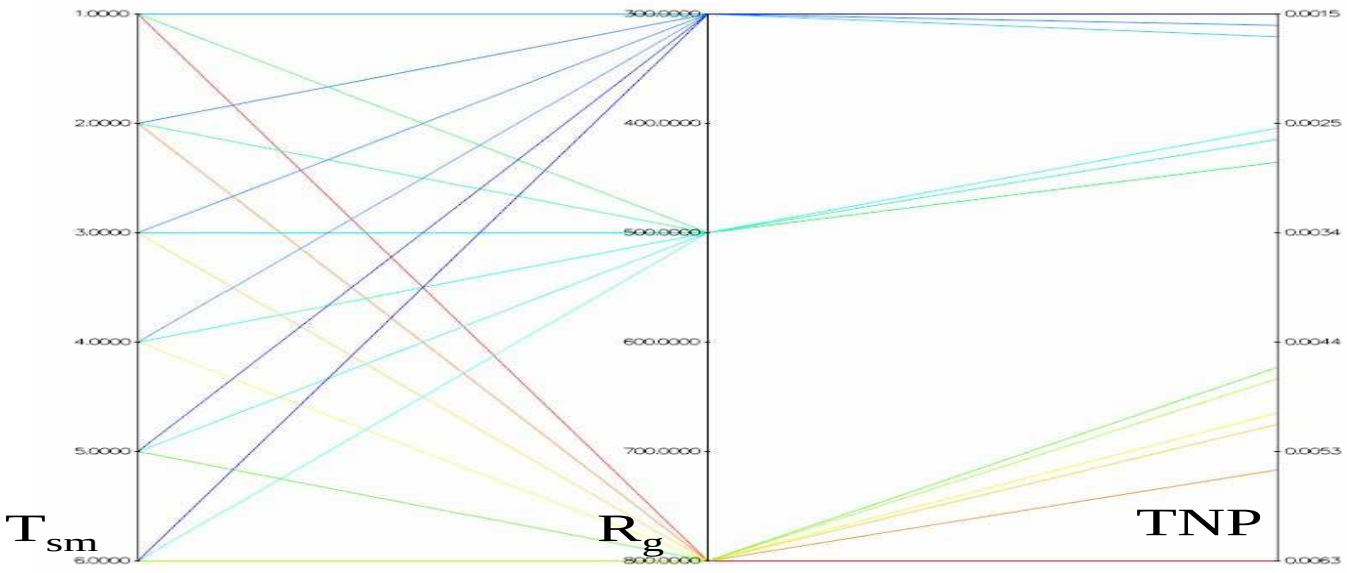

(d) EEMMASMH

Figure J.4: Influence of R_g and T_{sm} on the TNP objective for $N_G = 30$ (cont.)

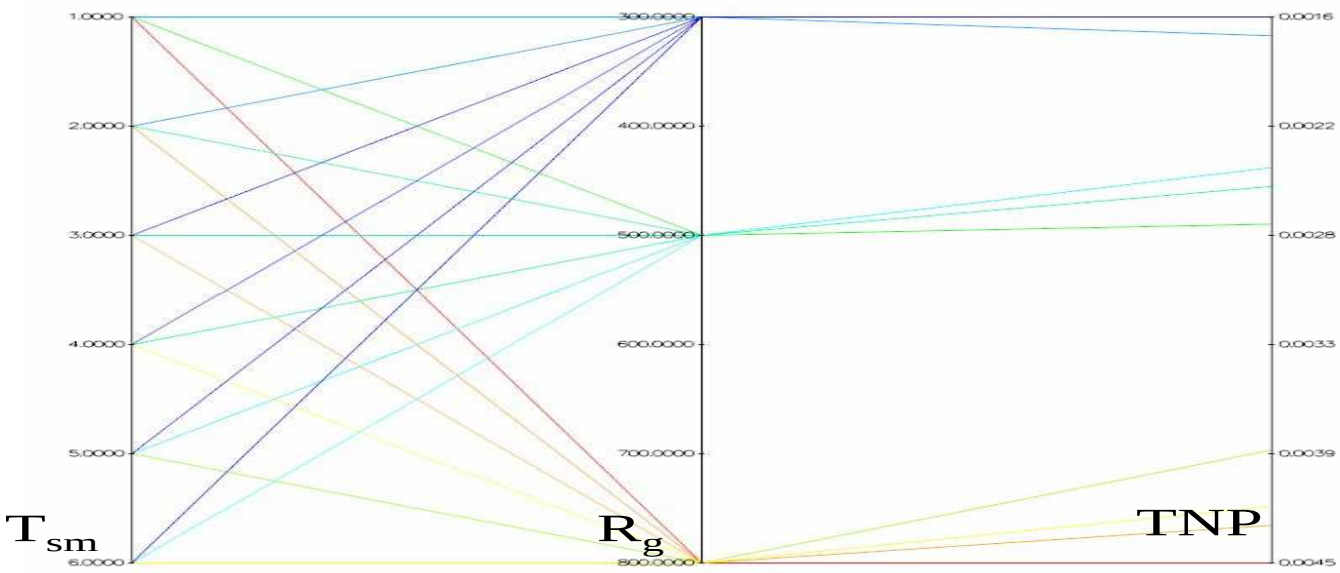

(e) EEMACOMC

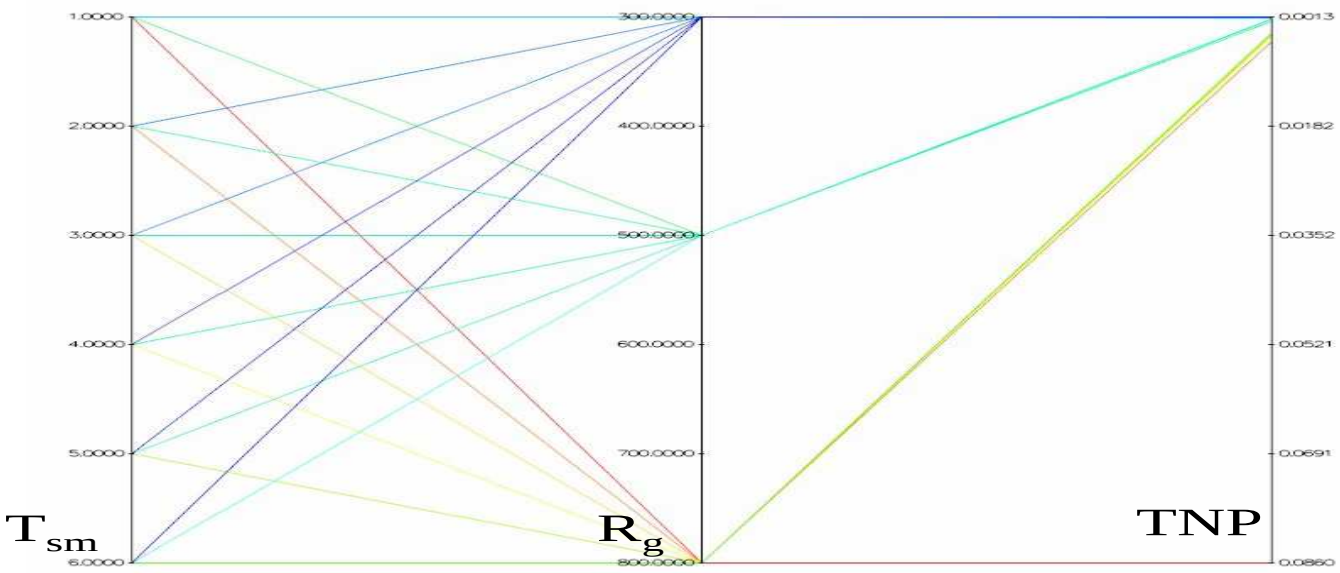

(f) NSGA-II-MPA

Figure J.4: Influence of R_g and T_{sm} on the TNP objective for $N_G = 30$ (cont.)

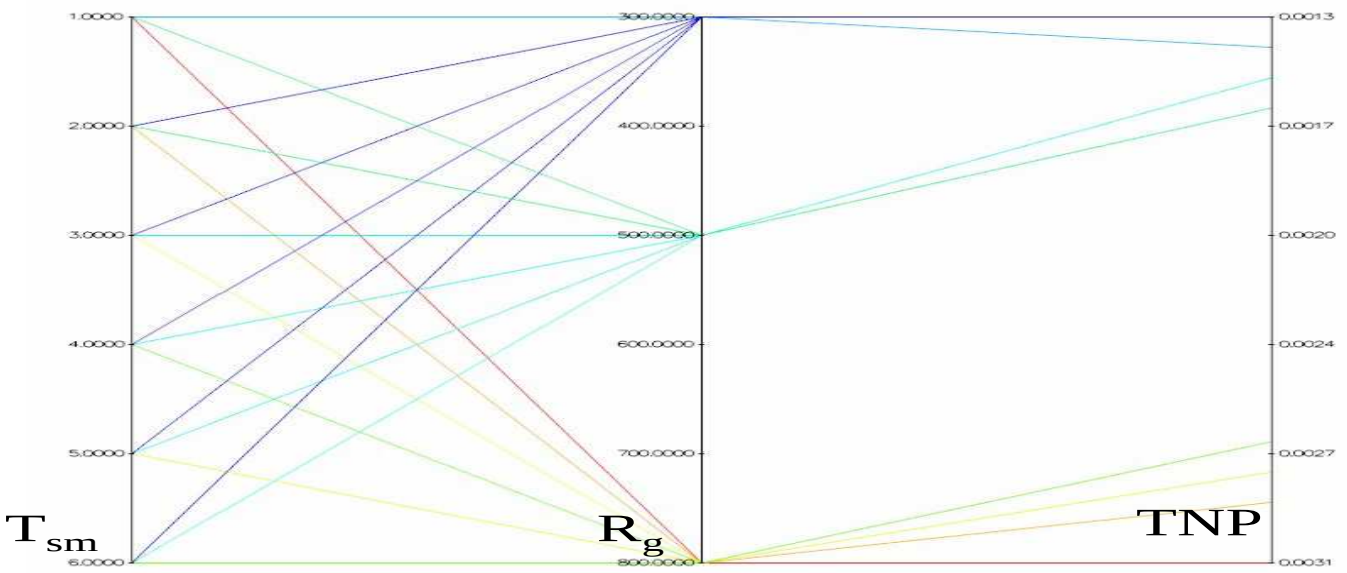

(a) EEMACOMP

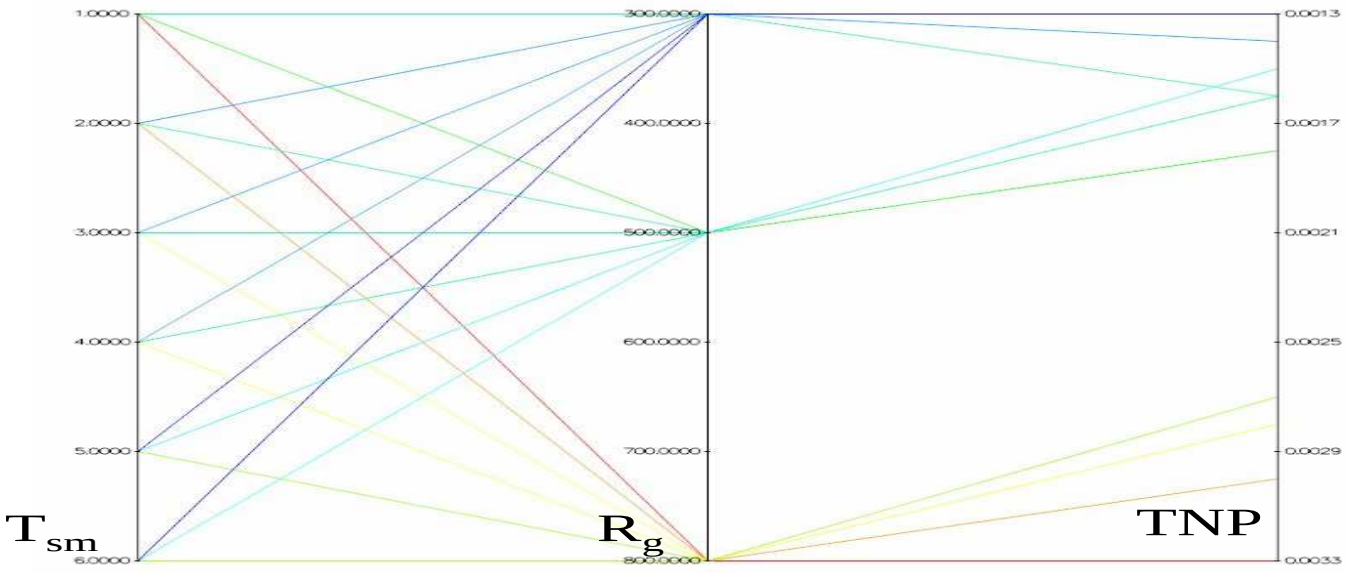

(b) EEMACOMH

Figure J.5: Influence of R_g and T_{sm} on the TNP objective for $N_G = 100$

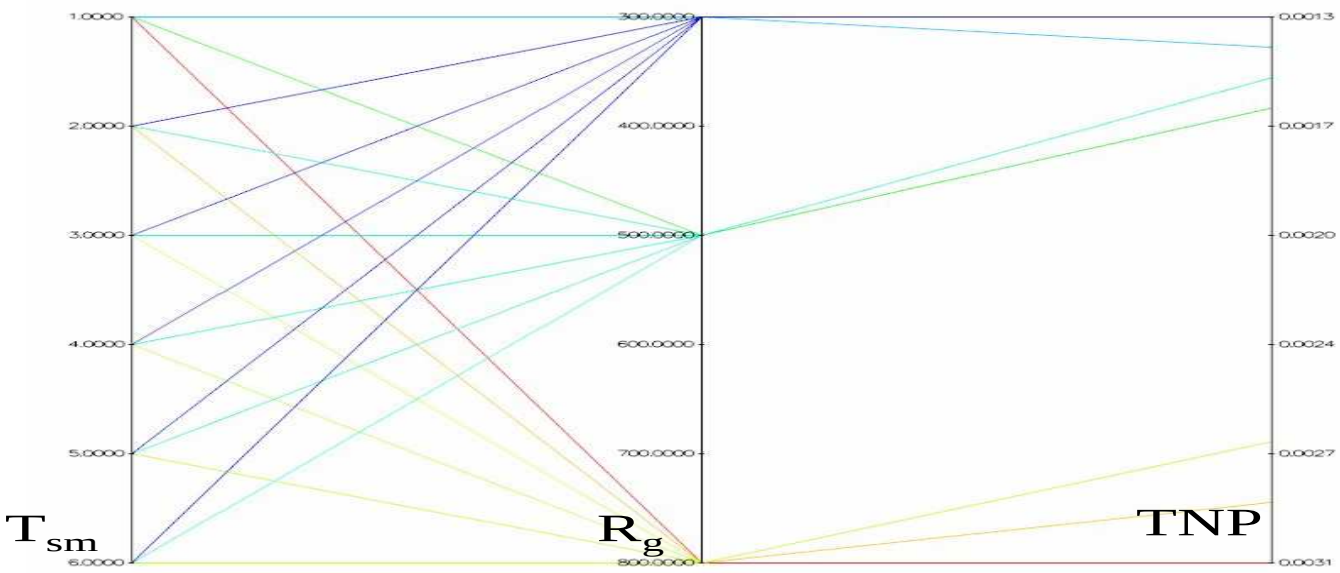

(c) EEMMASMP

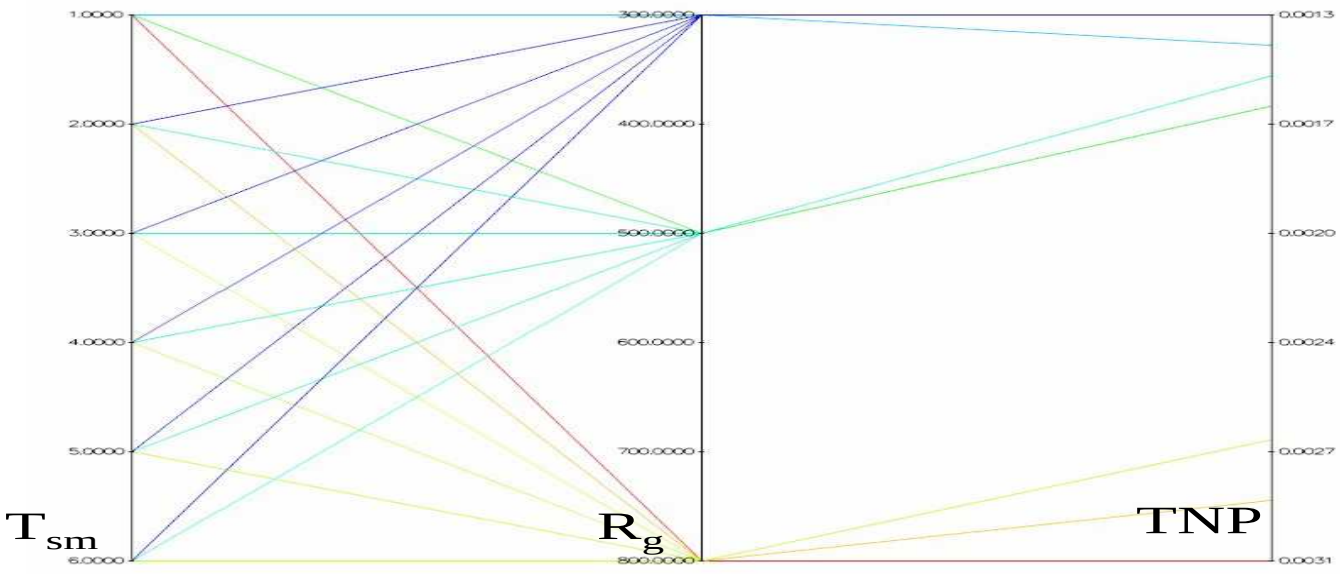

(d) EEMMASMH

Figure J.5: Influence of R_g and T_{sm} on the TNP objective for $N_G = 100$ (cont.)

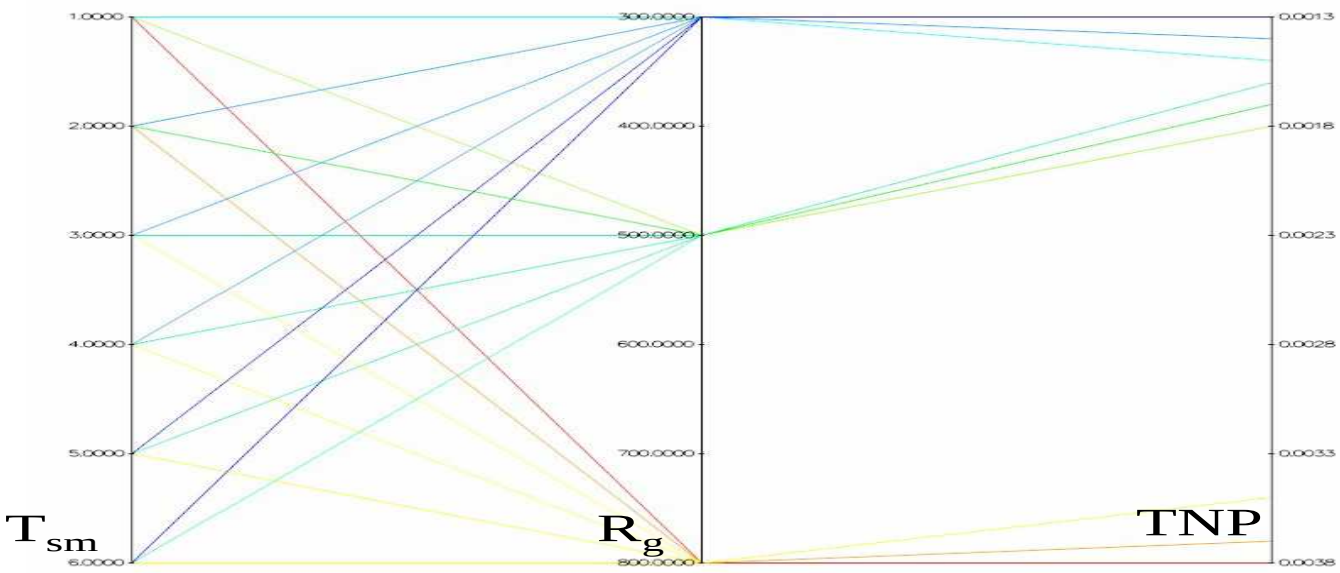

(e) EEMACOMC

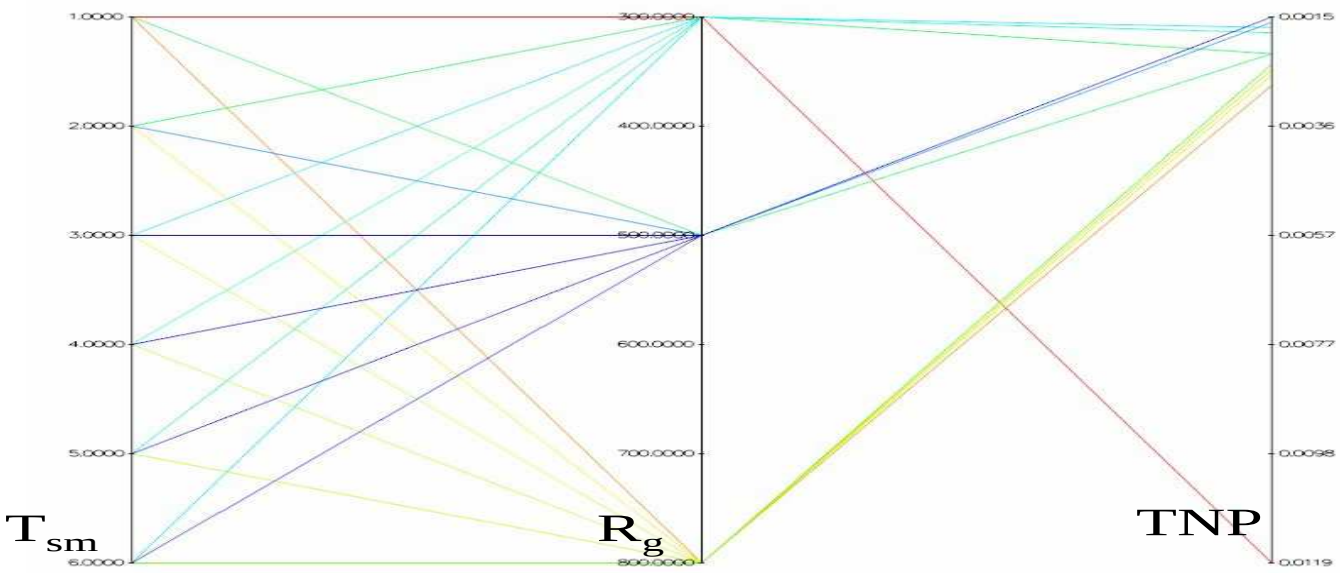

(f) NSGA-II-MPA

Figure J.5: Influence of R_g and T_{sm} on the TNP objective for $N_G = 100$ (cont.)

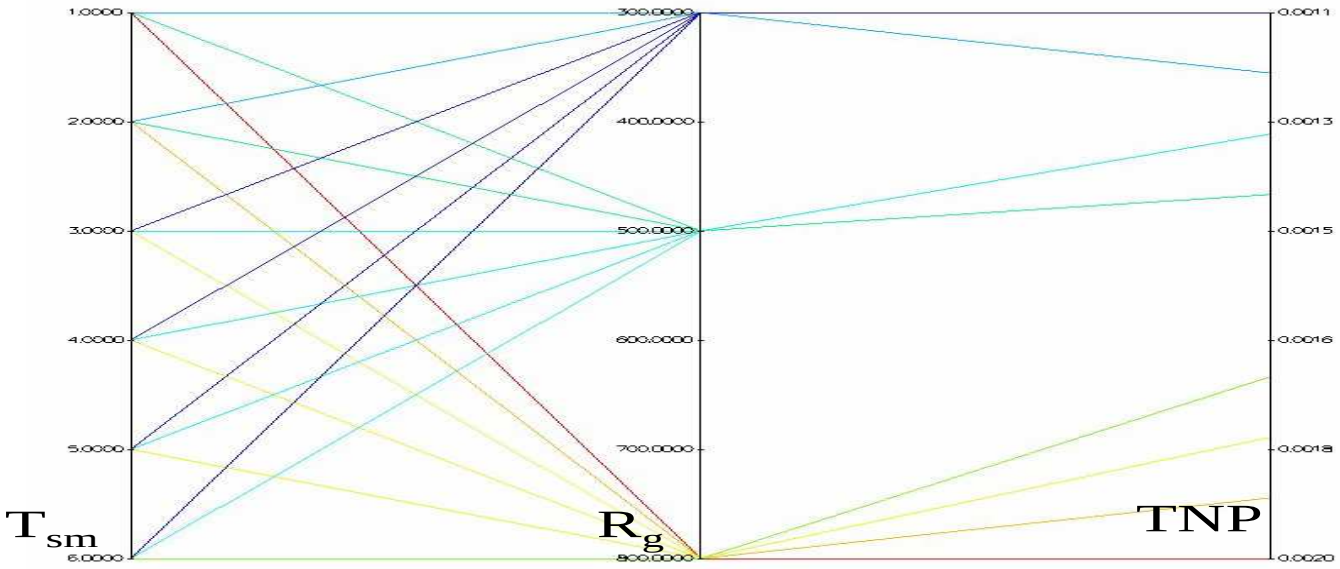

(a) EEMACOMP

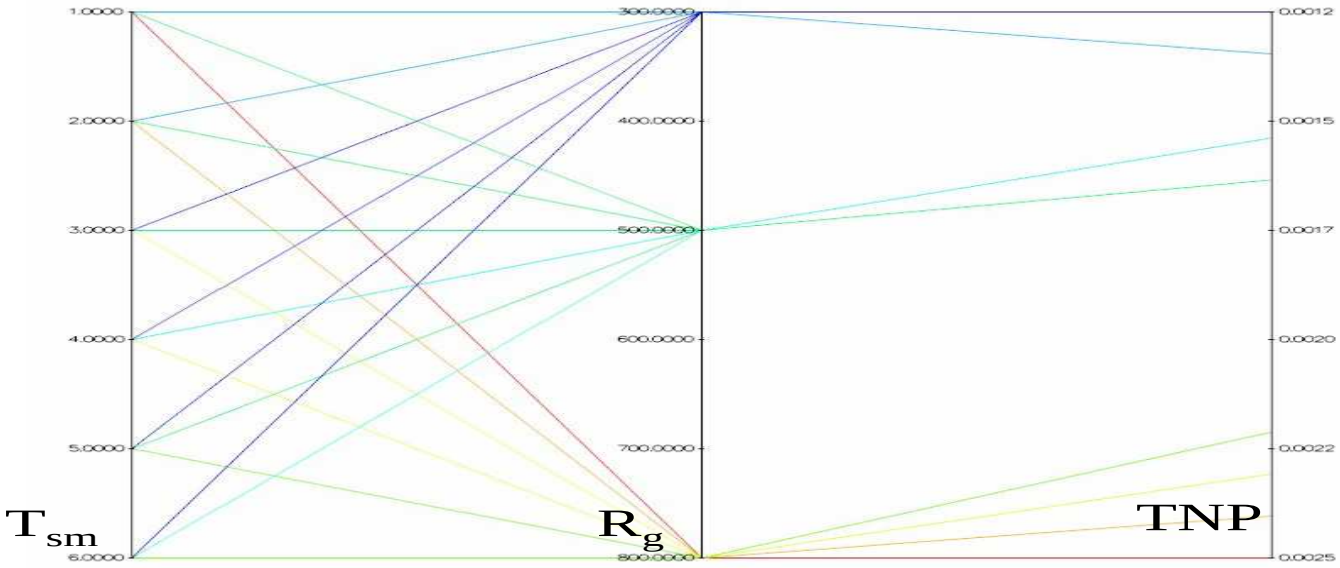

(b) EEMACOMH

Figure J.6: Influence of R_g and T_{sm} on the TNP objective for $N_G = 300$

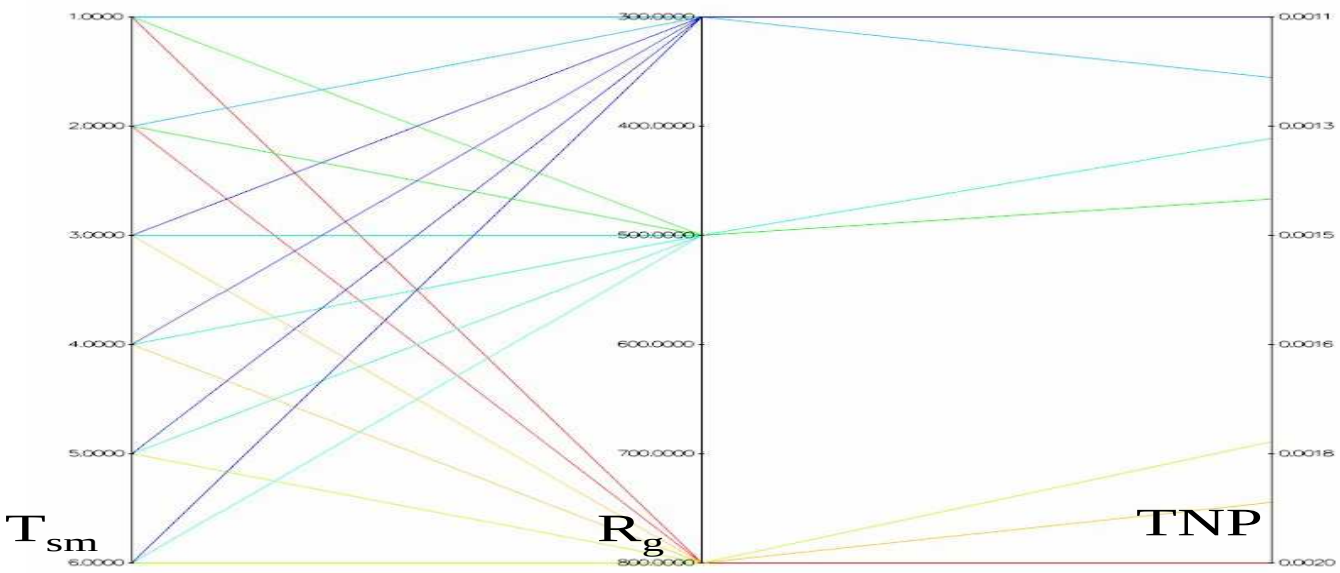

(c) EEMMASMP

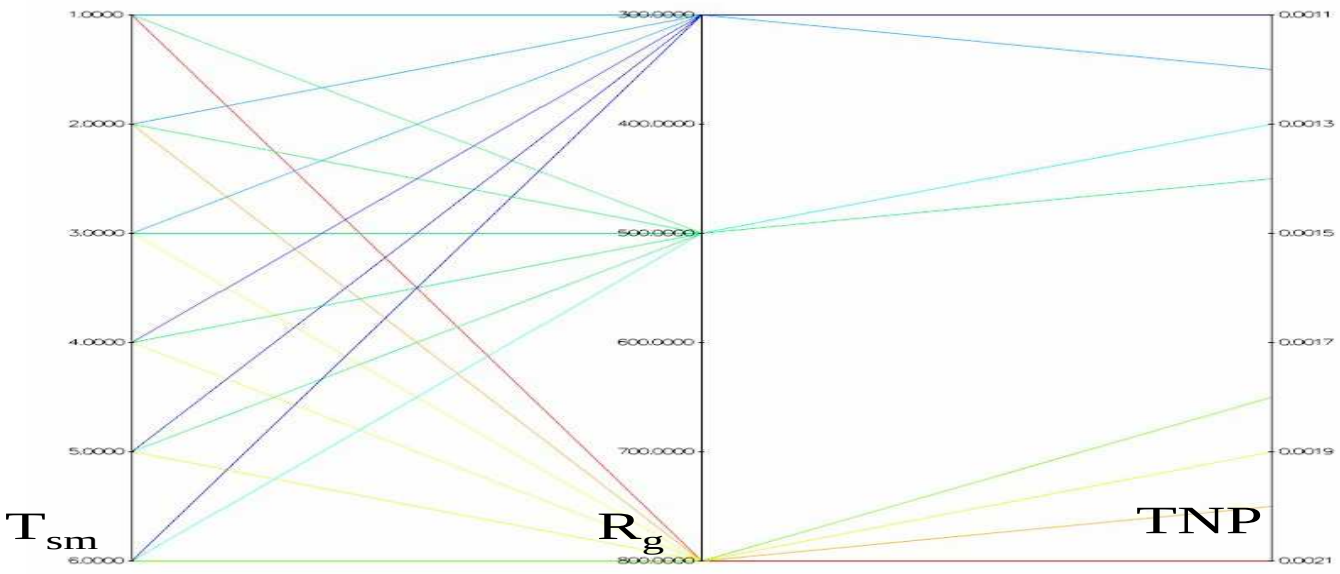

(d) EEMMASMH

Figure J.6: Influence of R_g and T_{sm} on the TNP objective for $N_G = 300$ (cont.)

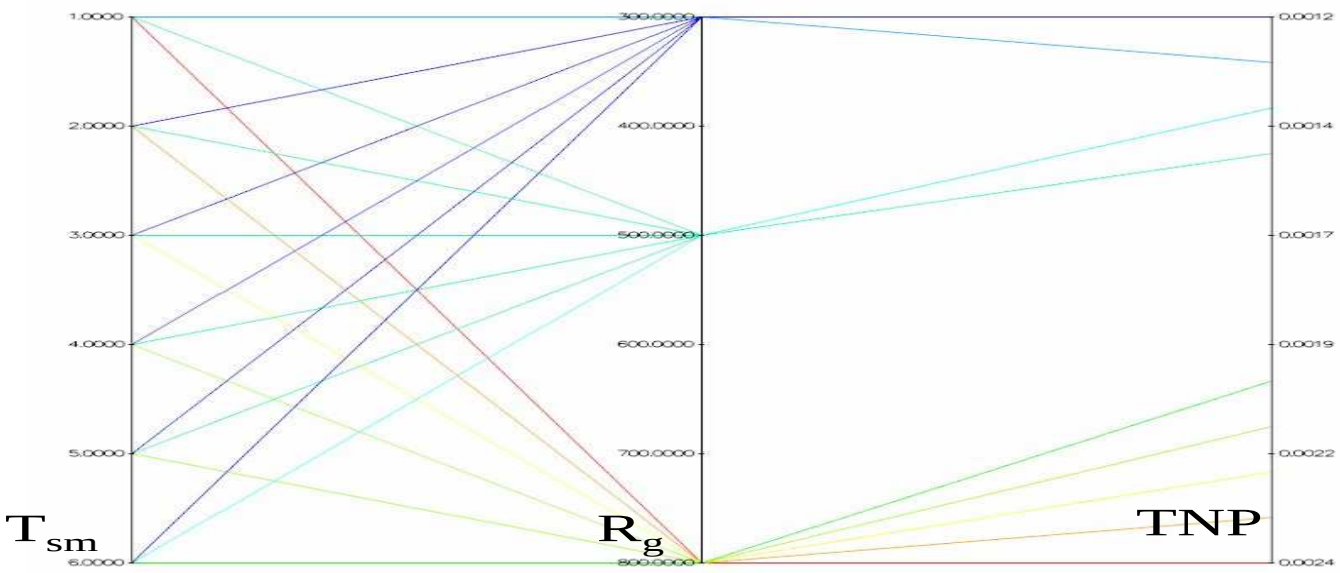

(e) EEMACOMC

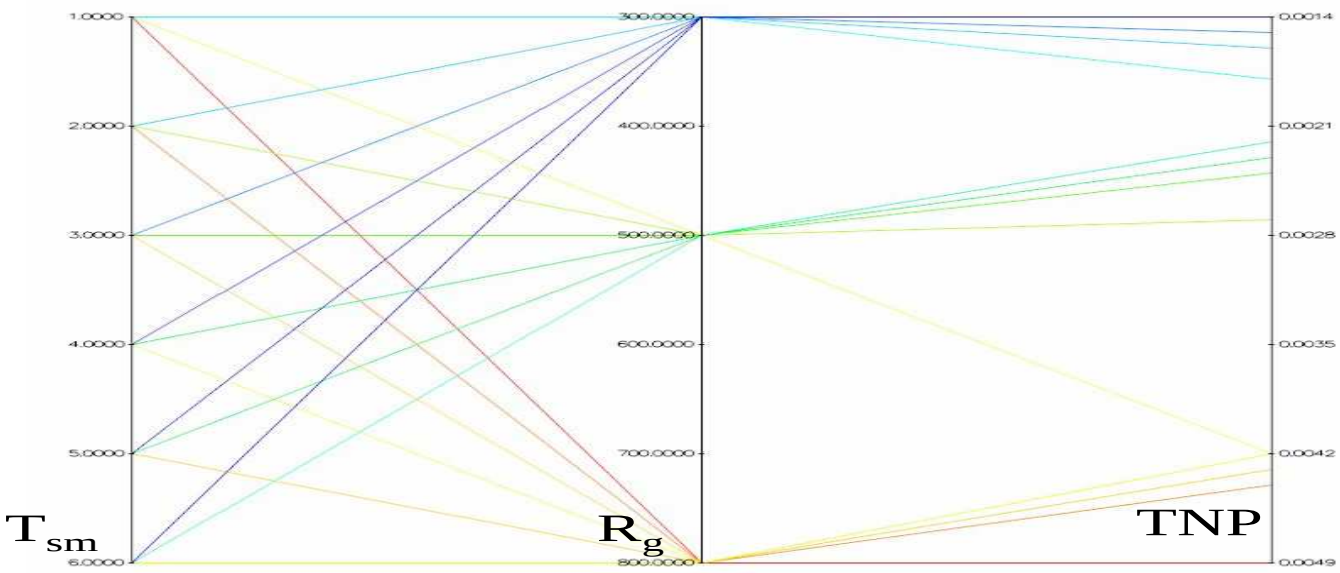

(f) NSGA-II-MPA

Figure J.6: Influence of R_g and T_{sm} on the TNP objective for $N_G = 300$ (cont.)

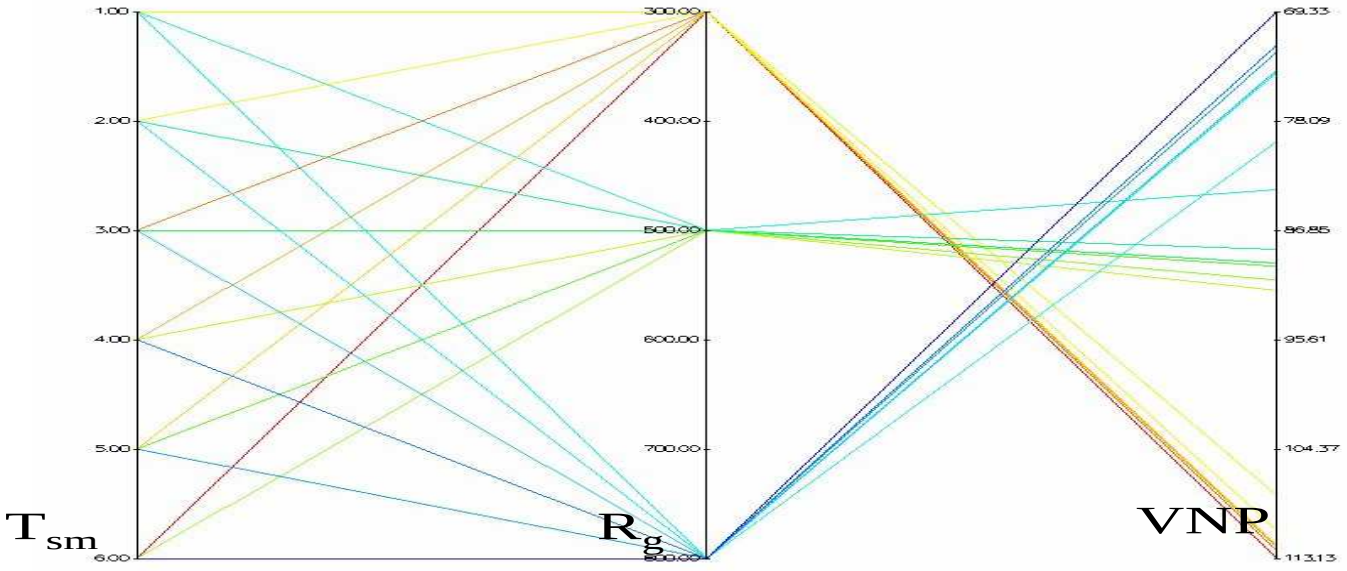

(a) EEMACOMP

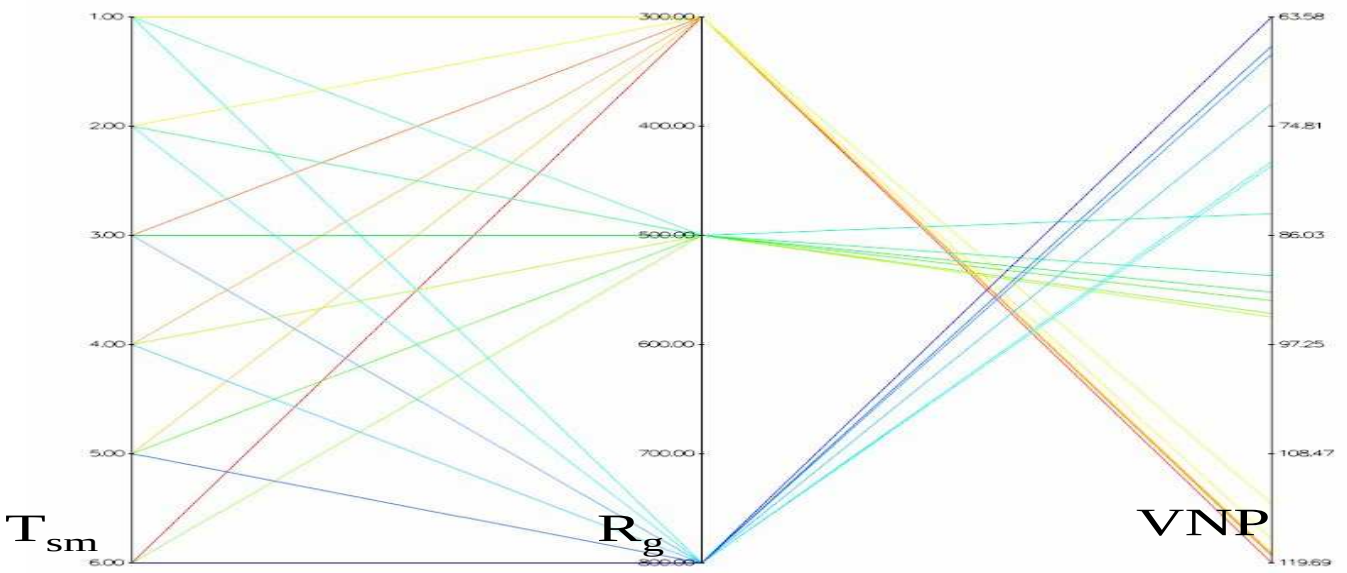

(b) EEMACOMH

Figure J.7: Influence of R_g and T_{sm} on the VNP objective for $N_G = 30$

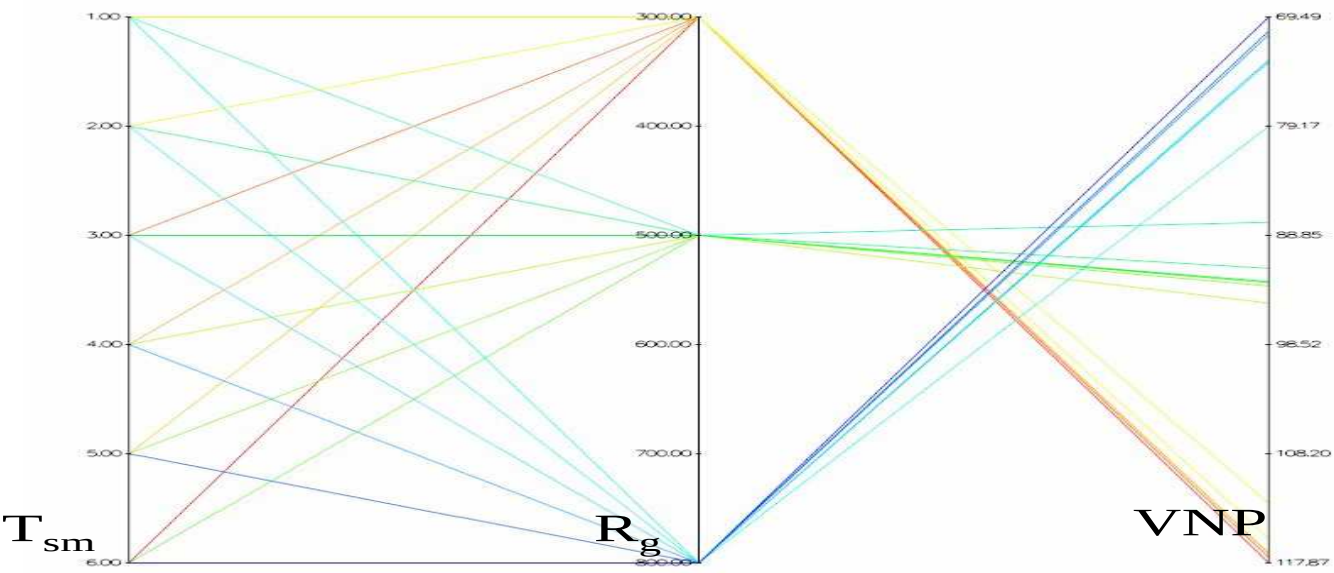

(c) EEMMASMP

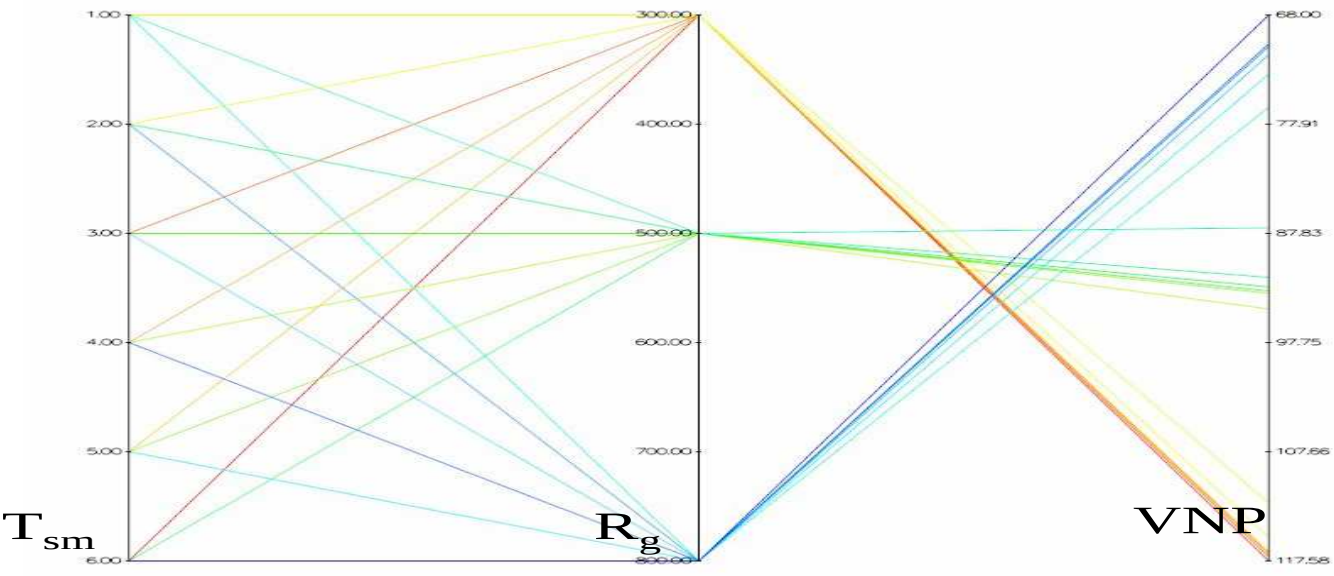

(d) EEMMASMH

Figure J.7: Influence of R_g and T_{sm} on the VNP objective for $N_G = 30$ (cont.)

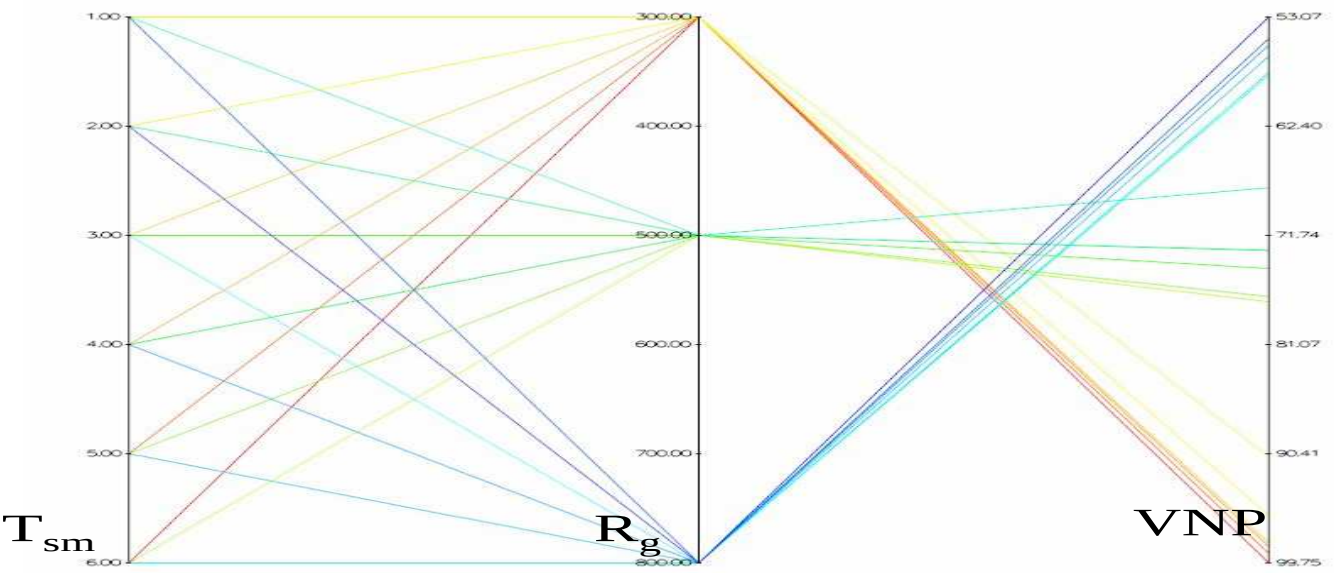

(e) EEMACOMC

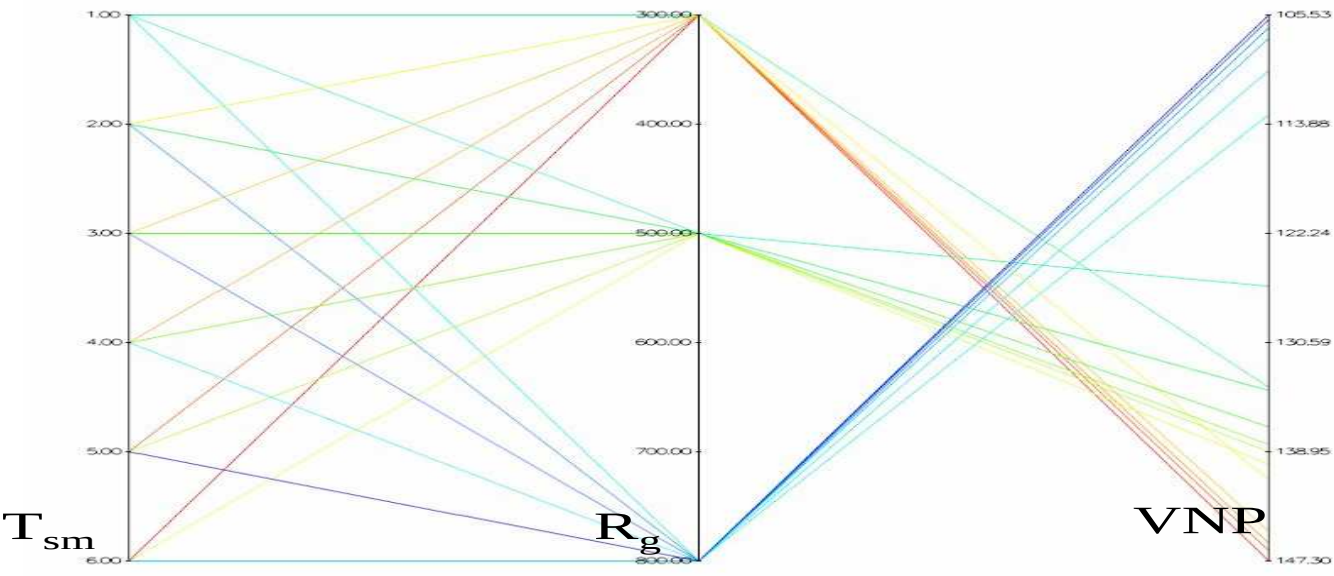

(f) NSGA-II-MPA

Figure J.7: Influence of R_g and T_{sm} on the VNP objective for $N_G = 30$ (cont.)

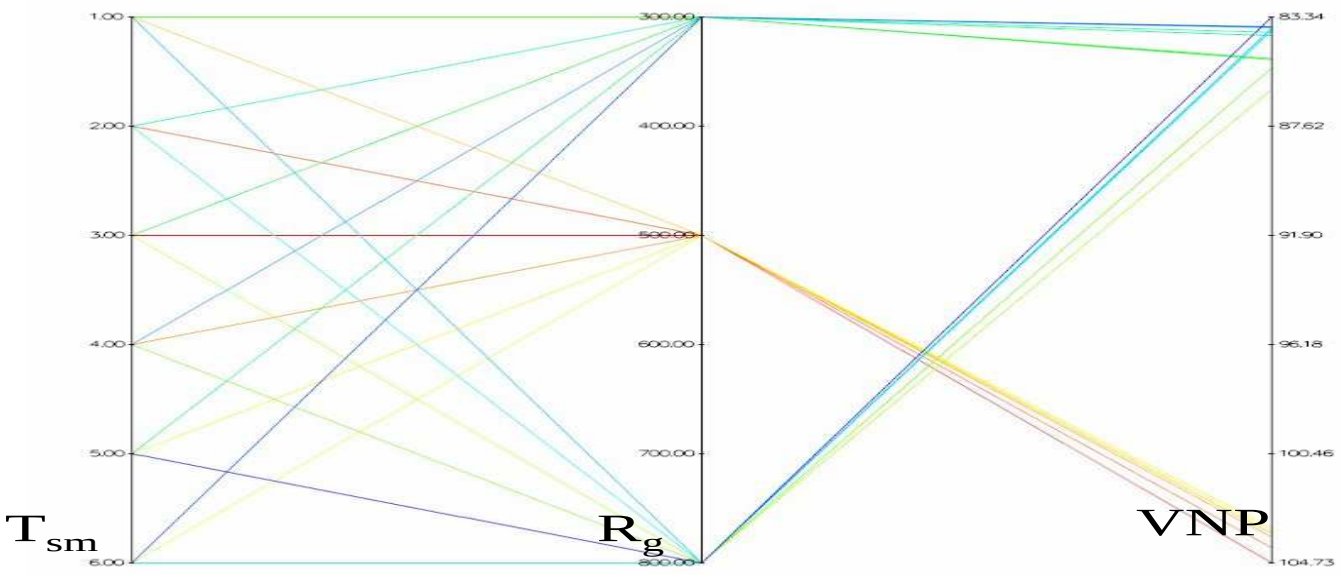

(a) EEMACOMP

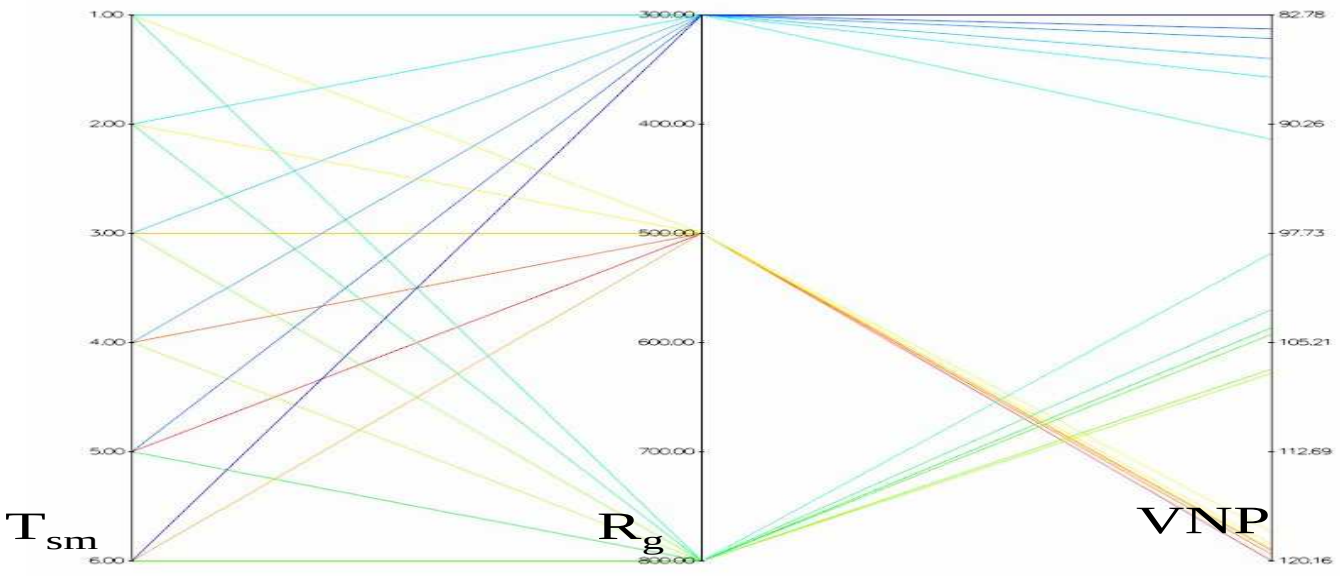

(b) EEMACOMH

Figure J.8: Influence of R_g and T_{sm} on the VNP objective for $N_G = 100$

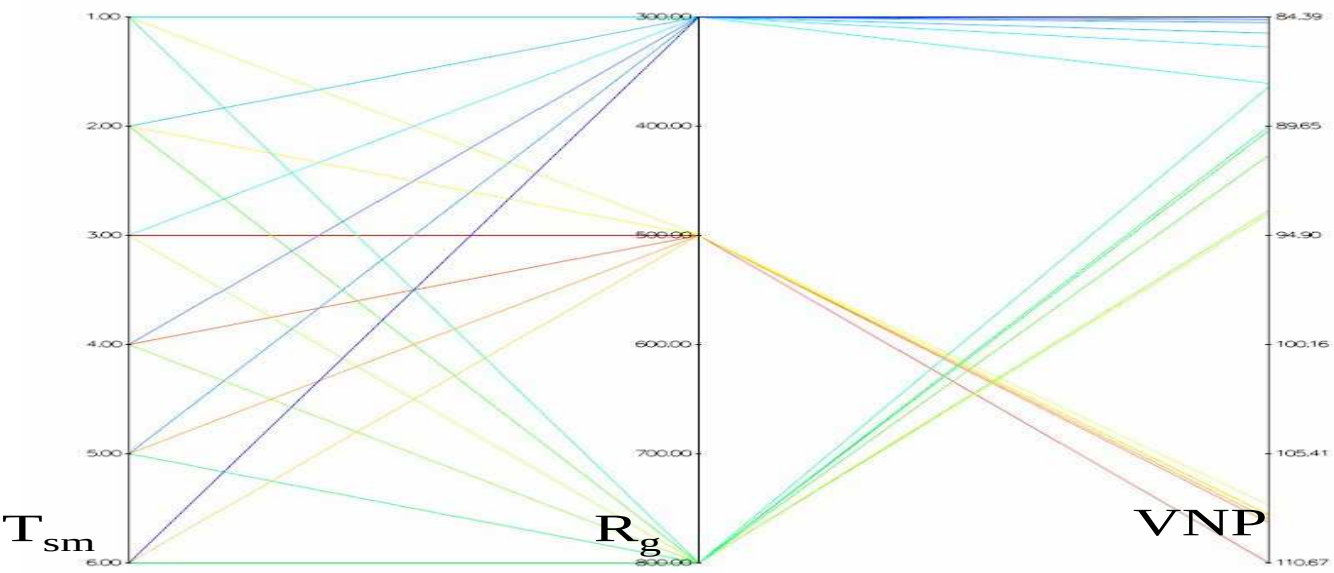

(c) EEMMASMP

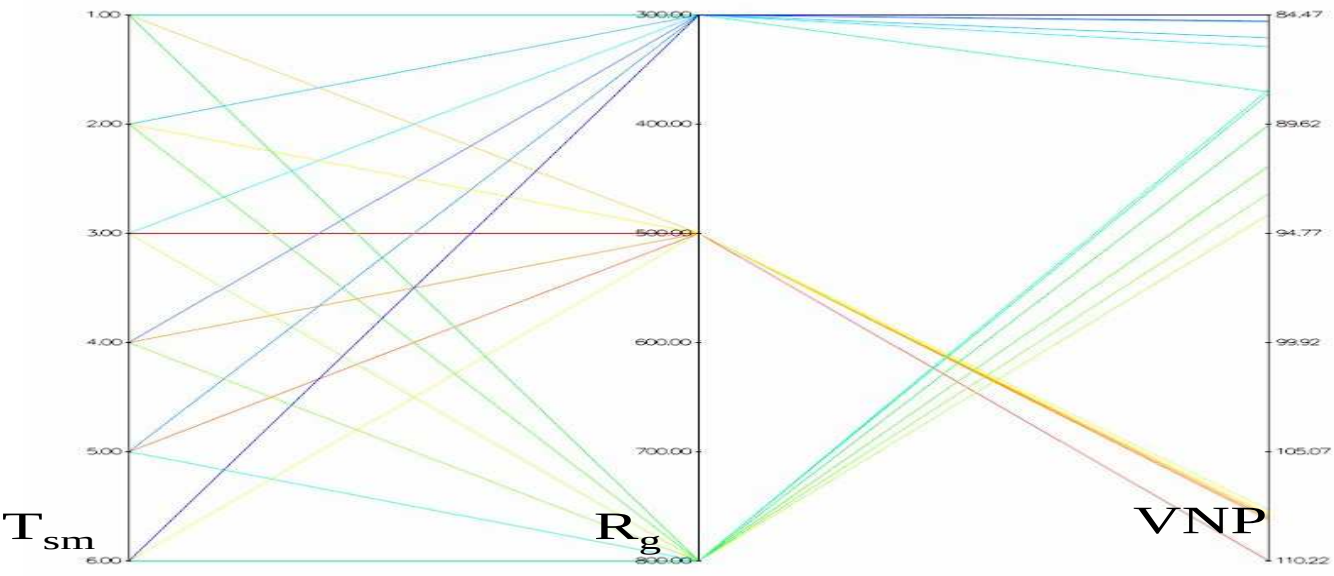

(d) EEMMASMH

Figure J.8: Influence of R_g and T_{sm} on the VNP objective for $N_G = 100$ (cont.)

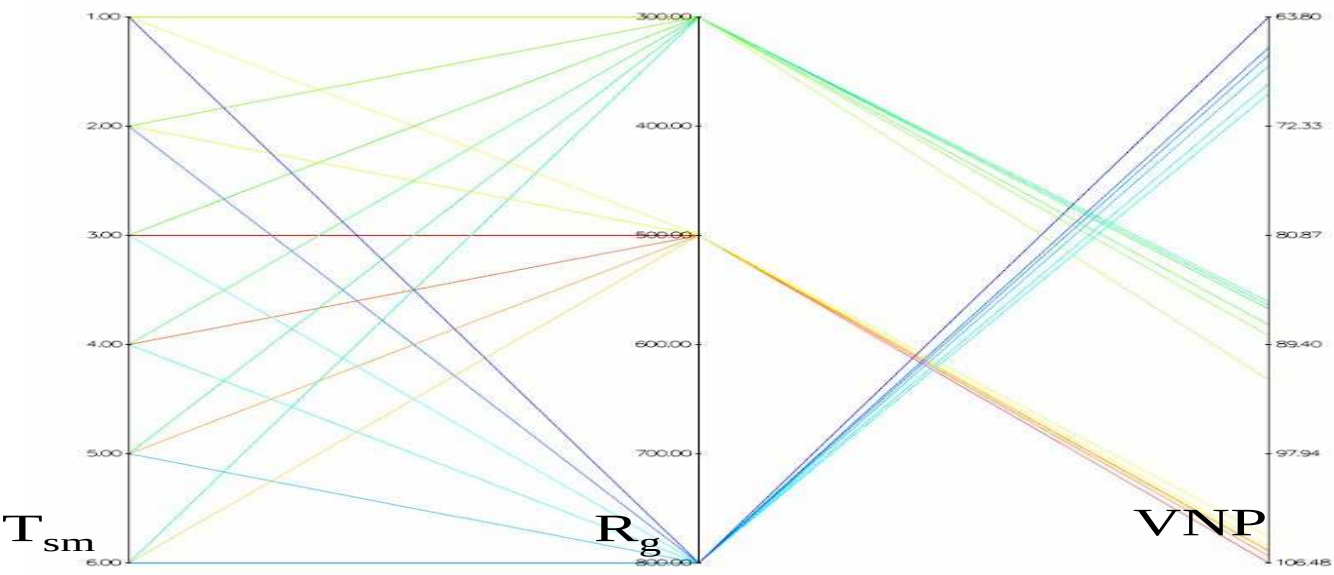

(e) EEMACOMC

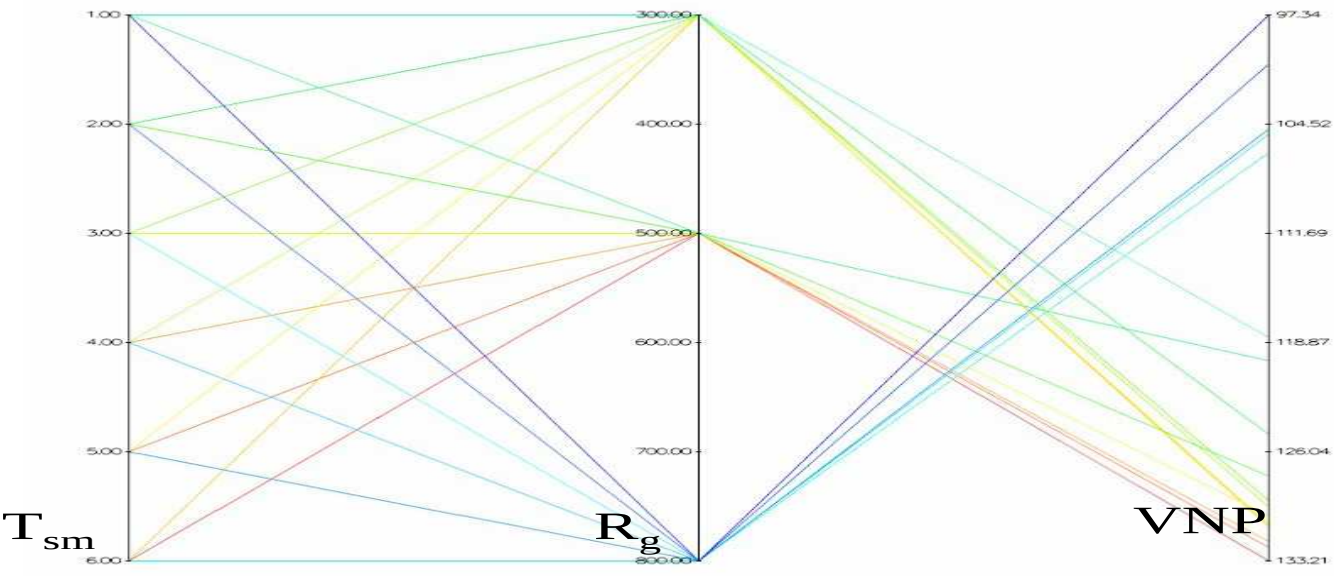

(f) NSGA-II-MPA

Figure J.8: Influence of R_g and T_{sm} on the VNP objective for $N_G = 100$ (cont.)

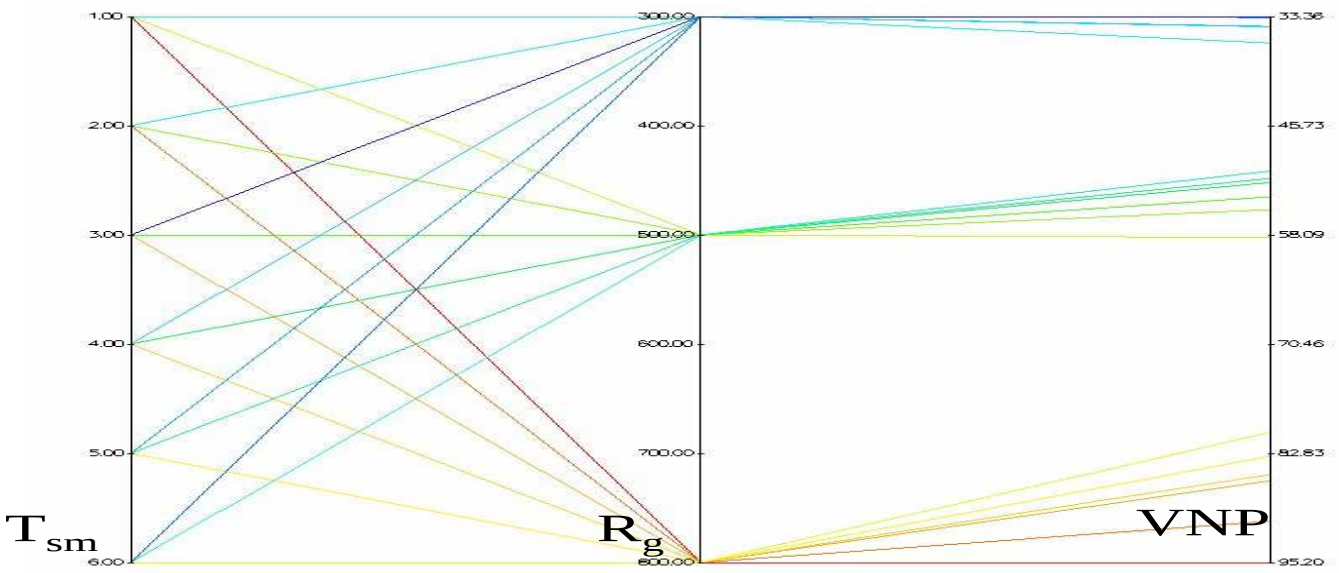

(a) EEMACOMP

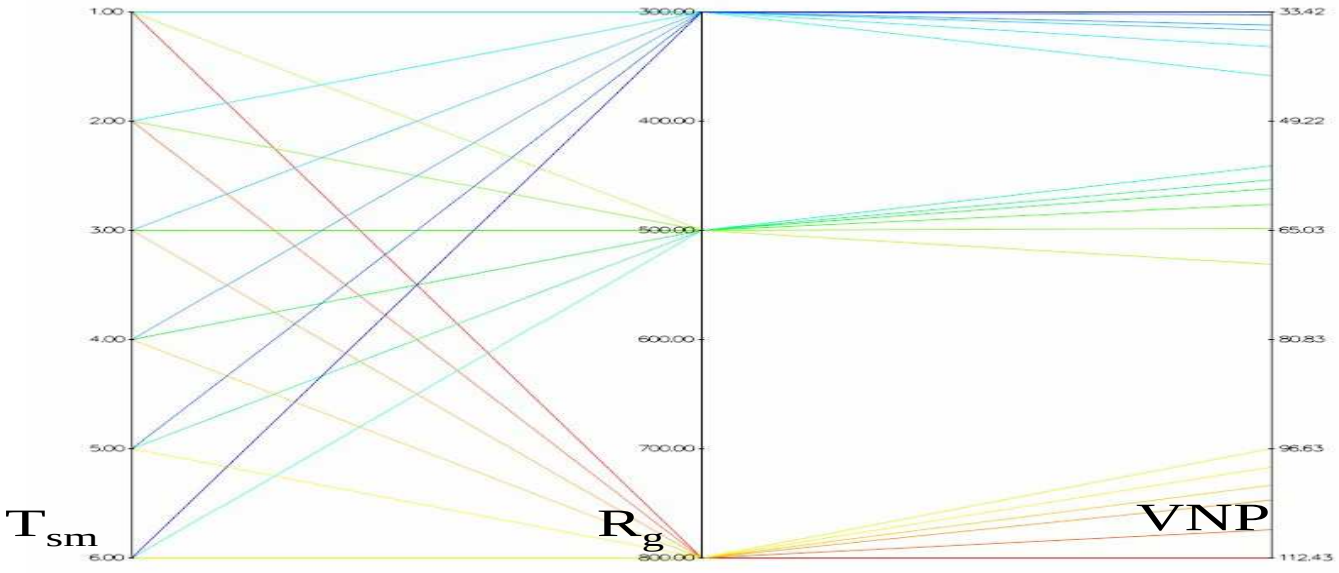

(b) EEMACOMH

Figure J.9: Influence of R_g and T_{sm} on the VNP objective for $N_G = 300$

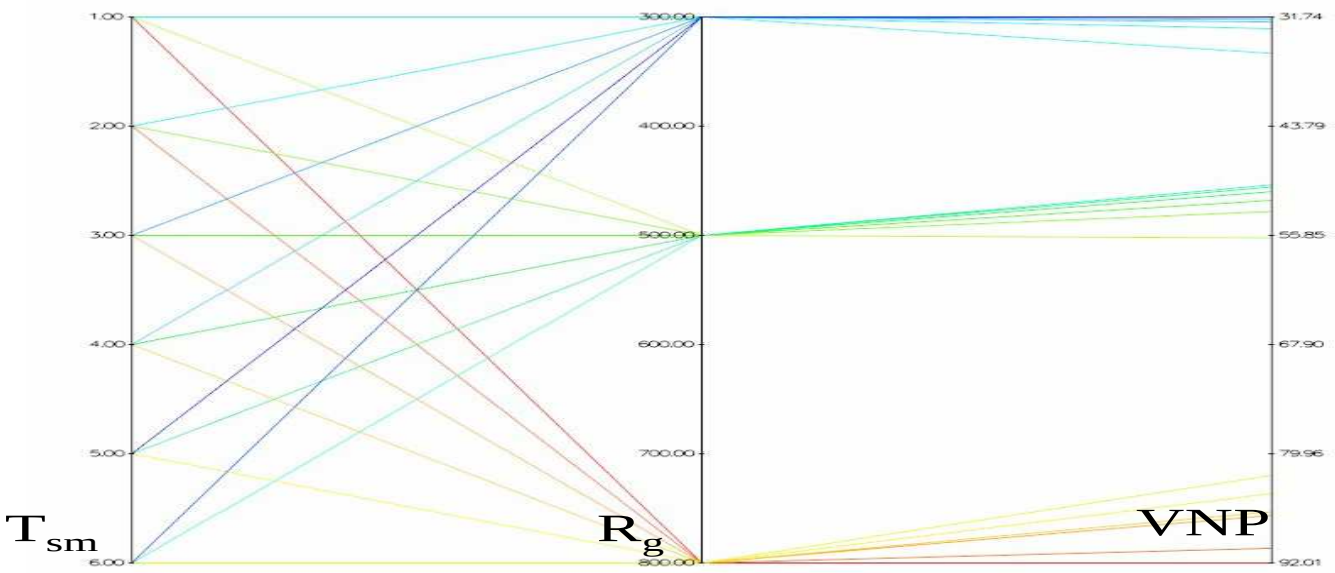

(c) EEMMASMP

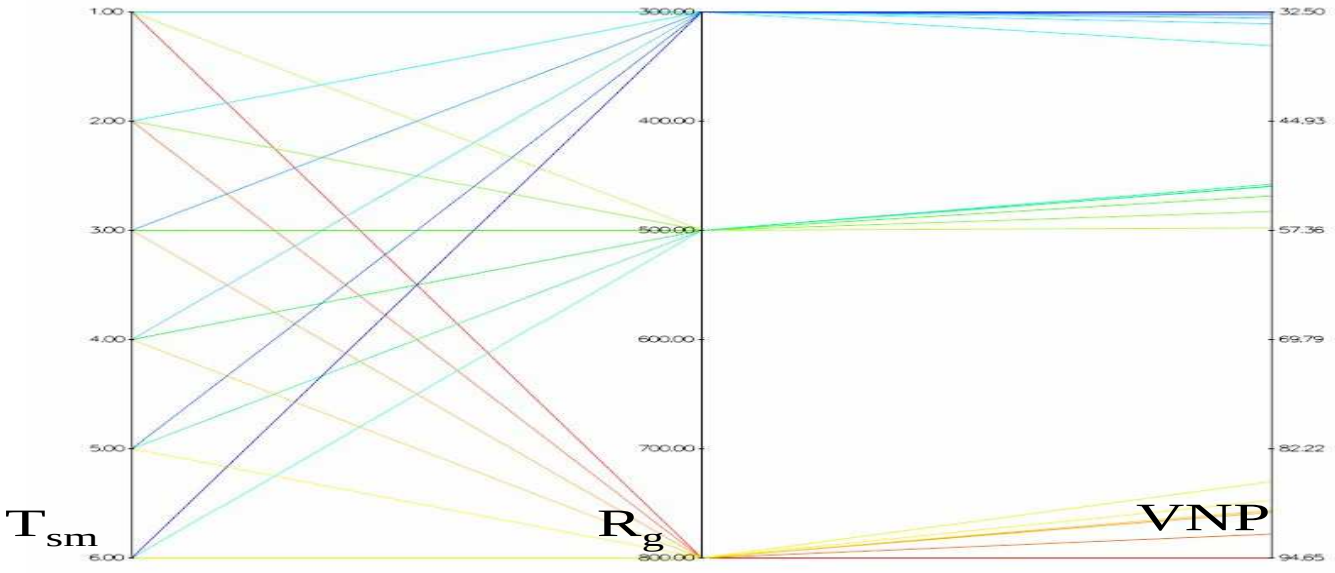

(d) EEMMASMH

Figure J.9: Influence of R_g and T_{sm} on the VNP objective for $N_G = 300$ (cont.)

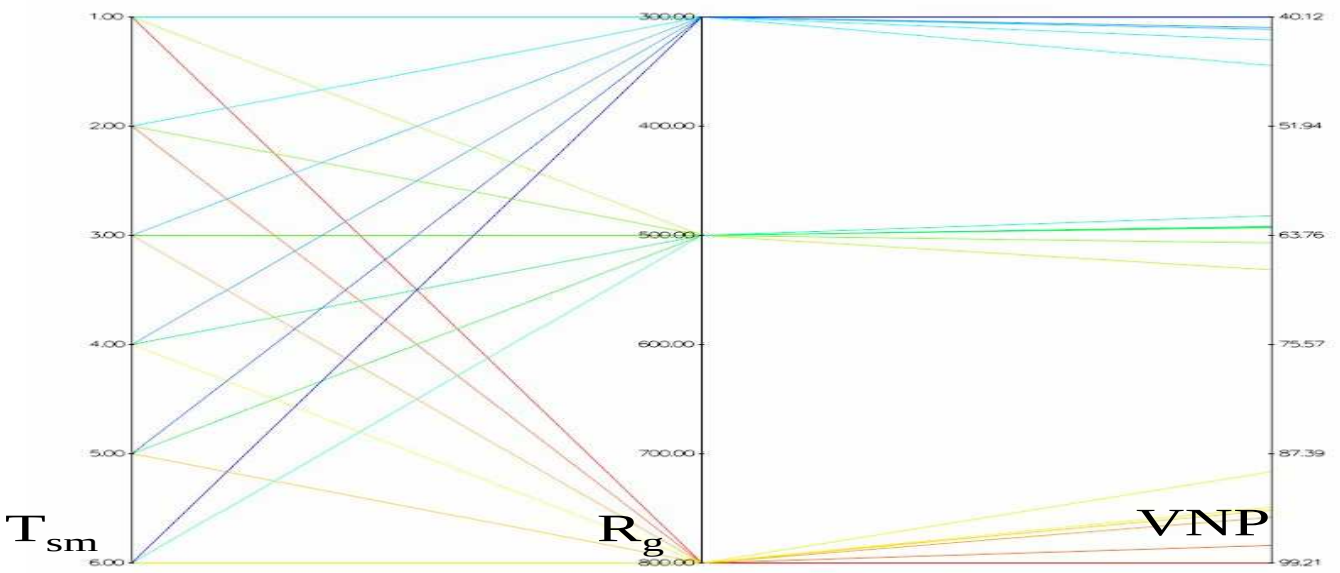

(e) EEMACOMC

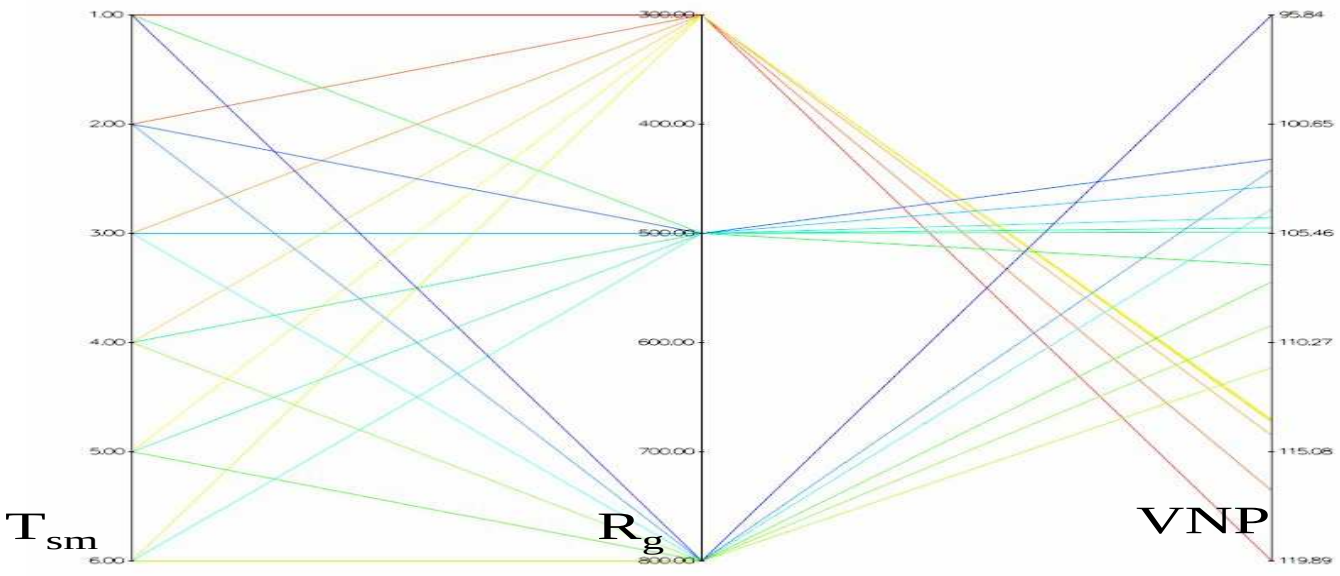

(f) NSGA-II-MPA

Figure J.9: Influence of R_g and T_{sm} on the VNP objective for $N_G = 300$ (cont.)

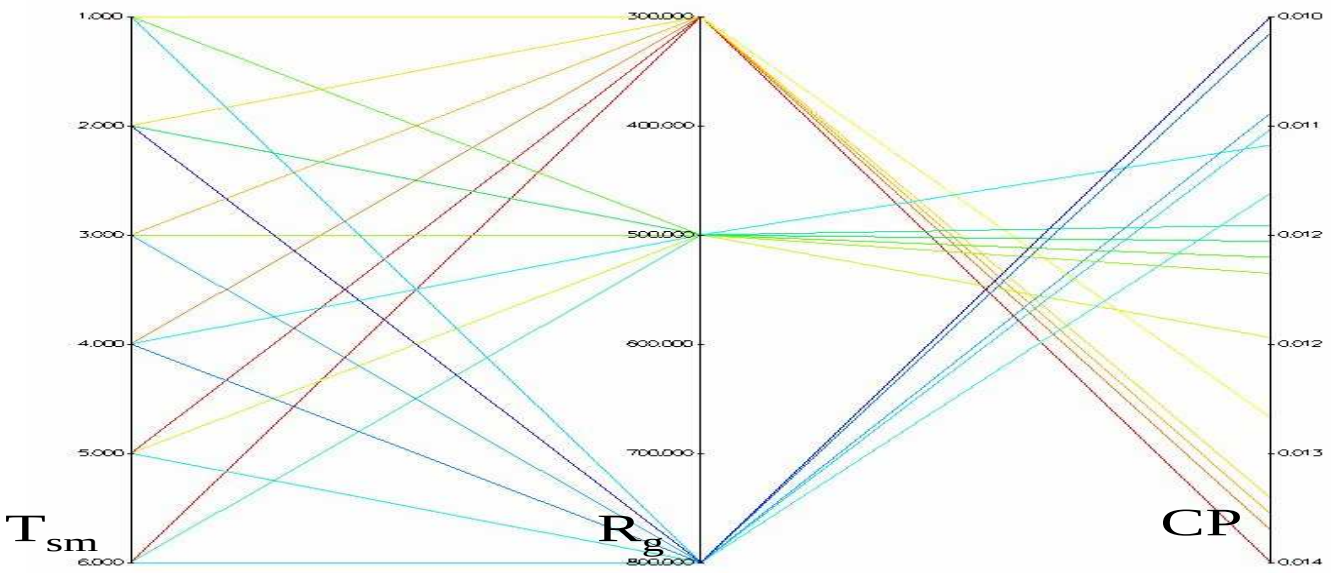

(a) EEMACOMP

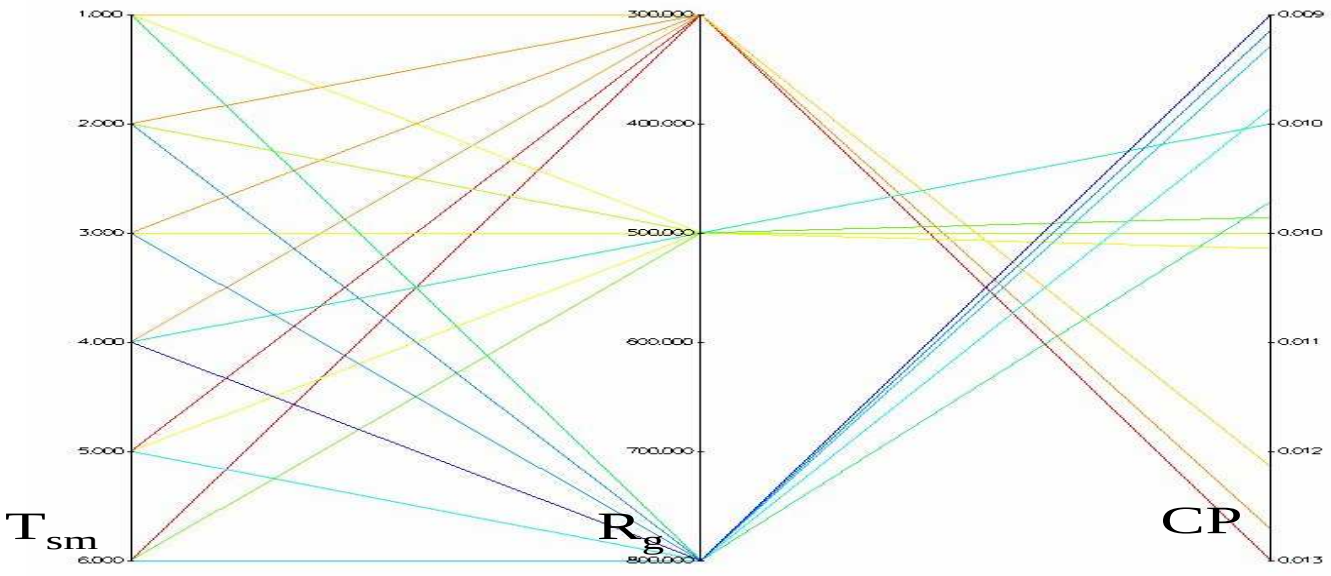

(b) EEMACOMH

Figure J.10: Influence of R_g and T_{sm} on the CP objective for $N_G = 30$

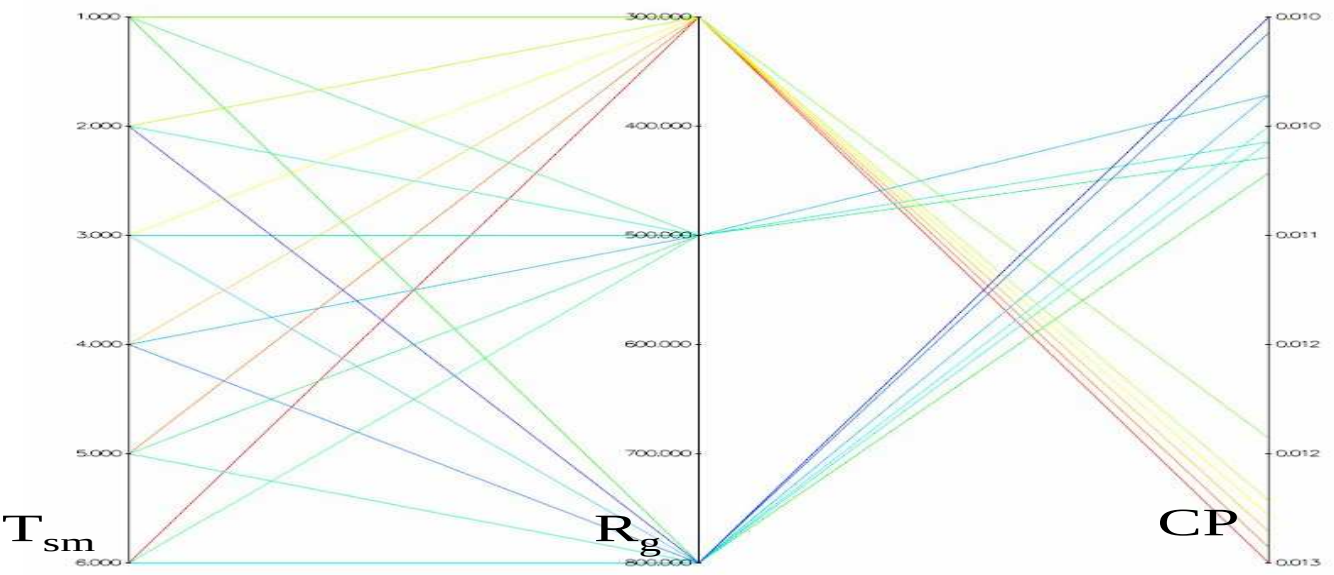

(c) EEMMASMP

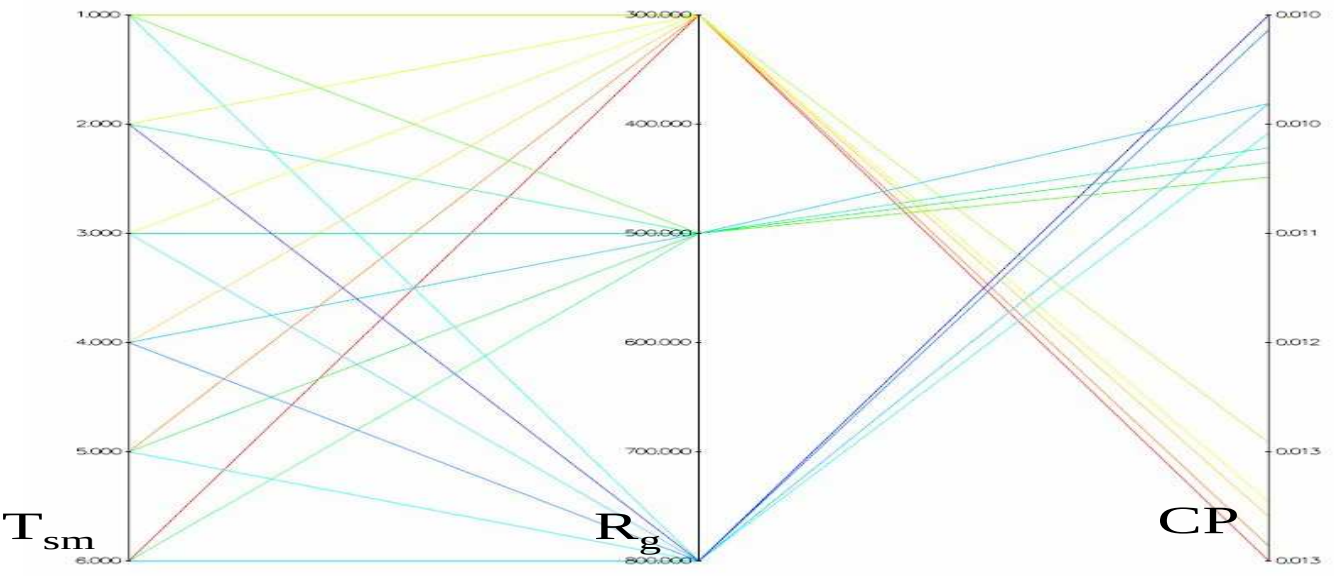

(d) EEMMASMH

Figure J.10: Influence of R_g and T_{sm} on the CP objective for $N_G = 30$ (cont.)

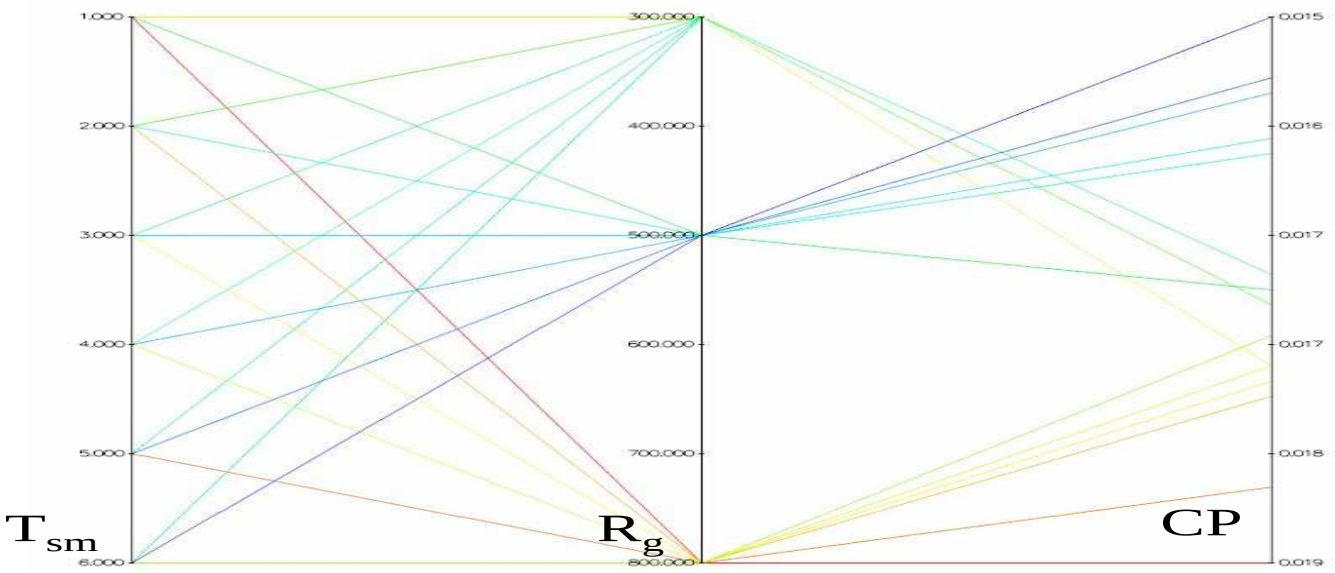

(e) EEMACOMC

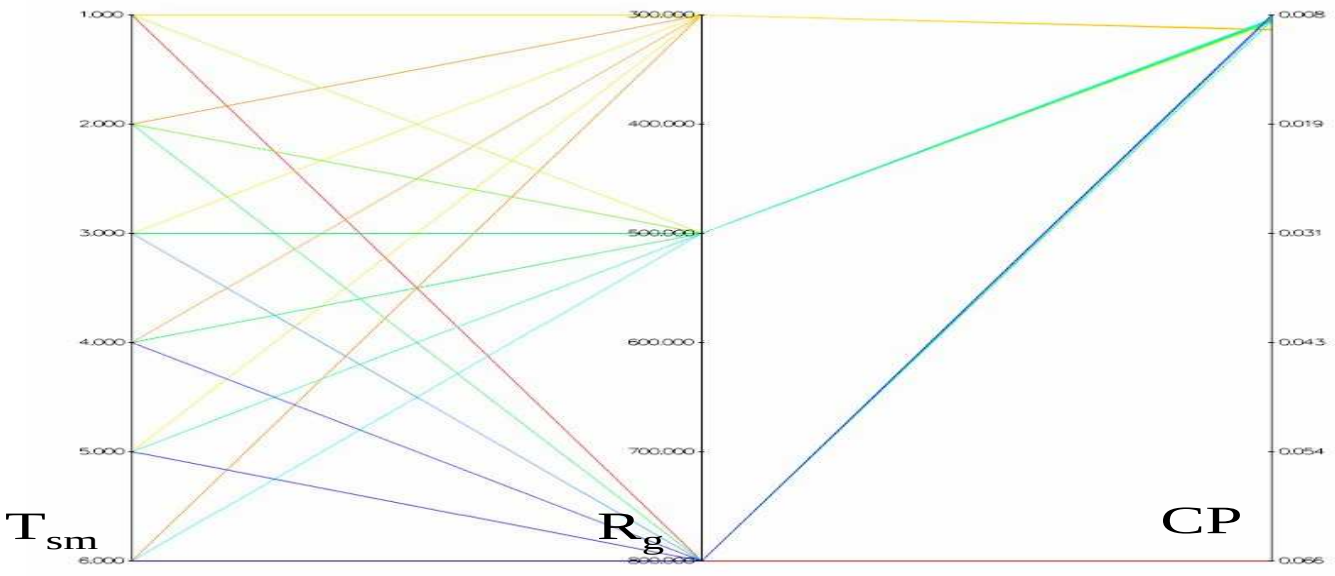

(f) NSGA-II-MPA

Figure J.10: Influence of R_g and T_{sm} on the CP objective for $N_G = 30$ (cont.)

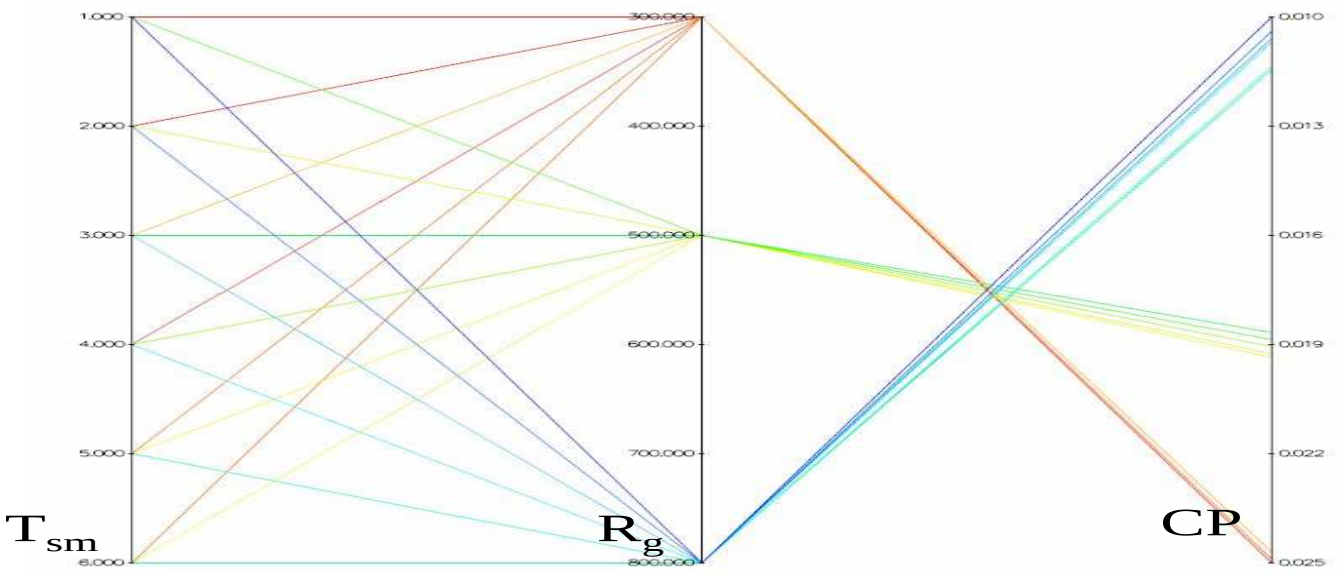

(a) EEMACOMP

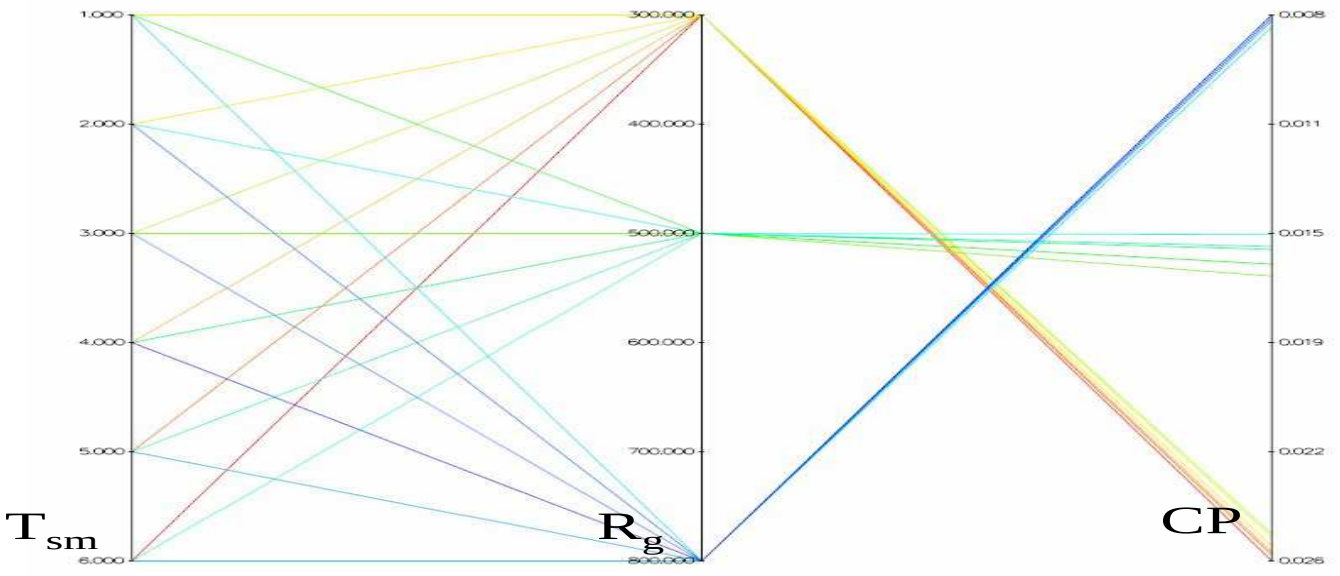

(b) EEMACOMH

Figure J.11: Influence of R_g and T_{sm} on the CP objective for $N_G = 100$

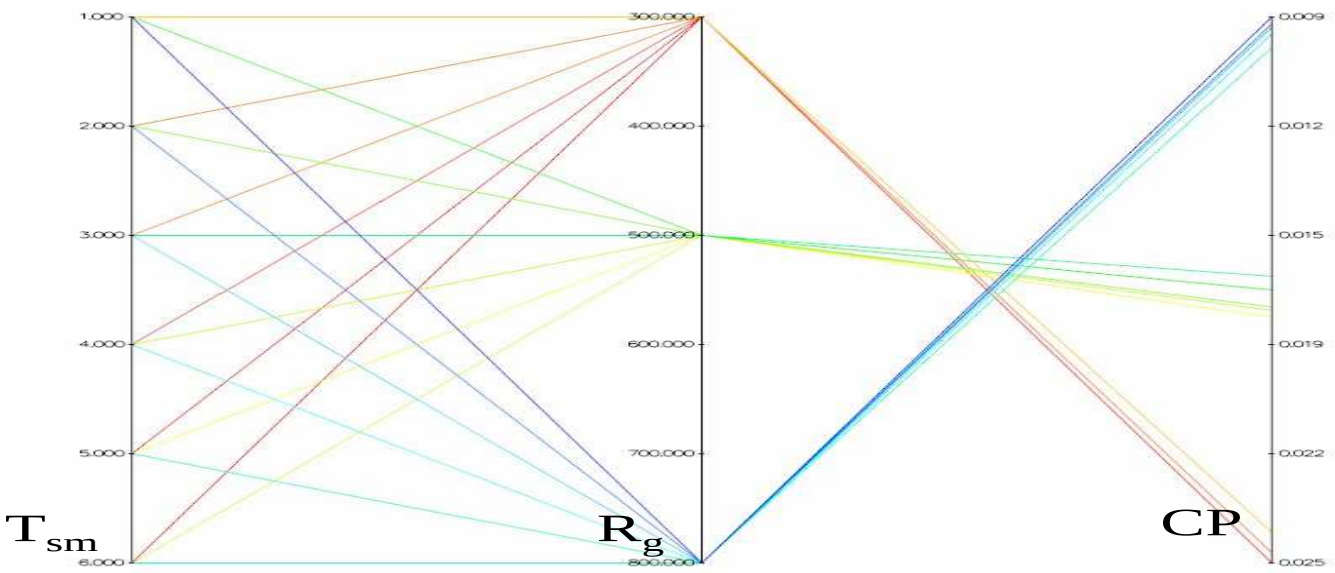

(c) EEMMASMP

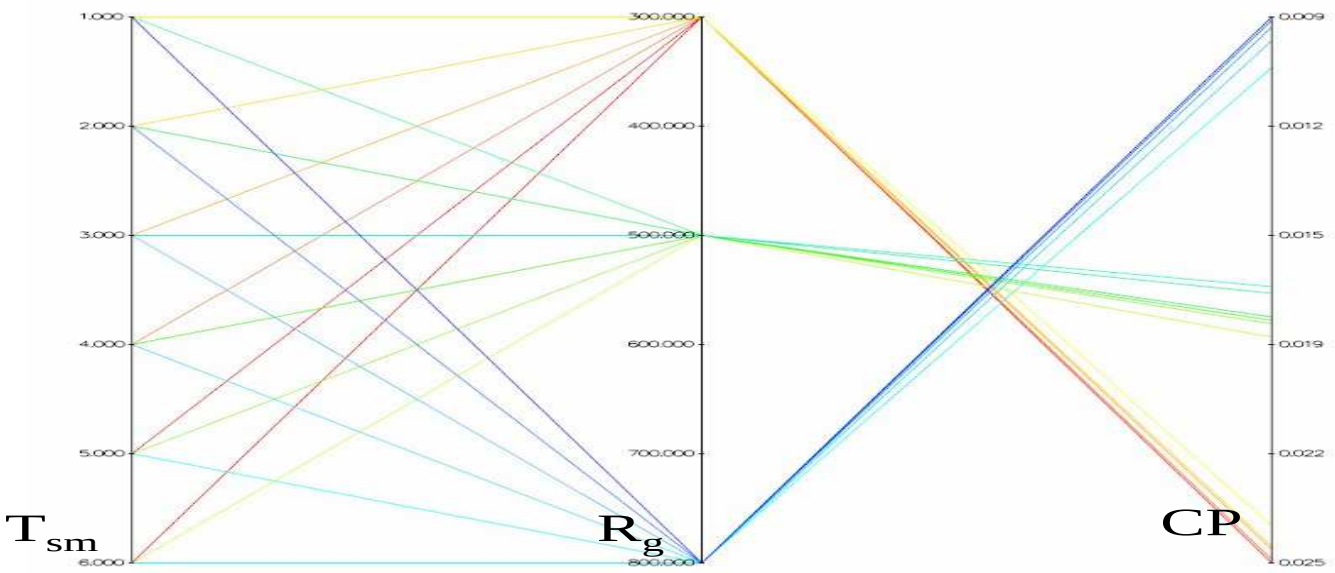

(d) EEMMASMH

Figure J.11: Influence of R_g and T_{sm} on the CP objective for $N_G = 100$ (cont.)

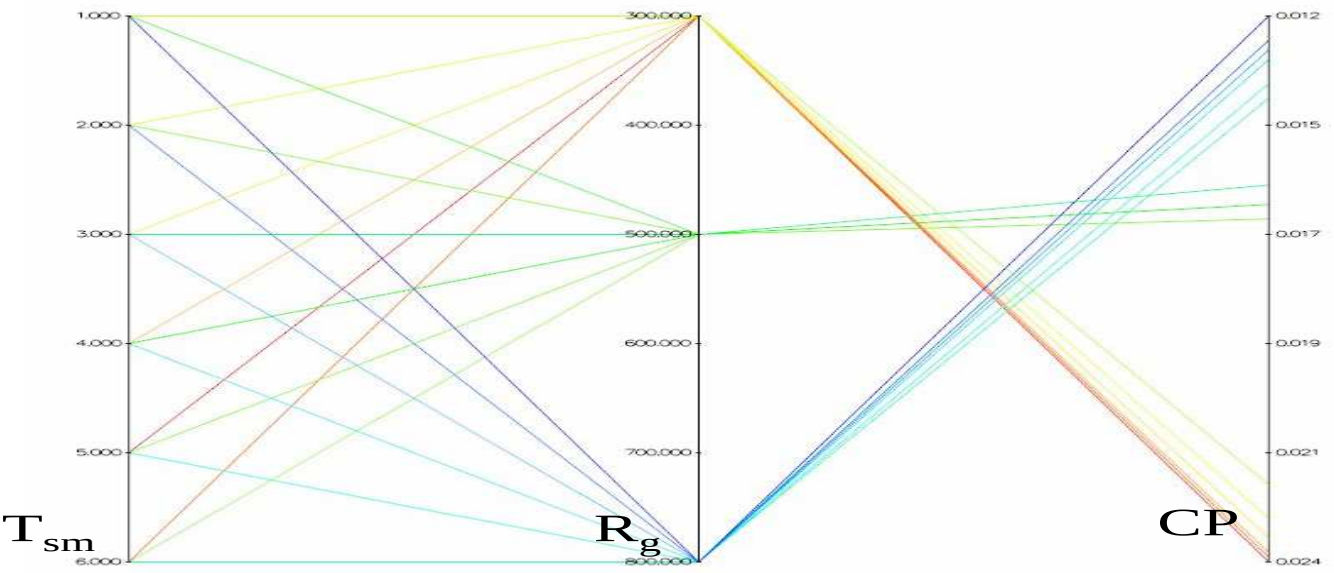

(e) EEMACOMC

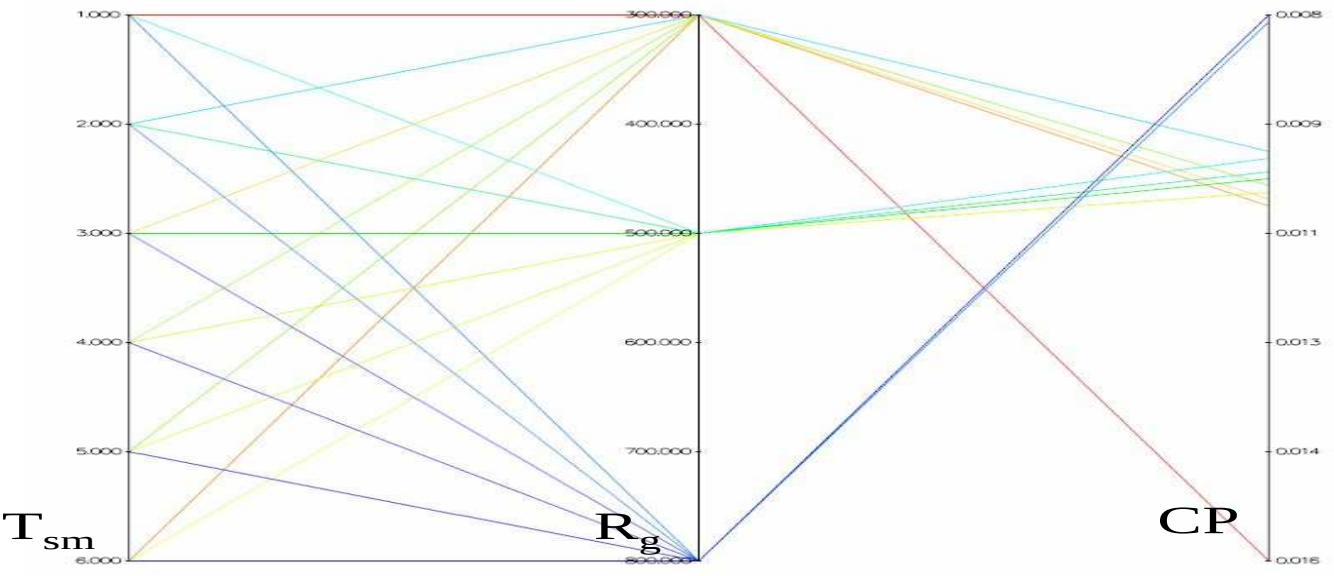

(f) NSGA-II-MPA

Figure J.11: Influence of R_g and T_{sm} on the CP objective for $N_G = 100$ (cont.)

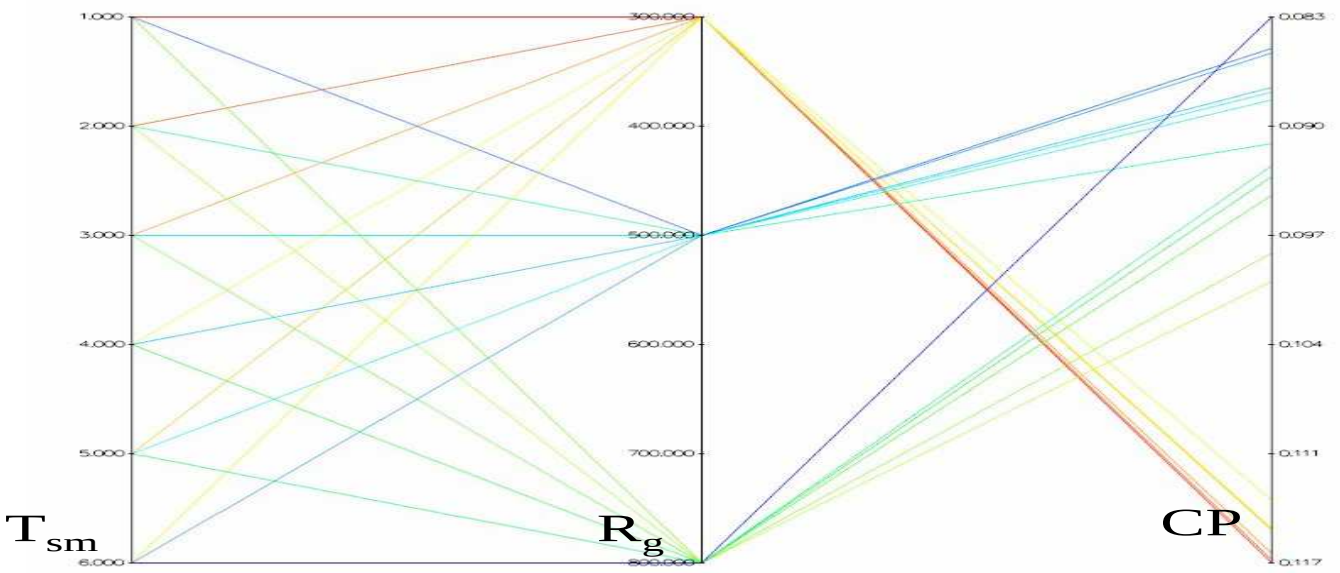

(a) EEMACOMP

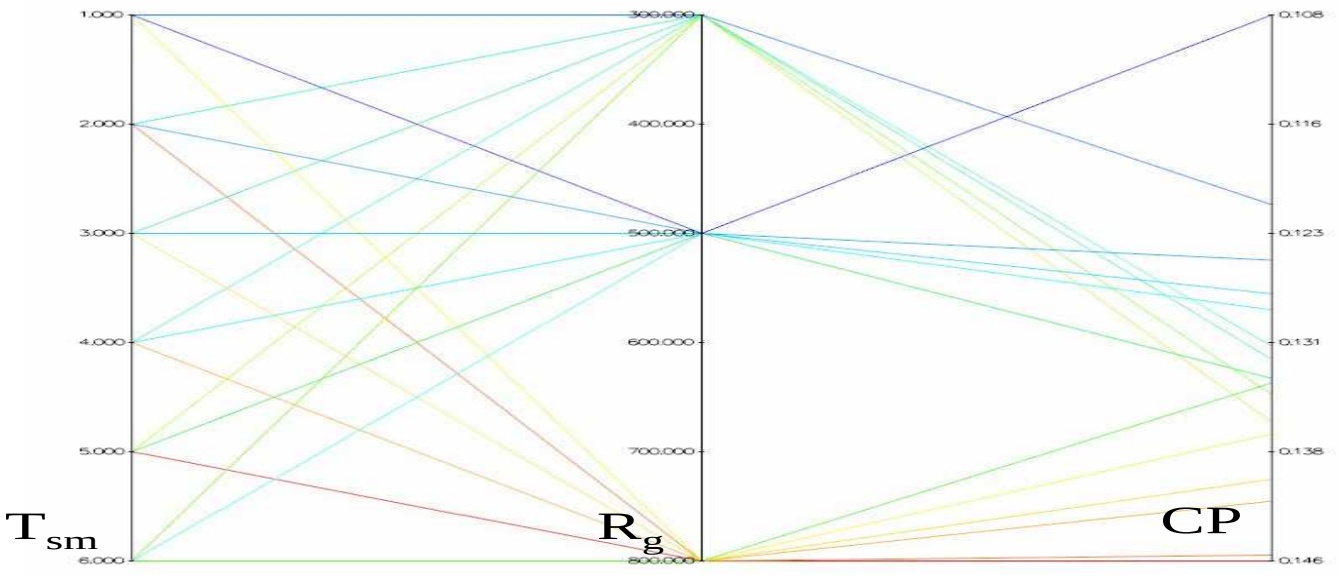

(b) EEMACOMH

Figure J.12: Influence of R_g and T_{sm} on the CP objective for $N_G = 300$

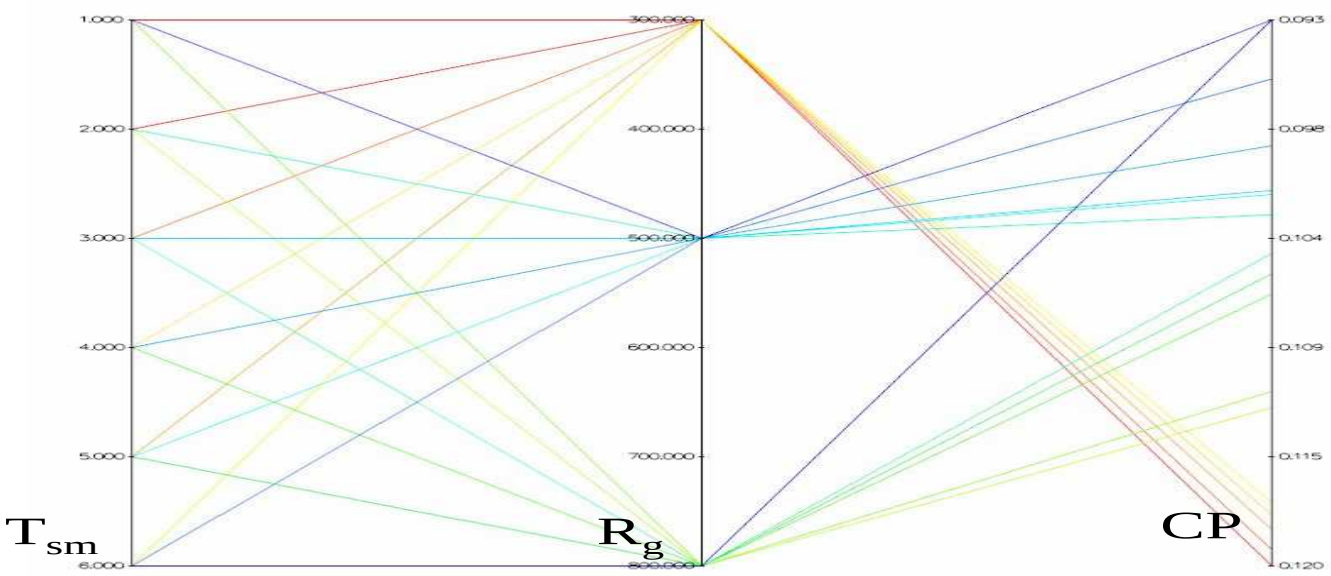

(c) EEMMASMP

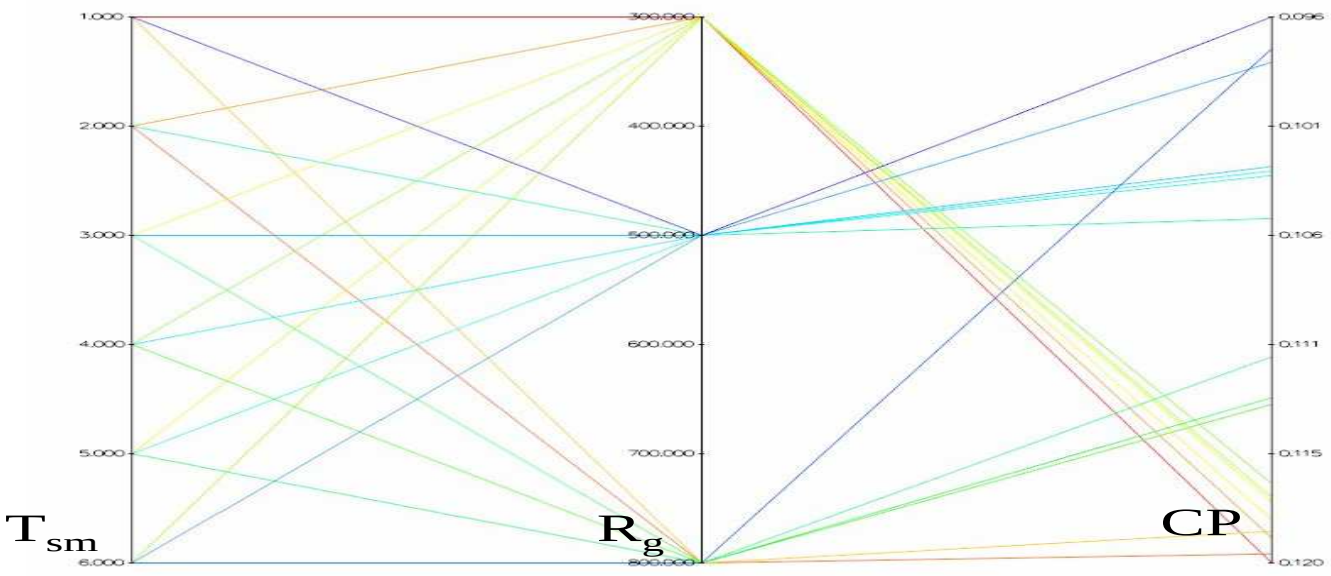

(d) EEMMASMH

Figure J.12: Influence of R_g and T_{sm} on the CP objective for $N_G = 300$ (cont.)

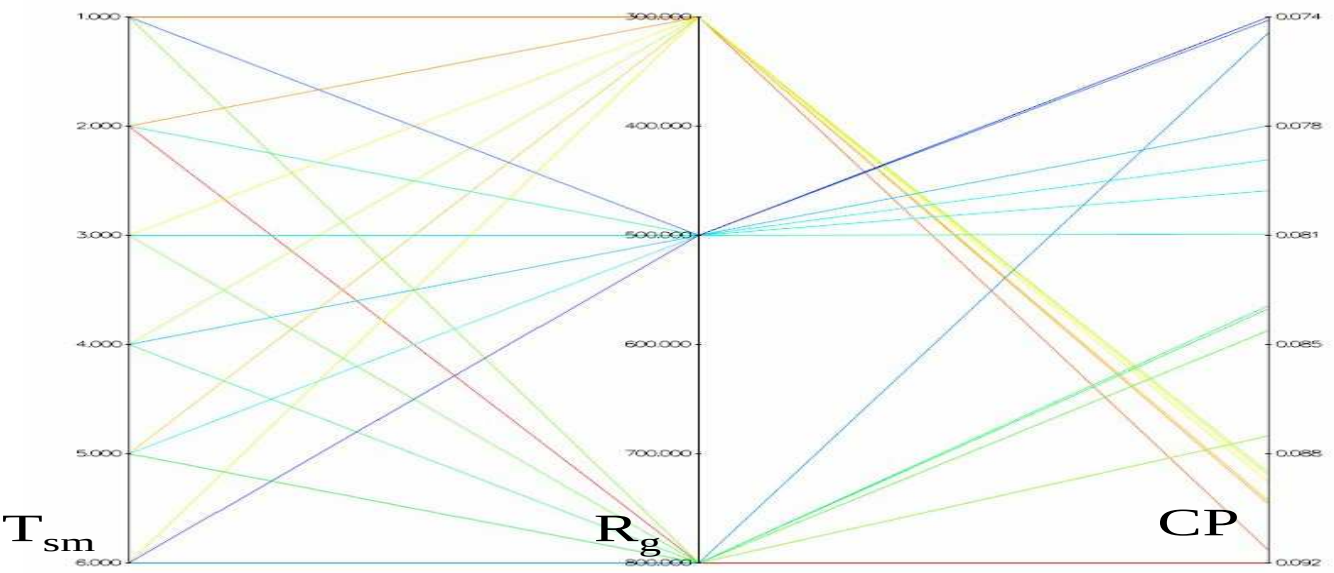

(e) EEMACOMC

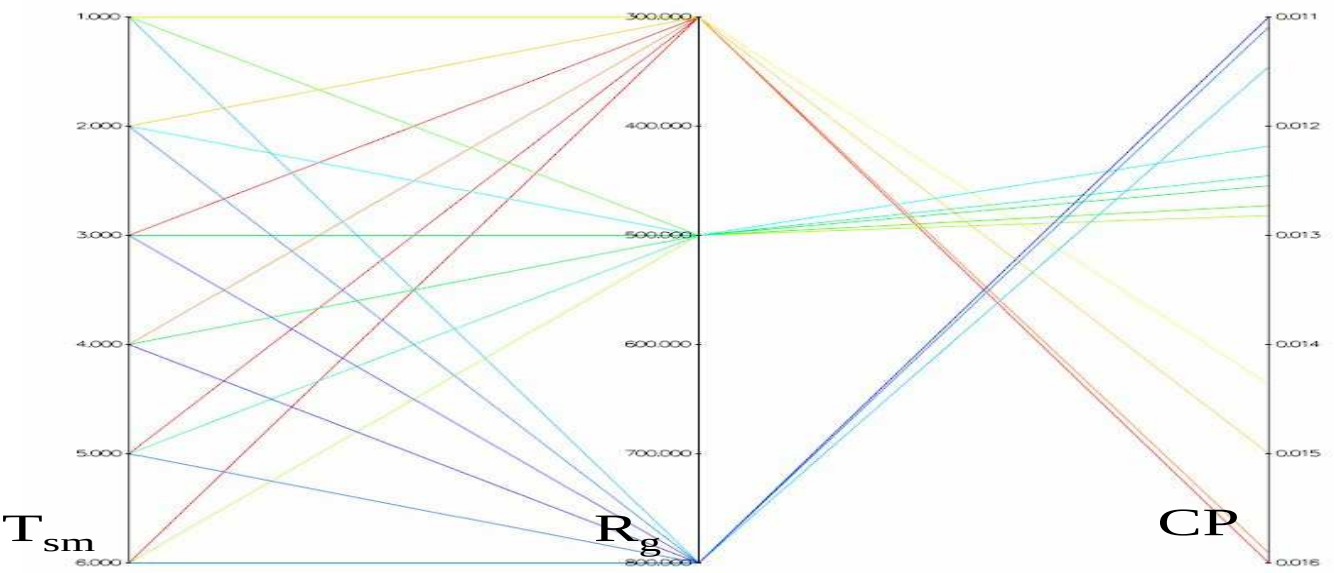

(f) NSGA-II-MPA

Figure J.12: Influence of R_g and T_{sm} on the CP objective for $N_G = 300$ (cont.)

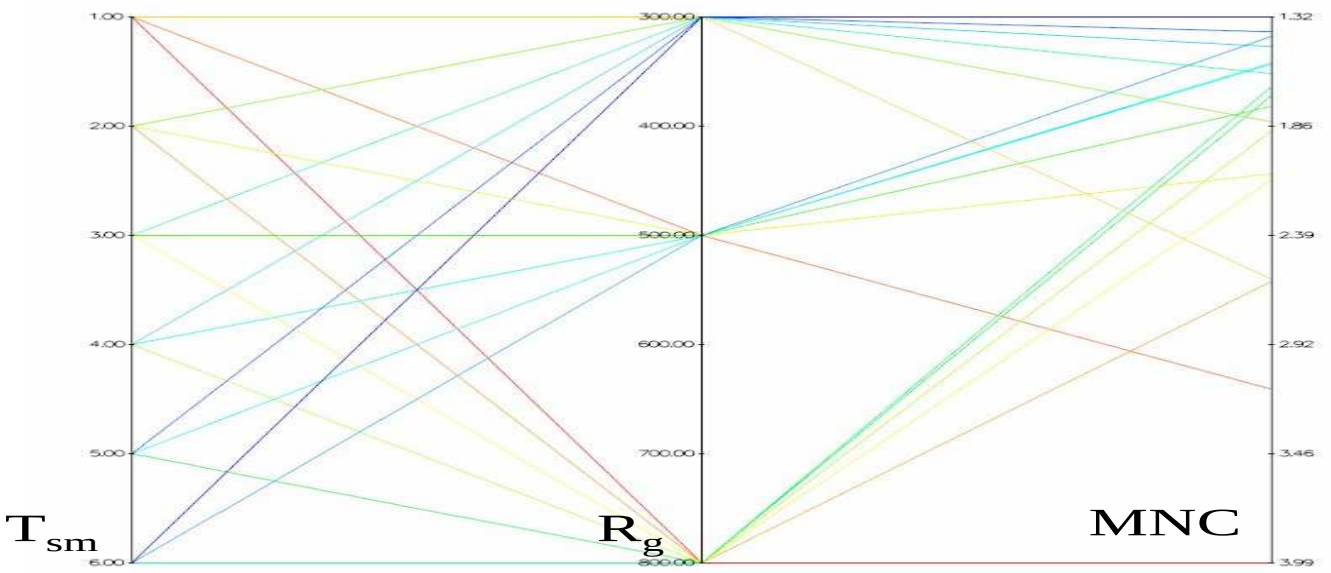

(a) EEMACOMP

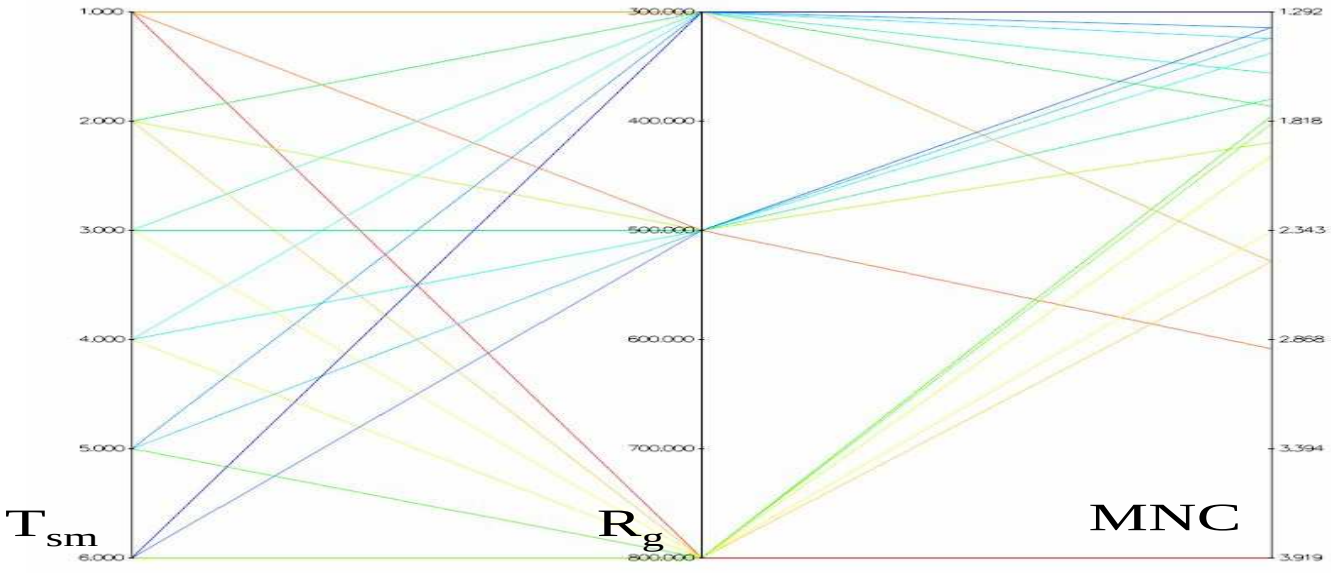

(b) EEMACOMH

Figure J.13: Influence of R_g and T_{sm} on the MNC objective for $N_G = 30$

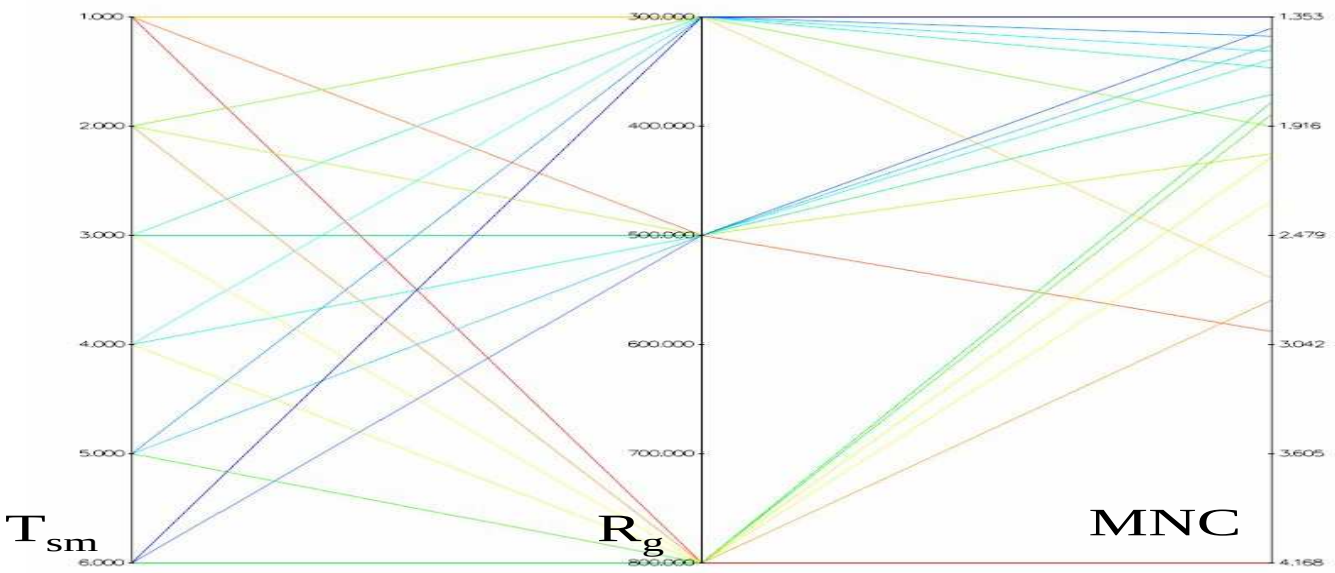

(c) EEMMASMP

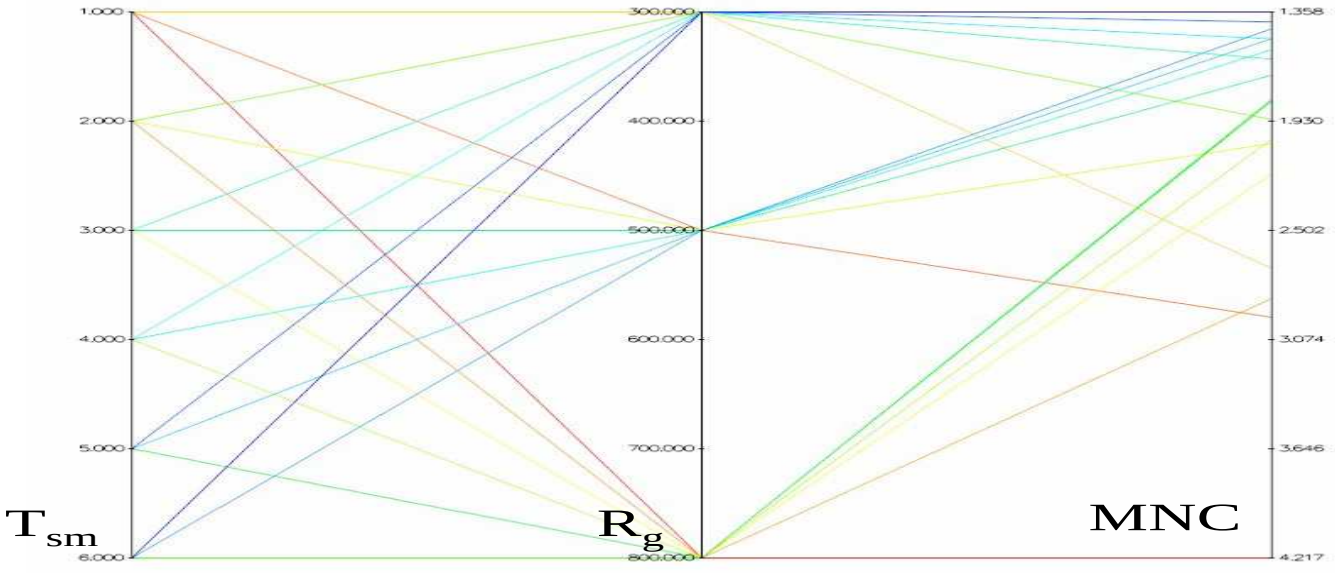

(d) EEMMASMH

Figure J.13: Influence of R_g and T_{sm} on the MNC objective for $N_G = 30$ (cont.)

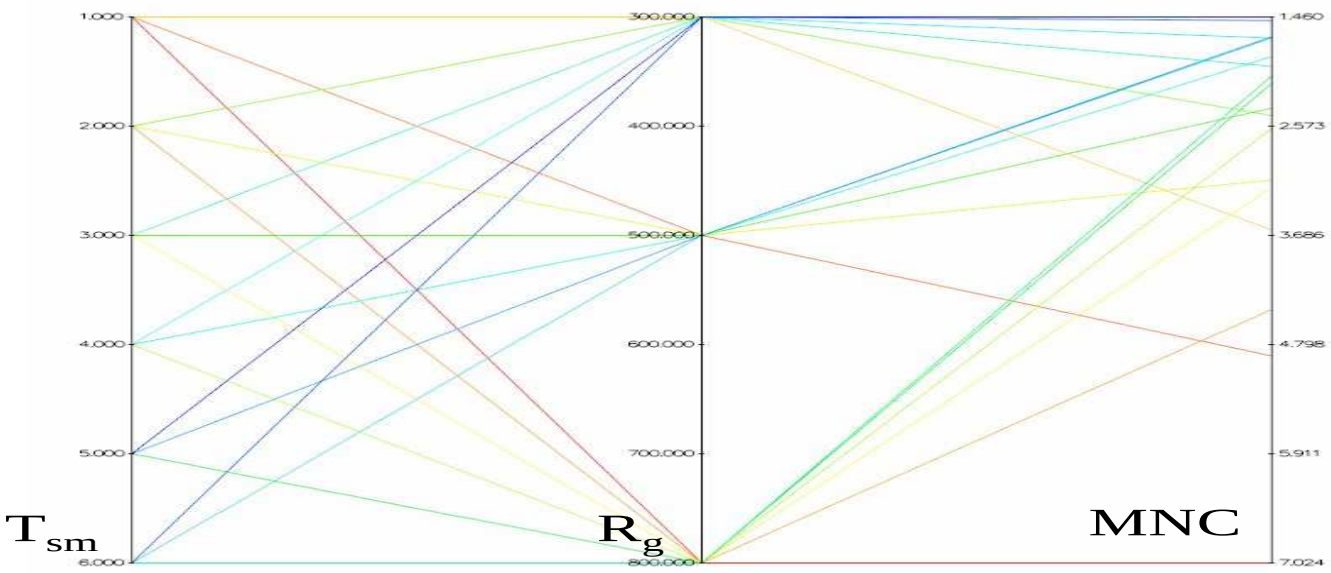

(e) EEMACOMC

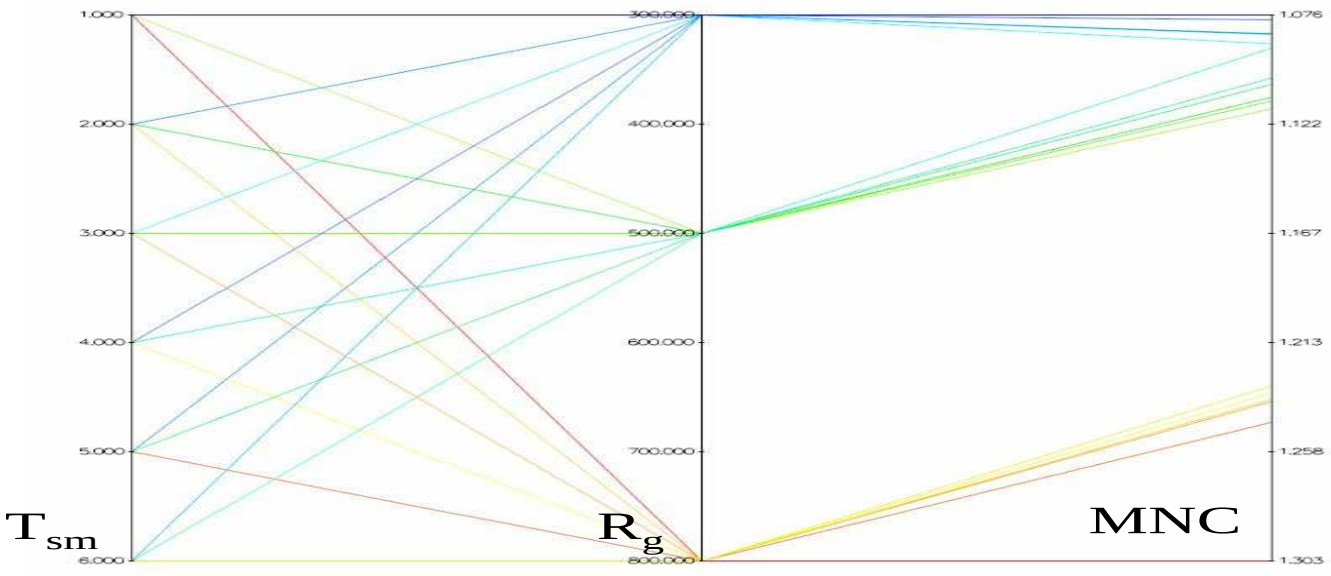

(f) NSGA-II-MPA

Figure J.13: Influence of R_g and T_{sm} on the MNC objective for $N_G = 30$ (cont.)

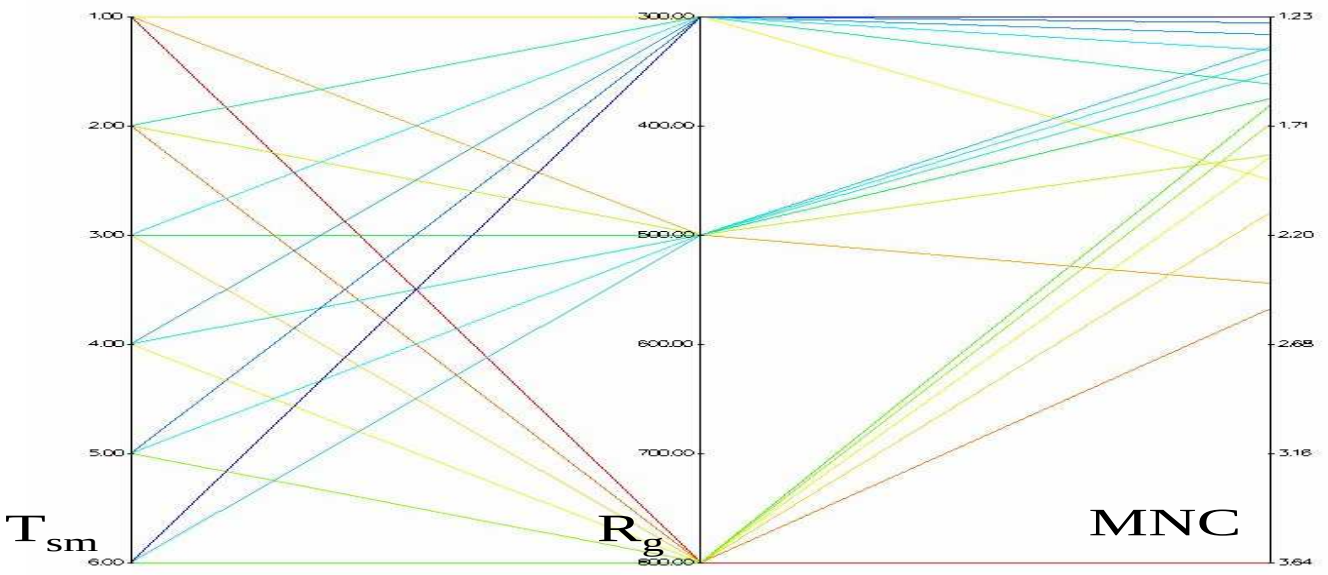

(a) EEMACOMP

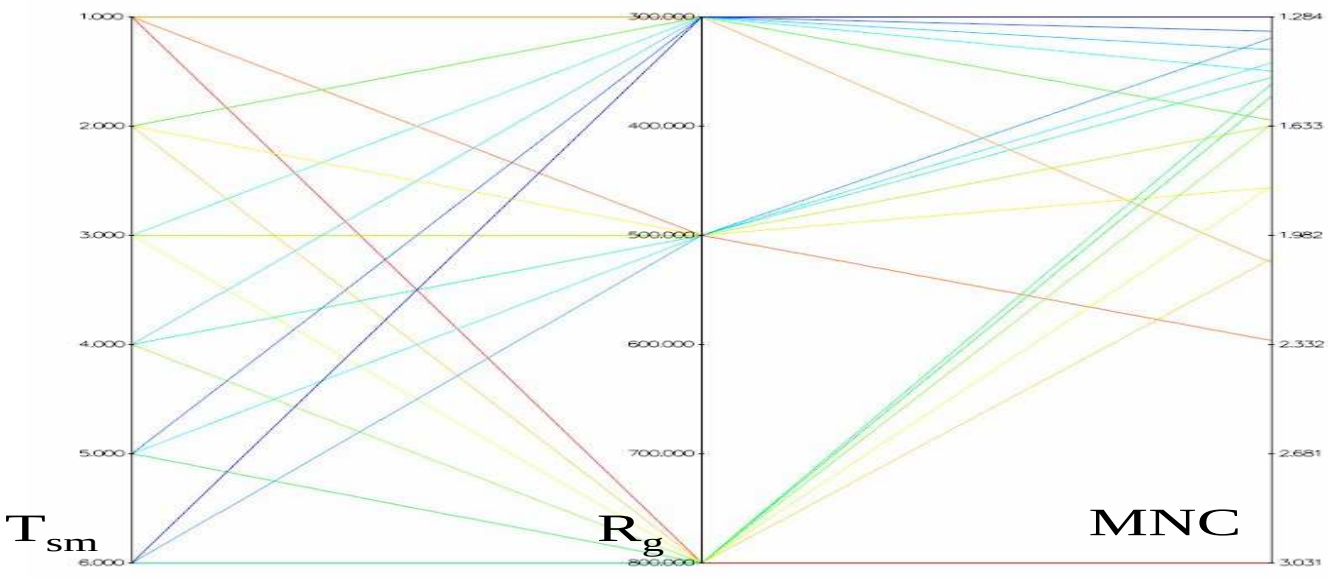

(b) EEMACOMH

Figure J.14: Influence of R_g and T_{sm} on the MNC objective for $N_G = 100$

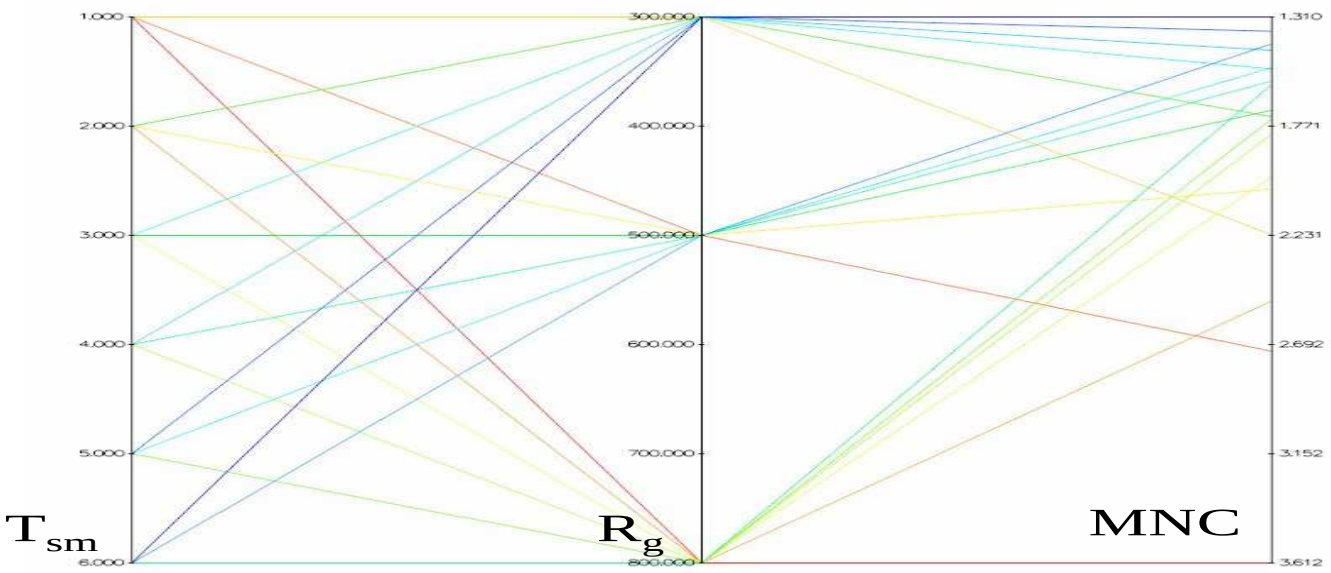

(c) EEMMASMP

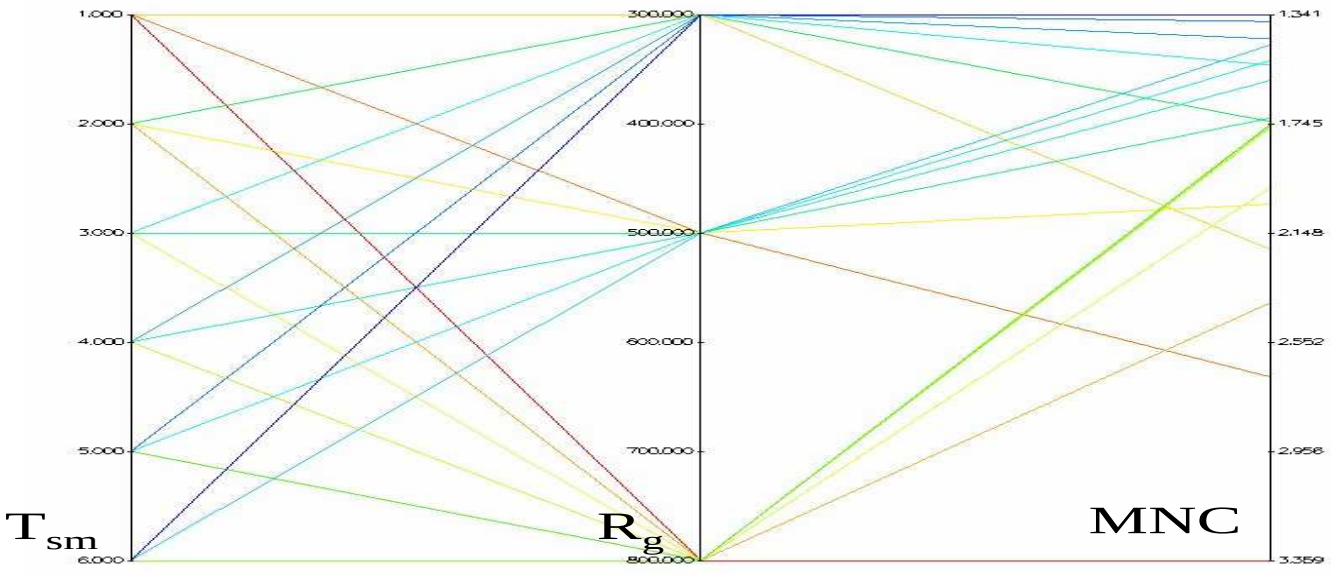

(d) EEMMASMH

Figure J.14: Influence of R_g and T_{sm} on the MNC objective for $N_G = 100$ (cont.)

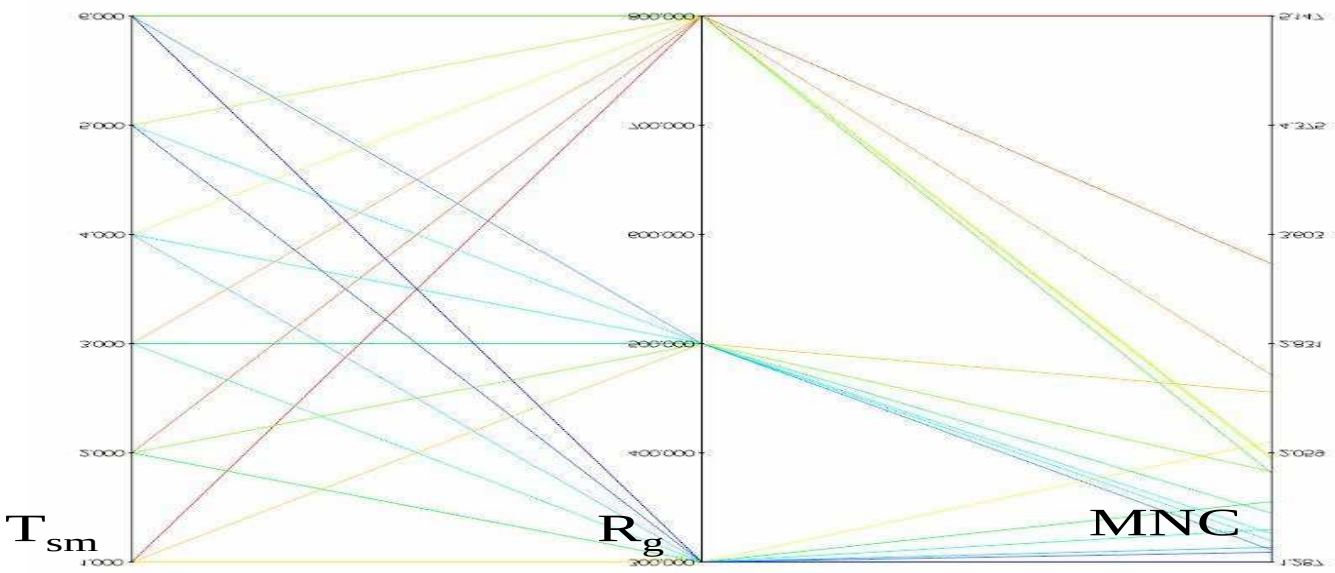

(e) EEMACOMC

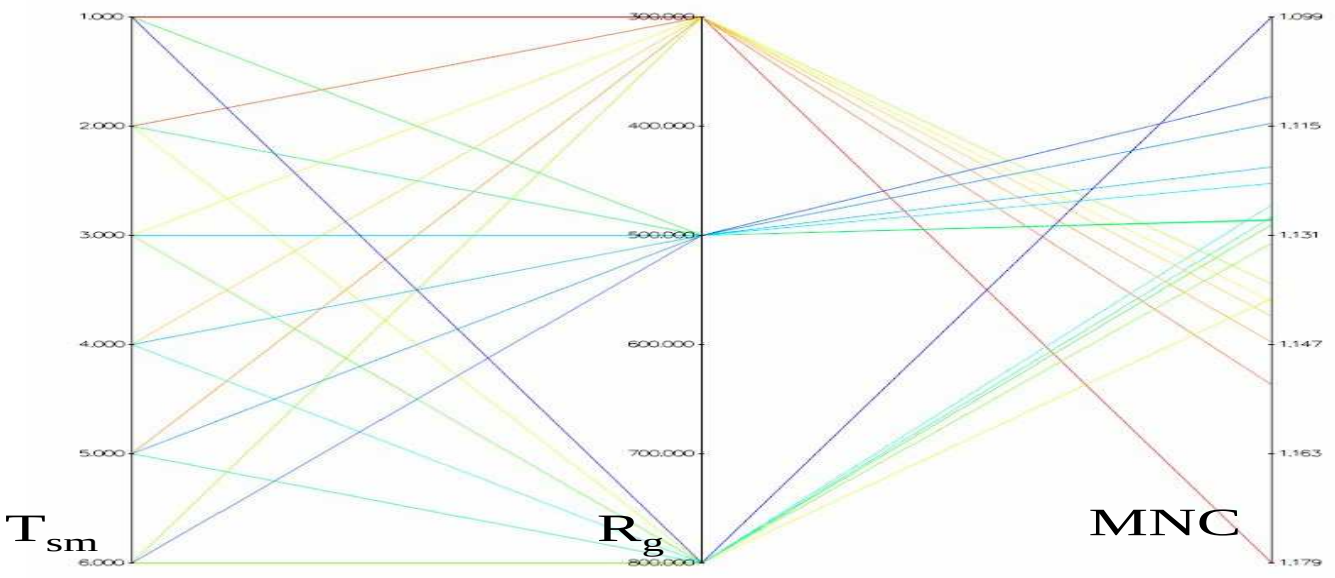

(f) NSGA-II-MPA

Figure J.14: Influence of R_g and T_{sm} on the MNC objective for $N_G = 100$ (cont.)

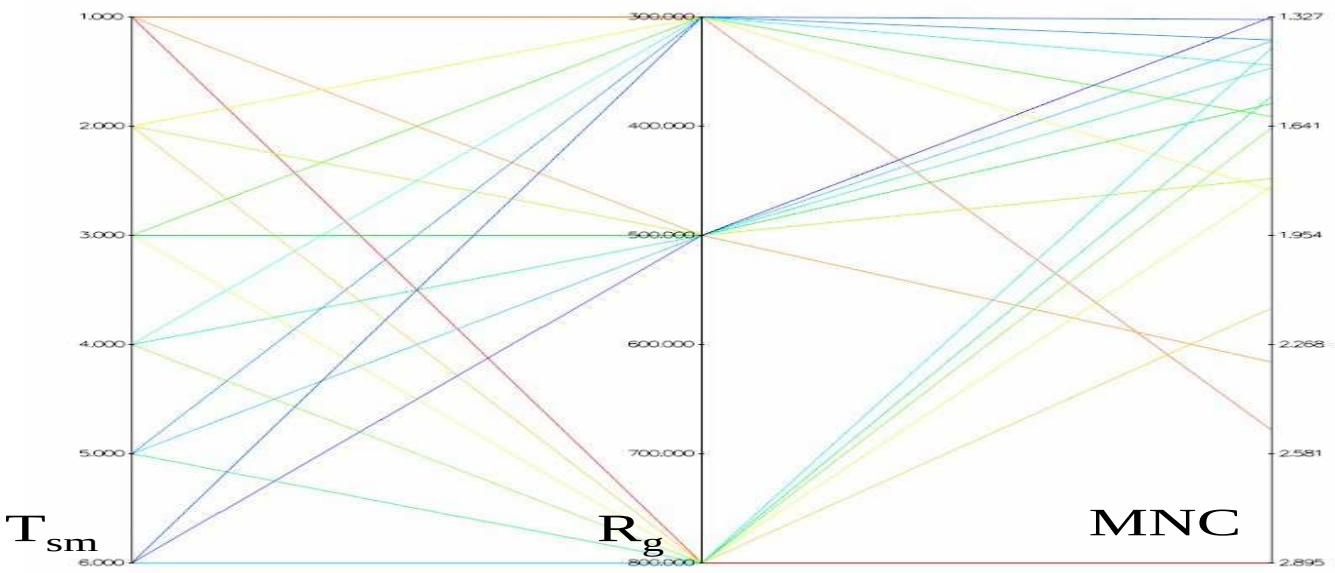

(a) EEMACOMP

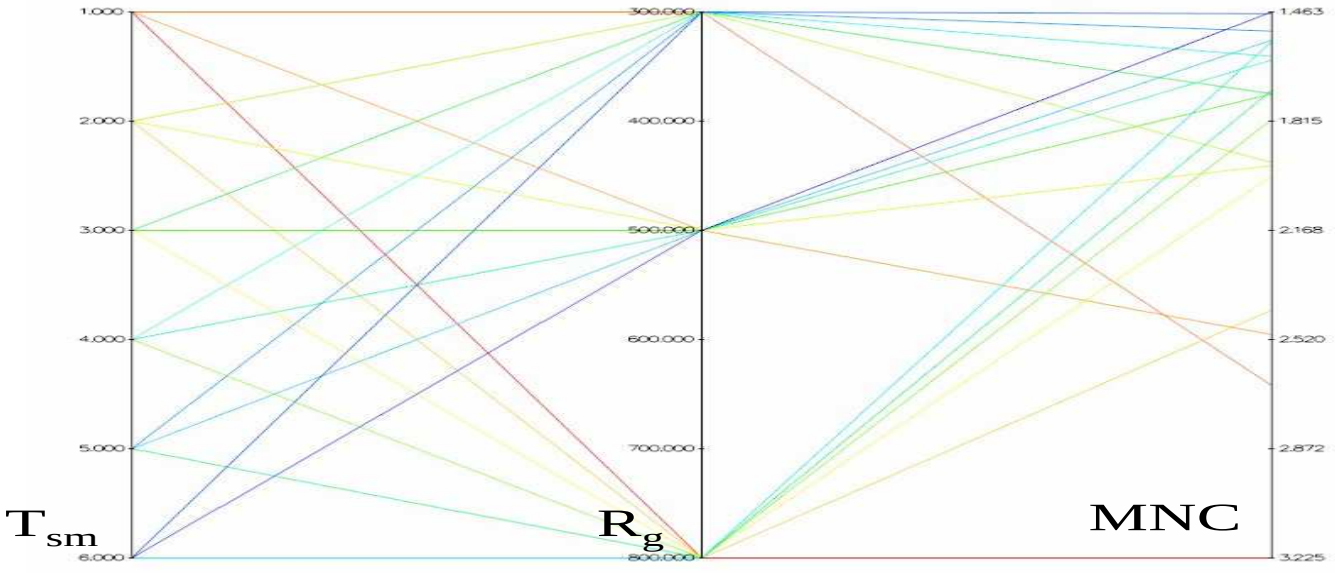

(b) EEMACOMH

Figure J.15: Influence of R_g and T_{sm} on the MNC objective for $N_G = 300$

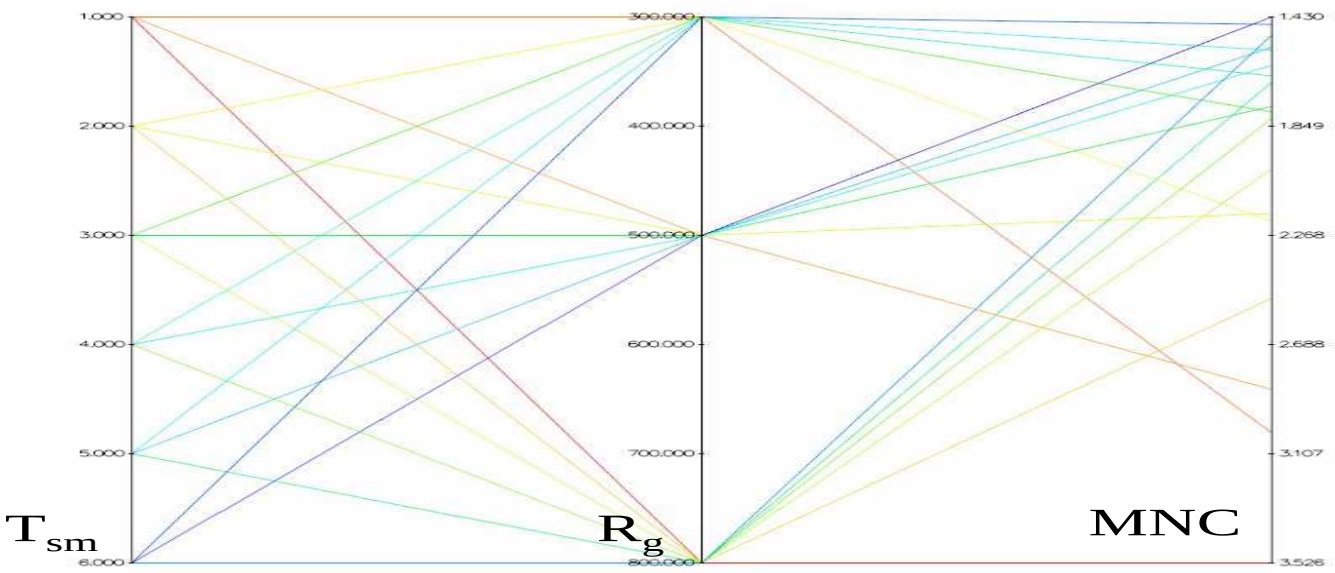

(c) EEMMASMP

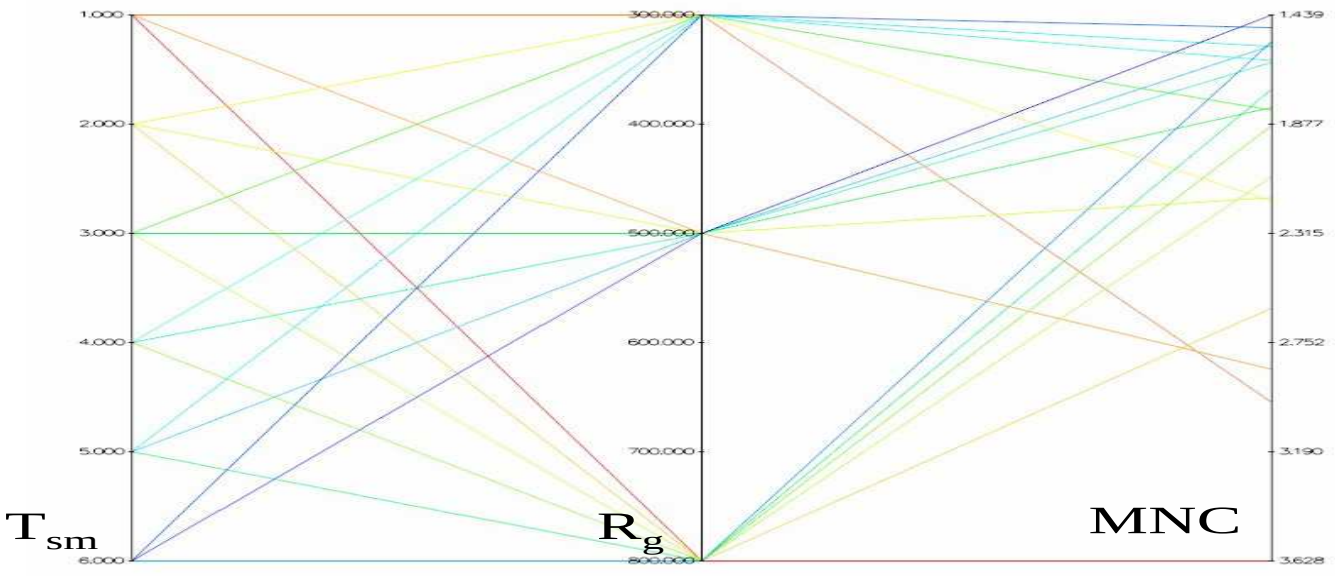

(d) EEMMASMH

Figure J.15: Influence of R_g and T_{sm} on the MNC objective for $N_G = 300$ (cont.)

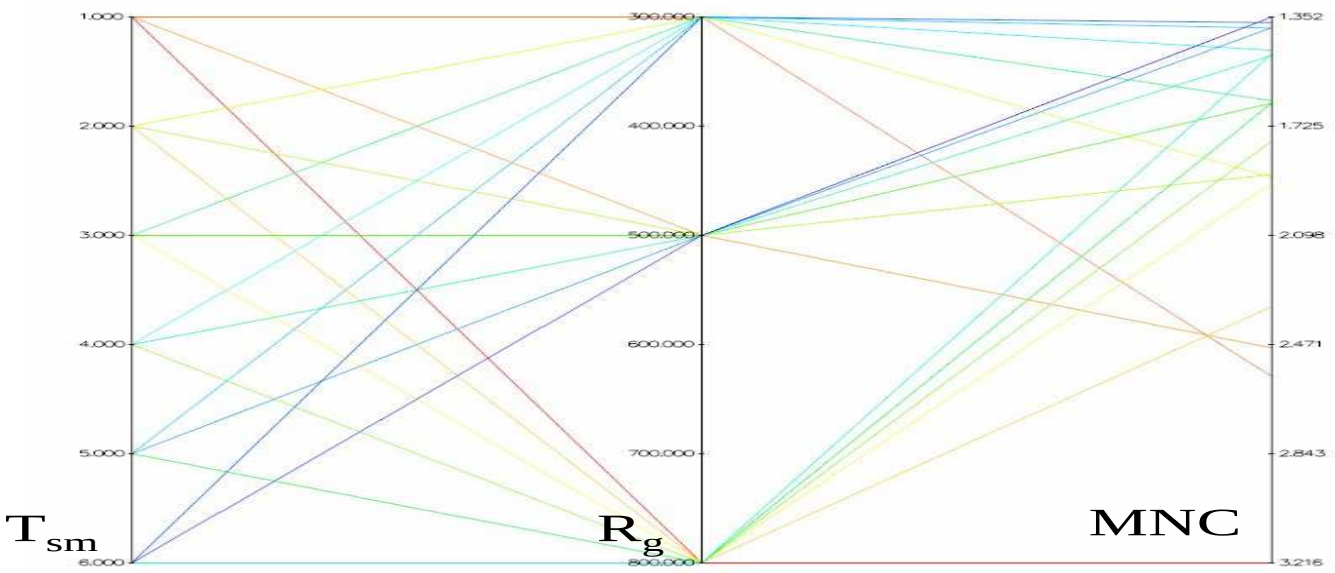

(e) EEMACOMC

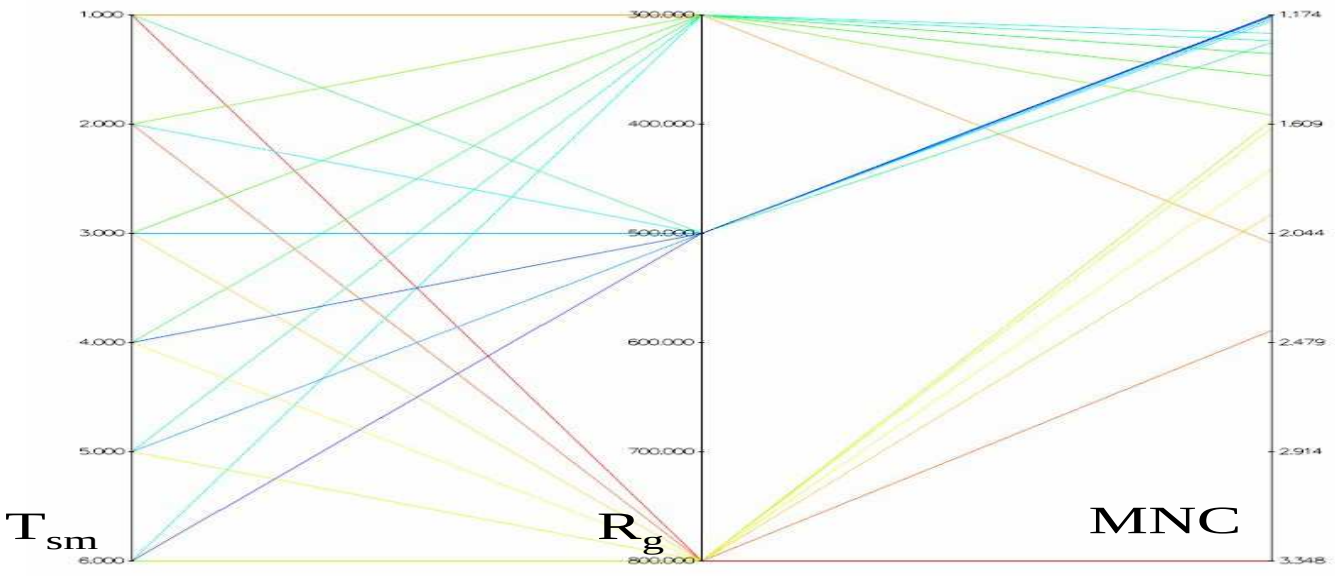

(f) NSGA-II-MPA

Figure J.15: Influence of R_g and T_{sm} on the MNC objective for $N_G = 300$ (cont.)